

Final Report to



Development of Subsurface Brine Disposal Framework in the Northern Appalachian Basin

11122-73.FINAL

September 25, 2015

Technical Points of Contact:

Mr. Joel R. Sminchak

(614) 424-7392

sminchak@battelle.org

Dr. Neeraj Gupta

(614) 424-3820

gupta@battelle.org

Contractual Point of Contact:

Ms. LaDonna F. James

(614) 424-5543

jamesl@battelle.org

Battelle

Battelle Memorial Institute

505 King Avenue

Columbus, Ohio 43201-2696

LEGAL NOTICE

THIS REPORT WAS PREPARED BY BATTELLE AS AN ACCOUNT OF WORK SPONSORED BY THE RESEARCH PARTNERSHIP TO SECURE ENERGY FOR AMERICA, RPSEA. NEITHER RPSEA MEMBERS OF RPSEA, THE NATIONAL ENERGY TECHNOLOGY LABORATORY, THE U.S. DEPARTMENT OF ENERGY, BATTELLE, NOR ANY PERSON ACTING ON BEHALF OF ANY OF THE ENTITIES:

- a. MAKES ANY WARRANTY OR REPRESENTATION, EXPRESS OR IMPLIED WITH RESPECT TO ACCURACY, COMPLETENESS, OR USEFULNESS OF THE INFORMATION CONTAINED IN THIS DOCUMENT, OR THAT THE USE OF ANY INFORMATION, APPARATUS, METHOD, OR PROCESS DISCLOSED IN THIS DOCUMENT MAY NOT INFRINGE PRIVATELY OWNED RIGHTS, OR
- b. ASSUMES ANY LIABILITY WITH RESPECT TO THE USE OF, OR FOR ANY AND ALL DAMAGES RESULTING FROM THE USE OF, ANY INFORMATION, APPARATUS, METHOD, OR PROCESS DISCLOSED IN THIS DOCUMENT.

THIS IS A FINAL REPORT. THE DATA, CALCULATIONS, INFORMATION, CONCLUSIONS, AND/OR RECOMMENDATIONS REPORTED HEREIN ARE THE PROPERTY OF THE U.S. DEPARTMENT OF ENERGY.

REFERENCE TO TRADE NAMES OR SPECIFIC COMMERCIAL PRODUCTS, COMMODITIES, OR SERVICES IN THIS REPORT DOES NOT REPRESENT OR CONSTITUTE AN ENDORSEMENT, RECOMMENDATION, OR FAVORING BY RPSEA OR ITS CONTRACTORS OF THE SPECIFIC COMMERCIAL PRODUCT, COMMODITY, OR SERVICE.

Signature of Submitting Official: *J.R. Sminchak*

Date: 9/25/15

ABSTRACT

The overall objective of this 2.5-year research project was to develop a geologic and operational framework for brine disposal in the Northern Appalachian Basin so that the produced fluids from unconventional onshore resource exploitation can be disposed safely and economically. Growth in shale gas production and associated brine and flowback water disposal needs has led to significant current and projected demand for brine disposal in the Appalachian Basin. This project addresses a crucial need of unconventional oil and gas production with an assessment of geologic and reservoir management aspects, source-sink analysis to predict the future capacity for brine disposal in the region, and guidance for operators, regulators, and public stakeholders. The project included compilation of geological and reservoir data for brine disposal, development of geocellular models, reservoir analysis, and advanced reservoir and geomechanical simulations. The methodology was designed to better understand the geologic setting, reservoir dynamics, geomechanical issues, and subsurface effects of brine disposal.

Many different geologic intervals are utilized for Class II brine disposal in the Appalachian Basin. The geologic parameters and injection well operational history of these zones may be used to better understand the impact of deep well disposal on groundwater systems in the region and support safe, reliable, and environmentally responsible brine disposal in the region. In this research, the study area was defined as eastern Kentucky, Ohio, Pennsylvania, and West Virginia. Operational data on injection rates and pressures were compiled for 2008-2012 for over 200 Class II brine disposal wells. This data showed that brine injection in the study area has increased from approximately 6-7 million barrels per year in the early 2000s to 17.6 million barrels in 2012, mostly due to shale gas activity. Injection was routed to about 324 wells as of August 2013, with median injection volume of 2,700 barrels per month. From 2013-2014, over 30 new Class II disposal wells were permitted in the study area, including five new permits in Pennsylvania. Four new commercial wells in Ohio had reported injection volumes over 1 million barrels per year each in 2014. Combined, these four wells provided a 33% increase in capacity over 2012. Several Class II brine disposal wells were monitored with continuous wellhead pressure loggers to estimate reservoir permeability from pressure fall-off cycles. Geomechanical analysis was also completed based on testing of ten rock cores from injection zones in the region to determine the potential for injection induce fracturing in the subsurface.

To define geologic properties of injection zones, 690 geophysical well logs from injection wells were analyzed. Geologic maps, cross sections, and descriptions were also completed for major injection zones. More detailed local analysis was completed for key injection units in each state to better understand the geologic features and distribution of the injection zones. Based on this information, local-scale geocellular models and injection simulations were developed for several key injection zones. Source sink analysis suggested there may be ultimate demand for brine disposal related to unconventional production of approximately 700-2,300 million barrels, while the capacity for brine disposal in depleted oil and gas zones and deep saline rock formations may be nearly 500 billion barrels.

Project results provide a catalog of injection rates for the various formations, which range from 100s of barrels per month to more than 100,000 barrels per month. For the period of 2008-2012, data showed that approximately 9,984 barrels of brine were injected for every billion cubic feet equivalent gas produced. Some reservoirs exhibit geologic boundaries which appear to limit long-term injection as reflected in operational data. Injection simulations suggest there is little potential for long-term migration of brine due to low permeability of the reservoirs and relatively minor contrast in density of formation and injection fluids. This project was supported by the Research Partnership to Secure Energy for America unconventional onshore program project #11122-73.

ACKNOWLEDGEMENTS

Support for this project was provided by the Research Partnership to Secure Energy for America under contract #11122-73. The project team thanks RPSEA for sponsoring this effort, which is an important issue for the Appalachian Basin region. Project guidance was provided by Mr. Kent Perry (RPSEA) and Mr. Joseph Renk III from U.S. Department of Energy-National Energy Technology Laboratory.

Project results reflect contributions from many people on the project team. The project lead was Battelle, and J.R. Sminchak was the project manager. Dr. Neeraj Gupta was technical advisor. The project team included the Kentucky Geological Survey (Tom Sparks and Marty Parris), Ohio Geological Survey (Ron Riley, Michael Solis, and Mohammed Fakhari), Pennsylvania Geological Survey (Brian Dunst, Katherine Schmid, and Robin Anthony), and the West Virginia Geological and Economic Survey (Philip Dinterman, Eric Lewis, and Jessica Moore). John Miller (Battelle) completed the geophysical log analysis and integration of geology across the region. The project benefited from previous geological research for the Appalachian Basin including: *The Atlas of Major Appalachian Gas Plays* (1996), *Midwest Regional Carbon Sequestration Partnership* (Phase I and Phase II), *A Geologic Play Book for Trenton-Black River Appalachian Basin Exploration* (2006), and other recent work on unconventional development in the project states.

The geomechanical analysis was conducted by NSI Tech (J.Y. Deng, Mike Smith, and Carl Montgomery) and Dr. Samin Raziperchikolaee from Battelle. Reservoir simulations were completed by J.R. Sminchak and Priya Ravi-Ganesh from Battelle. The source-sink analysis was completed by Ola Babarinde from Battelle. Isis Fukai (Battelle) was integral to developing the informational pamphlet. The Class II informational survey was led by Meghan Harley and Glenn Larsen (Battelle). Desiree Padgett provided technical editing for project reports. Support for the project was provided by Ohio Oil Gathering Corporation/ Crosstex. We'd also like to acknowledge several operators for allowing access to their wells for field monitoring, which was very useful in understanding real time operations for brine injection in the region.

Finally, we'd like to remember Mike Woolfe, a Battelle field technician who worked on the project and unexpectedly passed away in the winter of 2015.

TABLE OF CONTENTS

ABSTRACT.....	3
ACKNOWLEDGEMENTS.....	4
TABLE OF CONTENTS.....	5
List of Figures.....	9
List of Tables.....	17
List of Acronyms.....	20
EXECUTIVE SUMMARY.....	23
1. INTRODUCTION.....	25
1.1 Background.....	25
1.2 Project Overview.....	25
1.3 Description of the Northern Appalachian Basin.....	25
1.4 Assumptions and Limitations.....	28
2. OPERATIONAL DATA.....	30
2.1 Class II Brine Disposal Regulatory Framework.....	30
2.2 Data Sources.....	32
2.3 Survey of Class II Brine Disposal Wells in the Northern Appalachian Basin.....	34
2.3.1 Well Status.....	35
2.3.2 Injection Zones.....	35
2.3.3 Injection Well Construction Specifications.....	36
2.4 Operational Data Summary.....	38
2.4.1 Injection Well Trends.....	38
2.4.2 Injection Volumes, Rates, and Pressures.....	41
2.4.3 Class I UIC Injection Wells.....	49
2.5 Injection Performance Analysis.....	51
2.6 Class II Disposal Well Field Monitoring.....	55
2.6.1 Field Monitoring.....	55
2.6.1.1 ‘Clinton’-Medina.....	56
2.6.1.2 Newburg.....	57
2.6.1.3 Knox-Rose Run.....	58
2.6.2 Pressure Fall-off Interpretation.....	58
2.6.2.1 East-Central Appalachian Basin Clinton-Medina.....	58
2.6.2.2 East-Central Appalachian Basin Newburg.....	61
2.6.2.3 Central Appalachian Basin Knox-Rose Run.....	66
3. REGIONAL GEOLOGIC SETTING.....	70
3.1 Geologic Structural Framework Setting.....	70
3.2 Injection Zones/Formation Correlations.....	73
3.2.1 Cambrian Basal Sandstone Interval.....	75
3.2.2 Cambrian-Ordovician Interval.....	76
3.2.3 Lower Silurian Medina Group/‘Clinton’ Sandstone Interval.....	78
3.2.4 Middle Devonian-Middle Silurian Interval.....	79
3.2.5 Upper and Middle Devonian Interval.....	82
3.2.6 Mississippian-Pennsylvanian Interval.....	84
3.3 Regional Formation Maps.....	85
3.3.1 Precambrian.....	86
3.3.2 Cambrian Basal Sandstones.....	91
3.3.3 Basal Sandstones to Top of Copper Ridge Interval.....	93
3.3.4 Upper Cambrian Rose Run Sandstone.....	95

3.3.5	Knox Unconformity	98
3.3.6	Medina Group	99
3.3.7	Lockport Dolomite	101
3.3.8	Oriskany Sandstone	104
3.3.9	Devonian Shale and Sandstone	106
3.4	Well Log Analysis	108
3.5	Geotechnical Data	117
3.5.1	Hydraulic Core Test Data	117
3.5.2	Geomechanical Core Testing	119
3.6	Hydrologic Data	123
3.6.1	Reservoir Conditions	123
3.6.2	Injection Fluids	123
3.7	Regional Geocellular Model	128
4.	Local Geologic Analysis	131
4.1	Kentucky Class II Wells and Mississippian Weir Sandstone Case Study (KY)	131
4.1.1	Synopsis of Class II Wells in Kentucky	131
4.1.2	Geologic Setting	131
4.1.3	Weir Sandstone	134
4.2	West Virginia Class II Wells and Mississippian Big Injun Case Study (WV)	141
4.2.1	Synopsis of Class II Wells in West Virginia	141
4.2.2	Mississippian Big Injun Saltwater Disposal Wells in the Walton-Rock Creek Field, Roane County, West Virginia	145
4.2.3	Recommendations	151
4.3	Pennsylvania Upper Devonian Series Case Study	152
4.3.1	Introduction	152
4.3.2	Objective	154
4.3.3	Methodology	154
4.3.4	Results	155
4.3.5	Discussion	156
4.3.5.1	Depositional Environment	157
4.3.5.2	Porosity and Permeability	159
4.3.6	Seismic Data	159
4.3.7	Conclusions	162
4.4	Pennsylvania Lower Devonian Oriskany Sandstone Case Study	162
4.4.1	Introduction	162
4.4.2	Objectives	164
4.4.3	Methodology	164
4.4.4	Results	166
4.4.5	Discussion	167
4.4.6	Conclusions	168
4.5	Ohio Upper Silurian Lockport/Newburg Case Study	168
4.5.1	Introduction	168
4.5.2	Lockport Dolomite	173
4.5.3	Structural Consistency	178
4.5.4	Conclusion	180
4.6	Lower Silurian Medina Group Case Study	180
4.6.1	Introduction	180
4.6.2	Objectives	184
4.6.3	Methodology	184
4.6.4	Results	185
4.6.5	Dicussion	187

4.6.6	Conclusions.....	191
4.7	Central Ohio Cambrian-Ordovician Knox Unconformity to Basal Cambrian Sandstone Injection Well Case Study	192
4.7.1	Introduction.....	192
4.7.2	Regional Distribution.....	193
4.7.3	Stratigraphy.....	194
4.7.4	Well Completion.....	201
4.7.5	Operations.....	202
4.7.6	Injection Testing	203
5.	Injection Simulations.....	205
5.1	Weir Sandstone	205
5.1.1	Geocellular Model.....	205
5.1.2	Weir Sandstone Simulation.....	209
5.1.2.1	Input Parameters	209
5.1.2.2	Weir Sandstone Simulation Output	213
5.2	Lockport-Newburg.....	216
5.2.1	Lockport-Newburg Geocellular Model.....	216
5.2.2	Lockport-Newburg Simulation	221
5.2.2.1	Input Parameters	221
5.2.2.2	Lockport-Newburg Simulation Output.....	225
5.3	Clinton-Medina	232
5.3.1	Clinton-Medina Geocellular Model.....	232
5.3.2	Clinton-Medina Simulation.....	233
5.3.2.1	Input Parameters	233
5.3.2.2	Clinton-Medina Sandstone Simulation Output.....	237
5.4	Knox-Basal Sandstone	240
5.4.1	Knox-Basal Sandstone Geocellular Model	240
5.4.2	Knox-Basal Sandstone Simulation.....	242
5.4.2.1	Input Parameters	242
5.4.2.2	Knox-Basal Sandstone Simulation Output	245
5.5	Geomechanical Analysis of Brine Injection.....	248
5.5.1.1	Methods	248
5.5.1.2	Estimating Elastic Parameters	249
5.5.1.3	Estimating Overburden Stress	250
5.5.1.4	Estimating Minimum Horizontal Stress	250
5.5.2	Geomechanical Core Testing	250
5.5.3	Modeling Potential of Fracture Propagation	252
5.5.3.1	Big Injun Sandstone.....	252
5.5.3.2	Geomechanical Model	252
5.5.3.3	Geomechanical Analysis.....	253
5.5.3.4	Clinton-Newburg Zone	255
5.5.3.5	Geomechanical Model	255
5.5.3.6	Geomechanical Analysis.....	255
5.5.3.7	Knox Group Multiple Zone	258
5.5.3.8	Geomechanical Model	258
5.5.3.9	Geomechanical Analysis.....	259
5.5.4	Estimating Injectivity in Relation to Geomechanical Parameters in Western Flank of Appalachian Basin	262
5.5.4.1	Statistical Approach for Driving the Dynamic Rock Mechanical Parameters.....	263
5.5.4.2	Injectivity Potential in Different Zones of Appalachian basin	266

6.	Source-Sink Analysis	273
6.1	Brine Disposal Source Analysis.....	273
6.1.1	Assumptions and Limitations.....	273
6.1.2	Unconventional Resource Development in Northern Appalachian Basin	274
6.1.3	Wastewater Production and Trends in Brine Disposal.....	278
6.1.4	Ratio of Oil and Gas Production to Brine Disposal Volumes.....	283
6.2	Marcellus/Utica Resource Estimates and Long-Term Brine Disposal Demand	286
6.2.1	Brine Disposal Sink Capacity Analysis	286
6.2.2	Depleted Oil and Gas Formations	288
6.2.3	Deep Saline Formations.....	293
6.3	PA Recycle Reuse Case Study.....	296
6.4	Update of Brine Disposal Activity: 2012-2014.....	299
7.	Tools/Products for Industry/Operators	303
7.1	Injection Zone Summary.....	303
7.2	Wellhead Pressure Regression Estimator.....	304
7.3	Well Logging Options.....	309
7.3.1	Well Log Data Analysis.....	309
7.4	Well Testing Options (Pre-Injection).....	324
7.5	Injection Monitoring Options.....	331
7.5.1	Injection Tubing Monitoring.....	331
7.5.2	Injection Tubing/Casing Annulus Monitoring	332
8.	Survey of Information Sources for Produced Water Disposal	334
8.1	Class II Well Survey	334
8.1.1	Historical Background	335
8.1.2	Organizational Challenges and Current Data Availability.....	338
8.1.3	Geologic Considerations	341
8.1.4	Economics	342
8.1.5	Environmental Regulations (Policy Issues)	343
8.1.6	Unconventional Resources.....	344
8.1.7	Produced Water Management Practices.....	346
8.1.8	Underground Injection Program (Class II injection).....	347
8.1.9	Issues Related to Underground Injection	349
8.1.10	Other Associated Environmental Issues.....	350
8.1.11	State and Federal Regulations.....	352
8.1.12	Wellbore Integrity	354
8.1.13	Risk Based Data Management Solutions	355
8.1.14	Induced Seismicity	356
8.1.15	Current Research on Oil and Gas Wastewater Management	358
8.2	Class II Well Data Distribution Methodology	360
8.2.1	Model 1: Off-the-Shelf Document Management Software.....	361
8.2.2	Model 2: Existing Database Structure.....	364
8.2.3	Model 3: Web-Based Evaluation Tool.....	371
9.	Results and Discussion.....	375
9.1	Operational Data	375
9.2	Geologic Properties of Injection Zones.....	376
9.3	Source-Sink Analysis.....	377
10.	Impact to Producers.....	381
11.	Technology Transfer Efforts	383
12.	Recommendations	385
13.	REFERENCES.....	387

List of Figures

Figure 1-1.	General extent of the Appalachian Basin and Unconventional Marcellus and Utica Shale plays.	26
Figure 2-1.	Active Class II UIC brine disposal wells and other Class II EOR wells in the study area.	34
Figure 2-2.	Locations of Class II brine disposal wells, unconventional wells, and oil and gas fields in relation to the Marcellus and Utica shale.	39
Figure 2-3.	Brine disposal volumes and unconventional wells completed from 2008-2012. .	40
Figure 2-4.	Trends in brine disposal volume per number of unconventional wells.	41
Figure 2-6.	Average monthly injection pressure versus depth for 2012 for Class II brine disposal wells in the study area.	44
Figure 2-5.	Average monthly injection volume versus depth for 2012 for Class II brine disposal wells in the study area.	44
Figure 2-7.	Total injection volume for 2012.	45
Figure 2-8.	Average monthly injection volume for 2012.	46
Figure 2-9.	Average wellhead pressure for 2012.	47
Figure 2-10.	Class II brine disposal well count and total injection volume for 2012 by deepest injection formation.	48
Figure 2-11.	Class II brine disposal average monthly injection rate per well	49
Figure 2-12.	Sample injectivity analysis results for two Ohio wells.	54
Figure 2-13.	Wellhead logger installed on Class II injection well for field monitoring.	55
Figure 2-14.	Wellhead pressure monitoring results from four Clinton-Medina Class II brine disposal wells in the central Appalachian Basin.	56
Figure 2-15.	Wellhead pressure monitoring results from Clinton-Medina brine disposal well in the east-central Appalachian Basin.	57
Figure 2-16.	Wellhead pressure monitoring results from Newburg brine disposal well in the east-central Appalachian Basin.	57
Figure 2-17.	Wellhead pressure monitoring results from Knox-Rose Run brine disposal well in the central Appalachian Basin.	58
Figure 2-18.	Test data trends from plot of pressure increase versus time for each of the three test periods	59
Figure 2-20.	Injection test – 1 curve result.	60
Figure 2-19.	Fall-off test-2 curve result.	60
Figure 2-21.	Analysis plots for the 4-16-14 to 4-24-14 injection fall-off event.	63
Figure 2-22.	Analysis plots for the 4-24-14 to 4-28-14 injection fall-off event.	64
Figure 2-23.	Analysis plots for the 4-28-14 to 5-6-14 injection fall-off event.	65
Figure 2-24.	Injection rate and wellhead pressure for 10 injection cycles recorded Aug. 27 through Sept. 11, 2014.	66
Figure 2-25.	PTA diagnostic plots for cycle 5 fall-off period.	68
Figure 3-1.	Extent of the Appalachian Basin and neighboring basins with overlaid structural features in the eastern United States.	71
Figure 3-2.	Generalized geologic history of the Appalachian Basin.	72
Figure 3-3.	Schematic northwest to southeast section across the Appalachian Basin.	73
Figure 3-4.	Regional stratigraphic chart.	74
Figure 3-5.	Proterozoic tectonic provinces within the RPSEA study area.	87

Figure 3-6.	Major structural features within the RPSEA study area.	89
Figure 3-7.	Structure contours drawn on the Precambrian unconformity surface within the RPSEA study area.	90
Figure 3-8.	Structure contours drawn on top of the Cambrian basal sandstone surface within the RPSEA study area.	91
Figure 3-9.	Isopach contours of the Cambrian basal sandstone interval surface within the RPSEA study area.	92
Figure 3-10.	Structure contours drawn on top of the Copper Ridge Dolomite surface within the RPSEA study area.	94
Figure 3-11.	Isopach of the Rose Run Sandstone surface within the RPSEA study area.	95
Figure 3-12.	Structure contours drawn on top of the Rose Run Sandstone surface within the RPSEA study area.	96
Figure 3-13.	Structure contours drawn on the Knox unconformity surface within the RPSEA study area.	99
Figure 3-14.	Structure contours drawn on top of the Medina Group surface within the RPSEA study area.	100
Figure 3-15.	Isopach map of the Medina Group within the RPSEA study area.	101
Figure 3-16.	Structure contours drawn on top of the Lockport Dolomite surface within the RPSEA study area.	102
Figure 3-17.	Isopach map of the Lockport Dolomite within the RPSEA study area.	103
Figure 3-18.	Structure contours drawn on top of the Oriskany Sandstone surface within the RPSEA study area.	104
Figure 3-19.	Isopach map of the Oriskany Sandstone within the RPSEA study area.	105
Figure 3-20.	Structure contours drawn on top of the Devonian Shale surface within the RPSEA study area.	106
Figure 3-21.	Isopach of the Devonian Shale within the RPSEA study area.	107
Figure 3-22.	Clinton Sandstone porosity histogram.	111
Figure 3-23.	Balltown Sandstone type section, single thick sandstone bodies.	112
Figure 3-24.	Medina Sandstone type section with stacked sandstone bodies separated by shale.	113
Figure 3-25.	Upper Copper Ridge Dolomite type section showing thin injection intervals with high porosity.	114
Figure 3-26.	Lockport Dolomite (Newburg) porosity-feet isopach for 8% porosity cutoff in northeastern Ohio.	115
Figure 3-27.	Clinton Sandstone reservoir parameters vs injection data.	116
Figure 3-28.	Lockport Dolomite (Newburg) reservoir parameters vs injection data.	116
Figure 3-29.	Average monthly injection vs porosity feet for 8% porosity cutoff for the Clinton Sandstone and Lockport Dolomite (Newburg).	117
Figure 3-30.	Rock core with permeability and porosity data for Kentucky.	118
Figure 3-31.	Rock core with permeability and porosity data for Ohio.	119
Figure 3-32.	Salinity by county for produced water.	124
Figure 3-33.	Geologic fence diagram showing subsurface distribution of key injection zones for the study area.	128
Figure 3-34.	North-south view of geologic fence diagram showing subsurface distribution of key injection zones for the study area and wellpaths for Class II brine disposal wells.	129

Figure 3-35.	Location of shale gas wells (gray) and Class II brine disposal wells scaled according to 2012 total injection volume (bbl).....	130
Figure 3-36.	Location of shale gas wells (gray) and Class II brine disposal wells scaled according to 2012 average monthly injection rate (bbl/month).....	130
Figure 4-1.	Surface faults (left) of central and eastern Kentucky. Basement faults (right) identified from seismic investigations, and deep Precambrian–Early Cambrian grabens of central and eastern Kentucky.	132
Figure 4-2.	Wells completed in the Weir sandstone (dark green symbols).....	133
Figure 4-3.	Type log for Mississippian Weir sandstones, the Triad Resources Inc. No. 4 Ferguson, located in Elliott County (permit 103462).	134
Figure 4-4.	Permeability and porosity measurements of 164 Weir sandstone core samples (n > 7,700) from eastern Kentucky.....	135
Figure 4-5.	Structure map on base of Mississippian Sunbury Shale and top of Devonian Berea Sandstone.	136
Figure 4-6.	Detailed view of base of Sunbury Shale and top of Berea Sandstone structure from Figure 4-5 showing average daily injection rate for Weir wells.	137
Figure 4-7.	Detailed view of base of Sunbury Shale and top of Berea Sandstone structure from Figure 4-5 showing average monthly injection pressure for Weir wells. ..	137
Figure 4-8.	Detailed view of base of Sunbury Shale and top of Berea Sandstone structure from Figure 4-5 showing total volume of brine injected from 2008 through 2012 for Weir wells.	138
Figure 4-9.	Average and maximum injection pressures (psi), and monthly injection volumes (bbl) for the 60 month period from 2008 - 2012 in the Triad Resources, Albert Gillum No. G-1A.	139
Figure 4-10.	Average and maximum injection pressures (psi) and monthly injection volumes (bbl) over a 60 month period from 2008 through 2012 in the Pearlman Sparks, Noah Sparks No. 2 and No. 3 wells.	139
Figure 4-11.	Class II disposal wells in West Virginia.	141
Figure 4-12.	Disposal wells classified by geologic age of injection interval.	143
Figure 4-13.	Volume of fluids (in barrels) injected in 2012 and through September 2013 by geologic age.	144
Figure 4-14.	Volume of fluids (in barrels) injected in 2012 and through September 2013 by well.	145
Figure 4-15.	Location of Walton-Rock Creek field in Roane County, West Virginia.	146
Figure 4-16.	Walton Rock Creek Field with disposal wells, well status, and associated folds.....	147
Figure 4-17.	Injection volumes (in barrels) in and near the Walton Rock Creek field from January 2012 to September 2013.....	148
Figure 4-18.	Structural map of Walton-Rock Creek field.	149
Figure 4-19.	Isopach map of Walton-Rock Creek field.	150
Figure 4-20.	3D structure of Walton-Rock Creek field.	151
Figure 4-21.	Upper Devonian stratigraphic column.	153
Figure 4-22.	Stratigraphic column of the Chadakoin Formation and Bradford Group showing selected drillers' names for sandstones in the central column.	154

Figure 4-23.	Index map showing locations of Bradford Group disposal wells, cross sections, seismic lines, structure contours, and outcrop locations of the Bradford Group.	155
Figure 4-24.	Detailed cross section highlighting the interbedded shale in the sandstone packages.	156
Figure 4-25.	Appalachian foreland basin stratigraphic columns (northwest–southeast) from middle Devonian through lower Mississippian time.	157
Figure 4-26.	Depositional environment and paleogeography of the First Bradford sandstone, showing a portion of the model over the southern part of the case study area. ...	158
Figure 4-27.	2D seismic line with structural interpretation.	161
Figure 4-28.	Distribution of Oriskany Sandstone natural gas plays.	163
Figure 4-29.	Subsurface correlation diagram of Lower and Middle Devonian formations in Pennsylvania.	164
Figure 4-30.	Oriskany Sandstone structure map with cross section locations.	165
Figure 4-31.	Southwest-to-northeast cross section A–A’ in the case study area showing tilted imbricate fault blocks.	166
Figure 4-32.	Northwest-to-southeast cross section B–B’ across dip showing isolated fault-bound blocks.	167
Figure 4-33.	Total volume of fluid injected per year in Ashtabula, Mahoning, Portage, and Trumbull Counties, Ohio.	169
Figure 4-34.	Location of Class II wells in northeastern Ohio as of September 2014.	170
Figure 4-35.	Cumulative fluid injection by well, graduated symbol size, and color.	171
Figure 4-36.	Seven Class II permit application locations in Nelson and Windham Townships, Portage County, Ohio.	172
Figure 4-37.	Well locations used for initial mapping.	173
Figure 4-38.	Isopach contour map of the Lockport Dolomite in northeastern Ohio showing correlation lines.	174
Figure 4-39.	Correlation diagram I–I’ of the Lockport Dolomite in northeastern Ohio (no horizontal scale).	175
Figure 4-40.	Correlation diagram II–II’ of the Lockport Dolomite in northeastern Ohio (no horizontal scale).	176
Figure 4-41.	Correlation diagram III–III’ of the Lockport Dolomite in northeastern Ohio (no horizontal scale).	177
Figure 4-42.	Structure contour map on top of the Lockport Dolomite in northeastern Ohio. ..	178
Figure 4-43.	Structure contour map on top of the Dayton Formation in northeastern Ohio. ..	179
Figure 4-44.	Structure contour map on top of the Onondaga Limestone in northeastern Ohio.	180
Figure 4-45.	Stratigraphic column showing the rocks of the Medina Group in northwestern Pennsylvania and equivalent rocks in eastern Ohio, southwestern and central Pennsylvania.	181
Figure 4-46.	Northwest-southeast regional stratigraphic cross section, representing a 400-kilometer (250-mile) distance across the Appalachian Basin.	182
Figure 4-47.	Sands in the Medina showing spatial distribution of facies.	183
Figure 4-48.	Northwest to southeast structural cross section showing regional dip of the Medina Group from Erie through Crawford counties in the heart of Pennsylvania’s Medina play.	185

Figure 4-49.	Structure, isovol, and cross section in the Dewey Corners Medina gas pool.	187
Figure 4-50.	Calculated volume of total original gas reserves and cumulative production per field (left); GR, NPHI, and rhoB log from a depleted gas well 2,250 feet (690 meters) south of a Medina brine injection well in Warren County, Pennsylvania (right).	189
Figure 4-51.	Major tectonic lineaments, example wells with GR and core, and rate of subsidence and sediment supply.	190
Figure 4-52.	Regional distribution of Class II Cambrian reservoirs injection wells.	194
Figure 4-53.	General stratigraphy and injection intervals observed in Central Ohio Knox Unconformity to Basal Cambrian sandstone open-hole wells.	195
Figure 4-54.	General eastern Ohio log sections from proprietary wells.	196
Figure 4-55.	Cross section location and cross section with density, NMR, and sonic porosity showing decrease in porosity with depth in the Rose Run Sandstone.	198
Figure 4-56.	Lower Copper Ridge vugular porosity in AEP #1 well, Mason County, West Virginia.	199
Figure 4-57.	Porosity-feet map of the Lower Copper Ridge dolomite.	200
Figure 4-58.	Typical Beekmantown to top Basal Cambrian Sandstone open-hole well diagram of casing and tubing configuration.	202
Figure 4-59.	General injection operation schematic.	203
Figure 4-60.	Cross section of select open-hole logs (Tracks 1 and 2), spinner and temperature data (Tracks 3 through 5) for Silcor No. 1 SOS-D well.	204
Figure 5-1.	Berea Subsea structure with Albert Gillum #G1-a injection well and location of Sandy Creek Fault.	206
Figure 5-2.	Albert Gillum #G1-a well log suite with injection interval noted.	207
Figure 5-3.	Eastern Kentucky core permeability analysis from 164 wells with 7,700 total samples.	208
Figure 5-4.	Base Weir Sandstone subsea structure map.	209
Figure 5-5.	Weir Sandstone simulation model layers.	210
Figure 5-6.	Weir Sandstone simulation grid.	210
Figure 5-7.	Weir Sandstone simulated delta pressure (psi) over time.	214
Figure 5-8.	Weir Sandstone simulated pressure change (cross section).	214
Figure 5-9.	Weir Sandstone simulated salinity (mg/L) over time.	215
Figure 5-10.	Weir Sandstone simulated salinity over time (cross section).	216
Figure 5-11.	Lockport Newburg injection model wells surrounding the Victoria Lukey #1 injection well.	217
Figure 5-12.	Log suite for the Victoria Lukey #1 injection well with injection interval marked.	218
Figure 5-13.	West-to-east cross section of Lockport model wells.	219
Figure 5-14.	West-to-east cross section of two-zone Lockport porosity model.	220
Figure 5-15.	Lockport porosity model of layer in center of main injection zone (tartan grid cells displayed).	220
Figure 5-16.	Porosity-to-permeability transform from Johnson #1 (Pennsylvania) and Ocel #1 (Ohio) Lockport core data.	221
Figure 5-17.	Lockport-Newburg model permeability (cross section).	222
Figure 5-18.	Constant brine injection schedule trial.	223
Figure 5-19.	Variable brine injection schedule trial.	224

Figure 5-20.	Lockport model initial pressure map.	225
Figure 5-21.	Lockport porosity map indicating the injection zone (cross section).	225
Figure 5-22.	Lockport-Newburg brine injection simulation results at a constant injection rate over time.	226
Figure 5-23.	Salinity profile snapshots for the constant injection Lockport-Newburg GEM model (cross section).	227
Figure 5-24.	Aqueous salinity at the end of the 40-year post-injection monitoring period for the constant-injection Lockport-Newburg GEM model (cross section).	227
Figure 5-25.	Lockport-Newburg brine injection simulation results at variable injection rates over time.	228
Figure 5-26.	Salinity profile snapshots for the variable-injection Lockport-Newburg GEM model (cross section).	229
Figure 5-27.	Salinity at the end of the 20-year post-injection monitoring period for the variable-injection Lockport-Newburg GEM model (cross section).	229
Figure 5-28.	Pressure buildup at the end of the post-injection monitoring period in the variable-injection Lockport-Newburg GEM model.	230
Figure 5-29.	Results of the Lockport-Newburg model upper confining layer permeability sensitivity trial.	230
Figure 5-30.	Pressure and salinity at end of 20-year post-injection monitoring period in the variable-injection Lockport-Newburg GEM model.	231
Figure 5-31.	BHP through time for low and base-case variable-injection-rate trials.	231
Figure 5-32.	Pressure and salinity at 10 years of post-injection monitoring in the variable-injection Lockport-Newburg GEM model.	232
Figure 5-33.	Clinton-Medina section hung on top of the Clinton.	233
Figure 5-34.	Model layers and thicknesses (cross section).	235
Figure 5-35.	Model elevation of the Medina Sandstone surface.	236
Figure 5-36.	Clinton Sandstone simulation grid.	236
Figure 5-37.	Clinton-Medina simulated delta pressure (psi) over time.	238
Figure 5-38.	Clinton-Medina simulated delta pressure over time (cross section).	238
Figure 5-39.	Clinton-Medina simulated salinity (mg/L) over time.	239
Figure 5-40.	Clinton-Medina simulated salinity (cross section).	240
Figure 5-41.	Log curves and final porosity and permeability values from Knox to Basal Sandstone injection model.	241
Figure 5-42.	Basal Sandstone permeability derived from sidewall core, injection reservoir testing, and NMR logs.	242
Figure 5-43.	Knox-Basal Sandstone simulation model layers.	244
Figure 5-44.	Knox-Basal Sandstone simulation grid.	244
Figure 5-45.	Knox-Basal Sandstone simulated delta pressure (psi) over time.	246
Figure 5-46.	Clinton-Medina simulated delta pressure over time model cross section.	246
Figure 5-47.	Knox-Basal Sandstone simulated salinity (mg/L) over time.	247
Figure 5-48.	Knox-Basal Sandstone simulated salinity cross section.	248
Figure 5-49.	The effect of increasing pore pressure on rock failure (a), and the effect of poro-elasticity (b).	249
Figure 5-50.	Minimum horizontal stress (PcI) and Young's modulus of reservoir and surrounding formations (Big Injun Sandstone).	254

Figure 5-51.	BHP increase by water injection (a) and width and length of near borehole effects (b).	254
Figure 5-52.	Poro-stress changes away from wellbore (a) and total-stress changes away from wellbore (b).	255
Figure 5-53.	Minimum horizontal stress (PcI) and Young's modulus of reservoir and surrounding formations (Clinton-Newburg zone).	257
Figure 5-54.	BHP increase by water injection (a) and width and length of near borehole effects (b).	257
Figure 5-55.	Poro-stress changes away from wellbore (a) and total-stress changes away from wellbore (b).	257
Figure 5-56.	Width and length of fracture propagation (a) and total-stress changes away from wellbore (b).	258
Figure 5-57.	Minimum horizontal stress (PcI) and Young's modulus of reservoir and surrounding formations (Knox-Basal Sandstone).	261
Figure 5-58.	BHP increase by water injection (a) and width and length of near borehole effects (b).	261
Figure 5-59.	Poro-stress changes away from wellbore (a) and total-stress changes away from wellbore (b).	261
Figure 5-60.	Width and length of near borehole effects (a) and poro-stress changes away from wellbore (b).	262
Figure 5-61.	Study area of interest for investigation of Knox group reservoir injectivity.	263
Figure 5-62.	Depth variation of Rose Run and Copper Ridge across eight wells.	264
Figure 5-63.	Relationships among different petro-physical parameters.	264
Figure 5-64.	Relationship between compression – shear slowness and density.	265
Figure 5-65.	The predicted vs. measured compression and shear slowness.	265
Figure 5-66.	Compression and shear slowness at increasing depth in the Rose Run Sandstone (a) and Copper Ridge Dolomite (b).	266
Figure 5-67.	Dynamic Young's modulus and Poisson's ratio as a function of depth in the Rose Run Sandstone (a) and Copper Ridge Dolomite (b).	266
Figure 5-68.	Higher depth and higher margin between pore pressure and minimum horizontal stress.	267
Figure 5-69.	Construction of a model for geomechanics of one medium-depth-range well.	268
Figure 5-70.	Model schematic for one medium-depth-range well and variations in permeability and effective minimum horizontal stress between formations.	270
Figure 5-71.	Pressure distribution after one year of injection (a) and effective stress reduction after one year of injection (b).	271
Figure 5-72.	Injection capacity of different wells.	271
Figure 5-73.	Effect of higher Rose Run permeability on increased injectivity (a) and comparison of injectivity of different wells (b).	272
Figure 5-74.	Effective stress in three wells after one year of brine injection.	272
Figure 6-1.	Locations of unconventional wells in the study area (circa fall 2013).	275
Figure 6-2.	Density of unconventional wells in the study area.	277
Figure 6-3.	Direct distance between unconventional wells and Class II brine disposal wells in Appalachian Basin.	277
Figure 6-4.	Distance between unconventional wells and Class II disposal wells.	278
Figure 6-5.	Approximate number of brine disposal wells drilled by date.	280

Figure 6-6.	Class II brine disposal, natural gas production, and unconventional wells drilled (2008-2012).....	285
Figure 6-7.	Stratigraphic correlation chart for the study area.....	287
Figure 6-8.	Distribution of Class II brine disposal wells, hydrocarbon fields, and unconventional wells.	288
Figure 6-9.	Oil and gas fields in the Appalachian Basin and locations of active Class II injection wells.	290
Figure 6-10.	Locations of active Class II injection wells and related oil and gas fields in the Appalachian Basin.	291
Figure 6-11.	Recovery rate in the Appalachian Basin.....	292
Figure 6-12.	Annual horizontal and vertical shale well completion data for Pennsylvania. ...	296
Figure 6-13.	Example of hydraulic fracture water data included in a well completion report.....	297
Figure 6-14.	Total volume and recycled volumes used to treat shale wells in Pennsylvania.	297
Figure 6-15.	Disposal methods for wastewater from unconventional wells in Pennsylvania.	298
Figure 6-16.	Annual natural gas equivalent production and wastewater production from Pennsylvania shale gas wells.	299
Figure 6-17.	Locations of UIC Class II brine injection wells permitted since August 2012 in the Northern Appalachian Basin.	301
Figure 7-1.	Informational pamphlet for Class II brine disposal wells in the Appalachian Basin.	304
Figure 7-2.	2008-2012 average wellhead pressure versus depth.....	305
Figure 7-3.	2008-2012 average wellhead pressure versus average monthly injection rate. ...	306
Figure 7-4.	Observed average wellhead pressure versus regression model prediction.	308
Figure 7-5.	Observed average wellhead pressure versus regression model prediction for Clinton Sandstone Wells.....	309
Figure 7-6.	NMR water molecule response and processed log products.	312
Figure 7-7.	NMR-derived porosity and permeability with plotted sidewall core-derived porosity in Rose Run Sandstone.	313
Figure 7-8.	NMR-derived porosity and permeability with plotted sidewall core-derived porosity in Lower Copper Ridge Dolomite.	314
Figure 7-9.	Vugular carbonate zone in Lower Copper Ridge Knox Group dolomite.	315
Figure 7-10.	Natural fracture within vugular zone in Lower Copper Ridge Knox Group dolomite.	316
Figure 7-11.	Drilling-induced fractures.....	316
Figure 7-12.	Drilling-induced and natural fractures identified on image logs from central Ohio wells.	317
Figure 7-13.	Acoustic log responses in injection zones identified from spinner log.	318
Figure 7-14.	Comparison of porosity derived from density, NMR, acoustic, and neutron logs to sidewall core porosity in the Rose Run Sandstone.	320
Figure 7-15.	Comparison of porosity derived from density, NMR, acoustic, and neutron to sidewall core porosity in the Lower Copper Ridge Dolomite.	321
Figure 7-16.	Baker Hughes elemental spectroscopy RockView™ mineralogy log.....	322

Figure 7-17.	Porosity logs calculated from a matrix density porosity of 2.68 and a mineralogic matrix (variable matrix porosity) with core-derived porosity values plotted.	323
Figure 7-18.	Four-arm caged full-bore spinner-logging tool.....	325
Figure 7-19.	Example spinner-log flow profile for a 1,455-foot-long open-borehole interval, acquired at a 5-BPM injection rate.	327
Figure 7-20.	Example spinner-log flow profile for a 1,455-foot-long open-borehole interval, acquired at a 3-BPM injection rate.	328
Figure 7-21.	Example temperature logs collected before and after flow-meter logging.	329
Figure 7-22.	Injection rate and pressure history for a flow-meter logging test along with BHP fall-off data.....	330
Figure 7-23.	Time-history match analysis of injection/fall-off test to determine transmissivity of injection intervals.	331
Figure 7-24.	Injection well head configured with pressure monitoring equipment.	332
Figure 8-1.	Topics related to Class II injection summarized in this literature review.....	335
Figure 8-2.	Generalized timeline showing major oil- and gas-related events and regulatory response by government agencies.....	336
Figure 8-3.	Number of active Class II wells and regulatory enforcement authority, by state, as of 2012.	338
Figure 8-4.	Shale gas basins in the United States.....	345
Figure 8-5.	Past and projected (1990-2040) U.S natural gas production (TCF).	348
Figure 8-6.	Past and projected (1990-2040) electricity generation by fuel (trillion kilowatt-hours).	348
Figure 8-7.	Locations of induced seismic events in the United States.	357
Figure 8-8.	FracFocus.org home page.	365
Figure 8-9.	Texas-drilling.com home page.....	367
Figure 8-10.	rbdmsonline.org home page.....	369
Figure 8-11.	usgs.gov/water/ home page.....	370
Figure 8-12.	Example snapshot of the interface with operational data for a selected well	372
Figure 8-13.	Example of pop-up for well details in a sample zoomed-in AOR.....	373
Figure 9-1.	Map Showing Class II Brine Disposal Wells and Unconventional Well Density. ..	378

List of Tables

Table 1-1.	Oil and gas industry in the Northern Appalachian Basin.	27
Table 2-1.	USEPA UIC injection well class descriptions.	30
Table 2-2.	Class II regulatory agencies in the Northern Appalachian Basin.	31
Table 2-3.	Typical recording requirements for Class II UIC brine disposal wells.	32
Table 2-4.	Data sources for data collection task.	33
Table 2-5.	Class II injection well count.	35
Table 2-6.	Class II UIC brine disposal wells with active permits as of August 2013 classified by deepest injection formation.....	36
Table 2-7.	Well construction data compiled for Class II UIC brine disposal wells.....	37
Table 2-8.	Brine disposal volumes as reported for project study area for 2008-2012.	40
Table 2-9.	Summary of operational data for 2008-2012.	41
Table 2-10.	Summary of operational data for 2012.	42
Table 2-11.	Operating statistics distribution for 2008-2012.	42

Table 2-12.	Operating statistics distribution for 2012.....	43
Table 2-13.	Summary of Class I UIC injection into Mount Simon Formation.....	50
Table 2-14.	Parameters used to analyze pressure data and calculated parameters.....	61
Table 2-15.	Average injection rate for the three injection events analyzed.....	62
Table 2-16.	Reservoir and well properties for the PTA analysis.....	67
Table 2-17.	Estimates of reservoir and well properties from the radial analysis of the fall-off period for injection cycle #5.....	67
Table 3-1.	Common logs run in Appalachian Basin.....	108
Table 3-2.	Matrix density used for porosity calculations with mean and standard deviation for porosity.....	110
Table 3-3.	Summary of compressive strength properties compiled from existing wells in the study area.....	120
Table 3-4.	Summary of sonic properties compiled from existing wells in the study area.....	120
Table 3-5.	Rock core samples selected for geomechanical testing.....	121
Table 3-6.	Summary of geomechanical properties tested on rock samples from key injection intervals.....	122
Table 3-7.	Estimated fluid density by region, at a temperature of 25° C.....	125
Table 3-8.	Specific chemistry of fluid samples by region.....	126
Table 4-1.	Numbers of disposal wells classified by geologic age, geologic interval, and approximate depth.....	142
Table 4-2.	Porosity and permeability data for Bradford Group sandstones.....	159
Table 4-3.	Rose Run Sandstone and Basal Cambrian sandstone porosity and permeability.....	197
Table 5-1.	Weir Sandstone simulation input parameters.....	212
Table 5-2.	Lockport zone brine injection simulation input parameters.....	222
Table 5-3.	Clinton Sandstone simulation input parameters.....	234
Table 5-4.	Knox-Basal Sandstone simulation input parameters.....	243
Table 5-5.	Geomechanical static properties of rock samples from key injection intervals.....	251
Table 5-6.	Geomechanical dynamic properties of rock samples from key injection intervals.....	251
Table 5-7.	Tensile strength of rock samples from key injection intervals.....	252
Table 5-8.	Input data for the Big Injun geomechanical model.....	253
Table 5-9.	Input data for the Clinton-Newburg geomechanical model.....	256
Table 5-10.	Input data for the Rose Run-Copper Ridge geomechanical model.....	260
Table 5-11.	Parameters for building eight models at different depths.....	269
Table 5-12.	Injection depth, initial pressure, and initial effective stress for building eight models at different depths.....	269
Table 6-1.	Annual Class II brine disposal volumes (2008-2012).....	279
Table 6-2.	Summary of water use volumes for study area.....	281
Table 6-3.	Total pore volume estimate for Appalachian Basin.....	282
Table 6-4.	Estimated total pore volume, brine disposal volume, and annual recharge to groundwater in Appalachian Basin study area.....	283
Table 6-5.	Historical oil and gas production in the study area.....	283
Table 6-6.	Hydrocarbon production and oil and gas wells drilled in the study area (2001-2012).....	284
Table 6-7.	Class II brine injection volumes and hydrocarbon production (2008-2012).....	285

Table 6-8.	Brine disposal total demand estimates for Marcellus and Utica shale.....	286
Table 6-9.	Volumetric capacity in depleted oil and gas reservoirs penetrated by existing Class II brine disposal wells.	292
Table 6-10.	Volumetric capacity of Medina sandstone.....	294
Table 6-11.	Volumetric capacity of Rose Run sandstone.	294
Table 6-12.	Volumetric capacity of Oriskany sandstone.	294
Table 6-13.	Volumetric capacity of Potsdam sandstone.	295
Table 6-14.	Volumetric capacity of unnamed Conasauga sandstone.....	295
Table 6-15.	Volumetric capacity of unnamed Rome Trough sandstone.....	295
Table 6-16.	Volumetric capacity of Mount Simon sandstone formation.	295
Table 6-17.	Number of UIC Class II brine injection wells permitted post-August 2012 and the targeted injection zones reported in the study area.	302
Table 6-18.	Number of UIC Class II brine injection wells permitted post-August 2012 and the targeted injection zones reported in each state.	302
Table 7-1.	Correlation coefficients for regression analysis.....	307
Table 7-2.	Summary of regression fit coefficients.	307
Table 7-3.	Logging tools and analysis results.	309
Table 7-4.	Standard matrix density values for porosity calculations.	310
Table 7-5.	Standard matrix travel time values for sonic porosity calculation.....	319
Table 8-1.	Primary regulatory agencies and active Class II well inventories.	339
Table 8-2.	Primary regulatory agencies and data availability.	340
Table 8-3.	Geologic properties of injection zones in Alaska formations.	342
Table 8-4.	State distribution of the Marcellus Shale play.	342
Table 8-5.	Fracturing fluid additives, main compounds, and common uses.....	352
Table 8-6.	Class II well permitting requirements by state.	353
Table 8-7.	States and regulatory agencies using the RBDMS.	356
Table 8-8.	Number of induced seismic events in the United States by technology	357
Table 8-9.	Existing Document Management Software Options.....	363
Table 8-10.	Web-based evaluation tool features.	374
Table 9-1.	Summary of source-sink estimates for brine disposal.	380
Table 9-2.	Class II Brine Disposal Volumes for North American oil and gas regions.	380

List of Acronyms

3D	three-dimensional
AEP	American Electric Power
AOR	Area of Review
API	American Petroleum Institute
bbI	barrel
BCFG	billion cubic feet of gas
BHP	bottomhole pressure
BP	breakdown pressure
BPM	barrels per minute
BTGS	Bureau of Topographic and Geologic Survey
BVI	bulk volume irreducible
BVM	bulk volume movable
°C	degrees Centigrade
CBW	clay-bound water
CCUS	carbon capture, utilization, and storage
CFP	calculated formation fracture pressure
CFR	Code of Federal Regulations
CMG-GEM	Computer Modelling Group compositional and unconventional oil and gas reservoir simulator
CNP	compensated neutron porosity
CO ₂	carbon dioxide
CSD	cross-structural discontinuity
CWA	Clean Water Act
DLL	dual laterolog
DPM	diesel particulate matter
EF	efficiency factor
EOR	enhanced oil recovery
°F	degrees Fahrenheit
FOIA	Freedom of Information Act
g/cc	grams per cubic centimeter
GAO	U.S. Government Accountability Office
GIS	geographic information system
GR	gamma ray
GT	gigatonne
GWPC	Ground Water Protection Council

KGS	Kentucky Geological Society
km	kilometer
LAS	Log ASCII Standard
m/km	meters per kilometer
Ma	million years
MIP	maximum injection pressure
mD	millidarcy
mD-ft	millidarcy-foot
MD	measured depth
MDMS	Middle Devonian-Middle Silurian
mg/L	milligrams per liter
MMbbl	million barrels
MMbbo	million barrels of oil
MMBNGL	million barrels natural gas liquid
MMCF	million cubic feet
MRCSP	Midwest Regional Carbon Sequestration Partnership
MRex	Magnetic Resonance Explorer™
msl	meters above sea level
NORM	naturally occurring radioactive material
NPHI	neutron porosity geophysical log
NYSERDA	New York State Energy Research and Development Office
OCDO	Ohio Coal Development Office
ODNR	Ohio Department of Natural Resources
OOIP	original oil in place
PA DEP	Pennsylvania Department of Environmental Protection
PA*IRIS	Pennsylvania Internet Record Imaging System
PA GIS	Pennsylvania Geographic Information System
PaGS	Pennsylvania Geological Survey
PI	principal investigator
ppm	parts per minute
psi	pounds per square inch
psi/ft	pounds per square inch per foot
psig	pounds per square inch gage
PTA	pressure transient analysis
PTTC	Petroleum Technology Transfer Council
RBDMS	Risk Based Data Management Solutions
RF	recovery factor
RPSEA	Research Partnership to Secure Energy for America
rhoB	bulk density geophysical log
RPS	revolutions per second

SCFG	standard cubic feet of gas
SDR	Schlumberger Doll Research
SDWA	Safe Drinking Water Act
SEAWAT	Simulation of Three-Dimensional Variable-Density Ground-Water Flow and Transport
SG	specific gravity
Shmax	maximum horizontal stress
SNP	sidewall neutron porosity
SRI	secondary recovery injection
SRT	step rate test
STB	stock-tank barrel
SWD	salt water disposal
TCF	trillion cubic feet
TD	total depth
TORIS	Tertiary Oil Recovery Information System
TIFF	Tag Image File Format
UIC	underground injection control
USEPA	U.S. Environmental Protection Agency
USDW	underground source of drinking water
USGS	U.S. Geological Society
UTM	Universal Transverse Mercator
Vfs	fast shear wave velocity
Vp	compressional wave velocity
Vs	shear wave velocity
Vss	slow shear wave velocity
VDI	variable density image
WVDEP	West Virginia Department of Environmental Protection
WVGES	West Virginia Geological and Economic Survey

EXECUTIVE SUMMARY

This report presents results of the research project *Development of Subsurface Brine Disposal Framework in the Northern Appalachian Basin* (Research Partnership to Secure Energy for America Contract #11122-73). The 2-year effort was centered on providing operational ranges and geological properties for the Class II brine injection zones in the Northern Appalachian Basin. Data were collected on the status of brine disposal wells, geological conditions of injection zones, subsurface hydrologic conditions, geotechnical rock core test data, and operational data from injection wells. The information gathered was used to analyze injection performance, complete reservoir simulations of the injection process, and assess source-sink capacities. The project team included Battelle, the Kentucky Geological Survey, the Ohio Geological Survey, the Pennsylvania Bureau of Topographic and Geologic Survey, the West Virginia Geological and Economic Survey, and NSI Tech.

Research was focused on the Northern Appalachian Basin, a regional sedimentary basin that consists of thick sequences of mainly Paleozoic-age rocks overlying Proterozoic crystalline basement rock. The basin is over 500,000 square kilometers in area. The Northern Appalachian Basin study area included eastern Kentucky, Ohio, western Pennsylvania, and West Virginia. The region has a long history of oil and gas production, with thousands of hydrocarbon fields and over 900,000 wells. Cumulative production has been over 40 trillion cubic feet gas and 3.8 billion barrels oil. This history of oil and gas production has resulted in infrastructure to support disposal of fluids associated with oil and gas production and drilling operations.

Since 2003, development of unconventional organic shale plays has resulted in increased oil and gas activity in the Northern Appalachian Basin. Production in these unconventional plays has been driven by horizontal drilling and multi-stage hydraulic fracturing technology. This activity has resulted in higher volumes of drilling fluids and produced water to be disposed of after completion and during production of the well compared to conventional vertical wells. The main unconventional targets in the region have been the Marcellus and Utica-Point Pleasant shale, but operators are expanding to other organic shales.

Monthly operational data on injection volumes, wellhead pressure, and injection uptime from 2008-2012 were collected for Class II brine disposal wells in the study area and analyzed with statistics, graphs, and maps. Based on a survey of Class II UIC brine disposal wells in August 2013, there were 324 wells with active permits as of August 2013. The majority of the wells were in Ohio (211) and West Virginia (76); Kentucky had 30 and Pennsylvania had 7. The status of injection wells is fairly variable, with many wells being permitted or taken off-line due to demand or maintenance.

Geological data on the injection zones showed that many different rock formations are used for injection across the Appalachian Basin. Maps of these formations were compiled to depict the distribution of injection intervals. A total of 690 well logs were collected from the injection wells to better define the geologic layers and parameters. Hydrologic data were collected on reservoir conditions, but these data suggest that subsurface conditions must be evaluated on a site-specific basis. Data on injection fluids suggest that these fluids vary based on geographic location. The source-sink analysis task included review of unconventional shale wells, Class II wastewater production, trends in recycle/reuse of drilling fluids, and brine injection. Sink capacity was calculated for depleted hydrocarbon reservoirs and deep saline formations. A series of reservoir simulations were completed to investigate the pressure buildup and fluid migration effects of brine injection in reservoirs in the region. Additional geomechanical analysis was completed to determine the changes in subsurface stress conditions due to injection.

Overall, project results indicate there is adequate brine disposal capacity to meet demands related to unconventional hydrocarbon production in the Northern Appalachian Basin. The capacity is distributed across large areas in both depleted oil and gas fields and deep saline formations. Accessing the capacity may be limited by the injectivity of the injection zones, which is ultimately related to geologic properties and features of the rock layers. As such, brine disposal operations require careful, continued management.

Major conclusions of the project are summarized as follows:

- Operational records compiled under this study indicate that the total volume of brine being routed to Class II injection wells increased from 9.2 million barrels in 2008 to 17.6 million barrels in 2012. Provisional data suggests that disposal volumes continued to increase to over 20 million barrels in 2013.
- As of August 2013, a total of 324 Class II brine disposal wells were distributed throughout the region. Many of the wells were installed near hydrocarbon fields to manage produced water generated from local production. Other wells were completed within deep saline formations that are mostly saturated with dense brine fluid.
- Drilling records indicated that 10,164 unconventional horizontal shale wells have been drilled in the study area as of 2013. Unconventional wells are clustered in several areas that are located 100-500 km (60-300 mi) from many existing Class II brine disposal wells. A well density map illustrates areas of higher well activity that could benefit from closer injection wells.
- Trends in wastewater management in Pennsylvania indicate that more than 90% of unconventional operators were recycling/reusing fluids in their operations. For Pennsylvania unconventional Marcellus wells, the amount of wastewater recycled from 2010 to 2013 increased from 22% to 67%. Pennsylvania data indicated that operators used about 20% recycled wastewater for hydraulic fracturing treatment in 2013, versus 0% in 2006.
- Data from 2008-2012 indicate that an average of approximately 9,984 barrels of brine were injected per billion cubic feet of equivalent gas produced.
- Based on USGS resource estimates for the Marcellus and Utica shale, ultimate brine disposal demand for these unconventional plays may range from 706 million to 2,290 million barrels. Many factors (drilling technology, economy, etc.) may affect the development of these resources.
- Many different intervals are used for brine disposal in the region, including the Cambrian basal sandstone, the Cambrian Copper Ridge Dolomite and Rose Run Sandstone, the Silurian Medina Group/'Clinton' Sandstone, the Silurian Lockport-'Newburg' dolomite, the Devonian Oriskany Sandstone, and Mississippian sandstone units.
- Historical oil and gas production in Kentucky, Ohio, Pennsylvania, and West Virginia has totaled approximately 43 trillion cubic feet of gas and 3.8 billion barrels of oil, which is equivalent to approximately 47 billion barrels of brine void pore space in the depleted oil and gas reservoirs.
- Sink capacity based on volumetric calculations estimate brine disposal capacity at 2.8 billion barrels in depleted oil and gas fields penetrated by existing Class II brine disposal wells. Brine disposal capacity in deep saline formations was estimated at 480 billion barrels. The capacity is thousands of times greater than the 17.6 million barrels of brine injected in 2012 in the study area.
- Oil and gas production in the region has increased substantially to nearly ~8 trillion cubic feet of gas and ~22 million barrels of oil in 2014, which represents a ~10-fold increase since 2008.
- From 2013-2014, over 30 new Class II disposal wells were permitted in the study area, including five new permits in Pennsylvania. Four new commercial wells in Ohio had reported injection volumes over 1 million barrels per year each in 2014. Combined, these four wells provided a 33% increase in capacity over 2012.
- In general, it appears that subsurface brine disposal capacity is not a major limiting factor on unconventional development in the Appalachian Basin. Depleted oil and gas reservoirs and deep saline formations offer very large capacity for brine disposal in the region. Increased demand has been met with installation of 5-10 new wells per year.
- There are limiting factors related to transportation and costs of Class II wastewater disposal. The model of commercial disposal wells requires costly transport from well pads to distant injection wells. Trucking wastewater also creates a perception issue for the oil and gas industry because the trucks are visible to the general public along major interstates local roads near injection wells.
- There is benefit to tracking brine disposal across the whole Appalachian Basin versus state basis.

1. INTRODUCTION

This Final Technical Report describes the results of the project *Development of Subsurface Brine Disposal Framework in the Northern Appalachian Basin* (Research Partnership to Secure Energy for America [RPSEA] Contract #11122-73). The overall objective of the project was to examine operational and geological properties for the injection zones in the region. The project included a series of tasks to collect Class II brine disposal well operation data, characterize the injection zones, perform injection simulations, complete a source-sink analysis, and conduct an information survey for Class II brine disposal.

1.1 Background

Growth in unconventional shale development and its associated brine and flowback water disposal needs has led to significant current and projected demand for brine disposal wells in the Appalachian Basin. Addressing this demand in a safe and economically viable manner requires a systematic framework for managing fluids disposal in the Northern Appalachian Basin, an area that includes portions of Kentucky, Ohio, New York, Pennsylvania, and West Virginia. This project addresses a crucial need of unconventional oil and gas production by assessing the geologic and reservoir management aspects, conducting source-sink analysis to predict the future capacity for brine disposal in the region, and providing guidance for operators, gas producers, regulators, and public stakeholders. The project included compilation of geological and reservoir data for brine disposal, development of geocellular models from logs and seismic data, reservoir analysis, and advanced reservoir and geomechanical simulations. Research was centered on characterizing the geologic setting, reservoir dynamics, geomechanical issues, and subsurface effects of brine disposal.

1.2 Project Overview

The project was organized into series of technical tasks over a two-year period. The project team included Battelle (lead), the Kentucky Geological Survey (KGS), the Ohio Geological Survey, the Pennsylvania Bureau of Topographic and Geologic Survey, the West Virginia Geological and Economic Survey (WVGES), and NSI Technologies, LLC. The project was designed to provide detailed geologic and modeling analysis of multiple brine injection zones and share results with industry and regulators. Maps, geologic cross sections, inventory of reservoir parameters, and practical guidance for injection operations were prepared for industry and regulatory stakeholders.

1.3 Description of the Northern Appalachian Basin

This research focused on the Appalachian Basin, a regional sedimentary basin that stretches from Tennessee to Ontario, Canada (Figure 1-1). The Basin consists of thick sequences of mainly Paleozoic-age rocks overlying Proterozoic crystalline basement rock. It covers an area of approximately 500,000 square kilometers (km²). It is bordered by the Valley & Ridge/Blue Ridge Mountains to the southeast, Indiana-Ohio Plateau to the west, and crystalline rocks to the north. Relatively thin deposits of unconsolidated alluvial, fluvial, and glacial sediments overlie bedrock in the region.

The Northern Appalachian Basin includes areas in eastern Kentucky, eastern Ohio, western Pennsylvania, West Virginia, and southern New York. Sedimentary rocks form a clastic wedge

that thickens to depths over 8,000 meters in the Rome Trough in West Virginia (Beardsley and Cable, 1983; Quinlan and Beaumont, 1984; Ryder et al., 1992; Shumaker, 1996; Castle, 2001b; Greb et al., 2009). Rock formations include thick layers of shale, siltstone, limestone, dolomite, sandstone, salt, and coal (Patchen et al., 1985). The rocks form an elongated basin structure that dips gently toward the southeast with increasing deformation toward the Appalachian Mountains. In general, the rocks are saturated with mixtures of brine, oil, and gas. In fact, early settlers constructed salt furnaces along natural salt springs in the late 1700s to early 1800s to supply salt to the region.

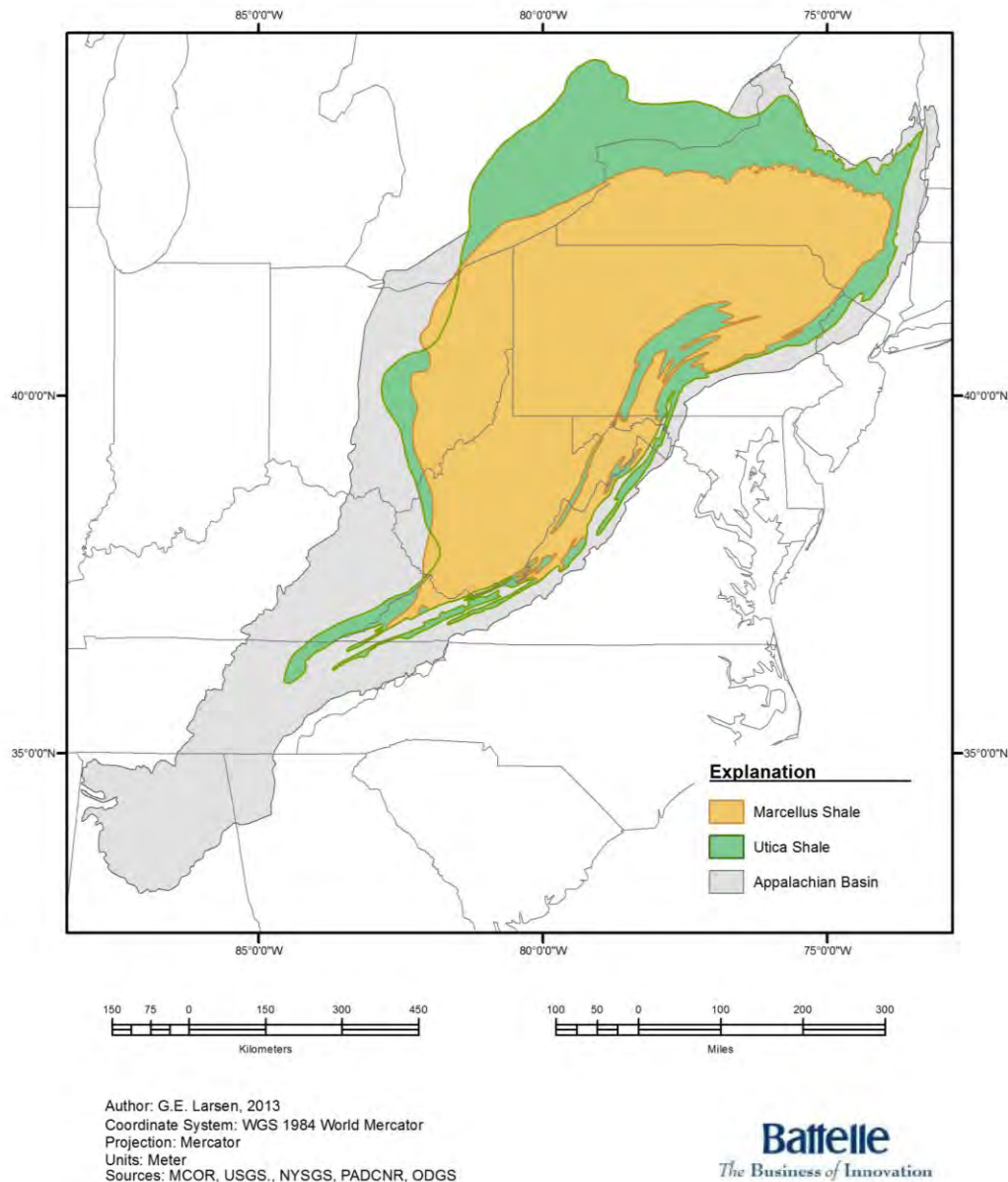


Figure 1-1. General extent of the Appalachian Basin and Unconventional Marcellus and Utica Shale plays.

The Northern Appalachian Basin has a long history of oil and gas production, dating back to the 1859 Drake discovery well in Venango County, Pennsylvania. Over time, thousands of oil and gas fields have been developed in the region (Milici, 1980; Roen and Walker, 1996). Table 1-1 summarizes general information on the oil and gas industry in the Northern Appalachian Basin. Over 900,000 wells have been drilled in the region over time. Cumulative production has been over 50 trillion cubic feet (TCF) of gas and 3 billion barrels (bbl) of oil. This history of oil and gas production has resulted in infrastructure to support disposal of fluids produced in association with oil and gas production and drilling operations.

Since 2003, development of unconventional organic shale plays has resulted in increased oil and gas activity in the Northern Appalachian Basin. Production in these unconventional plays has been driven by technology involving multiple horizontal wells and multi-stage hydraulic fracturing. These methods have resulted in higher volumes of drilling fluids and produced water to be disposed of after completion and during production of the well compared to conventional vertical wells.

The main targets in the region have been the Marcellus shale and the Utica-Point Pleasant shale, but operators are expanding to other organic shales like the Genesee, Rhinestreet, and Burket shales. Figure 1-1 shows the overall distribution of the Marcellus and Utica-Point Pleasant shale formations. Although the formations cover large areas, production has been generally concentrated in areas where the formations are deeper than 6,000 feet.

As of 2013, approximately 6,616 unconventional shale wells drilled in Pennsylvania (PA DEP, 2013), 2,109 unconventional wells drilled in West Virginia (WVGES, 2013), and 616 unconventional wells drilled in Ohio (ODNR, 2013). Eastern Kentucky does not have any unconventional Marcellus or Utica-Point Pleasant wells, but 957 lateral wells have been completed in the Upper Devonian shales. Approximately 24 Marcellus wells were drilled in New York from 2005-2010. As a result of the drilling activity, gas production in Pennsylvania in 2011 was over 1.3 TCF, more than Kentucky, Ohio, West Virginia, and New York combined (Table 1-1). Production continued to increase to around 8 TCF in 2014.

Table 1-1. Oil and gas industry in the Northern Appalachian Basin.

Parameter	KY	OH	PA	WV	NY	Source
Population (million)	4.4	11.5	12.8	1.9	19.6	EIA (2012)
Oil Reserves (thousand bbl)	17,000	41,000	24,000	21,000	1,200	EIA (2011); NYSM (2013)
Gas Reserves (million cu ft)	2,006,000	758,000	26,529,000	10,345,000	253,000	EIA (2011)
Oil Production (thousand bbl/year)	3,089	4,866	4,349	2,194	364	EIA (2012)
Dry Gas to Market (million cu ft/year)	124,243	78,858	1,310,592	394,125	31,124	EIA (2011)
Total Oil and Gas Wells	165,000	220,000	350,000	170,000	75,000	State Reports (approx.)
Unconventional Wells Drilled (~Fall 2013)	957	616	6616	1975	24	State Reports (approx.)
Rig Count (~Fall 2013)	5	34	57	31	0	State Reports (approx.)
Oil Consumption (thousand bbl/year)	117,000	219,300	233,100	35,800	238,700	EIA (2011)
Natural Gas Consumption (million cu ft/year)	222,577	820,485	962,961	115,363	1,216,532	EIA (2011)

Table 1-1. Oil and gas industry in the Northern Appalachian Basin (Continued)

Parameter	KY	OH	PA	WV	NY	Source
Refining Capacity (thousand bbl/day)	238	528	410	20	0	EIA (2012)
Residential Energy (MBTU)	381,838	937,436	923,592	168,568	1,070,000	EIA (2011)
Commercial Energy (MBTU)	253,256	711,507	638,225	111,624	1,183,000	EIA (2011)
Industrial Energy (MBTU)	804,302	1,230,021	1,211,577	275,615	347,000	EIA (2011)
Transportation Energy (MBTU)	471,980	948,592	951,930	168,425	1,015,000	EIA (2011)
Total CO ₂ Emissions (million metric tons)	150.7	249.1	256.6	98.9	172.8	EIA (2010)

1.4 Assumptions and Limitations

Data were analyzed from a variety of sources that collect information from operators, drillers, and service companies. Efforts were made to review the quality of the data, but the accuracy of the information relies on the agency databases. Efforts were focused on active Class II underground injection control (UIC) brine disposal wells. Class II enhanced oil recovery (EOR) wells were not addressed in the data collection task, because these wells typically inject fluid and/or gas for EOR operations.

The survey of wells identified Class II UIC brine disposal wells with active permits as of August 2013. Operational records were tabulated for a minimum period of 2008-2012 for wells with active permits. Data for West Virginia wells were available only for 2012. Other historical brine disposal wells were identified, but operational records were not compiled for those wells.

Operational records compiled in this study were based on UIC reporting data, which requires operators to report monthly operational parameters on injection volumes, injection rates, injection pressures, and operational uptime. This information was analyzed for indicators of injection performance; however, there are limitations to using the monthly data to calculate reservoir parameters. Injection performance analysis should be considered more of an indicator on reservoir conditions than a precise measurement. To address these limitations, the project included a task to monitor injection wellhead pressure in the field to record more continuous data on reservoir feedback from injection.

The status of Class II brine disposal wells is highly variable. This study focused on wells with operational data in the 2008-2012 time interval. When this study started, only operational data from 2012 and earlier were available. Many new Class II brine disposal wells have been permitted since then, although they are not all actually drilled or operating. Therefore, the data from this study may be considered a ‘snapshot’ of Class II activity. Data should not be considered a definitive list of Class II wells. This information is maintained by state or regional EPA UIC programs and changes frequently.

Maps, geologic cross sections, geophysical log analysis, and figures presented in this report are of a regional nature. Research focused on eastern Kentucky (east of the Kentucky River fault system), Ohio, Pennsylvania, and West Virginia. Areas outside this region were not reviewed in detail.

The analysis described in this report was based on the physical properties of geologic layers and historical trends in brine injection, drilling activity, and hydrocarbon production. Estimates related to brine disposal demand and capacity in this report are general in nature. Geologic features and hydraulic feedback are sometimes the first and last items to be considered for brine disposal. Many factors may affect brine disposal in the Appalachian Basin, including technology, economics, politics, regulations, weather, climate, world conflicts, public perception, transportation corridors, surface developments, and other issues. This study was focused on the geology and operations information, since other factors are more difficult to predict.

Injection simulation output from the project reflects simplified versions of real conditions, and the models described in this report represent averaged conditions to a large extent. Input data were compiled from a variety of sources that collect information from operators, drillers, and service companies. None of the simulations were based on existing brine disposal wells, and the input should not be considered specific to an existing well. Many of the injection intervals being examined under this project have relatively limited geotechnical data because they are not oil and gas reservoirs. Therefore, it was necessary to estimate some input parameters based on similar rock formations.

Site-specific projects would require field work such as seismic surveys, drilling, geophysical logging, reservoir tests, detailed reservoir modeling, and system design. The results of this report shall not be viewed or interpreted as a definitive assessment of suitability of candidate geologic injection formations, the presence of suitable caprocks, or sufficient injectivity to allow brine disposal to be carried out cost effectively.

2. OPERATIONAL DATA

2.1 Class II Brine Disposal Regulatory Framework

Underground injection wells are currently regulated by the U.S. Environmental Protection Agency (USEPA) under the Safe Drinking Water Act, which established the Underground Injection Control (UIC) program in 1979-1980. This program defined permitting, construction, operation, reporting, financial responsibility, and abandonment regulations for five classes (Classes I through V) of injection wells (Table 2-1). Class VI wells were introduced in 2012. UIC regulations were generally instituted in the early 1980s. States were allowed to petition for primacy enforcement authority to implement the UIC program, provided their UIC program is at least as stringent as federal standards.

Table 2-1. USEPA UIC injection well class descriptions.

Class	Use	National Inventory
I	Inject hazardous wastes, industrial non-hazardous liquids, or municipal wastewater beneath the lowermost USDW	680 wells
II	Inject brines and other fluids associated with oil and gas production, and hydrocarbons for storage.	172,068 wells
III	Inject fluids associated with solution mining of minerals beneath the lowermost USDW.	22,131 wells
IV	Inject hazardous or radioactive wastes into or above USDWs. These wells are banned unless authorized under a federal or state ground water remediation project.	33 sites
V	All injection wells not included in Classes I-IV. In general, Class V wells inject non-hazardous fluids into or above USDWs and are typically shallow, on-site disposal systems. However, there are some deep Class V wells that inject below USDWs.	400,000-650,000 wells
VI	Inject carbon dioxide (CO ₂) for long-term storage, also known as geologic sequestration of CO ₂	6-10 commercial wells expected to come online by 2016

Source: USEPA, 2013.

The UIC regulations are designed to protect underground sources of drinking water (USDW), defined as “an aquifer or portion of an aquifer that supplies any public water system or that contains a sufficient quantity of ground water to supply a public water system, and currently supplies drinking water for human consumption, or that contains fewer than 10,000 [milligrams per liter] total dissolved solids and is not an exempted aquifer.” Well operators must submit a permit application that summarizes an area of review, corrective action plan, USDW description, geologic formations, operating data, well construction, injection procedures, injection fluid, monitoring program, and financial responsibility.

Based on the application, the USEPA will write a permit and release it for a 30-day public comment period. After this comment period, the operator must demonstrate mechanical integrity with an annular pressure test to demonstrate that the well is not leaking. During injection operations, the operator must record information on daily total injection volumes, injection rates, injection pressures, annular pressures, and properties of the physical and chemical nature of the

injected fluid. The USEPA director has discretion to require additional characterization, monitoring, reporting, and well construction requirements. Permits are effective for five years and can be renewed every five years.

This study focuses on Class II UIC wells that inject brine and other wastes produced from the drilling, stimulation, and production of oil and natural gas. During drilling, fluids used to circulate cuttings and condition the well may require disposal. Similarly, flowback water from hydraulic fracturing may require disposal. These volumes have increased with the adoption of multi-stage lateral wells. Oil and gas operations often result in a portion of ‘produced water’ that is produced along with oil and gas. This ‘water cut’ is separated out from the oil and gas stream for disposal. The water cut may increase or decrease with the age of a field as oil and gas in the reservoir are depleted.

Before UIC regulations, oil and gas operations often utilized leaching pits, surface water discharge, discharge to drains, annular disposal, and/or injection wells to dispose of oil- and gas-related wastewater. The USEPA UIC program provided a framework for injection well permitting, construction, and operations. Table 2-2 summarizes the regulatory agencies for Class II UIC wells in the Northern Appalachian Basin.

Table 2-2. Class II regulatory agencies in the Northern Appalachian Basin.

State	Class II Status	Regulatory Agency	Comments
Kentucky	Regional Implementation	USEPA Region 4 UIC Program	Standard federal Class II UIC requirements
Ohio	State Primacy	Ohio Dept. of Natural Resources (ODNR) Division of Oil & Gas	Maximum bottom-hole injection pressure = $(0.75 \text{ psi/ft} - (0.433 \text{ psi/ft} * \text{SG})) * \text{top perf depth}$ $\frac{1}{4}$ -mile area of review for <200 bbl/day, $\frac{1}{2}$ -mile area of review for >200 bbl/day Ohio Administrative Code 1501:9-3-06 Amendment may require: (1) pressure fall-off testing, (2) geological investigation of potential faulting within the immediate vicinity of the proposed injection well location, (3) plan for monitoring seismic activity, (4) testing and recording of the original bottomhole injection interval pressure, (5) gamma ray, compensated density-neutron, and resistivity geophysical logging, (6) radioactive tracer or spinner survey, and (7) any other such tests that the chief deems necessary.
Pennsylvania	Regional Implementation	USEPA Region 3 UIC Program	Standard federal Class II UIC requirements
West Virginia	State Primacy	West Virginia Dept. of Environmental Protection Office of Oil & Gas	Maximum bottom-hole injection pressure = $0.80 \text{ psi/ft} - (0.433 \text{ psi/ft} * \text{SG} * \text{top perf depth})$ APT = 1.5-2.0 times MASIP for 20 minutes with <5% bleed off
New York	Regional Implementation	USEPA Region 2 UIC Program	Standard federal Class II UIC requirements (no active Class II wells in New York as of fall 2013)

Injection reporting requirements are defined in USEPA UIC regulations (40 CFR Part 146). These regulations require operators to provide USEPA with records on injection monitoring parameters. Regulations require continuous monitoring of injection, but only annual reporting of monthly records. States with primacy may require additional reporting requirements. In general, these requirements define the monitoring data available from Class II UIC brine disposal wells.

Table 2-3 summarizes the list of Class II UIC brine disposal reporting requirements. Reports are required on an annual basis, so there is often a time lag before records are available. Operators are required to report any exceedance of the assigned maximum allowable surface injection pressure. The UIC programs maintain databases of operational parameters.

Table 2-3. Typical recording requirements for Class II UIC brine disposal wells.

Parameter	Recording Frequency	Description
Required		
Injection Pressure	Monthly	Minimum, average, maximum wellhead injection pressure on injection tubing or casing
Injection Rate	Monthly	Minimum, average, maximum wellhead injection rate on injection tubing or casing
Annular Pressure	Monthly	Minimum, average, maximum wellhead annulus pressure
Injection Volume	Monthly	Monthly total injection volume and cumulative annual injection volume
Well Maintenance	----	Description of well work, changes in monitoring equipment
Optional		
Days Operating	Monthly	Days out of month injecting
Chemical and Physical Characteristics of Injected Fluids	Time intervals sufficiently frequent to yield data representative of their characteristics	Other fluid parameters (temperature, pH, density) may be required for states with primacy or at USEPA director's discretion

2.2 Data Sources

Table 2-4 summarizes the data sources for the data collection task. In general, well records were obtained from state oil and gas agencies. Injection operational records were obtained from the designated Class II UIC program for each state. Operational data for Kentucky Class II brine disposal wells were obtained from the USEPA Region 4 UIC program. A Freedom of Information Act release, dated August 16, 2013, of active Class II, Type D (brine or salt water disposal) wells identified 30 well locations in the Northern Appalachian Basin area of eastern Kentucky from the USEPA database list. Operational data for the wells were collected in late September from 14 of the Class II brine disposal wells. These data included scanned operator reports listing average pressure, maximum pressure, and total volume injected on a reported monthly basis from 2008 through 2012 calendar years. A total of 30 brine injection wells were identified; of these, operational data were collected for 21 wells.

Table 2-4. Data sources for data collection task.

State	Well Records	Injection Operational Data	Geotechnical Data
Kentucky	Kentucky Geological Survey	USEPA Region 4 UIC Program	Gas Atlas of the Appalachian Basin (1996), Midwest Regional Carbon Sequestration Partnership (2005), other technical papers, research, and databases
Ohio	ODNR Oil and Gas Division	Ohio Dept. of Natural Resources Division of Oil & Gas	
Pennsylvania	Pennsylvania Dept. of Cons. & Nat. Res. Bureau of Topographic and Geologic Survey	USEPA Region 3 UIC Program	
West Virginia	West Virginia Geologic and Economic Survey	West Virginia Dept. of Environmental Protection Office of Oil & Gas	

Operational data for Ohio Class II brine disposal wells were obtained from the Ohio Department of Natural Resources (ODNR) Oil and Gas UIC program. The ODNR database included records from 1978 to 2012. The data included monthly injection volumes, average injection pressure, maximum injection pressure, days operating, and casing/annulus pressures. A total of 211 Ohio Class II brine disposal wells were identified in the study.

Operational data for Pennsylvania Class II brine disposal wells were obtained from the USEPA Region 3 UIC program. Data were collected for seven Class II brine disposal wells in Pennsylvania. Data collected include annual injected volumes from 2001 to 2012; monthly injection volumes from January 2008 to December 2012; average monthly injection pressure; and monthly maximum injection volumes. The information was provided in both spreadsheet and scanned copies of operator reports.

Operational records were requested from West Virginia Department of Environmental Protection Office of Oil and Gas for Class II brine disposal wells. Personnel at the department indicated that these records are maintained in an older database format and are difficult to export. Data were provided for 2012-2013 for 76 wells.

Data were collected from a variety of sources that collect information from operators, drillers, and service companies. Efforts were made to review the quality of the data, but the accuracy of the information relies on the agency databases. The injection wells were installed over a time span of 1911-2013, so the quality of the records varies. Some information on wells was not available. Designation of the geologic formation for injection was retained as listed in regulatory agency documents. If the geologic formation was not available in regulatory records, the pertinent state geologic survey identified the injection formation based on well logs and geologic maps.

Efforts were focused on active Class II UIC brine disposal wells. Class II enhanced oil recovery (EOR) wells were not addressed in the data collection task, because these wells typically inject fluid and/or gas for EOR operations. There are a large number of Class II UIC EOR wells in the Northern Appalachian Basin (Figure 2-1). Basic information on Class I UIC injection wells was evaluated since these wells utilize similar injection zones to Class II brine disposal wells.

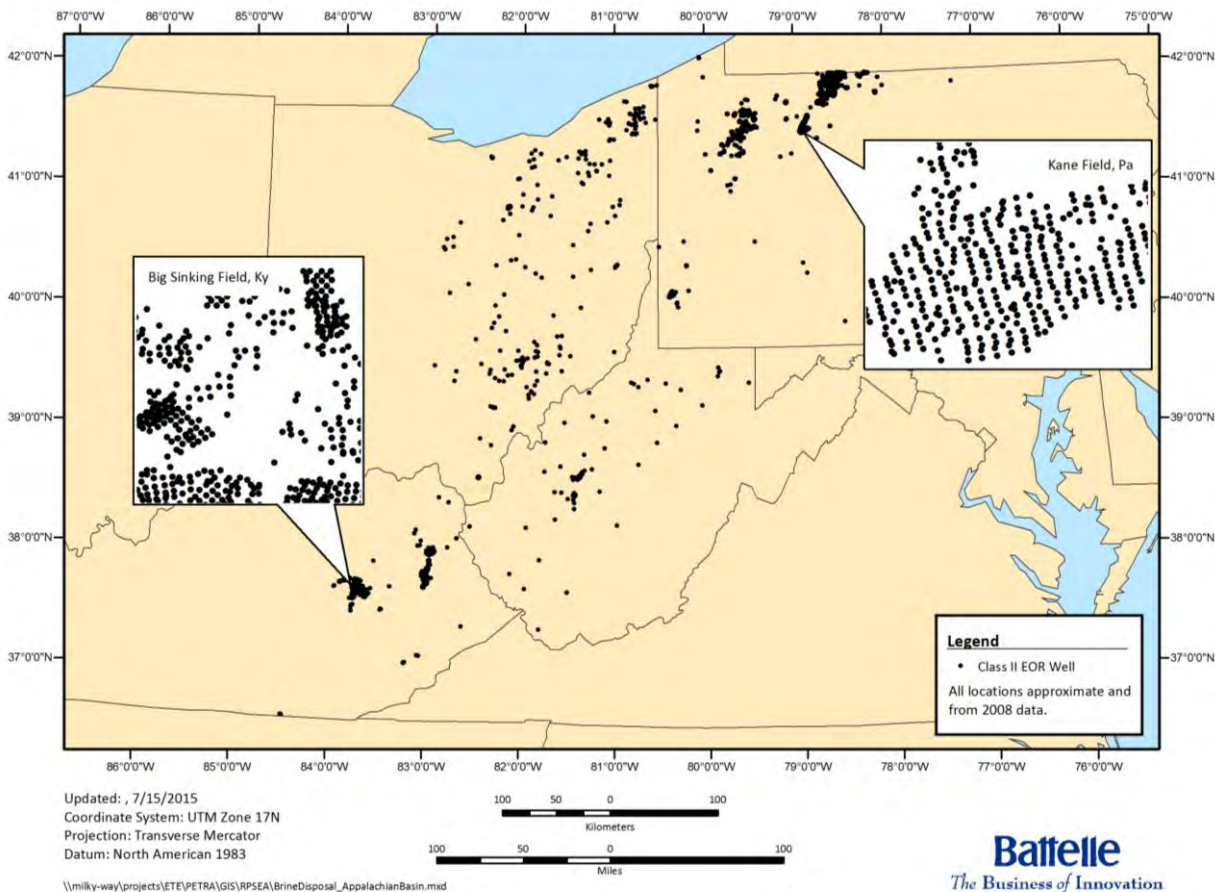


Figure 2-1. Active Class II UIC brine disposal wells and other Class II EOR wells in the study area.

The survey of wells identified active Class II UIC brine disposal wells as of August 2013. The status of injection permits is subject to change. Some wells are permitted but were never actually operated. Other well operations are temporarily suspended due to a permit violation such as failure to submit records on a timely basis. Many injection wells have permit applications pending completion of drilling or financial arrangements. Operational records were tabulated for a minimum period of 2007-2012 for wells with active permits. Other historical brine disposal wells were identified, but operational records were not compiled for these wells.

Injection records from other Class I UIC wells in the study area were reviewed, because these wells inject into some of the same formations as Class II UIC brine disposal wells. There were no active Class I UIC injection wells in Pennsylvania or eastern Kentucky. West Virginia had no active wells, although several wells were attempted in the 1960-1970s. Ohio had 10 active Class I UIC wells as of 2013.

2.3 Survey of Class II Brine Disposal Wells in the Northern Appalachian Basin

The objective of the brine disposal well survey was to identify and classify active Class II brine disposal wells in the Northern Appalachian Basin. A survey of active Class II brine disposal permits was performed for Kentucky, Ohio, Pennsylvania, and New York. Construction

information was tabulated for these wells. Finally, geophysical/wireline well logs were collected to aid in analysis of the wells.

2.3.1 Well Status

The status of Class II UIC brine disposal wells in Kentucky, Ohio, Pennsylvania, and West Virginia is subject to constant change, with new wells coming online and other wells being decommissioned. Data collection was limited to active permits as of August 2013. Many brine disposal wells in the region have been plugged and abandoned, have been reconverted for oil and gas production, or are otherwise inactive. For example, Ohio has over 400 brine disposal wells that are no longer active. Class II EOR wells were not included in the data collection task. However, the active wells best reflect current and future trends in brine disposal operations and demand in the region.

The status of Class II UIC brine disposal wells was obtained from the appropriate regulatory agency (see Table 2-2). Well records were collected from state databases on oil and gas wells. These records included permits, drilling reports, well completion reports, and other permit correspondence. Information was tabulated for general well status, location, and drilling parameters.

Table 2-5 summarizes the results of the Class II UIC well survey. The survey indicated that there were a total of 324 wells with active Class II UIC brine disposal permits as of August 2013. Most of the wells are located in Ohio and West Virginia. Records indicate that approximately 534 brine disposal wells have been abandoned or are otherwise inactive. In general, these inactive or abandoned wells have less complete data; therefore, they were not addressed in detail in the data collection task. The region also has over 5,000 EOR wells. Class II EOR and gas recovery wells may be either issued permits or authorized by rule, so they can be difficult to track accurately. New York had four Class II UIC brine disposal wells listed as active in 2013, but these wells were not addressed in this report.

Table 2-5. Class II injection well count.

Class II Injection Wells	E. KY	OH	PA	WV	Total
Active Brine Disposal Wells	30	211	7	76	324
Inactive/Abandoned Brine Disposal Wells	15	461	14	44	534
EOR Wells	~1,200	~1,700	~1,800	~650	~5,400

Source: USEPA (2011) Class II survey data.

2.3.2 Injection Zones

Wells were classified according to general deepest injection formation based on the well's screened interval or open-hole interval along with lithology denoted in each well. Deepest injection intervals were assigned based on overall geologic layers in the Appalachian Basin. More local analysis may be required to understand specific injection interval. Many wells inject into multiple formations, so the deepest injection formation may not portray the entire injection interval. Table 2-6 summarizes the list of active Class II brine disposal wells in the study area as of August 2013. The wells inject into a wide variety of rock formations.

Table 2-6. Class II UIC brine disposal wells with active permits as of August 2013 classified by deepest injection formation.

Deepest Injection Formation	KY	OH	PA	WV	Total
Pennsylvanian-Mississippian (Big Injun, Weir, Maxton, etc.)	12	2		46	60
Upper Devonian (Berea, Dev. Shale, Bradford)	1	26	2	18	47
Middle Devonian (Onondaga, Huntersville)		4		5	9
Lower Devonian (Oriskany-Helderberg-Huntersville, Bass Is.)		9	3	4	16
Upper Silurian (Lockport, Newburg, Corniferous)	9	60		2	71
Lower Silurian Clinton-Medina		48	2	1	51
Undifferentiated Knox	5	6			11
Rose Run	1	7			8
Copper Ridge, Trempealeau		21			21
Mount Simon, Basal sandstone		28			28
N/A	2				2
Total	30	211	7	76	324

2.3.3 Injection Well Construction Specifications

Available construction data for the active UIC Class II brine disposal wells for eastern Kentucky, Ohio, western Pennsylvania, and West Virginia were compiled from state well permit and completion records. Table 2-7 presents a statistical summary of the well construction data. Note that construction records were not available for all wells. Well construction specifications provide background on typical well dimensions, completion arrangements, and well treatments. For example, many wells are open-hole completion, which may allow better injection but be more difficult to re-enter and maintain long term. Many wells are completed with a typical acidization and fracture job, but these are lower volume (hundreds of barrels) treatments which likely only affect areas immediately surrounding the perforated borehole.

Table 2-7. Well construction data compiled for Class II UIC brine disposal wells.

Kentucky Class II Brine Disposal Wells							
Production Casing			Well Count	Completion	Well Count	Treatment	Well Count
Diameter	Min Depth	Max Depth					
4.5	753	5,743	14	Open hole	8	Fractured	6
6.375		480	1	Perforated	10	Shot	4
7	464	2,084	7	NA	12	Acidized	6
7.5		790	1			Frac & Acid	3
NA			7			Unknown	11
Ohio Class II Brine Disposal Wells							
Production Casing			Well Count	Completion	Well Count	Treatment	Well Count
Diameter	Min Depth	Max Depth					
2.875		1,860	1	Open hole	36	Fractured	61
4.5	795	8,794	157	Perforated	147	Acidized	68
5.5	963	8,215	19	NA	28	Frac & Acid	33
7	2,087	13,684	7			None	6
7.625		8,098	1			Unknown	43
8.625		4,095	1				
NA			25				
Pennsylvania Class II Brine Disposal Wells							
Production Casing			Well Count	Completion	Well Count	Treatment	Well Count
Diameter	Min Depth	Max Depth					
4.5	3,362	4,455	3	Unknown	7	Fractured	3
5.5		9,044	1			Acidized	1
7	6,993	8,470	2			Unknown	3
NA			1				
West Virginia Class II Brine Disposal Wells							
Production Casing			Well Count	Completion	Well Count	Treatment	Well Count
Diameter	Min Depth	Max Depth					
4.5	1,690	8,185	60	Open hole	9	Fractured	48
5.1875	1,383	2,025	3	Perforated	33	Acidized	4
5.5	2,005	6,556	5	NA	31	Frac/Acid	7
6.625		2,209	1			NA	17
7	1,333	6,595	6				
10.75		1,563	1				

Production casing sizes for the active wells range from 2 $\frac{7}{8}$ inches to 10 $\frac{3}{4}$ inches in diameter. In 80% of the wells, production casing sizes are 4 $\frac{1}{2}$ inches. For 65% of well completions, the injection zone was perforated through the casing and cement, and 18% were reported to be open-hole. Hydraulic fracturing and acidizing were the most common stimulation treatment of the injection zones, with 41% of the wells listed as fractured, 27% acidized, and 17% combination fracturing-acidizing completion.

2.4 Operational Data Summary

Class II UIC brine disposal well operations were analyzed to determine the working conditions observed for these injection wells in the Northern Appalachian Basin. The analysis was based on monthly operational information submitted to UIC programs. This information included injection volumes, pressures, and injection uptime. Parameters were analyzed based on injection formations, injection interval depth, and time trends.

2.4.1 Injection Well Trends

Data were evaluated for the five-year period of 2008-2012. In addition, data were analyzed separately for 2012 to summarize recent trends in injection. It should be noted that some wells listed as active by UIC programs did not have operational data available. Data were not available for West Virginia for 2008-2011. In addition, two West Virginia monthly injection volume records appeared to include a correction factor, possibly due to a meter malfunction or other issue with the injection system. In general, these items affected some of the statistics and maps, where we were forced to estimate average conditions or eliminate these outliers. West Virginia brine disposal volume was about 28% of the total volume for the study area in 2012, and this 28% portion was assumed in some trend analysis data for 2008-2011. At the time of analysis, data were not available from any state in the study area for 2013 forward, because operating data are generally compiled on an annual basis.

Information was described with statistics, graphs, and maps. Much of the data simply relate well activity rather than characterizing the reservoir. However, the operational data do provide some indicators of injection performance in the various reservoirs. Wells were classified by deepest injection formation, and many wells were screened across multiple formations. More detailed analysis of injection performance is presented in Section 2.5. Initially, a quality assurance/quality control check was completed on the dataset to identify any outliers or abnormal entries. The data were reviewed by graphing out injection parameters versus time for each well (Appendix). Basic statistics were also calculated. Some data points were corrected due to data export errors. Two wells in West Virginia (API#4701900508 and API#4707302540) had spikes in injection volume which appeared to be related to a record keeping correction rather than actual volume injected.

Figure 2-2 shows the locations of Class II injection wells in the study area along with unconventional wells and oil and gas fields. It also shows the extent of the Marcellus and Utica shale plays. As shown, the majority of brine disposal wells are located to the west of the unconventional gas well development, especially in northeastern Pennsylvania. Most wells are located near traditional oil and gas fields. In general, the wells follow the structure in the basin, with Silurian-Ordovician-Cambrian wells in the northwest portion of the basin and Mississippian-Devonian wells in the southeast portion of the basin.

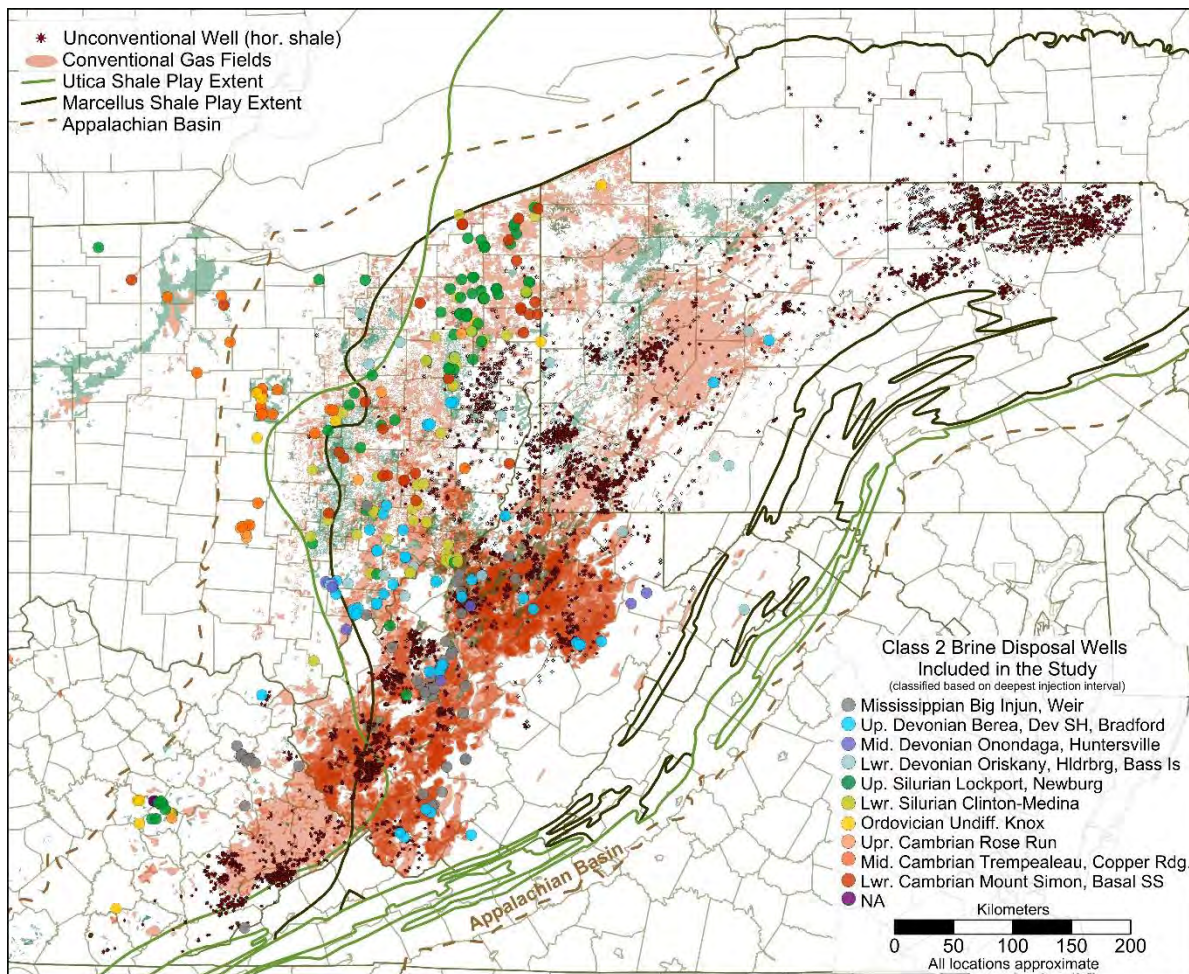


Figure 2-2. Locations of Class II brine disposal wells, unconventional wells, and oil and gas fields in relation to the Marcellus and Utica shale.

Table 2-8 and Figure 2-3 illustrate the overall injection trend from 2008-2012 for the study area. Records suggest that nearly 66 million bbl of fluid were injected in this period in the study area. As shown, most injection volume occurred in Ohio and West Virginia. Injection volumes in Kentucky increased in 2011-2012. There was a spike in injection volume in 2011, but some indication of a decrease or stabilization in 2012. Overall, total injection volume appears to follow the number of unconventional wells drilled in the region. A graph of total volume per well drilled from 2008-2011 is shown in Figure 2-4. These trends may reflect improved technology for well completion, reuse of flowback water, and water treatment followed by increases in produced water as the wells were brought online for production. The trends in produced water will likely follow the overall production curves for Marcellus and Utica-Point Pleasant wells; however, these trends are not particularly well defined at this point for these relatively new fields.

Table 2-8. Brine disposal volumes as reported for project study area for 2008-2012.

Year	KY	OH	PA	WV	Total Brine (bbl)
	(bbl)				
2008	135,815	6,946,806	138,723	2,007,534	9,228,877
2009	545,014	7,587,157	215,608	2,320,683	10,668,462
2010	220,667	8,469,500	169,149	2,462,890	11,322,206
2011	621,723	12,419,849	190,934	3,678,637	16,911,143
2012	709,835	12,980,726	110,488	3,838,821	17,639,870
*WV brine estimated as 28% of KY, OH, PA total for 2008-2011					

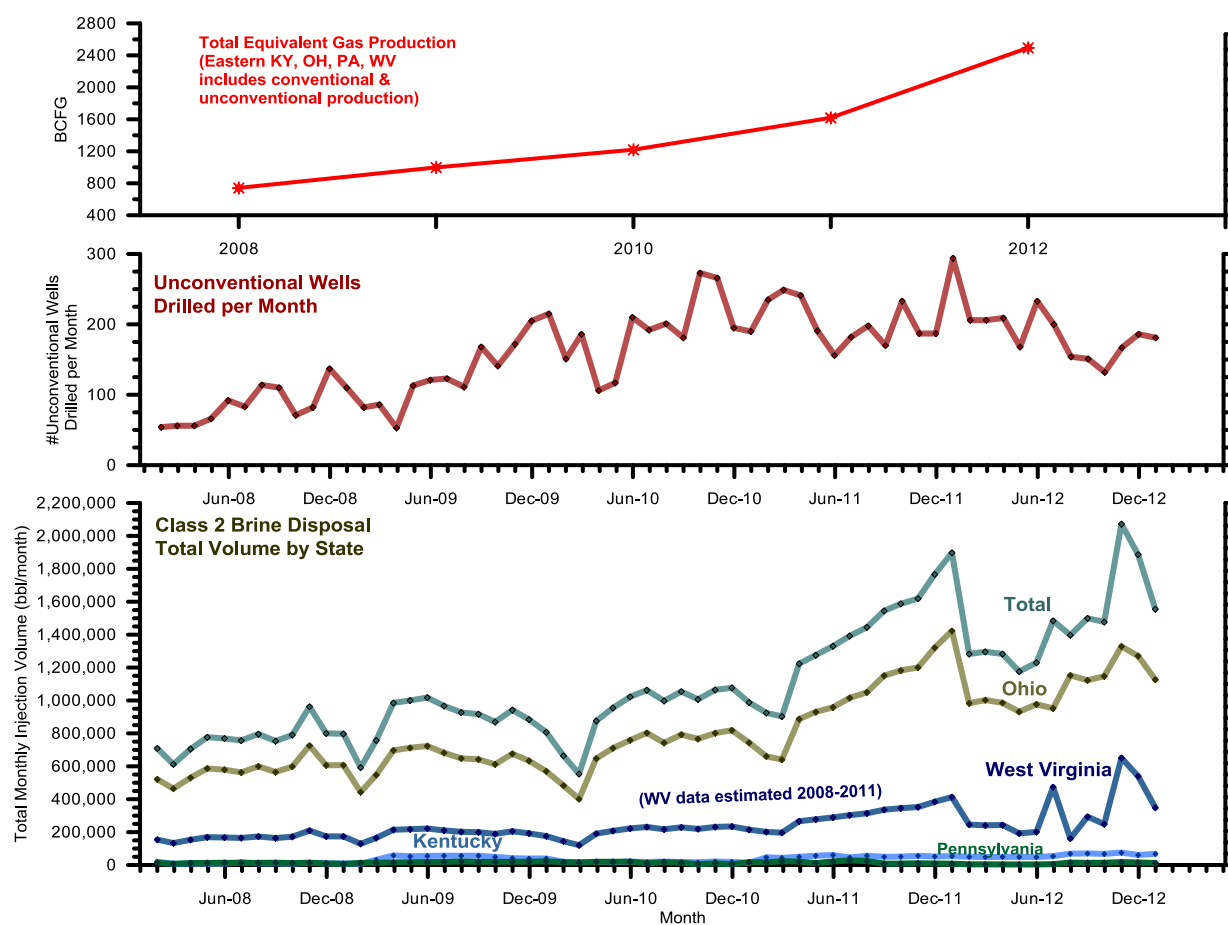


Figure 2-3. Brine disposal volumes and unconventional wells completed from 2008-2012.

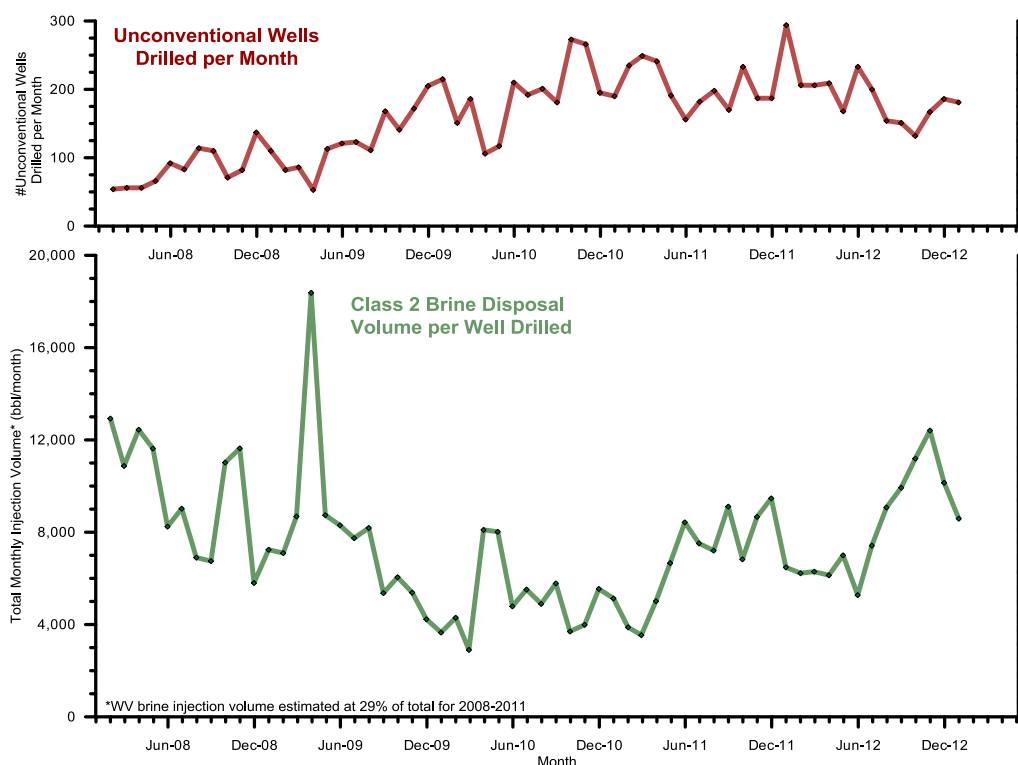


Figure 2-4. Trends in brine disposal volume per number of unconventional wells.

2.4.2 Injection Volumes, Rates, and Pressures

Table 2-9 summarizes general injection operational data for 2008-2012 (not including West Virginia data from 2008-2011). As shown, 246 wells reported injection volumes. The average injection per well was 224,522 barrels (bbl), median was 92,880, and the maximum total injection in a single well was 2,988,184 bbl. The average monthly injection volume per well was 6,713 bbl, the median was 2,607 bbl, and the maximum average monthly injection volume in a single well was 120,976 bbl. The lower median values suggests that the median statistic better represents the central tendency of the populations. Reported wellhead pressures averaged 578 pounds per square inch (psi), with a median of 518 psi and maximum of 2,660 psi.

Table 2-9. Summary of operational data for 2008-2012.

Statistic	Total Volume (bbl/well)	Avg. Monthly Volume (bbl/mo)	Avg. Wellhead Pressure (psi)
Count >0	246	246	205
Max	2,988,184	120,976	2,660
Mean	224,522	6,713	578
Median	92,880	2,607	518
STD	367,332	13,275	493
STD = standard deviation			

Table 2-10 summarizes general injection operational data for 2012. A total of 218 wells reported injection volumes. The average injection per well was 80,620 bbl, the median was 32,015, and

the maximum total injection in a single well was 766,596 bbl. The average monthly injection volume per well was 7,061 bbl, the median was 2,668, and the maximum average monthly injection volume in a single well was 120,976 bbl. Reported wellhead pressures averaged 628 psi, with a median of 543 and maximum of 2,384 psi. Again, the median values appear to represent the central tendency of the populations.

Table 2-10. Summary of operational data for 2012.

Statistic	Total Volume (bbl/well)	Avg. Monthly Volume (bbl/mo)	Avg. Wellhead Pressure (psi)
Count >0	218	218	174
Max	766,596	120,976	2,384
Mean	80,620	7,061	628
Median	32,015	2,668	543
STD	122,317	12,293	480
STD = standard deviation			

Table 2-11 shows the distribution of operational data for 2008-2012. Approximately 90% of the wells had less than 500,000 bbl total injection volume and less than 20,000 bbl/month injection rate. Most wells operated at average wellhead injection pressures of less than 1,000 psi.

Table 2-11. Operating statistics distribution for 2008-2012.

Total Volume (bbl)				Avg. Mo. Volume (bbl/mo)				Avg. Pressure (psi)			
Bin	Freq	%	Cum %	Bin	Freq	%	Cum %	Bin	Freq	%	Cum %
0	13	5.3	5.0	20	3	1.2	1.2	10	9	4.4	4.4
200	2	0.8	5.8	50	7	2.8	4.1	20	4	2.0	6.3
500	5	2.0	7.7	100	3	1.2	5.3	50	8	3.9	10.2
1000	1	0.4	8.1	200	6	2.4	7.7	100	10	4.9	15.1
5,000	13	5.3	13.1	500	23	9.3	17.1%	200	16	7.8	22.9
10,000	12	4.9	17.8	1,000	27	11.0	28.0	300	21	10.2	33.2
50,000	55	22.4	39.0	5,000	100	40.7	68.7	400	19	9.3	42.4
100,000	43	17.5	55.6	10,000	34	13.8	82.5	500	13	6.3	48.8
200,000	39	15.9	70.7	15,000	13	5.3	87.8	750	52	25.4	74.1
300,000	25	10.2	80.3	20,000	12	4.9	92.7	1000	23	11.2	85.4
400,000	10	4.1	84.2	50,000	15	6.1	98.8	1500	18	8.8	94.1
500,000	14	5.7	89.6	100,000	3	1.2	100	2000	7	3.4	97.6
1,000,000	17	6.9	96.1					2500	5	2.5%	100
1,500,000	6	2.4	98.5								
2,000,000	4	1.6	100								

Table 2-12 summarizes the distribution of operational data for 2012. Approximately 90% of the wells had less than 200,000 bbl total injection volume and less than 20,000 bbl/month injection rate. Most wells operated at average wellhead injection pressures of less than 1,000 psi.

Table 2-12. Operating statistics distribution for 2012.

Total Volume (bbl)				Avg. Mo. Volume (bbl/mo)				Avg. Pressure (psi)			
Bin	Freq	%	Cum %	Bin	Freq	%	Cum %	Bin	Freq	%	Cum %
				20	5	2.3	2.3	10	1	0.6	0.6
200	5	2.3	2.3	50	6	2.8	5.0	20	4	2.3	2.9
500	6	2.8	5.0	100	2	0.9	6.0	50	7	4.0	6.9
1000	2	0.9	6.0	200	8	3.7	9.6	100	4	2.3	9.2
5,000	26	11.9	17.9	500	21	9.6	19.3	200	15	8.6	17.8
10,000	20	9.2	27.1	1,000	22	10.1	29.4	300	17	9.8	27.6
50,000	76	34.9	61.9	5,000	79	36.2	65.6	400	16	9.2	36.8
100,000	31	14.2	76.1	10,000	27	12.4	78.0	500	17	9.8	46.6
200,000	27	12.4	88.5	15,000	14	6.4	84.4	750	40	23.0	69.5
300,000	9	4.1	92.7	20,000	14	6.4	90.8	1000	29	16.7	86.2
400,000	8	3.7	96.3	50,000	18	8.3	99.1	1500	12	6.9	93.1
500,000	4	1.8	98.2	100,000	2	0.9	100.0	2000	7	4.0	97.1
1,000,000	4	1.8	100.0					2500	5	2.9	100.0

Injection parameters were analyzed versus injection depth to examine any trends with depth. Figure 2-5 shows the average monthly injection volume versus depth in 2012. Most injection volume was below the 3,000-foot depth. There were some depth intervals with clusters of wells, but these may reflect a combination of geography and geologic structure more than some depth relationship.

Figure 2-6 illustrates the average wellhead pressure with depth in 2012 for wells in the study area. As might be expected, wellhead pressures are greater with depth to overcome hydrostatic pressures related to dense brine fluid present in the deeper rock intervals. These zones are also less likely to be depressurized from previous oil and gas production. Many wellhead pressure readings may be related to the volume of brine processed at the facility, so this information may not reflect injection performance.

Operating data were posted on maps to illustrate the spatial trends in parameters throughout the study area. As with other statistics, these maps may reflect well activity more than injection performance. Figure 2-7 shows total injection volume per well in 2012. As shown, many wells had injection volumes less than 100,000 bbl in 2012. There are some clusters of higher-volume wells near Washington County, Ohio/Pleasants County, West Virginia; Portage County, Ohio; and Estill/Lee County, Kentucky. Figure 2-8 shows average monthly injection volume in Class II brine disposal wells in the study area. As expected, this map shows similar trends.

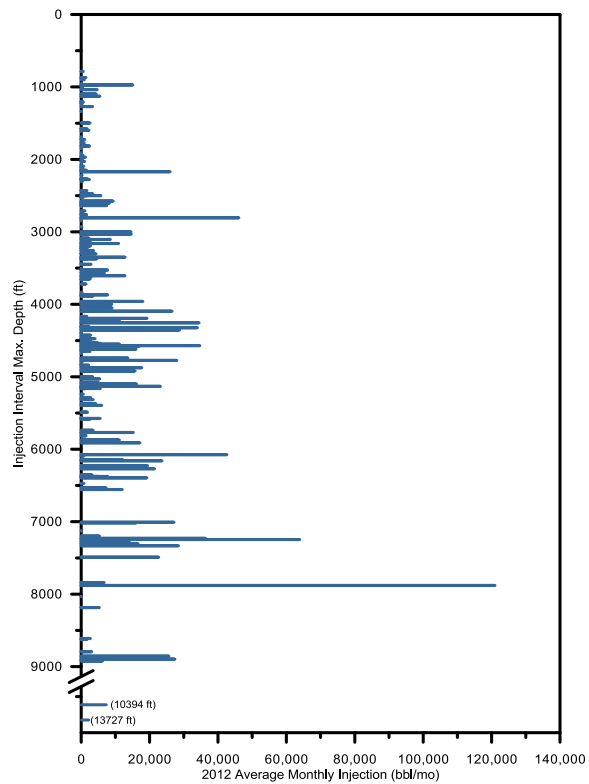


Figure 2-5. Average monthly injection volume versus depth for 2012 for Class II brine disposal wells in the study area.

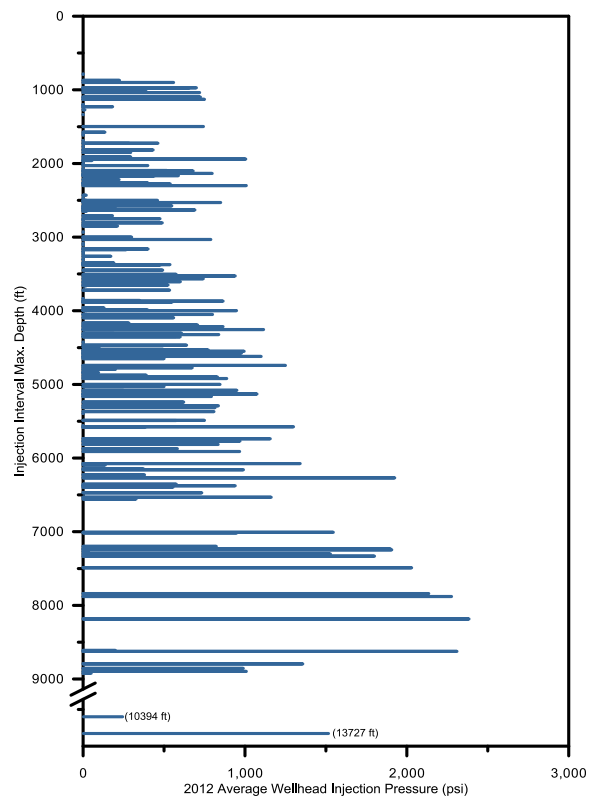


Figure 2-6. Average monthly injection pressure versus depth for 2012 for Class II brine disposal wells in the study area.

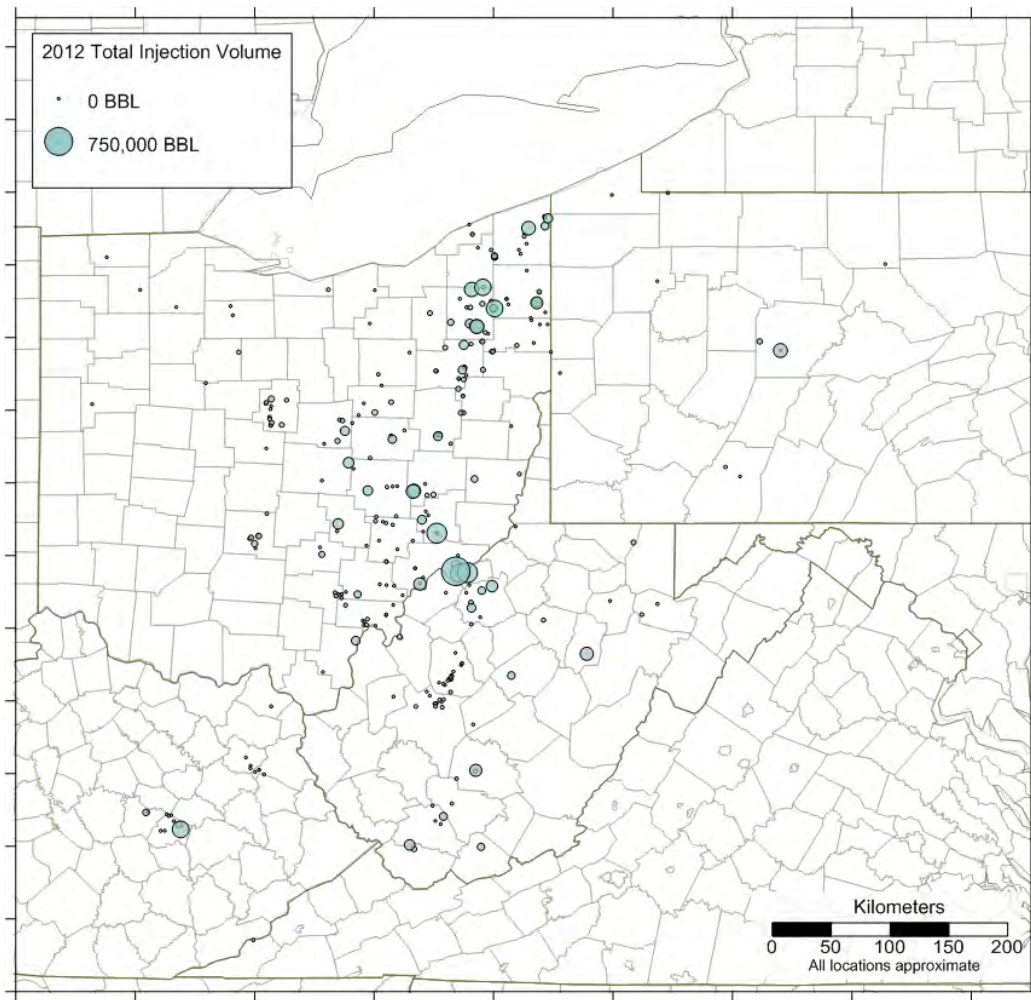


Figure 2-7. Total injection volume for 2012.

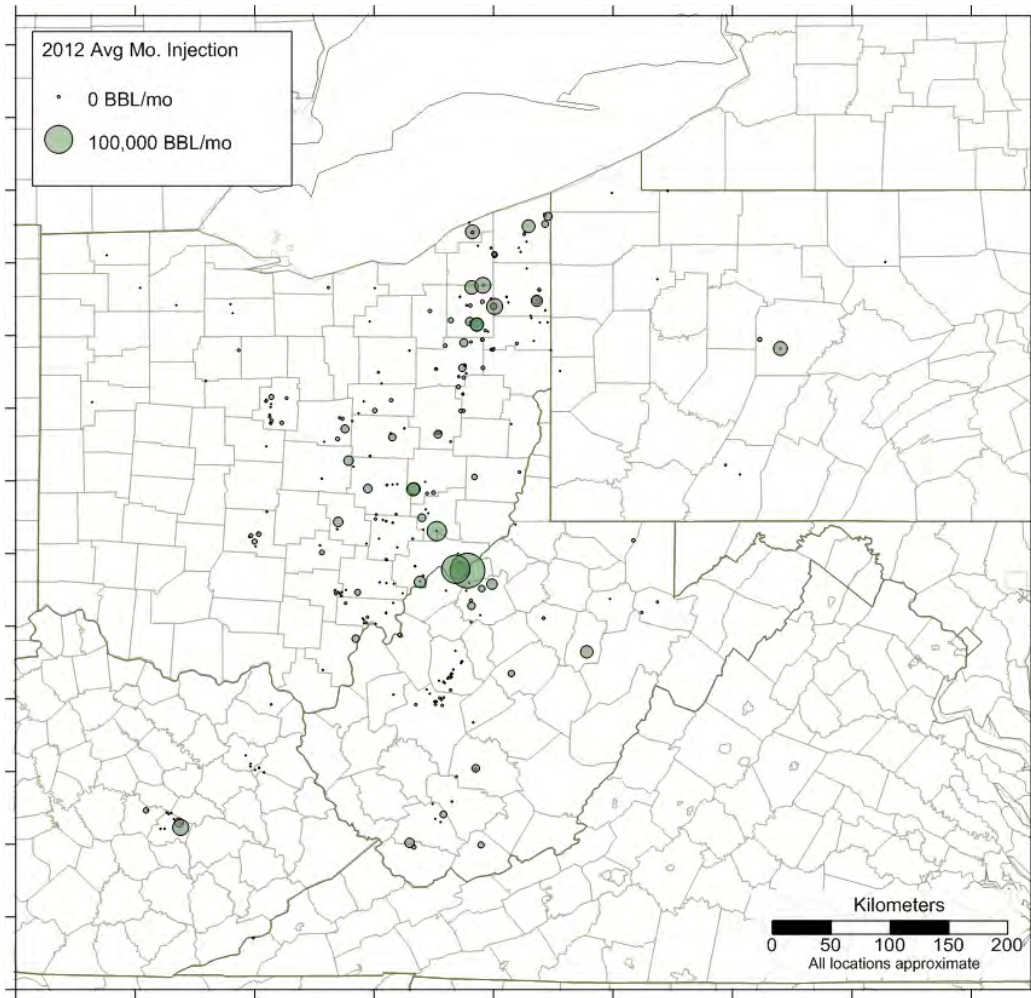


Figure 2-8. Average monthly injection volume for 2012.

Figure 2-9 shows average wellhead pressure in 2012 for the wells in the study area. A comparison of this map to injection volumes shows that many wells are operating at higher pressures but are injecting lower volumes.

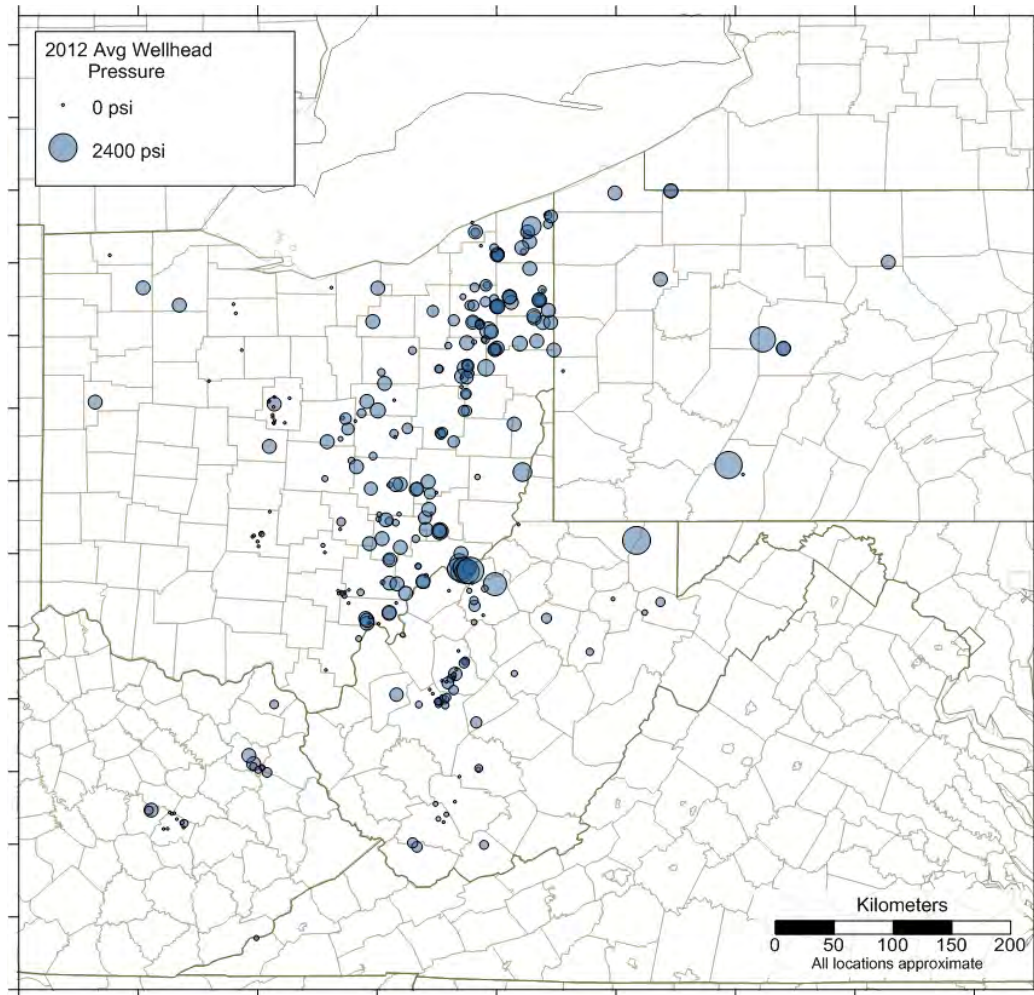


Figure 2-9. Average wellhead pressure for 2012.

General operating data were also evaluated based on rock formations to describe injection conditions in the various injection reservoirs. Figure 2-10 shows well count based on deepest injection zone for the wells in the study area. As shown, many wells inject in the ‘Clinton’-Medina and overlying Lockport-‘Newburg’ formations. There are also a fair number of wells completed in the Pennsylvanian-Mississippian Devonian formations, mainly in Kentucky and West Virginia. Figure 2-10 also shows total injection volume in 2012 by deepest injection formation. As shown, much of the injection volume occurred in wells that penetrate the ‘Clinton’-Medina, Lockport-‘Newburg’ Formation, and Mount Simon/Basal Sandstone.

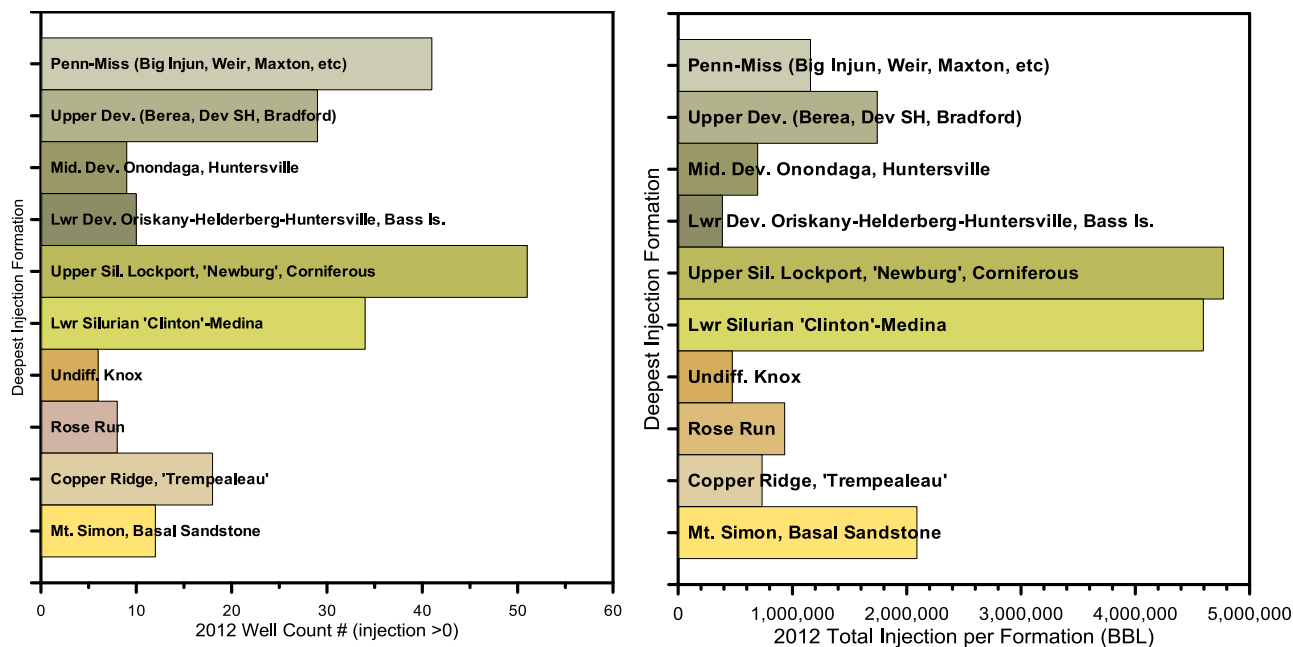


Figure 2-10. Class II brine disposal well count and total injection volume for 2012 by deepest injection formation.

Figure 2-11 shows average injection per well basis for 2012. This plot illustrates that many of the wells completed into the Mount Simon/Basal Sandstone unit had fairly high injection rates; however, there are not as many of these wells in the study area so the total volume is not as high as some other formations. 'Clinton'-Medina wells also had fairly high injection rates along with Knox and Rose Run formations. Figure 2-11 also shows average wellhead pressure for 2012 reported in the various rock formations. Average wellhead pressure for all formations is below 1,000 psi. The graph indicates that some wells in the Ordovician-Cambrian age formations have somewhat lower pressures.

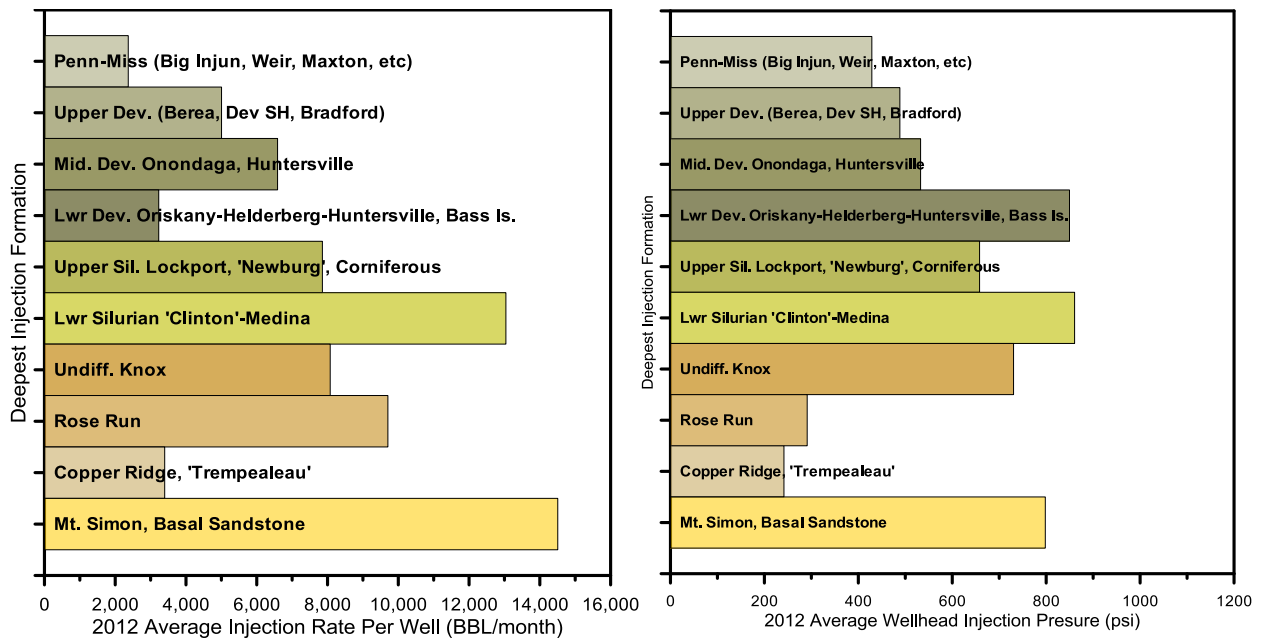


Figure 2-11. Class II brine disposal average monthly injection rate per well for 2012 by deepest injection formation.

2.4.3 Class I UIC Injection Wells

Injection records from other Class I UIC wells in the study area were reviewed, because these wells inject into some of the same formations as Class II UIC brine disposal wells. There are no active Class I UIC injection wells in Pennsylvania or eastern Kentucky. West Virginia has no active wells, although several wells were attempted in the 1960-1970s. Ohio has 10 active Class I UIC wells as of 2013. Sminchak et al. (2012) summarized Class I injection into the Mount Simon Sandstone in the western portion of the Midwest United States. The research found that 21 billion gallons (500 million bbl) of wastewater had been injected into the formation over the past 40 years (Table 2-13). Many of these wells were able to sustain injection rates of 5,000 to 10,000 barrels per day for several decades.

Table 2-13. Summary of Class I UIC injection into Mount Simon Formation.

Site/ Permit #	State	UIC Class	Operator/Lease	Total Depth (ft)	Total Injection (gallons)	Injection Period	Max. Inj. Pressure (psi)	Max. Inj. Rate (gpm)
127-1W-003	IN	I	ArcMit. Burns Hrb. WAL1	4298	2,073,773,736	1968-2012	NA	NA
127-1W-004	IN	I	ArcMit. Burns Hrb. WAL2	4301	1,449,430,497	1968-2012	NA	NA
127-1I-009	IN	I	IN DOT #1	4558	1,145,407,000	1999-2012	NA	NA
127-11-C007	IN	I	Cathay Deepwell Disp.	4538	1,038,498,287	1969-2012	500*	NA
03-02-003	OH	I	Ineos Lima #1	3125	1,900,000,000	1968-2008	843*	257
03-02-004	OH	I	Ineos Lima #2	3158	2,900,000,000	1969-2008	815*	266
03-02-005	OH	I	Ineos Lima #3	3157	2,200,000,000	1972-2008	800*	257
03-02-006	OH	I	Ineos Lima #4	3150	934,000,000	1991-2008	790*	257
M0002	MI	I	E.I.DuPontdeNemours #1	6514	47,211,266	1972-1982	NA	8.5
M0051	MI	I	Heinz N. Am. WDW#1	5915	956,606,100	1974-2007	1220	268
M0052	MI	I	Heinz N. Am. WDW#2	6189	1,029,360,211	1975-2007	1130	248
M0053	MI	I	Heinz N. Am. WDW#3	5913	653,436,009	1975-2007	1200*	184
M0069	MI	I	Detroit Coke Corp.#1	4112	257,774,260	1973-1995	1060	117
M0070	MI	I	Chemetron Corp.#1	5895	110,739,844	1966-1994	NA	122
M0071	MI	I	BASF Chemetron D-2	5910	205,063,274	1973-1994	NA	241
M0217	MI	I	BASF Chemetron D-3	9500	65,218,954	1979-1994	NA	NA
M0129	MI	I	Pfizer, Inc. #3	5945	452,816,909	1975-2007	1007	176
M0130	MI	I	Pfizer, Inc. #4	5946	450,746,358	1975-2007	671	94
M0373	MI	I	Pfizer, Inc. Park-Davis #5	6027	204,956,496	1992-2007	1180	236
M0137	MI	I	Pharmacia & Upjohn #3	5615	222,021,758	1977-2007	464	247
M0327	MI	I	Pharmacia & Upjohn #4	5600	119,562,178	1981-2007	718	31
M0155	MI	I	Honeywell Semet-Solvay#2	4112	169,429,102	1979-2007	860	101
M0226	MI	I	Honeywell Semet-Solvay#3	4127	75,334,789	1977-2007	920	106
M0184	MI	I	Ford Motor Company D-2	4308	81,525,102	1976-1987	NA	41
M0328	MI	I	Gelman Sci. StoferMarsh.1	5804	150,324,076	1982-2004	1405	133
M0357	MI	I	Bio-Lab, Inc IW#1	4856	266,164,922	1989-2007	624	48
M0430	MI	I	Bio-Lab, Inc IW#2	4850	70,014,896	1998-2007	NA	44
M0462	MI	I	Env. Disp. Sys. 1-12	4645	1,372,379	2005-2007	747	9.7
M0463	MI	I	Env. Disp. Sys. 2-12	4550	715,730	2005-2007	631	3.7
M0509	MI	I	Mirant Zeeland IW1	6775	68,904,979	2002-2008	1158	129
M0510	MI	I	Mirant Zeeland IW2	6632	58,583,483	2002-2008	1227	88
05-09-001	OH	I	AK Steel #1	3288	567,000,000	1967-2008	510*	100
05-09-002	OH	I	AK Steel #2	3281		1968-2008	550*	118
03-72-009	OH	I	Vickery Env. #2	2952	357,700,000	1977-2008	472*	68.6
03-72-011	OH	I	Vickery Env. #4	2902	189,800,000	1977-2008	677*	35.4
03-72-012	OH	I	Vickery Env. #5	2938	380,500,000	1981-2008	644*	90.5
03-72-013	OH	I	Vickery Env. #6	2922	319,200,000	1981-2008	401*	87.4
(source: Sminchak, 2013)				TOTAL	21,173,192,595 gallons			

2.5 Injection Performance Analysis

Field data were analyzed using simple methods to determine injectivity and attempt to examine injectivity behavior in different injection formations. Injectivity index is an effective way to determine the injection capacity of the injection wells during the planning phases of fluid injection projects and to monitor injection performance during operation. Underpressured depleted oil and gas reservoirs make up many of the brine disposal targets. Operators have been injecting fresh to brackish water into brine disposal wells in the Appalachian Basin for over 50 years at injection zone depths ranging from 1,000 feet to 13,000 feet.

Performance of the brine injection wells is critically influenced by operational parameters such as injection rate, pressure, and temperature; injection brine and resident fluid properties such as salinity, viscosity, and density; and geologic reservoir characteristics. From Darcy's law for radial flow, injectivity index (J) is defined in oilfield units as:

$$J = \frac{q}{(P_{BH} - P_e)} = \frac{k_w h}{141.2 \mu_w B_w (\ln \frac{r_e}{r_w} + s)} \quad (2.1)$$

where

- q = injection rate, barrels water per day
- k_w = effective reservoir permeability to water, millidarcies
- h = formation thickness, ft
- P_{BH} = bottomhole injection pressure, psi
- P_e = far-field reservoir pressure, psi
- μ_w = injected water viscosity, centipoise
- B_w = injected water formation volume factor
- r_e = drainage radius, ft
- r_w = wellbore radius, ft
- s = skin factor (total near-wellbore skin)

From a total of 324 active Class II wells, 10 Ohio wells, 6 West Virginia wells, 6 Kentucky wells, and 2 Pennsylvania wells were analyzed to calculate time-varying injectivity index. These active wells were selected for the first round of analysis based on the quality of data records (i.e., the degree of correlation between the reported injection rates and pressures) and the quantity of operational data (i.e., the number of continuous data records available). For these disposal wells, available input data consisted of wellhead pressures, brine injection volumes, and corresponding injection time periods. The injection zone depths, well completion, and regional brine salinity data were obtained from regional records.

The bottomhole pressures (BHP) were calculated from the available injection wellhead pressure data by using:

$$P_{BH} = P_{WH} + (\rho g \cdot TVD) - \Delta P_f \quad (2.2)$$

where P_{BH} = bottomhole pressure, psi
 P_{WH} = wellhead pressure, psi
 ΔP_f = frictional pressure drop in tubing and completion, psi
 $\rho g.TVD$ = hydrostatic pressure of fluid column to mid-point of perforations, psi

Assumptions for BHP calculations were:

1. Radial incompressible flow, immiscible displacement of injected brine, and native fluid phase are assumed.
2. Geochemistry and mineral precipitation are ignored.
3. The effect of various well completions is ignored to assume a single roughness factor and a standard tubing diameter (4.5 inches) where data were not available.

In general, frictional losses in the wellbore are found to be negligible compared to the hydrostatic potential for the given injection rates and tubing specifications. The wellhead pressure data were used for injectivity analysis after conversion into an equivalent BHP (see equation 2.2). The following two methods were used to calculate injectivity indices using the continuously monitored injection rates and pressures:

1. Darcy's law (ratio of injection rate and BHP differential with time)
 The injection rate, BHP, and calculated injectivity index (J from equation 2.1) are plotted together with time.

$$J = \frac{q}{(P_{BH} - P_e)} \quad (2.3)$$

Data fluctuations in the measured rates and pressures result in fluctuating injectivity indices that could be difficult to analyze.

2. Hall plot
 The modified Hall plot consists of plotting cumulative pressure difference-time product versus cumulative volume of brine injected. This plot yields a straight line with a slope equal to the reciprocal of the injectivity index based on equation (2.4) (obtained by integrating equation (2.1) with reference to time):

$$\sum_t \{P_{BH} - P_e\} \Delta t = \frac{141.2 \mu_w B_w (\ln \frac{r_e}{r_w} + s)}{k_w h} W_i \quad (2.4)$$

where, W_i is the cumulative water injected, bbl

From equation (2.4), the slope of the modified Hall plot, m_H , is given by the following expression, which represents the reciprocal of the injectivity index (equation 2.5).

$$m_H = \frac{141.2\mu_w B_w (\ln \frac{r_e}{r_w} + s)}{k_w h} \quad (2.5)$$

Hall plots are effective tools to process continuous water injection information. Any change in the slope of the Hall plot indicates a change in the injection behavior. Increasing slopes imply deteriorating performance (e.g., well plugging, skin) while decreasing m_H values indicate injectivity improvement (e.g., post-acid treatment). Considering the cumulative values reduces the effects of fluctuating measured data and helps us identify real changes in injectivity trends.

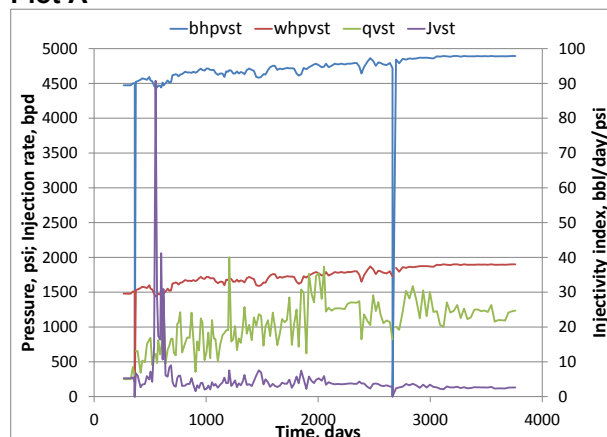
The value of the far-field reservoir pressure (P_e) critically affects the interpretation of this plot. An incorrect value of P_e could cause changes in m_H when no alteration of the formation properties has occurred or, conversely, may hide changing injectivity. To correctly estimate P_e in spite of the inevitable fluctuations in rates and pressures from the field, the calculation proposed in Silin et al. (2005) was used, where essentially the slope of the straight line plot between (P_{BH}/q) and $(1/q)$ gives P_e .

Sample results of an injectivity analysis for two Ohio wells are presented in Figure 2-12. One well is a Washington County brine disposal well that has injected 3,709,000 barrels brine into the Clinton sandstone since 1999. The second well is in Perry County, with 4,696,000 barrels brine injected into the Mount Simon Formation since 1985.

The trend in injectivity index with time was analyzed for these wells. Any change in either the pressure or the injection rate that is not accompanied by a similar change in the other is likely due to injectivity changes in the well under consideration. This is confirmed with corresponding slope changes in the Hall analysis plot. The decrease in injectivity index observed in Figure 2-12 (Plot B) indicates that the performance of the well is dropping. This decrease in the injectivity index needs to be analyzed in tandem with operators to determine the consequent course of action.

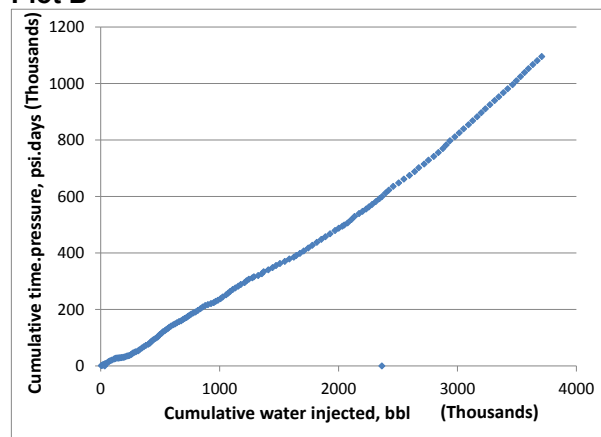
3416729395: Washington County, OH (CLINTON)

Plot A



Plot of injection rate, pressure differentials and injectivity index with time

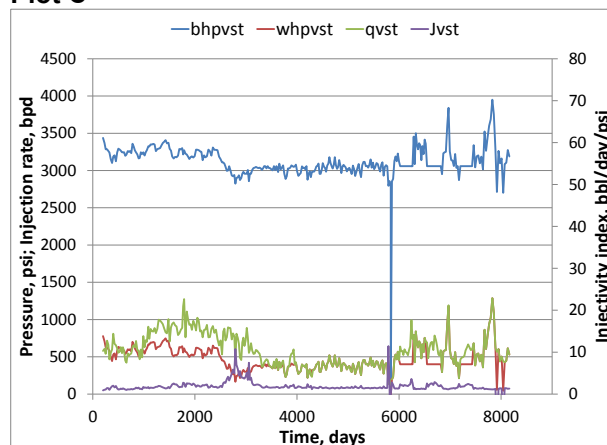
Plot B



Hall plot showing injectivity index trend during the injection period. Slope of the line gives reciprocal of J.

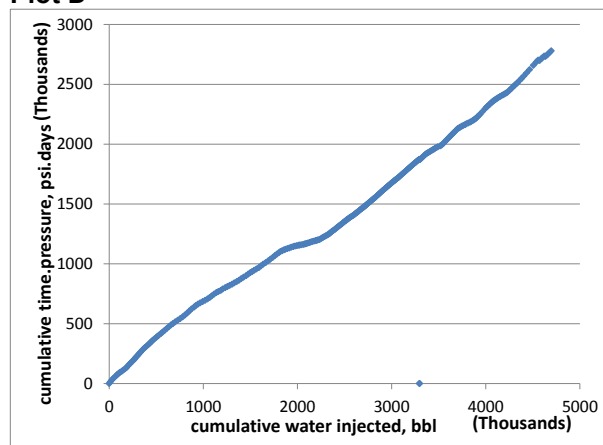
3412726595: Perry County, OH (MOUNT SIMON)

Plot C



Plot of injection rate, pressure differentials and injectivity index with time

Plot D



Hall plot showing injectivity index trend during the injection period. Slope of the line gives reciprocal of J.

Figure 2-12. Sample injectivity analysis results for two Ohio wells.

2.6 Class II Disposal Well Field Monitoring

To provide more information on hydraulic parameters for injection zones in the Appalachian Basin, field monitoring of eight Class II brine injection wells was completed. The field monitoring consisted of continuous logging of wellhead pressures during normal operations. Where possible, pressure transient analysis (PTA) was complete to estimate reservoir parameters and features like boundaries. Overall, the field monitoring of injection operations provided better understanding of typical brine injection operations in the region. Well testing estimates for reservoir permeability are valuable, since most of the brine disposal intervals are not well characterized in the region compared to hydrocarbon fields.

2.6.1 Field Monitoring

The field monitoring consisted of wellhead pressure logging for seven Class II brine injection wells in the study area. Well testing was facilitated by operators in the region. The project team provided wellhead pressure loggers, and they were installed by operators' well technicians (Figure 2-13). The loggers were set to record pressure every 1 minute. Actual well names and locations were kept confidential because operators did not want confidential information about their operations distributed. Wells were monitored for one to eight weeks. Flow rates were also recorded, where available from the operator. Continuous flow rates could not always be obtained because they would require significant modification of wellhead equipment. The monitoring was more general than a designed well test. Many wells exhibited typical pressure fall-off response during normal operational cycles. Field monitoring results are described as follows for the injection intervals.



Figure 2-13. Wellhead logger installed on Class II injection well for field monitoring.

2.6.1.1 'Clinton'-Medina

Five 'Clinton'-Medina Class II brine wells were monitored for wellhead pressures. Four of the wells were larger, commercial wells located in the central Appalachian Basin. These wells were monitored for one week each during typical injection operations. Figure 2-14 shows the wellhead pressure monitoring recorded for the four wells. As shown, three wells were operated continuously, so no pressure fall-off occurred that could be used for pressure fall-off analysis. The wells were run at fairly high wellhead pressures, because they were injecting commercial volumes of fluid. Well #4 was shut in during the monitoring period, because operators suspected it had been plugged with sediment from an unsuitable load of injection fluid. Overall, these wells reflect typical commercial brine disposal operations in the region, where wells inject a constant stream of fluid at fairly high pressure. The wells exhibit fairly continuous wellhead pressures with little fluctuation (10 to 20 psi). Most pressure fluctuations appeared related to pumping cycles and other minor adjustments in the injection system.

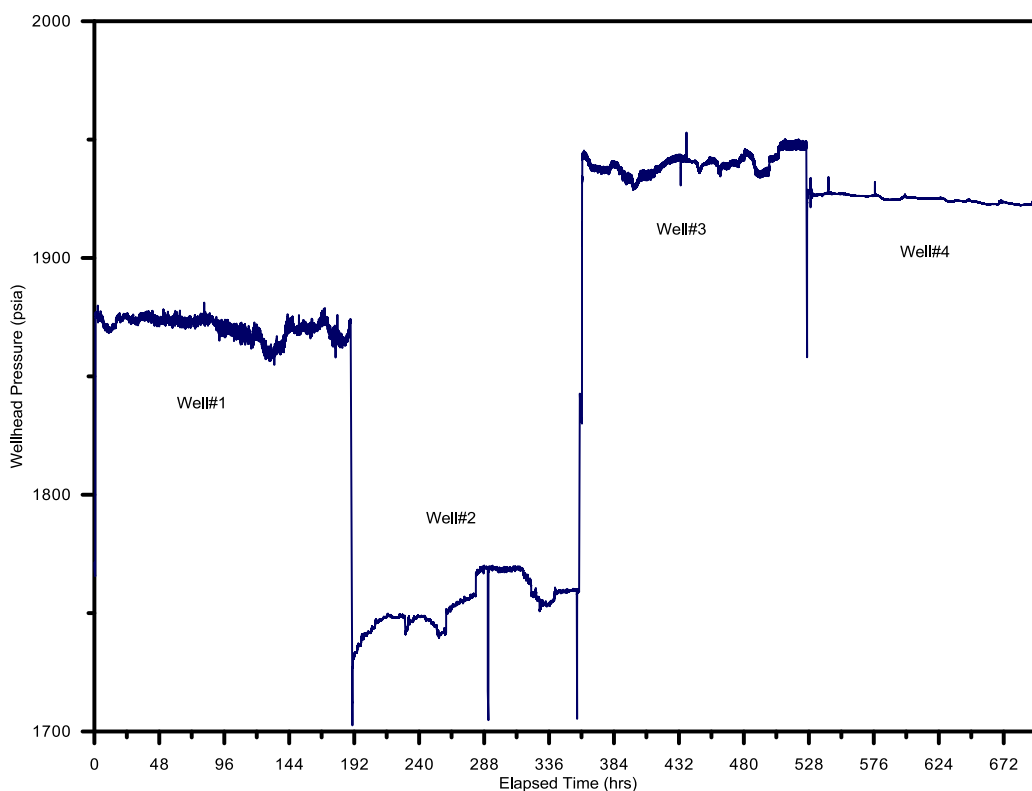


Figure 2-14. Wellhead pressure monitoring results from four Clinton-Medina Class II brine disposal wells in the central Appalachian Basin.

Another Clinton-Medina well in the east-central portion of the basin was monitored during well tests after the well was converted for injection. This well reflects acid job and short injection periods (Figure 2-15). The pressure fall-off was recorded after injection, but wellhead pressures dropped to below zero when the well went on vacuum. The well did show pressure buildup and fall-off curves that were analyzed for reservoir parameters.

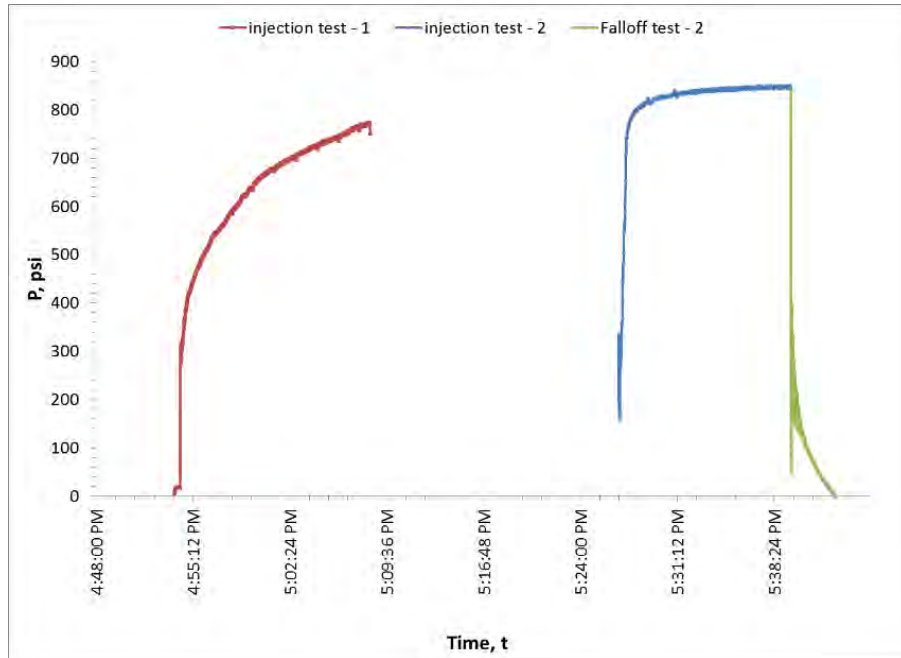


Figure 2-15. Wellhead pressure monitoring results from Clinton-Medina brine disposal well in the east-central Appalachian Basin.

2.6.1.2 Newburg

A Newburg Class II brine disposal well in the east-central portion of the Appalachian Basin was monitored for wellhead pressure over an eight-week period. During this period, the well was operated on a periodic basis at wellhead pressures between 400 and 700 psi (Figure 2-16). Injection rates were approximately 5 to 400 bbl/day. The well exhibited several pressure fall-off cycles that were analyzed for reservoir parameters.

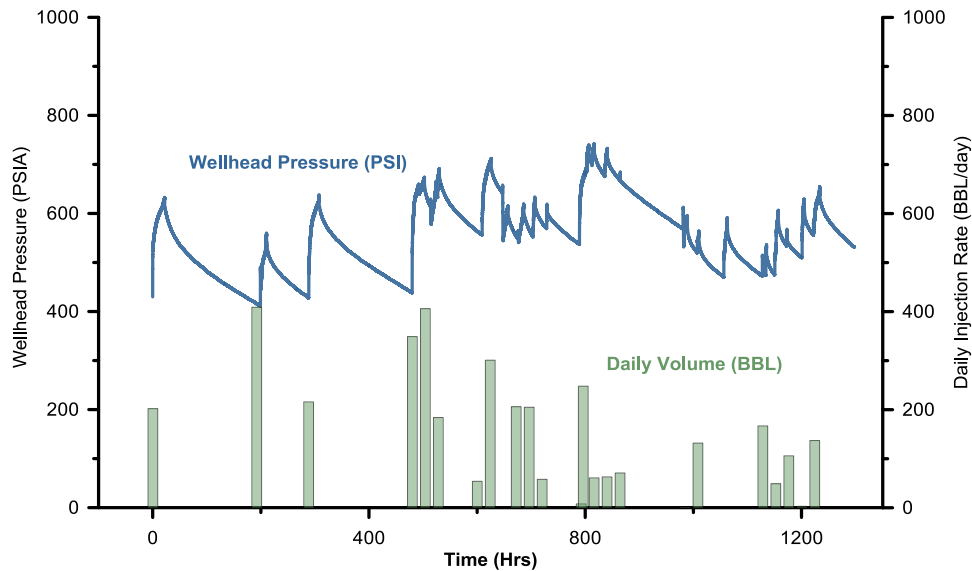


Figure 2-16. Wellhead pressure monitoring results from Newburg brine disposal well in the east-central Appalachian Basin.

2.6.1.3 Knox-Rose Run

A Knox-Rose Run well in the central Appalachian Basin was monitored for a period of approximately 14 days for wellhead pressures. The well was run at wellhead pressures of 600 to 1,100 psi with injection rates at around 1 bbl/min (Figure 2-17). The well showed numerous pressure fall-off cycles that were analyzed for reservoir parameters.

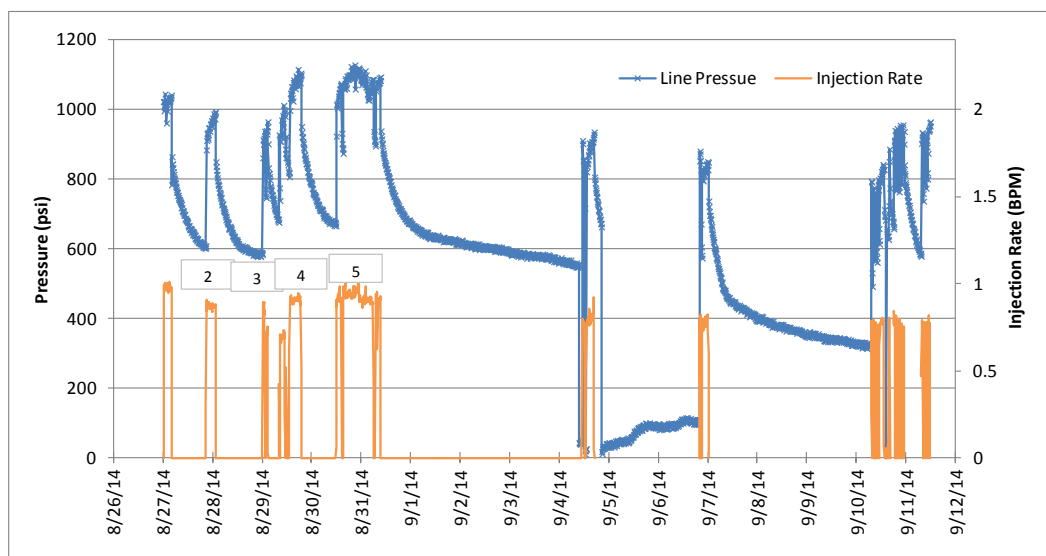


Figure 2-17. Wellhead pressure monitoring results from Knox-Rose Run brine disposal well in the central Appalachian Basin.

2.6.2 Pressure Fall-off Interpretation

Wellhead pressure data from a Clinton-Medina well, Newburg well, and Knox-Rose Run well were analyzed with pressure buildup/fall-off methods to estimate reservoir parameters and features. Most of these methods work better with downhole pressures. Since injection pressures were recorded at the wellhead, they may not be entirely consistent with downhole pressures. However, friction pressure loss calculations suggest that the downhole pressure loss is fairly minor for typical well configurations in the region. The main issue with monitoring occurred when the wellhead pressure declined to less than zero, and no further wellhead data could be recorded. Since most injection wells had been operating for several years, some background pressure trends may also have been present in the data.

2.6.2.1 East-Central Appalachian Basin Clinton-Medina

Data from the east-central Clinton-Medina well test were analyzed for effective formation permeability in the Clinton-Medina injection zone. The injection test was performed in a step rate test from approximately 3 to 5 bbl per minute. Injection periods lasted generally 5 to 10 minutes. Overall, it was difficult to establish stable pressures at the wellhead, possibly because the reservoir was depressurized after gas production. Pressure fall-off also showed oscillations as the well went on vacuum within 5 minutes of shut-in. Consequently, specific injection and fall-off periods were chosen when the data were considered more reliable than other periods. The test intervals selected for analysis are shown in Figure 2-17.

Given the fact that only the surface pressure data were available for these test periods, it was assumed that the rate of change of pressure at the surface and the bottomhole conditions are the same. Hence, surface pressures were used to analyze these well tests and determine formation permeability. Pressure increase was calculated as $|P_{init} - P_t|$ for each time period. Figure 2-18 shows the plot of pressure increase with time for each of the three chosen time periods.

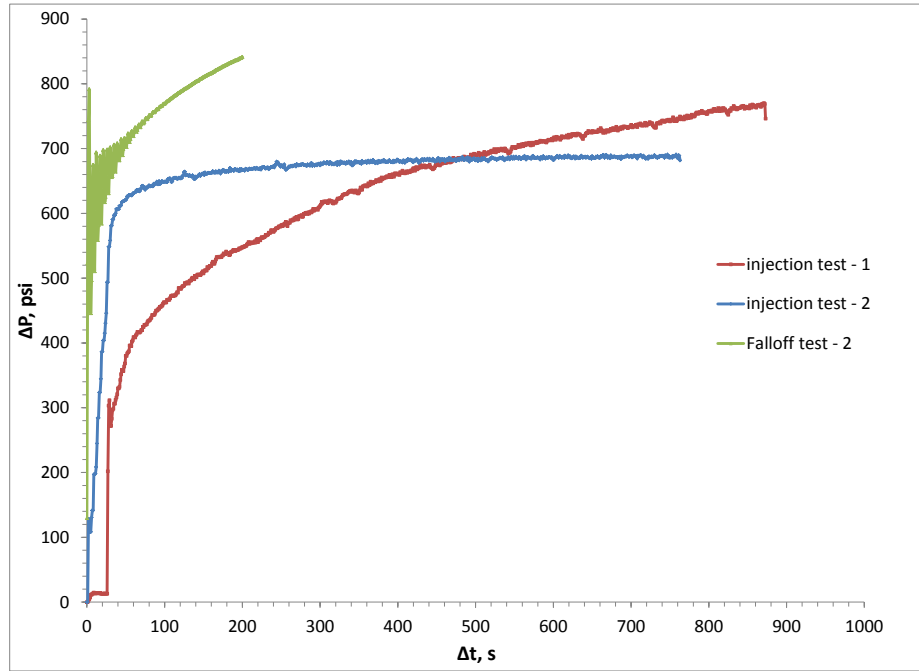


Figure 2-18. Test data trends from plot of pressure increase versus time for each of the three test periods

The pressure increase with time for the three chosen test periods suggests that injection test – 2 was not run long enough to allow steady (pressure) conditions necessary for formation characterization. The slope/trend of this test period was therefore different from the other two. We then analyzed injection test – 1 and fall-off test – 2 to obtain comparable permeabilities/transmissivities. Analysis equations to obtain the formation permeability were based on the log approximation solution for the radial flow diffusivity equation and Horner equation as:

$$P_{ws} = P_i - (162.6q\mu \frac{\beta}{kh})(\log \frac{tp + \Delta t}{\Delta t}) \quad (2.6)$$

This is the equation of a straight line with slope m when pressure is plotted with Horner time, $\frac{tp + \Delta t}{\Delta t}$.

Hence, formation permeability can be obtained for both pressure fall-off and injection tests as:

$$k = \left(162.6q\mu \frac{\beta}{mh} \right) \quad (2.7)$$

where

- k = formation permeability
- q = flow rate, bpd
- β = formation volume factor
- μ = fluid viscosity, cP
- m = slope of semilog plot between pressure and time
- h = formation thickness, ft
- P_i = initial pressure
- P_{ws} = well shut-in pressure
- C_t = total compressibility
- r_w = well radius.

Calculations for determining effective formation permeability from fall-off test – 2 and injection test – 1 are shown in Figures 2-19 and 2-20, respectively. Formation permeability in the injection zone was estimated to be 17-23 mD across a 160-foot perforated interval from the available data. Overall, the analysis suggests reservoir transmissivity of approximately 3,200 mD-ft.

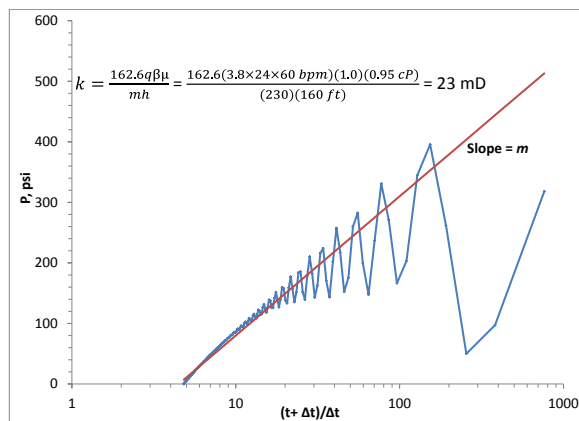


Figure 2-19. Fall-off test-2 curve result

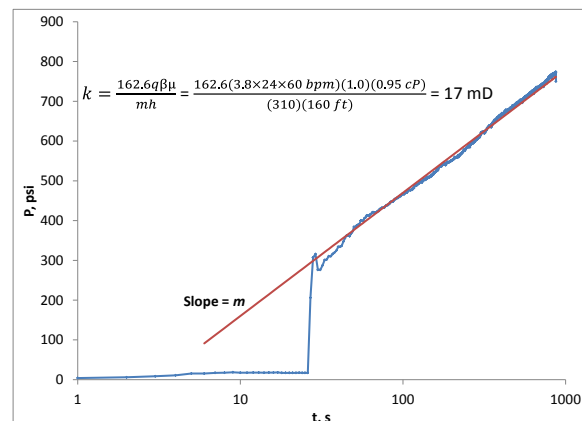


Figure 2-20. Injection test – 1 curve result

Analysis involved several assumptions related to input parameters and test conditions. The biggest assumption was that the test reached radial flow conditions, which may be unlikely in such a brief fall-off period. Due to rapid pressure fall-off, wellhead pressure measurements, and pressure oscillations, data were not suitable for additional reservoir test analysis such as pressure derivative plots that may provide information on reservoir features. Downhole gages would offer more stable pressure readings and longer fall-off data, but these gages are more intensive to install during injection tests.

2.6.2.2 East-Central Appalachian Basin Newburg

Wellhead operational data from a well in the east-central Appalachian Basin were analyzed for permeability in the Newburg-Lockport injection zone. Wellhead pressure data for the injection well were obtained for the period April 15 to June 10, 2014. During this period, 3637 bbl of brine were injected into the well during multiple injection events. Individual injection events followed by a fall-off period created a pressure transient response that could be analyzed to estimate reservoir and well properties, assuming sufficient information is known about the well and reservoir. A radial PTA was attempted for the first three injection events. Subsequent events were not analyzed because they were too closely spaced together. The radial PTA provides an estimate of reservoir permeability (k) and well skin (s).

The PTA analysis was conducted using the FAST WellTest™ software (Fekete, 2013). The analysis involved plotting the injection and fall-off data for each event on a log-log diagnostic plot ($\log \Delta P$ vs. $\log \Delta t$ plot) and on a straight-line plot (iP vs. $\log t$ plot) and fitting a straight line through the data region best corresponding to the infinite acting radial flow period (horizontal derivative). In the case of all three tests, radial flow was not indicated on the fall-off derivative; however, the injection derivative for all three tests did exhibit horizontal behavior. Therefore, the injection data were used to calculate permeability and well skin.

Parameters used in the analyses and calculated parameters are summarized in Table 2-14. Input parameters include injection rate (q), thickness (h), viscosity (μ), water formation volume factor (B), porosity (ϕ), total compressibility (C_t), and well radius (r_w). For each injection event, an average injection rate was calculated by dividing the total volume injected during the event by the duration of the pressure build-up period (Table 2-15). Straight-line and log-log diagnostic plots were developed for each of the three injection fall-off events (Figures 2-21 through 2-23).

Table 2-14 Parameters used to analyze pressure data and calculated parameters.

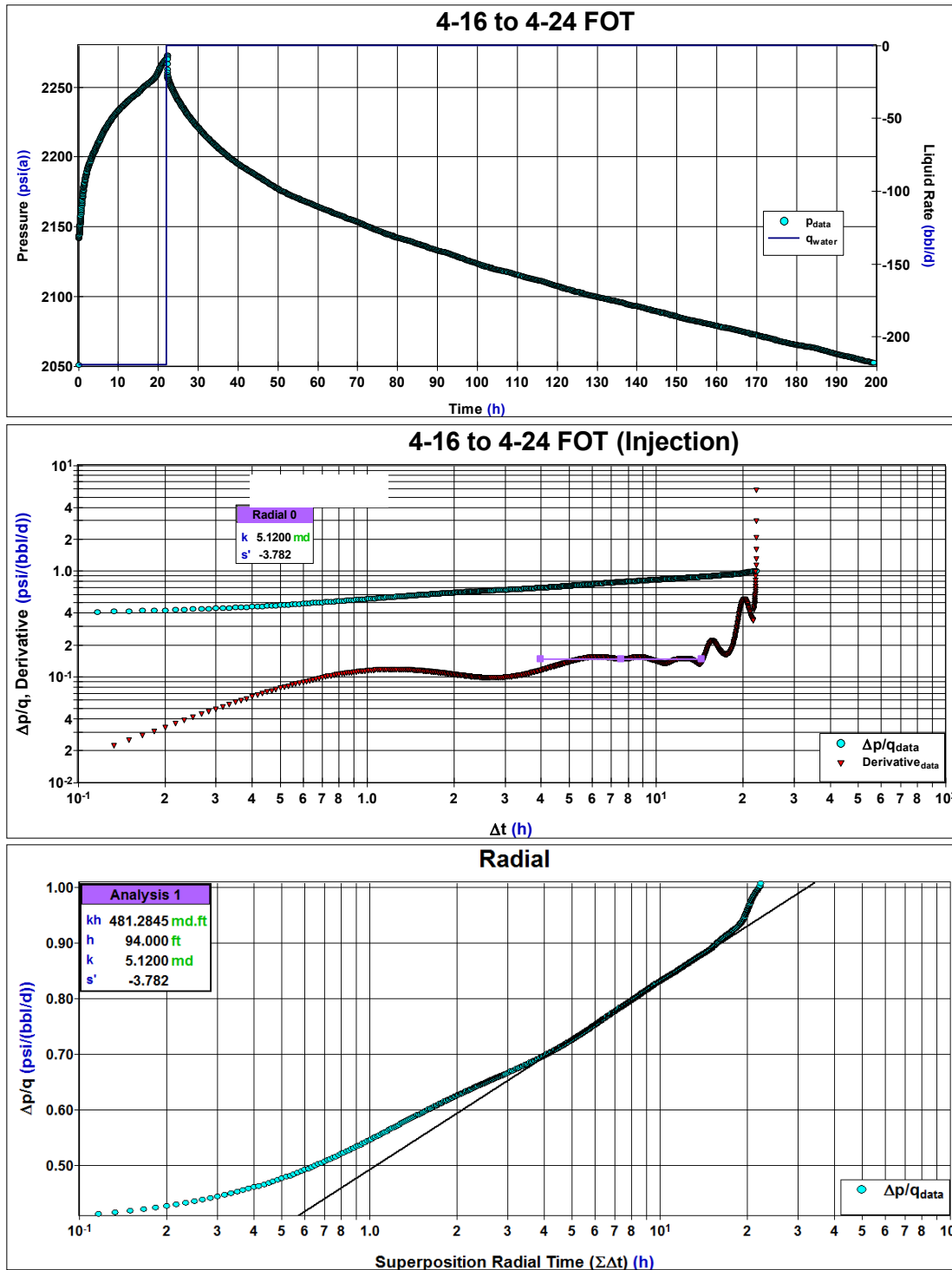
Parameter	Calculated Parameter		
Injection Fall-Off Event	4-16-14 to 4-24-14	4-24-14 to 4-28-14	4-28-14 to 5-6-14
Injection rate, q	219 STB/day	866 STB/day	274 STB/day
Thickness, h	94 ft	94 ft	94 ft
Viscosity, μ	1 cP	1 cP	1 cP
Formation Volume Factor, B	1 RB/STB	1 RB/STB	1 RB/STB
Porosity, ϕ	0.07	0.07	0.07
Compressibility, C_t	8.64e-06 1/psi	8.64e-06 1/psi	8.64e-06 1/psi
Well radius, r_w	0.3 ft	0.3 ft	0.3 ft
Permeability, k	5.1 mD	30	5.7
Skin, s	-3.8	-5	-4.3

STB = stock-tank barrel

Table 2-15. Average injection rate for the three injection events analyzed.

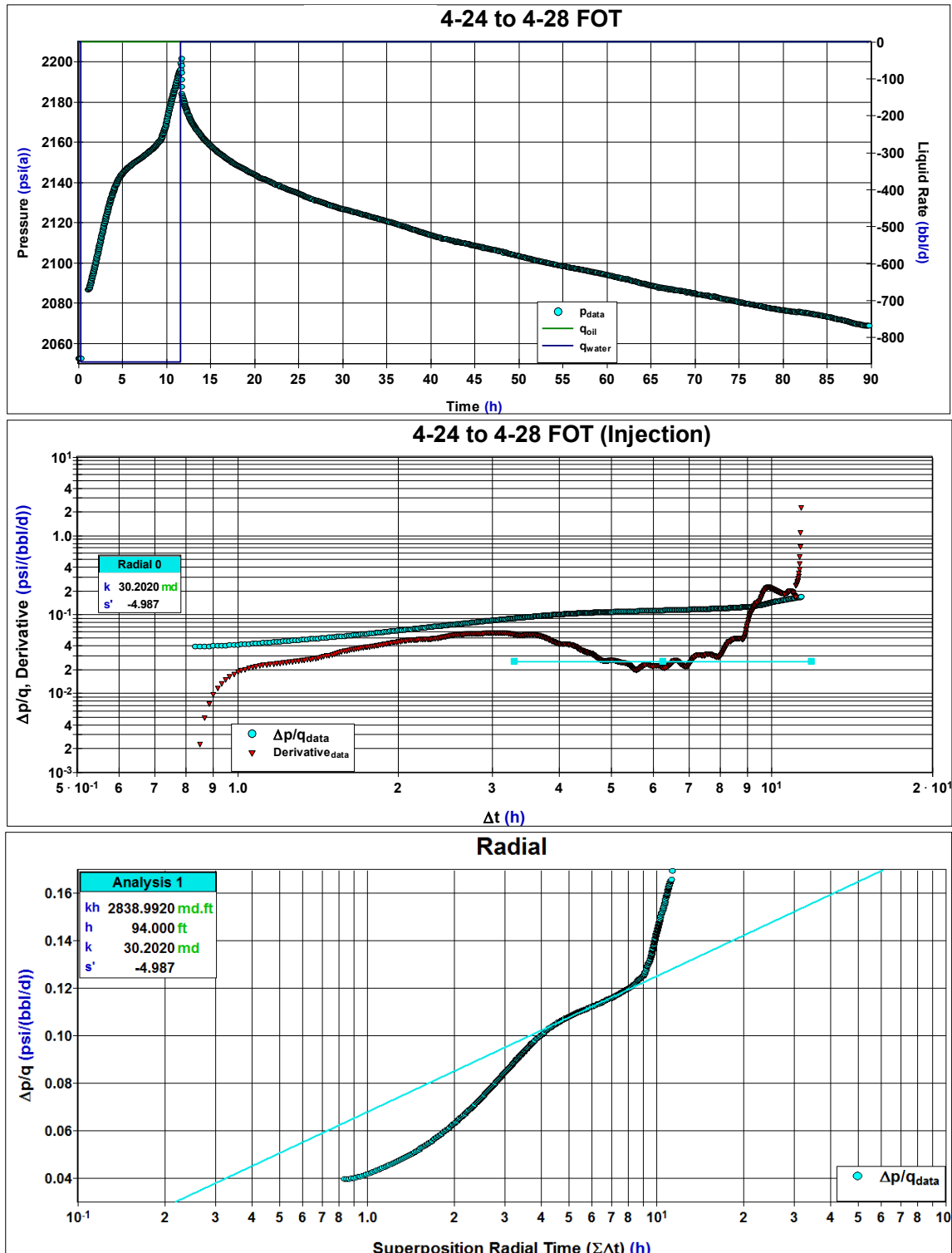
Start Injection	Stop Injection	Duration (hrs)	Avg Rate (bbl/day)	Avg Rate (gpm)	Fall-Off Duration (hrs)
4/16/2014 11:37	4/17/2014 9:44	22.1	219.20	6.4	177.1
4/24/2014 18:51	4/25/2014 6:11	11.3	866.12	25.3	78.15
4/28/2014 12:21	4/29/2014 7:14	18.9	274.53	8.0	172.3

The calculated permeability for two of the three tests analyzed was approximately 5 mD, while the calculated permeability for the third test was 30 mD (Table 2-14). The calculated average injection rate for this test is suspect because it is significantly higher (866 bbl/day) than the other two tests (219 to 274 bbl/day), yet the pressure response is similar. Calculated well skin was equal to approximately -5 for all three tests. A negative skin suggests that a zone exists immediately surrounding the well that has enhanced permeability relative to the reservoir. This could be due to well acid treatments or stimulation during well completion, which is normal for injection wells in the region.



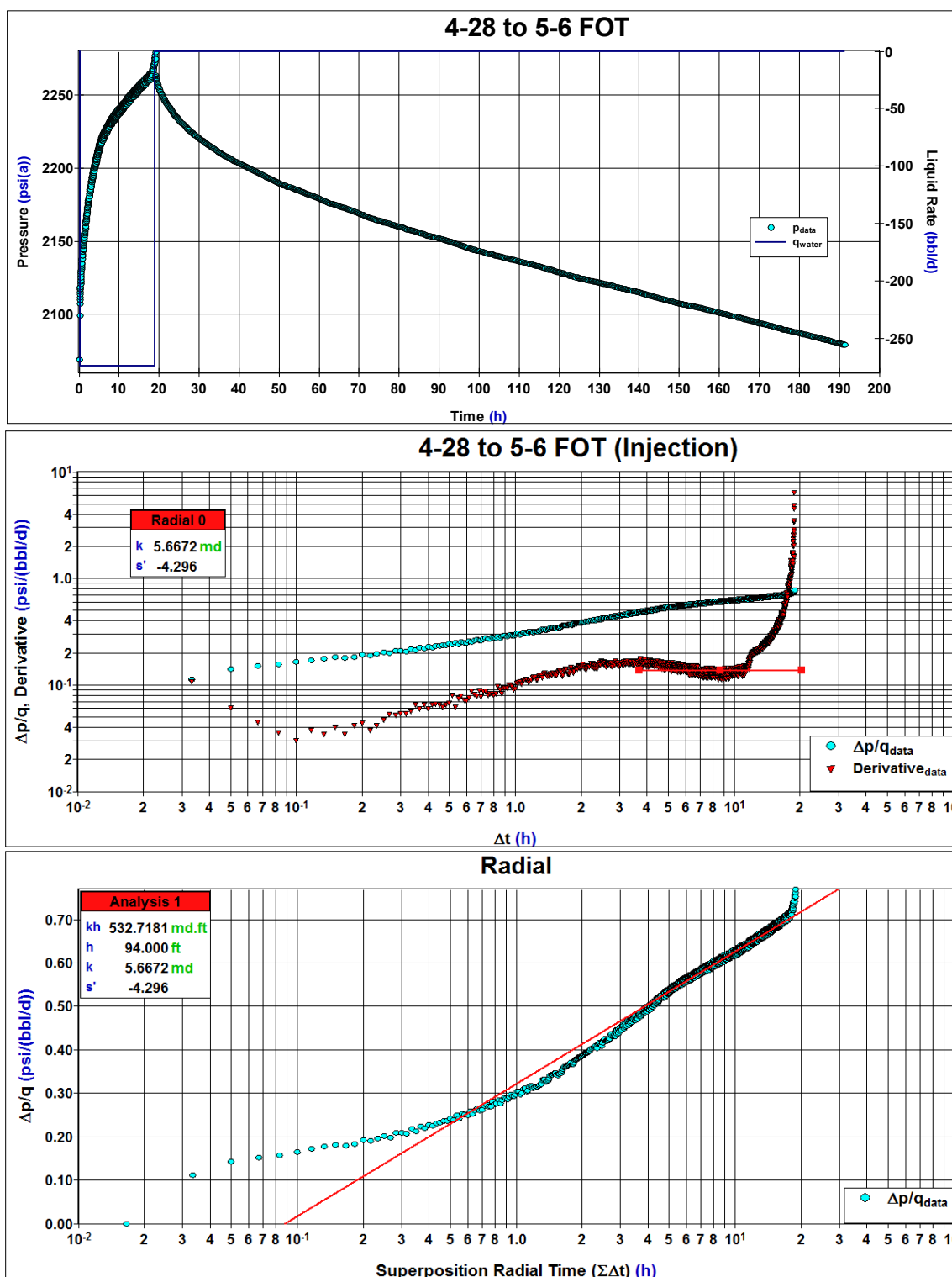
Note: Pressure data (top); injection data log-log plot (center); injection data straight-line plot (bottom).

Figure 2-21. Analysis plots for the 4-16-14 to 4-24-14 injection fall-off event.



Note: Pressure data (top); injection data log-log plot (center); injection data straight-line plot (bottom).

Figure 2-22. Analysis plots for the 4-24-14 to 4-28-14 injection fall-off event.

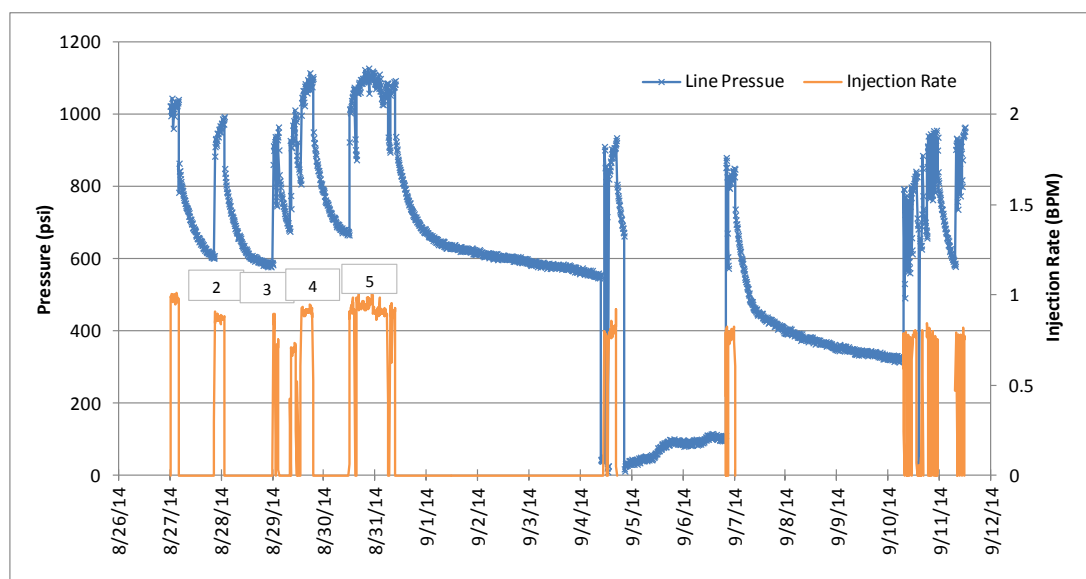


Note: Pressure data (top); injection data log-log plot (center); injection data straight-line plot (bottom).

Figure 2-23. Analysis plots for the 4-28-14 to 5-6-14 injection fall-off event.

2.6.2.3 Central Appalachian Basin Knox-Rose Run

Operational data from a central Appalachian Basin injection well were analyzed for formation permeability in the Knox-Rose Run injection zone. Surface injection pressure and injection rate data were recorded at 10-minute frequency during normal fluid injection operations during the period August 27 through September 11, 2014. During this time, 10 injection cycles were recorded, as shown in Figure 2-24. Surface injection pressure was measured in the injection line just upstream of the wellhead and upstream of a check valve in the injection line. If operating normally, the check valve would close when injection stopped, thus isolating the pressure logger from the well so that recorded pressures reflected the line pressure rather than wellhead pressure. However, except for one injection cycle on September 4, the valve remained in the open position after injection stopped, and recorded pressures during non-injection periods reflected wellhead (tubing) pressures for all but one injection cycle. As a result, the pressure data could be analyzed to estimate reservoir properties. Due to the problem with the check valve, only the data recorded before September 4 were analyzed.



Note: Data from Injection cycles 2 through 5 were analyzed.

Figure 2-24. Injection rate and wellhead pressure for 10 injection cycles recorded Aug. 27 through Sept. 11, 2014.

The well had 4½-inch production casing with a 124-foot open-hole section to approximately a 5,000-foot depth. The open borehole was drilled with a 7-7/8-inch bit. Injection was through 2-7/8-inch tubing with a packer set at a depth of approximately 4,800 feet. There are no well logs for the well; however, according to the well completion report, the open borehole extends across a portion of the Gull River Formation into the upper Knox Group-Rose Run formation.

The injection fall-off test was analyzed using the commercial well test analysis software program, FAST WellTest™. The analysis included PTA of the four-day fall-off period following injection cycle #5, and history-matching the pressure record for injection cycles #2 through #5 (injection cycle #1 was not included in the history match due to incomplete pressure data for this cycle).

The PTA of the final fall-off period for injection cycle #5 is shown in Figure 2-25. The PTA included: 1) a Cartesian plot showing the injection pressure and injection rate history for the portion of the test that was analyzed; 2) a log-log diagnostic plot of the fall-off pressure data and fall-off pressure derivative vs. time data; and 3) a straight-line semi-log plot of the fall-off pressure data vs. log time data. The log-log plot suggests that radial flow conditions were achieved, as indicated by the horizontal portion of the pressure derivative.

Input parameters used in the radial flow analysis are listed in Table 2-16. Radial flow analysis was performed to obtain an initial estimate of the permeability-thickness product, kh , and well skin, s_d (Table 2-17), as well as for use in the subsequent history-matching analysis.

Table 2-16. Reservoir and well properties for the PTA analysis.

Property	Units	Value	Comment
Transmissivity (Permeability x Thickness/Viscosity), kh/μ	mD-ft/cP	718	
Permeability-Thickness Product, kh	mD-ft	398	For $\mu=0.55$ cP
Thickness, h	ft	124	
Permeability, k	mD	3.2	For $h=124$ ft.
Well Skin, s_d	dimensionless	-4.7	
Wellbore Storage Coefficient, C_D	dimensionless	48	
Porosity, ϕ	%	5%	
Viscosity, μ	cP	0.55	
Well Radius, r_w	ft	0.328	
Compressibility of Water, C_w	psi ⁻¹	2.92e-06 psi ⁻¹	
Compressibility of the Rock, C_r	psi ⁻¹	6.48e-06 psi ⁻¹	

Table 2-17. Estimates of reservoir and well properties from the radial analysis of the fall-off period for injection cycle #5.

Parameter	Units	Value	Comment
Transmissivity (Permeability x Thickness/Viscosity), kh/μ	mD-ft/cP	751	
Permeability-Thickness Product, kh	mD-ft	413	For $\mu=0.55$ cP
Permeability, k	mD	3.3	For $h=124$ ft
Well skin, s_d	dimensionless	-6.5	

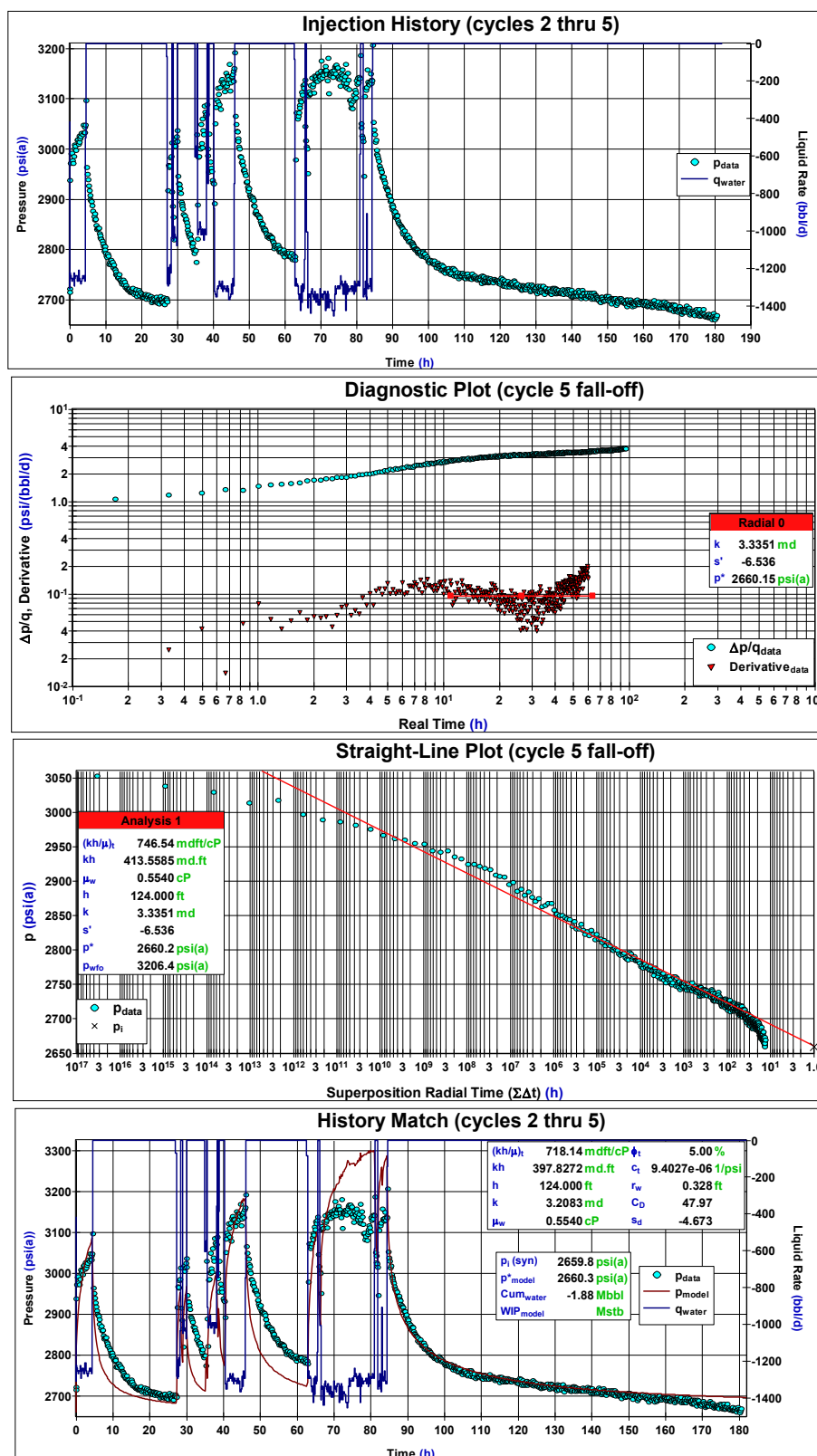


Figure 2-25. PTA diagnostic plots for cycle 5 fall-off period.

In the history-matching process, the injection rate history was simulated with an analytical radial-reservoir, vertical-well model in FAST WellTest™. Selected reservoir and well parameters, namely k , s_d , and dimensionless wellbore storage coefficient (C_D), were adjusted within reasonable limits until the best possible match was obtained between the simulated and measured pressures. The history-matching scenario yielded a $kh=167,360$ mD-ft for a $skin=6$. Other model parameters used in the history-match scenario are summarized in Table 2-16.

This analysis suggests that the hydraulically active portion of the open-borehole in this well has a transmissivity of 718 mD-ft/cP, which equates to a permeability-thickness product of 398 mD-ft for a viscosity of 0.55 cP. It should be noted that the viscosity value was estimated assuming a bottomhole temperature of 120° F (bottomhole temperature data were not available). It is unlikely that the entire 124-foot open-hole section is hydraulically active; however, without logs or flow-meter testing, it is not possible to identify the hydraulically-active interval(s) within the open-hole section. Without knowing the identity and true thickness of the hydraulically active interval(s), one can only conclude that the flow capacity (permeability-thickness product) represents the entire 124-foot section and that the permeability of this section is 3.2 mD. The history match that was achieved is an approximate simulation of the measured pressure data but does not honor it perfectly. In particular, injection cycles 2, 3, and 4 are better matched than injection cycle 5. The measured pressures for the injection period of injection cycle 5 appear suspect because they leveled off rather than continuing to increase with injection, as occurred during the previous injection cycles. Due to the approximate nature of the history match, the derived reservoir and well parameters should be considered estimates only.

3. REGIONAL GEOLOGIC SETTING

3.1 Geologic Structural Framework Setting

The Appalachian Basin is a multiple-stage, retroarc foreland basin that has undergone multiple rifting and orogenic events over its geologic history. The basin extends from Quebec in Canada to northern Alabama (Figure 3-1) and preserves sediments that have accumulated as the result of a series of tectonic events, mainly including:

1. Latest Precambrian to Early Ordovician synrift and postrift, passive margin clastic and carbonate sediments
2. Early Ordovician to Devonian Taconic Orogeny foreland basin marine carbonate, evaporate, and clastic sediments
3. Devonian Acadian Orogeny foreland basin marine clastic sediments
4. Mississippian to Early Permian Alleghanian Orogeny terrestrial and marginal marine clastic sediments

These major orogenic events (Figure 3-2) created the accommodation space which resulted in the preservation of a thick, relatively continuous stratigraphic succession with unconformities separating the major sequences (Figure 3-3). Sections 3.2 and 3.3 review the regional formations, structure, depositional history, and tectonics related to the injection zones that are the focus of this study.

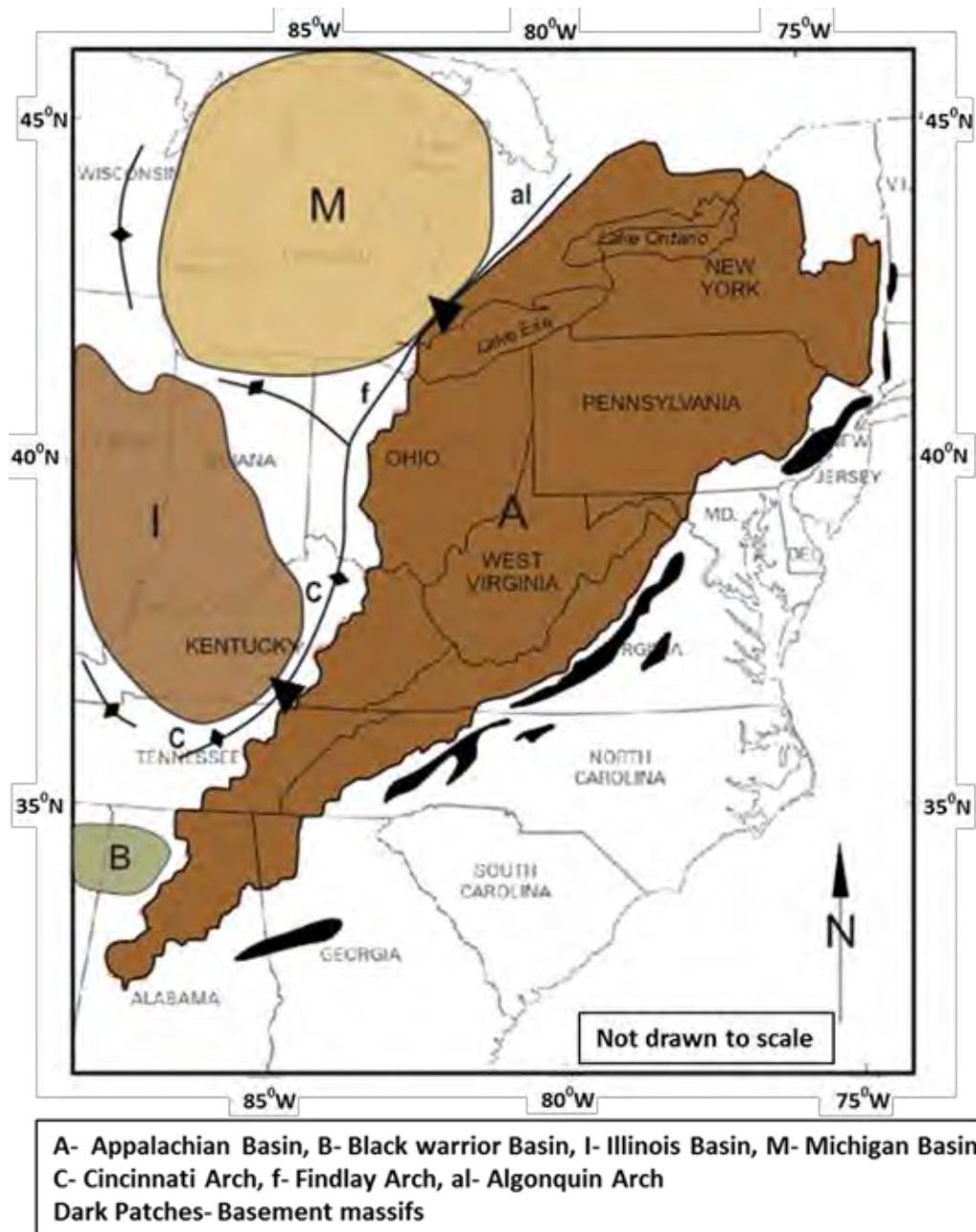
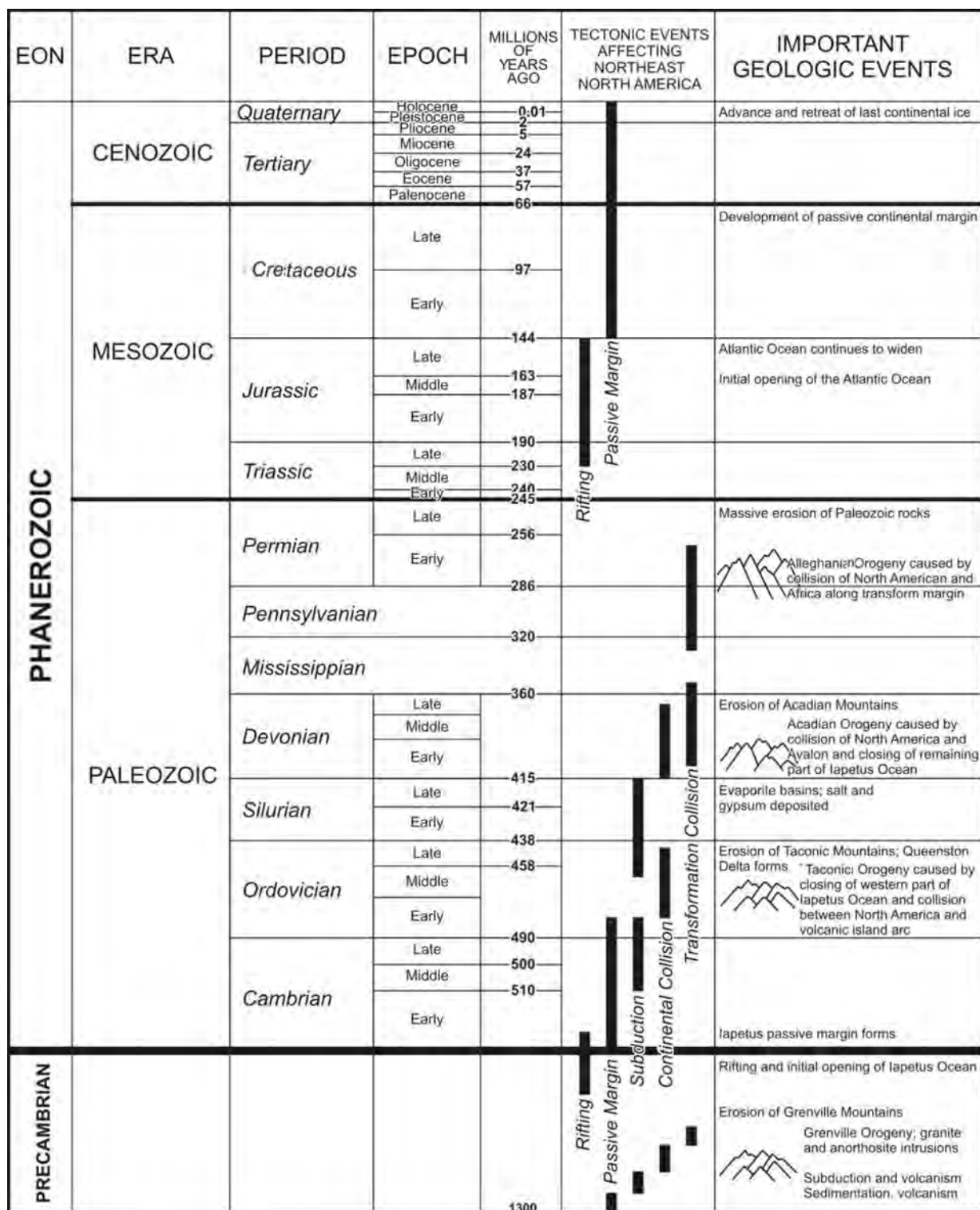
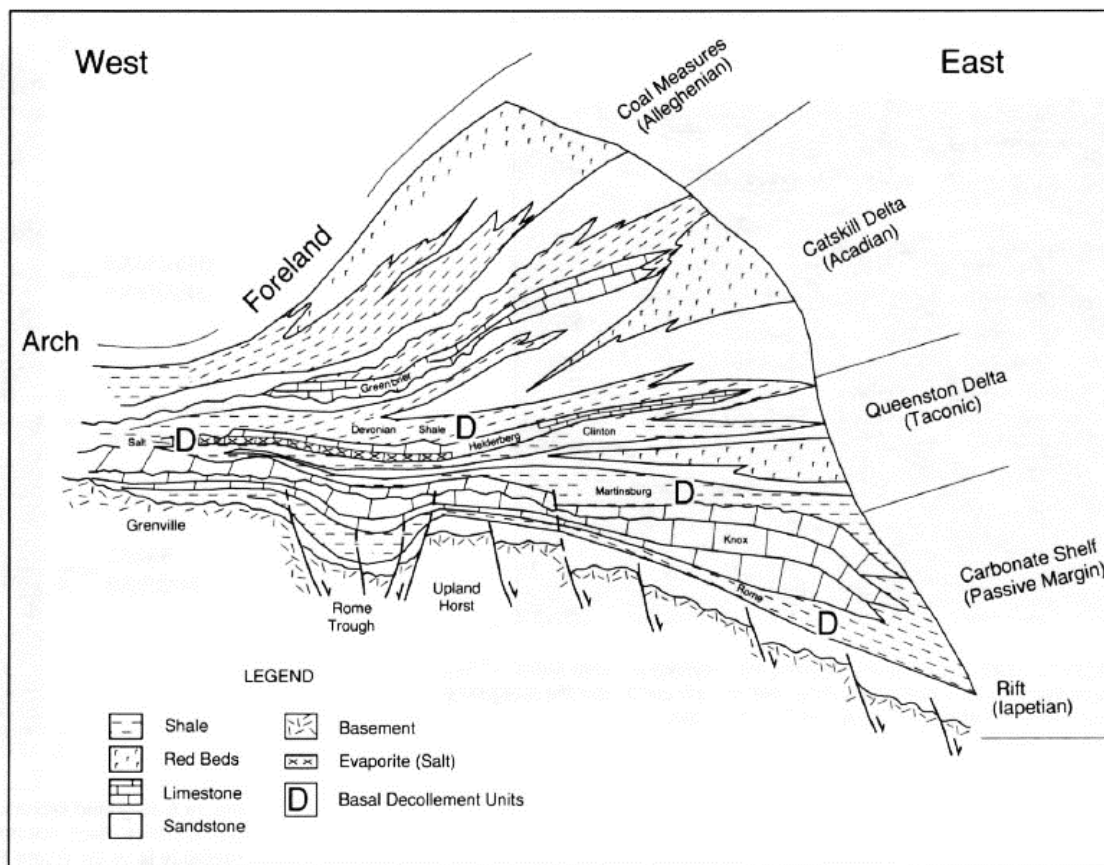


Figure 3-1. Extent of the Appalachian Basin and neighboring basins with overlaid structural features in the eastern United States.



Note: Geologic time is presented on the left. Major tectonic events and their effect on depositional and post-depositional processes are presented on the right. (modified from *Geologic History of New York*)

Figure 3-2. Generalized geologic history of the Appalachian Basin.

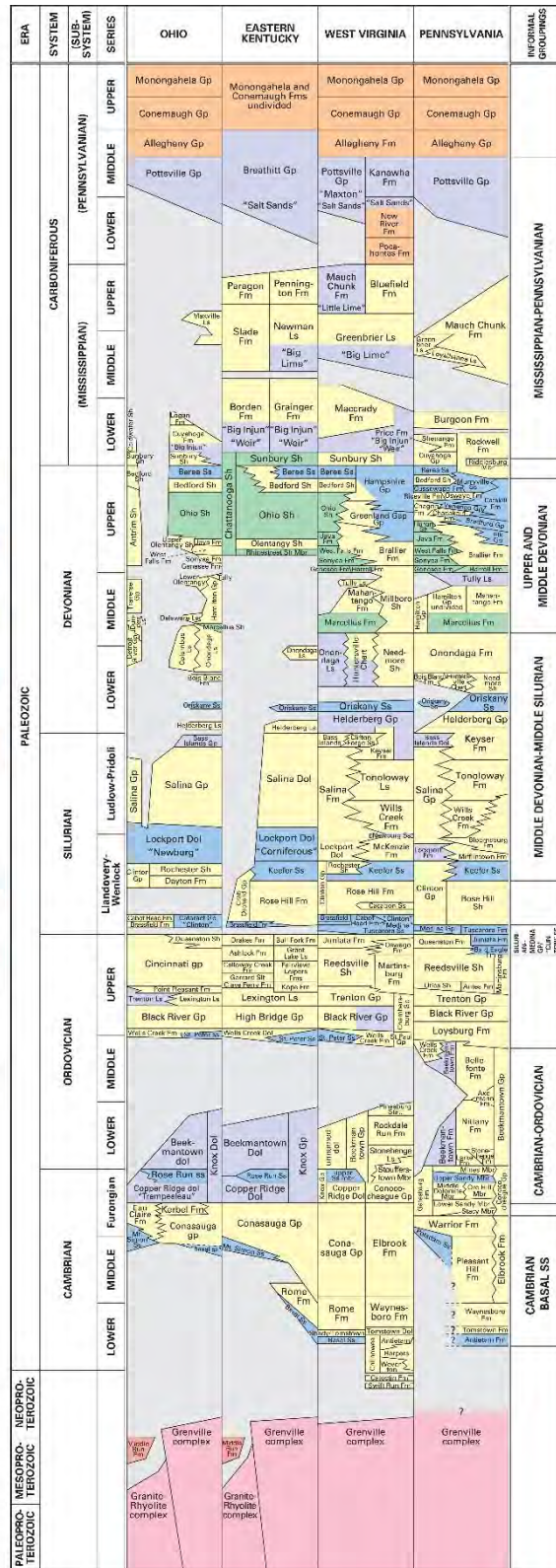


Source: From Roen and Walker, 1996.

Figure 3-3. Schematic northwest to southeast section across the Appalachian Basin.

3.2 Injection Zones/Formation Correlations

This study is focused on the Cambrian-Pennsylvanian interval, which contains the primary injection zones used for subsurface brine disposal in the northern Appalachian Basin. A correlation chart displaying the nomenclature used in the project area of Ohio, eastern Kentucky, West Virginia, and Pennsylvania is shown in Figure 3-4. Primary brine injection zones in the project area, based on the number of injection wells and injected volumes, are the Cambrian Basal Sandstone, the Cambrian Copper Ridge Dolomite and Rose Run Sandstone, the Silurian Medina Group/‘Clinton’ sandstone, the Silurian Lockport Dolomite, the Devonian Oriskany sandstone, and Mississippian sandstone units. These reservoirs comprise a heterogeneous assemblage of carbonates and siliciclastics with complex porosity development and variable geographic distribution and thickness. Key factors that influence reservoir quality and injection potential are effective porosity and pore size distribution, permeability, reservoir heterogeneity, lithology, diagenesis, and the presence and orientation of faults and fractures. Also critical to good injection reservoirs are the thickness and integrity of the overlying seal or confining interval. In this discussion, brine disposal zones within the project area have been grouped into the following six intervals, in ascending stratigraphic order: Cambrian Basal Sandstone, Cambrian-Ordovician, Silurian Medina Group/‘Clinton’ Sandstone, Middle Devonian-Middle Silurian, Upper and Middle Devonian, and Mississippian-Pennsylvanian (Figure 3-4).



Note: Major injection zones highlighted in blue.

Figure 3-4. Regional stratigraphic chart.

3.2.1 Cambrian Basal Sandstone Interval

The Cambrian basal sandstone interval includes some of the most promising targets for brine disposal within the northern Appalachian Basin region. Many of the deep injection wells in Ohio are completed open-hole from the top of the Knox to the base of the Cambrian basal sandstone. Thus it is difficult to determine precisely which zones are actually accepting fluid throughout this large stratigraphic interval.

The stratigraphically complex Cambrian basal sandstones lie unconformably on the Precambrian basement. There are four basic units within this interval (Figure 3-4), each with distinctive stratigraphic and injection reservoir characteristics: (1) the Mount Simon Sandstone of western Kentucky and western Ohio, (2) the unnamed dolomitic sandstones of the Conasauga Group (eastern Ohio, northern Kentucky, western Pennsylvania, and West Virginia), (3) Potsdam Sandstone (northern and north-central Pennsylvania), and (4) stratigraphically older unnamed basal Cambrian (Rome Trough) sandstones in the fault-bounded Rome Trough and eastern proto-Appalachian Basin (eastern Kentucky, West Virginia, and western Pennsylvania). This unnamed basal sandstone of the Rome Trough may be equivalent to the Antietam Formation as named in eastern Pennsylvania. The nature of the transition from the Potsdam Sandstone of northwestern Pennsylvania to the Antietam Sandstone and Rome Trough unnamed sandstones is unclear because of a lack of deep wells in southwestern Pennsylvania and West Virginia (Wickstrom et al., 2005).

Brine disposal is active in the Mount Simon Sandstone in Ohio, which has the largest injection potential of any individual geologic unit within the project area. The name “Mount Simon Sandstone” was first used by Walcott (1914) to designate a sandstone unit exposed near Eau Claire, Wisconsin (the type section). The Potsdam, described by Emmons (1838), was named for sandstone cropping out at Potsdam, New York.

The lithology of the Cambrian basal sandstone interval varies, from the typical Mount Simon Sandstone in western Ohio to the basal shaly and arkosic sandstones of the Rome Trough and the unnamed Conasauga sandstones. The Mount Simon Sandstone is a white, pink, or purple, fine- to coarse-grained, moderately to well-sorted quartz arenite that can be arkosic. The Mount Simon also contains thin interbeds of red, green, gray, or black, sandy to silty shale. Locally, thin beds of tight, silica-cemented quartz arenite occur. Bedding thickness ranges from thin to medium, and many beds contain thin laminae of finer-grained materials. Graded beds and cross bedding are common. Bioturbation is present but generally poorly developed. Grains are sub-rounded to rounded, commonly etched, and generally poorly cemented and friable. The lower portion is commonly conglomeratic and shaly and stained by hematite, some of which is mottled.

Based on core analyses and a 45-year history of relatively higher injectivity rates and volumes, the Mount Simon has overall higher porosity and permeability than the unnamed Conasauga sandstones. Data for the basal sandstones of the Rome Trough are scarce. The Mount Simon of the Indiana-Ohio platform has good to excellent reservoir quality with a gross thickness of 200 to 350 feet (60 to 100 meters), porosity averaging 14%, and permeability ranging from 10 to 200+ mD (Janssens, 1973; Clifford, 1975).

3.2.2 Cambrian-Ordovician Interval

The Knox interval (and equivalent units) is primarily a thick dolomitic succession, which is extensive across the eastern mid-continent region. Across much of Kentucky, Ohio, and West Virginia, the Knox strata are divided into the Cambrian Copper Ridge Dolomite and Ordovician Beekmantown Dolomite (Figure 3-4). In many portions of Ohio, Pennsylvania, Kentucky, and West Virginia, these units are separated by the much thinner Rose Run Sandstone (Upper Sandy Member of the Gatesburg Formation equivalent in Pennsylvania). Porosity development along the widespread, regional Knox unconformity is well documented, as are porous and permeable zones deeper within the Knox (Mussman et al., 1988; Smosna et al., 2005). The progressive westward truncation of Knox units along this regional unconformity created the Knox subcrop trends.

Copper Ridge Dolomite

Active brine disposal wells in the Copper Ridge Dolomite are present in Ohio and Kentucky. The Copper Ridge Dolomite was named by Butts (1940) for outcrops near Thorn Hill, Tennessee. This unit is a thick interval of dolostone with interbeds of sandstone and dark gray, argillaceous limestone in the eastern part of the Appalachian Basin (Ryder et al., 1996, 1997). Dolostones of the Copper Ridge in parts of northern Kentucky and Ohio range from dense to vuggy. Vuggy dolostones may occur throughout an interval of at least 400 feet (120 meters) in this area (Shrake et al., 1990). Farther eastward, in eastern West Virginia and Pennsylvania, the upper carbonate interval is equivalent to the Conococheague Group/Limestone and part of the Gatesburg Formation (Figure 3-4). Stose (1908) named the Conococheague for outcrops in Scotland, Pennsylvania. The Conococheague is a thick carbonate-dominated sequence that is divided into several formations in Pennsylvania (Kauffman, 1999). The Conococheague contains sandy dolostone, which may be argillaceous and contain local layers of dolomitic, quartzose sandstones near the base of the unit; limestones with chert; and thin interbeds of limestone and dolostone (Kauffman, 1999). The Middle Dolomite Member of the Gatesburg Formation beneath the Rose Run-equivalent in Pennsylvania is a dolostone similar to the Copper Ridge, which tends to be sandy toward the base (Ryder, 1991, 1992). The Copper Ridge thickens to more than 5,530 feet (1,690 meters) in the Rough Creek graben in Kentucky (Greb et al., 2009).

Zones of vuggy porosity have been encountered within the Copper Ridge in localized areas across the project area. The Copper Ridge dolomite of Morrow County, Ohio, consists of light-gray to light-brown, microcrystalline to medium-grained dolostone that locally contains well-developed, interconnected, vuggy to pinpoint porosity below or near the top of the Knox unconformity. Porosities range from 4 to 18%, and average 9% in productive oil and gas wells. Ryder (1994) describes paleotopographic relief (remnants) at the top of the Copper Ridge in Morrow County that is characterized by karst towers, karst cones, knob-like hills, and intervening karst plains resembling modern-day mature karst terranes. Karst forming and post-karst processes, including collapse features, diagenesis, mineralization, and fracturing, affected Copper Ridge reservoir development.

CO₂ injection was successfully demonstrated in the lower Copper Ridge at the AEP #1 Mountaineer well in Mason County, West Virginia, further attesting to this unit's disposal capability. Most of the Copper Ridge Dolomite is dominated by low-porosity (<5%) dolomite in the Mountaineer well. However, discrete porosity zones, from 8,176 to 8,284 feet (2,491 to 2,527

meters), have porosities greater than 15% (Greb et al., 2009, 2012). A porous zone with enhanced secondary vuggy porosity, in the same Copper Ridge stratigraphic interval, also is present in the Aristech core in Scioto County, Ohio, approximately 55 miles (88 kilometers) southwest of the Mountaineer well. The extent and origin of this porosity zone require further investigation.

Rose Run Sandstone

Brine disposal in the Rose Run Sandstone is active in Ohio and Kentucky. The Rose Run Sandstone was first described and named by Freeman (1949) from the Judy and Young #1 Rose Run Iron Co. well in Bath County, Kentucky. In that well, the unit consists of about 70 feet (20 meters) of poorly sorted sandstone approximately 300 feet (90 meters) below the Knox unconformity. Butts (1918) named the Upper Sandy Member of the Gatesburg Formation (Rose Run equivalent) from outcrop studies in central Pennsylvania.

The Rose Run interval, as described from subsurface core in Ohio, consists of white to light-gray, fine- to medium-grained, sub- to well-rounded, moderately sorted quartz arenites to subarkoses interbedded with thin lenses of nonporous dolostone (Riley et al., 1993; Baranoski et al., 1996). Glauconite and green shale laminae occur locally. Low-angle cross bedding, ripple marks, and polygonal mud cracks are sedimentary features present in cores. In core and outcrop in Pennsylvania, the Rose Run equivalent, the Upper Sandy Member of the Gatesburg Formation, contains three principal facies: (1) sandstone, (2) mixed sandstone and dolostone, and (3) dolostone (Riley et al., 1993). The sandstone facies consist of light-gray, fine-grained, well-sorted quartz arenites. The principal cement is silica. Cross bedding is present, including herringbone cross-stratification. The mixed sandstone and dolostone facies is dominated by sandstone that consists of fine- to medium-grained, moderately well-sorted quartz arenites. The principal cement is dolomite. The dolostone facies are light gray to olive gray and display nodular bedding and bioturbation.

Four major cementing agents occur in the Rose Run: (1) dolomite, (2) clays, (3) quartz overgrowths, and (4) feldspar overgrowths (Riley et al., 1993). Dolomite is the dominant cementing agent as observed in cores throughout Ohio and Pennsylvania. Five pore textures were observed in the Rose Run: (1) intergranular pores, (2) oversized pores, (3) moldic pores, (4) intraconstituent pores, and (5) fractures (Riley et al., 1993). Intergranular porosity is the most abundant porosity type in the Rose Run and appears to be mostly secondary based on corroded grain boundaries. Oversized pores are caused primarily by dissolution of dolomite and feldspar. Moldic pores occur in the more feldspathic samples and have the highest porosities and permeabilities. Intraconstituent pores occur most commonly in feldspar grains and appear to be more common toward the lower portion of the Rose Run. Fracture porosity is the least common porosity type observed in cores, but it may be locally significant in areas adjacent to major fault systems.

Within and adjacent to the Rose Run subcrop, reservoir quality is controlled by erosional truncation and paleotopography on the Knox unconformity. Reservoir quality within erosional remnants is often very good because of enhanced secondary porosity. Within the subcrop trend, average porosities measured from core and geophysical logs range from 6 to 12%, with values as high as 14% (Riley et al., 1993; Baranoski et al., 1996). Permeabilities vary widely from 0.01 to 198 mD, averaging 4 mD (Baranoski et al., 1996). Thickness of the Rose Run varies depending

on the size of the remnant. Wells with a complete section of Rose Run in the subcrop trend have a gross thickness of approximately 110 feet (30 meters) and a net thickness of about 50 feet (15 meters) of highly porous, permeable sandstone.

High porosities and permeabilities are not restricted to wells within the subcrop trend. Cores in Jackson and Scioto Counties, Ohio, approximately 40 to 50 miles (60 to 80 kilometers) down dip from the subcrop, indicate average porosities ranging from 6 to 12% and permeabilities often greater than 1.0 mD, with some values exceeding 100 mD. These porosities and permeabilities indicate good reservoir quality away from the highly drilled and explored subcrop trend.

Although the gross interval of the Rose Run thickens to the east, the sandstone-to-carbonate ratio decreases to the east and southeast, suggesting a clastic source to the north and northwest (Riley et al., 1993). Thus net sandstone generally decreases to the east and southeast. The AEP #1 well drilled in New Haven, West Virginia, encountered only 18 net feet (5 meters) of sandstone greater than 6% porosity within the Rose Run.

St. Peter Sandstone

Active brine disposal in the St. Peter Sandstone is present in Kentucky. The injection is often across extensive stratigraphic intervals spanning the St. Peter to the Copper Ridge. The St. Peter was named by Owen (1847) for sandstone outcrops along the St. Peter River (now Minnesota River) near Minneapolis/St. Paul, Minnesota. Within the project area, the St. Peter is recognized in Kentucky and West Virginia. A sandstone unit on the Knox unconformity also is present in localized areas in Ohio, but the stratigraphic relationship to the St. Peter is uncertain.

In general, the St. Peter Sandstone is a clean, relatively pure quartz arenite and yields a very low gamma ray value on geophysical logs (Wickstrom et al., 2005). Throughout Ohio, the Knox unconformity sandstone, where present, is a relatively clean, well-rounded, fine- to coarse-grained, friable quartz arenite. Drillers in Ohio encounter flows of brine from this thin, yet highly porous and permeable unit that typically washes out during drilling. Known cements include quartz overgrowths and dolomite in some areas. Authigenic clays also are present in matrix. In most areas, the St. Peter Sandstone is medium-grained, although small amounts of coarse- and fine-grained textures are present throughout the section. Cross bedding, bioturbation, and rare shell fossils have been observed in outcrop and core material. Porosity is usually good in outcrop and the shallow subsurface; however, burial compaction and cementation significantly reduce porosity in the deeper subsurface (Wickstrom et al., 2005).

The St. Peter Sandstone overlies an extensive erosional unconformity on top of dolostones of the Knox. This erosional surface can have significant topographic relief, especially across the major structural arches and reactivated faults in the region. The thickness of the St. Peter can vary significantly around such features. The St. Peter Sandstone is thinnest (10 to 100 feet [3 to 30 meters]) and shallowest (depths less than 2,500 feet [760 meters]) across the arches of Indiana and Ohio (Wickstrom et al., 2005).

3.2.3 Lower Silurian Medina Group/‘Clinton’ Sandstone Interval

Brine disposal in the Medina Group/‘Clinton’ sandstone interval is active in Ohio, West Virginia, and Pennsylvania. The stratigraphic nomenclature of this unit is somewhat complex, due to the influence of both facies changes across the Appalachian Basin and drillers’

terminology. Specifically, this sequence is known as the Medina Group in northwestern Pennsylvania, the Tuscarora in eastern Pennsylvania and West Virginia, the Cataract Group in eastern Ohio, and erroneously as the ‘Clinton’ and ‘Medina’ sandstone by drillers in eastern Ohio (Figure 3-4). Reference to the productive zones in this sequence as ‘Clinton’ originated in Fairfield County, Ohio, where drillers erroneously thought that limestone in the overlying Clinton Group was the source of gas in the Medina discovery well (McCormac et al., 1996). By the time it was established that the Medina Group sandstones were actually the producing units in these early wells, the ‘Clinton’ misnomer had become ingrained in basin operator terminology and is still in use today. The Medina Group was named by Vanuxem (1840) for its type locality in Medina, Orleans County, New York. The Tuscarora was named by Clark (1897) for exposures at Tuscarora Mountain in central-southern Pennsylvania.

The Medina Group/‘Clinton’ sandstone consists of interbedded sandstones, siltstones, and shales, with some carbonates (Laughrey, 1984; Laughrey and Harper, 1986; McCormac et al., 1996). The sandstones of the Grimsby Formation (part of the Medina Group in Pennsylvania) are very fine- to medium-grained quartzose rocks with subangular to subrounded grains, variable sorting, and thin, discontinuous, silty shale interbeds. These sandstones vary in color, from white to gray to red; hence, the reference to these units by drillers as ‘Red Clinton’ and ‘White Clinton,’ particularly in eastern Ohio. Cementing materials include secondary silica, evaporites, hematite, and carbonates (Piotrowski, 1981; McCormac et al., 1996). Gross thicknesses range from zero feet in the northwestern portion of the basin to more than 700 feet (210 meters) in eastern West Virginia. Pay zones in productive oil and gas wells range from 3 to 50 feet (1 to 15 meters) and average 23 feet (7 meters) in thickness (McCormac et al., 1996).

Porosity and permeability of the Medina Group varies due to depositional and diagenetic processes. Porosities range from 2 to 23% across the basin and average 7.8% (McCormac et al., 1996). Permeabilities are widely variable, ranging from less than 0.1 mD to 40 mD (McCormac et al., 1996). Typically, in eastern Ohio the Medina Group is a “tight” reservoir and requires conventional hydraulic fracturing for oil and gas production. However, the demonstrated use of this interval for gas storage in Ohio and Pennsylvania and widespread brine disposal in eastern Ohio indicates the potential of this interval for future brine disposal.

3.2.4 Middle Devonian-Middle Silurian Interval

The Middle Devonian-Middle Silurian (MDMS) interval (Figure 3-4) is a complex assemblage of Devonian and Silurian carbonates, clastics, and evaporites that are primarily an overall confining interval. Locally, however, this interval contains reservoirs that serve as important brine injection zones throughout the project area. The MDMS interval includes the following potential injection zones, in ascending stratigraphic order: the Keefer Sandstone, the Lockport Dolomite, the Bass Islands Dolomite, the Oriskany Sandstone, and the Huntersville Chert (Figure 3-4).

Keefer Sandstone

The Keefer Sandstone (“Big Six” of drillers) is used as a brine injection zone in Kentucky. The Keefer Sandstone was named by Ulrich (1911), who defined it as the basal member of the McKenzie Formation (Horvath, 1970). The type section is at Keefer Mountain near Hancock, Maryland (Horvath, 1970). The Keefer Sandstone is a poorly to very well-sorted, very fine- to

medium-grained sandstone and dolomitic sandstone with subangular to rounded grains. Conglomerate beds composed of quartz and occasional chert have been documented locally. This unit generally varies in color from light tan to pale brown but in some places may be greenish-tan. Quartz, calcite, dolomite, and ankerite serve as cementing agents (Noger et al., 1996). Drilling depths to the top of known Keefer Sandstone reservoirs range from 1,882 to 3,865 feet (574 to 1,179 meters) (Noger et al., 1996). Porous pay zones in the Keefer, with reservoir porosities greater than 4%, range from 3 to 63 feet (1 to 19 meters), averaging 14 feet (4 meters) (Noger et al., 1996).

Smosna (1983) documented the diagenetic history of the Keefer Sandstone in the subsurface of West Virginia and Kentucky. During early diagenesis, secondary quartz formed as syntaxial overgrowths on detrital grains. An initial stage of overgrowth development appears to be as meniscus cement around tangential grain contacts. As burial increased, a second generation of cement precipitated. In Roane County, West Virginia, this was anhydrite and gypsum precipitating from saturated brines. Formation waters were slightly less saline in Wayne County, where poikilotopic calcite cement developed (poikilotopic calcite cement refers to cement composed of calcite crystals of varied sizes that envelop or enclose other mineral crystals). Dolomitization was the last major diagenetic event. Dolomite mostly replaced earlier cements, but often it extended beyond these and replaced quartz grains (corrosion along margins), fossils, and clay minerals. Final porosity in the sandstones is low, ranging from 1% to 6%. Most primary pore space has been occluded by the two generations of cement and dolomite. Minor secondary porosity is due to the partial dissolution of calcite grains and cement. Secondary porosities between 9% and 14% are reported for some fields (Noger et al., 1996).

Lockport Dolomite

The Lockport Dolomite (“Newburg” of drillers in Ohio and West Virginia and “Corniferous” of drillers in Kentucky) is used as a brine injection zone in Ohio, Kentucky, and West Virginia. It is one of the primary brine injection zones in northeastern Ohio. Hall (1839) named the Lockport for exposures at Lockport, New York, but the best reference section is at the Niagara Stone Quarry at Niagara, New York (Brett et al., 1995). The Lockport Dolomite is widespread in the subsurface in the Appalachian Basin and outcrops in northwest Ohio.

Lithologically, this unit is a fine to coarsely crystalline, fossiliferous, slightly argillaceous dolostone throughout most of the Appalachian Basin. Portions of the Lockport are quartzose and even contain sandstone in northwestern Pennsylvania (Zenger, 1965; Rhinehart, 1979). Reported porosities for the Lockport Dolomite in the Appalachian Basin vary from 2 to 24%, with averages of 4 to 14% (Meglan and Noger, 1996; Noger et al., 1996). Porosities for core samples from the Midwest Regional Carbon Sequestration Partnership (MRCSP) work (Carter et al., 2010) vary from 1.5% to 9.0%, with respective permeabilities of 0.0004 to 920 mD to air (Klinkenberg permeabilities of 0.0001 to 0.920 mD, respectively). The latter value is a horizontal fracture permeability measured in core from the Johnson #1 well in the Kilgore pool, Mercer County, Pennsylvania. Vertical permeability in the same sample is 0.88 mD. Porous and permeable intervals in the Lockport Dolomite are largely restricted to thicker (greater than 15 feet [5 meters]) zones in the biohermal and biostromal lithofacies and to thinner skeletal shoals in Kentucky. The average pay thickness in eastern Kentucky is 12 feet (4 meters) (Meglan and Noger, 1996).

Bass Islands Dolomite

Brine disposal wells are drilled into the Bass Islands Dolomite in localized areas of eastern Ohio. The Bass Islands Dolomite was named for exposures on a group of islands in western Lake Erie (Lane et al., 1909). In the project area, the Bass Islands Dolomite and equivalent units underlie portions of Kentucky, West Virginia, Ohio, and Pennsylvania (see Figure 3-4).

Bass Islands lithologies vary laterally throughout the Appalachian Basin, from intervals dominated by dolostone lithologies in the east to primarily limestone lithologies in the west. In Pennsylvania, the Bass Islands is a carbonate unit that includes limestone, dolomitic limestone, and dolostone. Thin sections collected from the T. Goodwill #1 core from the Summit Storage pool, Erie County, Pennsylvania, illustrate that the Bass Islands Dolomite consists of cemented peloidal and intraclastic grainstones. Other Bass Islands lithologies in this well include fine to medium crystalline dolostone and dolomitic packed biopelmicrite. Lithodensity logs indicate that the rocks are often siliceous. Thin section analysis reveals that chert and quartz replace planar dolomite (Laughrey et al., 2007). Gross thicknesses range from less than 25 feet (8 meters) in western New York, western Ohio, and southwestern West Virginia to almost 100 feet (30 meters) in central New York, north-central Pennsylvania, and the West Virginia panhandle.

Although not as regionally persistent as other potential injection zones in the Appalachian Basin, the Bass Islands Dolomite possesses certain reservoir characteristics that make it an attractive injection target in parts of eastern Ohio and northwestern Pennsylvania. The porosity and permeability values reported for this unit, ranging from 2 to 15% and 10 to 230 mD, respectively, suggest that it could provide significant brine injection capacity; in some areas on its own, in others as part of a stacked reservoir scenario. Reservoir data suggest that, within fractured areas, the Bass Islands Dolomite has injectivity characteristics that could be favorable for brine injection. Even so, as production within the Bass Islands trend is defined by certain structural features that extend north and west from Erie County, Pennsylvania, to western New York, detailed studies regarding the integrity of lateral and vertical seals should be conducted prior to considering this unit for injection.

Oriskany Sandstone

The Oriskany Sandstone is used for brine disposal in Ohio, Pennsylvania, and West Virginia and was named for its type locality at Oriskany Falls, Oneida County, New York (Vanuxem, 1842). At this location, the Oriskany is a white, fossiliferous, clean, quartz-rich sandstone (Opritz, 1996; Patchen and Harper, 1996). The Lower Devonian Oriskany Sandstone of drillers' terminology actually encompasses several discrete and formal stratigraphic units within the Appalachian Basin (Heyman, 1977; Harper and Patchen, 1996), including (1) the type Oriskany Sandstone of New York, which also occurs in northwestern Pennsylvania and eastern Ohio; (2) the Ridgeley Sandstone of Pennsylvania, Maryland, Virginia, and West Virginia (where it is called Oriskany); (3) the Springvale Sandstone, a basal sandstone member or sandy aspect of the Bois Blanc Formation in Ontario, northeastern Ohio, and northwestern Pennsylvania (Oliver, 1967; Heyman, 1977); and (4) the Palmerton Formation, a sandstone in eastern Pennsylvania that is equivalent to a portion of the basal Onondaga Limestone (Sevon, 1968).

The Oriskany Sandstone is typically a pure, white, medium- to coarse-grained, monocrystalline quartz sandstone containing well-sorted, well-rounded, and tightly cemented grains (Diecchio,

1985; Harper and Patchen, 1996); it may be conglomeratic in places. Quartz and calcite are the most common cementing materials in the formation. In many areas of the basin, the formation contains such an abundance of calcite, both as framework grains and cement, that the rock is classified as a calcareous sandstone or sandy limestone.

In addition to the primary composition of quartz and calcite grains, minor proportions of pyrite, dolomite, rutile, zircon, and other minerals have also been observed (Harper and Patchen, 1996). Minerals that formed in place after the Oriskany was deposited include several clay minerals, sphalerite, and pyrite (Martens, 1939; Basan et al., 1980). Minor cements include pyrite, dolomite, ankerite, “glauconite,” and chalcedony (Basan et al., 1980).

The Oriskany Sandstone typically has low porosity and permeability. These low values make the identification of areas of good reservoir quality a necessity in considering brine injection in this unit. Calculated porosity values range from 0.5 to 14%, and measured porosities from five core analyses range from 0.02% to 8.8%. Measured permeabilities range from 0.0012 to 185 mD (Carter et al., 2010). Reduced intergranular, secondary dissolution, and to a lesser extent, fracture porosity are observed in these sandstones. Primary intergranular porosity is largely reduced by mechanical and chemical compaction and by extensive carbonate and silica cementation. Secondary porosity is associated with dissolution of carbonate grains and cement and other rock constituents and is the most common type observed. Where they occur, fractures increase porosity and permeability, but in many cases these fractures have been healed by mineralization so that data from individual wells are not useful in making basin-wide (or play-wide) characterizations.

Huntersville Chert

The Huntersville Chert along with the Oriskany Sandstone has been used as an injection zone in Pennsylvania. It was named by Price (1929) for exposures of highly silicified black chert in the vicinity of Huntersville, Pocahontas County, West Virginia. It is an important gas-producing unit in West Virginia and Pennsylvania (Flaherty, 1996). The Huntersville grades laterally to the west with the Bois Blanc in Pennsylvania and to the east with the Needmore Shale in central Pennsylvania and eastern West Virginia (see Figure 3-4).

The Huntersville Chert is characterized as typically massive, microcrystalline, and hard. It varies from translucent to opaque and from white to dark brown to dark gray in color. Often, it contains minor amounts of dolomite, quartz, glauconite, pyrite, calcite, and trace fossils. The sandy facies contains well-rounded quartz grains where the Huntersville lies directly on the Oriskany Sandstone. Like the Bois Blanc, the basal Huntersville comprises thin argillaceous sandstone beds, phosphatic nodules, and glauconite, indicating the presence of an erosional surface on the top of the Oriskany. Thickness of the Huntersville Chert varies from less than 100 feet (30 meters) in Elk and Forest Counties in northwest Pennsylvania to more than 250 feet (80 meters) in southwestern Pennsylvania and northern West Virginia. The best effective porosity is provided by fractures in the brittle chert (Flaherty, 1996).

3.2.5 Upper and Middle Devonian Interval

Brine disposal is active in clastics of the Upper Devonian Elk Group/Brallier Formation (Benson) in West Virginia; the Upper Devonian Bradford Group (Balltown and Speechley) in

Pennsylvania and West Virginia, the Upper Devonian Venango Group/Greenland Gap Formations (Thirty-Foot, Gordon, and Fifth) in West Virginia and Pennsylvania, and the Upper Devonian Berea Sandstone in Ohio and West Virginia and in organic-rich black shales of the Middle Devonian Marcellus Shale in Ohio and West Virginia, the Upper Devonian Genesee Formation in West Virginia, and the Upper Devonian Ohio Shale and Rhinestreet Shale in Ohio and West Virginia (see Figure 3-4). For a detailed discussion of stratigraphy and nomenclature of the Upper and Middle Devonian units, see Tomastik (1996), Boswell et al. (1996a, 1996b), and Donaldson et al. (1996).

Upper Devonian Clastics

The Elk Group/Brallier (Benson) sandstones and siltstones represent the lower portion of the Acadian clastic wedge of the Catskill delta. A regional net sandstone isopach map of the Benson shows the thicker sandstones are restricted to the eastern margin of this oil and gas play (Donaldson et al., 1996). In the subsurface, the Benson consists of fine-grained sandstone and siltstone beds that occur mainly west of the 70-foot-thick contour of the Benson isopach map. A typical Benson reservoir in northern West Virginia is a coarse, silt-size rock containing greater than 18% matrix (mostly illite), 5 to 10% porosity, and permeabilities of 0.1 to 2.0 mD (Donaldson et al., 1996). Primary porosity is intergranular.

The Bradford reservoirs, the middle clastic progradational episode of the Catskill delta, are typically siltstones and thick-bedded, fine-grained sandstones (Boswell et al., 1996b). Bradford reservoirs in northern West Virginia are typically siltstones and thin-bedded, fine-grained sandstones. Sandstone units may be narrow in geographic size. A single mapped Balltown channel sandstone in Harrison County, West Virginia, is less than 1,000 feet (300 meters) wide and less than 5 feet (1.5 meters) thick (Boswell et al., 1996b). Balltown reservoirs in West Virginia have low porosities and permeabilities and are typically hydraulically fractured. Petrographic analyses of a Balltown reservoir in Taylor County, West Virginia, had a porosity of 10% with permeabilities ranging from 0.2 to 0.3 mD (Boswell et al., 1996b). The role of natural fractures for enhancing porosity and permeability is uncertain.

The Venango is the shallowest and most sandstone-rich of the three clastic progradational episodes of the Catskill delta complex (Boswell et al., 1996a). Total thickness of sandstone reservoirs in the Venango Group varies from zero feet to more than 200 feet (60 meters). Thickness decreases rapidly westward and more slowly eastward away from the main sandstone belt in western West Virginia and western Pennsylvania (Boswell et al., 1996a). Individual sandstone beds in excess of 50 feet (15 meters) are rare, with 15 to 20 feet (5 to 6 meters) being common. Within this main sandstone belt, porosities range as high as 18 to 25%. Permeabilities are also high and range from 10 to 500 mD with values that exceed 1,000 mD (Harper and Laughrey, 1987). However, away from this main sandstone trend, porosity and permeability diminish and are rarely above 6% and 0.1 mD, respectively.

The Berea Sandstone is a fine- to medium-grained, clay-bonded quartz sandstone with a thickness ranging from a few feet to greater than 235 feet (72 meters) in the Appalachian Basin (Pepper et al., 1954). Porosities from cores and logs range from 2% to 26% and average 12%. Permeability from cores ranges from 0.01 to 480 mD and average 3.84 mD (Tomastik, 1996). Cementation, compaction, and feldspar dissolution are diagenetic processes that have influenced porosity and permeability (Larese, 1974). The dominant pore type is intergranular. Secondary

porosity from dissolution of potassium feldspar and replacement of framework minerals also is present. Dominant cementing agents are dolomite, quartz, and siderite. Kaolinite, illite, and chlorite are the most abundant clays present.

Middle-Upper Devonian Black Shales

Middle-Upper Devonian organic-rich black shales between the Berea Sandstone and Onondaga Limestone were deposited within a well-defined foreland basin and pinch out westward to non-deposition upon a positive Cincinnati Arch. Brine disposal units include the Marcellus Shale, the Genesee Formation, the Rhinestreet Shale Member, and the Ohio Shale (Cleveland Member and Huron Member) units (see Figure 3-4). These black shales are deeper-water facies equivalent to the clastics deposited from the Catskill delta to the east. Organic-rich shale units are unique in that they are the source, seal, and reservoir rocks for unconventional reservoirs in the Appalachian Basin. Matrix porosity is low, ranging from 1.0 to 5.0%, and permeabilities are extremely low, ranging from 10E-8 to 10E-9 mD (Boswell, 1996). Oil and gas production from black shale intervals has been successful following massive hydraulic fracturing in horizontal wells. Detrital materials represent 60 to 98% in eastern Kentucky with the following proportions: silt- and clay-sized quartz (42%), illite (34%), kaolinite (6%), and feldspar (4%). Interconnected natural fractures are important to create porosity and permeability for brine disposal. Depths to these black shale units increases eastward as these black shale tongues grade into more siltstone-rich facies.

3.2.6 Mississippian-Pennsylvanian Interval

The Mississippian-Pennsylvanian interval contains the shallowest zones used for brine disposal in the northern Appalachian Basin. This interval consists of a complex, heterogeneous mixture of interbedded sandstones, limestones, and coal beds. Within the project area, brine disposal occurs in the sandstone and limestone units of the Mississippian-age Price Formation/Cuyahoga Formation/Borden Formation/Grainger Formation (“Weir” and “Big Injun”), the Greenbrier Limestone/Newman Limestone (“Big Lime”), the Mauch Chunk Formation (“Little Lime”), and the Pennsylvanian-age New River Formation/Breathitt Group/Pottsville Group (“Salt Sands” and “Maxton”) (see Figure 3-4).

Mississippian Units

Active brine disposal occurs in localized areas in the Mississippian Price Formation/Cuyahoga Formation/Borden Formation/Grainger Formation (“Weir” and “Big Injun”) in Ohio, West Virginia, and Kentucky. The “Weir” sandstone was named in 1911 for a sandstone bed encountered while drilling an oil and gas well near Weir, West Virginia (Krebs and Teets, 1914). The “Weir” sandstone beds occur within the Price Formation in West Virginia and the Borden and Grainger Formations in Kentucky. These sandstone beds occur at several stratigraphic intervals between the base of the “Big Injun” and the top of the Sunbury Shale. In West Virginia, “Weir” sandstones that are located 350 feet (100 meters) or more above the Sunbury are named by drillers as the “upper Weir”; those between 150 and 350 feet (50 and 100 meters) above the Sunbury, the “middle Weir”; and those within 100 feet (30 meters) of the Sunbury, the “lower Weir” (Matchen and Vargo, 1996). In central and southern West Virginia, “Weir” sandstones are fine- to medium-grained, and in Kentucky, they are described as parallel-bedded, very fine-grained to fine-grained and moderately well-sorted (Matchen and Vargo, 1996). The “Big Injun” has not been defined in outcrop, and the stratigraphic terminology is somewhat variable and

confusing. The term “Big Injun” was first used when drillers encountered a thick sandstone beneath the Greenbrier Limestone (“Big Lime”). As the play developed, “Big Injun” has been used for any productive sandstone near the base of the “Big Lime” or the top of the Mississippian clastics. In outcrop in the northern part of the basin, the “Big Injun” equivalent rocks are fine- to medium-grained, light-gray sandstones. In southern West Virginia, “Big Injun” correlative rocks are medium- and fine-grained sandstones (Vargo and Matchen, 1996). The “Big Injun” in eastern Kentucky is considered part of the Borden Formation and is a distal equivalent to the “Big Injun” of West Virginia (Vargo and Matchen, 1996). Lithologically, this interval in eastern Kentucky varies from shale to very fine-grained sandstone.

The Mississippian Greenbrier/Newman Limestones (“Big Lime”) are active brine injection zones in West Virginia and Kentucky (see Figure 3-4). The Greenbrier was named for exposures on the Greenbrier River in south-central West Virginia (Rogers, 1879). Lithologically, “Big Lime” carbonates in the Greenbrier are ooid grainstones and also serve as gas reservoirs. The type section for the Newman Limestone is Newman Ridge, Tennessee (Campbell, 1893). Natural gas reservoirs occur in two zones: an unnamed basal unit consisting of medium- to thick-bedded, cherty, skeletal, dolomitic limestone and finely crystalline dolomite (Smosna, 1996), and scattered ooid grainstones that are locally dolomitized.

The “Little Lime” is considered to be part of the lower Mauch Chunk Formation in West Virginia (Barlow, 1996), where it serves as a brine injection zone. It is a brown to gray-brown, argillaceous to silty limestone, which grades upwards into shale. In Gilmer and Braxton Counties, West Virginia, this unit is an oolitic to skeletal grainstone (Carpenter, 1976).

Pennsylvanian Units

The Pennsylvanian New River Formation/Breathitt Group/Pottsville Group (“Salt Sands” and “Maxton”) are the shallowest brine disposal zones in the project area and are used for injection disposal in West Virginia and Kentucky (see Figure 3-4). The “Maxton” is an informal drillers’ term that is used for a basal Pottsville sandstone. The name was taken from the Maxton farm near the Sistersville field in West Virginia (White, 1904). Drillers apply the term “Salt Sands” to various stratigraphic sandstone units in the lower Pennsylvanian. Up to three of these sandstone units may be recognized: the “First Salt” correlates with the Homewood; the “Second Salt” correlates with the Upper Connoquenessing Sandstone; and the “Third Salt” correlates with the Lower Connoquenessing Sandstone (Hohn, 1996). Units within the Breathitt Group in Kentucky and the New River Formation in West Virginia have been called “Salt Sands.” The gas-producing in this interval are hard, massive, gray to white sandstones that can be locally soft and friable. The producing reservoirs consist of one or more massive quartz arenites separated by gray to black silty shales, siltstones, sandstones, or thin coals. Porosities in these reservoirs range from 2 to 20% and average 12% (Hohn, 1996).

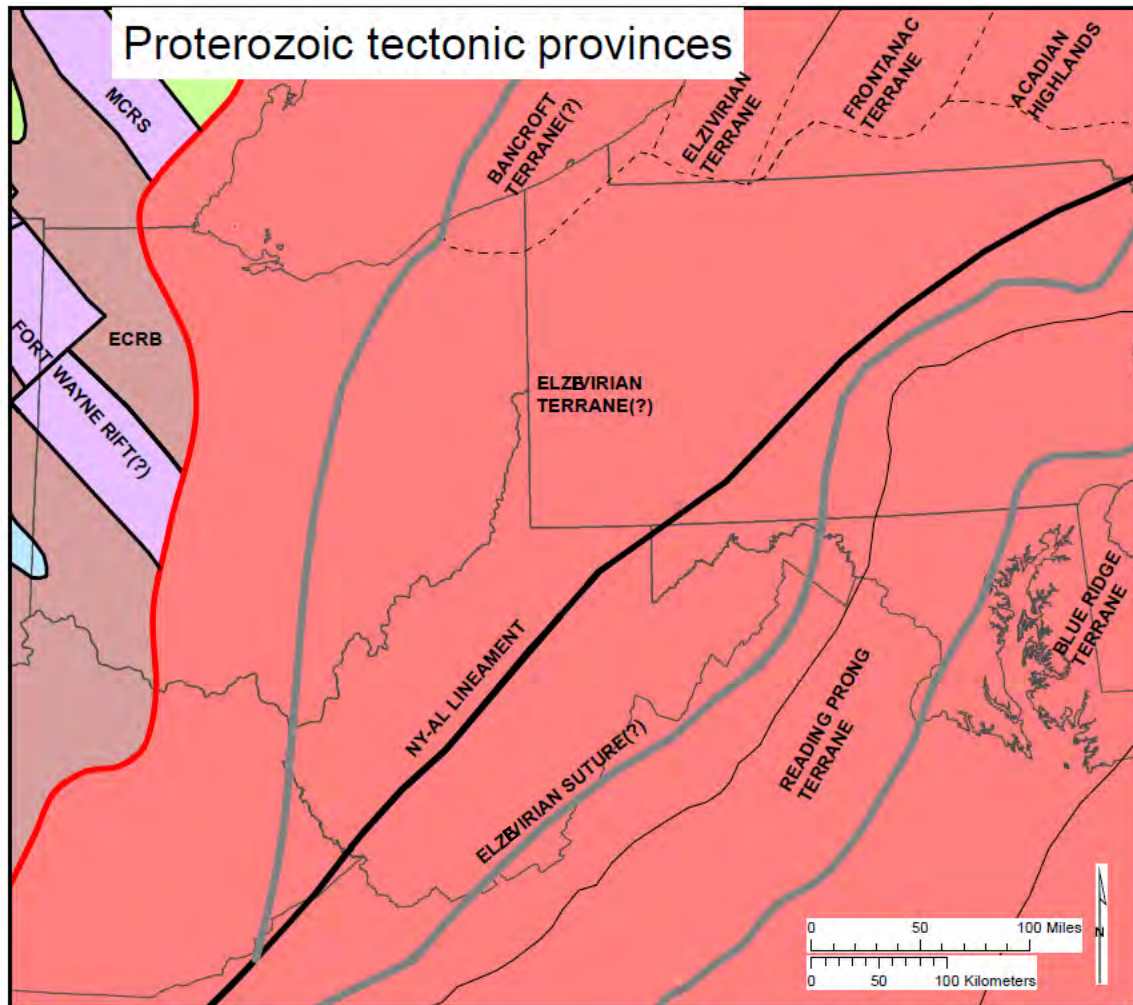
3.3 Regional Formation Maps

This section discusses the regional formation maps of interest for the major injection intervals covered in this study. Each section reviews the depths, thickness, depositional environments, paleogeography, and tectonism for each interval.

3.3.1 Precambrian

The Precambrian unconformity map displays the surface which separates the overlying Paleozoic strata from the underlying Proterozoic strata (Wickstrom et al., 2005). While the Precambrian is not considered an injection interval, it provides context for the overall distribution of overlying sedimentary rocks in the Appalachian Basin. The underlying Proterozoic rocks are composed of various lithologies but are collectively referred to as Precambrian basement. Basement is the general term used to describe crystalline rocks (igneous or metamorphic) below sedimentary rocks.

Composition of the Proterozoic rocks below the Precambrian unconformity is varied within the RPSEA study area and reflects several tectonic events culminating in the formation and subsequent breakup of the supercontinent Rodinia (Thomas, 2006). The major tectonic provinces include the Granite-Rhyolite Province, to the west, and the Grenville Province, to the east, which are separated by the northeast–southwest-trending Grenville Front. Major tectonic features within the Granite-Rhyolite Province include the Midcontinent rift system and the East Continent Rift Basin (Figure 3-5). The Grenville Province reflects three tectophases of the Grenville orogeny and may include accreted terranes prior to the Grenville orogeny. These terranes are incorporated within the Grenville Province; for example, the Elzeverian terrane. After a period of extended stability Rodinia rifted apart, forming Laurentia and the Iapetus Ocean.



Notes: ECRB = East Continent Rift Basin; MCRS = Midcontinent rift system.

Grenville front = thick red line; New York-Alabama lineament = thick black line; possible suture or terrane boundary = thick gray line.

Mazatzal Province = green; Granite-Rhyolite Province = blue; Grenville Province = red, East Continent Rift systems=purple & brown.

Sources: Modified after Whitmeyer and Karlstrom, 2007; Baranoski et al., 1996; Bartholomew and Hatcher, 2010.

Figure 3-5. Proterozoic tectonic provinces within the RPSEA study area.

Granite-Rhyolite Province (1,480–1,450 Ma)

The Granite-Rhyolite province is an extensive Proterozoic terrane that consists of various types of Mesoproterozoic igneous and dominantly felsic volcanic rocks (Wickstrom et al., 2005). Age dating of rocks from this province indicate they are of a similar age to the Grenville protoliths, ranging in age from 1,480 to 1,450 Ma (Lidiak and Zietz, 1976; Hoppe et al., 1983; Denison et al., 1984; Bickford et al., 1986).

Elzevirian (1,245–1,220 Ma)

The pre-Grenville Elzevirian orogeny is well documented in eastern North America from outcrop to basement massif outliers (McLelland et al., 2010), but the extent of the Elzevirian terrane under the Paleozoic cover strata is not well defined (Figure 3-5). A dominant magnetic boundary may mark the western extent of the Elzevirian terrane under Ohio and Kentucky

(Whitmeyer and Karlstrom, 2007). As shown, the Elzevirian terrane boundary is truncated by the New York-Alabama lineament (Bartholomew and Hatcher, 2010). The pre-Grenville terranes, which underlie the RPSEA study area, may be demarked by the Coshocton zone (Pratt et al., 1989). The Coshocton zone is a zone of west-dipping reflectors beneath the Paleozoic cover strata in eastern Ohio and is in contrast to east-dipping bedding observed in outcrop.

The East Continent Rift Basin (1,500–600 Ma)

East Continent Rift Basin is a Middle to Late Proterozoic rift basin that lies west of the Grenville Front. The Grenville Front partially covers the East Continent Rift Basin (Figure 3-5) (Wickstrom et al., 2005). Rocks within the East Continent Rift Basin consist mainly of sedimentary clastics interbedded with felsic and mafic volcanics (Shrake et al., 1990; Drahovzal et al., 1992; Wickstrom et al., 1992). Sedimentary and volcanic rocks of this province are known through boreholes and range in age from more than 1,500 to 600 Ma (Drahovzal et al., 1992; Drahovzal, 1997; Santos et al., 2002; Drahovzal and Harris, 2004).

Mid-Continent Rift System (1,200–1,100 Ma)

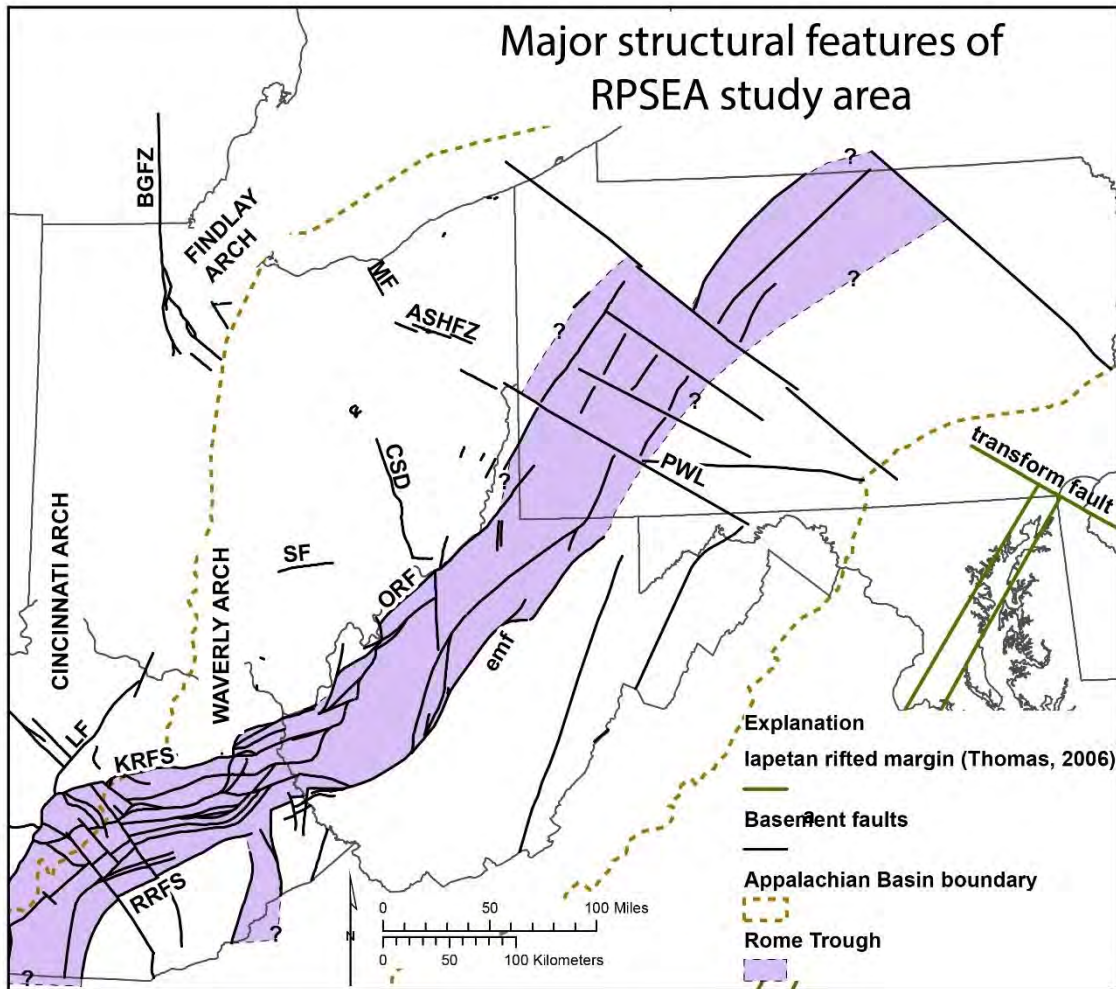
The Middle Proterozoic Mid-Continent rift system traverses Kansas, Iowa, Minnesota, Michigan, and apparently terminates just north of the RPSEA study area (Figure 3-5). Lithologies within this rift system consist of rocks similar to the East Continent Rift Basin with ages of 1,200 to 1,100 Ma (Green, 1982; Van Schmus and Hinze, 1985; Dickas, 1986). Even with the similar lithologies and ages, the relationship of the Mid-Continent rift system and the East Continent Rift Basin is unknown (Drahovzal et al., 1992).

Grenville Province (1,200–880 Ma)

The Grenville Province was accreted during the Grenville orogeny (Figure 3-5). The Grenville orogeny is broken into three distinct orogenic events: the Shawinigan, the Ottawan, and the Rigolet (Bartholomew and Hatcher, 2009). The Shawinigan phase (1,200 to 1,150 Ma) is marked by orogen-wide terrane accretion, magmatism, and deformation from Texas to Canada. The Ottawan phase (1,080 to 1,020 Ma) is also marked by extensive terrane accretion, magmatism, and deformation from North Carolina (Mars Hill terrane) to Canada. The final phase of the Grenville orogeny is the Rigolet (1,020 to 880 Ma). The Rigolet is marked by widespread extension in the Appalachian Region (Forsythe et al., 1992). Much of this extension is thought to be related to strike-slip movement along the New York-Alabama lineament (Bartholomew and Hatcher, 2009).

Iapetan Rifting (620–535 Ma)

Following a long period of uplift and exhumation of the Grenville Province, Iapetan rifting began (Figure 3-6). The Laurentian continental margin and associated stratigraphic succession are a direct result of the continental margin configuration (Thomas and Astini, 1999). A second rift system formed cratonward of the main Iapetan rift. This rift system failed and is partially occupied by the Rome Trough (Harris et al., 2004; Thomas, 2006).



Notes: The Rome Trough is in purple.

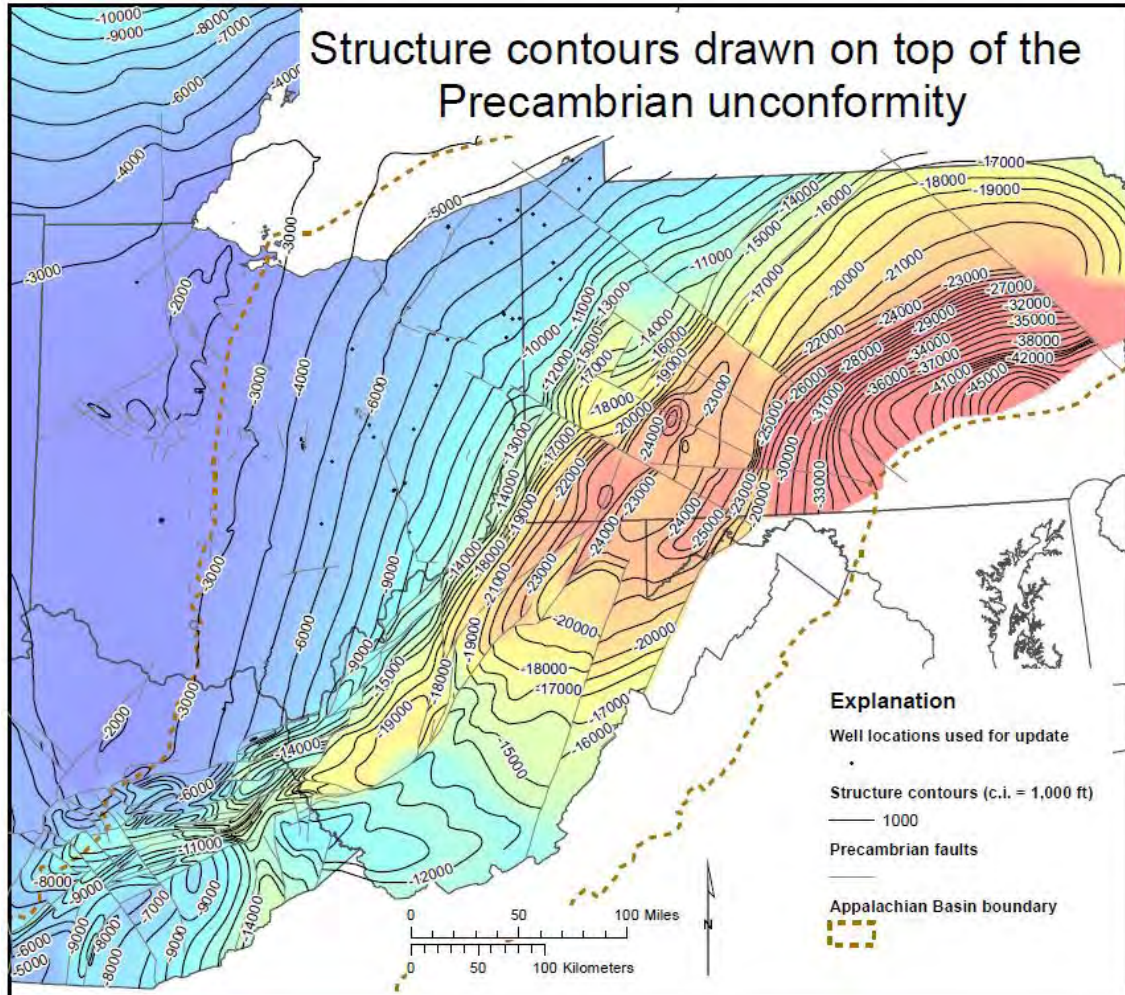
ASHFZ = Akron-Suffield-Highlandtown fault zone; BGFZ = Bowling Greene fault zone; CSD = Cambridge Structural Discontinuity; emf = eastern margin fault; KRFS = Kentucky River fault system; LF = Lexington fault; MF = Middleburg fault; ORF = Ohio River fault; PWL = Pittsburg-Washington lineament; RRFS = Rockcastle River fault system; SF = Star fault.

Sources: Modified after Wickstrom et al. (2005) and Harris et al. (2004).

Figure 3-6. Major structural features within the RPSEA study area.

Depth of Proterozoic Rocks

The Precambrian surface ranges from less than 2,000 feet (600 meters) below sea level in western Ohio and east-central Kentucky to greater than 48,000 feet (15,000 meters) below sea level in eastern Pennsylvania (Figure 3-7). Throughout the study area, the Precambrian surface dips to the southeast until it is broken by the Rome Trough bounding faults. Where the basement is shallowest, two topographic highs underlie the Paleozoic strata: the Cincinnati and Findlay Arches (Figure 3-6). These arches remained relatively stable during Appalachian Basin subsidence; however, during major Appalachian orogenic events, some arching did occur and is reflected locally by the distribution of facies (Wickstrom et al., 2005). Most of the arching is thought to be a result of differential subsidence rather than tectonically induced (Wickstrom et al., 1992).



Note: Contours hand-edited to reflect recent well data.

Source: Modified from Wickstrom et al. (2005).

Figure 3-7. Structure contours drawn on the Precambrian unconformity surface within the RPSEA study area.

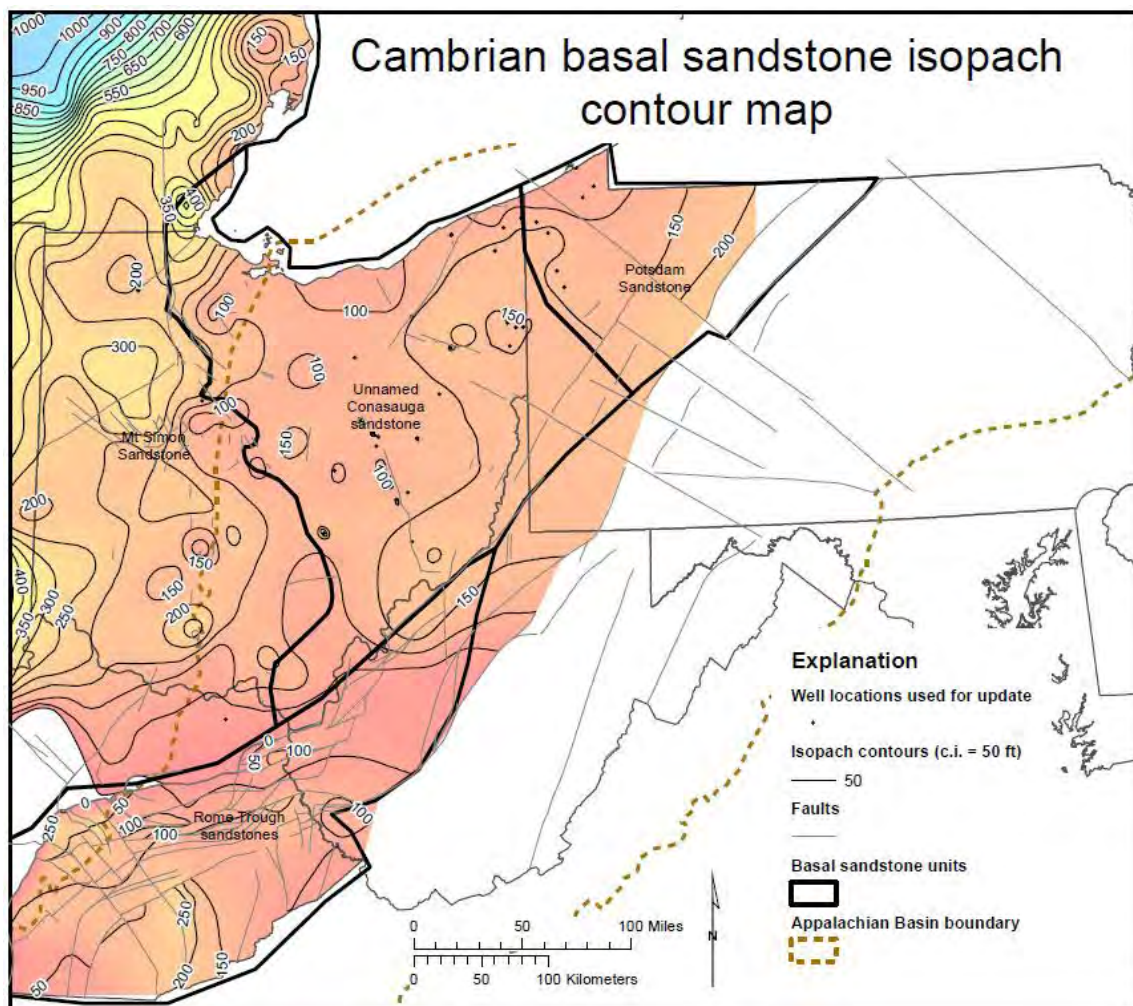
The dominant structural feature within the region is the Rome Trough, an extensional graben system which breaks the Precambrian unconformity surface from Tennessee to Pennsylvania (Figures 3-6 and 3-7). As mapped, the Rome Trough graben structure is relatively symmetrical in Kentucky and changes to an asymmetric half-graben, dipping to the southeast in West Virginia. The half-graben character extends into western Pennsylvania until it is truncated by the Pittsburgh-Washington lineament (Parrish and Lavin, 1982). North of the lineament, the trough changes to a southeast-dipping monocline cut by down-to-southeast dipping normal faults (Wickstrom et al., 2005). Subsequent Appalachian orogenic events have caused some reactivation and reverse motion along some of the faults within the Rome Trough (Drahovzal and White, 2002; Harris et al., 2004).

The configuration of the Precambrian surface is a record of the Proterozoic events leading to the assemblage and breakup of the supercontinent Rodinia (Thomas, 2006). The tectonic history of

the underlying basement has resulted in a faulted and fractured crust. These pre-existing weaknesses have reactivated as faults and subtle fold axes or have influenced facies distribution. Understanding the Precambrian structure is critical in understanding the overlying Paleozoic section.

3.3.2 Cambrian Basal Sandstones

The Cambrian basal sandstone interval is often targeted as a brine disposal unit within the RPSEA study area (Figure 3-4). The Mount Simon Sandstone, which is part of the mapped basal sandstone interval, pinches out in central Ohio (MRCSP, 2005). East of this pinch-out, thinner, less-continuous sandstones are found in the same stratigraphic position as the basal sandstones. For the RPSEA assessment, these sandstone intervals have been mapped as one group across the entire region (Figure 3-8).



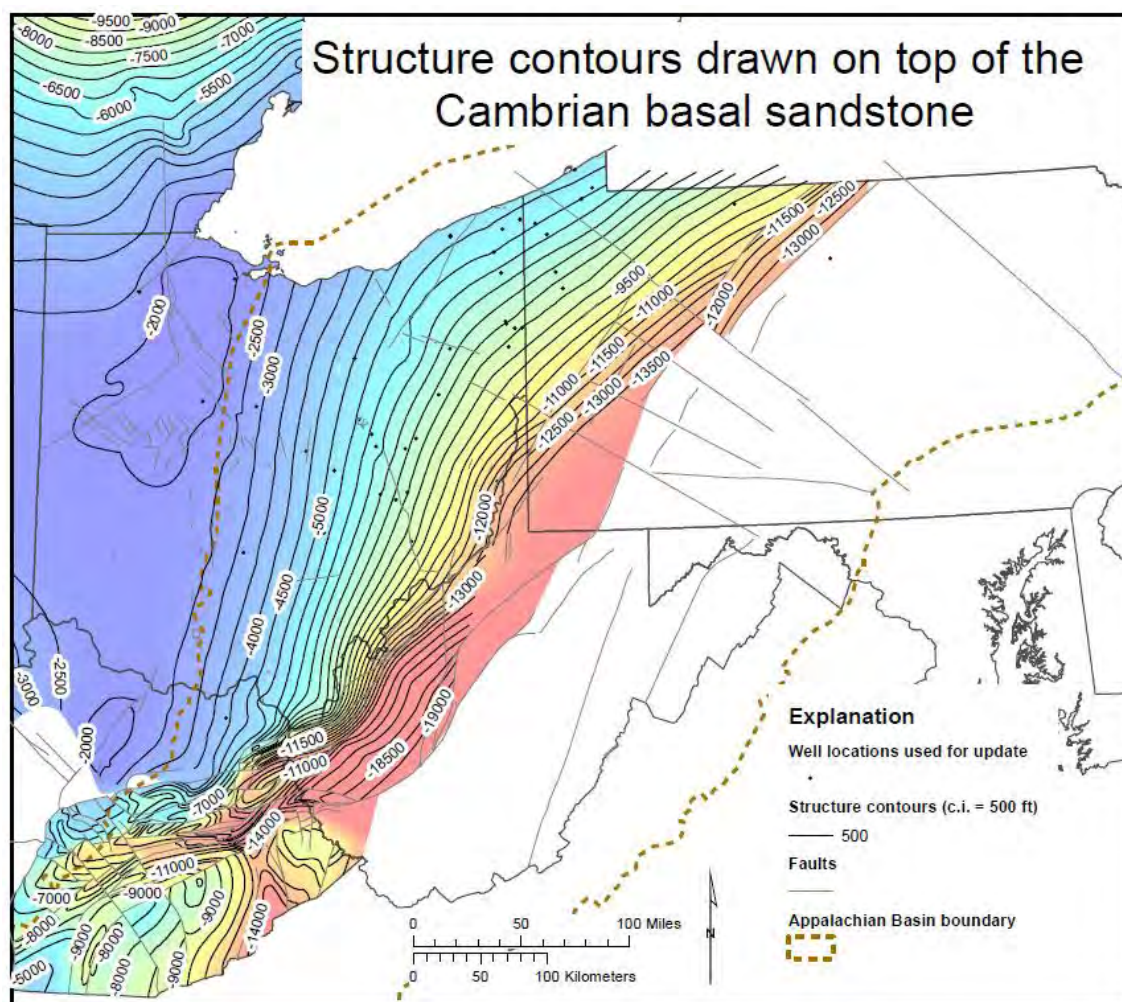
Source: Modified from Wickstrom et al. (2005).

Figure 3-8. Structure contours drawn on top of the Cambrian basal sandstone surface within the RPSEA study area.

Depth and Thickness Ranges

The top of the Cambrian basal sandstone interval ranges from approximately 2,000 feet (600 meters) below sea level in northern Ohio to greater than 19,000 feet (5,800 meters) below sea level in the Rome Trough of West Virginia and southwestern Pennsylvania (Figure 3-9).

Thickness of the basal sandstone interval ranges from zero feet, where local Precambrian topography exists (Janssens, 1973; Baranoski, 2002, 2013), to more than 300 feet (90 meters) in western Ohio (Figure 3-8). Generally, the basal sandstone interval maintains a range of thickness from 50 to 300 feet (15 to 90 meters) in the RPSEA study area. In eastern Kentucky, the basal sandstone gradually thins eastward toward the Rome Trough but abruptly thickens within the trough.



Source: Modified from Wickstrom et al. (2005).

Figure 3-9. Isopach contours of the Cambrian basal sandstone interval surface within the RPSEA study area.

Within the Rome Trough, the basal sandstones appear to thicken southward independent of major faults, indicating that the sandstones may be pre-Iapetian rift deposits unaffected by movement on the major bounding faults of the Rome Trough; however, post-depositional

structural movement influenced depth and local thickness preservation (Harris et al., 2004; Wickstrom et al., 2005). Some of the variability in thickness may also indicate structural influences from localized faulting, especially where there are substantial thickness changes in the basal sandstone interval across relatively short distances.

Depositional Environments/Paleogeography/Tectonism

During Late Precambrian and Early Paleozoic time, the RPSEA region was part of a large continent, named Rodinia, which straddled the equator (Wickstrom et al., 2005). During Late Precambrian time, the Laurentian plate rifted away from Rodinia, creating the Iapetus Ocean between them (Dietz, 1972). At this time, the southern margin of Laurentia became a passive continental margin. During Early and Middle Cambrian time, the Grenville rocks were deeply eroded in what is now the Appalachian Basin. Deposition of sand on the Precambrian unconformity began late during the Middle Cambrian as sea level rose and the southern margin of Laurentia began to subside in response to the sediment loading and thermal subsidence (Thomas and Astini, 1999). During Early or Middle Cambrian time, the Rome Trough formed along the southern margin of Laurentia. The Rome Trough is part of a failed rift system, extending from the Mississippi embayment through Kentucky to Pennsylvania (Thomas, 2006). The rift is thought to have originated on incipient Precambrian crustal-block faults derived from stresses during the opening of the Iapetus Ocean. Thus, the Cambrian basal sandstone interval of the RPSEA study area is a transgressive sequence of sandstones, shales, and carbonates deposited on the regional Precambrian unconformity surface. Both lower and upper boundaries are highly diachronous, making regional correlations difficult and tenuous at best. The basal sandstones in the Rome Trough are not correlative to the Mount Simon and unnamed Conasauga sandstones, which are considered younger than the unnamed basal sandstones within the trough.

Depositional environments for the Cambrian basal sandstones vary widely, from marginal marine to marine, littoral, fluvial, and estuarine (Janssens, 1973; Driese et al., 1981; Haddox and Dott, 1990; Wickstrom et al., 2005). The marine influence is evident where sandstone intertongues with dolostone in the Appalachian Basin region. In the Rome Trough, red and green shales and siltstones with nodular evaporates interlayer with the sandstones, suggesting very shallow, subtidal to intertidal deposition with restricted marine circulation (Harris et al., 2004). The regional shoreline generally migrated northward from the proto-Illinois/Michigan Basin, Rome Trough and eastern proto-Appalachian Basin to the Canadian Shield during transgression (Milici and de Witt, 1988).

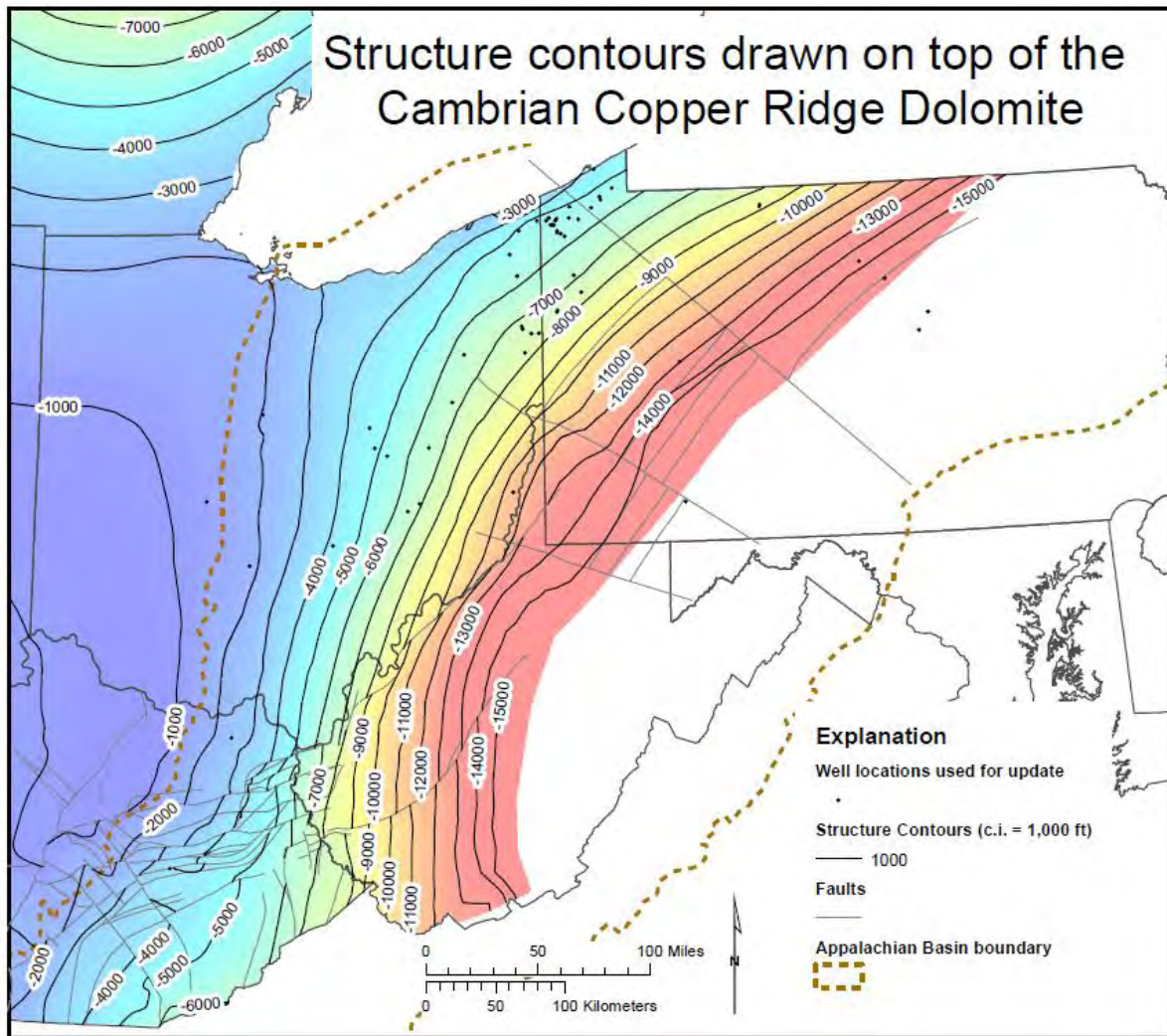
3.3.3 Basal Sandstones to Top of Copper Ridge Interval

The stratigraphic interval from the top of the Cambrian basal sandstones to the top of the Copper Ridge Dolomite (Figure 3-4) is not a widely targeted brine disposal interval within the RPSEA study area. Isolated, local porosity may be available in some units within this interval and may provide opportunities for stacked brine disposal (multiple downhole injection targets).

Depth and Thickness Ranges

The Copper Ridge Dolomite ranges from less than 1,000 feet (300 meters) below sea level in western Ohio and eastern Kentucky to more than 15,000 feet (4,600 meters) below sea level in eastern Pennsylvania (Figure 3-10). In Kentucky and West Virginia, faults within the Rome Trough disrupt the surface of the Copper Ridge Dolomite. Thickness from the top of basal

sandstone to the top of the Copper Ridge interval varies from less than 1,000 feet (300 meters) in the vicinity of the Cincinnati Arch to more than 9,000 feet (3,000 meters) within the Rome Trough (Wickstrom et al., 2005). Most of the thickness variation within the trough occurs within the Rome Formation and lower part of the Conasauga Group (Ryder et al., 1996, 1997; Harris et al., 2004).



Source: Modified from Wickstrom et al. (2005).

Figure 3-10. Structure contours drawn on top of the Copper Ridge Dolomite surface within the RPSEA study area.

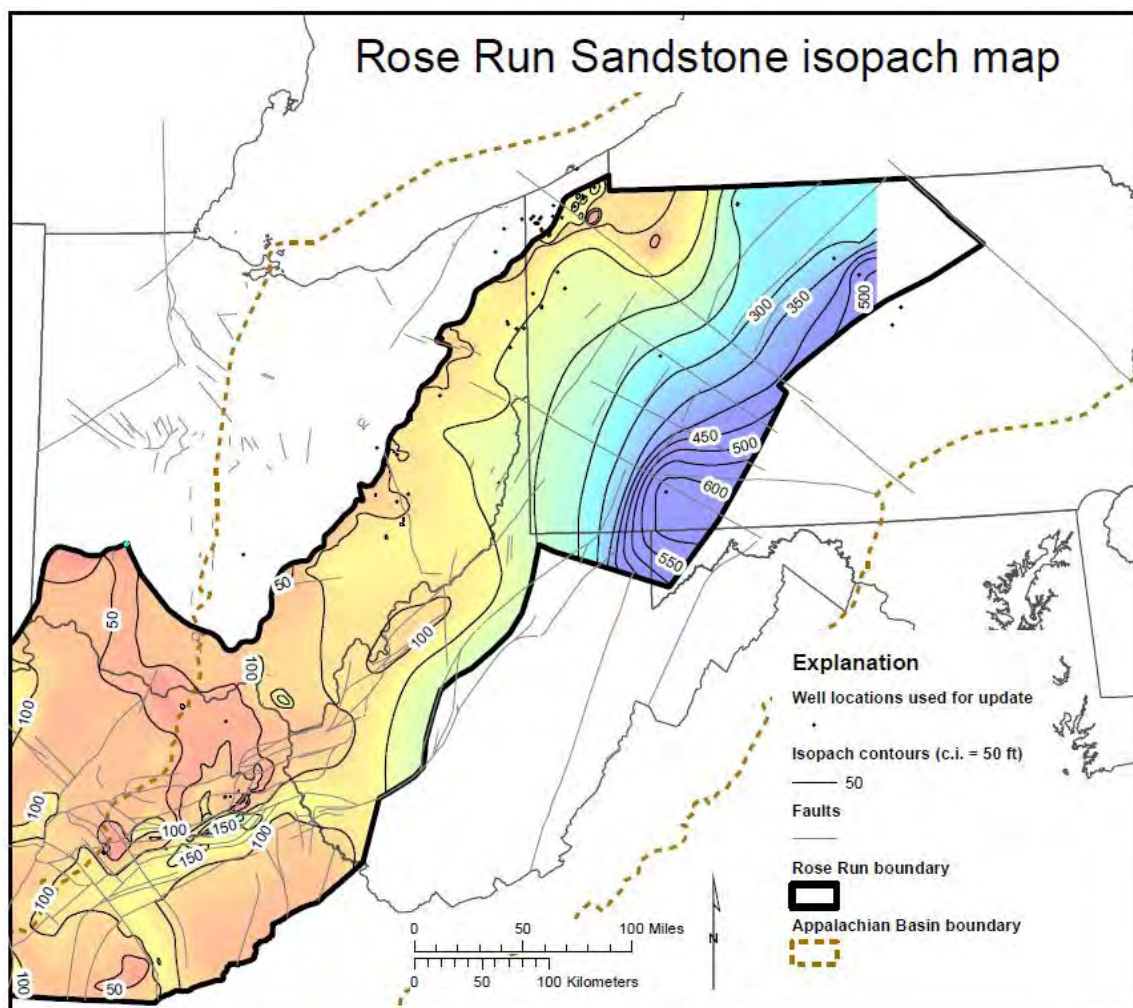
Depositional Environments/Paleogeography/Tectonism

During deposition of the top basal sandstone to the top of the Copper Ridge interval, a shallow epicontinental sea covered the RPSEA study area (Wickstrom et al., 2005). Subsidence of the Rome Trough and lesser subsidence in the Appalachian Basin influenced depositional facies as well as sea-level fluctuations. The pervasive dolomitization of the upper part of this interval (Copper Ridge equivalents) throughout the North American continent continues to be enigmatic,

although it may be related to the expulsion and migration of fluids from the Ordovician Sevier or Late Paleozoic Alleghenian orogenies (Montanez, 1994).

3.3.4 Upper Cambrian Rose Run Sandstone

In Ohio and eastern Kentucky, the Cambrian-Ordovician Knox interval is subdivided, in ascending stratigraphic order, into the Copper Ridge Dolomite, Rose Run Sandstone, and Beekmantown dolomite. The Cambrian Rose Run Sandstone is the only laterally persistent sandstone within the Knox Group. This sandstone interval can be correlated in the subsurface (Figure 3-4) from eastern Ohio, where it subcrops beneath the Knox unconformity (Figure 3-11), to eastern Kentucky and into western West Virginia (upper sandstone member of the Knox), Pennsylvania (Upper Sandy member of the Gatesburg Formation), then extending into New York (partial equivalent of the Theresa Formation).



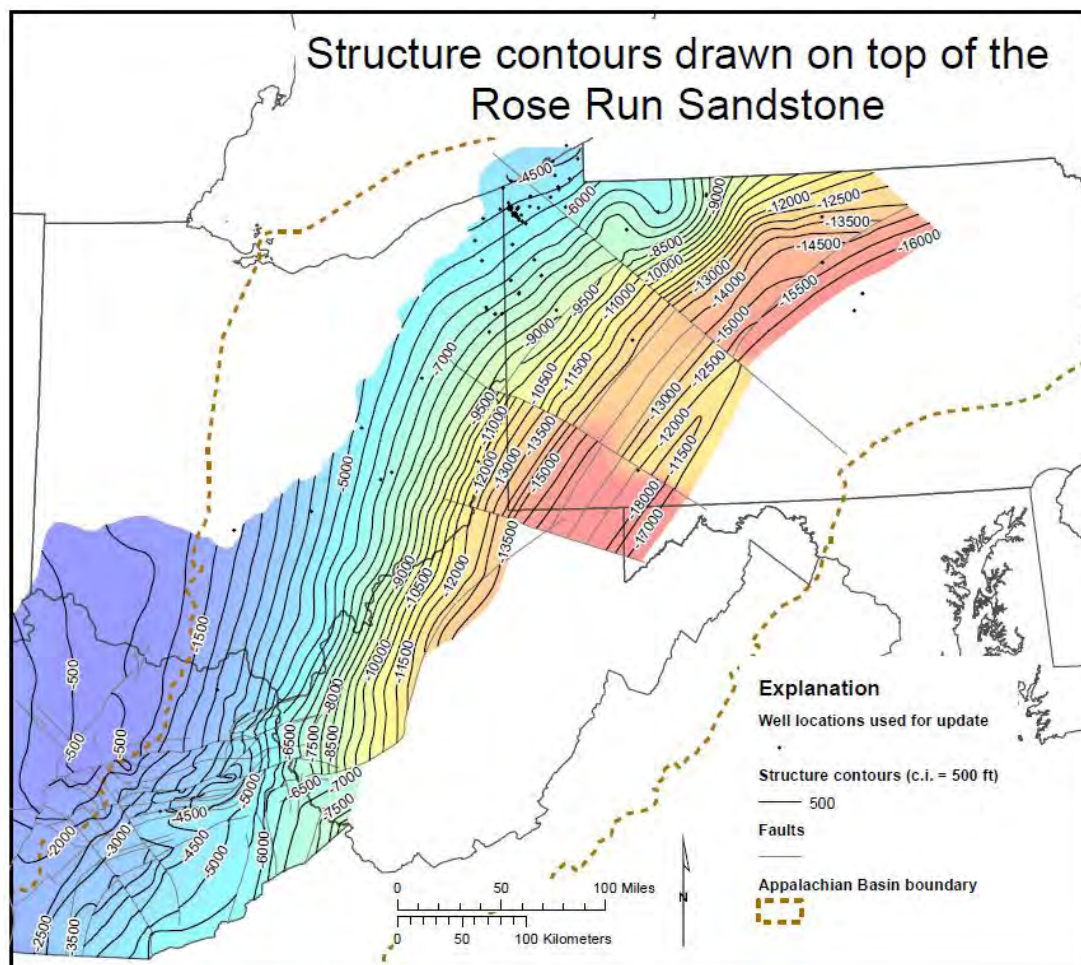
Note: Simplified in the zone of outliers.

Source: Modified from Wickstrom et al. (2005).

Figure 3-11. Isopach of the Rose Run Sandstone surface within the RPSEA study area.

Depth and Thickness Ranges

Generally, the Rose Run Sandstone dips to the east and southeast with strike trending northeast–southwest (Figure 3-12). Subsea elevations range from 400 feet (120 meters) above sea level in north-central Kentucky to greater than 17,000 feet (5,200 meters) below sea level in south-central Pennsylvania. Dips range from approximately 50 feet (15 meters) per mile in northeastern Ohio and northwestern Pennsylvania to approximately 100 feet (30 meters) per mile in southeastern Ohio and western West Virginia. Faults of the Rome Trough disrupt the Rose Run surface in Kentucky and West Virginia. The Rose Run Sandstone interval thickens gradually from zero feet at the western limit of the subcrop to more than 600 feet (200 meters) in northeastern West Virginia and southwestern Pennsylvania (Figure 3-11). Typically, the Rose Run is about 100 feet (30 meters) thick throughout the area of eastern Ohio and northwestern Pennsylvania (Figure 3-11). In Kentucky, relatively abrupt variation of thickness along Rome Trough faults may reflect syntectonic deposition of the Rose Run. The irregular nature of the Rose Run isopach contours in Ohio near the subcrop is a result of erosion on the Knox unconformity. Various paleotopographic features, including numerous erosional remnants, are present along the subcrop trend as a result of paleodrainage (Riley et al., 1993).



Note: Simplified in the zone of outliers. Source: Modified from Wickstrom et al. (2005).

Figure 3-12. Structure contours drawn on top of the Rose Run Sandstone surface within the RPSEA study area.

Depositional Environments/Paleogeography/Tectonism

Following the Rome Trough rifting and deposition of the basal sandstones, Late Cambrian recycled sands, including those of the Rose Run, continued to be deposited across the present-day Appalachian Basin region. These sands were mixed with shelf carbonates that eventually dominated this passive margin (Riley et al., 1993). Provenance studies of the Rose Run Sandstone suggest that they are compositionally mature and were derived from the crystalline Precambrian shield complexes and overlying platform rocks (Riley et al., 1993). The widespread Knox unconformity developed during the initial collision of the passive margin and the lowering of eustatic sea level during the Middle Ordovician (Mussman et al., 1988; Read, 1989). The progressive westward truncation of Knox units along this regional unconformity created and exposed the Rose Run subcrop trend.

Deposition of the Rose Run and adjacent Knox units has been attributed by various authors to represent a peritidal to shallow subtidal marine environment (Mussman and Read, 1986; Anderson, 1991; Ryder, 1992; Riley et al., 1993; Ryder et al., 1997). The Rose Run is part of a heterogeneous assemblage of interbedded and carbonate facies in the Knox that were deposited on a carbonate shelf (Ginsburg, 1982). The Rose Run represents lowstand deposits of siliciclastic sediments that were transported onto the peritidal platform and reworked during subsequent sea-level rises (Read, 1989).

Many authors have interpreted tidal flat deposition for the Rose Run and equivalent strata (Mussman and Read, 1986; Anderson, 1991; Riley et al., 1993), based upon core and outcrop description. Sedimentary features supporting this include herringbone cross bedding and basal lags of dolostone and shaly dolostone, indicating scour along tidal channel thalwegs. In outcrop in central Pennsylvania, a shallowing-upward tidal flat sequence is recognized. Subsurface cores in Ohio also indicate a supratidal facies from the presence of digitate algal stromatolites, mud cracks, and nodular anhydrite and chert replacing evaporites. Throughout the Rose Run and adjacent Knox units is extensive mottling from bioturbation, which is indicative of intertidal and subtidal environments.

The major tectonic features affecting Rose Run structure occur in northeastern Ohio, western Pennsylvania, eastern Kentucky, and western West Virginia. In western Pennsylvania, these include the Tyrone-Mount Union and Pittsburgh-Washington lineaments, which have been interpreted as northwest-southeast-trending wrench faults (Riley et al., 1993). In addition, numerous growth faults above basement rifts have been proposed that have been offset by movement along these major wrench faults (Laughrey and Harper, 1986; Harper, 1989; Riley et al., 1993). In northeastern Ohio, the major tectonic features indicated by regional mapping are the northwest-southeast-trending Akron-Suffield-Smith and the Highlandtown fault systems, which also have been suggested to be wrench faults (Riley et al., 1993). These are extensions of the Pittsburgh-Washington lineament in Pennsylvania. In eastern Kentucky and western West Virginia, the Rose Run structure is truncated by the east-northeast-trending Rome Trough. Locally, small-scale features are present that are not evident on the regional-scale maps.

East of this broad zone of gradual thickening, the contours become narrower in western Pennsylvania as a result of the rapid thickening that is present in the Rome Trough. Various authors have indicated that the Rome Trough was actively subsiding during Rose Run deposition (Wagner, 1976; Harper, 1991). Approximately 470 feet (140 meters) of Rose Run was

encountered in the Amoco #1 Svetz well in Somerset County, Pennsylvania, before drilling was stopped at 21,640 feet (6,600 meters); most of that thickness occurred in the uppermost sandstone body.

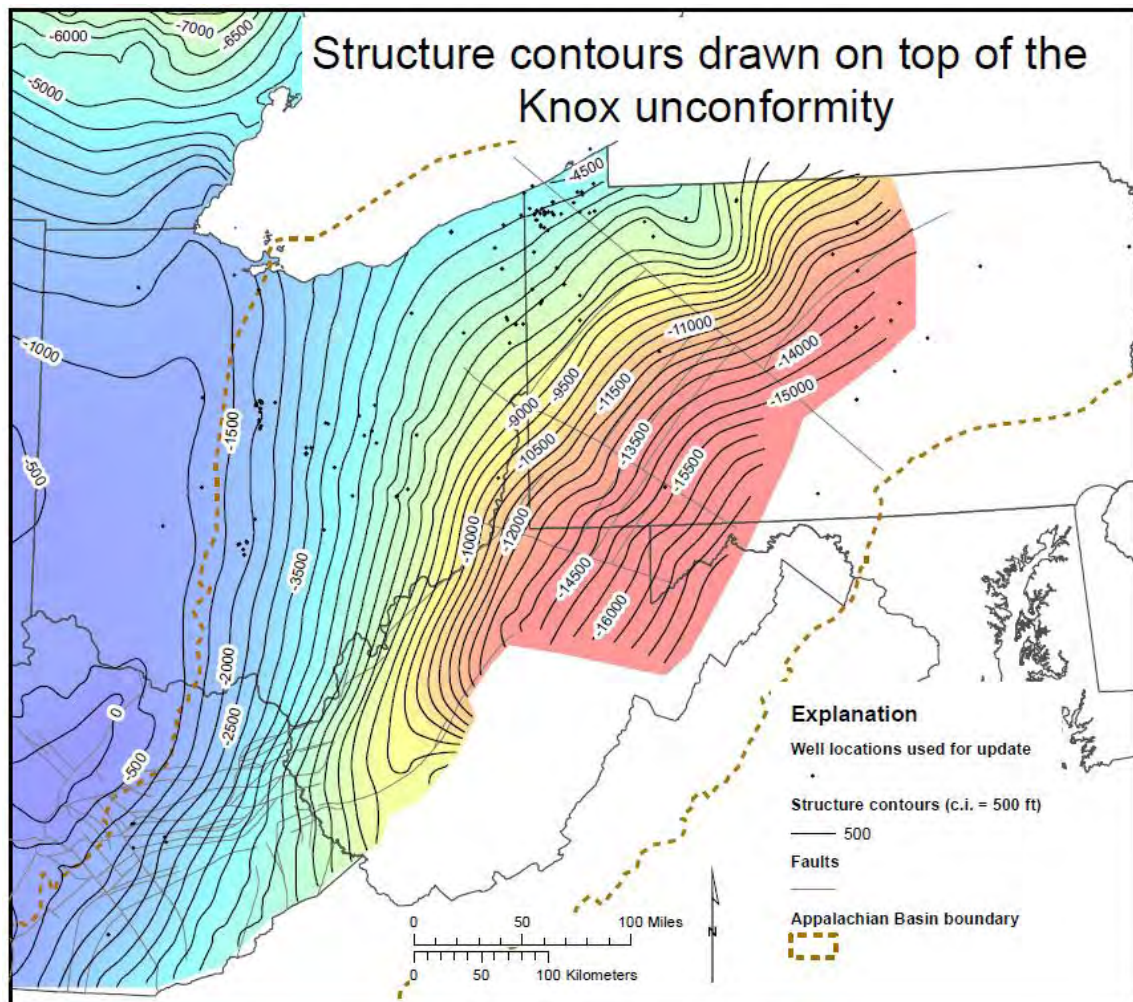
The depositional pattern of the Rose Run in south-central Ohio and north-central Kentucky suggests control by the Waverly Arch, a north–south-trending feature that was first identified by Woodward (1961). Isopach maps of the Knox by Janssens (1973) and the Prairie du Chien by Shearrow (1987) indicate thinning over the arch. This thinning also is coincident with a facies change in the Rose Run where the facies is sandstone-dominant on the east side and carbonate-dominant on the west side of the Waverly Arch (Riley et al., 1993). A rather abrupt thinning is demonstrated on the isopach map across the state line of Ohio and Kentucky. This is, in part, an artifact of how the base of the Rose Run is interpreted differently in Ohio and Kentucky as discussed previously. Abrupt thickening in the Rome Trough of Kentucky suggests syntectonic deposition of the Rose Run.

3.3.5 Knox Unconformity

The Knox unconformity is a widespread regional unconformity which eroded the Beekmantown dolomite, the Rose Run Sandstone, and the Copper Ridge Dolomite (see Figure 3-4). The Beekmantown dolomite is at the top of the Knox Group and cannot be consistently identified from the Copper Ridge without the Rose Run Sandstone separating the two dolomites. Locally, some porosity is available within the Beekmantown, indicating potential for brine disposal.

Depth and Thickness Ranges

The Knox unconformity dips to the southeast. Depth ranges from greater than zero feet above sea level along the Lexington fault system, in Kentucky, to more than 18,000 feet (5,500 meters) below sea level in northern West Virginia (Figure 3-13). Some localized faulting may offset the surface, but at this scale no faults significantly displace the surface. Thickness of the Beekmantown ranges from zero feet in eastern Ohio (Rose Run subcrop) (Figure 3-11) to more than 1,000 feet (300 meters) in central Pennsylvania.



Source: Modified from Wickstrom et al. (2005).

Figure 3-13. Structure contours drawn on the Knox unconformity surface within the RPSEA study area.

Depositional Environments/Paleogeography/Tectonism

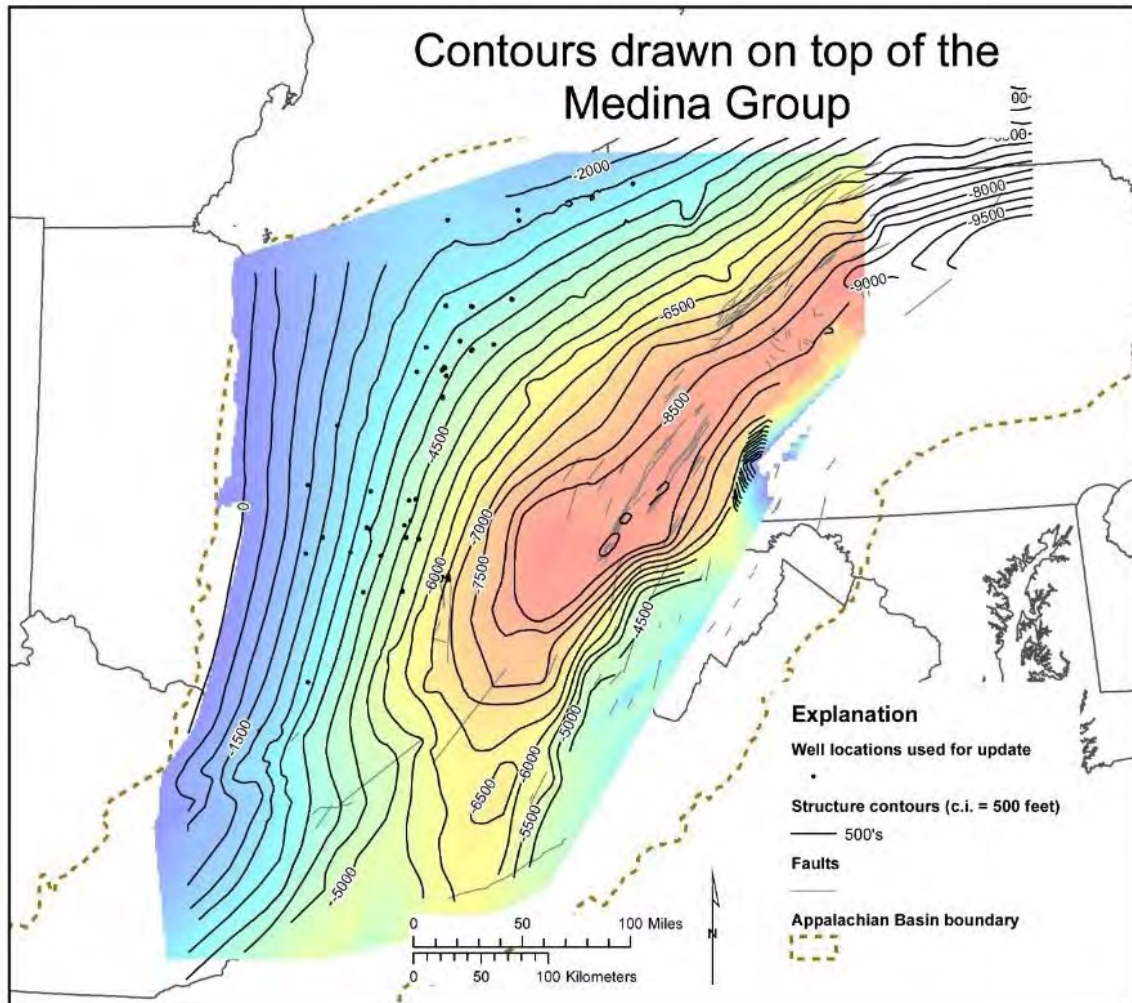
The Beekmantown Dolomite was deposited in a tidal flat to shallow marine environment along a broad, subsiding, continental shelf (Riley et al., 1993). Carbonates are the most dominant, although siliciclastics are more common in Pennsylvania. Locally, evaporate deposition occurred where restricted circulation and high salinity existed. Development of the Knox unconformity marks the transition from passive to convergent margin at the beginning of the Taconic orogeny and lowering of eustatic sea level (Mussman et al., 1988).

3.3.6 Medina Group

Depth and Thickness Ranges

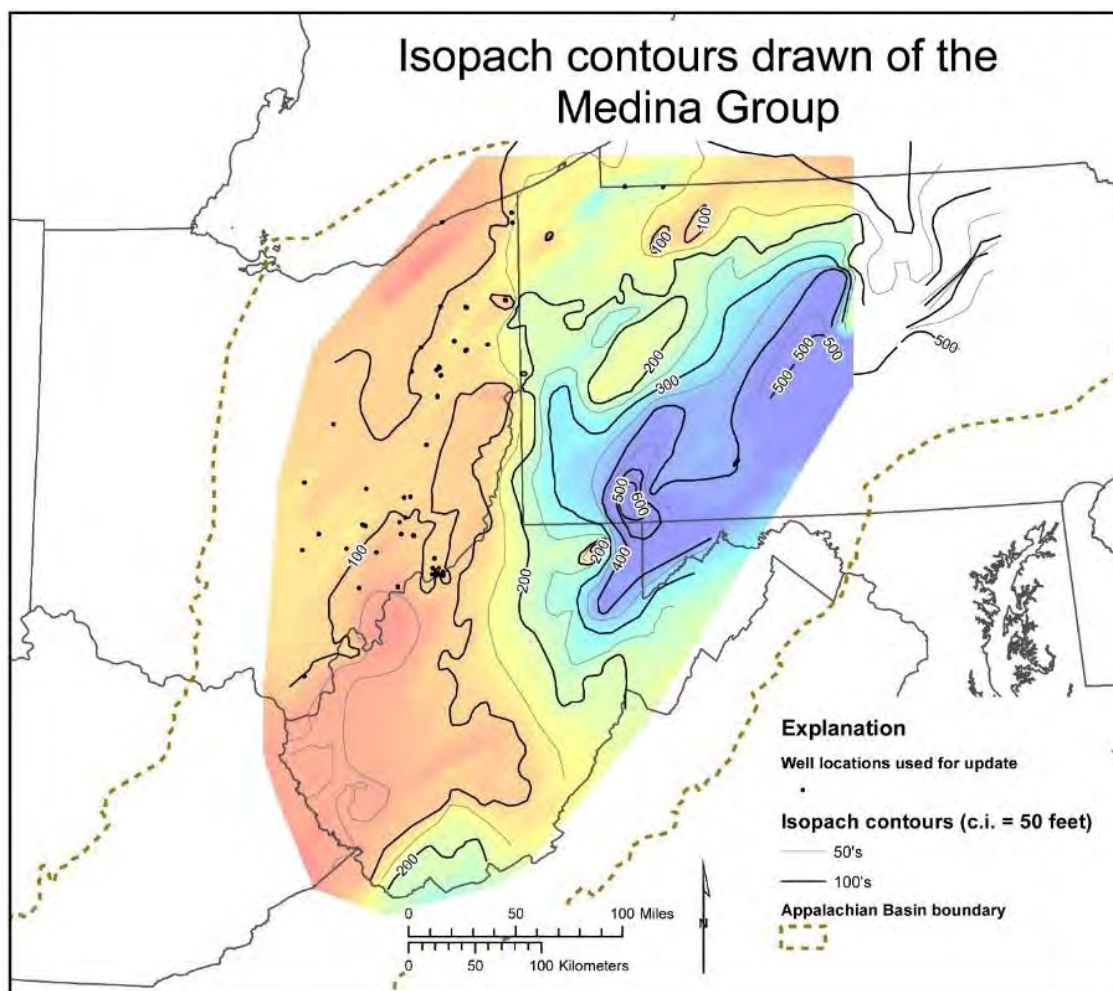
The Medina Sandstone ranges from less than zero feet below sea level in western Ohio and eastern Kentucky to more than 10,000 feet (3,000 meters) below sea level in eastern Pennsylvania (Figure 3-14). Some local faulting can control hydrocarbon accumulations or can

be associated with areas of poor production in the Medina (McCormac et al., 1996). Thickness of the Medina Group ranges from zero feet in eastern Ohio to more than 600 feet (180 meters) in central Pennsylvania (Figure 3-15).



Source: Modified from Wickstrom et al. (2005).

Figure 3-14. Structure contours drawn on top of the Medina Group surface within the RPSEA study area.



Source: Modified from Wickstrom et al. (2005).

Figure 3-15. Isopach map of the Medina Group within the RPSEA study area.

Depositional Environments/Paleogeography/Tectonism

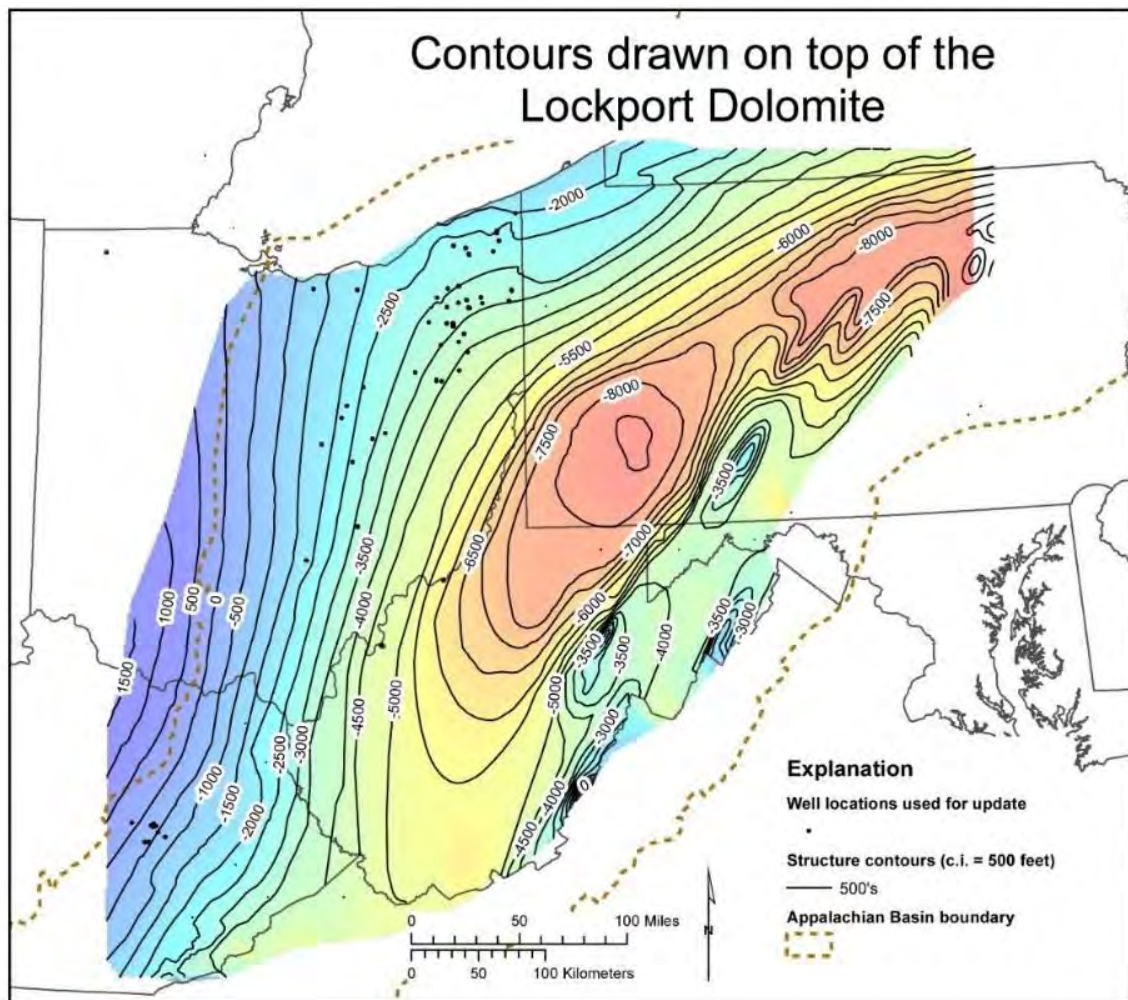
The Medina Group Sandstones consist of an interbedded sequence of sandstones, siltstones, and shales which transition from a basal transgressive, marine sandstone member at the base of the group to a complex deltaic to shallow marine-dominated system in which the main producing sandstone units were deposited. The deltaic sedimentation generally prograded from the east to the west (McCormac et al., 1996) and represents the final stages of foreland basin infill resulting from the Taconic Orogeny. In general, the individual sandstone members are not blanket sandstones, but a complex system of varying sandstone morphology.

3.3.7 Lockport Dolomite

Depth and Thickness Ranges

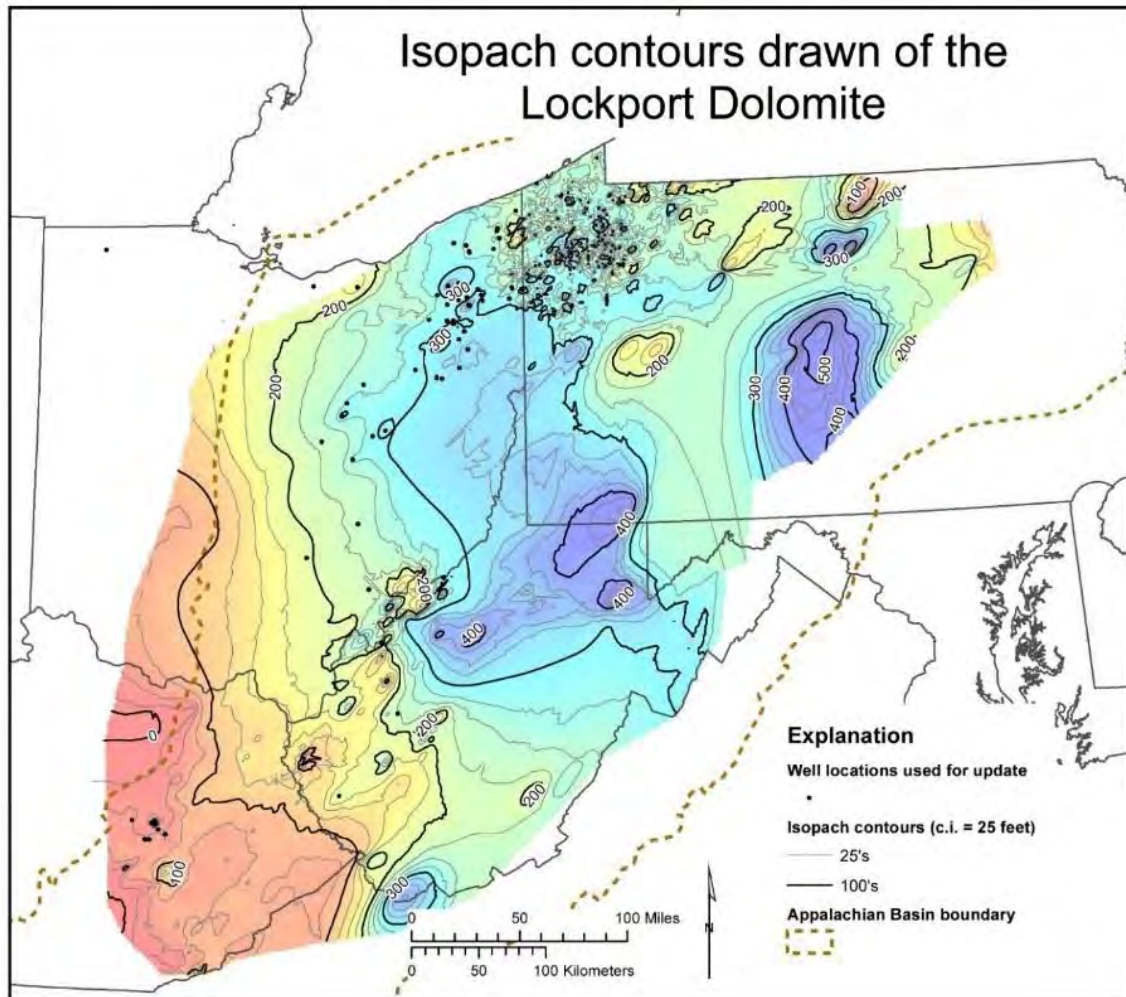
The Lockport Dolomite ranges from less than 1,500 feet (450 meters) above sea level in western Ohio and eastern Kentucky to more than 8,500 feet (2,600 meters) below sea level in western

Pennsylvania (Figure 3-16). Thickness of the Lockport Dolomite ranges from zero feet in eastern Kentucky to more than 500 feet (150 meters) in central Pennsylvania (Figure 3-17).



Source: Modified from Wickstrom et al. (2005).

Figure 3-16. Structure contours drawn on top of the Lockport Dolomite surface within the RPSEA study area.



Source: Modified from Wickstrom et al. (2005).

Figure 3-17. Isopach map of the Lockport Dolomite within the RPSEA study area.

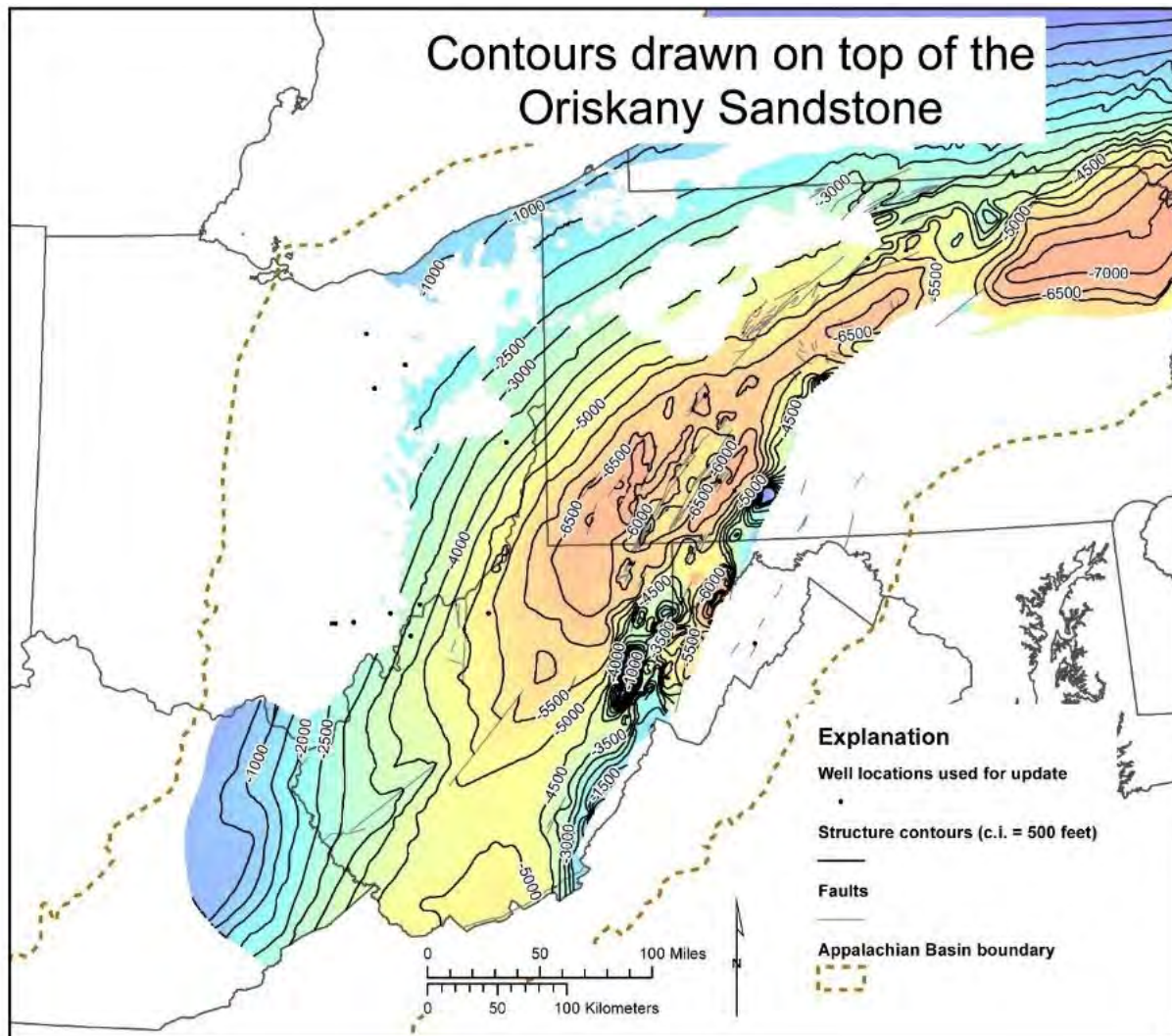
Depositional Environments/Paleogeography/Tectonism

The Lockport Dolomite is a fine to medium crystalline dolomite that was deposited on a carbonate shelf after the Taconic foreland basin was filled and prior to the onset of Acadian deformation. In the southern portion of the study area, the Lockport is underlain by the Keefer Sandstone, which represents an early siliciclastic-dominated, coastal to shallow marine environment (Noger et al., 1996). Locally within the Lockport, patch reef bioherms are developed that may be associated with changes in sea level, paleohighs, and syndepositional faulting (Noger et al., 1996).

3.3.8 Oriskany Sandstone

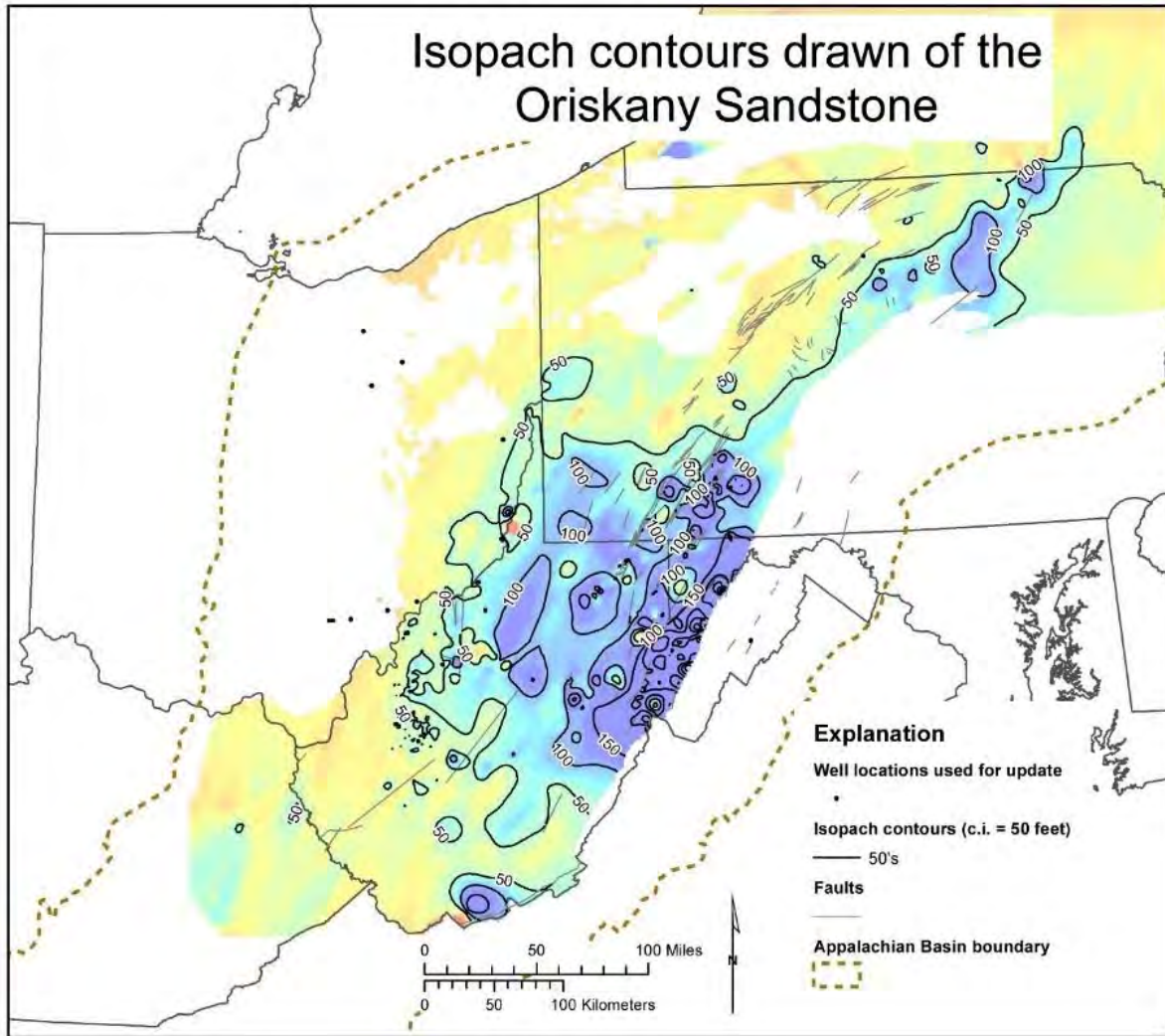
Depth and Thickness Ranges

The Oriskany Sandstone ranges from less than 500 feet (150 meters) below sea level in western Ohio and eastern Kentucky to more than 7,000 feet (2,130 meters) below sea level in northeastern Pennsylvania (Figure 3-18). Thickness of the Oriskany Sandstones ranges from zero feet where the sandstone pinches out to the west to more than 150 feet (45 meters) in central Pennsylvania (Figure 3-19).



Source: Modified from Wickstrom et al. (2005).

Figure 3-18. Structure contours drawn on top of the Oriskany Sandstone surface within the RPSEA study area.



Source: Modified from Wickstrom et al. (2005).

Figure 3-19. Isopach map of the Oriskany Sandstone within the RPSEA study area.

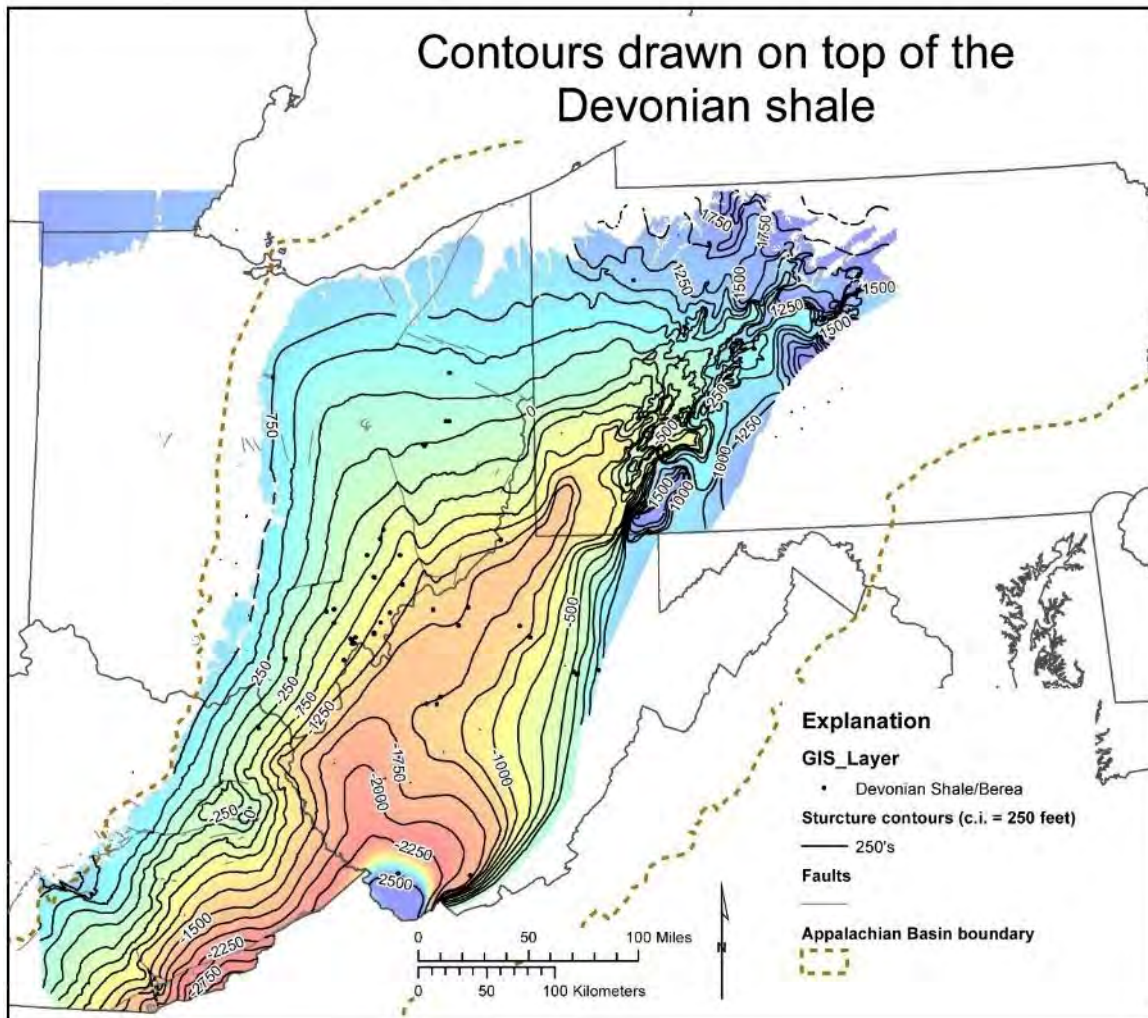
Depositional Environments/Paleogeography/Tectonism

The Oriskany Sandstone is a conformable to unconformity bound marine sandstone overlying the Helderberg formation that marks a regional transition from marine carbonate and evaporate deposition below to marine clastic-dominated deposition in the Devonian above. There are portions of the study area where the Oriskany is absent that may have had little or no sand originally deposited, or where the Oriskany was potentially eroded during an unconformity event related to the initiation of Acadian deformation. After deposition and burial, the Oriskany was displaced in the eastern portion of the study area into anticlines and synclines with associated faulting by Alleghenian thrust faults in the Silurian salts and potentially the Orovician shales (Harper et al., 1996).

3.3.9 Devonian Shale and Sandstone

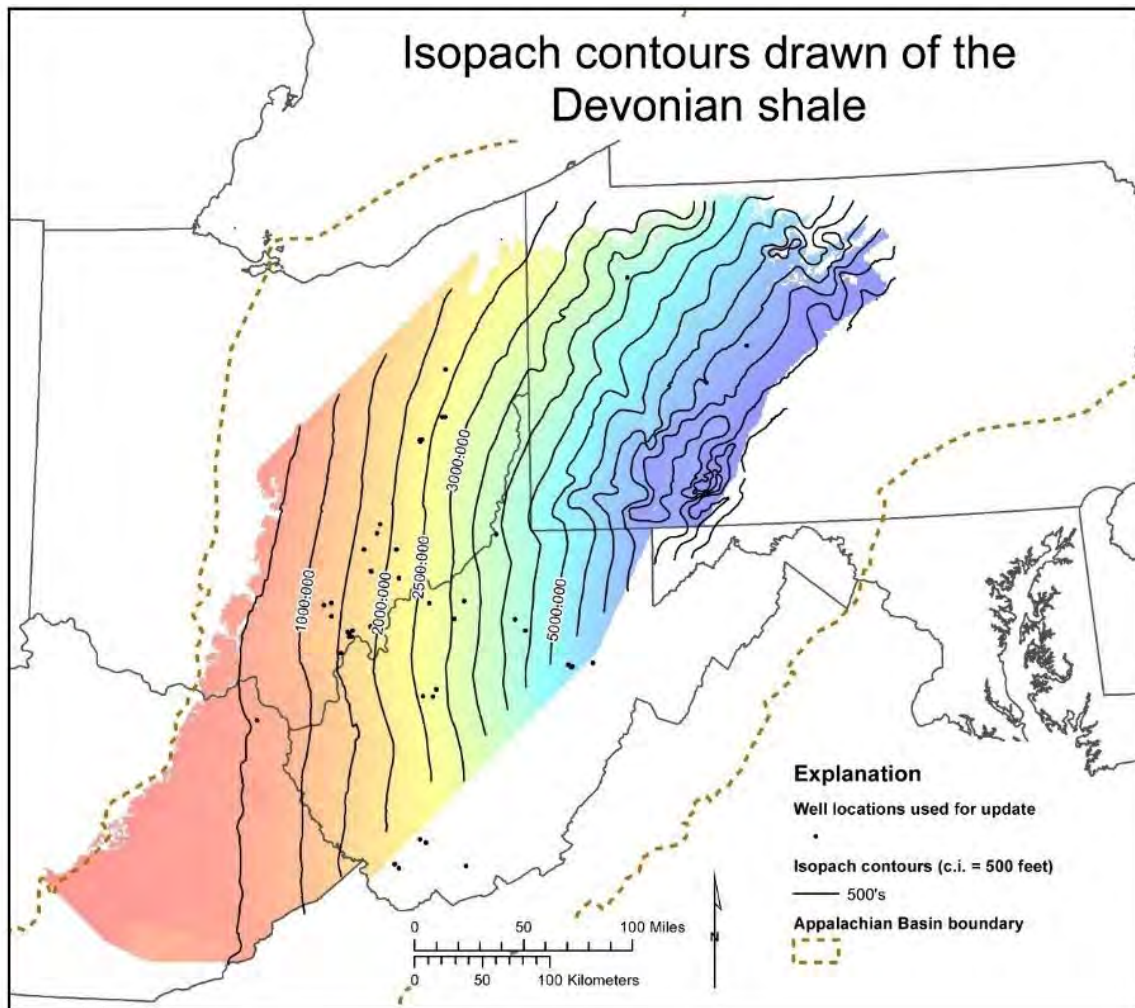
Depth and Thickness Ranges

The Devonian Shale ranges from outcropping at the surface along the northern and western portions of the study area to more than 2,500 feet (760 meters) below sea level in southern West Virginia (Figure 3-20). Thickness of the Devonian Shale ranges from zero feet where the shale outcrops to the west to more than 7,000 feet (2,100 meters) in central Pennsylvania (Figure 3-21).



Source: Modified from Wickstrom et al. (2005).

Figure 3-20. Structure contours drawn on top of the Devonian Shale surface within the RPSEA study area.



Source: Modified from Wickstrom et al. (2005).

Figure 3-21. Isopach of the Devonian Shale within the RPSEA study area.

Depositional Environments/Paleogeography/Tectonism

The Devonian Shale as mapped in this study represents a thick marine shale-dominated Catskill Delta clastic wedge that was the result of accommodation space created during the main foreland basin development during the Acadian Orogeny. The eastern portion of the deltaic clastic wedge which fans out to the west is more dominated by gray shales, siltstones, and sandstones being shed from the collision boundary to the east, whereas the western portion of the study area is dominated by gray and black shales deposited along the basin margin away from the clastic supply. Ettensohn (2008) proposed as many as four tectophases within the Acadian Kaskaskia sequence which encompass the various shale and quartzose reservoirs. The distribution of reservoir facies within the Devonian Shales siltstones of the Venango, Bradford, and Elk Groups is mainly controlled by the deltaic lobe channel distributions, but sand and siltstone development may have been influenced in some areas underlying Silurian Group salt movement and/or basement faulting. After deposition and burial, the Devonian Shale was displaced in the eastern

portion of the study area into anticlines and synclines with associated faulting by Alleghenian thrust faults in the Silurian salts and potentially the Ordovician shales.

3.4 Well Log Analysis

The objective of the well log analysis was to provide a basic understanding of general reservoir parameters for the injection zones and determine local and regional variability. The analysis involved a systematic review of all available geophysical logs for Class II brine disposal wells in the study area. Gross and net thickness, average porosity, and porosity-feet estimates for each injection zone were calculated. This information was then tabulated with the injection data for analysis.

The initial log data set included 688 raster TIFF images; 26 digital LAS files provided by the State Geologic Survey Partners for the wells which had logs in the state files; and 18 LAS data files from previous Battelle projects. The log suites were reviewed to see which images and log suites had sufficient numbers to be used for the study. For many of the older, pre-1970s drilled wells, very few or no logs were available. The common logs run on wells within the Appalachian Basin (Table 3-1) vary regionally and by formation, but gamma ray, bulk density, and neutron logs were present on most of the wells within the study area. For the wells with log images, the injection intervals were evaluated, and the curves for gamma ray, bulk density, neutron, and photoelectric effect were digitized over the injection interval and surrounding formations. Digilog Services was subcontracted to do the curve digitizing from the images. The current working well set with digital logs is 180 wells, most of which are in Ohio.

Table 3-1. Common logs run in Appalachian Basin.

Type of Log
Gamma Ray
Bulk Density
Neutron Porosity
Induction
Laterolog
Cement Bond
Perforation

The basic log curves used for the project are a gamma ray log for formation correlation and bulk density log for porosity and thickness evaluation. The carbonate injection intervals may have a more complex porosity profile that may need multiple logs for porosity calculations, but bulk density was used in this study for time considerations and to maintain consistency with many of the older, limited log suites available on the majority of the wells. The rock matrix densities used to calculate porosity from bulk density were chosen based on general formation lithology (Table 3-2). Formation porosity cutoffs of 6%, 8%, and 10% were used to calculate gross, net, average porosity, and porosity feet for each zone. Histograms of the porosity for each injection interval were generated for interval description and comparison (Figure 3-22).

Formation tops were compiled from the Ohio Geologic Survey for the Ohio wells, and tops from previous studies for the sub-Knox Unconformity wells were also used for the reservoir zone top and bottom distinctions (Greb et al., 2009; Battelle, 2013). Most of the sandstone units have gross and net thicknesses generally ranging from 20 to 110 feet within a single sandstone body,

such as the Balltown Sandstone (Figure 3-23), or a series of stacked sandstone bodies over a short interval, such as the Medina Sandstone (Figure 3-24). The carbonate injection intervals generally encompass thicker gross formation intervals with thin net thicknesses of high porosity, as in the Upper Copper Ridge Dolomite (Figure 3-25). Isopach maps for the injection interval gross thickness, net thickness, and porosity feet were generated to look at the distribution of reservoir parameters (Figure 3-26).

The reservoir parameters were compiled along with the general injection data for the wells to evaluate correlations and trends in different injection intervals. Appendix includes cross plots of cumulative injection vs 8% porosity feet for a reservoirs and type groupings for wells within the study area. The analyses for the Clinton Sandstone (Figure 3-27) and the Lockport Dolomite (Newburg) (Figure 3-28) show general characteristics of two different reservoir types in similar depth ranges. The Clinton Sandstone has higher porosity-feet values than the Lockport, but in general has smaller average injection rates (Figure 3-29). This trend indicates potential higher permeability within thin carbonate injection intervals as compared to sandstone intervals.

The wells with multiple injection zones, in either open holes or perforated through casing, present some challenges in identifying which zones are potentially taking fluid and how to sum reservoir parameters for analysis with the injection data. The limited log set of spinner logs and other flow tests, which are used to evaluate the injection intervals and identify consistent methods for reviewing the multiple-zone wells, is covered in Sections 4.7.6 and 7.4.

Table 3-2. Matrix density used for porosity calculations with mean and standard deviation for porosity.

6% Porosity Cutoff Values			
Injection Zones	Matrix Density	Mean Porosity	Standard Deviation
Salt Sandstone	2.68	0.121	0.036
Greenbrier LS	2.71	0.122	0.078
Maxton SS	2.68	0.076	0.011
Big Injun	2.68	0.184	0.071
Weir SS	2.68	0.116	0.04
Berea SS	2.68	0.166	0.084
2ND Berea SS	2.68	0.165	0.093
Bradford Group SS	2.68	0.195	0.052
Gordon SS	2.68	0.154	0.081
Balltown SS	2.68	0.1	0.024
Onondaga LS	2.71	0.126	0.055
Oriskany SS	2.68	0.081	0.014
Bass Island Dolomite	2.83	0.096	0.021
Lockport (Newburg Zone) Dolomite	2.83	0.092	0.042
Clinton SS	2.68	0.095	0.037
Medina SS	2.68	0.096	0.035
Beekmantown Dolomite	2.83	0.105	0.04
Rose Run SS	2.71	0.101	0.036
Upper Copper Ridge Dolomite	2.83	0.1	0.042
Copper Ridge B	2.71	0.102	0.033
Lower Copper Ridge Dolomite	2.83	0.103	0.042
Conasauga	2.71	0.104	0.038
Rome	2.83	0.103	0.042
Basal Sandstone	2.71	0.114	0.043

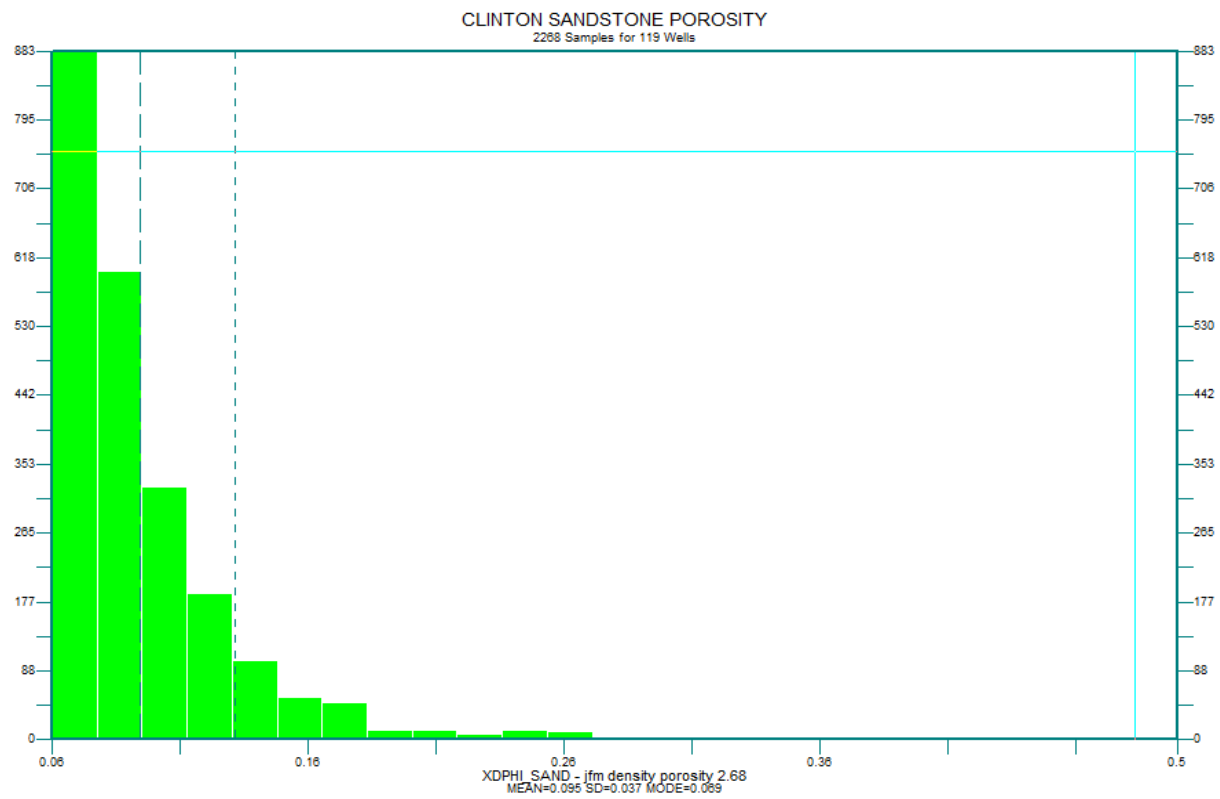
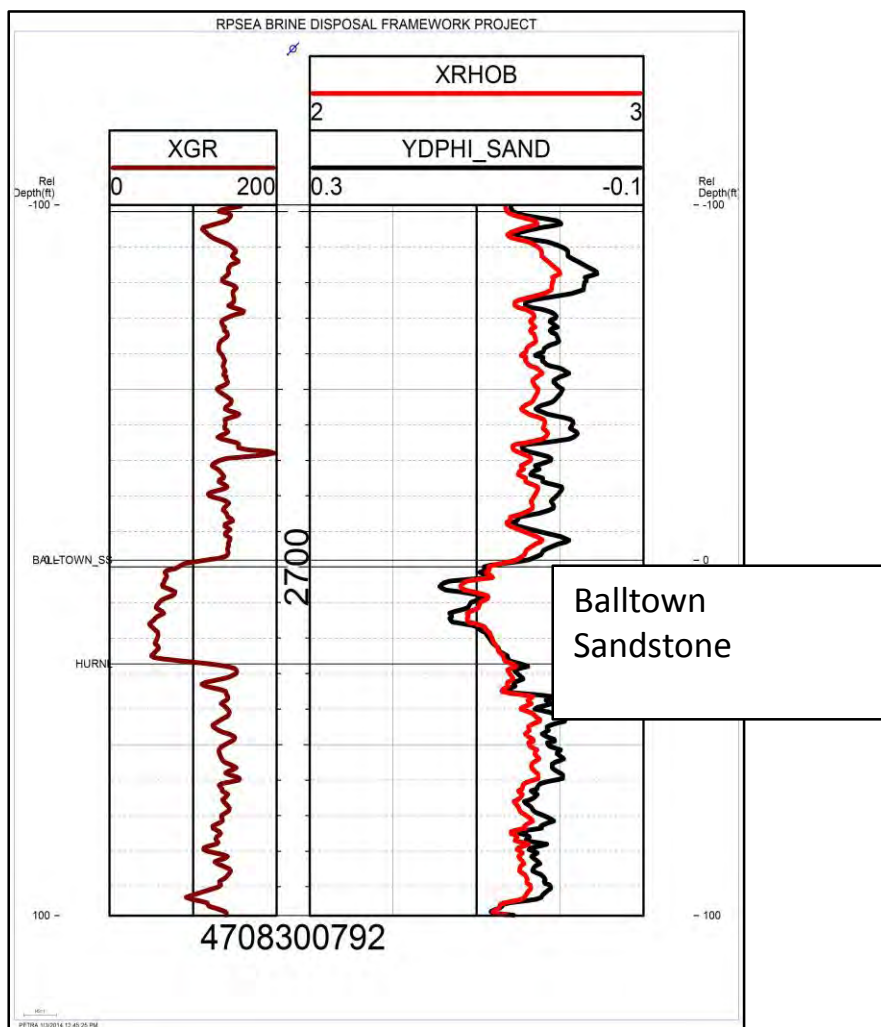
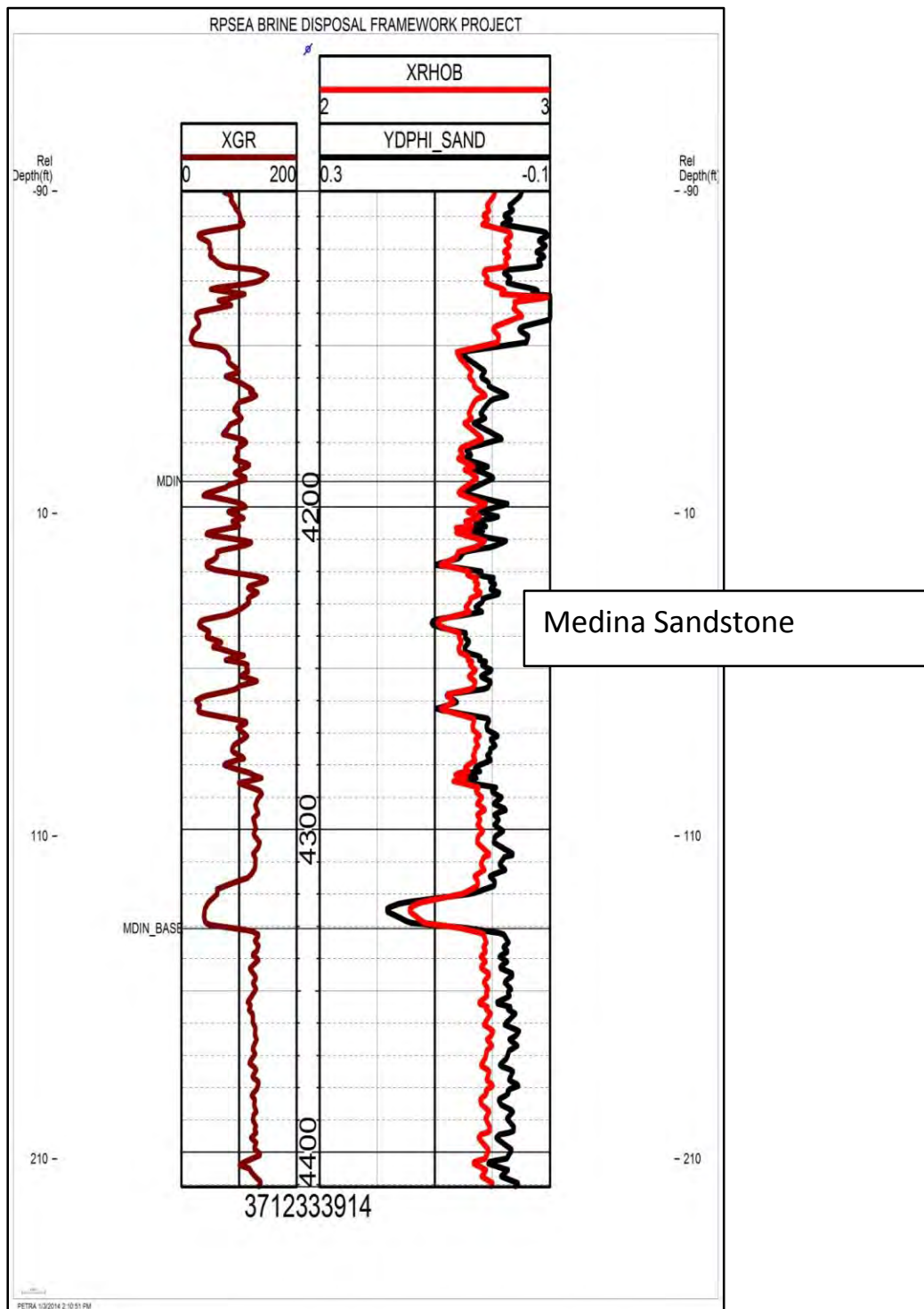


Figure 3-22. Clinton Sandstone porosity histogram.



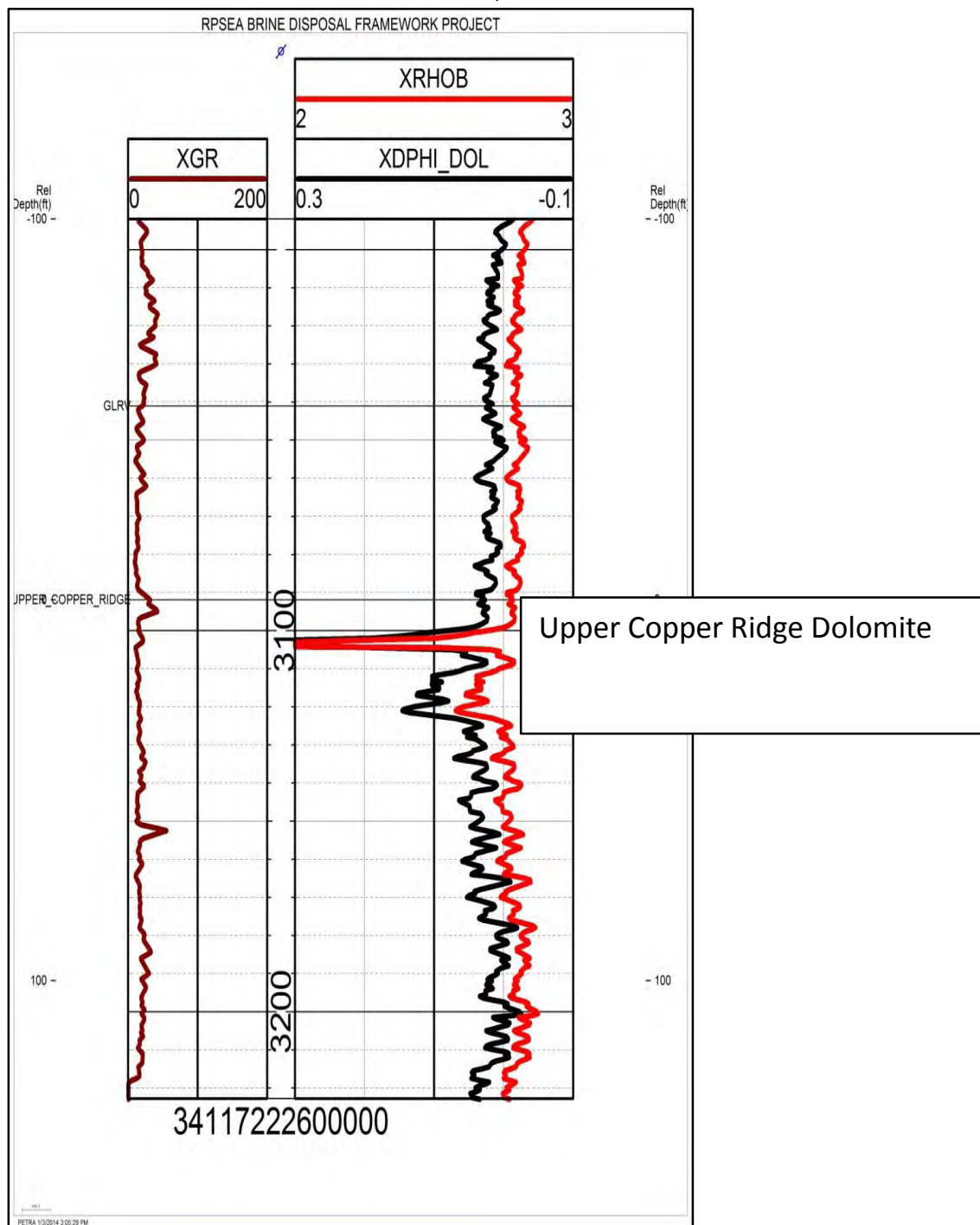
Note: XGR=gamma ray, XRHO=bulk density,
YDPHI_Sand=calculated porosity.

Figure 3-23. Balltown Sandstone type section, single thick sandstone bodies.



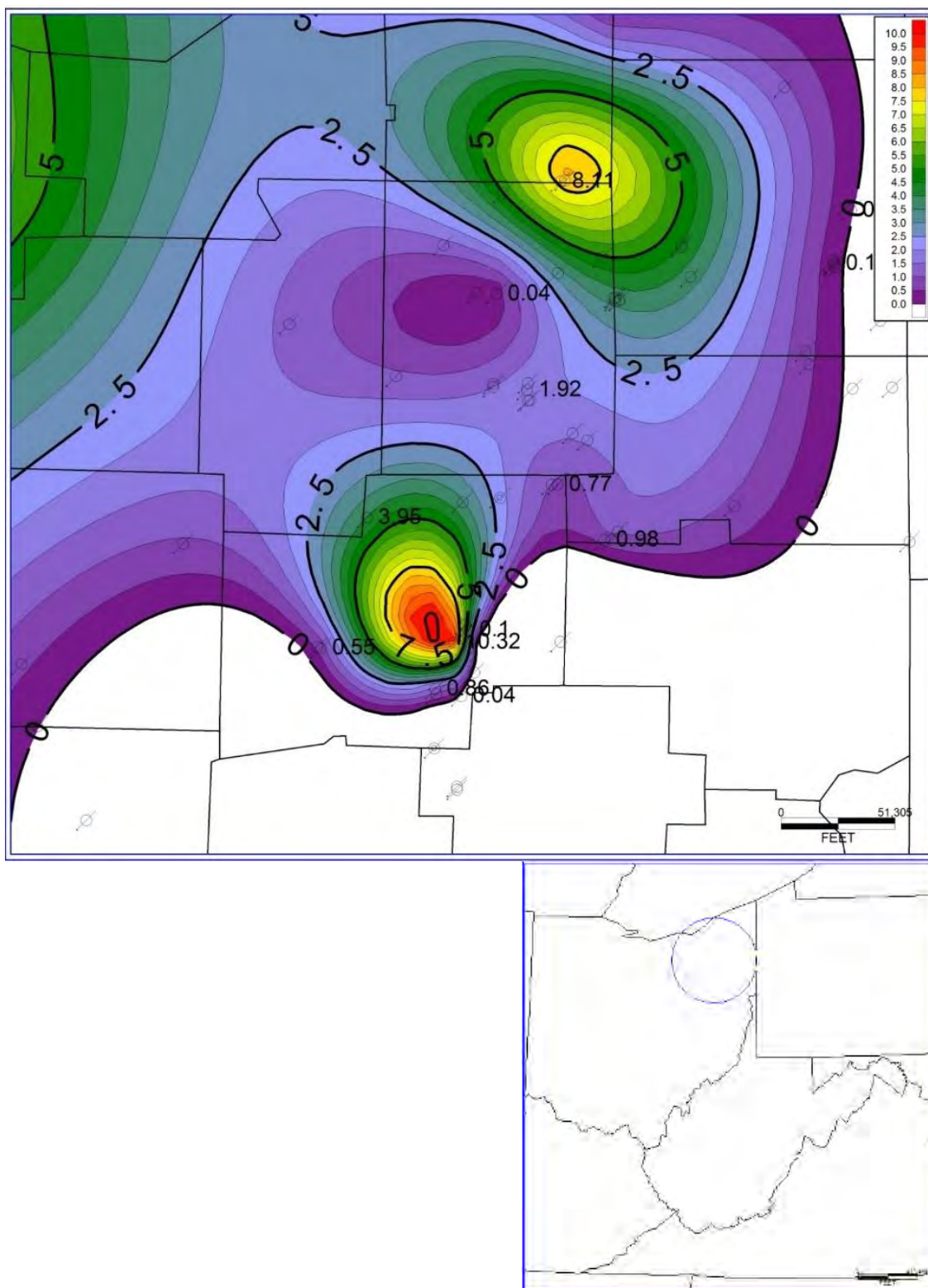
Note: XGR=gamma ray, XRHO=bulk density, YDPHI_Sand=calculated porosity.

Figure 3-24. Medina Sandstone type section with stacked sandstone bodies separated by shale.



Note: XGR=gamma ray, XRHO=bulk density, XDPHI_Dol=calculated porosity.

Figure 3-25. Upper Copper Ridge Dolomite type section showing thin injection intervals with high porosity.



Note: Contour interval = 0.5 porosity feet.

Figure 3-26. Lockport Dolomite (Newburg) porosity-feet isopach for 8% porosity cutoff in northeastern Ohio.

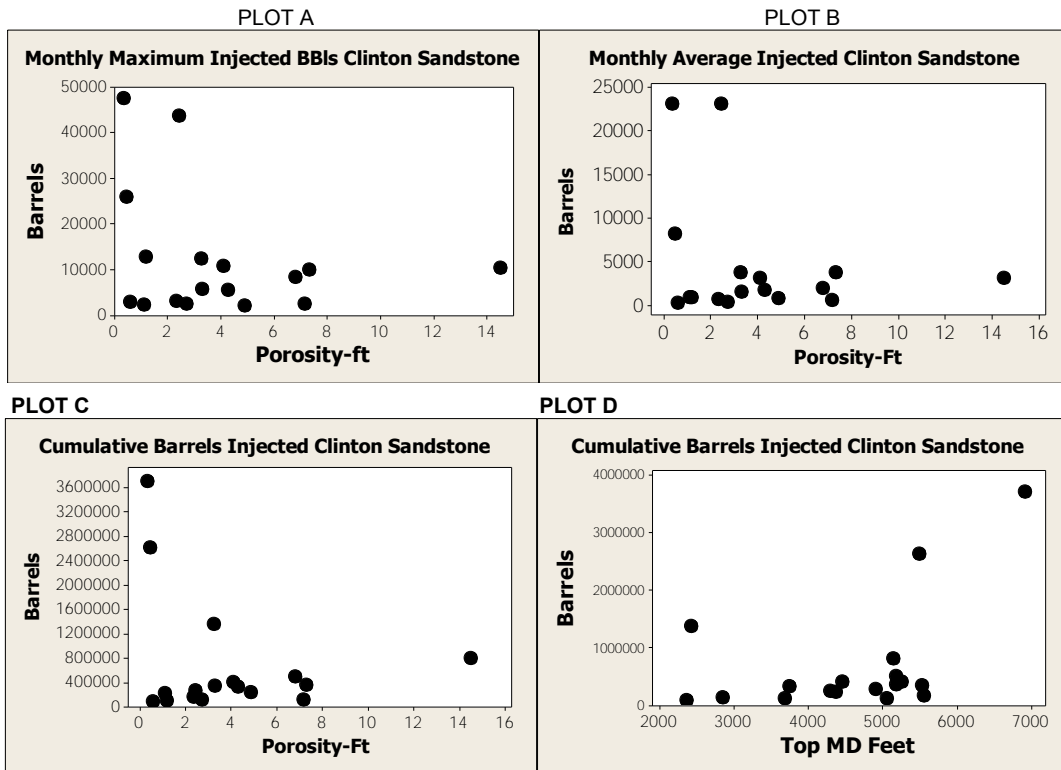


Figure 3-27. Clinton Sandstone reservoir parameters vs injection data.

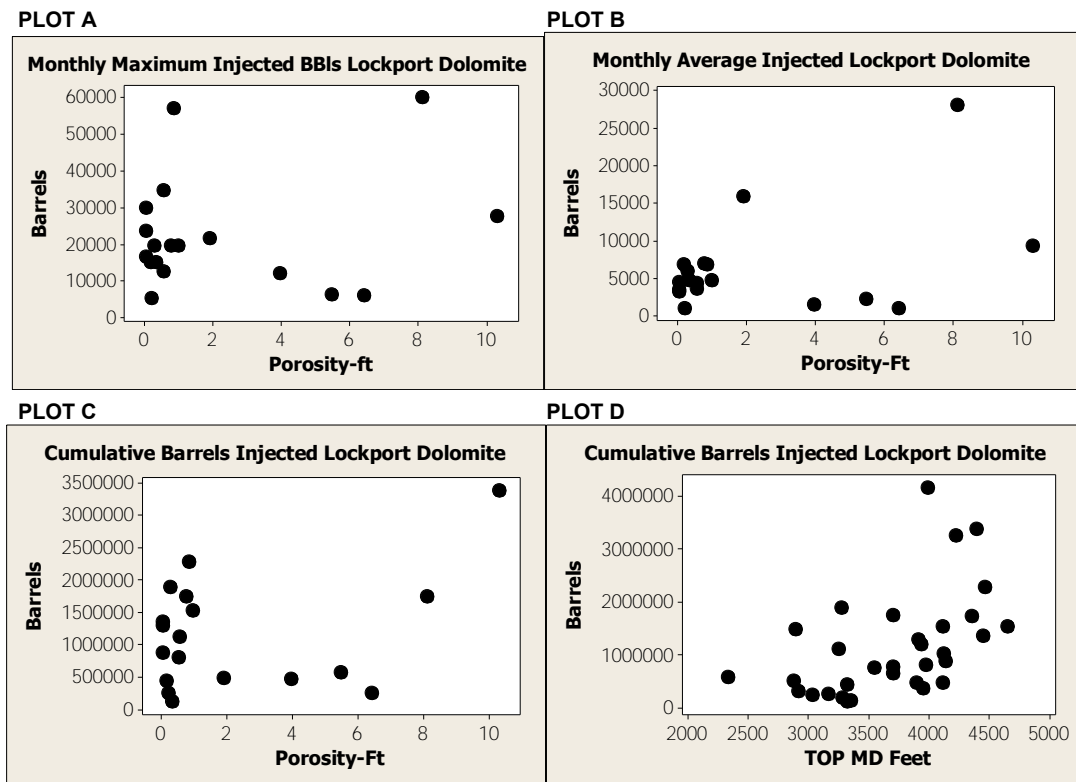


Figure 3-28. Lockport Dolomite (Newburg) reservoir parameters vs injection data.

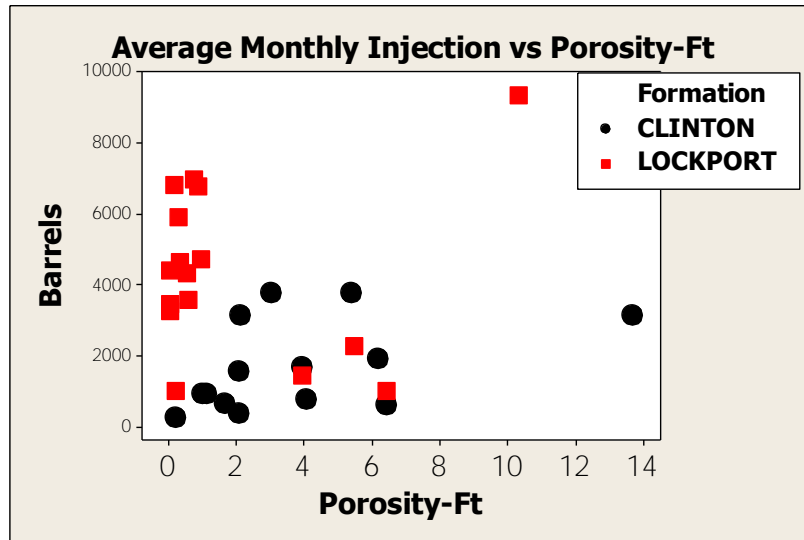


Figure 3-29. Average monthly injection vs porosity feet for 8% porosity cutoff for the Clinton Sandstone and Lockport Dolomite (Newburg).

3.5 Geotechnical Data

Geotechnical data were collected for key injection zones to aid in characterizing injection intervals and providing input for injection simulations. Hydraulic rock core test data were compiled from reports and state databases. These data were supplemented by ongoing efforts to collect and analyze pressure fall-off. Geomechanical data were collected from other research projects and rock core tests on samples from the state core repositories.

3.5.1 Hydraulic Core Test Data

Hydraulic rock core test data were compiled from key injection intervals. The hydraulic rock tests include laboratory measurements of rock porosity, density, and permeability. Geotechnical core test data for Kentucky were mainly available from the Kentucky Geological Survey KYCCS test well drilled in Carter, County, Kentucky, in 2013. In addition, data were compiled from the Weir sands and the ‘Corniferous’ Lockport Dolomite/Keefer (Figure 3-30). A total of 453 feet of whole core was collected from the well from intervals in the Beekmantown, Rose Run, Copper Ridge, and Mount Simon formations. Selected intervals were tested for permeability and porosity. Permeability and porosity core test data were available from 358 wells in Ohio, including both injection and other oil and gas wells (Figure 3-31). Much of this information was available from ‘Clinton’-Medina wells (140) and Berea wells (71). In Pennsylvania, 77 core test data were obtained from a ‘Clinton’-Medina well in Venango County. In West Virginia, geotechnical test data were obtained (95 whole core and 23 sidewall cores) from a well in Mason County that penetrated the Knox-Basal sandstone interval (Sminchak et al., 2006). Hydraulic rock core test data for the northern Appalachian Basin were also reviewed from other research.

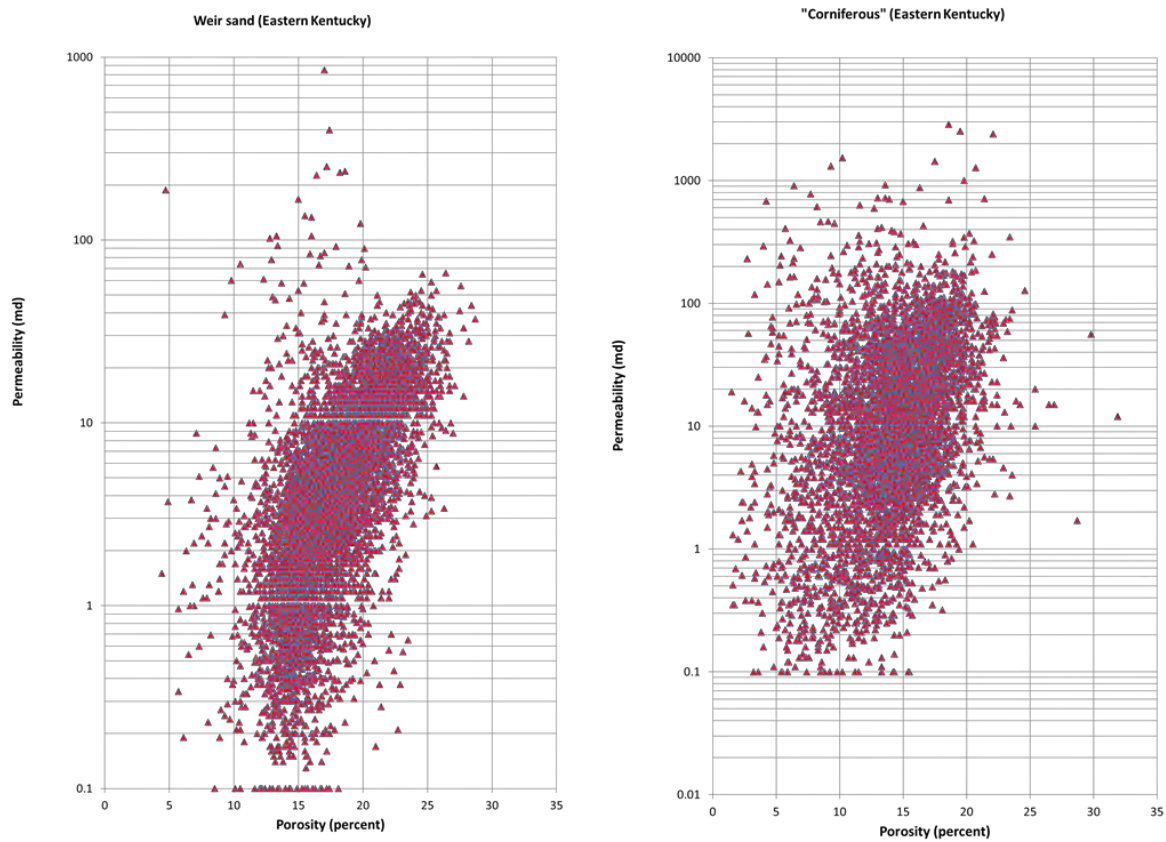


Figure 3-30. Rock core with permeability and porosity data for Kentucky.

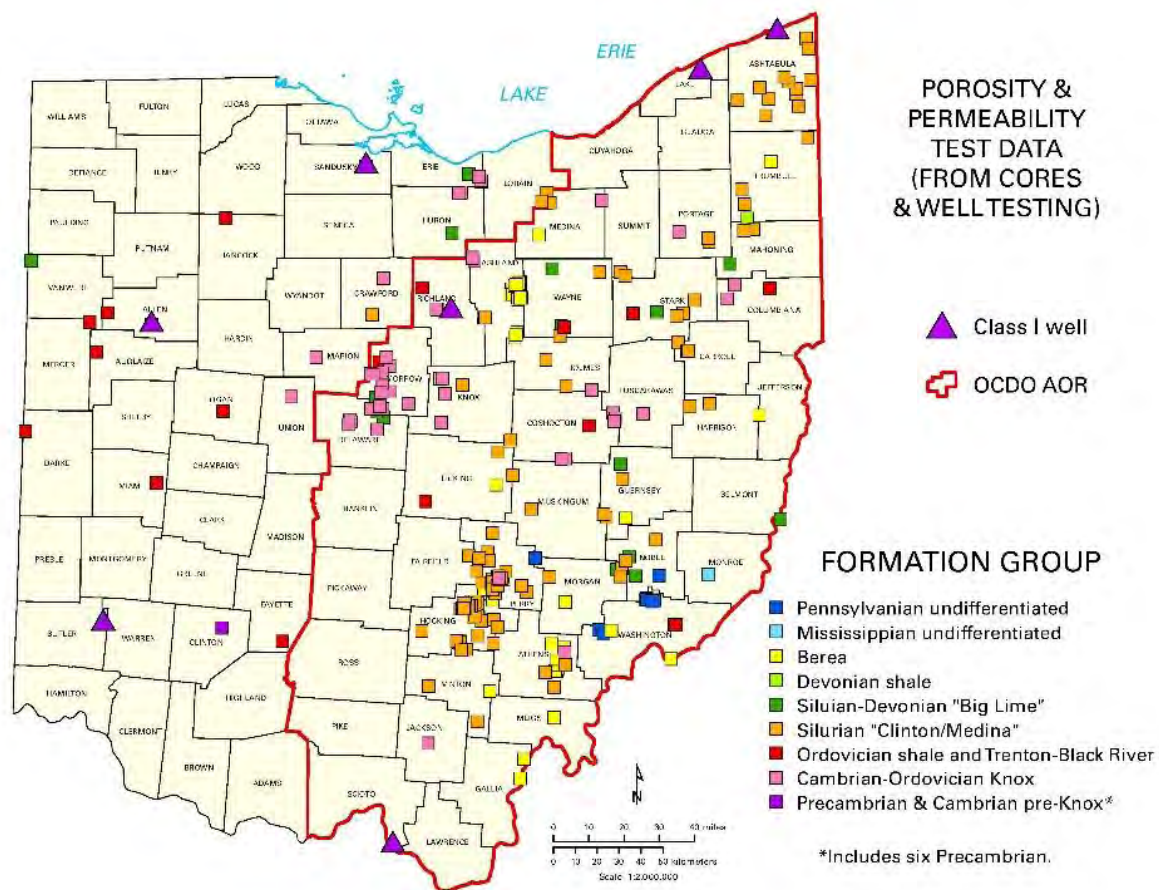


Figure 3-31. Rock core with permeability and porosity data for Ohio.

3.5.2 Geomechanical Core Testing

Geomechanical properties (Poisson's ratio, Young's modulus, and compressibility) measured on rock core samples were compiled from other research for the Northern Appalachian Basin for the geomechanical analysis of the effect of brine injection. In general, few geomechanical data are available, because the tests have only recently become more common as test methods and hydraulic fracturing methods have progressed. Consequently, samples from state core repositories were collected and tested under this project to supplement the existing dataset.

Existing geomechanical test results were obtained from three wells in the study area. Results were obtained for 10 tests completed on rocks from the Knox-Basal Sandstone interval for a well in Mason County, West Virginia (Sminchak et al., 2006). Test data were also obtained on samples from the Rose Run and Basal Sandstone formations from a well in Tuscarawas County, Ohio, and four samples from the Rose Run Sandstone formation from a well in Coshocton County, Ohio. Table 3-3 summarizes the results of compressive strength properties. Compressive strength is lower for shale zones (Utica), moderate in the Rose Run Sandstone, and

higher in the deeper dolomite zones (Beekmantown and Mount Simon). Table 3-4 summarizes the sonic properties collected from existing wells.

Table 3-3. Summary of compressive strength properties compiled from existing wells in the study area.

Well	Formation	Depth (ft)	Confining Pressure (psi)	Compressive Strength (psi)	Static Young's Modulus ($\times 10^6$ psi)	Static Poisson's Ratio
Fred Barth #3	Utica	5661.50	2500	19493	1.87	0.23
Fred Barth #3	Utica	5680.50	2500	19921	2.15	0.23
Fred Barth #3	Utica	5683.50	2500	25790	3.11	0.25
Fred Barth #3	Trenton	5790.00	2500	19397	1.93	0.25
AEP#1	Wells Ck	7166.10	1300	50972	9.48	0.28
AEP#1	Beekmantown	7745.00	1400	51600	10.51	0.30
AEP#1	Rose Run	7763.00	1400	34484	7.65	0.23
AEP#1	Rose Run	7818.60	1400	32753	6.09	0.20
ODGS CO2 No. 1	Rose Run	7441.00	2600	41110	4.818	0.384
ODGS CO2 No. 1	Mount Simon	8561.00	2950	45360	5.649	0.252

Table 3-4. Summary of sonic properties compiled from existing wells in the study area.

Well	Formation	Depth (ft)	Confining Pressure (psi)	Bulk Density (g/cc)	Ultrasonic Wave Velocity				Dynamic Elastic Parameter			
					Compressional		Shear		Young's Modulus ($\times 10^6$ psi)	Poisson's Ratio	Bulk Modulus ($\times 10^6$ psi)	Shear Modulus ($\times 10^6$ psi)
					ft/sec	μ sec/ft	ft/sec	μ sec/ft				
Redman-Barth #3	Utica	5661.50	2500	2.56	13418	74.53	7636	130.96	5.06	0.26	3.52	2.01
Redman-Barth #3	Utica	5680.50	2500	2.55	13789	72.52	8172	122.37	5.64	0.23	3.47	2.29
Redman-Barth #3	Utica	5683.50	2500	2.59	15272	65.48	8801	113.62	6.78	0.25	4.54	2.71
Redman-Barth #3	Trenton	5790.00	2500	2.61	14293	69.96	8074	123.85	5.79	0.27	4.12	2.29
AEP#1	Black River	6825.00	1200	2.71	18885	52.95	9560	104.60	8.56	8.85	3.33	0.33
AEP#1	Gull River	7025.00	1200	2.69	17721	56.43	9147	109.32	7.34	8.00	3.03	0.32
AEP#1	Beekmantown	7700.00	1400	2.80	18788	53.23	9785	102.19	8.51	9.51	3.62	0.31
AEP#1	Copper Ridge	8219.00	1500	2.83	19950	50.13	10315	96.95	9.75	10.68	4.05	0.32
AEP#1	Nolichucky	8575.00	1500	2.79	19227	52.01	10074	99.27	8.81	10.00	3.81	0.31
AEP#1	Maryville	9004.00	1600	2.61	17284	57.86	8957	111.65	6.76	7.44	2.83	0.32
ODGS CO2 No. 1	Rose Run	7441.00	2600	2.50	15282	65.44	9261	107.98	7.00	0.21	4.02	2.89
ODGS CO2 No. 1	Mount Simon	8561.00	2950	2.45	14839	67.39	9176	108.98	6.62	0.19	3.56	2.78

Additional rock samples were collected and tested for geomechanical tests under this project. Each state reviewed available rock core in its state repositories and identified samples suitable for testing from key injection zones. Ten samples (plus one backup sample) were selected and sent to a geotechnical laboratory for geomechanical testing (Table 3-5). The samples were tested for compressive strength and sonic properties by a geotechnical laboratory. Table 3-6 presents results from the testing on rock cores collected in this study.

Table 3-5. Rock core samples selected for geomechanical testing.

Formation	State	County	Well API	Depth (ft)	General Description
Big Injun/MS	WV	Roane	4708700963	2186.87-2187.63	Tan-pinkish fine- to medium-grained sandstone
Clinton	OH	Hocking	3407321968	2917	Light tan silty fine sandstone
Medina	PA	Somerset	3711120087	8885.65-8886.15	Gray, fine-grained carbonate
Oriskany	PA	Venango	3712136455	5292-5292.35	Dk gray shale
Newburg	WV	Kanawha	4703902571	5155.5	Tan-gray silty fine sandstone
Rose Run	OH	Coshocton	3403124092	6926.7	Brown-gray fine sandstone
Rose Run	KY	Carter	1604300150	3312.75-3313.10	Tan, fine-grained sandstone
Copper Ridge	KY	Carter	1604300150	3790.30-3790.80	Tan vugular dolomite
Copper Ridge/ Trempealeau	OH	Morrow	3411721478	2950.5-2951	Tan vugular dolomite
Mount Simon SS	KY	Carter	1604300150	4686.35-4686.80	Gray dense sandstone
Bradford ^a	PA	Clarion	3703120165	1930-1930.4	Gray silty shale

a. Backup sample.

Table 3-6. Summary of geomechanical properties tested on rock samples from key injection intervals.

Sample No.	Formation	Depth (ft)	Confining Pressure (psi)	Compressive Strength (psi)	Static Young's Modulus (x10 ⁶ psi)	Static Poisson's Ratio
5-RMV	Big Injun	2186.87	730	30749	5.53	0.15
6-RMV	Clinton	2543.00	850	18882	3.65	0.23
7-RMV	Trempealeau	2950.50	1050	17473	5.43	0.16
1-RMV	Rose Run	3312.81	1350	24111	5.43	0.19
2-RMV	Copper Ridge	3790.30	1350	24544	8.33	0.19
3-RMV	Mount Simon	4686.35	1560	23254	4.56	0.30
8-RMV	Newburg	5155.76	1720	39265	6.63	0.16
9-RMV	Oriskany	5292.00	1760	50279	7.13	0.16
10-RMV	Rose Run	6926.70	2310	32949	5.78	0.16
11-RMV	Medina	8885.65	3160	43004	7.09	0.28

Sample No.	Depth (ft)	Formation	Confining Pressure (psi)	Bulk Density (g/cc)	Ultrasonic Wave Velocity				Dynamic Elastic Parameter			
					Compressional		Shear		Young's Modulus (x10 ⁶ psi)	Poisson's Ratio	Bulk Modulus (x10 ⁶ psi)	Shear Modulus (x10 ⁶ psi)
					ft/sec	μsec/ft	ft/sec	μsec/ft				
5-RMV	2186.87	Big Injun	730	2.65	16544	60.44	10630	94.07	9.28	0.15	4.40	4.04
6-RMV	2543.00	Clinton	850	2.25	12500	80.00	7966	125.54	4.44	0.16	2.17	1.92
7-RMV	2950.50	Trempealeau	1050	2.65	16788	59.57	8655	115.54	7.04	0.32	6.49	2.67
1-RMV	3312.81	Rose Run	1100	2.41	16075	62.21	8295	120.56	5.89	0.32	5.41	2.23
2-RMV	3790.30	Copper Ridge	1350	2.71	21770	45.93	11010	90.82	11.74	0.33	11.38	4.42
3-RMV	4686.35	Mount Simon	1560	2.35	14209	70.38	8961	111.60	5.96	0.17	3.01	2.55
8-RMV	5155.76	Newburg	1720	2.56	14150	70.67	8867	112.77	6.39	0.18	3.29	2.71
9-RMV	5292.00	Oriskany	1760	2.55	13945	71.71	9391	106.48	6.59	0.09	2.65	3.03
10-RMV	6926.70	Rose Run	2310	2.58	17417	57.42	10050	99.50	8.78	0.25	5.86	3.51
11-RMV	8885.65	Medina	3160	2.59	16778	59.60	9949	100.51	8.48	0.23	5.21	3.45

* Velocities determined after applying 1000 psi differential stress.

Sample No.	Depth (ft)	Formation	Thickness (inch)	Diameter (inch)	Density (g/cc)	Max. Load (lb)	Brazilian Tensile Strength (psi)
5-BZ	2,186.87	Big Injun	0.599	0.996	2.64	1597	1704
6-BZ	2,543.17	Clinton	0.565	0.972	2.21	542	628
7-BZ	2,950.58	Trempealeau	0.552	0.973	2.62	913	1081
1-BZ	3,312.84	Rose Run	0.532	0.972	2.14	586	721
2-BZ	3,790.57	Copper Ridge	0.529	0.973	2.78	1064	1315
3-BZ	4,686.45	Mount Simon	0.567	0.972	2.26	362	419
8-BZ	5,155.81	Newburg	0.603	0.973	2.55	1416	1538
9-BZ	5,292.08	Oriskany	0.456	0.973	2.53	1233	1771
10-BZ	6,926.74	Rose Run	0.588	0.972	2.61	1012	1127
11-BZ	8,885.73	Medina	0.597	0.974	2.37	1233	1351

3.6 Hydrologic Data

Hydrologic data were collected to better define subsurface conditions and characterize the fluids being injected into brine disposal wells in the Northern Appalachian Basin. Reservoir conditions and injection fluids were summarized for the study area.

3.6.1 Reservoir Conditions

Reservoir conditions include the temperature, pressure, salinity, and fluid saturation conditions in the injection zones. These parameters affect injection performance and fluid flow. Temperature data were reviewed from bottomhole temperatures recorded in geophysical well logs and other research (Muffler, 1979; NREL, 2013). Reservoir pressure data were reviewed from sources on oil and gas reservoirs and other research (Rennick and Whieldon, 1970; Clifford, 1973; Warner, 1988; Roen and Walker, 1996). Similarly, the salinity of formation fluids was summarized from research on brine properties in the Appalachian Basin (Hoskins, 1947; Sanders, 1991; Dresel and Rose, 2010). Fluid saturation was also derived from geophysical well logs where possible. In general, most reservoir parameters in the Appalachian Basin are related to depth. Temperature, pressure, and salinity increase with depth. In addition, many depleted oil and gas fields being utilized for injection are highly depressurized. Consequently, conditions need to be evaluated on a site- or field-specific basis for detailed reservoir evaluation.

3.6.2 Injection Fluids

Data on injection fluids were compiled to provide input for simulations of the injection process. Sources of information on injection fluids included Ohio Department of Natural Resources (ODNR) inspection reports, the United States Geological Survey (USGS) Database, the Marcellus Shale Commission Report, and a New York State Energy Research and Development Authority (NYSERDA) report, which provided in-depth produced water characteristics in the Appalachian Basin (USGS, 2002; Hayes, 2011; AMTV, 2012; URS, 2011; Cramer, 2011; ProChemTech, 2013; Tomastik, 2013). These characteristics were tabulated and organized into geographical regions (Figure 3-32). Pennsylvania was divided into four quadrants (northwest, northeast, southwest, and southeast). Ohio was divided into five regions (northwest, northeast, southwest, southeast, and central Ohio characteristics). West Virginia was divided into a north and south region. New York had only one region, because most samples were from southwest New York.

The average and standard deviation for each water parameter were calculated across geographical regions and for the sample set as a whole. The Marcellus Shale Commission report provided time-dependent water characteristics, so the latest occurring sample (typically 14 or 90 days after the fracturing event) was used in the average. The concentration of the formation fluid parameters increases drastically with time, while the volume of flowback produced decreases. The current trend in the industry is to recycle as much flowback water as possible. The latest available sample was therefore used, since this highly concentrated brine is the water most likely to be disposed of in a UIC well.

The regional and overall averages and standard deviations were then taken, and the water quality parameters were pared down to two types: those relevant to creating charge balances and

performing geochemical analyses, and those of concern for scaling or fouling of the injection well.

Additionally, data were found for the density, compressibility, and viscosity of sodium chloride solutions of varying concentrations and at various temperatures and pressures. The total dissolved solids (TDS) values were assumed to be primarily sodium chloride, and simple correlations were made to estimate density, compressibility, and viscosity of produced brines in the Marcellus (Kestin et al., 1981; Rogers and Pitzer, 1982; The Salt Institute, 2013).

The correlations for density, compressibility, and viscosity can be combined with the data assembled and used to perform modeling of the geochemistry for injection wells that accept water from a specific region. An example of this process is provided in Table 3-7, which provides an estimate of the fluid density from the correlation, given TDS and temperature (assumed to be 25° Celsius [C]). The average and standard deviation of estimated fluid density are provided by region. This will allow for reservoir modeling of injection wells that accept water from one of the regions listed in Table 3-7. Table 3-8 summarizes data on specific chemistry of the fluid samples.

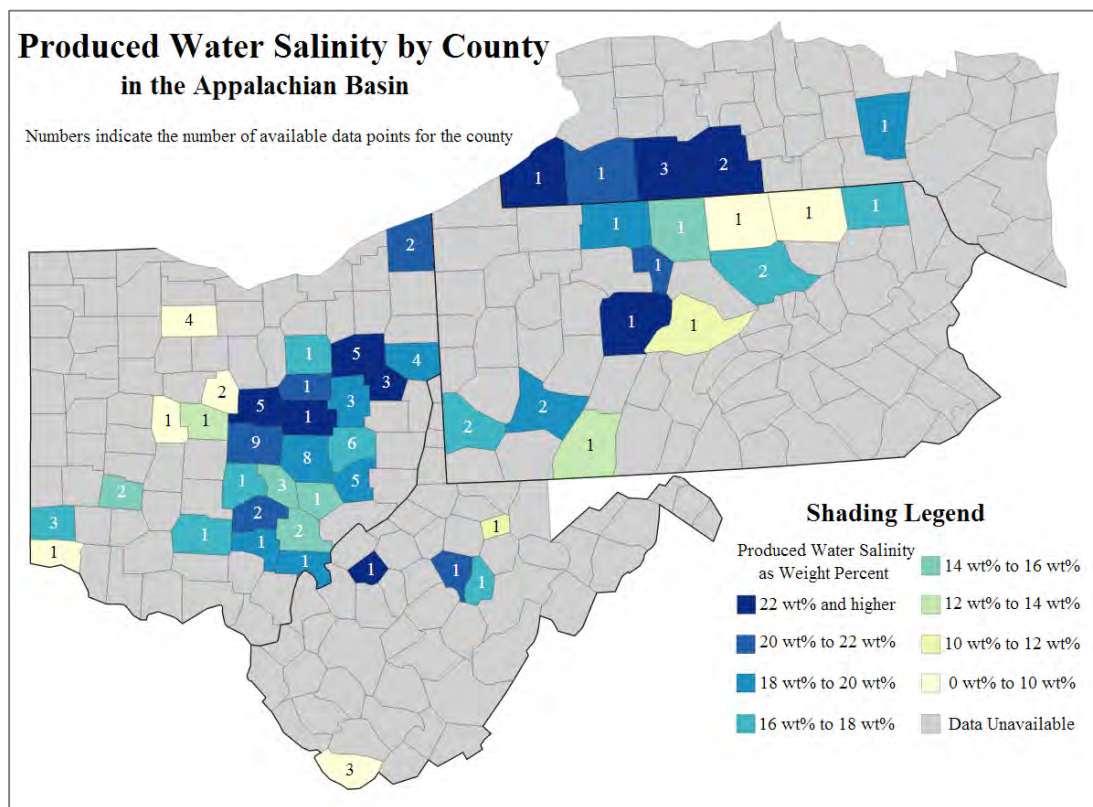


Figure 3-32. Salinity by county for produced water.

Table 3-7. Estimated fluid density by region, at a temperature of 25° C.

Region	Number of Samples	Estimated Fluid Specific Gravity @ 25° C	
		Average	Standard Deviation
Overall	113	1.13	0.05
Central Ohio	31	1.14	0.04
NE Ohio	19	1.15	0.03
NE Pennsylvania	5	1.07	0.07
NW Ohio	4	1.04	0.01
NW Pennsylvania	5	1.13	0.04
NY	8	1.17	0.01
SE Ohio	20	1.13	0.03
Southern WV	3	1.04	0.00
SW Ohio	1	1.01	
SW Pennsylvania	10	1.12	0.05

Table 3-8. Specific chemistry of fluid samples by region.

Description (mg/L)	Aluminum (Total)	Barium (Total)	Bicarbonate Alkalinity (as CaCO ₃)	Boron	Bromide (Total)	Calcium (Total)	Chloride (Total)	Hardness (CaCO ₃)	Iron (Total)	Magnesium (Total)
Overall Average	8.63	2,283	79.33	185.93	944.17	25,113	132,815	60,604	137.90	3,041
Overall Std Dev	21.71	2,946	61.75	828.50	519.44	14,282	54,929	33,115	108.34	2,138
Central Ohio Average	17.50	3	21.55		1,580.00	30,844	147,551	103,500	181.50	4,642
Central Ohio Std Dev	1.98	2	11.67		14.14	13,469	48,898	3,536	75.66	2,029
NE Ohio Average	4.41	64	169.00		509.00	30,461	159,684	23,500	82.00	3,496
NE Ohio Std Dev						9,141	38,589			1,311
NE Pennsylvania Average	4.21	3,501	91.90	835.59	376.16	10,297	74,446	42,466	166.46	740
NE Pennsylvania Std Dev	5.42	3,410		1858.41	448.57	9,825	73,082	46,957	110.99	736
NW Ohio Average						3,345	37,523			1,396
NW Ohio Std Dev						1,344	10,313			383
NW Pennsylvania Average	28.73	4,892	30.90	11.34	1,158.80	23,780	142,964	78,000	100.14	1,568
NW Pennsylvania Std Dev	56.18	4,448		5.90	427.00	12,274	52,975	32,023	42.04	642
NY Average						40,718	182,112			4,208
NY Std Dev						18,219	21,805			2,899
SE Ohio Average	9.75	96	49.00	5.64	974.00	24,231	133,742	48,100	197.00	2,547
SE Ohio Std Dev	2.34	13	0.99	5.33	36.77	7,874	30,211	1,414	15.56	1,928
Southern WV Average						4,828	41,948			569
Southern WV Std Dev						383	2,343			46
SW Ohio (One Sample)						477	7,100			249
SW Pennsylvania Average	0.81	1,230		32.74	1,132.43	18,019	115,406	65,875	172.78	1,686
SW Pennsylvania Std Dev	0.77	1,380		45.52	523.49	12,556	55,409	25,682	165.98	1,105
Northern WV Average	0.59	2,846		39.62	982.67	16,920	120,425	55,333	80.97	1,915
Northern WV Std Dev	0.39	1,816		40.37	336.72	9,195	47,914	23,714	29.92	1,528

Table 3-8. Specific chemistry of fluid samples by region. (cont)

Description (mg/L)	Manganese (Total)	pH	Potassium (Total)	Sodium (Total)	Strontium (Total)	Sulfate (Total)	TDS	Total Acidity (CaCO ₃)	Total Alkalinity (CaCO ₃)	TSS
Overall Average	10.30	6.04	1,182	50,335	2,981	530.39	218,944	325.25	66.81	312.80
Overall Std Dev	8.86	0.68	1,446	20,036	2,429	430.25	88,058	214.22	47.43	277.33
Central Ohio Average	26.35	5.88	1,185	52,655	929	706.27	240,867	407.50	21.55	253.00
Central Ohio Std Dev	5.30	0.63	636	15,096	10	469.55	78,862	88.39	11.67	19.80
NE Ohio Average	5.99	5.87	1,268	62,411	914	599.82	261,211	236.00	169.00	125.00
NE Ohio Std Dev		0.51	296	15,408		295.43	61,722			
NE Pennsylvania Average	5.12	6.28	343	27,852	2,653	186.39	127,822	298.10	76.02	494.30
NE Pennsylvania Std Dev	4.49	0.43	353	26,090	2,653	262.49	125,378	350.04	36.98	427.16
NW Ohio Average		7.15		18,317		908.00	61,570			
NW Ohio Std Dev		0.91		4,468		386.26	16,325			
NW Pennsylvania Average	14.03	5.90	1,257	50,360	5,786	362.57	226,800	296.64	50.32	160.96
NW Pennsylvania Std Dev	12.76	0.69	969	29,353	1,841	560.72	77,186	151.86	32.27	142.02
NY Average		6.04	1,586	63,293		327.88	294,195			
NY Std Dev		0.94	1,768	10,900		504.69	30,057			
SE Ohio Average	20.60	5.80	1,110	56,050	454	627.35	221,077	349.00	49.00	190.00
SE Ohio Std Dev	7.35	0.50	492	11,843	325	321.49	49,157	16.97	0.99	4.24
Southern WV Average		6.44	360	18,609		0.00	66,788			
Southern WV Std Dev		0.24	30	1,038		0.00	3,748			
SW Ohio		7.99	115	3,800		310.00	13,400			
SW Pennsylvania Average	8.21	5.93	707	43,256	2,926	43.19	196,443	304.75	52.84	369.25
SW Pennsylvania Std Dev	5.05	0.30	1,167	19,710	2,178	25.59	88,743	189.23	33.02	340.54
Northern WV Average	4.83	6.03	1,289	49,832	3,360	79.10	223,299	572.50	70.87	272.67
Northern WV Std Dev	4.28	0.39	1,025	19,433	336	89.95	78,534	498.51	64.65	150.86

3.7 Regional Geocellular Model

Geologic maps and cross sections were integrated into a 3D framework model for the region. The model is based on maps of key injection formations for the region. The map data for the key injection zones were input into EarthVision© geologic visualization software. These maps were based on stratigraphy determined in well logs from oil and gas wells in the region. The model illustrates the geologic structure, formation thickness, and subsurface features for the region in relation to injection wells.

Figure 3-33 shows a geologic fence diagram based on the model. The model shows key injection formation top layers for the ground surface, Devonian Shale, 'Clinton'-Medina sandstone, Cambrian basal sand, and Precambrian. Figure 3-34 shows an east-west view of the diagram.

Overall, the regional framework helps to depict the general setting for Class II brine disposal wells in the region. The injection wells generally penetrate older Silurian-Cambrian age formations in the northwestern portion of the Appalachian Basin. Wells in the eastern portion of the basin are completed in younger Mississippian-Devonian age formations, because the rock layers thicken substantially in Kentucky and West Virginia where the Rome Trough is present. The regional diagrams provide general information on formation depth and thickness, but detailed geologic maps are more suitable for site-specific assessments.

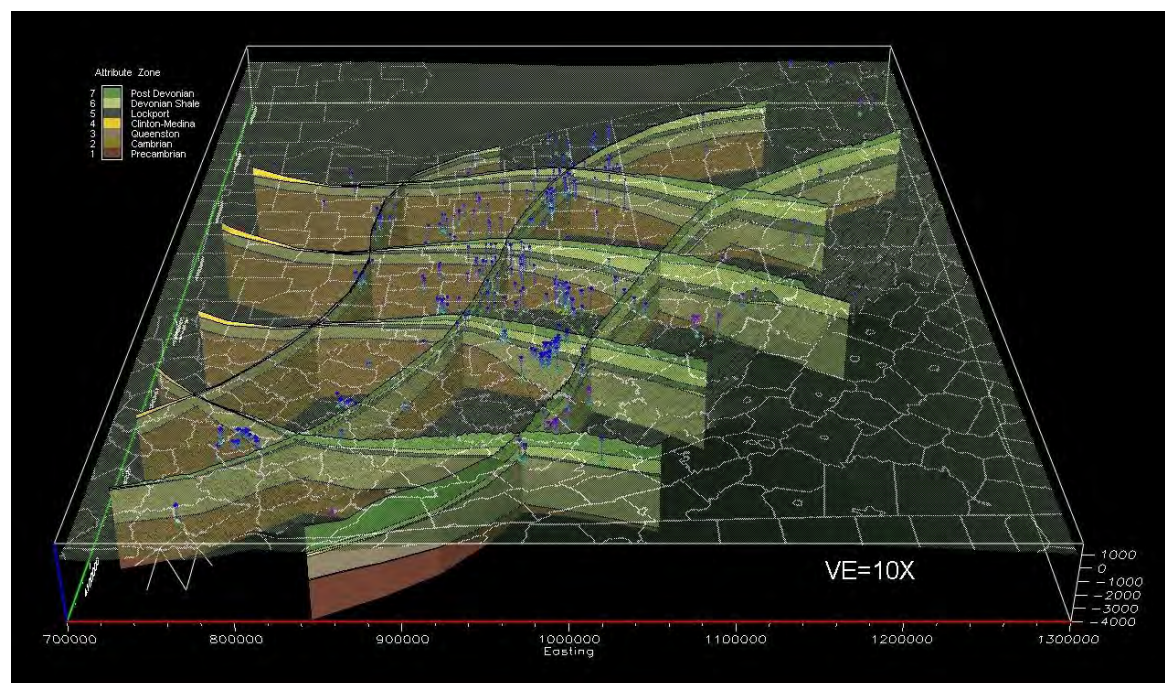


Figure 3-33. Geologic fence diagram showing subsurface distribution of key injection zones for the study area.

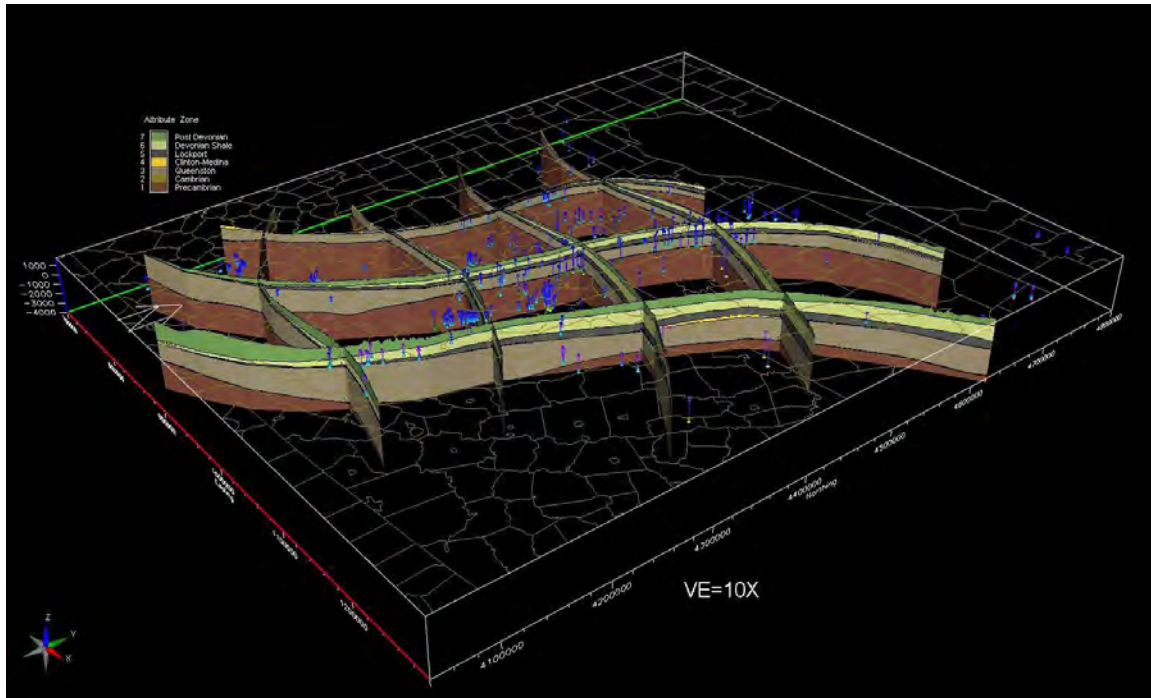


Figure 3-34. North-south view of geologic fence diagram showing subsurface distribution of key injection zones for the study area and wellpaths for Class II brine disposal wells.

The location of shale gas wells, brine disposal wells, and geologic injection zones were also posted with injection well operating statistics to further delineate the relationship between brine sources and sinks. Figure 3-35 shows a 3D image of the brine injection wells' total volume in 2012, along with geologic layers and shale gas wells. The diagram illustrates the spatial distribution of the numerous shale gas wells along with the injection wells. Figure 3-36 shows a 3D image of the brine injection wells' scaled monthly injection rate from 2012. This diagram illustrates which wells have higher injection rates. Note that the posted data for injection wells are not scaled to reservoir parameters, so the size of the spheres do not reflect radius of influence at each injection well.

Overall, the geocellular model helps depict the distribution of Class II brine disposal wells along with the subsurface geologic layers in the region. Into the eastern portion of the Appalachian Basin, the rock layers become much deeper, so shallower zones are utilized for injection. The deeper layers may also be denser and compacted, with less suitable properties for injection. The geocellular model also portrays the location of the shale gas wells along with the brine disposal wells. The geocellular model provide an illustration of the regional features. More detailed, local analysis of geologic zones and properties would be necessary to properly site an injection well.

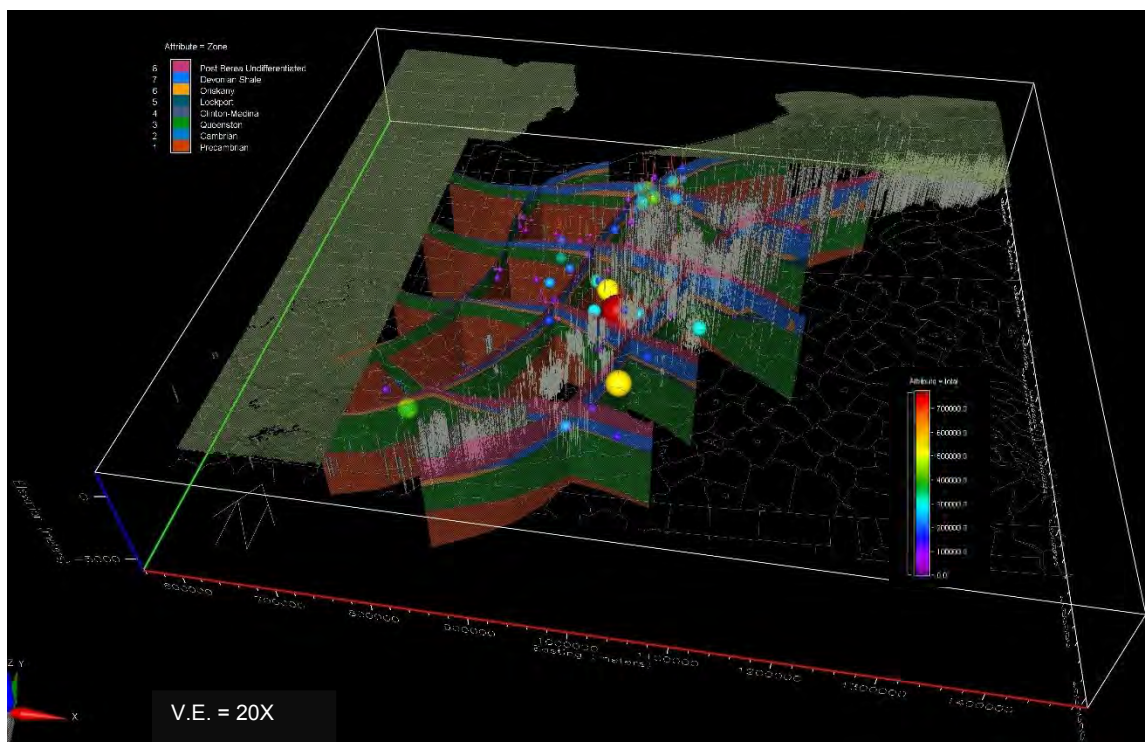


Figure 3-35. Location of shale gas wells (gray) and Class II brine disposal wells scaled according to 2012 total injection volume (bbl).

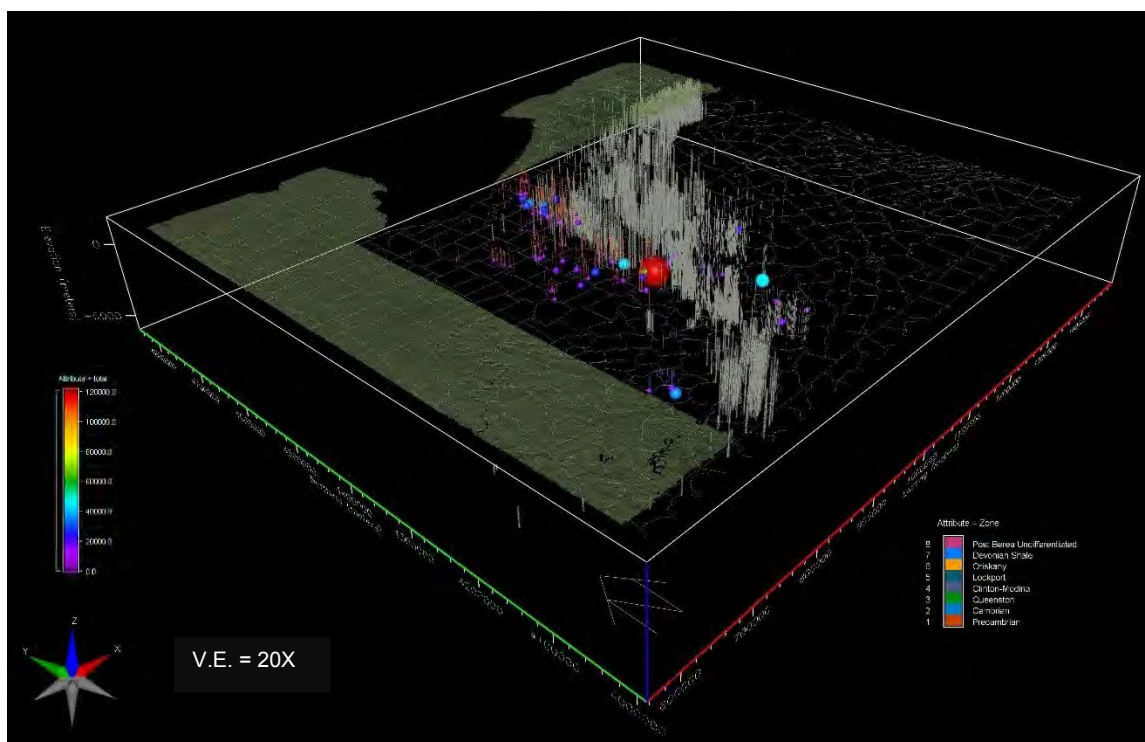


Figure 3-36. Location of shale gas wells (gray) and Class II brine disposal wells scaled according to 2012 average monthly injection rate (bbl/month).

4. Local Geologic Analysis

4.1 Kentucky Class II Wells and Mississippian Weir Sandstone Case Study (KY)

4.1.1 Synopsis of Class II Wells in Kentucky

Recently, a detailed summary of Class II wells in Kentucky was discussed with the Kentucky Geological Survey (KGS) publication *Class I Waste-Disposal Wells and Class II Brine-Injection Wells in Kentucky* (Sparks et al., 2013). The name, type, location, and status of disposal wells were obtained through multiple Freedom of Information Act (FOIA) requests to the USEPA in 2012. A total of 11 Class I industrial waste disposal wells and 87 Class II brine (salt water) disposal wells were compiled and mapped. The map identified plugged, inactive, and operating (i.e., active) disposal wells.

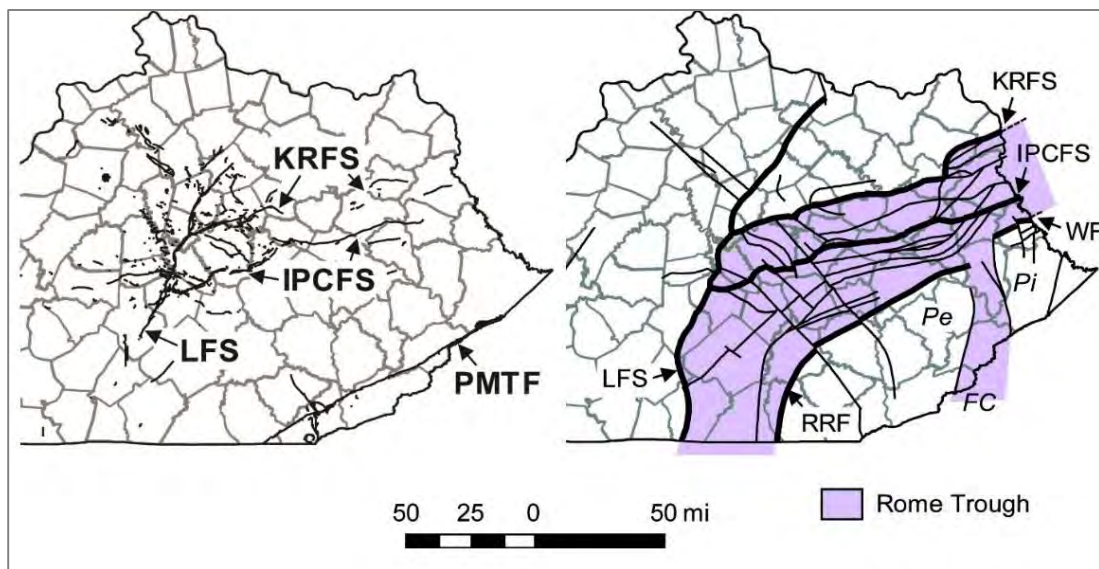
For this research, KGS submitted a more comprehensive FOIA request to USEPA for administrative and operations data for active-only Class II wells for the Appalachian Basin of eastern Kentucky. From the request, a total of 30 active wells were identified among seven stratigraphic reservoirs; 21 of the 30 wells included monthly operational data (volumes injected, average and maximum injection pressures). In early 2014, two Class II disposal wells were permitted in the deeper Knox Dolomite section (Beekmantown to Copper Ridge). In addition, a well completed dry in March 2012 is scheduled to be reclassified as a Class II disposal well in the Knox Dolomite. Thus, the total number of active brine disposal wells in eastern Kentucky currently is 33.

A new online map service developed in late 2014 at the KGS provides locations and detailed information for all disposal wells in Kentucky. These data were secured as a previously released document available on the USEPA FOIA web site. The map service, Class I and Class II Wells in Kentucky, is an updated and interactive version of the KGS publication by Sparks et al. (2013). The Class II brine disposal well number increased to 135 wells with the inclusion of 34 previously unreported permanently abandoned wells and seven newly permitted wells. In addition, the map service documents considerably more USEPA-regulated injection wells, with the addition of 2,937 Class II enhanced recovery or secondary recovery injection wells. Although the increase in overall Class II well numbers initially sounds impressive, it should be noted that that nearly two-thirds are abandoned, shut in, or temporarily abandoned.

4.1.2 Geologic Setting

The surface geology of the Appalachian Basin in Kentucky consists of gently to steeply dipping sedimentary rocks of Upper Pennsylvanian through Upper Devonian age overlain by unconsolidated sediments of Tertiary and Quaternary age. These rocks are underlain in the subsurface by Silurian, Ordovician, and Cambrian strata (Harris and Baranoski, 1996; Harris and Drahovzal, 1996). Bedrock consists of Pennsylvanian and Mississippian interbedded sandstone, siltstone, shale, coal, and limestone; Devonian black, organic-rich shale with minor gray shale and sandstone; and limestone, dolomite, sandstone, and shale for the remaining lower Paleozoic strata.

The geologic structure is characterized by east-to-southeast dipping strata that are cut by several structural features and associated faults. The features include the Rome Trough, Pine Mountain Thrust, and Paint Creek uplift. The Rome Trough is an overall east-west trending Cambrian rift that extends beneath portions of the Appalachian Basin from Kentucky into West Virginia and Pennsylvania (McGuire and Howell, 1963; Ammerman and Keller, 1979). The trough is bounded on the west and north by the Lexington–Kentucky River Fault Systems, and on the south by the Rockcastle River and Warfield Faults. The Irvine–Paint Creek Fault System is located along the axis of the Rome Trough approximately 20 miles south of and subparallel to the Kentucky River Fault System (Figure 4-1). These major fault zones have southwest-northeast oriented faults with down-to-the-south, high-angle normal offsets (Black and Haney, 1975; Black, 1986; Dever, 1999). Displacements on the faults into the rift range 300 to 5,000 feet (Drahovzal and Noger, 1995; White and Drahovzal, 2002). In addition to the southwest-northeast oriented faults, the Rome Trough contains a smaller number of southeast-northwest oriented faults.

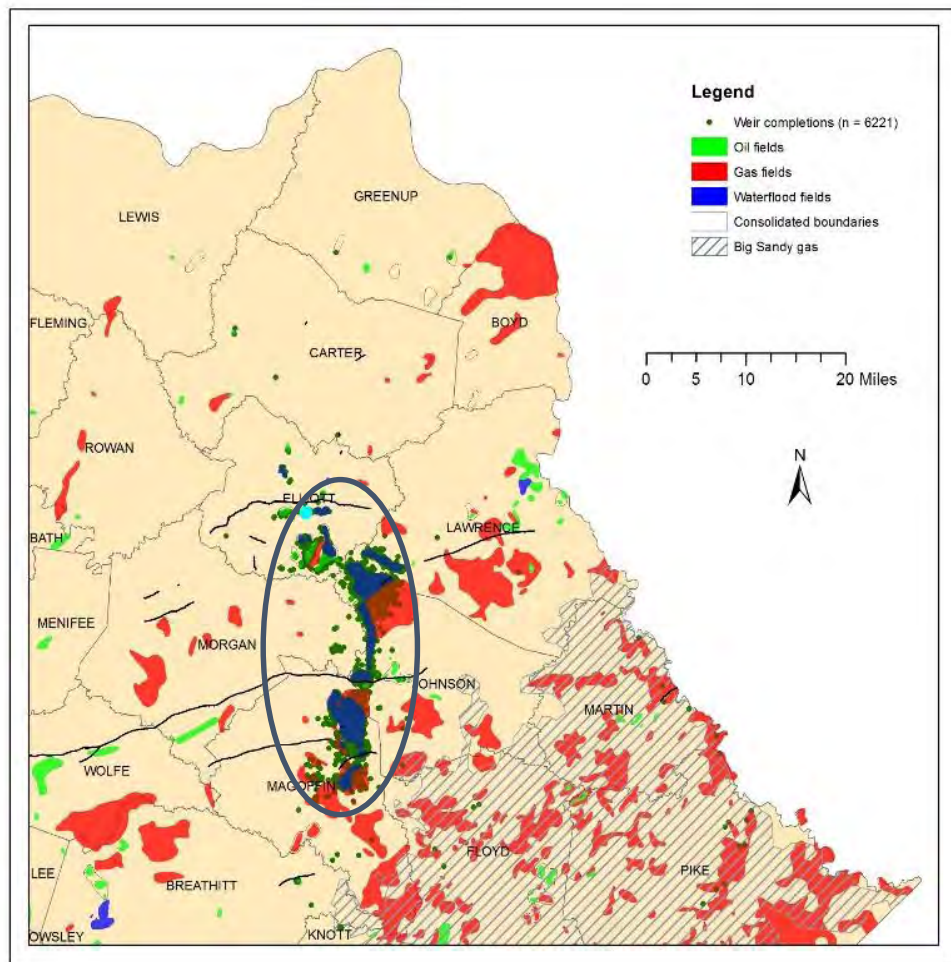


Note: Major fault zones and structural features include the Irvine–Paint Creek Fault System (IPCFS), Kentucky River Fault System (KRFS), Lexington Fault System (LFS), Pine Mountain Thrust Fault (PMTF), Floyd County Channel (FC), Perry County Uplift (Pe), Pike County Uplift (Pi), Rockcastle River Fault (RRF), and the Warfield Fault (WF). Maps adapted from Greb and Solis (2010).

Figure 4-1. Surface faults (left) of central and eastern Kentucky. Basement faults (right) identified from seismic investigations, and deep Precambrian–Early Cambrian grabens of central and eastern Kentucky.

The Pine Mountain Thrust Fault is located along the southeastern margin of Kentucky along the Virginia and Tennessee borders (Figure 4-1). The thrust fault is 125 miles wide southwest-northeast and 25 miles long southeast-northwest; it is the westernmost feature of the Valley and Ridge Province (Hatcher et al., 1989; Greb and Solis, 2010). The thrust fault is exposed along the northwest flank of Pine Mountain, where it dips to the southeast and cuts the Devonian Ohio Shale.

The Paint Creek uplift is a narrow, north-south trending anticline that is cut by the east-west trending Kentucky River and Irvine–Paint Creek Fault Systems in Elliott, Lawrence, Johnson, and Magoffin Counties (Matchen and Vargo, 1996; Noger et al., 1996) (Figure 4-2). Near the surface, the uplift has about 250 feet of closure at the level of the Pennsylvanian Fire Clay coal bed (McFarlan, 1943). The uplift serves as the primary structural trap for the Oil Springs, Isonville, Ivyton, and Keaton-Mazie oil and gas fields. These fields have been primarily developed in the Mississippian Weir Sandstone; however there has also been significant gas production (Isonville, Redbush, Mine Fork fields) in the deeper Silurian Lockport Dolomite-Keefer (Big Six) Sandstone (Noger et al., 1996).

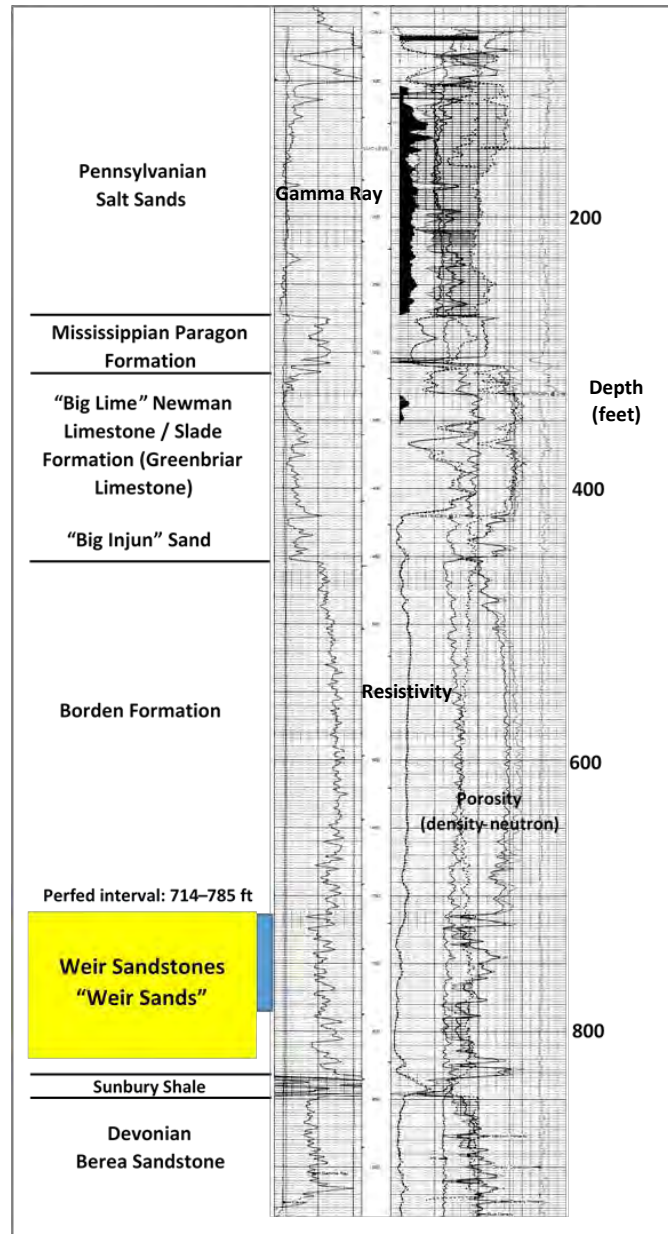


Note: Area inside of oval is location of Paint Creek uplift and Weir oil and gas fields. Gas, oil, and waterflood fields are shown with red, green, and blue shading respectively. The Big Sandy gas field (Devonian Ohio Shale) is shown with gray hachure. The light blue filled circle shows the location of the type log, the Triad Resources Inc. No. 4 Ferguson.

Figure 4-2. Wells completed in the Weir sandstone (dark green symbols).

4.1.3 Weir Sandstone

The Weir sandstones or “Weir sands” of eastern Kentucky is a driller’s term for thin sandstones and siltstones of the Farmers Member of the Borden Formation (Figure 4-3). The sands are named, in descending order, the Stray Weir Gas, 1st Weir, and 2nd Weir (Matchen and Vargo, 1996). In addition, a lowermost 3rd Weir is sometimes recognized and recorded on well completion logs by local drillers. The sandstones are parallel-bedded, very-fine grained to fine-grained, and moderately well-sorted (Chaplin, 1980). Reservoir quality is variable, with porosity ranging from 5 to 28% and permeability from less than 0.1 to greater than 200 mD (Figure 4-4).



Note: For location, see Figure 4-2.

Figure 4-3. Type log for Mississippian Weir sandstones, the Triad Resources Inc. No. 4 Ferguson, located in Elliott County (permit 103462).

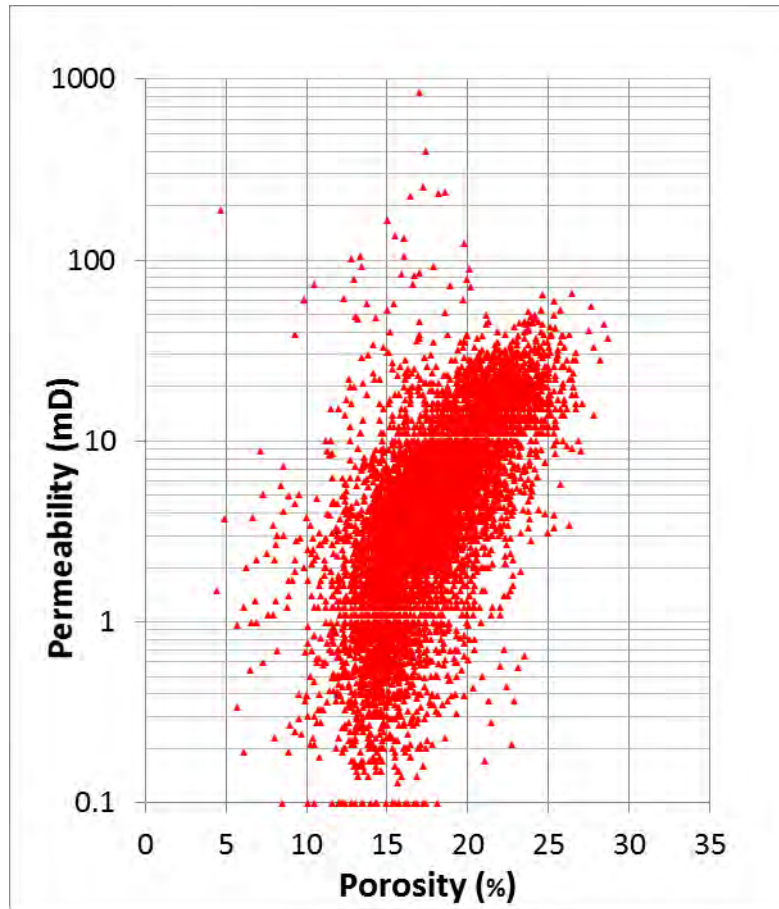


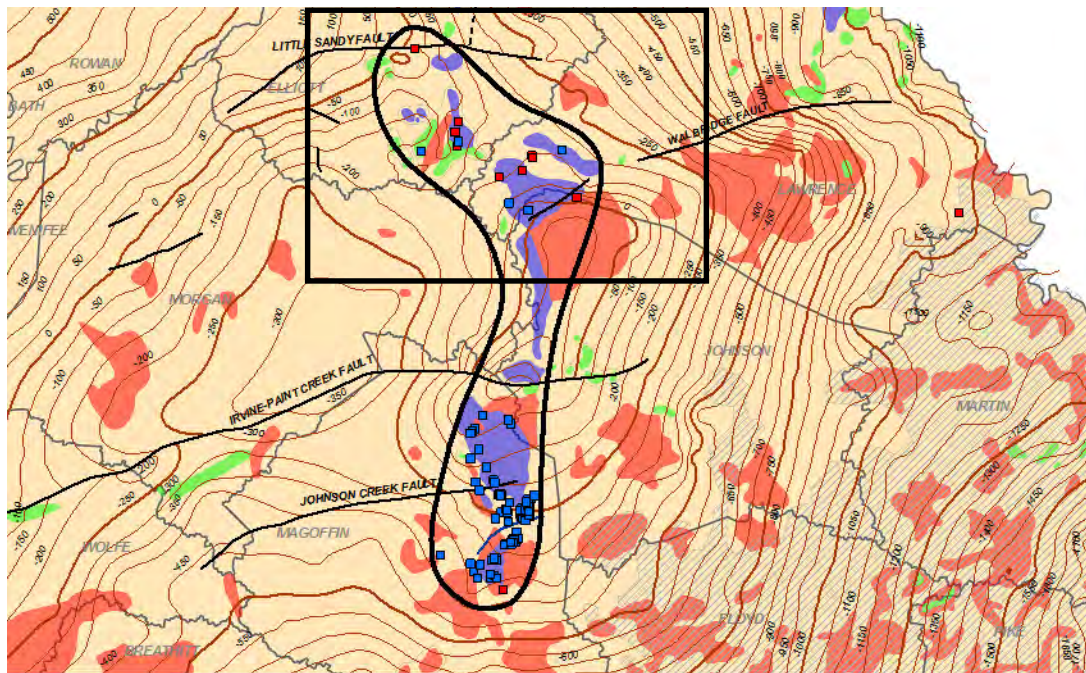
Figure 4-4. Permeability and porosity measurements of 164 Weir sandstone core samples (n > 7,700) from eastern Kentucky.

Stratigraphy for the Weir varies from stacked north-south oriented deltaic sandstones in West Virginia to prodeltaic turbidite siltstones, shales, and sands in eastern Kentucky (Matchen and Vargo, 1996). The Weir overlies the lower Mississippian Sunbury Shale, a dark-gray to black, carbonaceous, fissile shale, which represents the uppermost transgressive phase of the widespread Devonian-Mississippian black shale sequence (Boswell, 1996). The Weir sandstones are, in turn, overlain by sandstones, siltstones, and shales of the upper Borden Formation and then by the “Big Lime” carbonates of the Slade Formation/Newman Limestone section (Figure 4-3). Locally, Weir sand reservoirs tend to occur at regular stratigraphic position near the base of the Borden, although individual sands are not likely continuous over a large area.

Over 6,200 oil or gas wells have been completed in nine fields along the crest of the Paint Creek uplift (Figure 4-2). Weir oil and gas fields and their associated waterfloods include Isonville, Martha, Keaton-Mazie, Redbush, Elna, Mine Fork, Win, Oil Springs, and Ivyton, most of which are characterized in the Gas Atlas (Matchen and Vargo, 1996) and in the TORIS database (KGS, 2015). Records for many wells completed in Weir sandstones only contain drillers’ logs. Beginning with the discovery of the Redbush and Win fields in 1917 (Jillson, 1937), most oil and gas development in the Paint Creek area occurred from 1917 to 1930 and 1960 to 1990. Anticlinal closure along the north-south oriented Paint Creek uplift is the main trapping feature;

however, stratigraphic pinchouts are also present, along with faulted structure closure. Cumulative production, as reported in the TORIS database, from Weir oil fields totals approximately 72 million bbl (KGS, 2015).

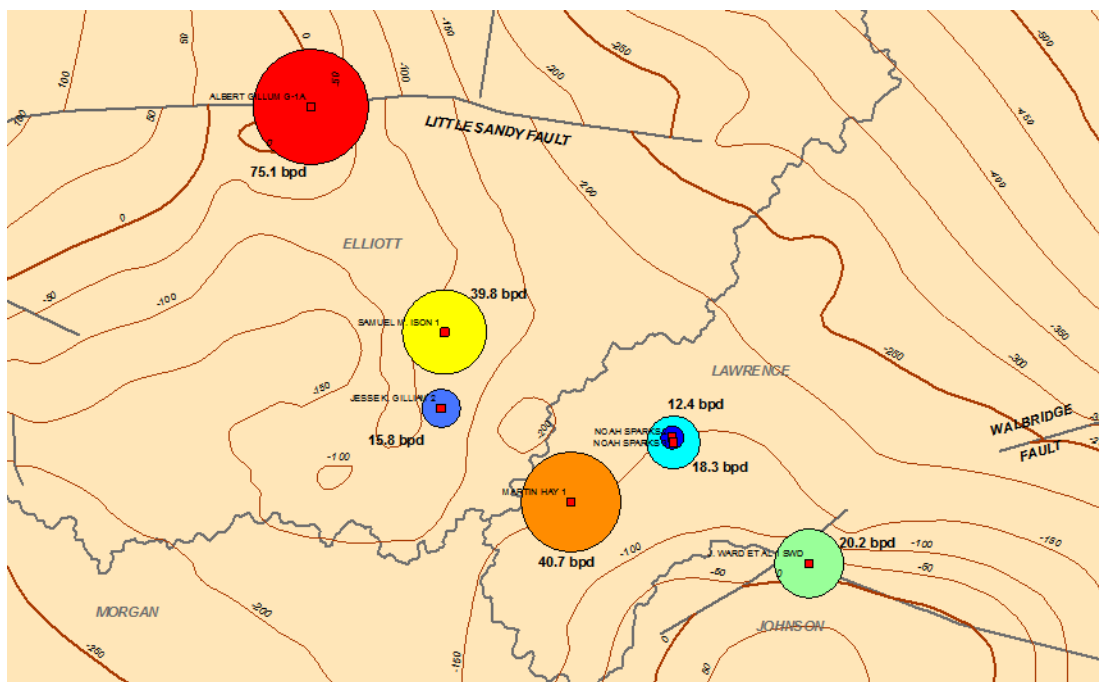
Nine wells are actively injecting brine (salt water) into Weir sandstones along the northern edge of the Paint Creek uplift adjacent to or within Isonville, Keaton-Mazie, and Martha Fields (Figure 4-5). One salt water disposal (SWD) well in Magoffin County (Ivyton Field) was reported active during 2013, but no electric logs and injection data are available. The reservoir depth for the Weir is relatively shallow (665 to 1,164 feet, measured depth) in Elliott and Lawrence Counties, and slightly deeper (800 to 1,407 feet, measured depth) in Magoffin County.



Note: Oil, gas, and waterflood fields illustrated with green, red, and blue shading, respectively. Heavy black line shows location of Paint Creek uplift and area of active Weir injection wells. Red symbols (n= 10) are salt water disposal (SWD) wells, and blue symbols (n = 99) are EOR and secondary recovery injection (SRI) wells. Box outlines area for detailed view in Figures 4-6, 4-7, and 4-8.

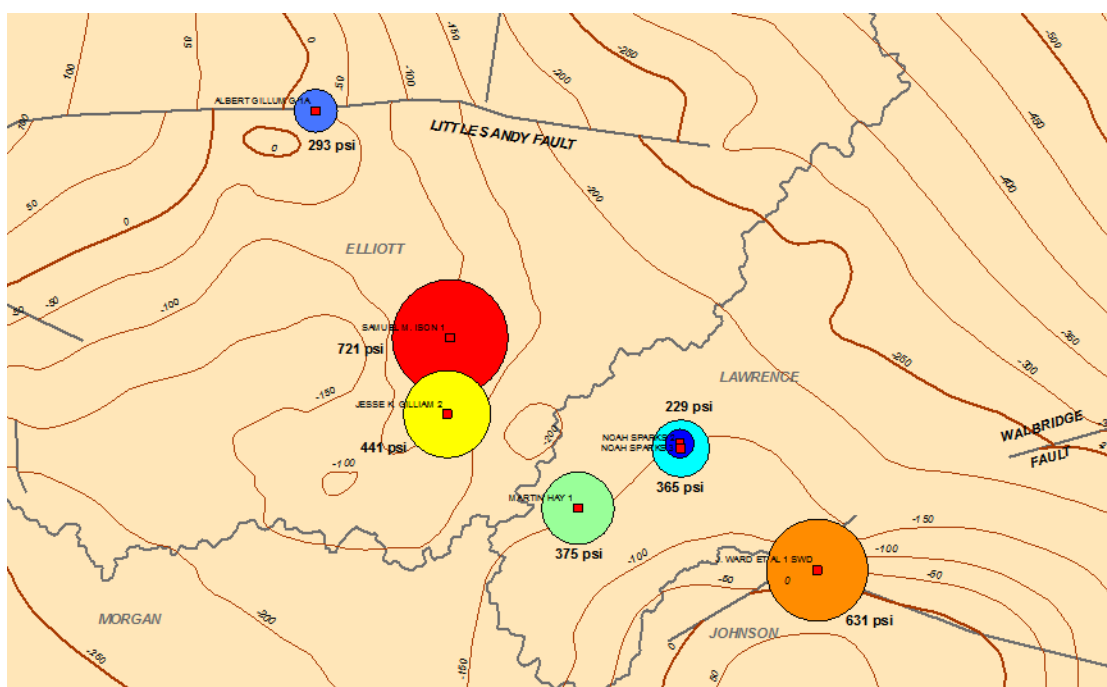
Figure 4-5. Structure map on base of Mississippian Sunbury Shale and top of Devonian Berea Sandstone.

Detailed monitoring and operations data, reported on a monthly basis, were obtained from the USEPA for seven of the nine wells in the Weir. Data were obtained for the period 2008 through 2012 through a FOIA request. Injection rates, based on dividing monthly volumes by days in the month, are low, ranging from 12 to 75 bbl per day (Figure 4-6). Monthly average injection pressures range from 229 to 721 psi (Figure 4-7). Over the 2008 to 2012 period, total brine volumes injected per well ranged from about 8,000 to over 100,000 bbl (Figure 4-8). Monthly injection volumes ranged from 0 (no activity) to 5,000 bbl. It was not unusual, however, to have months or years when no data were reported. It is not clear whether the absence of data reflects no activity or poor documentation.



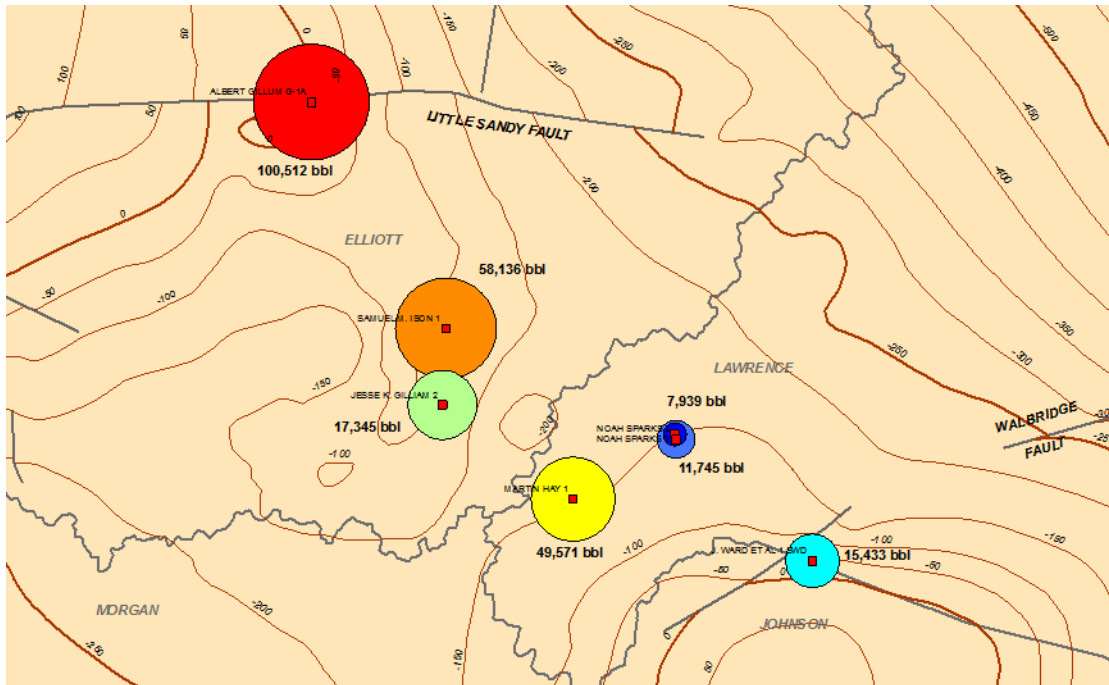
Note: Bubble diameter correlates to magnitude of injection rate (bpd = barrels per day).

Figure 4-6. Detailed view of base of Sunbury Shale and top of Berea Sandstone structure from Figure 4-5 showing average daily injection rate for Weir wells.



Note: Bubble diameter correlates to magnitude of injection pressure (psi = pounds per square inch).

Figure 4-7. Detailed view of base of Sunbury Shale and top of Berea Sandstone structure from Figure 4-5 showing average monthly injection pressure for Weir wells.



Note: Bubble diameter correlates to magnitude of injected volume (bbl = barrels).

Figure 4-8. Detailed view of base of Sunbury Shale and top of Berea Sandstone structure from Figure 4-5 showing total volume of brine injected from 2008 through 2012 for Weir wells.

To better understand the reservoir behavior of the Weir sandstones, time-series plots of average and maximum injection pressures and total injected volumes were plotted and examined for trends (see Figure 4-9 for an example). Significant variations in injection volume with modest variations in pressure were observed in four of the seven wells. The behavior could be attributed to good permeability, poor pressure documentation, or inadequate pressure gauge resolution. In the example provided in Figure 4-9, the well behavior could signify enhanced permeability associated with fractures, as the Triad Gillum No. G-1A is located in the Little Sandy fault zone (Figures 4-6, 4-7, 4-8). In contrast, the Sparks No. 2 and 3 wells likely represent twin wells, and both show marked pressure increases in response to injection (Figures 4-7 and 4-10). Though not shown, the time-series plot for the Ison No. 1 well (Figure 4-6) shows little variation in pressure with varying injection volume. Such behavior likely represents inaccurate reporting.

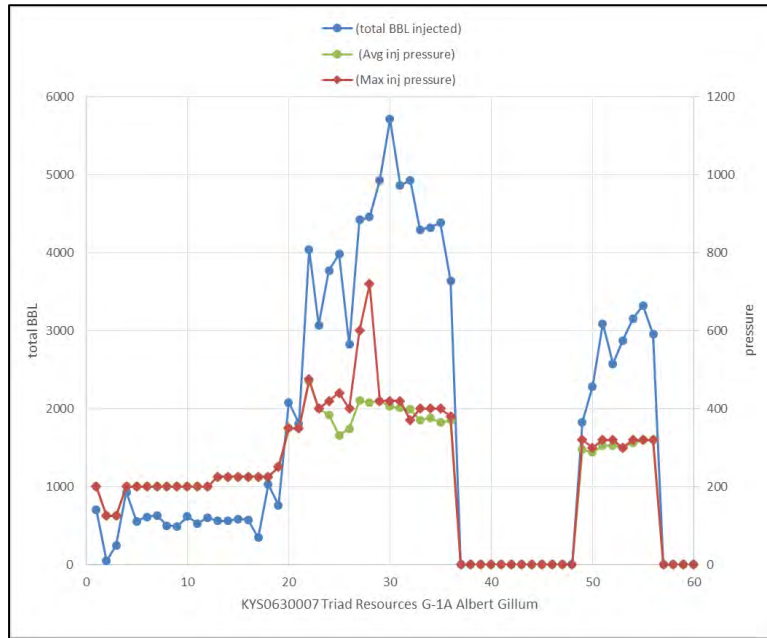


Figure 4-9. Average and maximum injection pressures (psi), and monthly injection volumes (bbl) for the 60 month period from 2008 - 2012 in the Triad Resources, Albert Gillum No. G-1A.

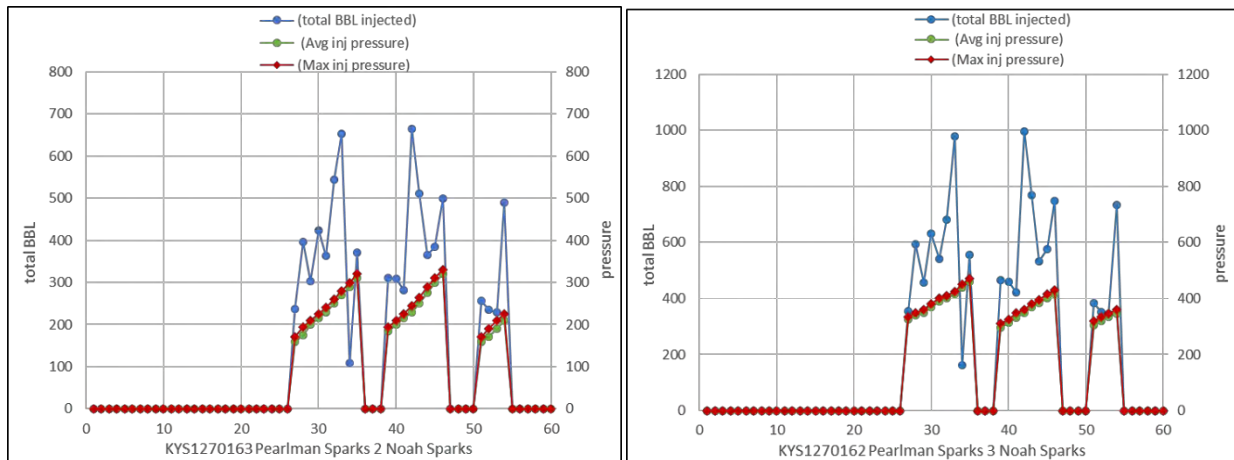


Figure 4-10. Average and maximum injection pressures (psi) and monthly injection volumes (bbl) over a 60 month period from 2008 through 2012 in the Pearlman Sparks, Noah Sparks No. 2 and No. 3 wells.

Laboratory analysis of injection fluids is required to be performed by operators on a yearly basis. Our FOIA request yielded water chemistry records for three wells. TDS for injected salt water ranged from 135,000 to 234,000 mg/L in the Isonville waterflood (Elliott County) and approximately 180,000 mg/L in the Keaton-Mazie waterflood (Lawrence County). In contrast, TDS values from the KGS brine database are lower for the Weir (100,000 mg/L in Elliott County to 150,000 mg/L in Lawrence County). The higher TDS values in the injection wells appear to reflect a mixture of produced waters from the Weir and the deeper “Corniferous” section (Silurian Lockport Dolomite and Keefer Sandstone), which has higher salinity.

The scope of underground injection and disposal activities in the Weir waterflood fields may not be adequately realized without a discussion of other important well operations in the area. The USEPA regulates oil- and gas-related injection wells in Kentucky under the Underground Injection Control Program as Class II, Type D or Type R wells (USEPA, 2015a). SWD wells, as discussed above, are Type D wells, and are for the safe disposal of brines (salt water) that are brought to the surface with oil and gas production. These brines are injected back into the same or similar porous underground formation from which they were initially produced. This practice of brine disposal also ensures the protection of USDWs. Type R wells, on the other hand, inject brine, water, steam, polymers, or CO₂ into oil-bearing formations to recover residual oil and gas (USEPA, 2015b). Often called EOR or secondary recovery injection (SRI) wells, Type R wells make up a significant portion of the existing service wells in waterflood fields.

In the northern Paint Creek uplift of Elliott, Johnson, and Lawrence counties, where the nine brine disposal wells are active, five enhanced recovery wells are also actively injecting fluids into the Isonville, Martha, and Keaton-Mazie waterfloods. In the southern portion of the Paint Creek uplift south of the Irvine-Paint Creek fault, there are a significant number of active enhanced recovery injection wells; only one active brine disposal (SWD) well in contrast to approximately 100 enhanced recovery wells (EOR, SRI) in northeastern Magoffin County (Oil Springs and Ivyton waterflood fields) (see Figure 4-5). Because of the nature of injection fluids used in EOR and SRI wells, they may serve dual purposes (both brine disposal and enhanced injection). However, for this study no operational data were requested for Type R wells from the USEPA, nor was any injection data available for these recovery wells; thus, injection volumes are currently unknown. However, the potential volume of total brines injected into the Weir could be significant.

As noted, injection into Weir sandstones occurs at relatively shallow depth in some areas (665 to 1,407 feet). Consequently, contamination of the potable water zone is of concern. Mapping by Hopkins (1966) and more recently by Grider and Parris (2014) shows that approximately 470 to 770 feet of sedimentary strata separate the Weir sandstones from the potable water zone. Included in this interval is 250 to 300 feet of interbedded siltstones, shales, and mudstones of the upper Borden Formation, which should provide an adequate confining interval. The confining interval is penetrated, however, by more than 6,200 wells, many of which date to the 1920s and could have questionable casing integrity. In addition, the previously mentioned and other faults in the area (Figure 4-1) could provide leakage pathways, although their conductivity and sealing character remains unknown.

Active oil and gas operations likely help to avoid development of significant overpressure as fluids are removed from Weir reservoirs. This fluid and pressure balance reduces the risk of out-

of-zone leakage. KGS does not, however, consider the Weir a viable target for large-scale commercial brine injection involving “out-of-zone” fluids due to the above-mentioned risks. Deeper reservoirs, such as the Ordovician Rose Run Sandstone and porous Cambrian Copper Ridge Dolomite, appear to be to be more prospective.

4.2 West Virginia Class II Wells and Mississippian Big Injun Case Study (WV)

4.2.1 Synopsis of Class II Wells in West Virginia

The West Virginia Geological & Economic Survey (WVGES) has compiled information on Class II disposal wells in West Virginia. Through this research, there are 136 documented disposal wells on record (Figure 4-11). As of September 2013, there are 78 active disposal wells in the state. Fifteen of these wells are classified as commercial disposal wells, where the well operator accepts fluids from various oil and gas operators. Fourteen of the active wells are classified as combination wells, where there is a disposal interval in one part of the well and a separate formation producing oil elsewhere in the well. The combination wells are generally older and currently are not injecting high volumes of fluids, but the permits have been renewed through time to keep these wells as an option for disposal. Several disposal wells lack classifying information. Six wells are permitted to come online as injection wells after September 2013.

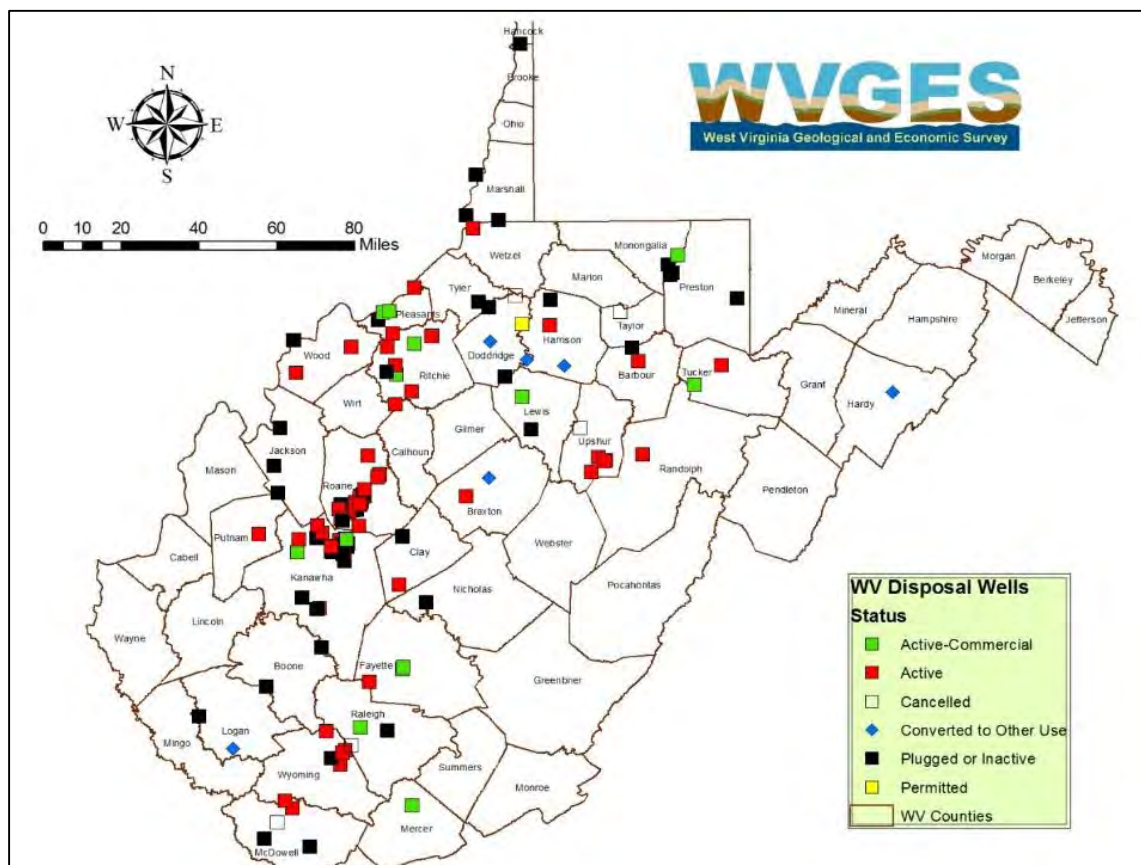


Figure 4-11. Class II disposal wells in West Virginia.

Sources of data used to compile information on Class II injection wells in West Virginia included well permits, plats, and completions; the WVGES oil and gas well database; core and cuttings data; structural data; geophysical logs; and West Virginia Department of Environmental Protection (WVDEP) disposal permits. WVDEP has primacy in West Virginia. For some older wells, WVGES has historical injection data, but the dissemination of these data to WVGES ceased in the 1980s and was consolidated under the WVDEP Office of Oil & Gas. Injection parameters were acquired for active disposal wells from WVDEP from January 2012 through September 2013. A challenge for classifying older disposal wells included a lack of historical records and/or incomplete well records as well as a lack of history on wells that were originally drilled for a different purpose and then converted to disposal wells.

Injection Parameters

Many injection intervals are utilized in West Virginia. Different factors are involved to determine the injection interval; in addition to geology, these factors include geography and proximity to a producing area. Within West Virginia, the shallowest and deepest disposal intervals are the Pennsylvanian Salt Sands and the Silurian Clinton-Medina, respectively (Table 4-1, Figure 4-12). The vast majority of disposal wells in West Virginia are in the Mississippian interval, with most of those wells injecting fluids into the Big Injun sandstone. Due to structural and stratigraphic changes, depths of injection intervals of the same unit vary widely across the state (Table 4-1).

Table 4-1. Numbers of disposal wells classified by geologic age, geologic interval, and approximate depth.

Age	Units	Status	Approx. Depth (ft)
Pennsylvanian	Salt Sands	19 wells, 12 active	1,200-1,700
Pennsylvanian & Mississippian	Salt Sands, Little Lime, Big Injun, Maxton	5 wells, 4 active	1,200-2,200
Mississippian	Princeton, Maxton, Squaw, Weir, Big Lime, Big Injun, Sunbury, undiff. Price, Berea	62 wells, 37 active	1,200-4,000
Mississippian & Upper Devonian	Little Lime, Big Lime, Huron	1 well, 1 active	2,500
Upper Devonian	Gantz, 30Ft, Gordon, Fifth, Balltown, Rhinestreet, Geneseo	14 wells, 9 active	2,600-6,200
Upper & Middle Devonian	Rhinestreet, Marcellus	2 wells, 1 active	4,100-5,100
Middle Devonian	Marcellus, Onondaga, Huntersville	6 wells, 5 active	3,500-6,500
Middle Devonian & Silurian	Marcellus, Newburg	1 well, 0 active	4,300-5,100
Middle & Lower Devonian	Marcellus, Huntersville, Oriskany	3 wells, 2 active	7,800-8,000
Lower Devonian	Oriskany	4 wells, 3 active	6,500-6,700
Upper-Lower Devonian	Rhinestreet, Onondaga, Oriskany	1 well, 0 active	4,900-5,100
Silurian	Salina, Newburg, Clinton, Medina	6 wells, 3 active	5,100-7,300

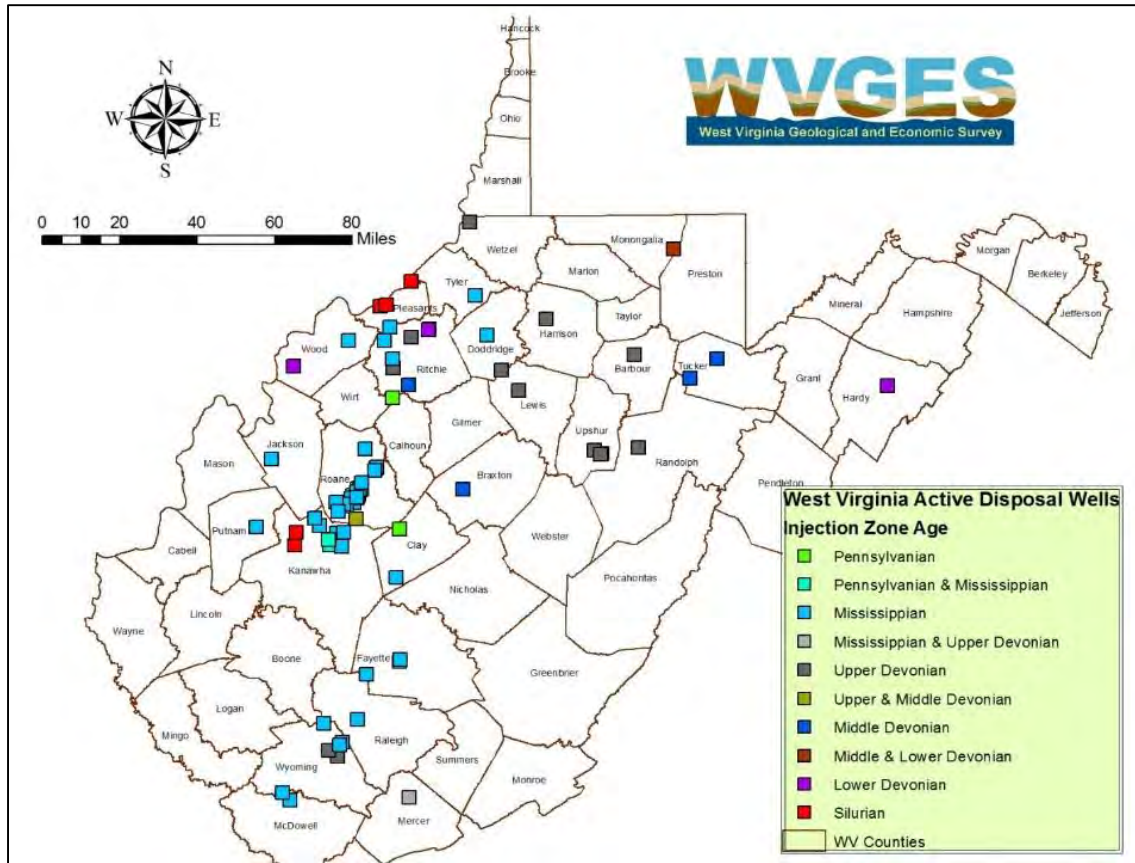


Figure 4-12. Disposal wells classified by geologic age of injection interval.

From January 2012 through September 2013, 6.3 million bbl of fluids were injected into disposal wells in West Virginia. Though the greatest number of injection wells is in the Mississippian Big Injun, the total volume injected is dispersed through various other geologic formations (Figure 4-13). Mississippian, Upper Devonian, and Silurian age formations are responsible for housing most of the fluids injected (Figure 4-13). The majority of fluids injected in 2012-2013 were in wells near the active Marcellus oil and gas production areas in north-central West Virginia (Figure 4-14); however, significant volumes are injected into disposal wells in southern West Virginia (Figure 4-14), some of which are commercial disposal wells. The highest single well volume over this time period was a commercial well in Pleasants County, West Virginia, that injected 1.3 million bbl of fluids into the Silurian Clinton-Medina interval.

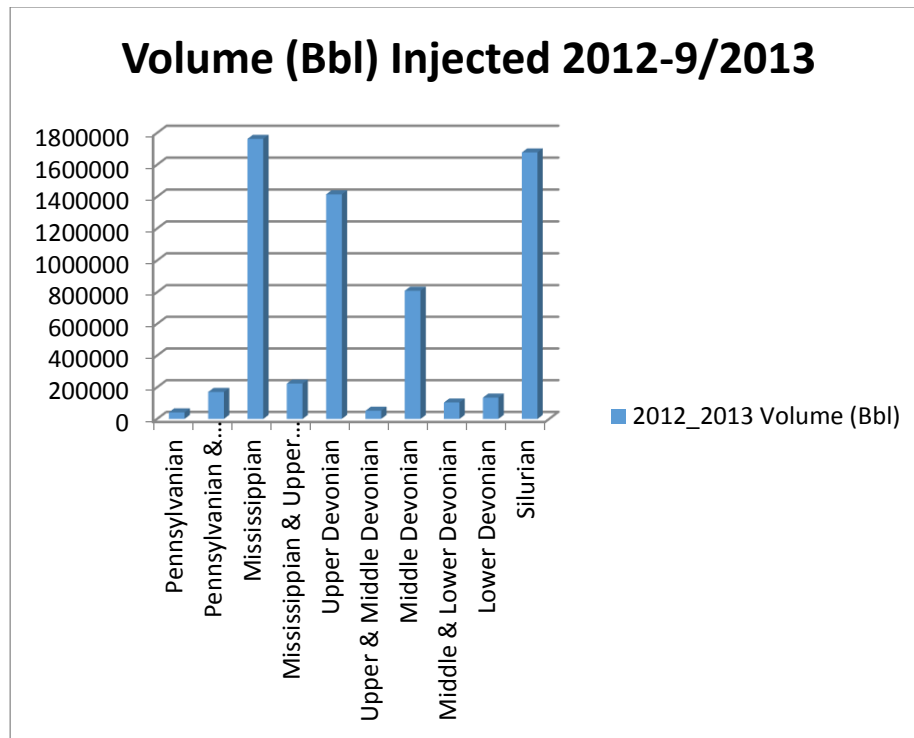


Figure 4-13. Volume of fluids (in barrels) injected in 2012 and through September 2013 by geologic age.

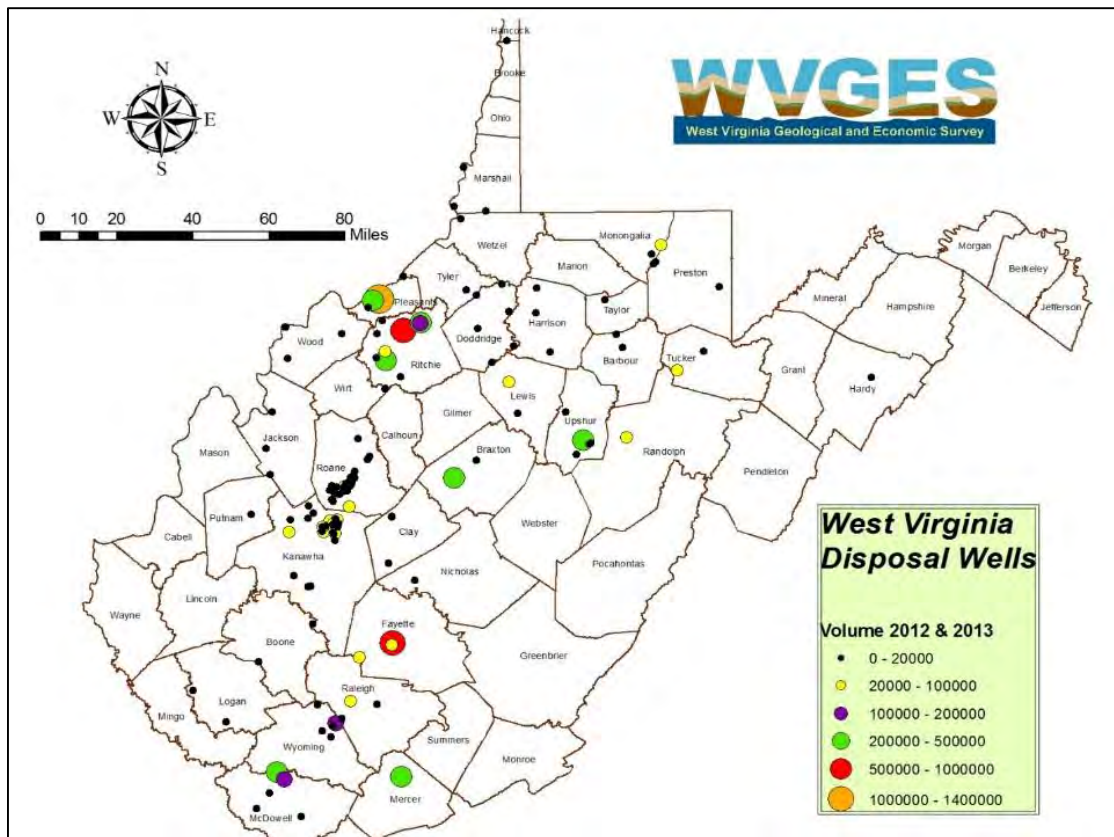


Figure 4-14. Volume of fluids (in barrels) injected in 2012 and through September 2013 by well.

4.2.2 Mississippian Big Injun Saltwater Disposal Wells in the Walton-Rock Creek Field, Roane County, West Virginia

The Walton-Rock Creek oil field in Roane County, West Virginia (Figure 4-15), discovered in 1907, was the most active oil field in West Virginia during the late 1960s and early 1970s (Cardwell and Avary, 1982). The primary reservoir is the Mississippian Big Injun sandstone of the Price Formation (Hohn et al., 1993) with a depth of ranging between 1,950 and 2,150 feet (Whieldon & Eckard, 1963). The field also has the following characteristics: American Petroleum Institute (API) oil gravity = 43.5, reservoir temperature = 75° F, and an average porosity = 22% (Cardwell and Avary, 1982). The trapping mechanism in the field consists of a permeability barrier bounded by anticlines (Cardwell and Avary, 1982). The Jarrett Syncline runs through the field, while the Milliken and Arches Fork anticlines bound the field to the west and northeast, respectively (Hohn et al., 1993) (Figure 4-16).

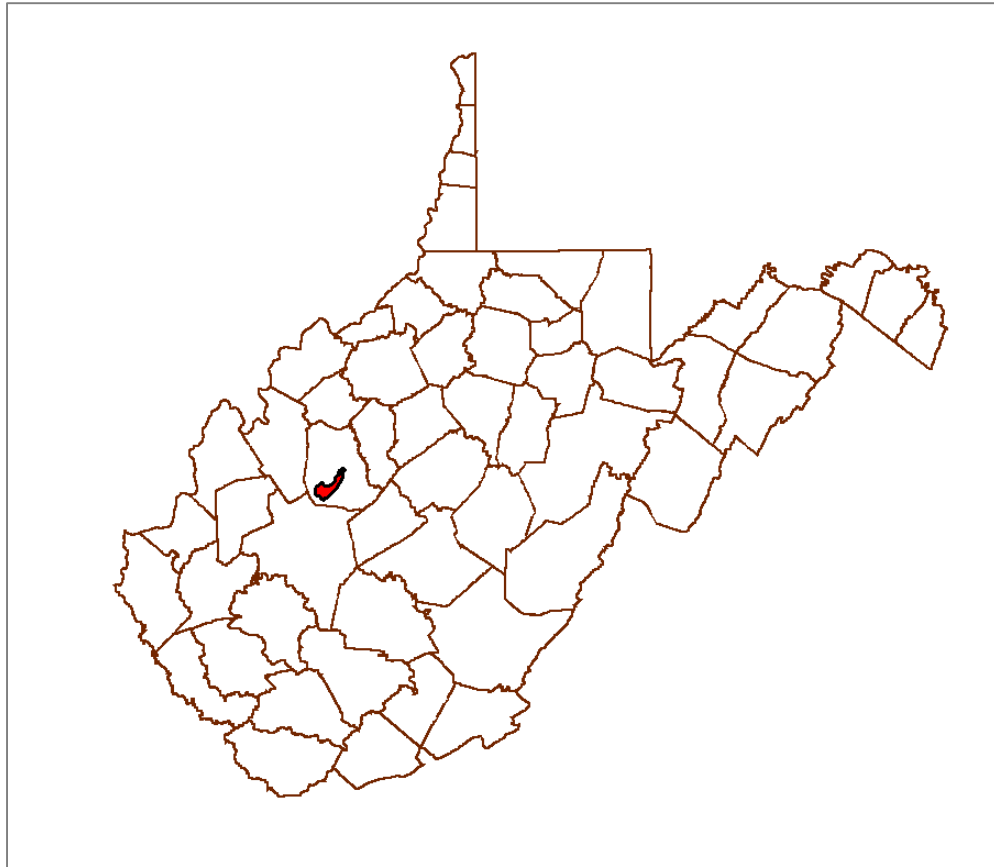


Figure 4-15. Location of Walton-Rock Creek field in Roane County, West Virginia.

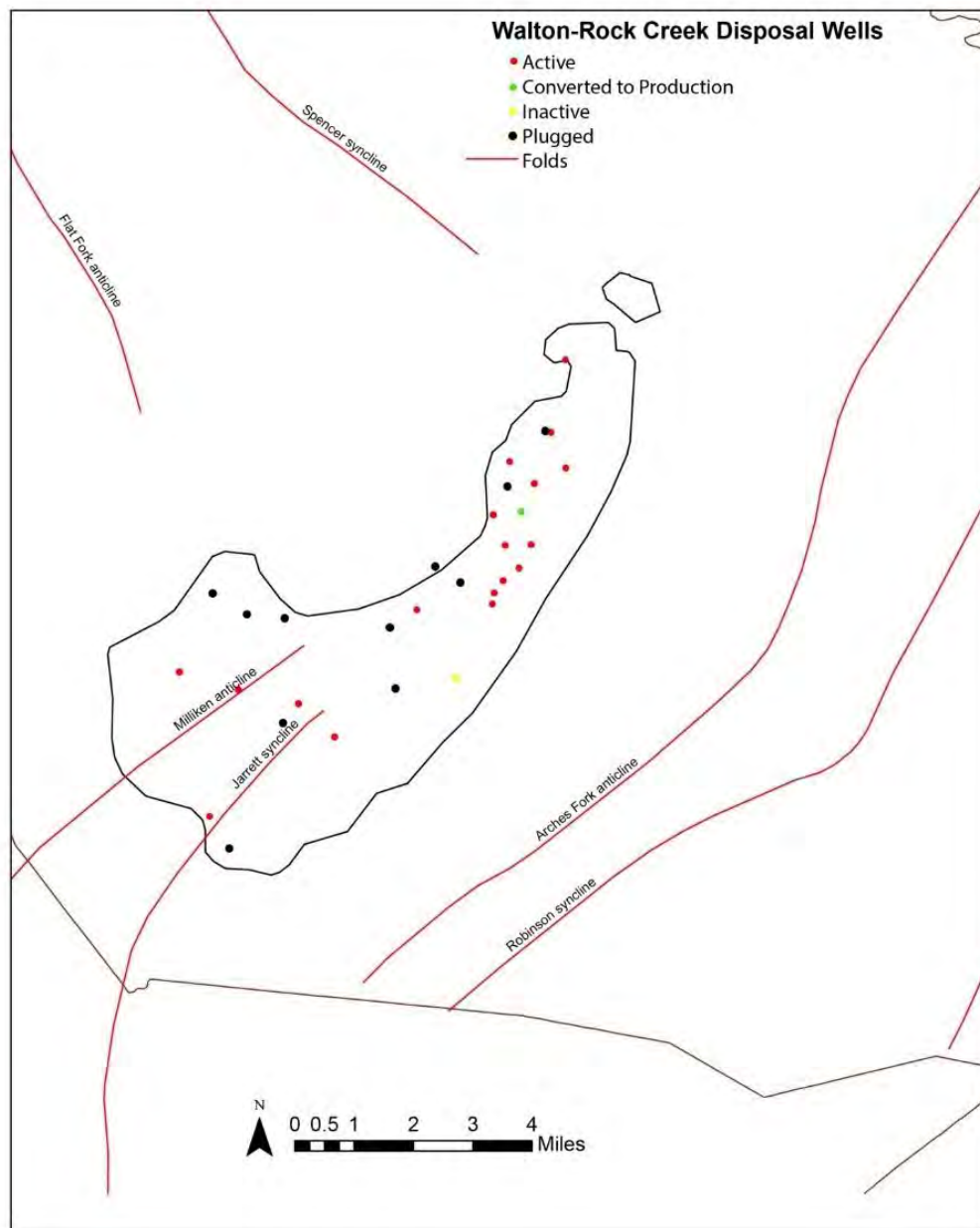


Figure 4-16. Walton Rock Creek Field with disposal wells, well status, and associated folds.

Compared to other areas in West Virginia, there is a high density of SWD wells within the Walton-Rock Creek field. On record, there are 30 disposal wells within the field (Figure 4-16) with 18 classified as “active,” one that has been converted to “production only,” one classified as “inactive,” and 10 that have been plugged. Several of the disposal wells are considered “combination wells,” with known disposal at depths between 1,310 and 1,724 feet into the Pennsylvanian Salt Sands and oil production from the Middle/Lower Mississippian Big Injun sandstone. Injection zones within the Big Injun range from 1,850 to 2,216 feet. Other zones of

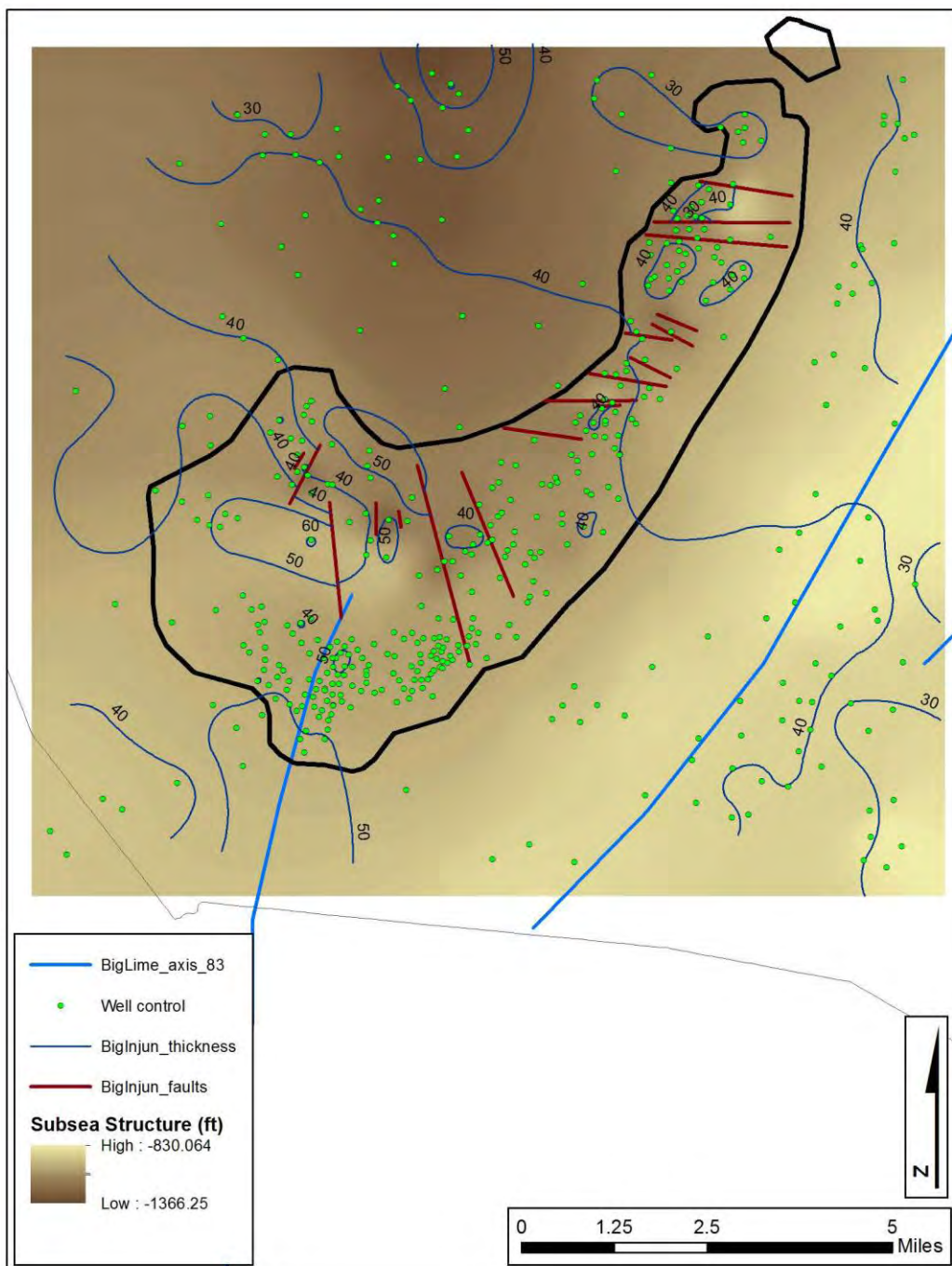


Figure 4-18. Structural map of Walton-Rock Creek field.

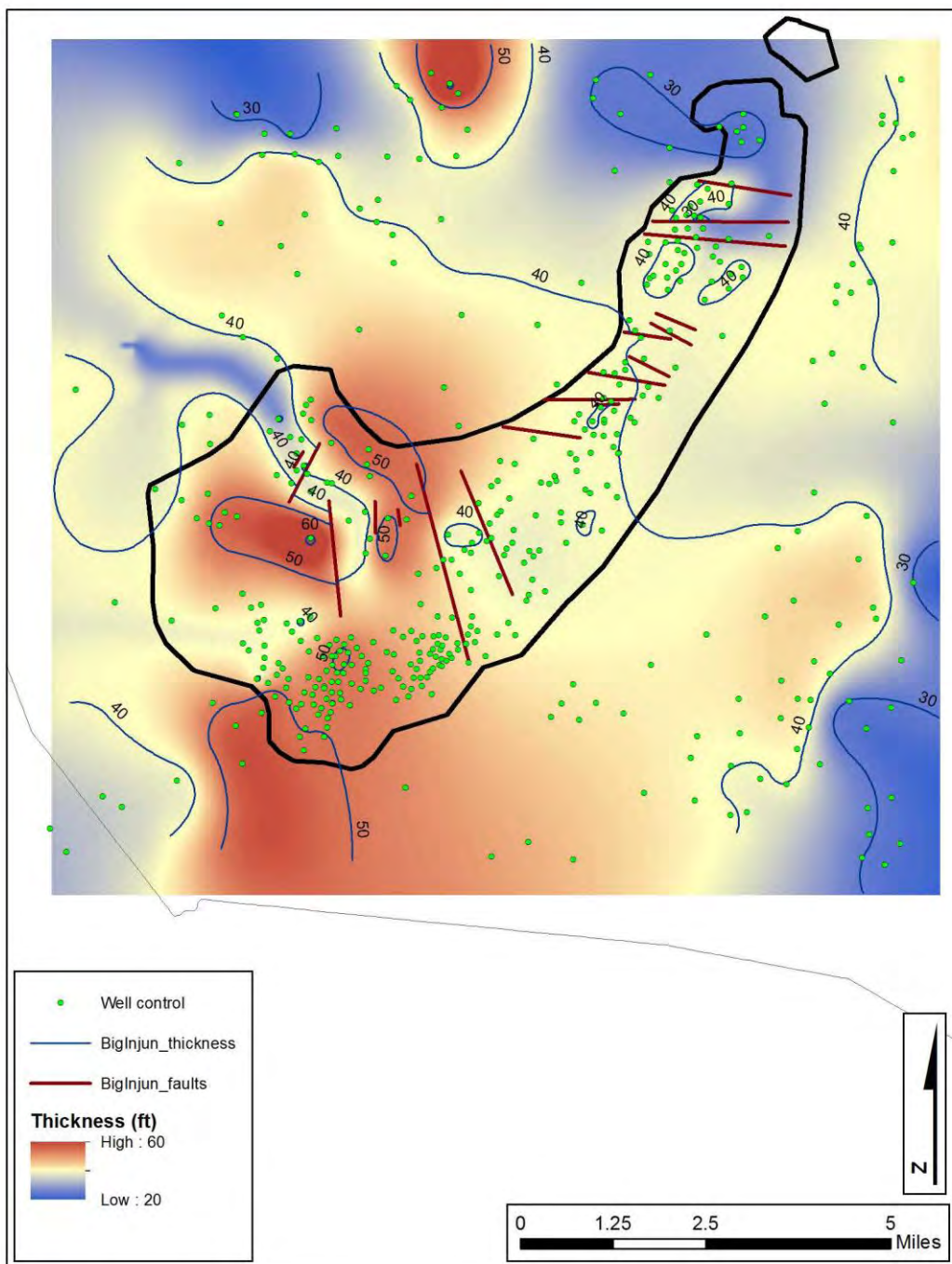


Figure 4-19. Isopach map of Walton-Rock Creek field.

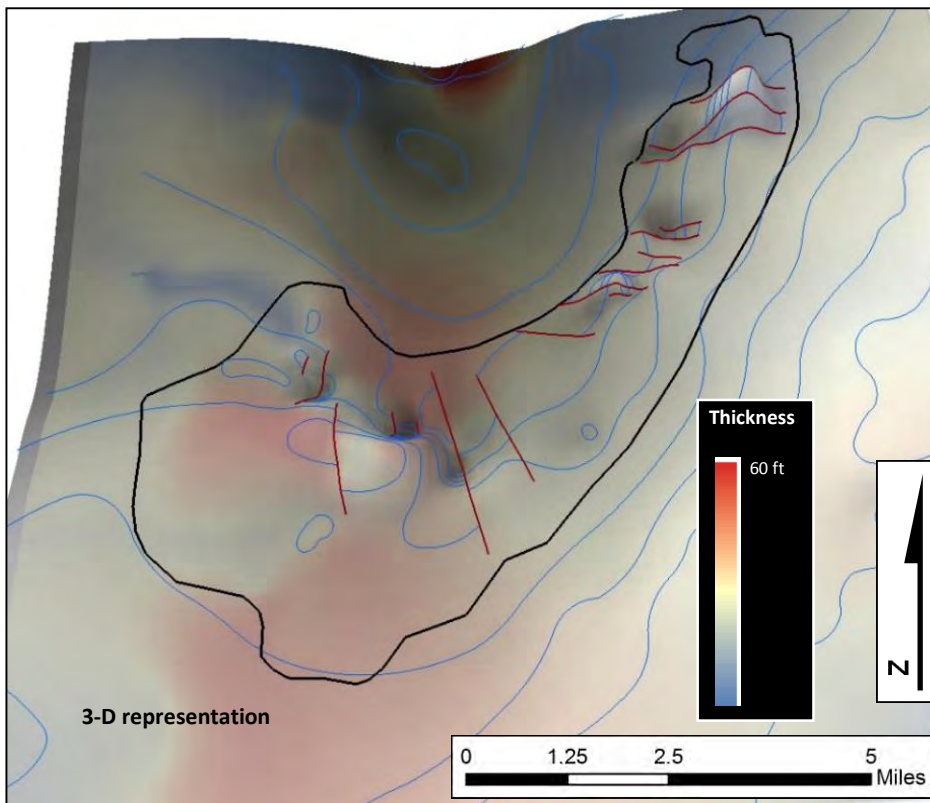


Figure 4-20. 3D structure of Walton-Rock Creek field.

Many of the disposal wells were first brought online during peak oil production in the late 1960s and early 1970s. The need for disposal wells was due to the large amount of produced water from conventional oil and gas wells. The wells would commonly produce at least 2 bbl of water per barrel of oil; however, some wells produced over 20 bbl of water per barrel of oil (Hohn et al., 1993). High water saturation within the field has been attributed to the lack of successful EOR operations (Hohn et al., 1993).

Many of the permits for disposal wells have been renewed; therefore, many of these disposal wells remain active. Currently, on a well-to-well basis, total injected volume into the Walton-Rock Creek wells is lower than other disposal wells in West Virginia. This may indicate that these disposal wells are not being heavily used to dispose of wastewater from the current Marcellus drilling activity in the state.

4.2.3 Recommendations

WVGES has had an informal policy of recommending an injection interval at or below the active production interval. Since the majority of activity in West Virginia is in the Marcellus Shale, injection into, or deeper than, the Marcellus may be in the best interest of the state. However, depth to some potential intervals would likely be cost prohibitive; therefore, anything below the Silurian was not considered for West Virginia.

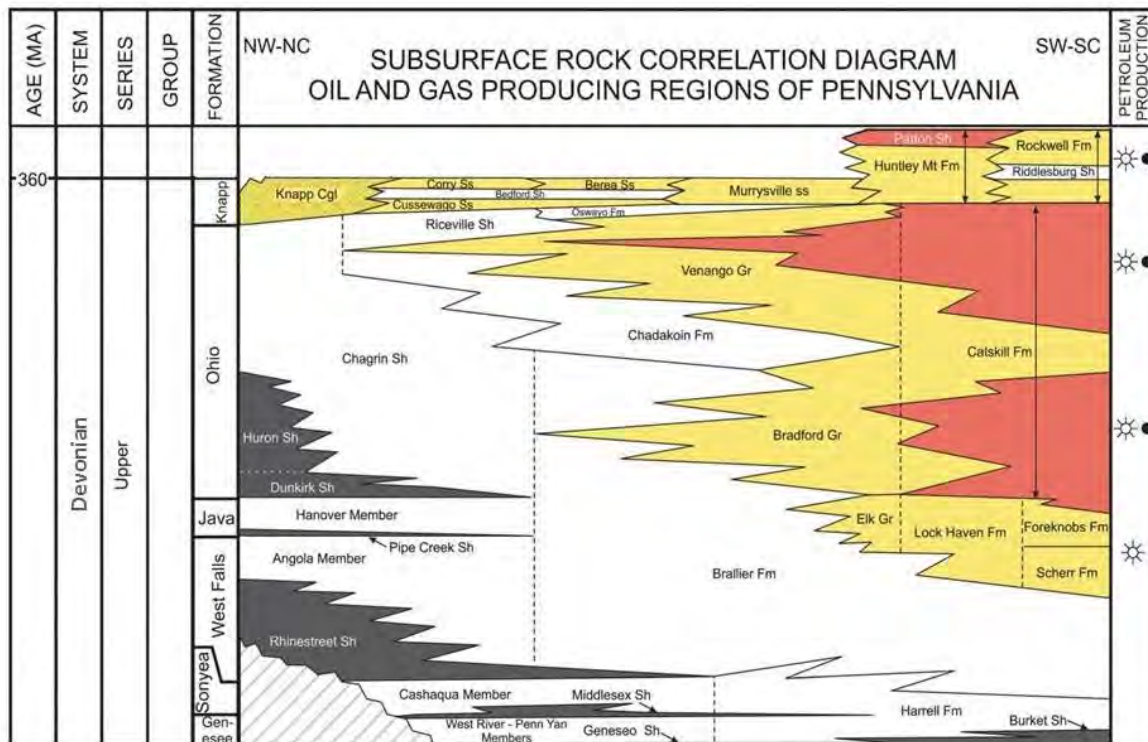
Five intervals below the Marcellus may provide safe and effective injection zones, but each interval presents some operational challenges. The first unit, the Oriskany Sandstone, has favorable porosity but is still being developed in many areas for production and/or storage of natural gas. Down section, the Silurian Salina Group is both a current and historic target for commercial salt water production, predominantly in Marshall County, West Virginia. An active solution mining production and disposal well infrastructure exists in this area, which is also in very close proximity to the active Marcellus and Utica shale fairway. The Newburg interval, perhaps the most favorable target, may be able to accept large volumes of fluids, is not currently a major producing interval, and has well-defined stratigraphic and structural traps Lewis (2013). Below the Newburg, the Clinton-Medina interval is another potential target with a recently permitted disposal well in Tyler County, West Virginia. Finally, the Lower Silurian Tuscarora could prove to be an acceptable target, but would likely have to be examined on a local scale due to low porosity, except where fractured.

The Silurian Newburg and Clinton-Medina intervals are likely the most promising disposal targets. Geologic structures, however, must be taken into account. Economics will certainly play a role but, in general, deeper injection intervals provide the best targets when seeking to avoid contact with fresh water aquifers and/or contamination of active producing reservoirs.

4.3 Pennsylvania Upper Devonian Series Case Study

4.3.1 Introduction

Upper Devonian sandstones were the first geologic units targeted for the extraction of oil and gas in Pennsylvania. Potentially productive Upper Devonian sandstones underlie most of western Pennsylvania and east-central West Virginia (Boswell et al., 1996a), where oil and gas production has been reported since the late 1800s. The Upper Devonian section thicknesses in Pennsylvania range from 9,000 feet (2,750 meters) in east-central Pennsylvania to less than 3,000 feet (900 meters) in the northwestern part of the state. This section is composed mostly of interbedded shales, siltstones, and sandstones (Harper, 1999). These Upper Devonian sandstones are broken up into the Venango, Bradford, and Elk groups (Figure 4-21). In Pennsylvania, more than 34,500 wells have produced oil or natural gas from the Venango Group sandstones; over 69,500 wells have produced oil or natural gas from Bradford Group sandstones; and over 2,500 wells have produced oil or gas from sandstones in the Elk Group (PA*IRIS/WIS, 2015).



Source: From Carter, 2007.

Figure 4-21. Upper Devonian stratigraphic column.

Five Bradford Group wells in Pennsylvania have been used for oil and gas wastewater injection, and permits are being sought for additional brine injection wells in this horizon. Drillers' names for sandstones noted in this study and their relative depths are shown in Figure 4-22. To date, brine disposal wells in the Bradford Group have injected into the Speechley, Balltown, and First Bradford sandstones. This case study examined an area in the central portion of western Pennsylvania that included three active or formerly active brine disposal wells. There were two active brine injection wells disposing into Bradford Group sandstones as of the end of 2014 (Johnson, 2015).

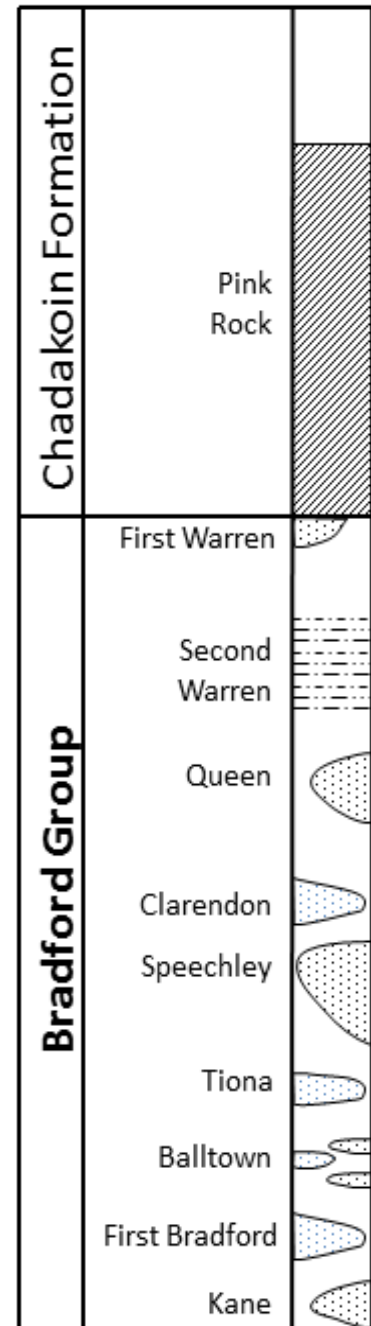
4.3.2 Objective

The objective of this case study was to evaluate Bradford Group sandstones in an area that included three injection disposal wells. Cross sections have been constructed to assess the variability of potential injection horizons and seals in the Bradford Group.

4.3.3 Methodology

North-south and east-west cross sections were constructed using PETRA[®] software for an area that encompasses three Upper Devonian disposal wells in western Pennsylvania (Figure 4-23). Wells were selected depending on the availability of geophysical logs that included, at a minimum, a gamma ray (GR) curve with an API scale. The east-west cross section (A–A') (Appendix) was constructed between a former disposal well in Butler County and an active disposal well in Clearfield County. This cross section traverses approximately 60 miles (95 kilometers). The north-south cross section (B–B') (Appendix) originated at an active injection well in Elk County, bisected the A–A' cross section, and ended at a gas well in Westmoreland County. Cross section B–B' runs a length of about 90 miles (145 kilometers). Sandstones in the Bradford Group crop out approximately 9 miles (14.5 kilometers) north of the northernmost B–B' well and approximately 22 miles (35 kilometers) east of the easternmost A–A' well. These cross sections were constructed as measured depth sections to illustrate an interval that includes the Chadakoin Formation through either the First Bradford sandstone or to the base of the logged interval.

Two sandstone intervals in the Bradford Group, two shale marker beds, and the top of the Chadakoin Formation were correlated in these cross sections. The two shale marker beds were used to verify sandstone correlations. The lower marker bed is the same horizon used in a study of the sedimentology and structure of the First Bradford sandstone (Murin, 1988), a productive sandstone in the Bradford Group. The other shale marker has been used by the Pennsylvania Geological Survey (PaGS) in Upper Devonian correlations. The cross sections highlight the Speechley and the First Bradford sandstones. The Speechley sandstone was assessed to be one of the most continuous sandstones in the Bradford Group by Piotroski and Harper (1979). The First Bradford sandstone correlation relies heavily on Murin (1988).



Source: Modified from Harper, 2009.

Figure 4-22. Stratigraphic column of the Chadakoin Formation and Bradford Group showing selected drillers' names for sandstones in the central column.

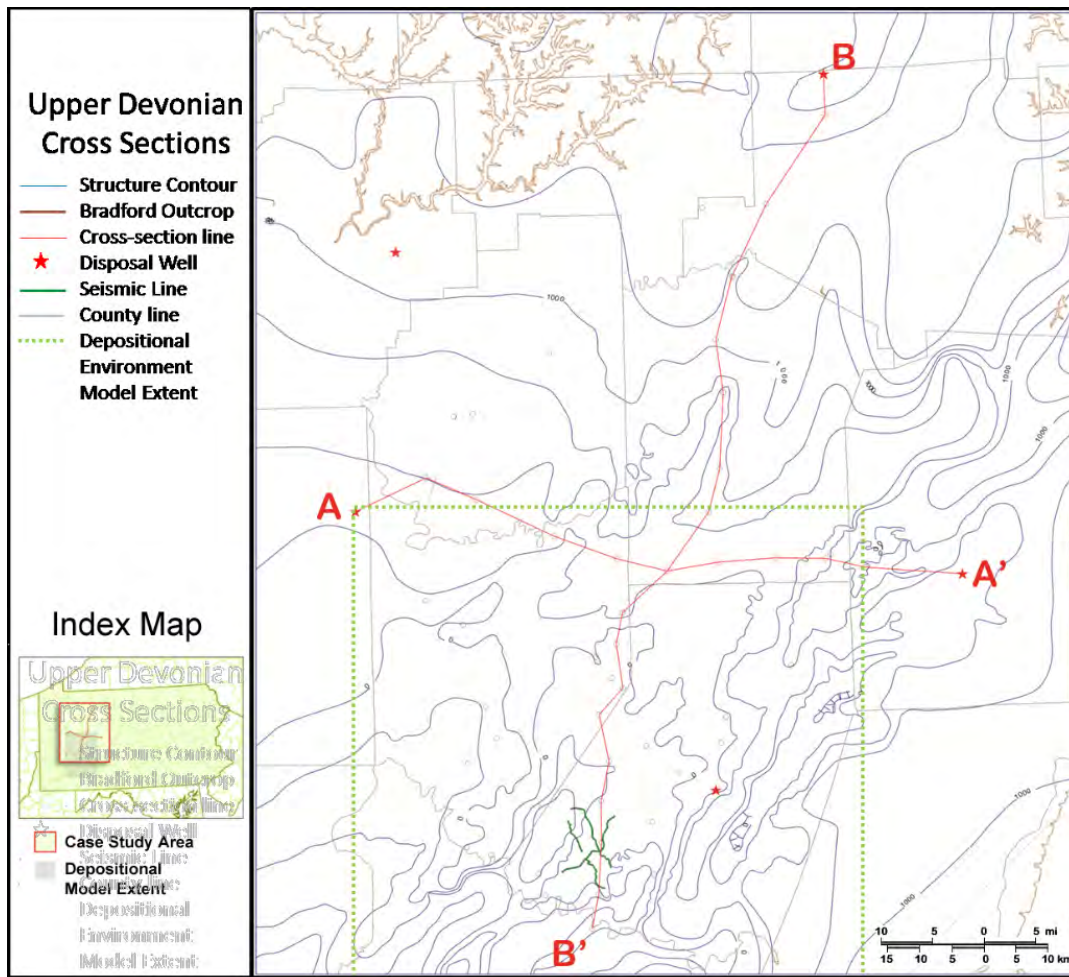


Figure 4-23. Index map showing locations of Bradford Group disposal wells, cross sections, seismic lines, structure contours, and outcrop locations of the Bradford Group.

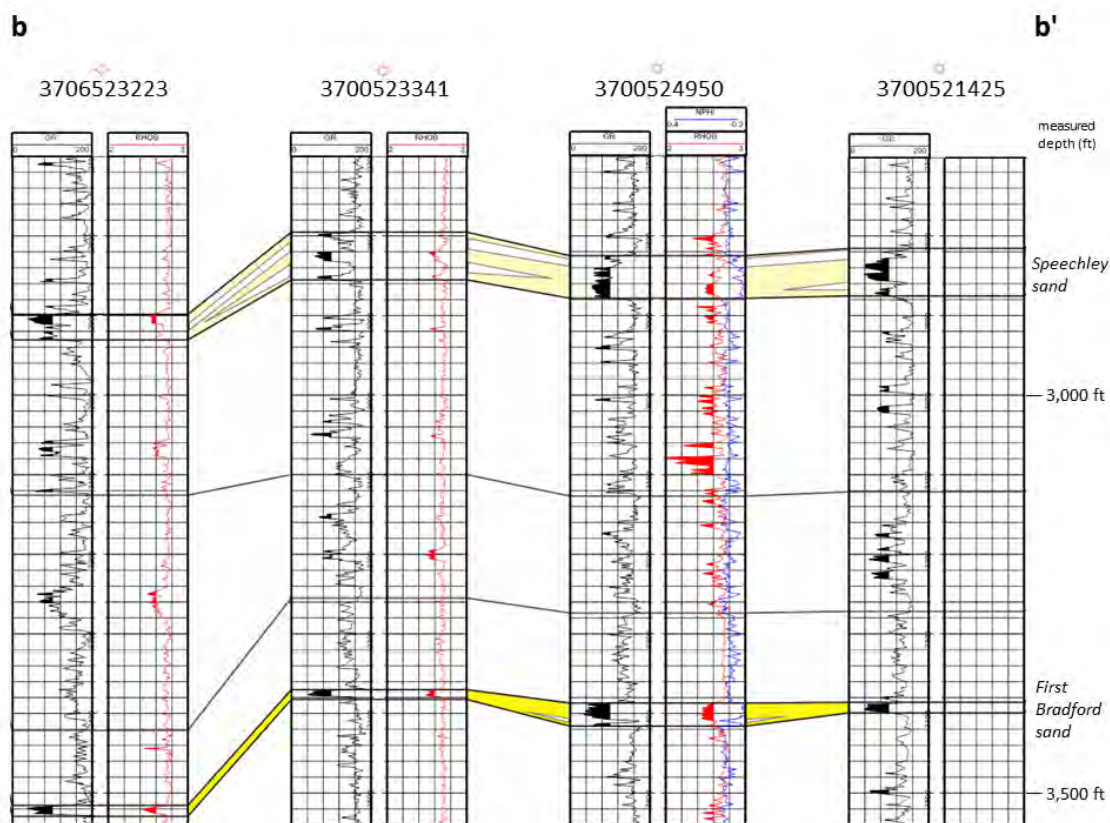
Various density (RhoB) and GR values can be used to determine potential productive zones in subsurface sandstone bodies. A cutoff of 100 API units on the GR log was used to highlight (in black) intervals composed of at least 50% sandstone. This falls midway between the GR value for clean sandstone (32 API units) and the GR value for typical shale (165 API units) in southwestern Pennsylvania (Murin, 1988) in the cross sections. The red shading on the density (RhoB) logs highlights densities of 2.55 grams per cubic centimeter (g/cc) or less. Due to the shaly nature of this formation, higher GR and lower RhoB cutoffs have been used by operators to determine potential productive horizons than cutoffs used for other formations.

4.3.4 Results

The brine disposal wells included in this case study have injected into either the Speechley or the First Bradford sandstone. Measured depth ranges of Bradford Group sandstones in the cross sections range from 1,900 feet (580 meters) at the top of the highest Speechley sandstone to 3,600 feet (1,100 meters) at the base of the lowest First Bradford sandstone. Injection depths

vary from 2,100 feet (640 meters) to 2,600 feet (800 meters). The injection intervals of these wells include over 50% sandstone and less than 2.5 g/cc calculated bulk density.

In western Pennsylvania, the Bradford Group consists mostly of interbedded shale, siltstone, and sandstone. The two sandstone bodies examined in this study vary in thickness and extent. These cross sections show the sandstones thickening and thinning over tens of miles. Figure 4-24 enlarges a sandy zone from the B-B' section. This cross section shows the variability of the sandstones over a small area and the thin shale interbeds that sometimes divide the sandstones.



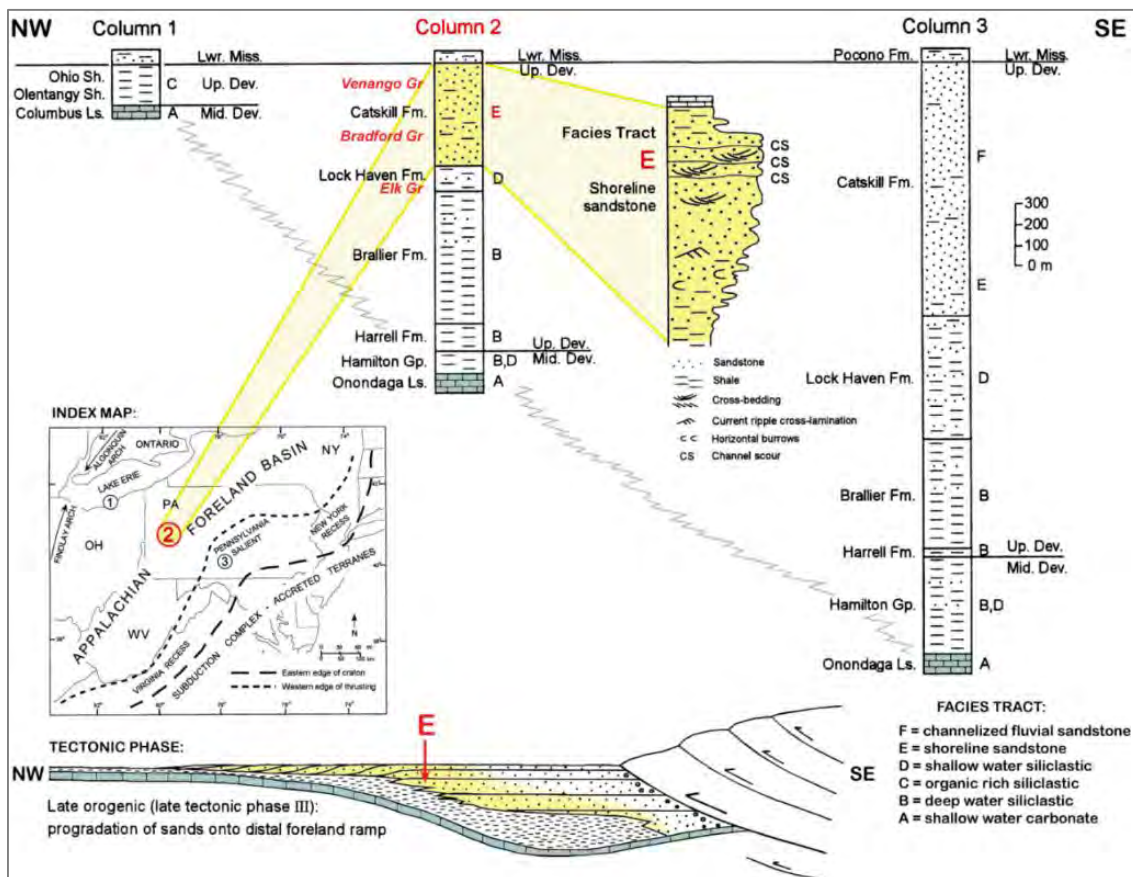
Note: This section is an enlarged segment of the B-B' cross section (Appendix). The location of this section is shown by the letters at the base of the cross section. Measured depths (feet) and sandstone names are shown on the right side of this figure.

Figure 4-24. Detailed cross section highlighting the interbedded shale in the sandstone packages.

4.3.5 Discussion

The Bradford Group in western Pennsylvania is part of the Catskill clastic wedge (Figure 4-25), which formed during the Acadian orogeny as sediments from the mountain-building (orogenic) event were deposited into the shallow Catskill Sea between the mountain belt to the east and the craton to the west. Over time, as the orogeny continued, the sea filled with sediments and the basin margin migrated westward, resulting in coarser alluvial fan deposits above basin floor deposits (Woodrow, 1985). Coarser sandstones may intrude basin floor deposits locally, as turbidites, but in general the older, underlying Bradford Group deposits are finer-grained than the

overlying Venango Group sandstones in the Catskill Delta sequence in western Pennsylvania (Harper, 1999; Lundegard, et al., 1985; Woodrow, 1985). The Bradford Group is a progradational shoreline facies tract deposited in response to filling of the proximal foreland (Figure 4-25). It consists of thick, upward coarsening sand-dominated sequences, with nearshore marine and deltaic facies grading upward to coastal and alluvial-plain sands (Castle, 2001a).



Note: The Bradford Group sands (Column 2) in western Pennsylvania (Area 2) were deposited in a shoreline facies tract (E) during the late phase of the Acadian orogeny, when the sands prograded onto the distal foreland ramp of the Appalachian foreland basin (modified from Castle, 2001a).

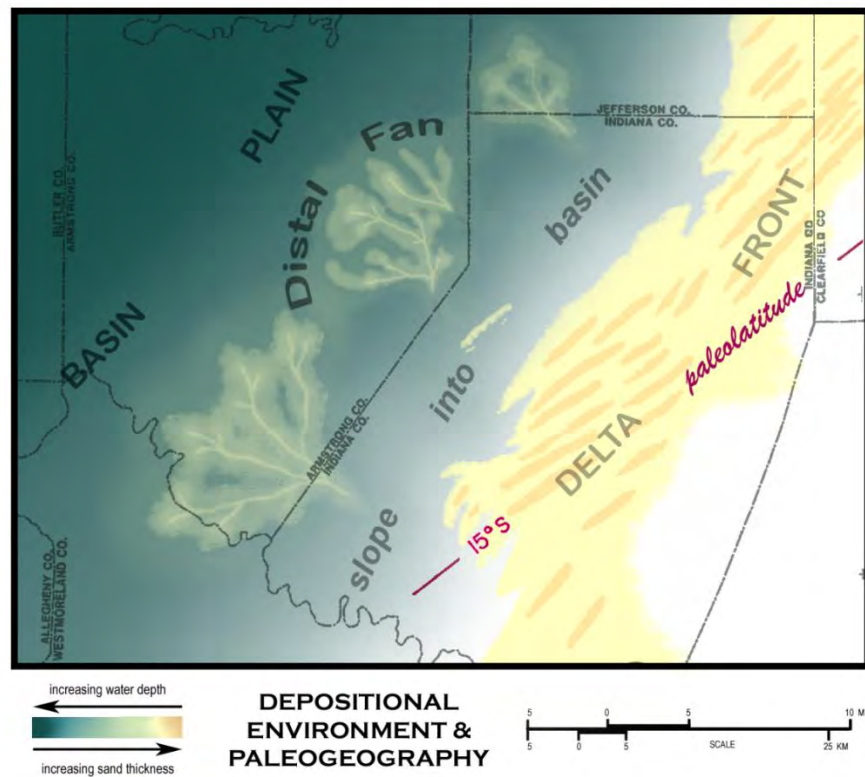
Figure 4-25. Appalachian foreland basin stratigraphic columns (northwest-southeast) from middle Devonian through lower Mississippian time.

4.3.5.1 Depositional Environment

Bradford Group sands in the case study area were deposited as submarine channels and in near-shore delta front environments (Boswell et al., 1996a), as shown in Figure 4-26 for the First Bradford sand. A modern analogue is the epeiric Arafura Sea between the tectonic lands of New Guinea and the stable Australian craton (Murin, 1988).

The fluvial-deltaic facies of the Bradford Group form discontinuous sand bodies that vary both vertically and laterally. However, they possess a common depositional energy, water depth, and sediment supply (Castle, 2001b). This creates recognizable patterns of deposition. These patterns can be mapped using the closely spaced geophysical well log control that exists in many

Bradford development fields to find facies suitable for brine injection, as well as stratigraphic traps including permeability pinchouts and seals.



Sources: Modified from Boswell et al. (1996a) and Murin (1988).

Figure 4-26. Depositional environment and paleogeography of the First Bradford sandstone, showing a portion of the model over the southern part of the case study area.

4.3.5.2 Porosity and Permeability

Porosity and permeability values of sandstones in the Bradford Group are highly variable (Table 4-2). Porosity measurements from core analysis range from 0.04% to 11%. In some areas, compaction has reduced porosity (Murin, 1988). Although permeability measurements of less than 0.01 mD have been found to be common (Murin, 1988), measurements as high as 44 mD have been recorded (Glohi, 1984). High permeability measurements usually occur in fractured zones. In addition, dissolution of cements and/or grains caused high permeability in the Kane sandstone in Cush Cushion field (Hussing, 1994), which lies on the eastern side of the area examined here. The porosity and permeability variability encountered in these sandstones depend on the initial depositional environment and post-depositional factors including compaction, fracturing, and dissolution of cements and/or grains.

Table 4-2. Porosity and permeability data for Bradford Group sandstones.

Well ID	Driller's Sandstone	Number of Samples Analyzed	Interval Measured (feet)	Range of Porosity from Core Analysis (%)	Average Porosity from Core Analysis (%)	Range for Permeability to Air (mD)
063-25084 ^a	Warren	14	30	0.04 - 8.4	2.92	0.01 - 44.0
	Upper Speechley	13	25	2.7 - 7.5	5.25	0.01 - 1.8
	Second Balltown	13	25	0.05 - 8.7	3.42	0.01 - 0.03
	Sheffield	23	25	2.6 - 8.5	7.13	0.01 - 11.8
005-22349 ^b	Speechley	26	28	3.3 - 9.0	5.85	<0.1 - 28.0
	Balltown	13	17	1.3 - 4.9	3.65	<0.1 - 33.0
	First Bradford	16	23	1.2 - 10.2	6.81	<0.1 - 3.0
129-21640 ^b	First Bradford	11	12	6.8 - 12.0	9.74	<0.1 - 263.0
129-21642 ^b	Speechley	15	28	8.6 - 10.6	9.63	<0.1 - 957.0
	Balltown	21	26	1.2 - 11.1	8.49	<0.1 - 57.0

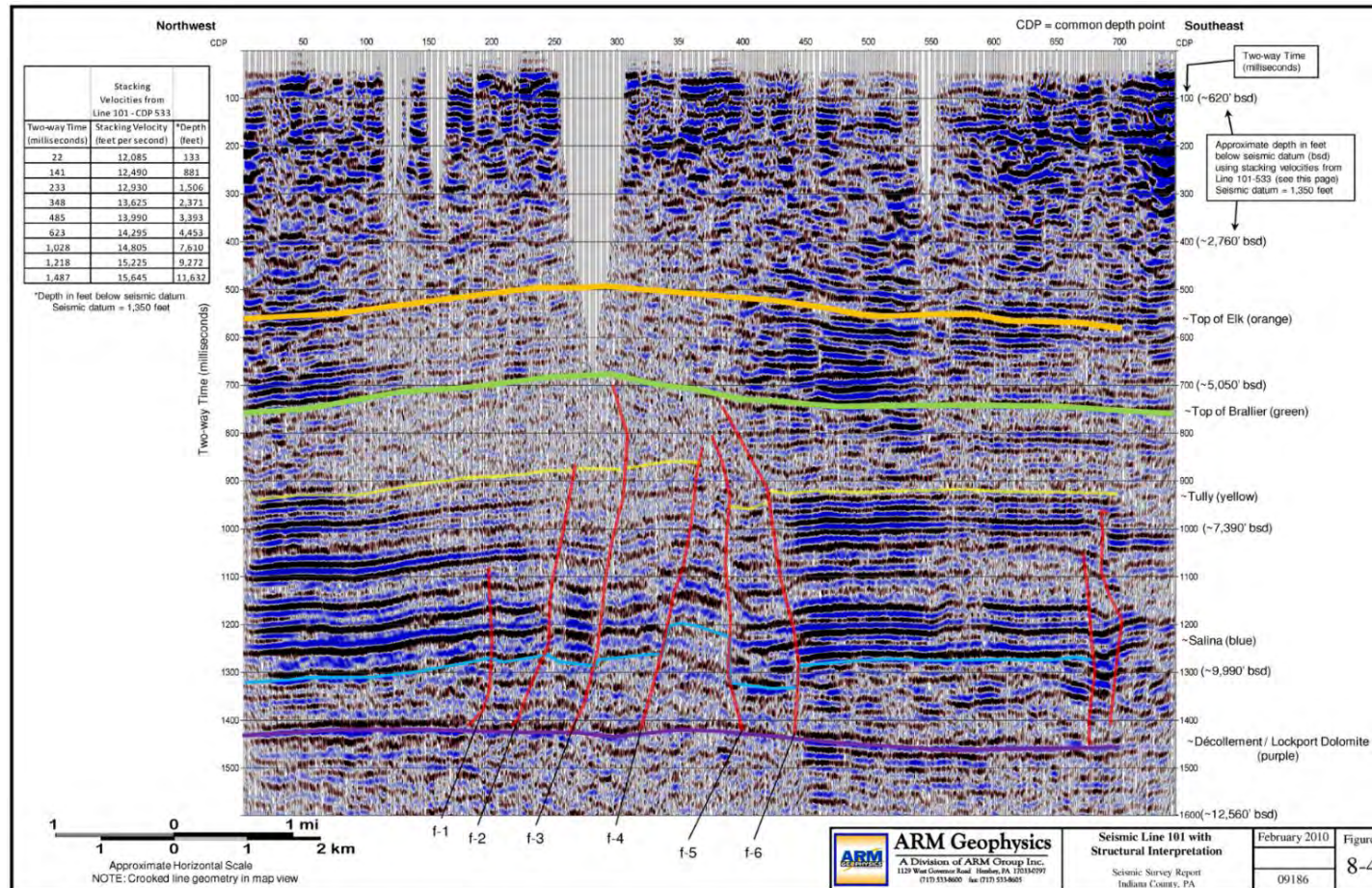
Data from Glohi (1984).

Data from core analysis reports on file at Bureau of Topographic and Geologic Survey, Pittsburgh, Pennsylvania.

4.3.6 Seismic Data

In 2009, the Pennsylvania Bureau of Topographic and Geologic Survey oversaw the collection of approximately 25 miles (40 kilometers) of seismic lines in southern Indiana County. One seismic line was run approximately parallel to the axis of the Jacksonville anticline, and two lines were run perpendicular to that line (Carter et al., 2014). These seismic lines were planned along the Jacksonville anticline in Indiana County, an area known for its oil and gas production. The seismic lines lie within the southern extents of this case study (see Figure 4-23).

The seismic study revealed a series of en echelon low-angle normal faults affecting the Tully Limestone (yellow line) and the Salina salts (blue line) (Figure 4-27). The seismic line shown in Figure 4-27 was run approximately perpendicular to the anticline. These faults were interpreted by ARM Geophysics (Vogel et al., 2010) to rise from a décollement zone at the top of the Lockport Dolomite (purple line). The Bradford Group is not shown on this seismic survey. It lies above the Elk Formation (orange line). Because these interpreted faults die out in either the Brallier Formation (green line) or in the Hamilton Group (Carter et al., 2014), there does not appear to be significant risk to injecting brine into the Bradford Group in the vicinity of this anticline.



Source: From Vogel et al. (2010).

Figure 4-27. 2D seismic line with structural interpretation.

4.3.7 Conclusions

Oil and gas has been produced from Bradford Group sandstones for decades, and there is potential for the conversion of depleted fields to brine injection. Detailed maps using geophysical log control will be necessary to identify sandstone lenses with sufficient porosity, permeability, and areal extent for injection. Because these Bradford Group sandstones tend to be discontinuous, a sufficient degree of log control is needed to understand the depositional environment in order to interpret the pattern of facies development. Using the injection wells shown in these cross sections as examples, it is recommended that higher GR and lower RhoB values be used to evaluate these potential injection zones rather than the cutoffs used in this case study.

The First Bradford and Speechley represent the culmination of a period of rapid progradation and were deposited over a wide areas, with each being followed by deposition of shale during periods of transgression. The sands underlying the First Bradford, deposited as submarine fans to shallow marine, tend to be thinner, although they can be productive locally. However, in the Balltown stratigraphic interval between the First Bradford and Speechley, the increase in depositional energy in response to shoreline progradation (Castle, 2001b), combined with the rapid progradation that occurred during deposition of the Balltown sands, result in reservoir-quality sands that have good vertical and lateral seals. Occurrence of sand in the Warren interval also tends to be contained by transgressive shales both vertically and laterally.

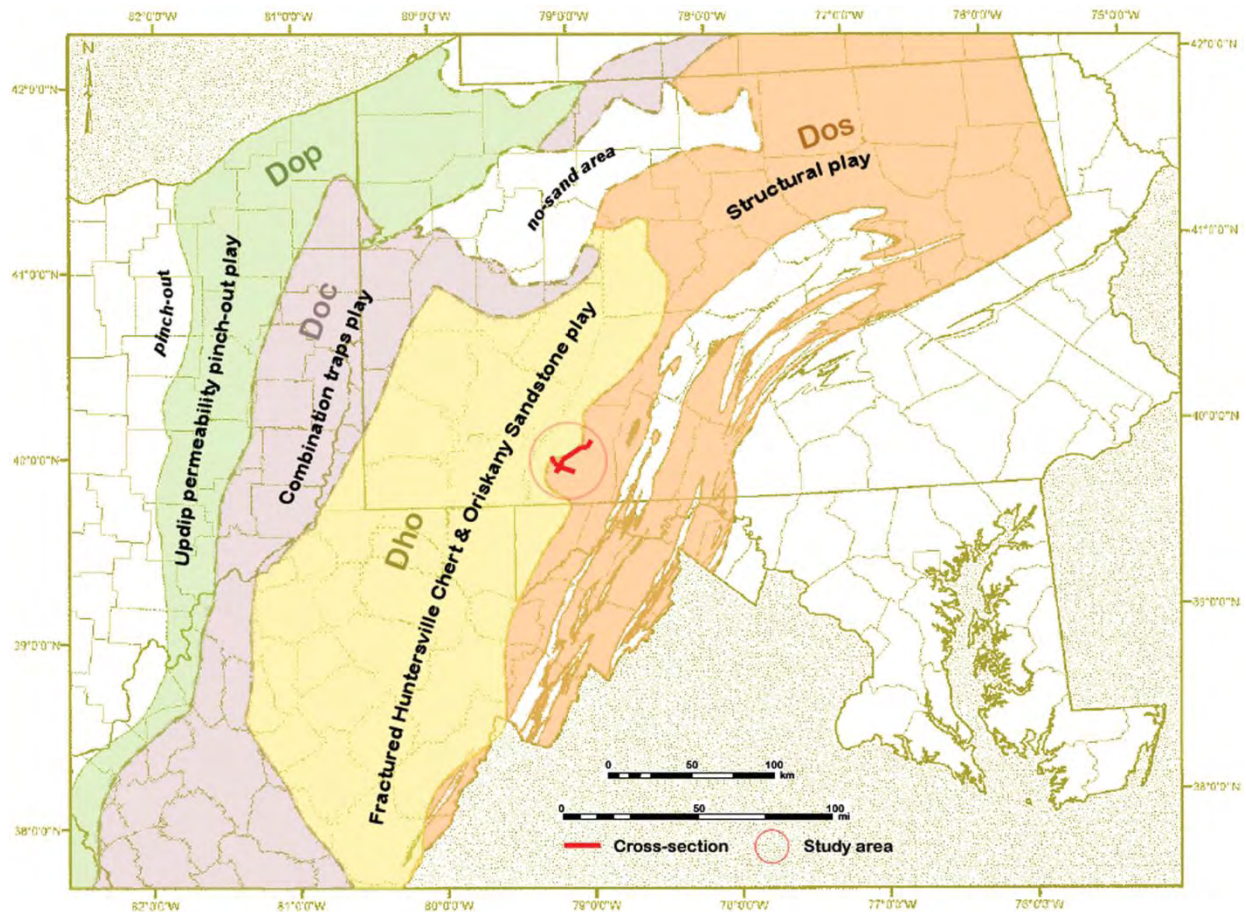
The potential proximity of faults needs to be taken into account when planning an injection well, especially in the vicinity of surface anticlines. The Onondaga-Salina interval is faulted extensively in the area of surface anticlines (Beardsley et al., 1999). The risk does not appear to be significant around the Jacksonville Anticline, but faults do exist beneath this anticline. Higher resolution data may be necessary to prove that there is no risk from faults in the Bradford Group sandstones.

4.4 Pennsylvania Lower Devonian Oriskany Sandstone Case Study

4.4.1 Introduction

Currently, over half of the active brine disposal wells in Pennsylvania inject into the Oriskany Sandstone. The Oriskany Sandstone has remained an important target for oil and gas development in Pennsylvania since the North Penn Gas Company No. 1143 well was completed in Tioga County on September 11, 1930 (Kostelnik and Carter, 2009a). The majority of the development of the Oriskany Sandstone play in Pennsylvania has taken place on anticlines within 50 miles (80 kilometers) of the Allegheny structural front (Harper and Patchen, 1996).

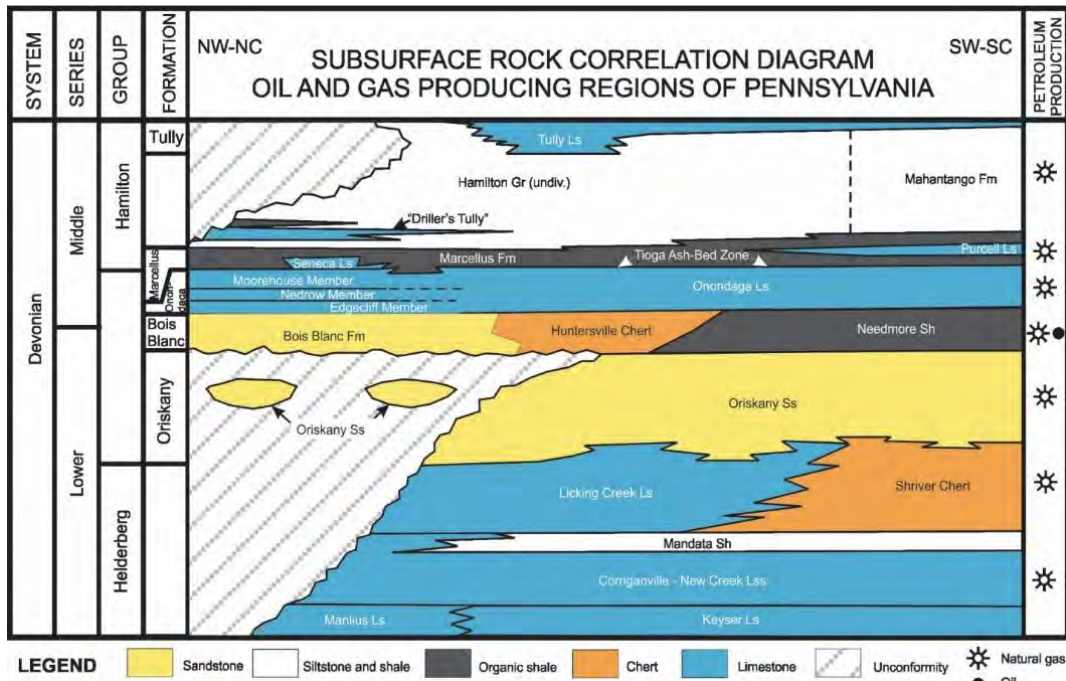
The Oriskany Sandstone in the Appalachian basin has been divided into four distinct natural gas plays, as described by Harper and Patchen (1996), Flaherty (1996), Patchen and Harper (1996), and Opritza (1996). These plays can be identified by their various trapping mechanisms and are: (1) Dos: Lower Devonian structural play; (2) Dho: fractured Middle Devonian Huntersville Chert and Lower Devonian Oriskany Sandstone; (3) Doc: Lower Devonian Oriskany Sandstone combination structural and stratigraphic traps; and (4) Dop: Lower Devonian Oriskany Sandstone up-dip permeability pinch-out. This case study looks at wells within the Dho and Dos reservoirs in Somerset County, Pennsylvania (Figure 4-28).



Source: Modified from Kostelnik and Carter, 2009a.

Figure 4-28. Distribution of Oriskany Sandstone natural gas plays.

Oriskany completions and production are often commingled with the overlying Huntersville Chert in Pennsylvania (Figure 4-29). Within this interval, drilling companies seldom differentiate between these formations and will stimulate zones with the highest porosity. Oriskany production is most often commingled with the Huntersville Chert in the fractured (Dho) play and the southwest part of the structural (Dos) play. Geologic logs of these three formations indicate various combinations of sandstone, limestone, and chert. These formations have been subjected to numerous periods of alteration, with post-diagenetic fractures having left the most significant overprint (Harper and Patchen, 1996), which often leads to the commingled production.



Source: From Carter, 2007.

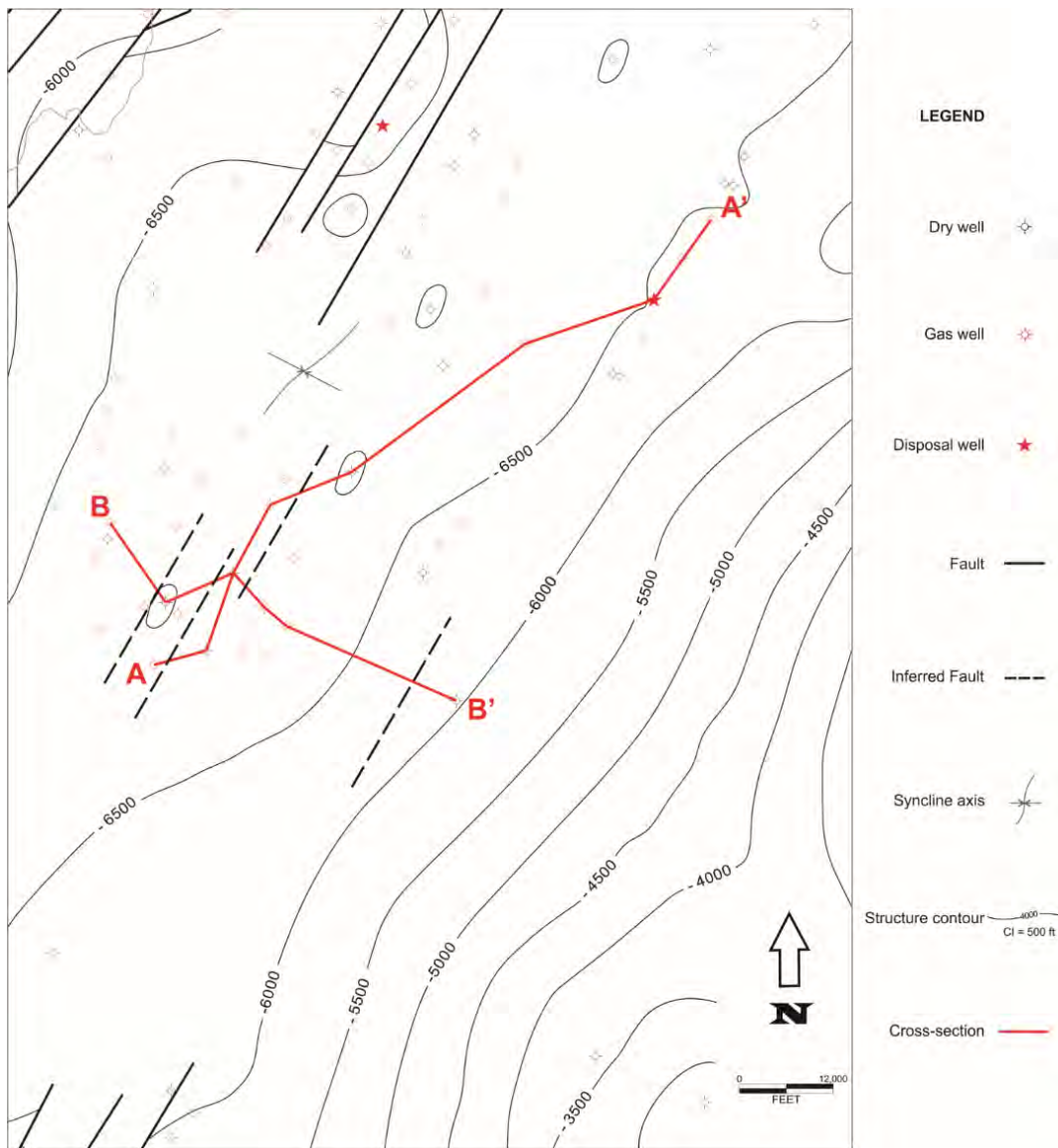
Figure 4-29. Subsurface correlation diagram of Lower and Middle Devonian formations in Pennsylvania.

4.4.2 Objectives

Currently, four UIC Class II wells are disposing into the Oriskany Sandstone in Pennsylvania. The purpose of this case study was to evaluate the Oriskany Sandstone as a reservoir for injection of brine fluids in the geographical area surrounding two of these active disposal wells. Located in Somerset County, they are API No. 3711120006 and API No. 3711120059.

4.4.3 Methodology

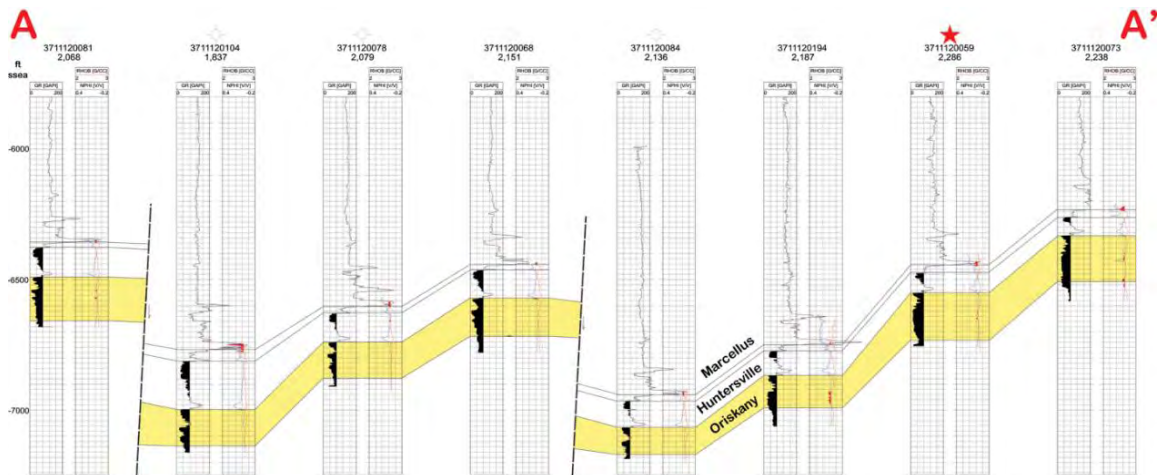
GR, neutron porosity (NPHI), and bulk density (ρ_B) geophysical logs were utilized to identify Oriskany Sandstone intervals with injection potential. GR of ≤ 80 API units and a ρ_B of ≤ 2.65 g/cc were used to highlight $\geq 50\%$ sand with $\geq 5\%$ porosity. Well-to-well cross section correlations were made using geophysical logs and were run both parallel and perpendicular to regional strike using PETRA[®] software. Cross section locations and the local Oriskany structure are shown in Figure 4-30. Faults in these two cross sections (Figures 4-31 and 4-32) were inferred by the change in stratigraphic position of the correlated formations. The dashed fault lines shown on these cross sections represent offset between neighboring wells and not the precise fault locations or offsets. The approximate locations were then located on the structure map and the faults were oriented parallel to previously mapped faults.



4.4.4 Results

The mapped faults in this area trend roughly parallel to the strike of the mapped syncline (Figure 4-30). These faults formed as a result of imbricate thrust-faulting. The strike cross section (Figure 4-31) is most likely to cross faults where it deviates from the true strike orientation. In Figure 4-31, it can be observed that the dry wells were encountered on the downward side of the fault blocks. The dip cross section (Figure 4-32) is oriented roughly perpendicular to these faults.

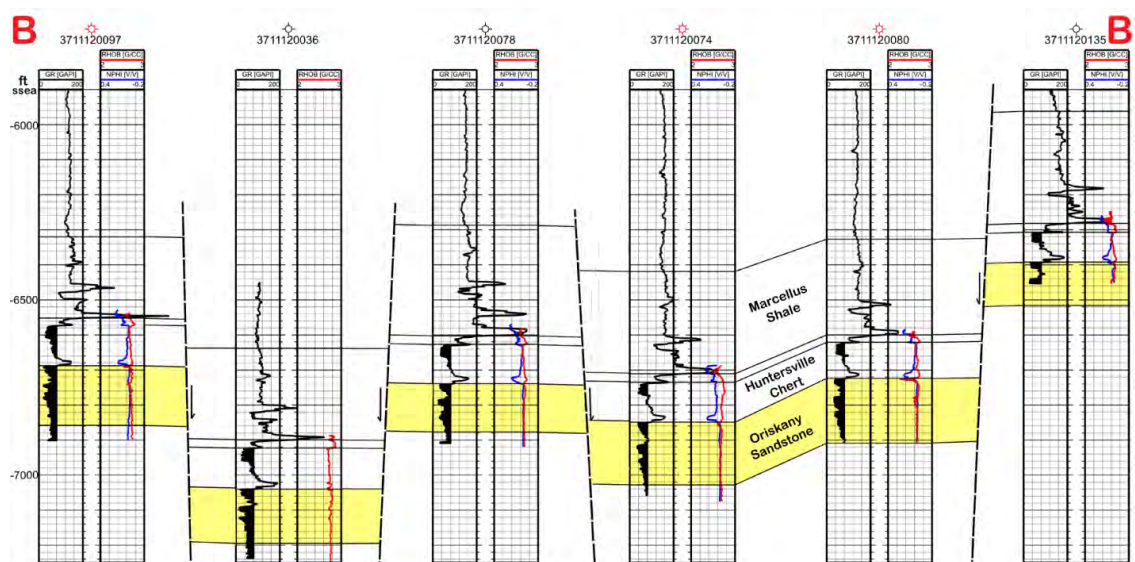
Figure 4-31 illustrates A–A', a southwest-to-northeast cross section that contains logs from the Rockwood, Shamrock, Somerset West, and Shanksville fields in Somerset County, Pennsylvania. This cross section is parallel to basin strike and crosses three tilted fault blocks that are sub-parallel to basin strike. Completion reports show 3711120104, 3711120078 and 3711120084 to be dry, which suggests that these wells encountered the Oriskany Sandstone below their fault block's gas-water contact.



Note: Structurally lower wells on the fault blocks are dry holes, suggesting that these wells encountered the Oriskany Sandstone below their fault blocks' gas-water contact. Subsea (ssea) depths (feet) are shown at the left of the figure.

Figure 4-31. Southwest-to-northeast cross section A–A' in the case study area showing tilted imbricate fault blocks.

Figure 4-32 illustrates B–B', a northwest-southeast cross section that contains logs from the Kimmel, Rockwood, and Shamrock fields in Somerset County, Pennsylvania. Oriskany Sandstone gas production is contained in isolated pools in separate, tilted fault-bound blocks.



Note: Secondary fracture porosity will likely play a key role in injectivity and overall storage capacity.

Figure 4-32. Northwest-to-southeast cross section B–B' across dip showing isolated fault-bound blocks.

4.4.5 Discussion

In the central Appalachian Plateau Province, it became apparent early in the development of the Oriskany structural traps play (Dos) that the overlying Huntersville Chert was at least as important a gas reservoir as the Oriskany (Harper and Patchen, 1996). Thus, Flaherty (1996) assigned most of the Oriskany structural reservoirs in the central Plateau to the fractured Middle Devonian Huntersville Chert and Lower Devonian Oriskany Sandstone play (Dho). The location of this case study is near the border of these two sandstone plays. Well production in this area is controlled by a combination of fractures and structural traps.

Kostelnik and Carter (2009b) report that the distribution of porosity and permeability varies depending upon type of Oriskany play. While the highest porosity values based on geophysical log data and core analysis occur in Dop and Doc plays (see Figure 4-28), well data from the Dho play shows high fracture porosity. Although the Dos play shows the lowest measured permeabilities, and a wide variability in lithologies and porosities, well control and cumulative gas production in this play can be used to target individual wells with permeability suitable for injection.

In the case study area in Somerset County, upper Oriskany arenites are extensively cemented by calcite and secondary quartz (Basan et al., 1980). With low porosity and the lack of good fracture permeability, production zones rely heavily on fractures that accrued post-diagenesis, most likely as a result of the Alleghanian Orogeny.

With respect to structure, the wells in the case study area are positioned on tilted imbricate fault blocks. Gas will be trapped in the high portion of the fault block, with the low portion of each fault block tending to be wet. Thus, dry holes may not be truly indicative of lack of porosity or permeability.

4.4.6 Conclusions

The Oriskany Formation is divided into four different natural gas plays in the Appalachian basin. Kostelnik and Carter (2009b) report that the distribution of porosity and permeability varies depending upon type of Oriskany play. Active injection wells in Pennsylvania are disposing fluids in the Oriskany Sandstone in three of these plays. The highest porosity values based on geophysical log data and core analysis occur in Dop and Doc plays (see Figure 4-28); the disposal well in Beaver County is injecting into the Oriskany Sandstone in the Doc play. No Oriskany wells in Pennsylvania are injecting into the Dop play. Three disposal wells and one recent brine injection permit are targeting the Oriskany Sandstone in the Dho play. Well data from this play shows high fracture porosity. Two active injection wells are injecting into the sandstone in the Dos and Dho plays in southwestern Pennsylvania. Although the Dos play shows the lowest measured permeabilities, and a wide variability in lithologies and porosities, well control and cumulative gas production can be used to target individual wells with permeability suitable for injection.

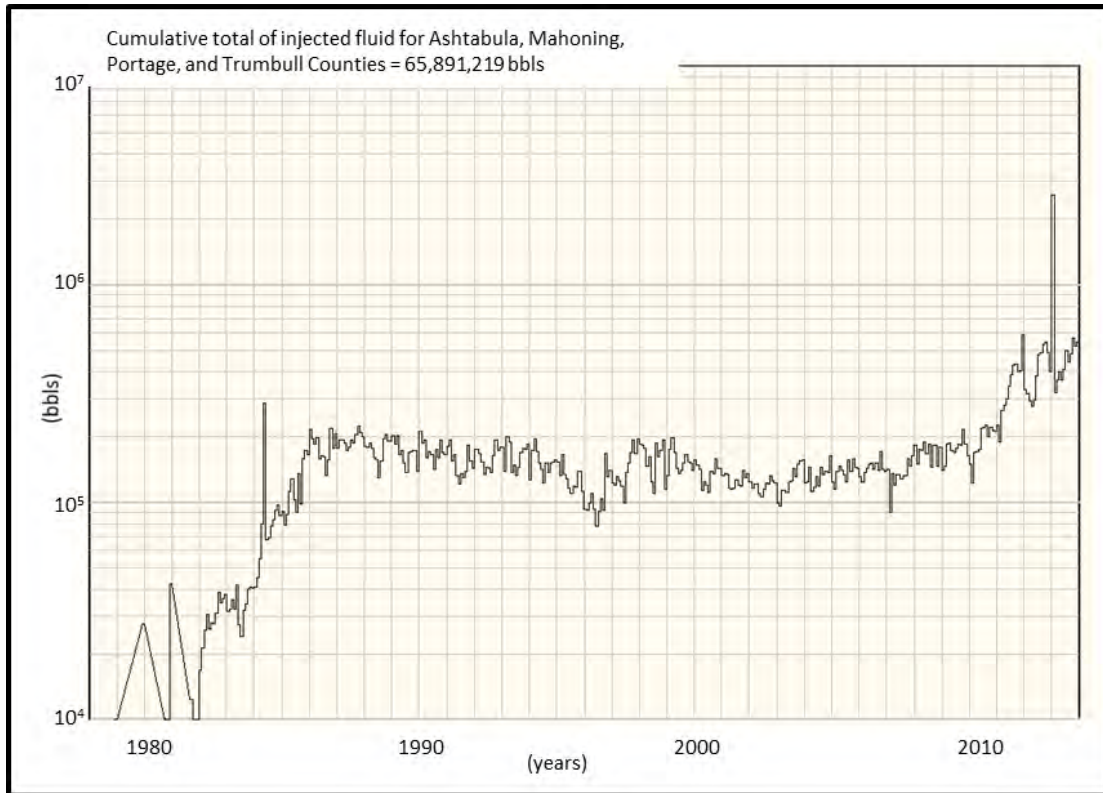
Both geologic structure and fracturing account for gas production in the area of this case study, and vertical communication with the Huntersville Chert must be considered. Structurally, these wells are positioned on tilted imbricate fault blocks. Gas will be trapped in the high portion of the fault block, with the low portion of each fault block tending to be wet. The downdip contact with water in these tilted fault blocks may function as the seal to gas migration with respect to adjacent fault blocks.

Fracture permeability is not evident in geophysical log data and is not easily measured using core data. Cumulative production and production decline curves in depleting/depleted gas wells may be more useful when considering wells for possible conversion to brine injection, prior to testing injectivity in these wells. Even so, non-productive wells that exist below the gas-water contact may also have good fracture permeability.

4.5 Ohio Upper Silurian Lockport/Newburg Case Study

4.5.1 Introduction

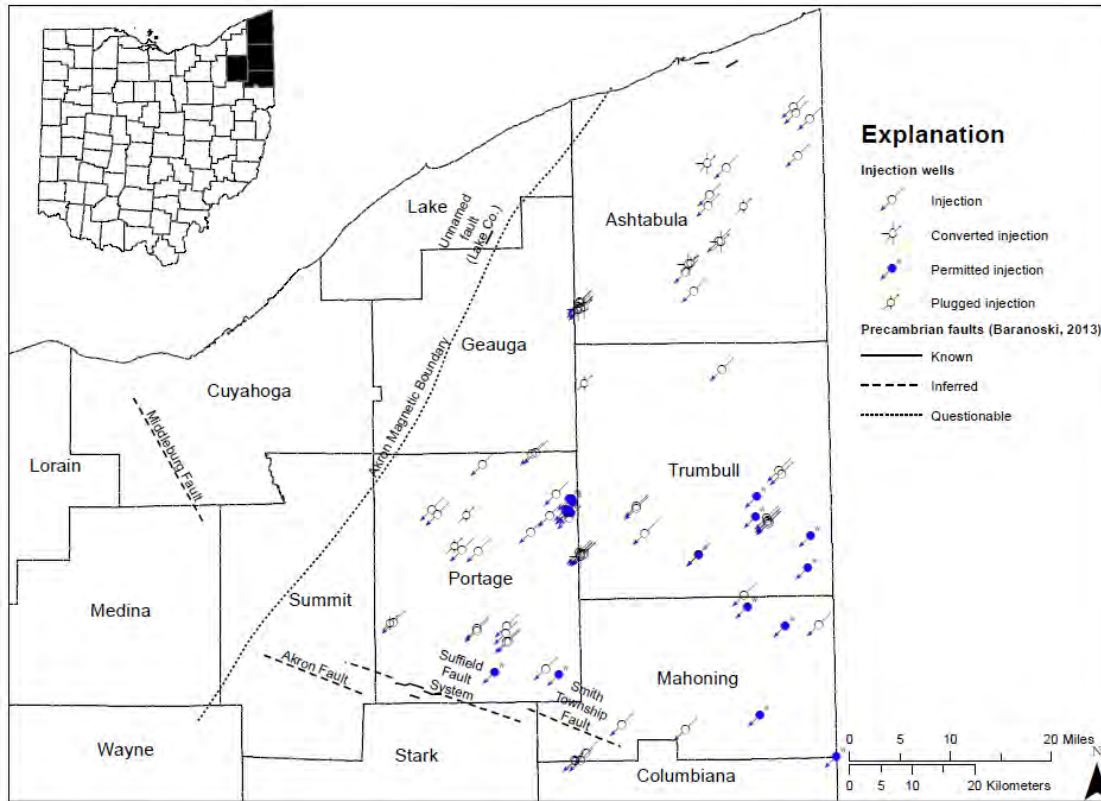
Beginning in 1983, oil, gas, and saltwater production, as well as disposal volumes, have been reported to the State of Ohio. Since that time, over 65 million barrels (MMbbl) of fluid associated with oil and gas production have been injected into Class II wells in northeastern Ohio counties, specifically, 16 MMbbl in Ashtabula, 4 MMbbl in Mahoning, 32 MMbbl in Portage, and 13 MMbbl in Trumbull (Figure 4-33).



Note: Limited injection volume reports were turned in to the State of Ohio prior to 1983, when state law first required operators to report injection volumes. Data spikes may be a result of inaccurate volumes records or poor injection practices; however, the increase of fluid injection is coincident with the increase in Marcellus Shale drilling activity.

Figure 4-33. Total volume of fluid injected per year in Ashtabula, Mahoning, Portage, and Trumbull Counties, Ohio.

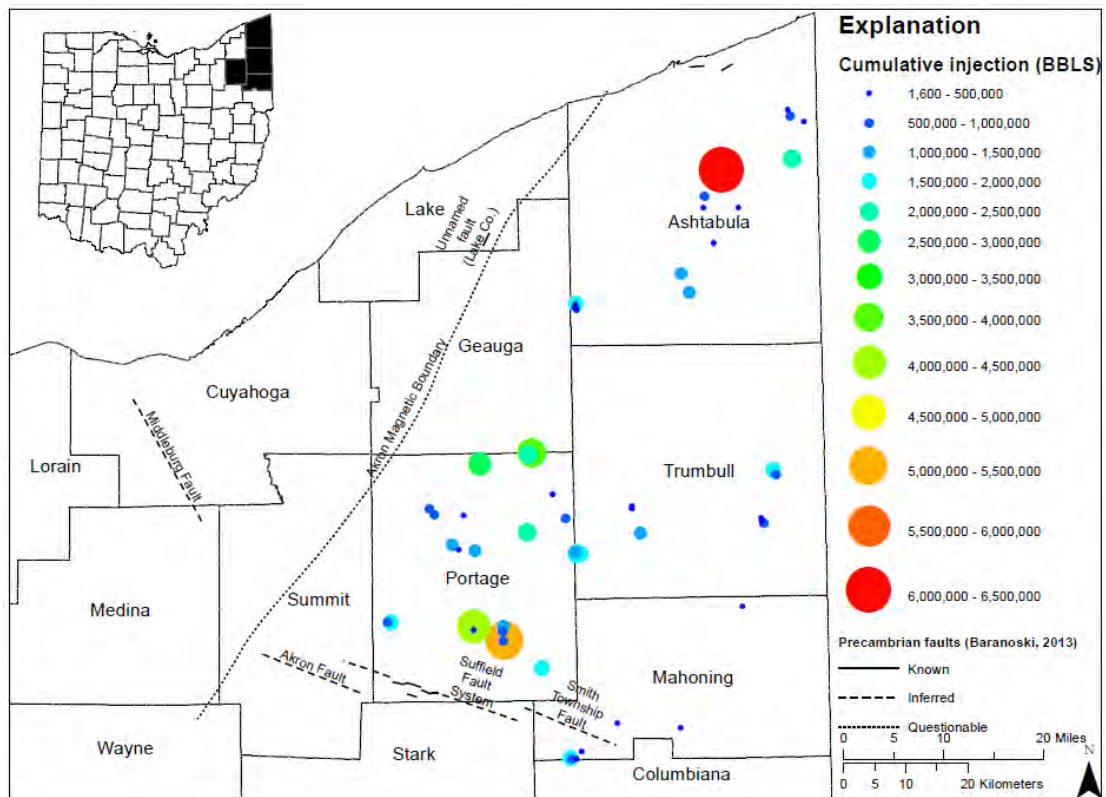
After the 2011 seismic events in Youngstown Township of Mahoning County, which were closely related to Class II disposal, the Division of Geological Survey created supplemental maps for 31 Class II permit application locations, in relation to known structural features of northeastern Ohio, to aid Ohio's UIC Program for Class II permit application approval. Of the 31 Class II permit application locations mapped—3 in Ashtabula, 3 in Mahoning, 9 in Portage, and 16 in Trumbull Counties—17 of the permit applications proposed 'Newburg' as the injection target. In northeastern Ohio, 'Newburg' typically refers to the Silurian Lockport Dolomite (Figure 4-34).



Source: DOGRM, 2014.

Figure 4-34. Location of Class II wells in northeastern Ohio as of September 2014.

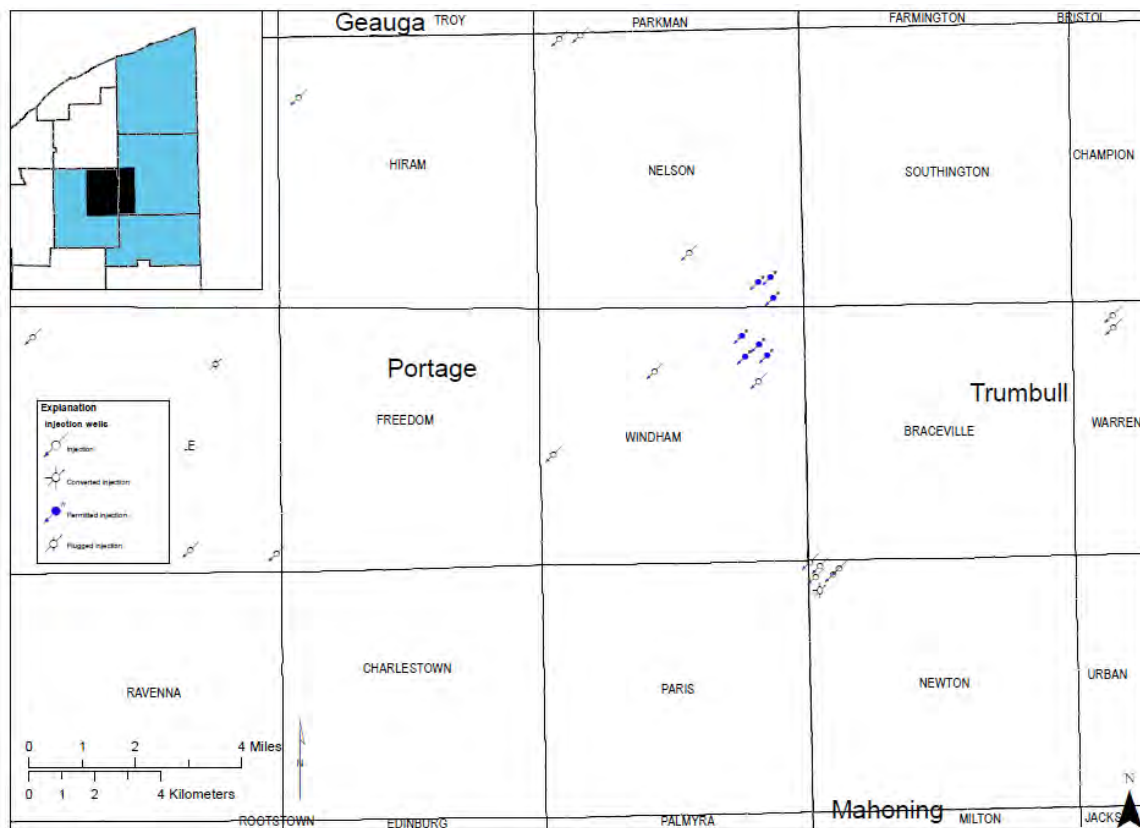
The majority of fluid injection in northeastern Ohio is in Portage County and targets the Wenlockian-Ludlowian (middle Silurian) Lockport Dolomite (Figure 3-4, Figure 4-35). In 2014, four Class II permit applications targeted the Lockport Dolomite in Windham Township, Portage County, Ohio (Figure 4-36). Initial indications suggested the potential of targeting fracture porosity. Windham Township lies just northwest of and is consistent with the trend of the Mahoning River Valley lineament (ODNR, 2012). However, the potential for high-porosity reefal structures within the Lockport Dolomite has also been recognized (Carman, 1927; Floto, 1954; Kahle and Floyd, 1972; Smosna et al., 1989; Noger et al., 1996). To determine the underlying structure and Lockport stratigraphic properties, a number of petrophysical wells logs in the vicinity of Windham Township were depth registered, formations were correlated, and selected horizons were mapped (Figure 4-37).



Source: DOGRM, 2014.

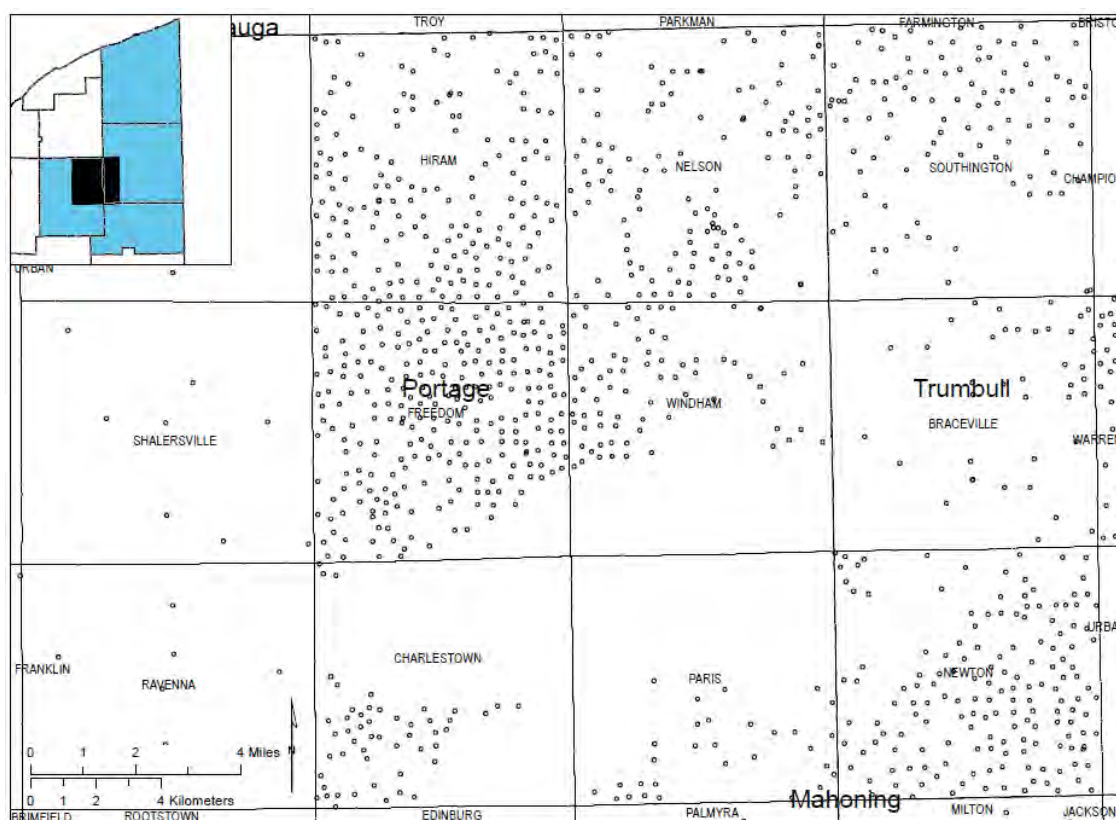
Note: Majority of injection in Portage County, Ohio (32 MMbbls).

Figure 4-35. Cumulative fluid injection by well, graduated symbol size, and color.



Note: Area of interest focused on a nine-township block around Windham Township.

Figure 4-36. Seven Class II permit application locations in Nelson and Windham Townships, Portage County, Ohio.



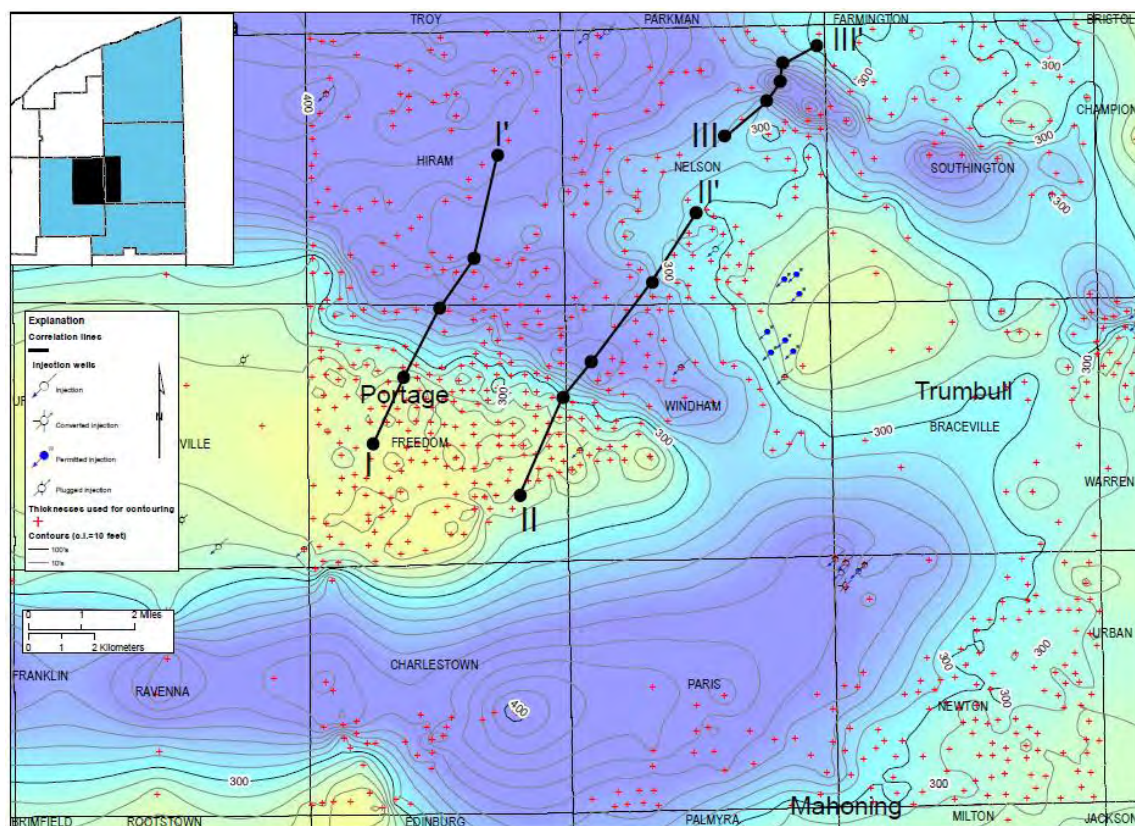
Note: Not all wells were used due to time constraints. There are no drilled wells which penetrate the Dayton Formation in blank areas of Charlestown, Paris, and Windham Townships, Portage County, Ohio.

Figure 4-37. Well locations used for initial mapping.

4.5.2 Lockport Dolomite

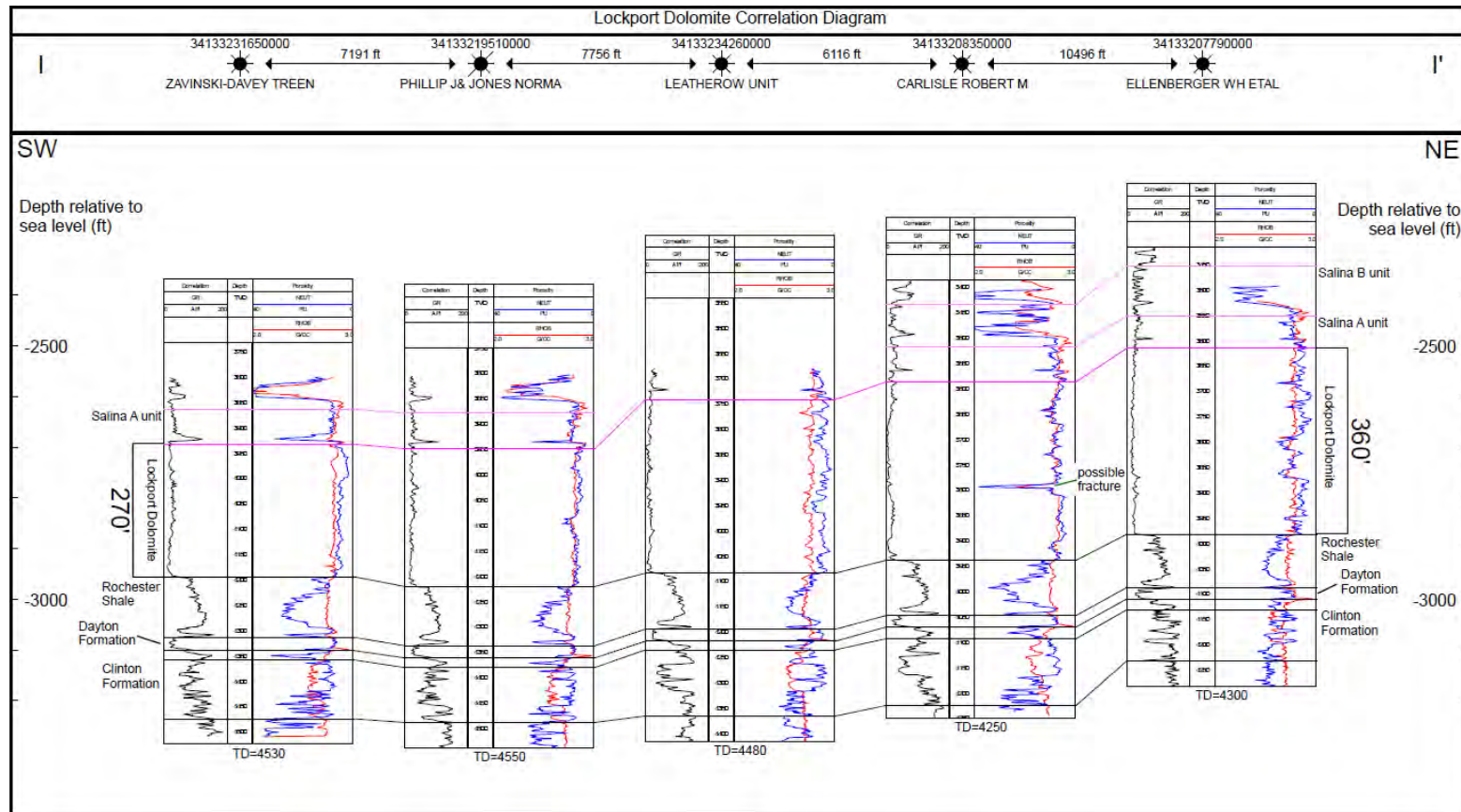
At outcrop in western Ohio, carbonate mounds identified as reefs have been described within the Lockport Dolomite (Carman, 1927). These reefal mounds are typically composed of packstones, wackestones, and grainstones (Kahle and Floyd, 1972). Many of the mounds are bound by stromatoporoids, tabulate corals, bryozoans, and algae. The binding is most extensive in the centers of the reefs/bioherms. Few petrological studies of the Lockport Dolomite in eastern Ohio have been conducted; however, areas of potential Lockport reef development have been identified (Smosna et al., 1989; Noger et al., 1996).

An isopach map of the Lockport Dolomite in the vicinity of Windham Township (Figure 4-38) demonstrates a range of thickness from 270 to 400 feet (80 to 120 meters). The majority of thickening occurs in linear east–west and northwest–southeast trends. Well-developed porosity zones are thickest in the thickest part of the build-up and thin on the flanks of the build-up (Figures 4-39, 4-40, and 4-41). Cuttings from wells yielded very few fossils because of cutting size (API#s 34133206530000, 34133209220000, and 34133200760000), but the abrupt, linear thickness changes suggest macroreef development within the area of interest.



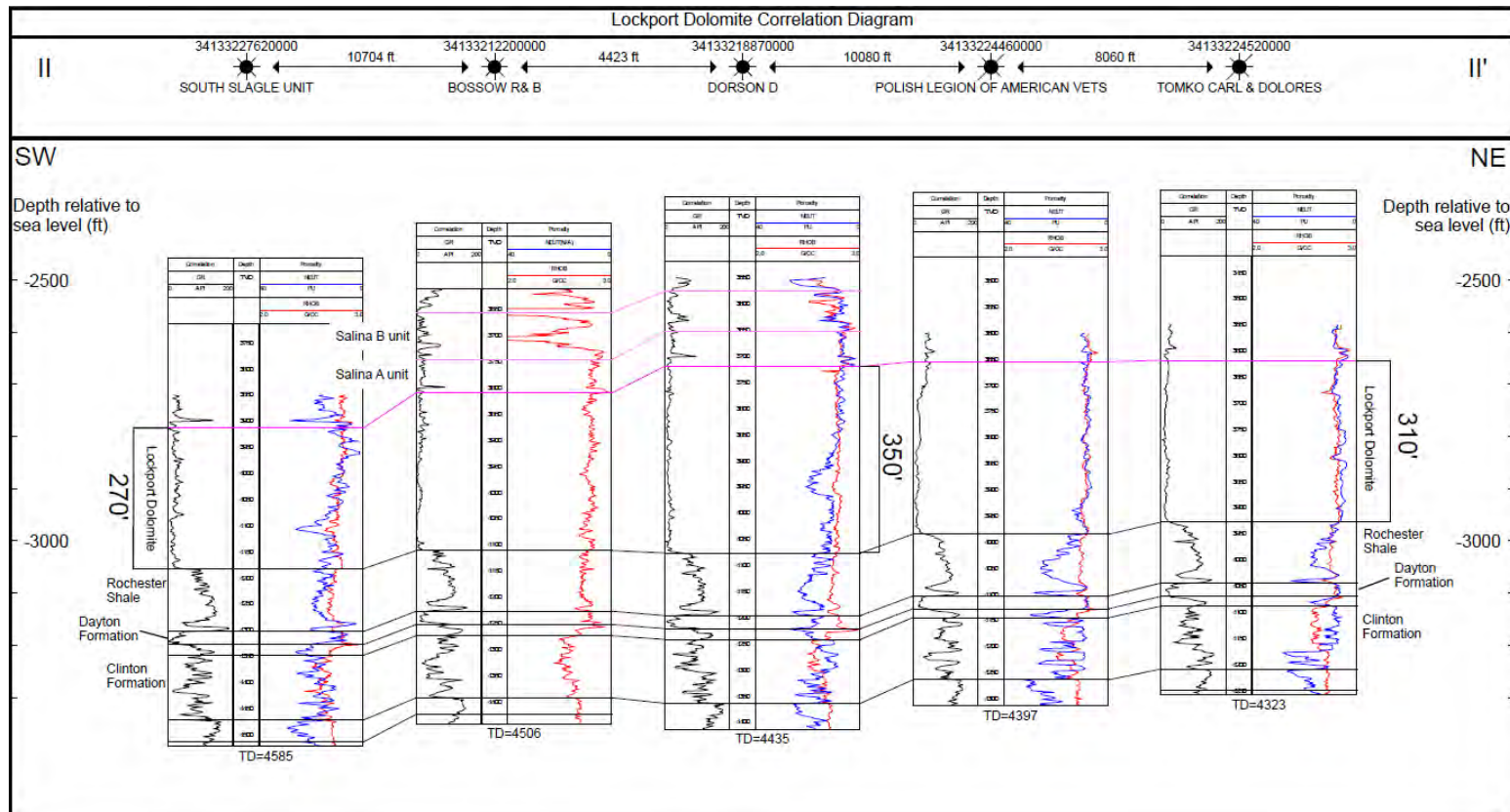
Note: Correlation lines are diagrammed in Figures 4-39, 4-40, and 4-41.

Figure 4-38. Isopach contour map of the Lockport Dolomite in northeastern Ohio showing correlation lines.



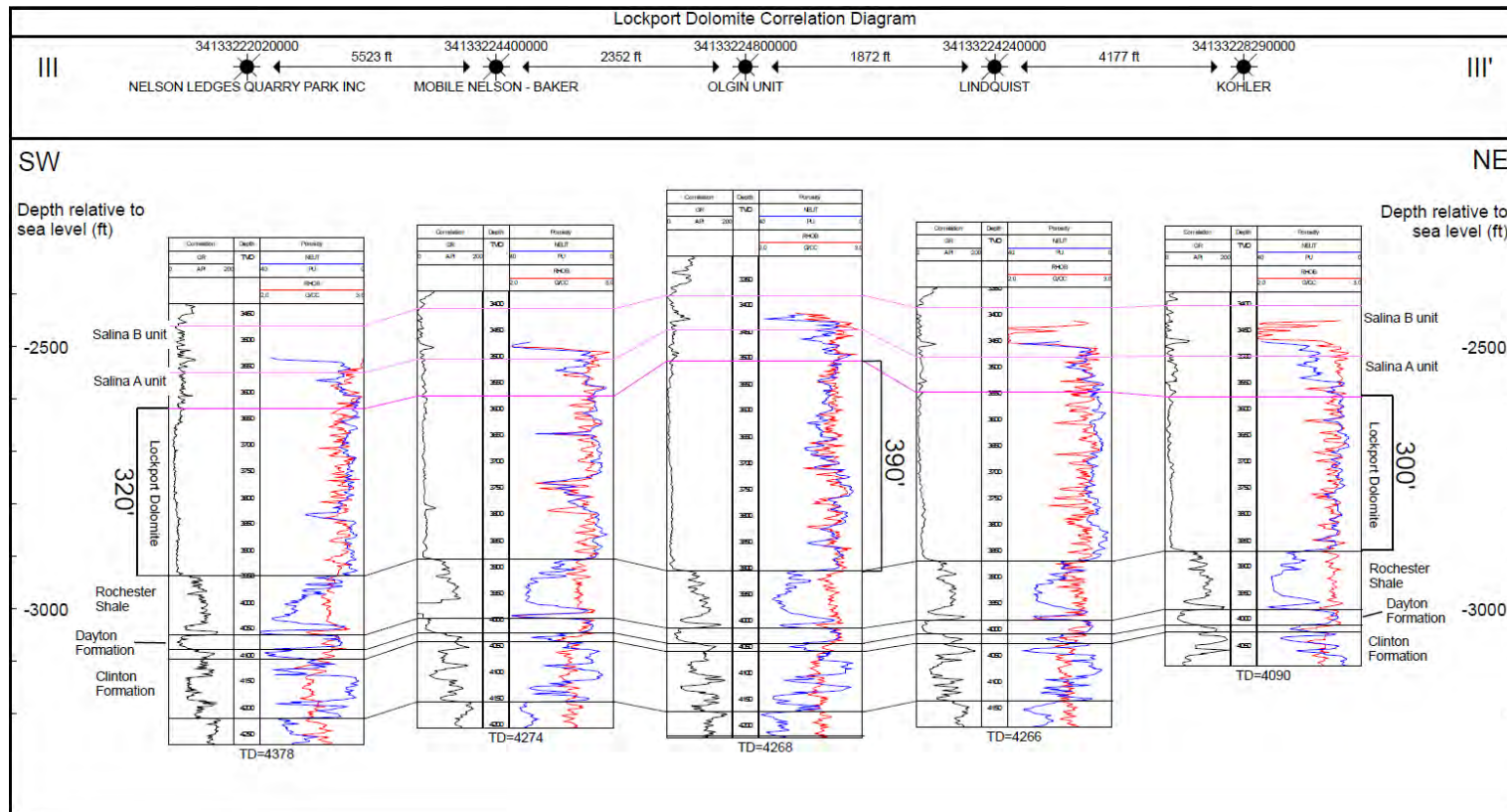
Note: See Figure 4-38 for location.

Figure 4-39. Correlation diagram I-I' of the Lockport Dolomite in northeastern Ohio (no horizontal scale).



Note: See Figure 4-38 for location.

Figure 4-40. Correlation diagram II-II' of the Lockport Dolomite in northeastern Ohio (no horizontal scale).



Note: See Figure 4-38 for location.

Figure 4-41. Correlation diagram III–III' of the Lockport Dolomite in northeastern Ohio (no horizontal scale).

Structurally, the Class II permit applications in Windham Township are located approximately 17 miles southeast of the Akron magnetic boundary and 19 miles northeast of the Akron-Suffield fault system (Figure 4-34). No other known structural features are within the area of interest.

The top of the Lockport Dolomite ranges in elevation from 2,440 feet (740 meters) below sea level to 3,160 feet (960 meters) below sea level (Figure 4-42). Overall, the Lockport dips to the southeast, although the surface displays some relatively consistent east–west/northwest–southeast variations of strike trends from the dominant southwest–northeast strike. The Lockport structure closely mimics the trends displayed on the Lockport isopach map (Figure 4-38). Where structural lows occur on the Lockport surface, the Lockport is thin; where structural highs occur, the Lockport is thick, suggesting the Lockport surface variations are a result of Lockport depositional patterns.

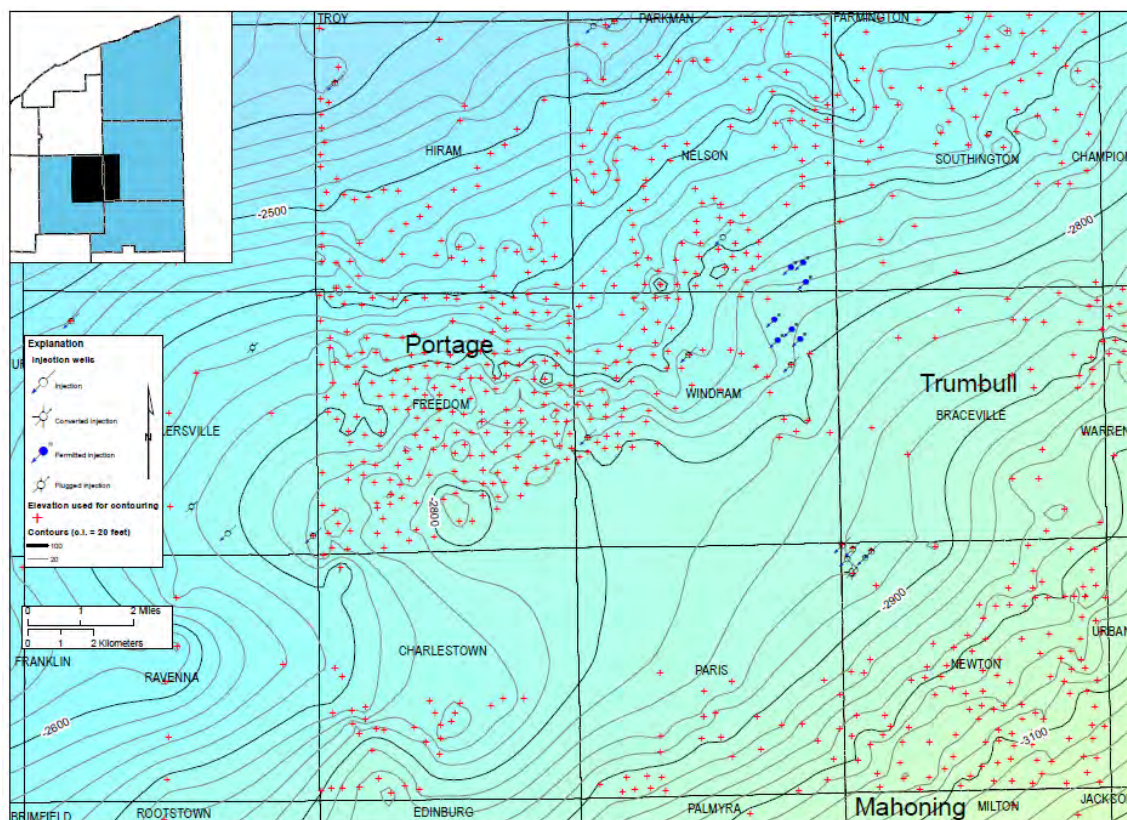


Figure 4-42. Structure contour map on top of the Lockport Dolomite in northeastern Ohio.

4.5.3 Structural Consistency

To ascertain any consistent structural trends, the Wenlockian (middle Silurian) Dayton Formation (Packer Shell) and Middle Devonian Onondaga Limestone were mapped. The Dayton Formation in the vicinity of Windham Township dips to the southeast and ranges in elevation from 2,800 to 3,600 feet (850 to 1,100 meters) below sea level (Figure 4-43). Several localized variations in strike are evident, but they are not persistent throughout the study area. The overlying Onondaga Limestone surface ranges in elevation from 1,000 to 1,800 feet (300 to 550

meters) below sea level (Figure 4-44). The surface of the Onondaga strikes northeast–southwest and dips to southeast. The Onondaga surface shows some subtle variation of strike consistent with variations seen on the Lockport surface (see Figure 4-42). These consistent fluctuations of strike on the Onondaga surface may be a result of depositional patterns in the Lockport Dolomite (see Figure 4-38).

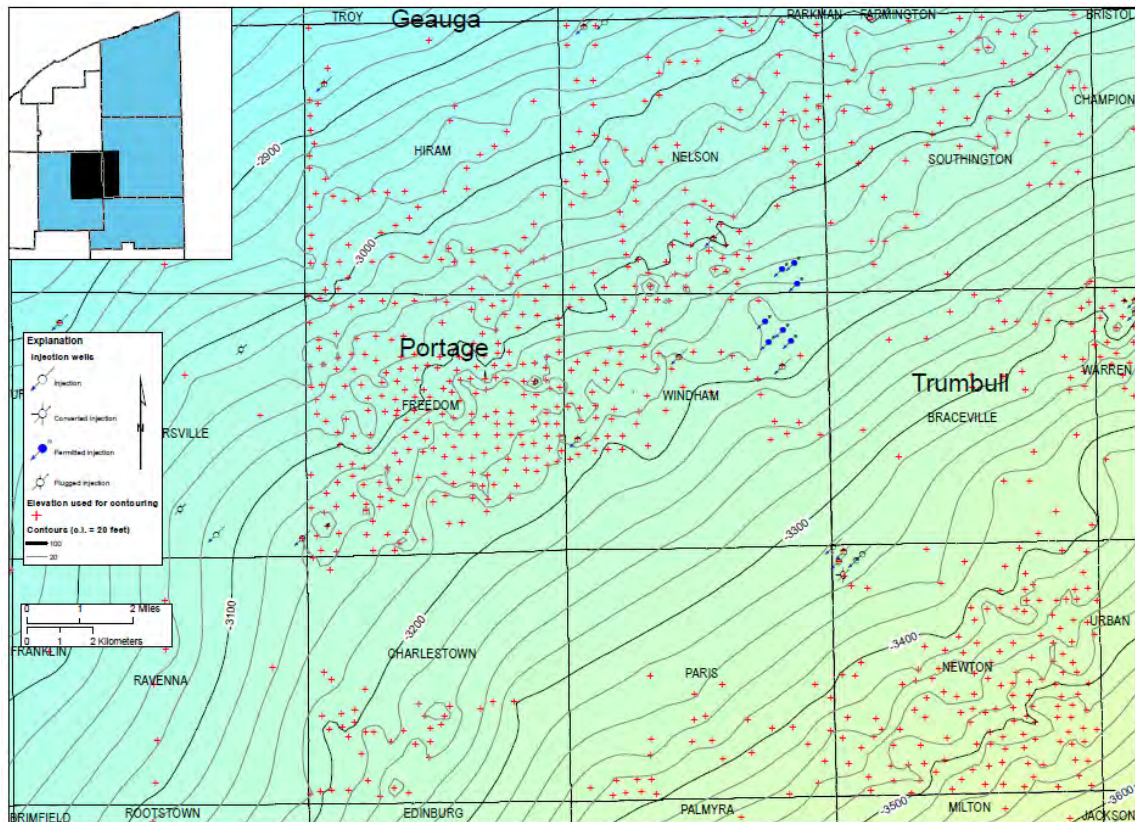


Figure 4-43. Structure contour map on top of the Dayton Formation in northeastern Ohio.

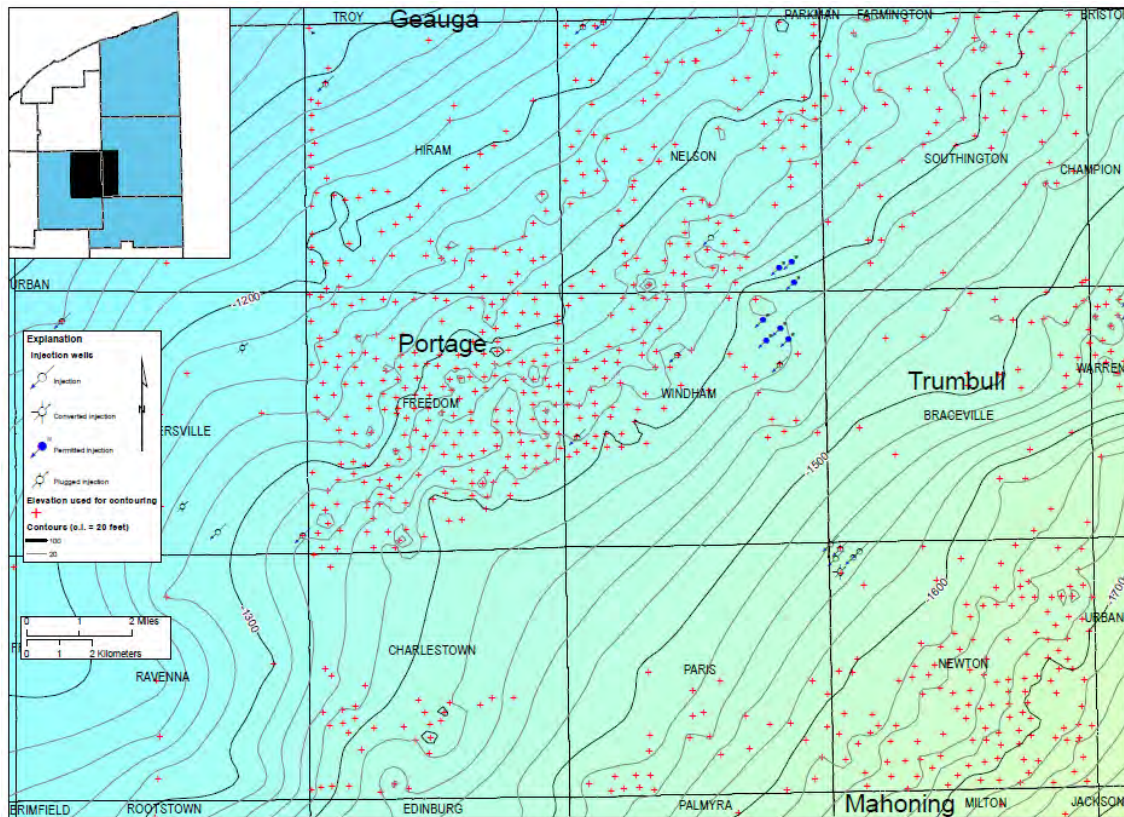


Figure 4-44. Structure contour map on top of the Onondaga Limestone in northeastern Ohio.

4.5.4 Conclusion

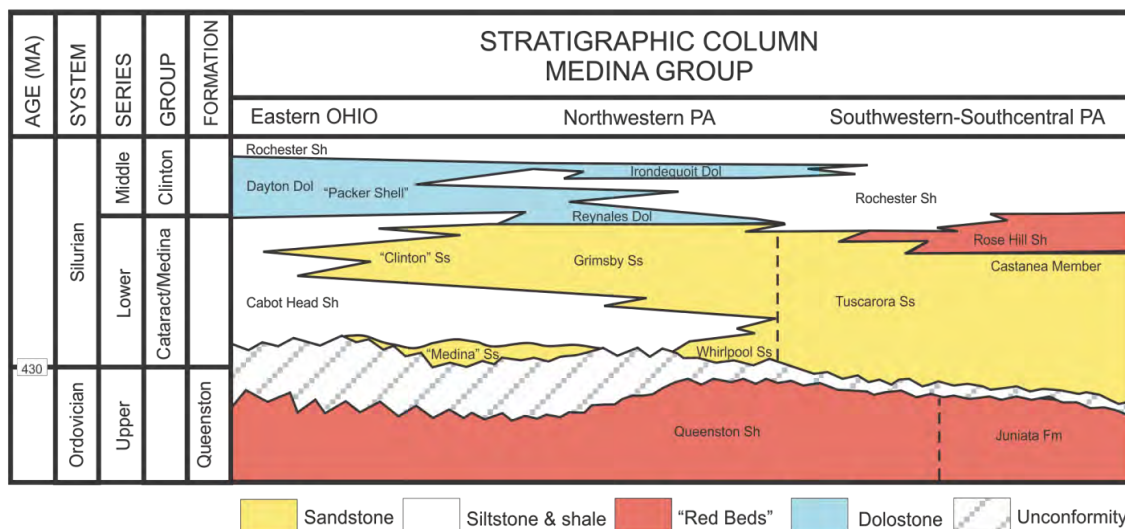
In the vicinity of Windham Township, Portage County, Ohio, existing Class II wells have targeted high-porosity reefs within the Lockport Dolomite. Targeting the thickest portions of Lockport Dolomite build-up for Class II brine disposal would enhance porosity prospects in the subsurface. Further Lockport mapping would help predict Class II permit application locations with high potential porosity. Opportunities for secondary fracture porosity may exist if there is any structural influence on Lockport reef development.

4.6 Lower Silurian Medina Group Case Study

4.6.1 Introduction

Two wells in Pennsylvania are currently permitted as Class II-D to inject wastewater 4,300 feet (1,310 meters) deep into the Lower Silurian Medina Group. These wells had each produced 335 million cubic feet (MMCF) of natural gas over 20 years prior to being converted to brine disposal. Depleted oil and gas fields are candidates for brine injection in the Appalachian Basin because of their demonstrated fluid and gas storage capacity, as documented by regional carbon sequestration studies (e.g., Venteris and Carter, 2009). The Medina Group is regionally extensive across several states, with approximately 30 trillion cubic feet in recoverable gas reserves (Castle, 1998). In Pennsylvania, the productive zones have been correlated and mapped as the Grimsby and Whirlpool formations. Where sandstone beds are present in the intervening Cabot Head shale, probably as storm-deposited shelf bars formed below normal wave base

(Castle, 1998), they are included in the Grimsby Formation (Venteris and Carter, 2009). In Ohio, with more than 30 wells disposing brine waters into the Medina Group, it is known as the 'Clinton/Medina,' with the 'Clinton' of Ohio being equivalent to the Grimsby Formation in Pennsylvania, and the Medina of Ohio being equivalent to the Whirlpool sandstone (Figure 4-45).

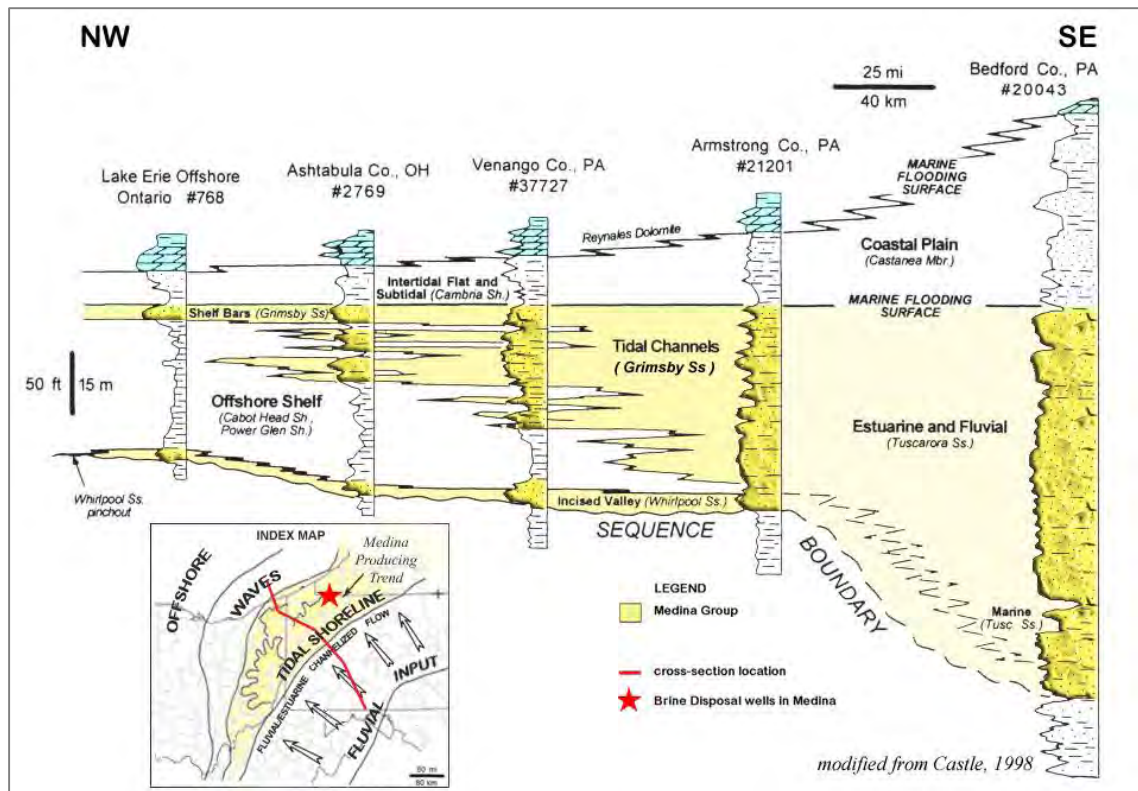


Source: Modified from Carter, 2007.

Figure 4-45. Stratigraphic column showing the rocks of the Medina Group in northwestern Pennsylvania and equivalent rocks in eastern Ohio, southwestern and central Pennsylvania.

The Medina Group produces oil, gas, and condensate from sandstone facies in a tide-dominated shoreline extending through northeastern Kentucky, eastern Ohio, northwestern Pennsylvania, and western New York. Castle (1998, 2001a and b) interprets deposition in the Grimsby as having occurred in a coarsening-upward sequence during regression. The thickest sandstones, and most important hydrocarbon reservoirs, are in this unit (Figure 4-46).

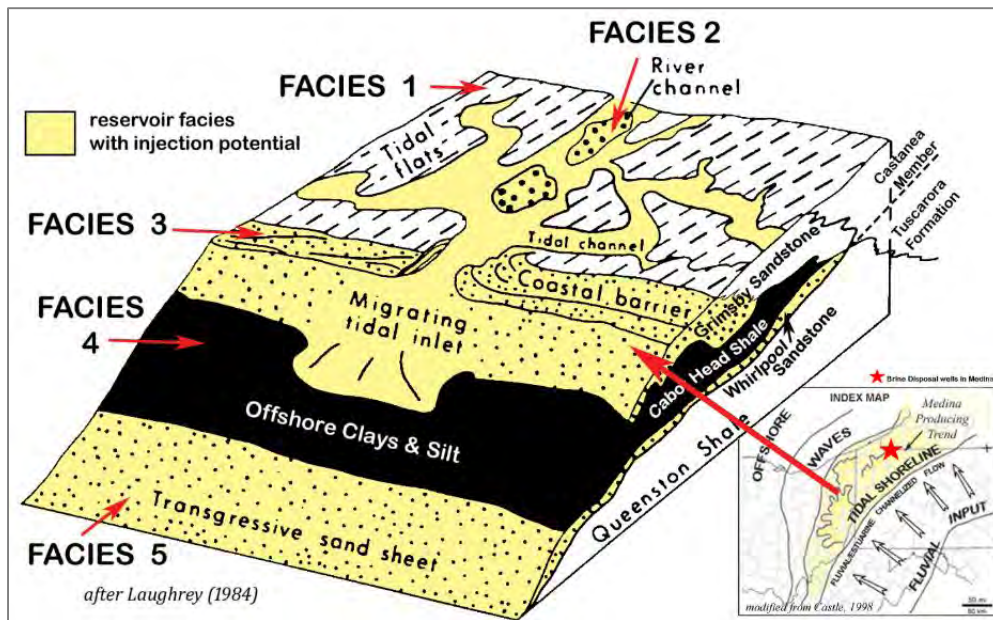
Above a sequence-bounding unconformity at the base of the Medina Group, the Whirlpool sandstone consists of a lower cross-bedded interval and an upper ripple-laminated interval. Interpreted by Castle (1998) as a channel deposit of an incised-valley fill that was reworked during sea level rise, the lower cross-bedded interval has been interpreted by Laughrey (1984) as a channel deposit during sea level lowstand, while the upper unit represents marine reworking during the initial transgression. Castle (1998) interprets the lower Whirlpool as being deposited either during late lowstand or initial sea-level rise. The transgressive systems tract is represented by the Whirlpool and the overlying Cabot Head shale. Occurring in Pennsylvania and New York, this lower Whirlpool facies is well-developed in the vicinity of the brine disposal wells, where it is a significant contributor of porosity and permeability in the Class II-D injection and surrounding producing wells.



Note: Cross section shows relationship of Pennsylvania and Ohio's Medina productive area to depositional environment and sequence stratigraphic framework. Lobe-shaped sandstone bodies shown on the index map are areas of sediment input to the shoreline. A high degree of local lateral variability in sand thickness and orientation on these lobes represent deposition along a tide-dominated shoreline due to mixed influence of channel transport of sediment, tidal-current reworking, and wave modification (Castle, 1998).

Figure 4-46. Northwest-southeast regional stratigraphic cross section, representing a 400-kilometer (250-mile) distance across the Appalachian Basin.

As in oil and gas exploration, reservoir characterization is a key task in planning injection projects, to ensure sufficient porosity and permeability to support a practical injection rate. Accordingly, rock characteristics critical to characterizing a potential reservoir include thickness, porosity, permeability, and lateral and vertical heterogeneity of these parameters (Venteris and Carter, 2009). Reservoir characteristics vary considerably, both vertically and laterally, and depositional environment is an important control on orientation and morphology of Medina Group reservoirs (Laughrey, 1984). Castle and Byrnes (2005) identified upper shoreface, lower shoreface, tidal flat, tidal channel, tidal flat, fluvial, and estuarine depositional facies in the Lower Silurian Medina Group and its laterally equivalent formations. Laughrey (1984) divided the Medina Group's depositional system into the five facies shown in Figure 4-47. They are: (1) tidal-flat, tidal-creek, and lagoonal sediments; (2) braided fluvial-channel sediments; (3) littoral deposits; (4) offshore bars; and (5) sublittoral sheet sands. The high degree of variability that is shown in the distribution of facies in the diagram below is reflected in the morphology of the lobes shown in yellow on the index map. The mixed influence of channel transport of sediment, tidal-current reworking, and wave modification is what makes the reservoir characteristics of the Medina vary so considerably, both vertically and laterally.



Note: Facies that develop reservoir porosity and permeability in yellow (after Laughrey, 1984). These facies occur throughout the Medina play, highlighted in yellow on the index map (from Castle, 1998). The location of brine disposal wells in Pennsylvania is shown as the red star on the index map.

Figure 4-47. Sands in the Medina showing spatial distribution of facies.

Extensive well control exists in the mature, depleted hydrocarbon pool where current brine disposal wells are located. Many such fields are present throughout the Medina play, with wells located on spacings of 1,000 feet to 2,500 feet (300 meters to 760 meters). This high degree of well control can be used in conjunction with identification of facies tracts that are linked through common depositional energy, water depth, and sediment supply (Castle, 2001a) to identify a facies complex consisting of uniform and widespread similarities in sedimentation. As such, these depleted Medina fields and pools make potential candidates for brine injection.

The initial phase of Medina drilling, which began in the late 1800s, discovered high-quality reservoirs, many of which have since been converted into gas storage fields. Improvements in drilling techniques (1940s) and the advent of hydraulic fracturing and modern well logging technology (1950s) expanded the extent and depths of economically recoverable reserves from Medina reservoirs (McCormac et al., 1996). Injection potential may favor these earlier high-yield discovery areas.

Pursuant to the Natural Gas Policy Act of 1978, Medina reservoirs with average permeability less than 0.1 mD qualified for tight formation designation and have been drilled since the 1980s, greatly expanding the number of Medina wells. As these hydrocarbon reservoirs deplete, they may be candidates for conversion to brine disposal. Although measured porosity and permeability average less than 6% and 0.1 mD, infrequent values as high as 18% and 1,048 mD do occur (Castle and Byrnes, 1998). Advancements in logging suites, petrographic analyses, and geostatistical studies, combined with years of documented oil and gas production histories, allow for more precise targeting of potential brine disposal.

4.6.2 Objectives

Wells drilled on 1,300- to 2,000-foot (400- to 600-meter) spacing in the Dewey Corners gas pool, where two Class II-D brine disposal wells are permitted, provide a unique opportunity to examine a mature field that produced an average of 20 years, has geophysical log control, and two depleted wells currently being used for brine injection. This case study assessed the available data to determine: (1) stratigraphy, depositional environment, and facies tract; (2) structural controls and diagenesis; (3) how these criteria influence production in an area with history and well control; and (4) how this information may be applied to injection potential in the Medina play in Pennsylvania for the purposes of wastewater brine disposal.

4.6.3 Methodology

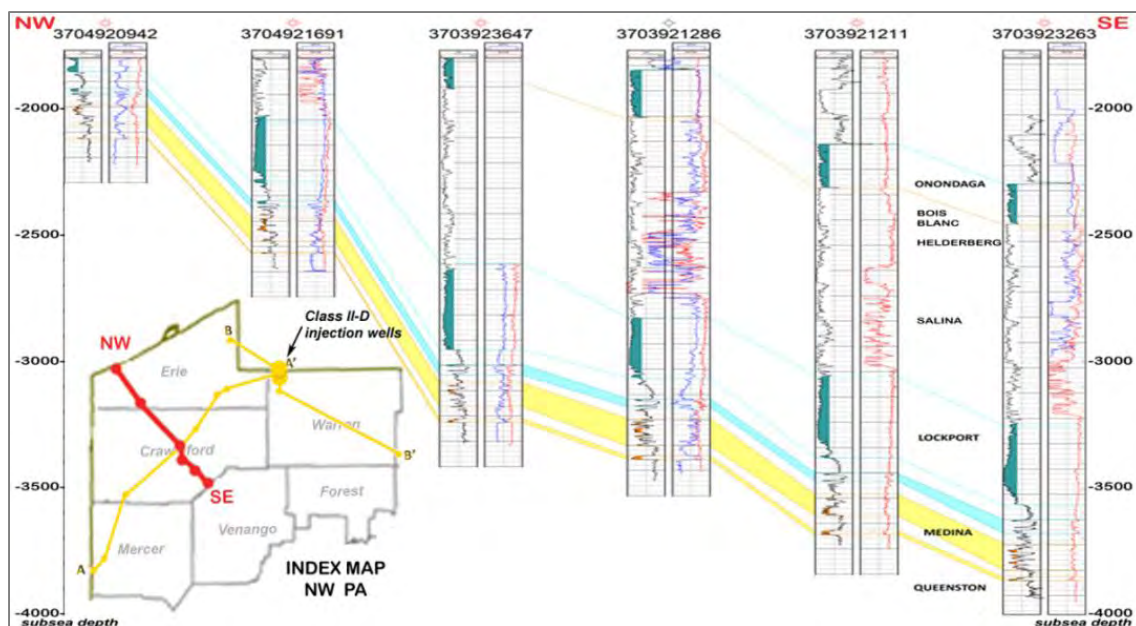
Cross sections constructed from existing well log control were used to examine variability in sand and porosity development in order to estimate the vertical and lateral extent of potential injection zones. Approximately 630 wells with digital logs penetrating the Medina Group in Pennsylvania, Ohio, Kentucky, and West Virginia were culled from the ~71,000 well record PETRA[®] database created for this project. From the database, six wells from eastern Ohio and 40 wells in northwestern Pennsylvania with a full standard geophysical log suite consisting of GR, NPHI, and rhoB were selected for further cross section analysis. In order to assess the extent of zones with potential injection capability, a GR of ≤ 75 API units and a rhoB of ≤ 2.60 g/cc were used to highlight $\geq 50\%$ sand containing $\geq 6\%$ porosity.

Cross sections were hung stratigraphically on the base of the Reynales Dolomite to facilitate correlations. The Reynales is a regionally consistent carbonate facies in the Clinton Group immediately overlying the Medina Group in northwestern Pennsylvania. Along with the overlying Dayton and Irondoquoit dolomites, it intertongues with thin lenses in the Rochester shale. Typically referred to as the “Packer Shell”—a familiar driller’s term in the northern Appalachian Basin for these dolomite formations in the Clinton Group—these stacked dolomites form a stratigraphic seal on top of the injection zone. The Reynales pinches out in eastern Ohio, so the Dayton dolomite overlies the Medina Group there (see stratigraphic column in Figure 4-45). Incorporating the Class II-D brine disposal wells, stratigraphic cross section A–A’ along the basin strike in northeastern Ohio through northwestern Pennsylvania and B–B’ following basin dip were created and incorporated in the Appendix.

The Class II-D brine disposal wells permitted in 2012 are located in the Dewey Corners gas pool of Columbus field in Warren County, Pennsylvania, near the state line where the Medina productive area extends into New York. Wells in this pool were drilled in the 1980s through the early 1990s and completed in the Medina sands for gas development on spacings of 1,300 to 2,000 feet (400 to 600 meters). These wells averaged 20 years of cumulative gas production; well and production records from PA*IRIS/WIS show that these wells are now depleted. An isovol (i.e., contours of equal volume) was developed from the cumulative gas (MMCF) production records. Sixteen Medina wells in this pool, including the current Class II-D wells, were evaluated for relationships between production and structure, sand, porosity, and/or facies development, as determined from GR, NPHI and rhoB logs.

4.6.4 Results

The top of the Medina Group occurs from 2,000 feet (600 meters) below sea level (northwest Erie County, Pennsylvania) to more than 5,000 feet (1,500 meters) below sea level (southeast Warren County, Pennsylvania). Measured depth to the top of the Queenston Formation averages 3,800 feet (1,160 meters) (northwest Erie County), increasing southeast to 6,800 feet (2,100 meters) (southeast Warren County). The Pierce field discovery well in northwest Erie County produced from a measured depth of 2,737 feet (834 meters) (Kelley and McGlade, 1982). To the east, the brine disposal wells in northwestern Warren County are injecting from 4,150 to 4,330 feet (1,270 to 1,320 meters). Strike is N75°E (Kelley and McGlade, 1982) to N60°E, and Venteris and Carter (2009) report that the Medina Group dips southeastward at a rate of 30 to 50 feet per mile (6 to 9 meters per kilometer) in the study area in northwestern Pennsylvania (Figure 4-48).



Note: Several well-documented hydrocarbon producing Medina fields are located in this region, including the Pierce (Kelley and McGlade, 1982), Conneaut (Venteris and Carter, 2009), Cooperstown (Zagorski, 1991), Athens, and Geneva fields (Laughrey, 1984). Cross section location shown in red. Location of stratigraphic cross sections included in the Appendix is shown in yellow.

Figure 4-48. Northwest to southeast structural cross section showing regional dip of the Medina Group from Erie through Crawford counties in the heart of Pennsylvania's Medina play.

The thickness of the Medina Group ranges from 213 feet (65 meters) in eastern Ohio to 177 feet (54 meters) at the injection wells in northwestern Pennsylvania in cross section A–A' (Appendix). The gross sand interval in the Grimsby, referred to as the “Grimsby Sand,” is encountered approximately 35 to 40 feet (10 to 12 meters) below the top of the Medina Group and ranges from 75 to 100 feet (20 to 30 meters) thick. Between 40 and 80 feet (10 and 20 meters) of Cabot Head shale lies between the Grimsby and Whirlpool. The Whirlpool sandstone

at the base of the Medina Group ranges from 5 to 20 feet (2 to 6 meters) in gross interval thickness.

Total thickness of the Medina interval is fairly consistent from eastern Ohio to northwestern Pennsylvania. However, the quantity and quality of net sand varies considerably from well to well. While it was possible to recognize facies in the regional cross sections A–A' and B–B' from the facies models of Castle (1998, 2001a and b, 2005) and Laughrey (1984), it was not possible to trace individual sand development in wells this far apart.

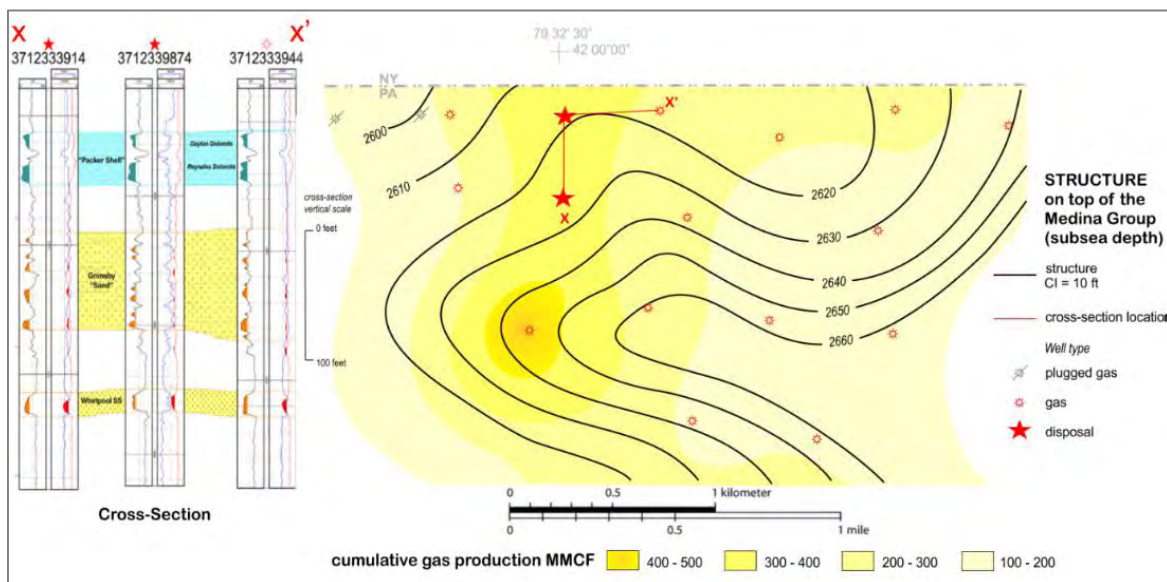
The regional cross section A–A' along basin strike (Appendix) from eastern Ohio to northwestern Pennsylvania showed a repeatable frequency of sand development and characterization that was correlative with depositional environments in the shoreline tract (facies tract B) of Castle (1998, 2001a and b). Comparing strike section A–A' to dip section B–B' (Appendix) showed a coarsening-upward sequence and similar variety of facies types in both strike and dip direction. It was not possible to resolve any real difference between the amount of variability or types of facies encountered in the strike section as compared to the dip. However, this could be due to most, if not all, of the cross section area falling within the progradational deposits of the shoreline facies tract as described by Castle (2001a and b). Since they are in the same facies tract, the cross sections should look consistent in their variability and be similar to each other.

It was possible to see thinning and thickening in individual sands in wells that were 1,300 to 2,000 feet (400 to 600 meters) apart in the same pool as the two brine disposal wells. There was good correlation between facies in the Whirlpool sand identified by Castle (1998, 2001a and b) and Laughrey (1984) to what was encountered on the geophysical logs and also a good correlation of net Whirlpool sand to the spatial geostatistical models of Venteris and Carter (2009). Fair correlation was found between cumulative production to encountering channel incised-valley fill facies development in the basal Whirlpool and tidal channel facies in the Grimsby.

The Class II-D brine disposal wells associated with this case study have experienced variable injection activity. Bittering #1 (API 37-123-39874) had 65,691 bbl brine injected in 2013 and Bittering #4 had 12,677 bbl injected in 2013. These wells are reported to be injecting under gravity flow and have not been operating at a full capacity of 30,000 bbl per month as of the date of this report.

Both the Grimsby and Whirlpool sands are developed in this pool. Producing Medina gas wells averaged more than 200 MMCF per well when the lower sand facies in the Whirlpool was encountered having at least 6 to 8 feet of 10% or better porosity ($\rho_B < 2.50$). Neutron gas effect appears attenuated in this zone, possibly due to saline drilling mud filtrate invasion on the walls of the wellbores. One well that had produced nearly 500 MMCF also had 26 feet (8 meters) of sand having an average ρ_B of 2.6 in the upper portion of the Grimsby sandstone. Wells with the highest cumulative production, and therefore the best injection potential, have cleaner sand development coupled with higher porosity. These are located on the edge of a structural low between structural nosings, which may represent a cross-structural discontinuity (CSD). Pool terminations commonly occur at CSDs in the Medina (Harper, 1989), while Laughrey (1984) reported that lineaments and fracture traces can be zones of secondary

permeability. Wells having cumulative production less than 150 MMCF were downdip and lacked porosity or sand development in the lower Whirlpool (Figure 4-49).



Note: Production relates to porosity and permeability development and preservation in the incised fluvial facies of the lower Whirlpool sandstone and localized tidal channel facies in the upper Grimsby Formation.

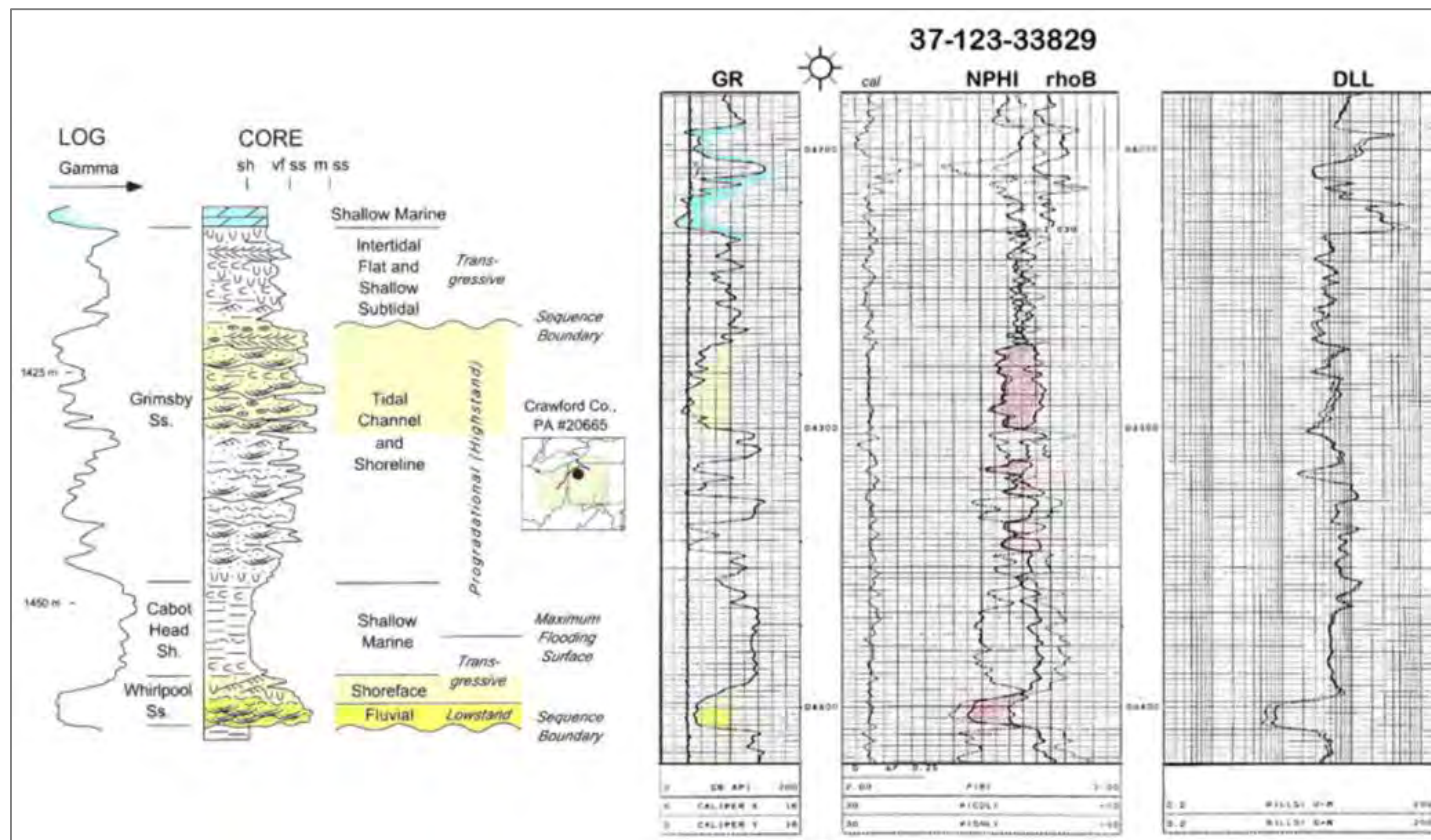
Figure 4-49. Structure, isovol, and cross section in the Dewey Corners Medina gas pool.

4.6.5 Discussion

Wells drilled on 1,300 to 2,000 feet (400 to 600 meters) spacing in the Dewey Corners gas pool where the Class II-D brine disposal wells are located allowed an opportunity to examine a mature field that has produced for an average of 20 years, has geophysical log control, and has two depleted wells that are currently being used for injection. Geophysical log control can be used to identify reservoir facies and facies tracts that are linked through common depositional energy, water depth, and sediment supply (Castle, 2001a and b). Comparison of geophysical well logs in this pool to regional cross sections in northwest Pennsylvania and eastern Ohio (Appendix) show similarity in character and variation, which appear to be widespread.

The Medina play is composed primarily of tide-dominated shoreline facies. The greatest calculated volume of total original gas reserves and greatest cumulative production per field are associated with coarsening-upward progradational shoreline sequences. However, because of the large number of wells typically needed to deplete the reserves in these fields, the per-well original gas reserves and cumulative production are less for these tide-dominated shoreline sequences than for other types of sequences (Castle and Byrnes, 2005). As fields and pools in the Medina play become depleted, they will likely also require a greater number of injection wells to dispose of brine in the volume previously occupied by hydrocarbons. This appears to be the case with the two current brine disposal wells. They are located within 1,320 feet (400 meters) of each other, and another well 1,500 feet (460 meters) away from the first well is currently in the permitting process.

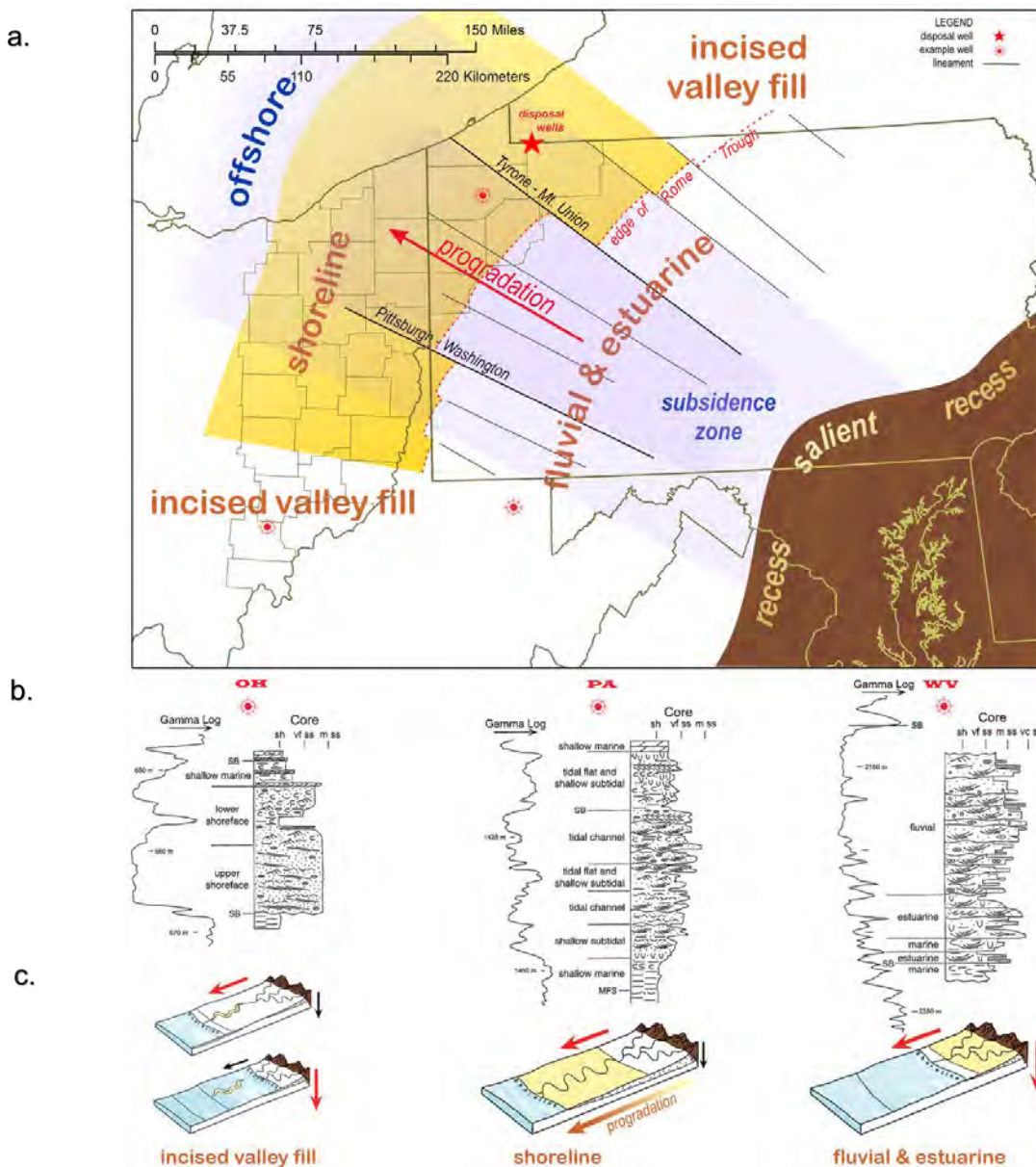
The most favorable reservoir petrophysical properties and the best estimated production from Lower Silurian sandstones are associated with fluvial and upper shoreface facies of incised-valley fills, which Castle and Byrnes (2005) interpret to have formed predominantly in areas of structural recesses along a collisional margin during the Taconic orogeny (Ordovician time). As rate of sediment supply and subsidence influences deposition, this facies can also form in the distal foreland basin during late highstand or initial transgression, as with the lower Whirlpool sand in the Dewey Corners pool. (Figures 4-50 and 4-51).



Note: Left: the greatest calculated volume of total original gas reserves and greatest cumulative production per field are associated with prograding coarsening-upward shoreline sequences (Castle, 2001a). This sequence is shown for the Grimsby sandstone in GR log and core (left) from Crawford County, Pennsylvania.

Right: GR, NPHI, and rhoB log from a depleted gas well 2,250 feet (690 meters) south of a Medina brine injection well in Warren County, Pennsylvania, shows this sequence in the Grimsby Formation. This well produced 500 MMCF. Note tidal channel facies in the upper Grimsby which develops clean sand on the GR and good cross-over between the NPHI and rhoB logs. Also note attenuated neutron response in the basal Whirlpool sand and the invasion profile in this same zone on the dual laterolog (DLL) (resistivity) log to the right, indicative of high permeability.

Figure 4-50. Calculated volume of total original gas reserves and cumulative production per field (left); GR, NPHI, and rhoB log from a depleted gas well 2,250 feet (690 meters) south of a Medina brine injection well in Warren County, Pennsylvania (right).



Note: Map of major tectonic lineaments (a), which provide a mechanism for extending subsidence (blue zone) onto the foreland ramp. This mechanism is proposed for most of the sand deposition in the productive Medina play (modified from Castle, 2001a). Red arrow shows direction of sediment progradation. Red dotted line shows approximate western boundary of the Rome trough (after Harper, 1989). Example wells are located in each type of depositional sequence, or facies tract. Red star is location of brine disposal wells. The brine disposal wells are located just north of the Tyrone-Mount Union lineament.

Example wells (b) with GR and core illustrate shoreline (Pennsylvania), incised-valley fill (Ohio) and fluvial/estuarine (West Virginia) sequences (Castle and Byrnes, 2005), which are controlled by (c) rate of subsidence and sediment supply. Rate of subsidence (vertical arrows) and rate of sediment supply (arrow points from proximal toward distal) have relative values. Thick red arrows represent higher rates, thin black arrows are lower rates. Mountains (brown) are proximal, ocean (blue) is distal.

Figure 4-51. Major tectonic lineaments, example wells with GR and core, and rate of subsidence and sediment supply.

Laughrey (1984) reported that lineaments and fracture traces in the Athens and Geneva fields are zones of secondary permeability. This can be due to enhanced fracture porosity, which functions as a conduit for gas migration into the formation. Fluid migration along these lineaments can also create seals by dissolving minerals and re-precipitating as diagenetic cements. Harper (1989) reported that field and pool terminations commonly occur at northwest-southeast trending lineaments (CSDs). According to Castle (2008), downdropping of crustal blocks along CSDs provides a mechanism for extending differential subsidence (and clastic progradation) onto the distal foreland. These tectonically induced variations in deposition occur along strike, as well as in the dip direction (see Figure 4-51).

Lytle et al. (1971) reported that regional Medina Group structure is characterized by a southeasterly dip of approximately 45 feet (14 meters) per mile with local interruptions by minor folds and small faults. These minor fold axes trend northeast and southwest, paralleling the long axis of the Appalachian Basin. Structural noseings, which represent mild paleohighs, are associated with hydrocarbon accumulation in the Medina Group in the Athens and Geneva fields (Laughrey, 1984) and the Pierce pool, Conneaut field (Kelley and McGlade, 1969). If gas was entrapped in these paleohighs before cementation and destruction of the secondary voids, the pores may have been preserved, inasmuch as hydrocarbon emplacement inhibits further diagenesis (Laughrey, 1984). Diagenesis is defined as the compositional and textural changes that occur post-depositionally in sediments and sedimentary rocks under low temperatures and pressures. Diagenesis controls the type and amount of porosity and the variety of minerals precipitated in pores and pore throats. Much of the secondary porosity in Medina Group sandstones was subsequently occluded by late diagenetic cements. Gas migration into paleohighs keeps pore throats open, while diagenesis in the form of quartz overgrowths and other cements form a lateral seal that would keep brine disposal waters from migrating in depleted gas reservoirs with this trapping mechanism.

4.6.6 Conclusions

Good well control exists in the mature, depleted gas fields that have years of production histories and offer optimum potential for quantifying injection capabilities for brine disposal. The fluvial-deltaic facies of the Medina Group form discontinuous sand bodies that vary both vertically and laterally. However, they possess a common depositional energy, water depth, and sediment supply (Castle, 2001a and b). This creates recognizable patterns of deposition. These patterns can be mapped using the closely spaced geophysical well log control in Medina development fields to find facies suitable for brine injection.

The greatest calculated volume of total original gas reserves and greatest cumulative production per field are associated with the coarsening-upward progradational shoreline sequences. However, because of the large number of wells typically needed to deplete the reserves in these fields, the per-well original gas reserves and cumulative production are less for these sequences than for other types of sequences (Castle and Byrnes, 2005). Multiple injection wells in close proximity may be necessary.

The most favorable reservoir petrophysical properties and the best estimated production from the Lower Silurian sandstones are associated with fluvial and upper shoreface facies of incised-valley fills, which Castle and Byrnes (2005) interpret to have formed predominantly in areas of

structural recesses along a collisional margin during the Taconic orogeny. The basal Whirlpool sandstone in the Class II-D injection wells in Warren County are believed to be in this facies, which formed either during late highstand or initial transgression.

Neutron (NPHI) log gas effect is attenuated in the lower Whirlpool zone in the Dewey Corners pool where the injection wells are located. Resistivity logs in the form of dual laterolog (DLL) show separation between shallow and deep penetrating laterologs, indicative of saline drilling mud filtrate invasion. The combined response of both NPHI and DLL indicates permeability in the lower Whirlpool (interpreted as fluvial/valley fill facies). Resistivity is a downhole geophysical tool that is recommended for assessing permeability and therefore injection potential, especially in sands that develop rhoB porosities in excess of 8%.

Reservoir characteristics (i.e., porosity, water saturation, fluid sensitivity, and geophysical-log response) of Medina Group reservoirs vary considerably, both vertically and laterally. Although it may be possible to identify a facies complex, post-depositional diagenetic effects, which have altered the pore systems of Medina sandstones, are superimposed on the physically deposited spectrum of sandstone types. Diagenesis may cause large differences in injection volumes in wells with geophysical logs which look very similar to each other volumetrically. Core data in conjunction with geophysical logs and production histories would be advised.

Diagenesis can render a formation sensitive to acids or fresh water. The Medina sandstones have two principal engineering problems: (1) acid sensitivity (due to the presence of chlorite, hematite, and dolomite); and (2) mobilization and migration of fines (i.e., illite). The possibility of a minor swelling-clay problem exists in zones that contain corrensite and illite/chlorite mixed-layer clays (Laughrey, 1984). These clays may prove problematic to brine injection, particularly injection of less saline waters.

4.7 Central Ohio Cambrian-Ordovician Knox Unconformity to Basal Cambrian Sandstone Injection Well Case Study

4.7.1 Introduction

The Cambrian-Ordovician Knox Unconformity to Basal Cambrian Sandstone reservoirs have been previously used as Class I and II injection targets in the Appalachian Basin and are the current focus of new commercial-scale injection of completion and produced water from the unconventional Marcellus and Utica Shale development activity. The combined injection reservoir wells are looked at here in central Ohio due to the open-hole completions and injection into carbonate and clastic formations from the Knox Unconformity to the Basal Cambrian Sandstones. The Mount Simon/Basal Cambrian Sandstone has been utilized in western Ohio, where reservoir quality and injectivity have proved to be highly effective for large-volume injection of waste fluids. Class I Mount Simon injection wells in the Ohio, Michigan, and Indiana Arches Province have a total injection volume of 500 million barrels over the last four decades (Sminchak, 2012). Reservoir data collected from new wells drilled for development of Class II brine disposal and for reservoir characterization for CO₂ sequestration has shown that the Basal Cambrian Sandstones decrease in quality as an injection target in eastern Ohio (Gupta, 2013). This trend is also similarly observed in the Rose Run Sandstone with increased depth. Research over the last decade and newer Class II injection wells have shown that while the sandstone reservoirs lose porosity and permeability with increasing depth in the Appalachian

Basin, the Knox Group and Conasauga Group carbonate units below the Knox Unconformity have zones of vugular and fracture porosity with exceptional permeability values (Gupta, 2013). The carbonate injection zones in these units are less continuous and require a more intense characterization program, including running acoustic, image, nuclear magnetic resonance, and production logs, acquiring cores, and performing pressure fall-off or injection testing to fully characterize reservoir extent and quality.

The risks associated with induced seismicity in the Precambrian Basement rocks have also triggered the need to find and characterize injection zones in the deeper portion of the Appalachian above the Basal Cambrian Sandstone that can accept large volumes of water in a single commercial-scale facility. Several injection wells in northeastern Ohio have been shown to correlate to induced seismicity in the Precambrian Basement during injection into the Basal Cambrian Sandstone (Seeber et al., 2004; Kim, 2013). This section summarizes the general stratigraphy, well completion, operational data, and log and pressure analysis in wells in the southeastern Ohio portion of the Appalachian Basin.

4.7.2 Regional Distribution

The regional distribution of Class II injection wells utilizing Knox Unconformity to Basal Cambrian Sandstone reservoirs is focused in eastern Ohio along the western flank of the Appalachian Basin (Figure 4-52). Most of these wells were drilled to dispose of completion and produced water from conventional wells, but newer wells drilled since 2005 have been drilled in deeper portions of the Appalachian Basin in closer proximity to the unconventional Marcellus and Utica Shale plays. This is mainly done to reduce trucking time and lower the costs of fluid transportation.

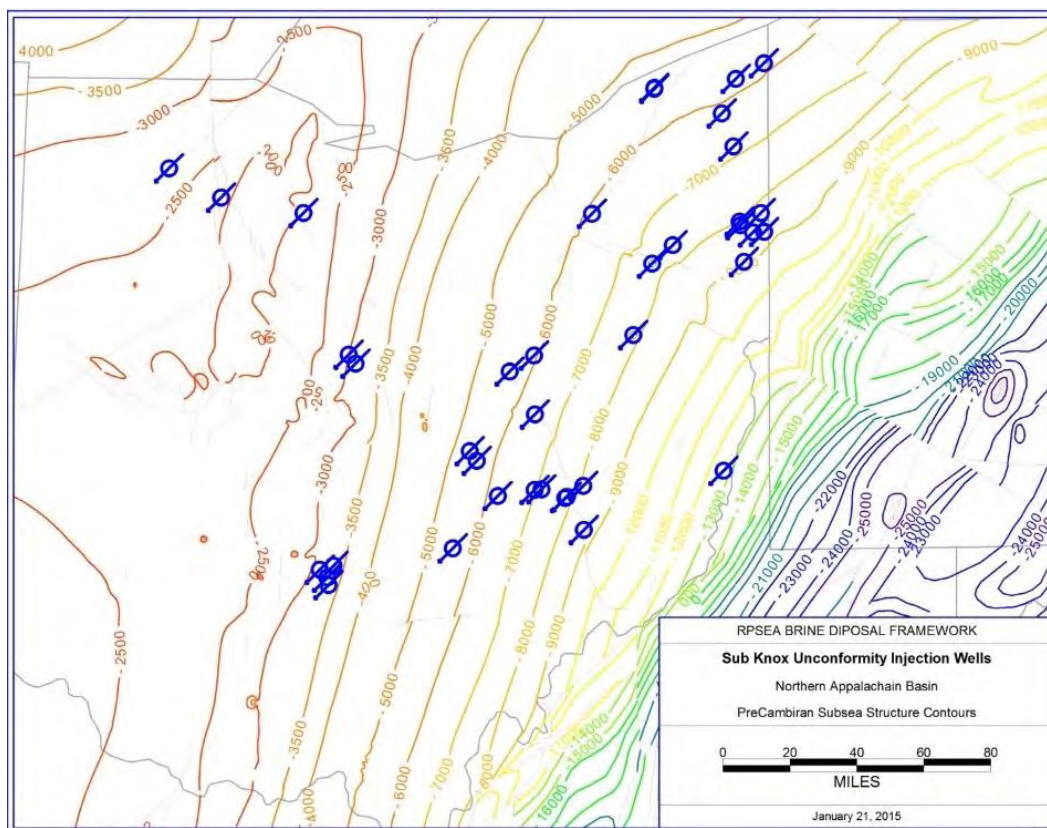


Figure 4-52. Regional distribution of Class II Cambrian reservoir injection wells.

4.7.3 Stratigraphy

The formations that have been the focus of deep injection in descending order are the Beekmantown Dolomite, Rose Run Sandstone, Copper Ridge Dolomite, Conasauga Dolomite, and Basal Cambrian Mount Simon/ Basal Sandstones (see Figure 3-4). These formations have been researched and characterized since 2001 through research efforts managed by Battelle conducted for the MRCSP and the Ohio Coal Development Office (OCDO). This research has been focused on finding regional CO₂ sequestration targets in the Midwest, but has also provided brine disposal operators the chance to partner with these major research projects to better understand the porosity and permeability distribution of the brine injection reservoirs throughout the region. The general zones where injectivity has been identified in central Ohio include a range of clastic and carbonate lithologies (Figure 4-53). The bulk density and neutron porosity logs are a general first-pass qualifier for identification of potential injection zones (Figure 4-54). The following subsections summarize, by formation, some of the key findings for wells studied in the Ohio Valley region and general details related to operation of these wells.

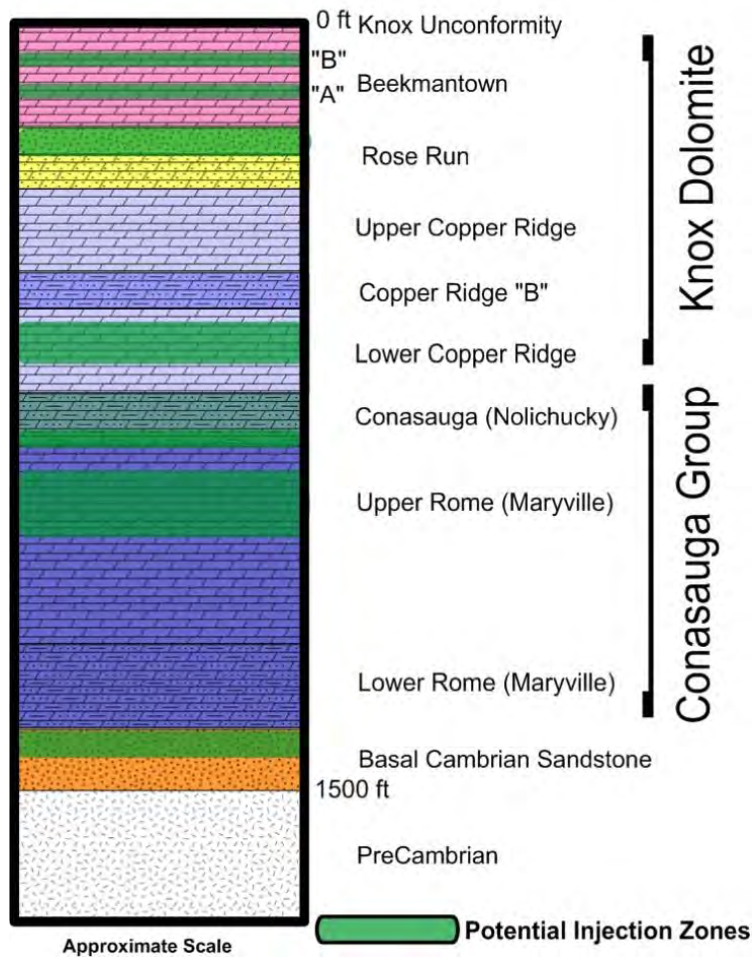


Figure 4-53. General stratigraphy and injection intervals observed in Central Ohio Knox Unconformity to Basal Cambrian sandstone open-hole wells.

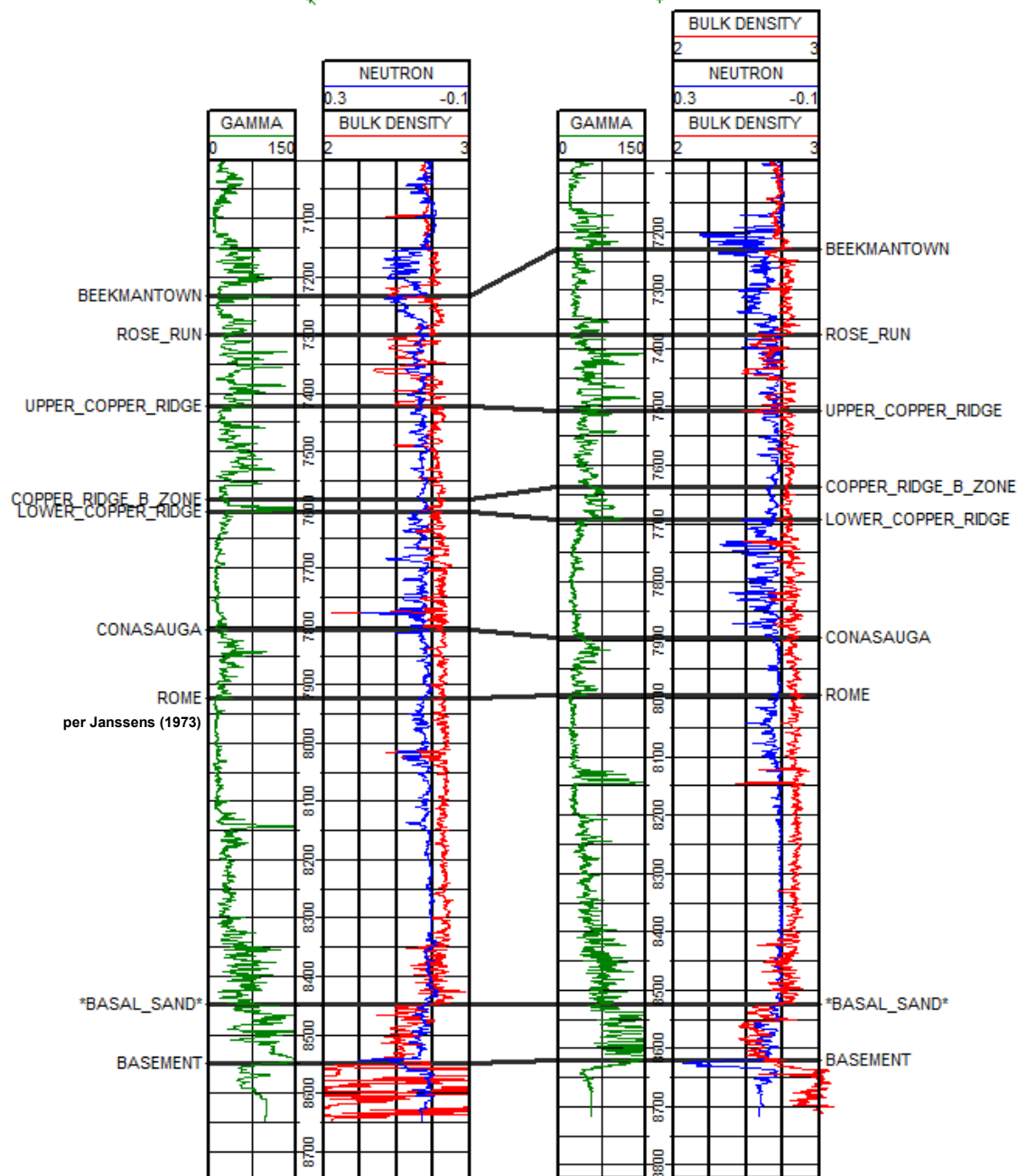


Figure 4-54. General eastern Ohio log sections from proprietary wells.

Beekmantown Dolomite

The Beekmantown Dolomite is a light- to medium-brown, fine- to medium-crystalline dolomite with zones of higher porosity associated with potential subaerial exposure associated with the Knox Unconformity (Wickstrom et al, 2010). The Beekmantown has well-developed porosity in the lower 220 feet in two regionally correlated stratigraphic zones (called the A and the B) associated with the Knox Unconformity remnants. These zones of porosity can also be identified down dip from the subcrop in eastern Ohio, and show porosity and vug development from

11,387 to 12,285 feet in the Georgetown Marine #1 API # 34-013-20611 well in Belmont County, Ohio, where the Beekmantown is 941 feet thick (Gupta, 2013). While there are currently no wells injecting into the Beekmantown at these depths, the regional potential for injection is present.

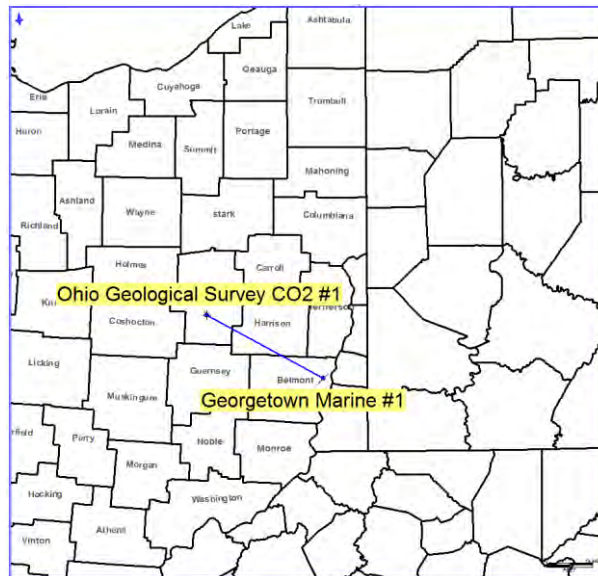
Rose Run Sandstone

The Rose Run Sandstone is a laminated to cross-bedded, fine- to coarse-grained subarkose composed primarily of monocrystalline quartz and k-feldspar interbedded with dolomite (Janssens, 1973, Riley et al., 1993, and Perry, et al., 2013). The Rose Run is a major hydrocarbon producer in eastern Ohio, where it is associated with remnants created by the Knox Unconformity, subcropping individual sandstone members, and in structural trap settings. Porosity and permeability are enhanced where the Rose Run is closely associated with the Knox Unconformity. The general trend for porosity and permeability in the Rose Run is to decrease with depth. In the Ohio Geological Survey CO₂ #1 well in Tuscarawas County, Ohio, the core derived porosity ranges between 1.3 and 10.8% and permeability ranges between 0.001 and 31.6 mD at a depth of 7,377 to 7,506 depth MD (Perry et al., 2013). In the Georgetown Marine #1 well in Belmont County, Ohio, the porosity is 0.4% to 3.0% and the permeability is below 0.017 mD at 12,292 to 12,416 depth MD, and the sandstone is well cemented (Gupta, 2013) (Table 4-3). The cross section of log porosity estimates from the density, nuclear magnetic resonance (NMR), and sonic tools show the decrease in porosity from the Ohio Geologic Survey #1 well to the Georgetown Marine #1 (Figure 4-55). The cementation with depth reduces permeability and makes the Rose Run Sandstone a potential poor target for injection at depth away from the subcrop.

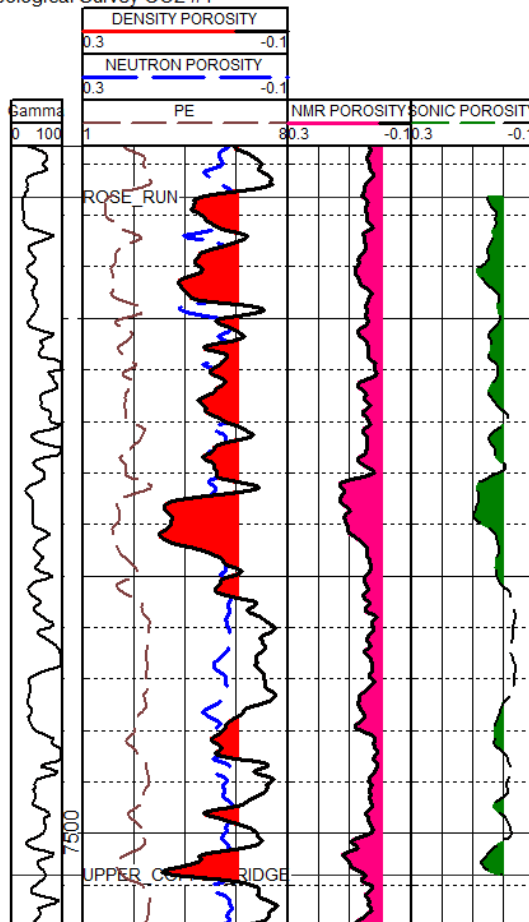
Table 4-3. Rose Run Sandstone and Basal Cambrian sandstone porosity and permeability.

Well	Rose Run		Basal Cambrian Sandstone	
	Porosity (PU)	Permeability (mD)	Porosity (PU)	Permeability (mD)
Ohio Geologic Survey CO ₂ #1	1.3-10.8	0.001-31.6	1.2-10.7	0.0005-1.06
Georgetown Marine #1	0.4-3.0	<0.017	0.6	0.0014

Note: PU = porosity unit.



Ohio Geological Survey CO2 #1



Georgetown Marine #1

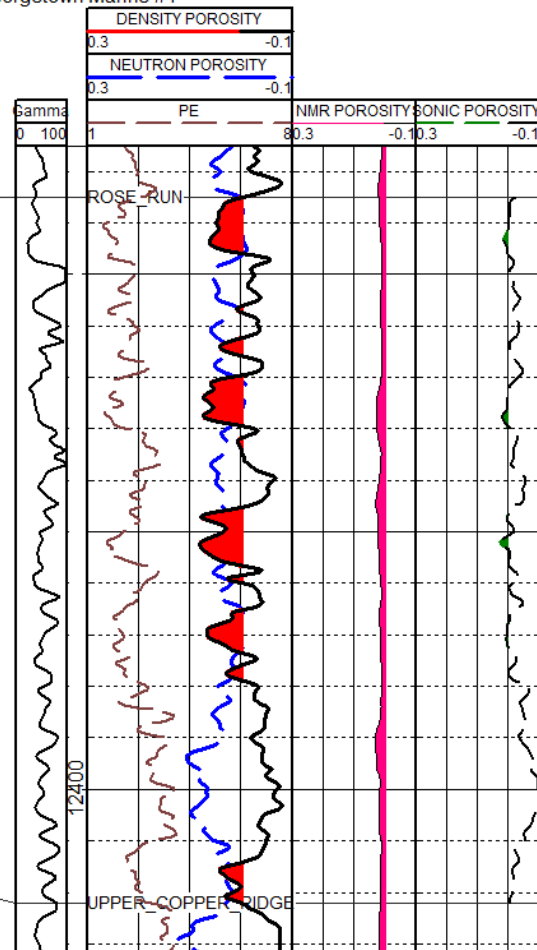


Figure 4-55. Cross section location and cross section with density, NMR, and sonic porosity showing decrease in porosity with depth in the Rose Run Sandstone.

Copper Ridge Dolomite

The Copper Ridge Dolomite can be broken down into an Upper, Middle “B-Zone,” and Lower Unit composed of low-porosity, very fine to coarse crystalline dolostone (Gupta, 2013). The B-Zone is a mix of interbedded dolomitic siltstones, dolomicrite, and argillaceous siltstones which thickens to the north of the Highland Town fault system (Janssens, 1973). North of the Highland Town Fault system in the Northstar #1 well, the Copper Ridge B was shown to have modest injectivity based on NMR log analysis (Gupta, 2013). In southeast Ohio, the Lower Copper Ridge shows vugular zones with potential high porosity and injectivity (Gupta, 2013). The porosity has been developed through secondary enhancement of primary porosity by multiple stages of dolomitization and dissolution (Gupta, 2013). Image logs collected in the AEP #1 well in Mason County, West Virginia, show a variety of vug sizes and enhanced fractures in the upper portion of the Lower Copper Ridge (Figure 4-56). Net porosity maps generated for injection reservoirs below the Knox Unconformity showed that the Lower Copper Ridge has the highest net porosity feet in the southeast Ohio region (Gupta, 2013) (Figure 4-57).

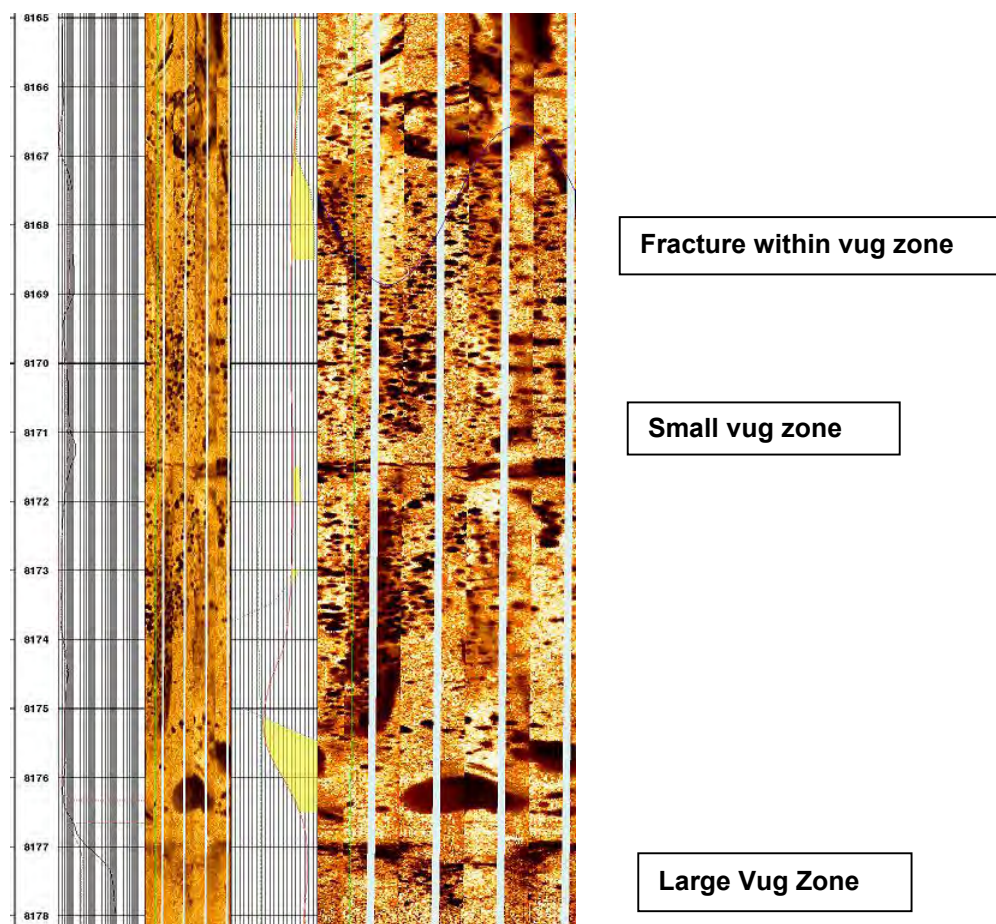
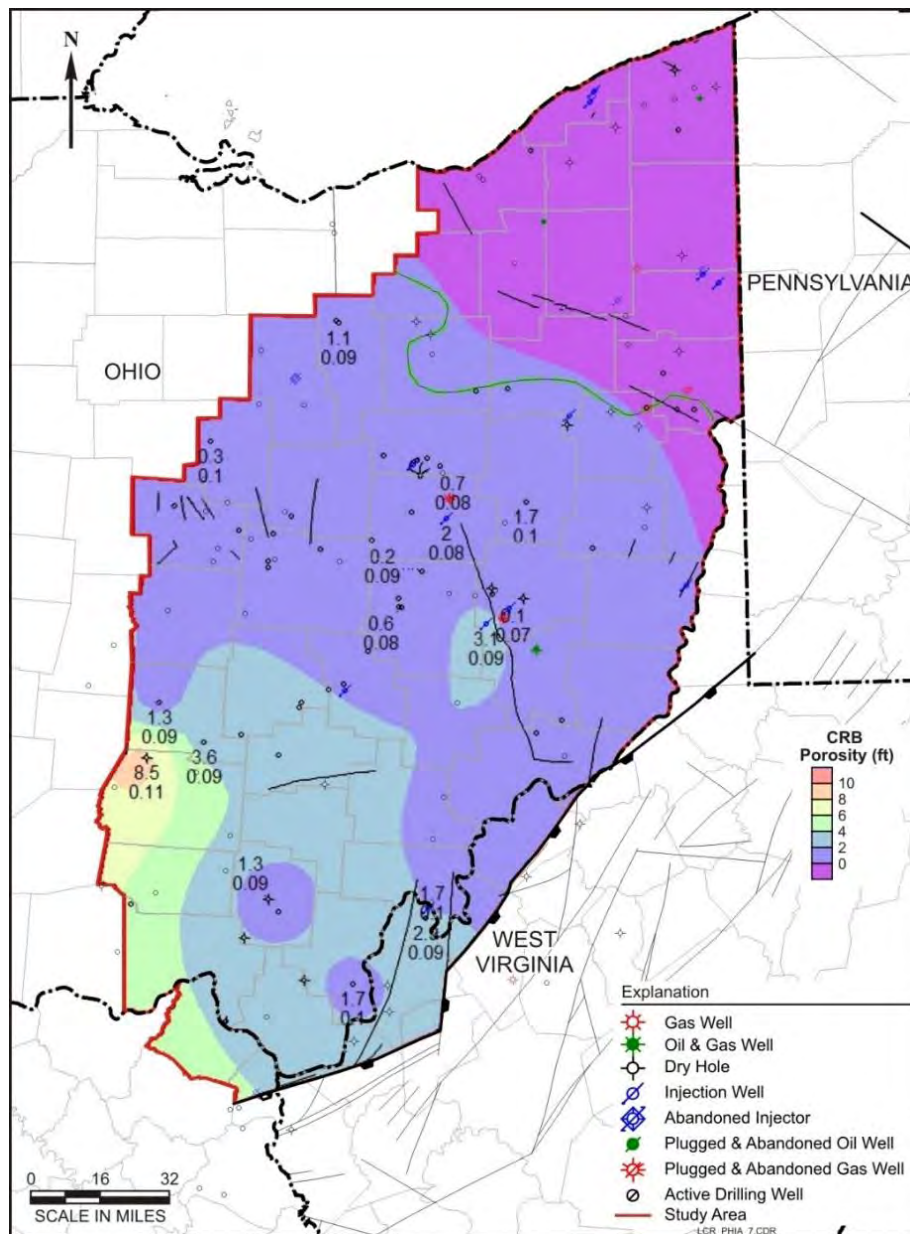


Figure 4-56. Lower Copper Ridge vugular porosity in AEP #1 well, Mason County, West Virginia.



Source: From OCDO (2013).

Figure 4-57. Porosity-feet map of the Lower Copper Ridge dolomite.

Conasauga Group

The Conasauga Group in southeast Ohio generally consists of dense, argillaceous, light-colored micro- to finely grained crystalline dolomite interbedded with thin shale and sandstone (Gupta, 2013) which can be correlated to the Nolichucky. In general, the Nolichucky does not show reservoir development in the central Ohio region, but the Nolichucky/Maryville boundary and upper Maryville have shown minor to excellent injectability in several wells tested in the central Ohio region (Gupta, 2013).

Maryville Dolomite

The Upper Maryville is light- to medium-gray, cryptocrystalline to fine- and medium-crystalline, laminated to irregular, massively bedded, slightly arenaceous dolostone. The lower part is transitional to the underlying Cambrian Basal Sandstone, is very argillaceous, and contains thin shale stringers which are transitional to the underlying Cambrian Basal Sandstones (Gupta, 2013). Several wells within the Central Ohio region show excellent injectability into the upper portion of the Maryville (Gupta, 2013).

Basal Cambrian Sandstones

The Basal Cambrian Sandstone is an arkose that consists of 51% mono- and polycrystalline quartz and 21% feldspars (Perry, 2013). The reservoir quality in eastern Ohio is reduced as compared to the Mount Simon Sandstone in western Ohio due to pore-lining clays and quartz and feldspar overgrowths (Perry, 2013). Porosity and permeability derived from core in the Ohio Geological Survey CO₂ #1 and Georgetown Marine wells show a similar trend as the Rose Run Sandstone, decreasing reservoir quality with depth (see Table 4-3). Of particular concern with injection into the Basal Cambrian Sandstone is the potential for induced seismicity within the Precambrian Basement. Kim (2013) concluded that a series of 109 small earthquakes detected in 2011 and 2012 near Youngstown, Ohio, were the result of fluid injection that increased pore pressure and activated pre-existing subsurface faults in the Precambrian basement. The Northstar #1 well that was the site of injection was completed open hole and drilled through the Basal Cambrian Sandstone and into the Precambrian Basement.

4.7.4 Well Completion

Typical well completions in central Ohio consist of setting conductor, surface casing, and 5½- to 7-inch final casing in or at the top of the Beekmantown Dolomite and completing the remaining portion of the well open-hole (Figure 4-58). Where the Beekmantown or Rose Run is in a hydrocarbon-producing area, these zones may be cased off to protect producing zones from the injection operations. Where wells in the past have been drilled into the Precambrian Basement, current trends are to penetrate only the top of the Basal Cambrian Sandstone due to induced seismicity concerns in the low-porosity Precambrian crystalline rocks. After the production string has been cemented, the open-hole section of the well is circulated clean and acid jobs are performed to clean out near wellbore damage. Tubing 3½- to 5½-inch in diameter is set in the hole with a packer placed within 50 feet of the open hole in either a tension or compression set.

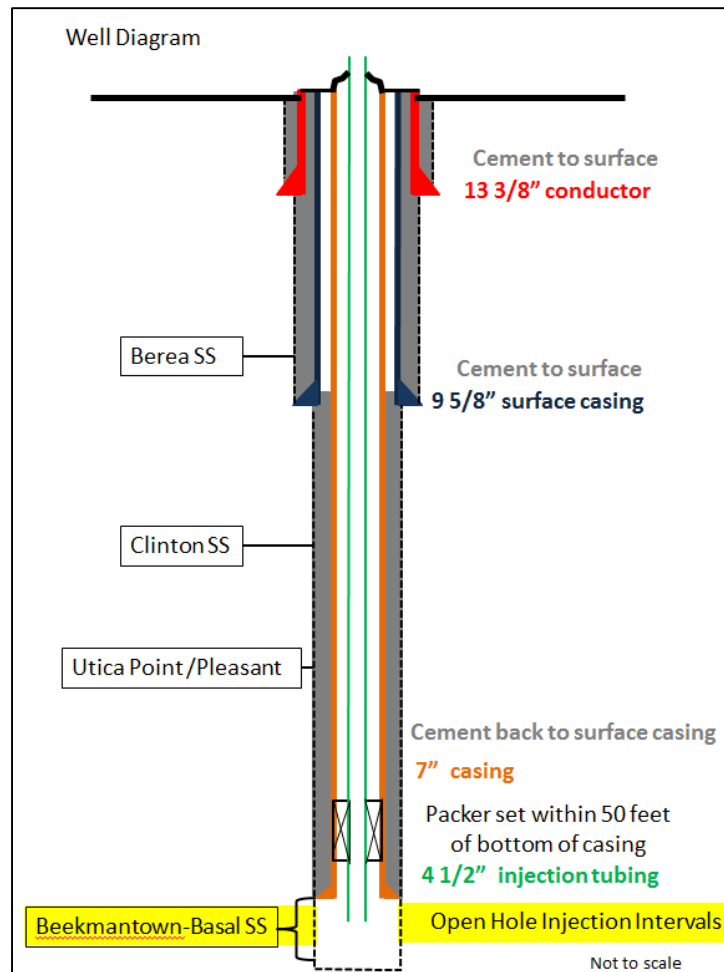


Figure 4-58. Typical Beekmantown to top Basal Cambrian Sandstone open-hole well diagram of casing and tubing configuration.

4.7.5 Operations

Since 2010, the trend with the open-hole commercial scale injection wells in eastern Ohio is toward larger facilities with the capabilities to unload brine into facilities that can process multiple thousands of barrels of water daily and effectively settle, screen, and filter solids out of the fluid column before injection occurs. The facilities generally consist of five main components: an unloading pad, an offloading tank, main tank series, pump house, and injection well (Figure 4-59). The main components have secondary containment systems composed of concrete or other berm materials to enclose the various stages of the water processing from potential leakage into ground. The offloading tanks are used to initially settle solids and monitor for quality control of the fluids received. The number of tanks in the main tank series is designed to provide adequate water storage for volumes to be injected on a daily basis, depending on the scale of the operation. Within the pump house, final filtering of the water down to the micron level occurs to ensure that the fewest possible solids are injected into the formation. Filters are monitored manually and through automated systems to maintain filter integrity for injection into the formation. Once the injection water passes through the final filter process, it is pumped to the well, where pressures are monitored during injection to stay within

the permitted injection pressure limits as determined by the initial well testing and formation depth. Processed volumes can be metered at the unloading pad or pump house (or both) to track volumes processed and injected.

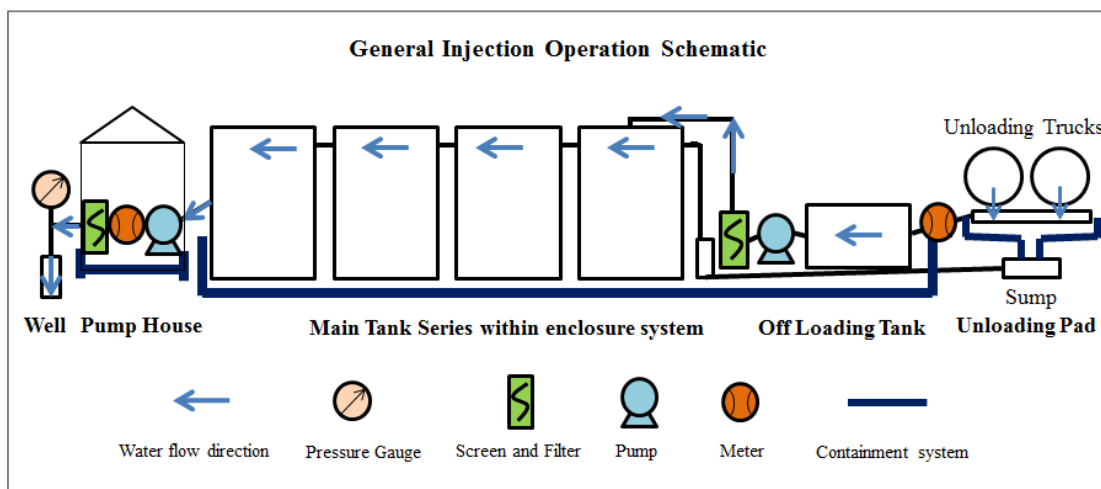


Figure 4-59. General injection operation schematic.

4.7.6 Injection Testing

In the open-hole completion wells, spinner or flowmeter logging is critical in identifying those zones into which injection is occurring. In eastern Ohio, it is typical to do an injection test after completion, where flowmeter logs are run over the entire open hole and fluid flow and temperature logs identify injection zones. See Section 7.4 for more in-depth discussion of the logging procedure.

The Silcor No. 1 SOS-D well (API 34-059-2-420) is a UIC Class II brine disposal well located in Guernsey County, Ohio. Temperature surveys conducted simultaneously with spinner logs confirmed that multiple flow zones exist in the open-hole section (Figure 4-60). The temperature anomalies and changes in spinner rates indicate that the majority of injection occurred in the Lower Copper Ridge (7,970 and 8,060 feet) and the Rome Dolomite formations (8,350 feet), with a small component in the lower Beekmantown and Rose Run (Gupta, 2013). In this well, the thin injection zones in the carbonate formations show much better injection potential than the Rose Run Sandstone.

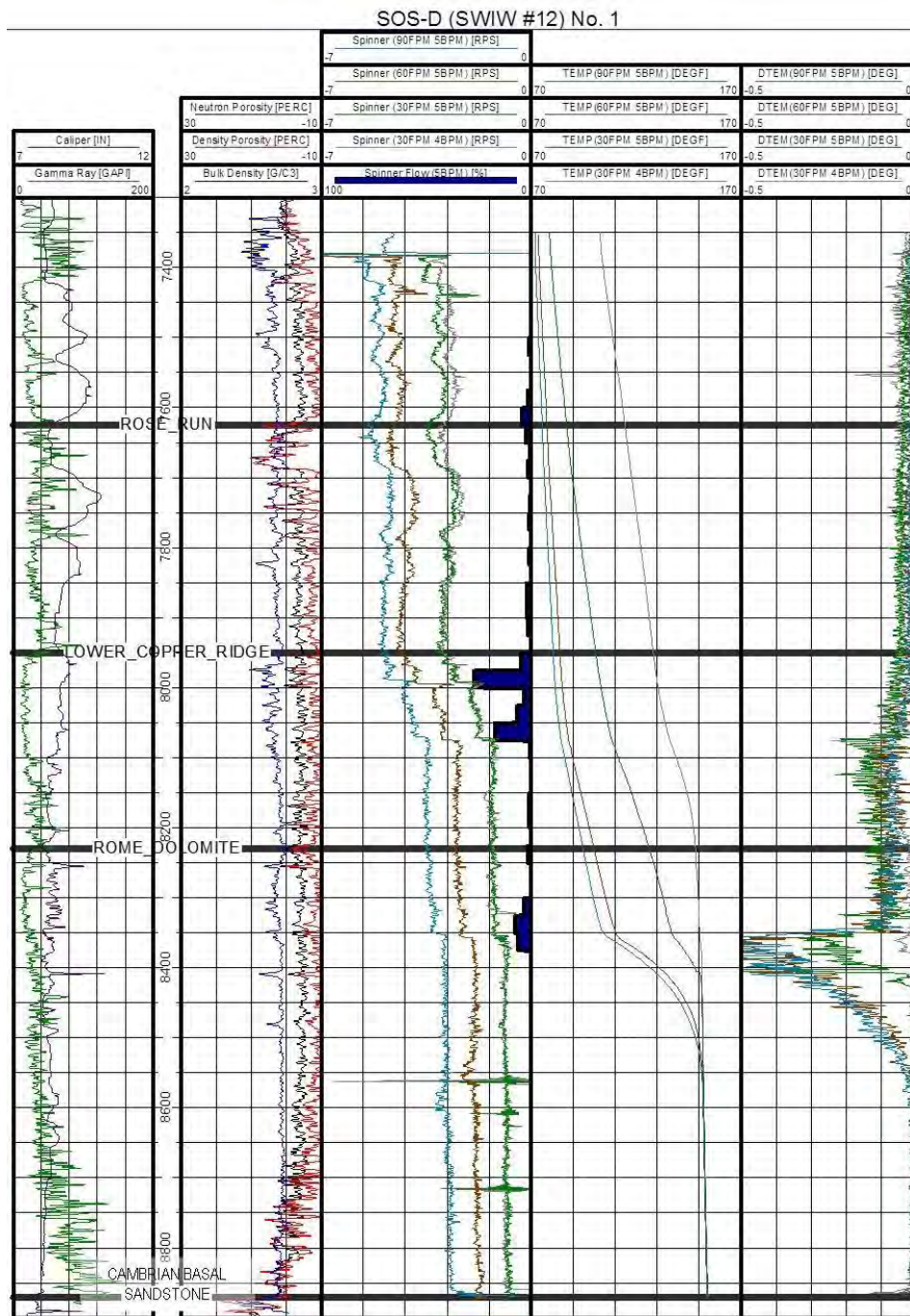


Figure 4-60. Cross section of select open-hole logs (Tracks 1 and 2), spinner and temperature data (Tracks 3 through 5) for Silcor No. 1 SOS-D well

5. Injection Simulations

This section describes numerical simulations of brine injection. The objective of the simulations was to analyze the subsurface pressure buildup and fluid migration due to brine injection. Four simulations were completed for major injection intervals in the region: Mississippian Weir Sandstone, Silurian Lockport-‘Newburg’ zone, Silurian ‘Clinton-Medina,’ and Cambro-Ordovician Knox-Basal sandstone interval. These intervals represent the major injection zones in the Appalachian Basin. Geocellular models were developed for each simulation to represent the subsurface distribution and properties of the injection zones and adjacent layers. The models were based on general log and operational data for the reservoirs. The distribution of the models includes a variety of reservoir types and depths across the northern Appalachian Basin region. Geocellular model information was ported to simulation codes to simulate the injection process.

The Weir, Clinton-Medina, and Knox-Basal sandstone simulations were run with the USGS computer program SEAWAT, and the Lockport-‘Newburg’ model was run with the CMG-GEM computer program. SEAWAT is designed to simulate three-dimensional (3D), variable-density, saturated groundwater flow (Langevin et al., 2008). The program is often used to investigate saltwater intrusion in aquifers, but it may also be applied to brine injection. The program includes a coupled version of MODFLOW (Harbaugh et al., 2000) to compute groundwater flow and MT3DMS (Zheng et al., 1999) to compute solute transport. The model is generated by assigning a finite difference grid of geotechnical parameters (permeability, storage, thickness), initial conditions (salinity, pressure), and boundary conditions. CMG-GEM is a finite element reservoir simulation computer program with similar input (CMG, 2012). The program includes options to model complex, heterogeneous, faulted reservoirs. Additional geomechanical analysis was completed to investigate the effect of brine injection on subsurface stress and strain conditions. To facilitate the analysis, ten rock cores from injection zones were tested for static geomechanical parameters. Further geomechanical analysis was completed with the StimPlan™ software package.

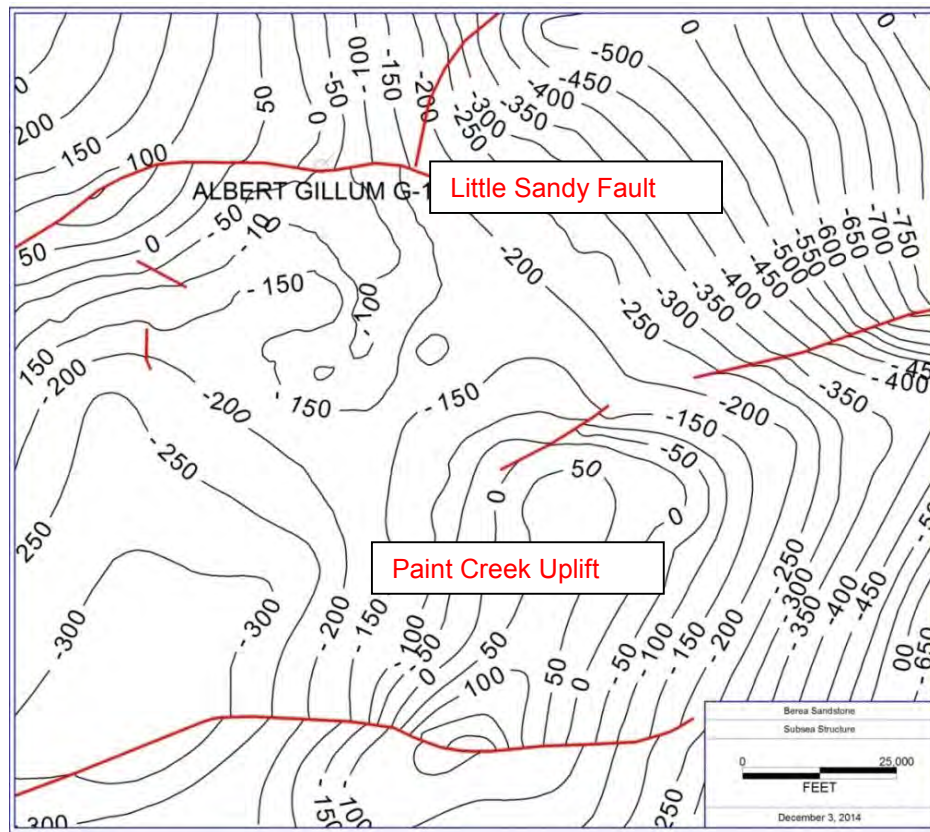
5.1 Weir Sandstone

The Weir sandstone simulation is representative of Mississippian age injection wells, which are common in Kentucky and West Virginia. These injection wells typically inject at lower rates for local disposal, but collectively have significant injection volumes.

5.1.1 Geocellular Model

The location for the Weir Sandstone geocellular injection model is in Elliot County, Kentucky. The Weir model was built using a single well for sandstone porosity distribution along with three surrounding wells to build a simple anticlinal structure with a bounding fault to the north. The Albert Gillum #G1-a API # 16063001600000 is located north of the Paint Creek Uplift and adjacent to Little Sandy Fault (Figure 5-1). The structural complexity of the area surrounding the well made this location a good candidate for a Weir Sandstone model because the area’s mapped faults are in close proximity to the injection location. The log suite (Figure 5-2) included gamma ray, neutron porosity, and bulk density curves. A density porosity curve was calculated over the Weir Sandstone interval using a 2.68 matrix density. The log porosity values were then used to estimate permeability for the Weir Sandstone using the core analysis data collected from the Kentucky Geologic Survey analysis of over 7,700 samples from 164 different

Weir Sandstone samples (Figure 5-3). Structure grids were created that include a small anticlinal feature to the south of the Albert Gillum well (Figure 5-4) and a bounding fault on the northern side of model.



Note: Red lines are interpreted faults.

Figure 5-1. Berea Subsea structure with Albert Gillum #G1-a injection well and location of Sandy Creek Fault.

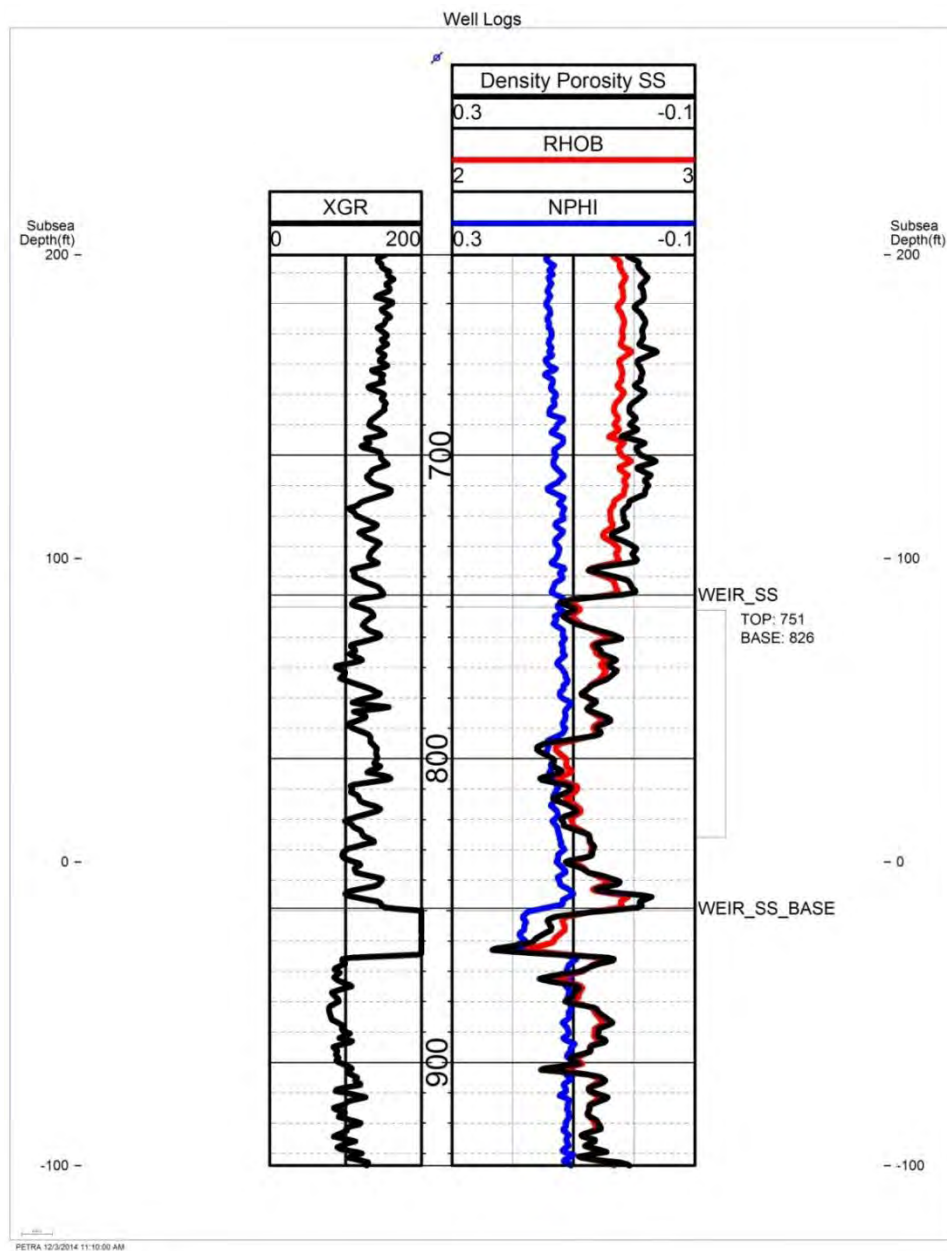


Figure 5-2. Albert Gillum #G1-a well log suite with injection interval noted.

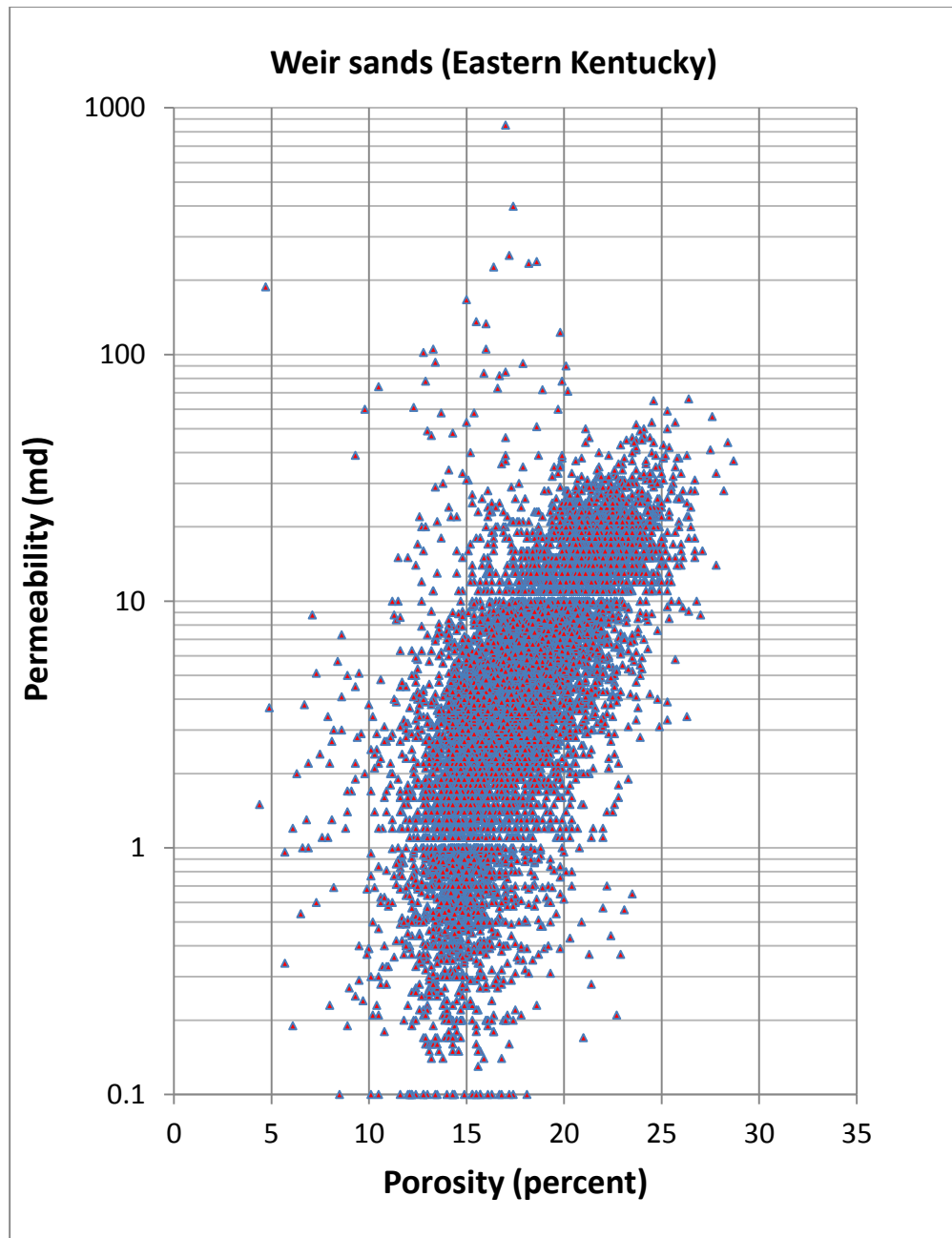
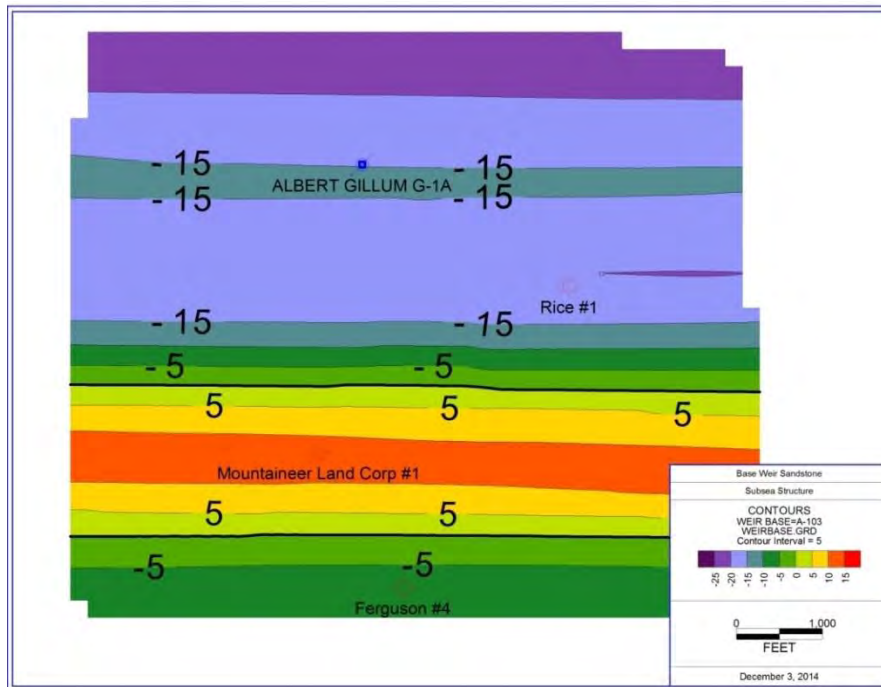


Figure 5-3. Eastern Kentucky core permeability analysis from 164 wells with 7,700 total samples.



Note: Color contours mark boundaries of the model.

Figure 5-4. Base Weir Sandstone subsea structure map.

5.1.2 Weir Sandstone Simulation

5.1.2.1 Input Parameters

The Weir Sandstone simulation was based on the geocellular model described in Section 5.1.1. Table 5-1 summarizes the model setup parameters. The model domain was specified as 2 km by 2 km with 21 model layers. The model covers a depth range of approximately 95 meters from the Borden Shale to the Sunbury Shale over a depth range of 65 to -30 meters msl. Layer thickness and structure were imported from the geocellular model and include the anticline structure and sealing fault (Figure 5-5).

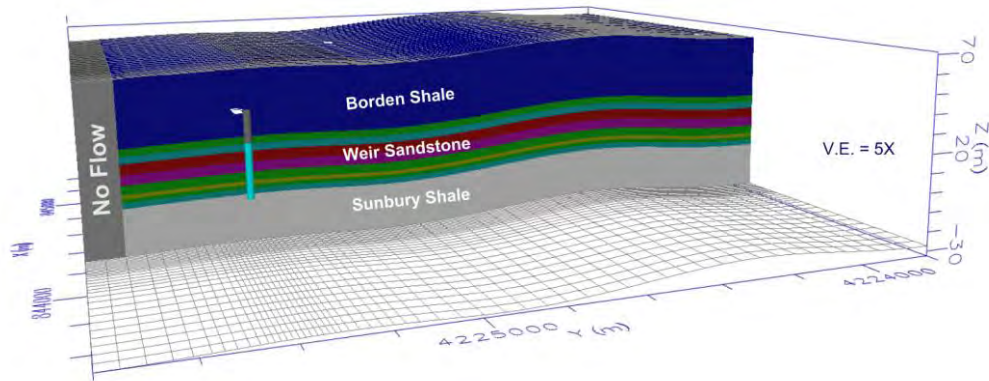


Figure 5-5. Weir Sandstone simulation model layers.

The model grid consisted of 56 rows and 56 columns designed to include the sealing fault and anticline structure, with the injection well on the downdip portion of the anticline (Figure 5-6). Grid size ranged from 50 meters by 50 meters at the edges of the model domain to 12.5 meters by 12.5 meters near the injection well. Total grid cells in the model numbered 65,856.

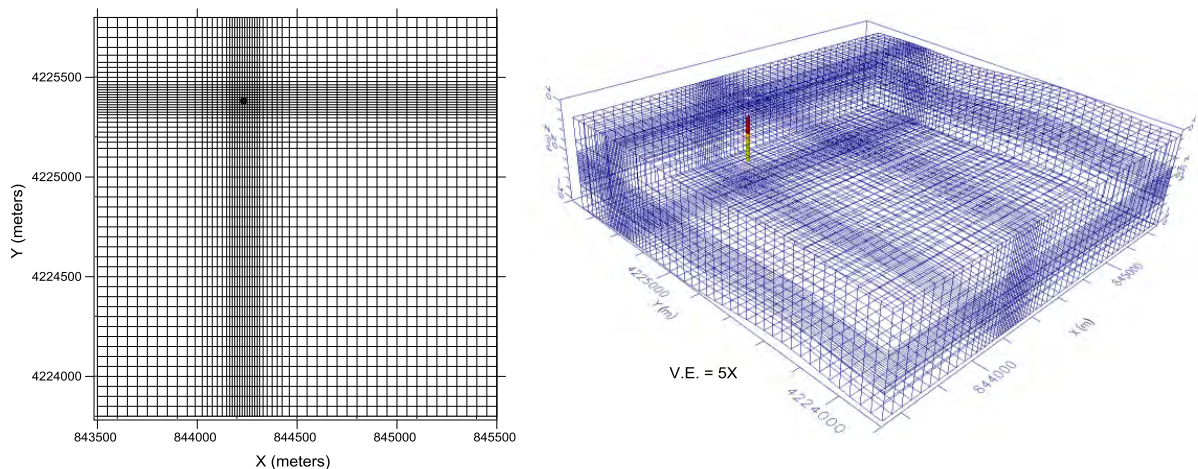


Figure 5-6. Weir Sandstone simulation grid.

Permeability was input as homogeneous by layer. The permeability in the Weir zone was based on porosity-permeability from rock core test data and model calibration to wellhead pressure for a brine disposal well in the area. In the model calibration process, reservoir permeability was increased 1.5 times the value suggested on the porosity-permeability curve. For example, permeability in layers 4-5 was increased from 10 mD to 15 mD to obtain a better pressure calibration. As such, model development suggests the reservoir may be on the higher end of the permeability data for the Weir Sandstone.

The constituent species was specified as salt. Fluid density range was 1.00 to 1.25 with a density/concentration slope of 0.7143. Initial salinity was set at 125,000 mg/L based on produced water in the area. Initial pressure was set at hydrostatic conditions based on 0.433

psi/ft pressure gradient. Constant head boundary conditions were assigned at the model edges based on this pressure gradient.

The injection well was designated to row 17, column 23 with the well module in the SEAWAT program. The well was screened across the Weir interval in layers 4-18. A pumping rate of 79 bbl/day was scheduled for 10 years followed by 10 years of post-injection. The pumping rate was the average rate from Mississippian-Devonian injection wells in operational data from the Appalachian Basin. At the injection well, point source was assigned with salt concentrations of 180,000 mg/L based on data on injection fluid for brine disposal wells in the area.

Table 5-1. Weir Sandstone simulation input parameters.

Parameter	Value	Comment
Flow Model	MODFLOW/SEAWAT	MODFLOW 2000, transient simulation, total simulation time = 7,300 days (20 years)
Domain	2 km x 2 km x 93 m	Includes anticline structure with sealing fault
Rows	56	None
Columns	56	None
Layers	21 Top = ~63 m Bottom = ~ -30 m	Variable thickness based on structure maps: Layer 1-3 = Borden Shale Layer 4-18 = Weir Layer 19-21 = Sunbury Shale
Grid Spacing	Max = 50 x 50 m Min = 12.5 x 12.5 m	Resolution increased near injection well (65,856 grid cells)
Permeability (mD)	Homogeneous by layer Based on porosity-permeability transform $K_x:K_z = 1:1$	Layer 1-3 = 0.0005 Layer 4-5 = 15 Layer 6-7 = 1.5 Layer 8-10 = 0.3 Layer 11-13 = 30 Layer 14-15 = 15 Layer 16 = 7.5 Layer 17 = 15 Layer 18 = 1.5 Layer 19-21 = 0.0001
Bulk Compressibility	Constant value for layers 1-21	1.5E-6 1/m
Boundaries	Constant head, no flow	Constant head nodes specified at N,S,E,W model boundaries based on 0.433 psi/ft gradient
Injection Well	Row 17 Col 23	+78 bbl/day for 3,650 days
Solution Parameters	Bi-Conjugate Gradient Stabilized acceleration routine, head change criterion = 0.001	<0.05% cumulative volumetric budget error
Transport Model	SEAWAT2KT	Species = Salt
Initial Salt Concentration	125,000 mg/L	Based on general produced water data for eastern Kentucky
Source Term	Constant Concentration Source	Injection fluid salinity = 180,000 mg/L based on local injection fluid analysis

5.1.2.2 *Weir Sandstone Simulation Output*

The Weir Sandstone simulations were designed to analyze lower injection rates in a more structurally complex injection zone. The model is representative of the many Mississippian-Devonian age injection wells in the region. Most of these injection wells are used for brine disposal from local oil and gas fields at fairly low injection rates. The model includes a subtle anticline structure and sealing fault. The sealing fault was assigned as no-flow boundary in the model. No fractures systems were included in the simulation. Model layers were homogenous with permeability based on approximate transform of porosity-permeability from Weir Sandstone rock core testing.

The SEAWAT model was run in transient mode for 10 years of injection at 79 bbl/day followed by a 10-year post-injection period. A central-in-space weighted algorithm solution scheme was used to calculate fluid density terms. Model net mass balance showed 'in-out' cumulative mass error less than 0.05% for all simulation runs. Simulations were run for injection fluid with a salinity of 180,000 mg/L, based on fluid analysis data from Class II brine disposal wells in the general area. The model was calibrated to nearby injection wells, which have historical wellhead pressures of 300 to 500 psi and injection rates ranging from 50 to 200 bbl/day.

Simulation pressure, salinity, and flow vectors were output at various time steps to examine the effects of subsurface injection. To calibrate the model to pressures observed in local injection wells, the reservoir zone permeability was scaled by a factor of 1.5X. Overall, this permeability remains within the range of permeability from Weir rock core tests. Based on the calibrated model, the maximum simulated pressure change was 403 psi, which compares to the historical wellhead pressures measured in a nearby Class II disposal well (332 psi on average). The model simulates pressure change in the reservoir, so there may be some additional pressure at the wellhead due to friction loss through the tubing. The model was sensitive to permeability scaling, such that a small change in permeability resulted in a several-hundred psi pressure change at the injection well.

Figure 5-7 shows the simulated pressure change over time in model layer 12. The simulation illustrates the effects of the boundary on the pressure buildup pattern. Results suggest the pressure front extending a maximum of 220 meters from the injection well at >100 psi after 10 years of injection. After injection was stopped, the simulation showed pressure decreasing within six months to near initial conditions. The simulation suggests that a minor pressure pulse may continue to migrate upgradient along the anticline. Figure 5-8 shows the pressure profile in cross section at 3,650 days. As shown, the pressure front is more of a thick, tabular pattern due to the relatively homogenous nature of the injection zone.

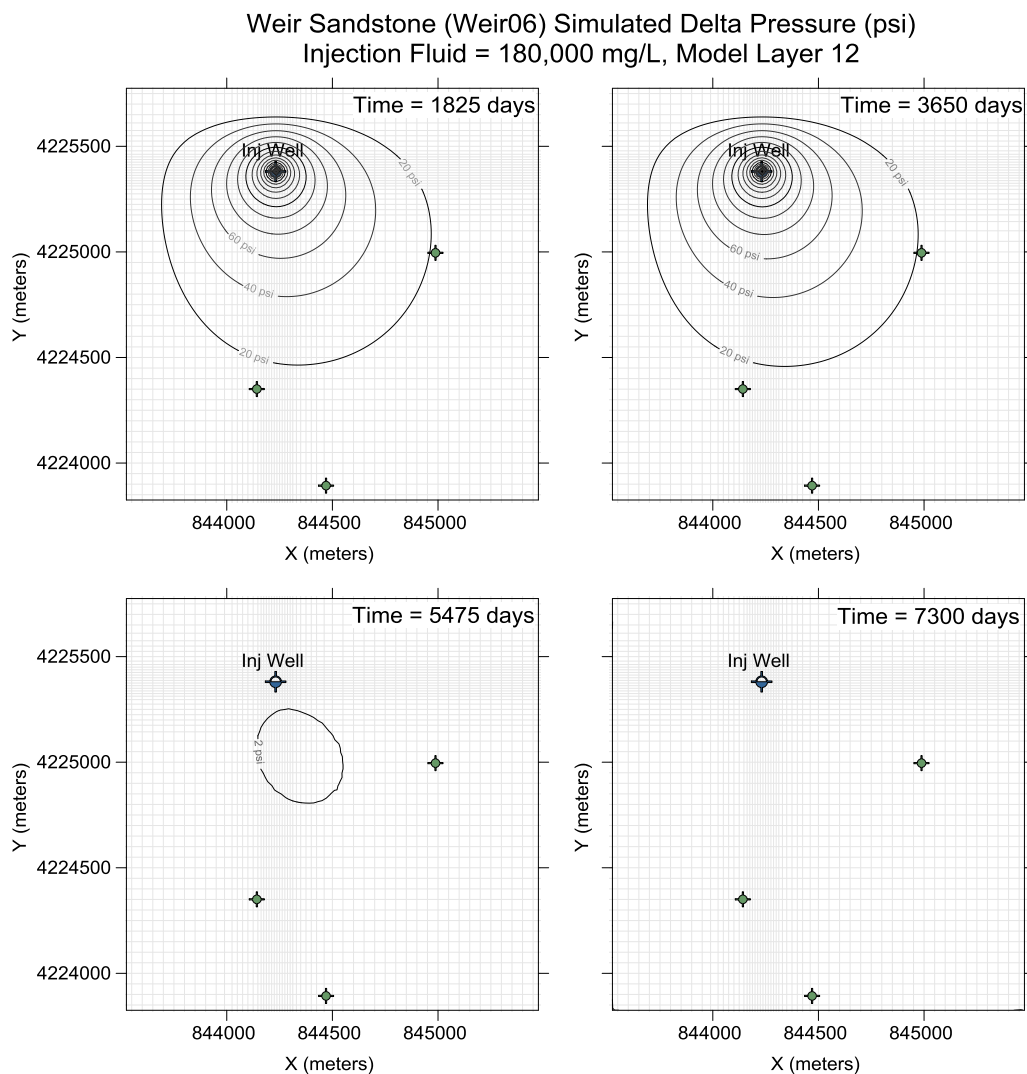


Figure 5-7. Weir Sandstone simulated delta pressure (psi) over time.

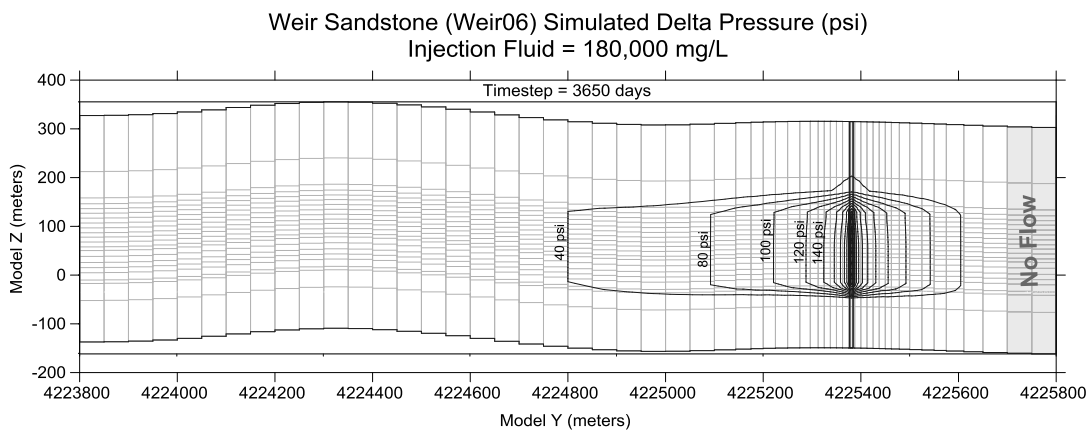


Figure 5-8. Weir Sandstone simulated pressure change (cross section).

Simulated changes in salinity were analyzed to illustrate the variable density effects of injection. In the model, the injected fluid was specified as 180,000 mg/L and the in-situ formation fluid was set at 125,000 mg/L. Figure 5-9 shows simulated salinity over time. As shown, the salinity front extended to a maximum of 150 meters from the injection well. The injected brine did not extend to any model boundaries, so it does not appear to be affected by the specified features. There was minimal brine migration related to variable density effects in the 10-year period after injection. Additional long-term simulations were run to investigate the potential for brine migration. These simulations indicated that it would take hundreds of years to observe any significant brine migration. Figure 5-10 shows the simulated salinity at time step 3,650 days. Results indicated a smaller brine front than the simulated pressure front.

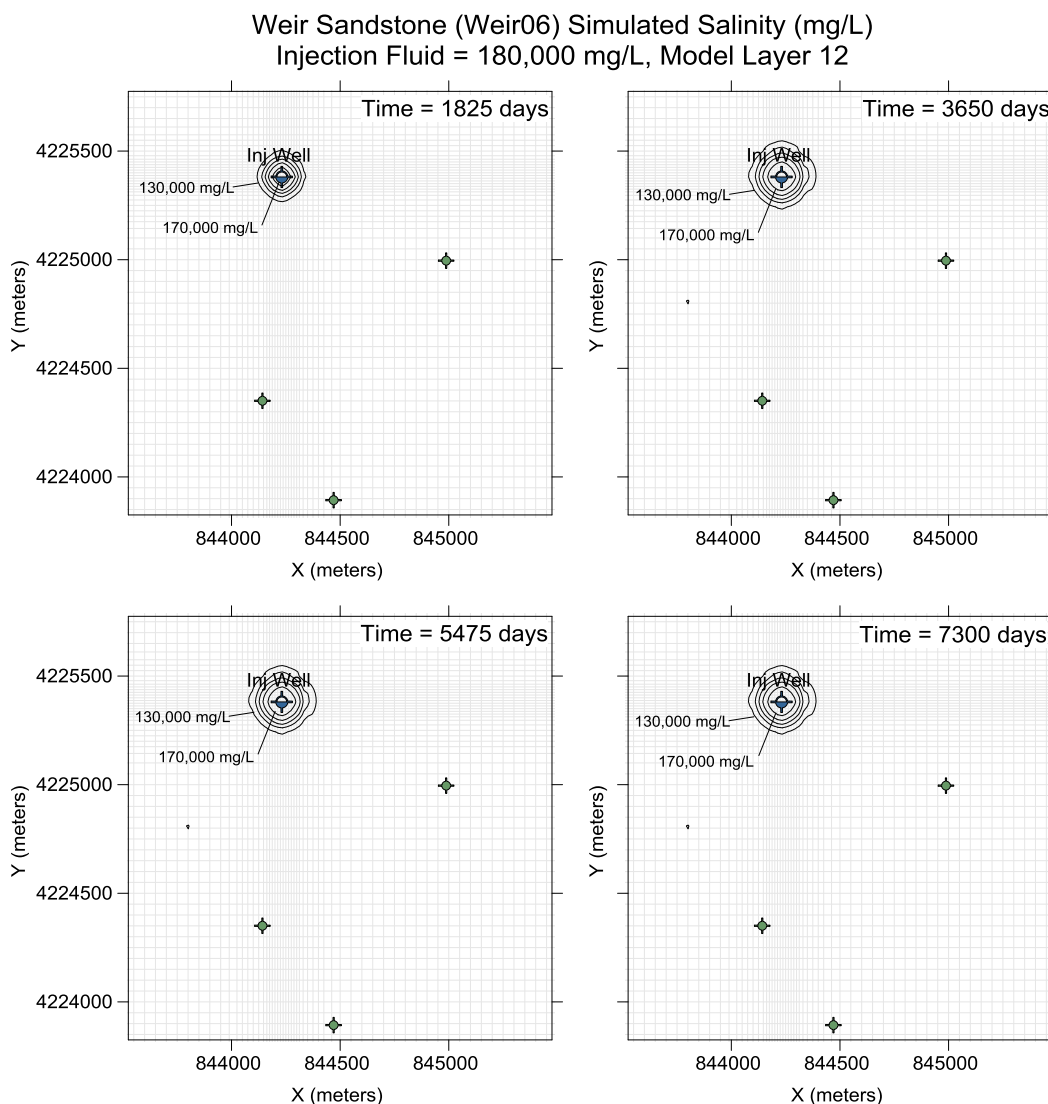


Figure 5-9. Weir Sandstone simulated salinity (mg/L) over time.

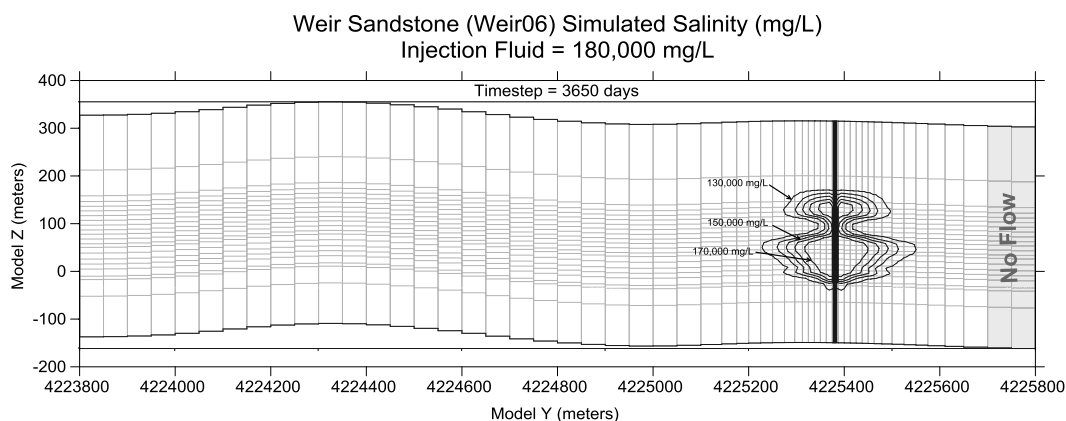


Figure 5-10. Weir Sandstone simulated salinity over time (cross section).

5.2 Lockport-Newburg

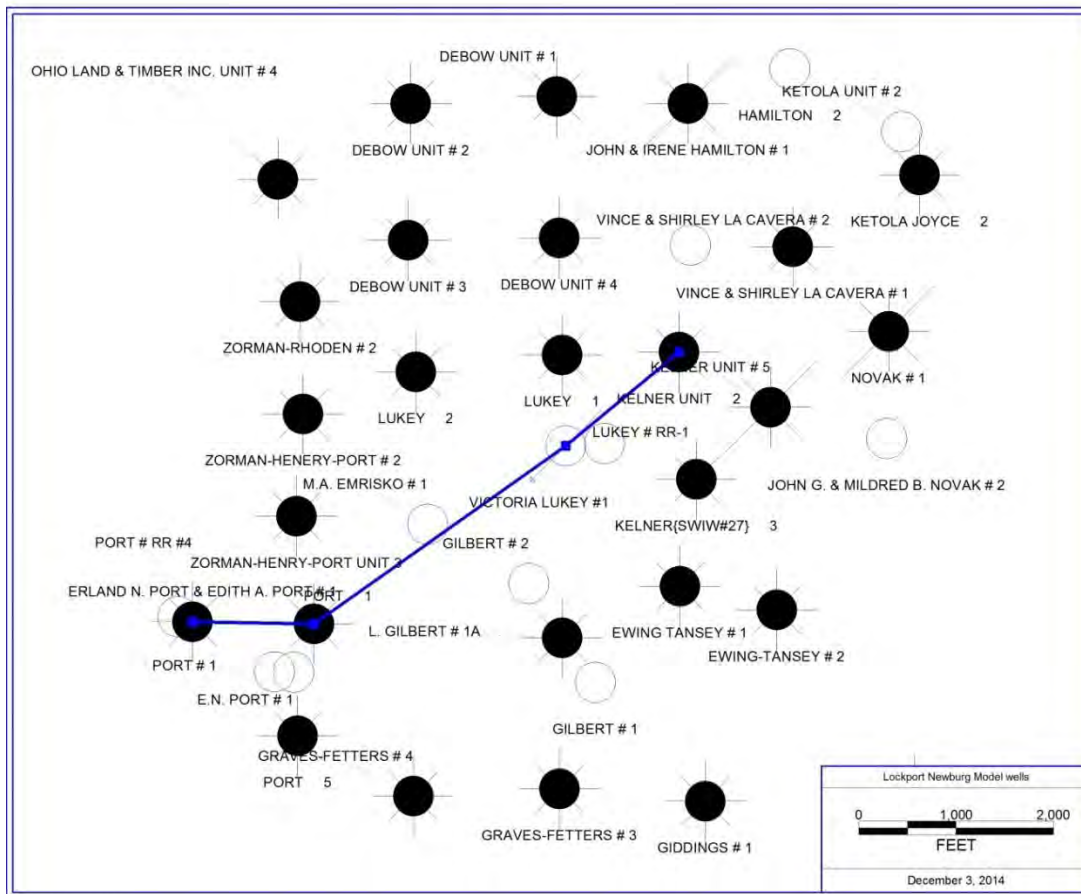
The Lockport-Newburg is a common formation for injection in northeast Ohio. The formation is a carbonate rock type with variable properties reflecting deposition of patchy reefal mounds. Many wells penetrate the formation because the “Clinton”-Medina hydrocarbon reservoir underlies the Lockport-Newburg.

5.2.1 Lockport-Newburg Geocellular Model

The Lockport-Newburg geocellular model was developed to evaluate brine injection in a shallow permeable carbonate zone that is commonly used in the region, with a focus in northeastern Ohio. The Newburg zone within the lower Lockport Dolomite commonly shows zones of very high porosity and permeability. These reservoir properties vary laterally from well to well in the Ashtabula area. A complex 3D model was built for this reservoir to evaluate the potential effects of this lateral heterogeneity.

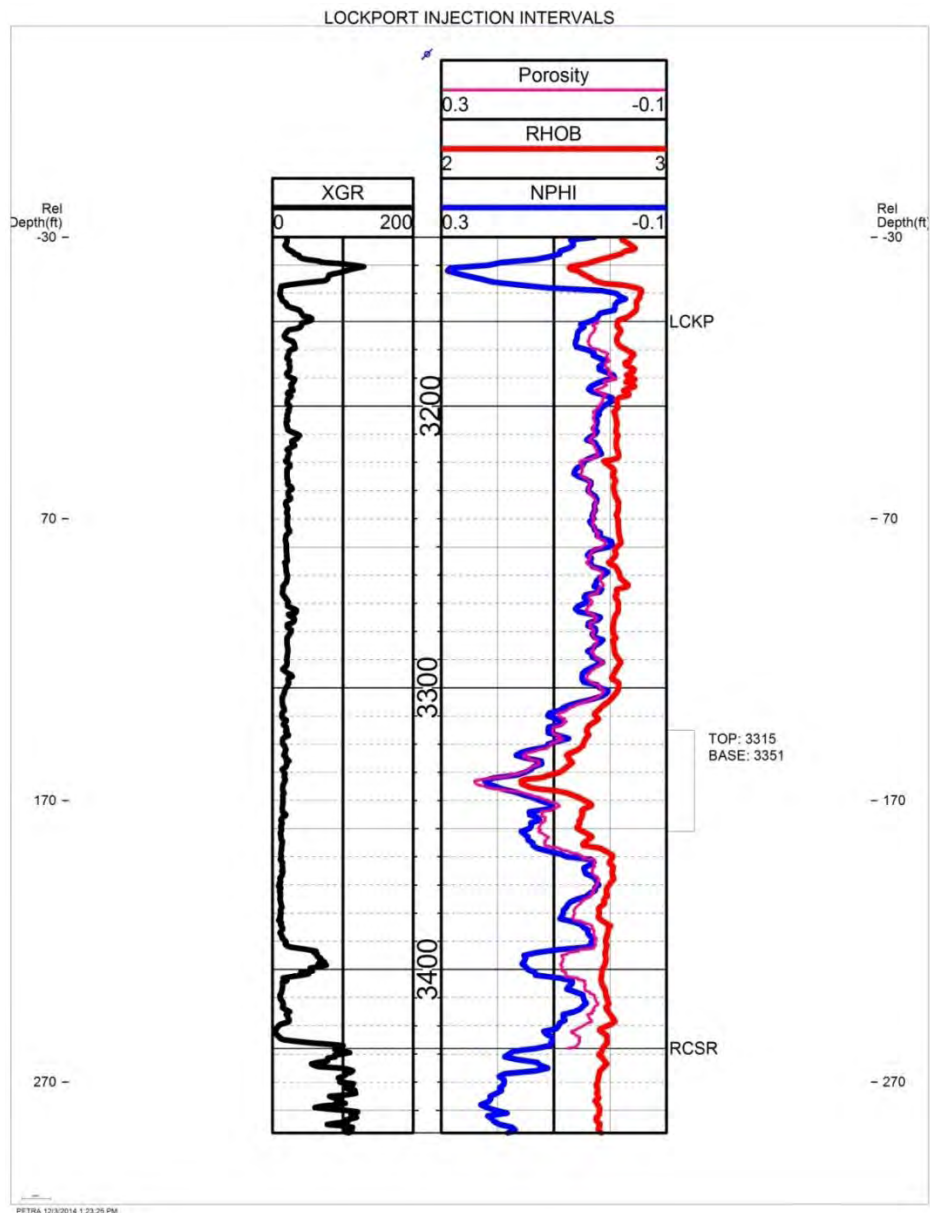
The model location was based on an area in southeastern Ashtabula County, Ohio. The Lockport model was built from log data in the Victoria Lukey #1 API 3400720245 injection well and 25 surrounding Clinton wells (Figure 5-11). The log data included gamma, density, and neutron logs over the Lockport Dolomite.

After the log data were digitized, a dolomite-corrected neutron porosity curve was generated from the original limestone neutron porosity curves. The typical neutron porosity curves in the study are Sidewall Neutron porosity logs, so the shift involved a 2.5% decrease in neutron porosity. A density porosity curve was then calculated from the bulk density curve using a 2.83 dolomite matrix. The average of the dolomite-corrected neutron porosity and dolomite density porosity was used as the final porosity estimate in the model (Figure 5-12). The injection interval in the Victoria Lukey #1 well is located in the lower portion of the Lockport typically called the Newburg. A cross section of the study area shows the lateral variability present in this zone (Figure 5-13).



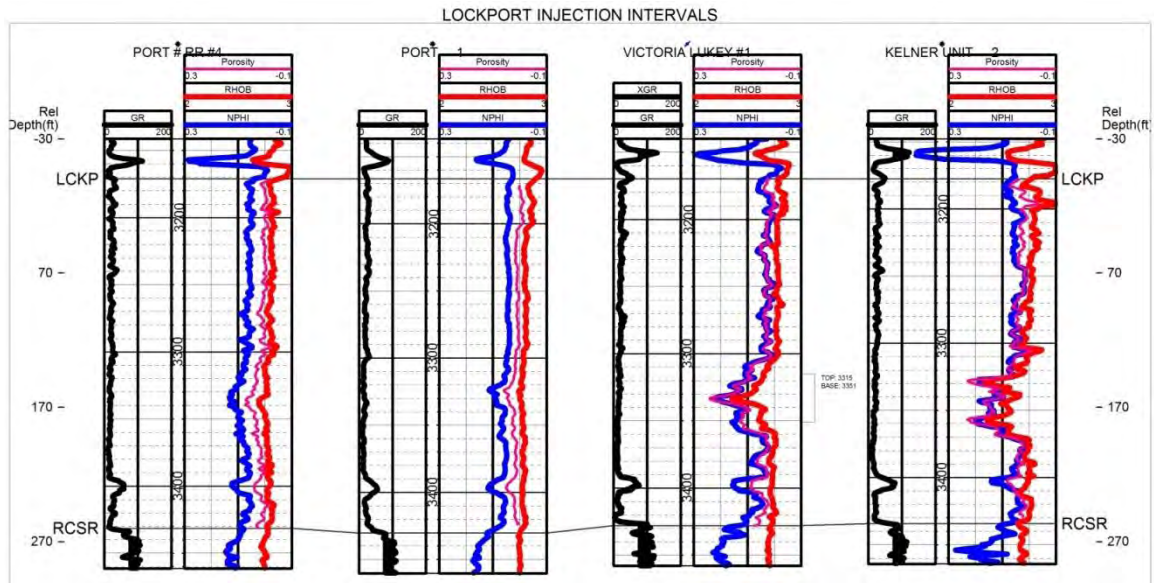
Note: Blue line indicates cross section.

Figure 5-11. Lockport Newburg injection model wells surrounding the Victoria Lukey #1 injection well.



Note: Porosity curve generated from average of the dolomite-corrected neutron and density porosity curves.

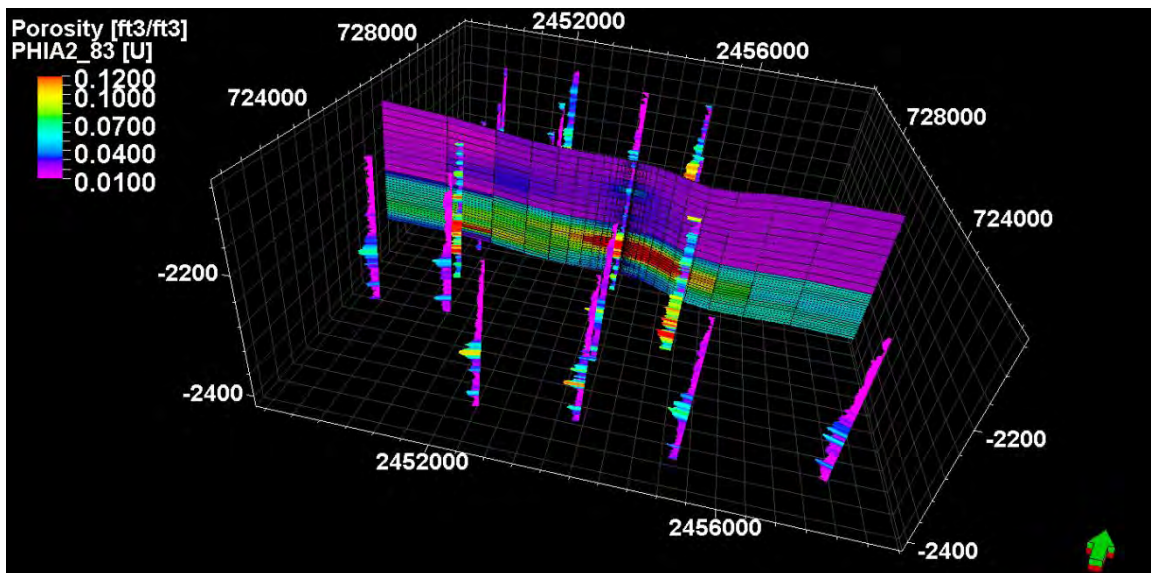
Figure 5-12. Log suite for the Victoria Lukey #1 injection well with injection interval marked.



Note: Section line shown in Figure 5-11.

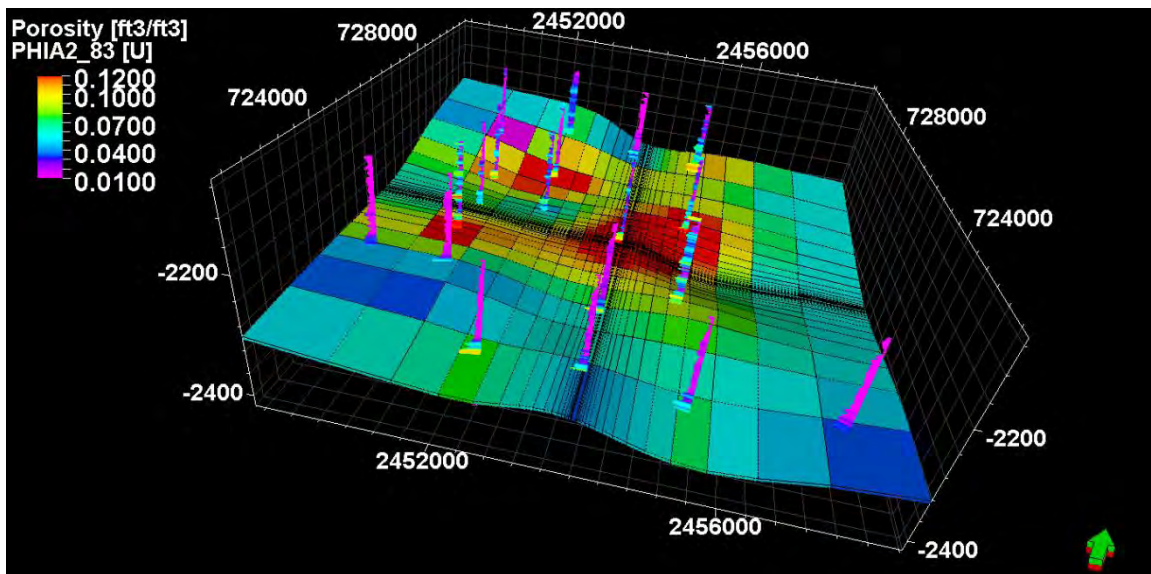
Figure 5-13. West-to-east cross section of Lockport model wells.

A two-zone static earth model was constructed in Petrel® modeling software consisting of a 10-layer upper, less porous zone and a 20-layer lower, high-porosity zone. The Victoria Lukey #1 well injection interval is located in the lower zone. An 8,000-foot-wide grid was centered on the injection well. A logarithmic tartan grid was created with a 50-foot inner cell and 35 total-width cells, for a total of 36,750 cells. The final porosity model shows the lateral variability present in the area surrounding the injection well (Figures 5-14 and 5-15). The mean porosity in the upper zone is 2.1% and in the lower zone is 7.1%. The porosity was transformed into permeability using the core data analyzed in the Midwest Regional Carbon Sequestration Partnership (MRCSP) Middle Devonian-Middle Silurian Formations report (MRCSP, 2008) (Figure 5-16).



Note: Log curves are displayed along well paths. Coordinates in Ohio North NAD 27 feet and depth in subsea feet. North arrow in lower right corner.

Figure 5-14. West-to-east cross section of two-zone Lockport porosity model.



Note: Log curves are displayed along well paths. Coordinates in Ohio North NAD 27 feet and depth in subsea feet. North arrow in lower right corner.

Figure 5-15. Lockport porosity model of layer in center of main injection zone (tartan grid cells displayed).

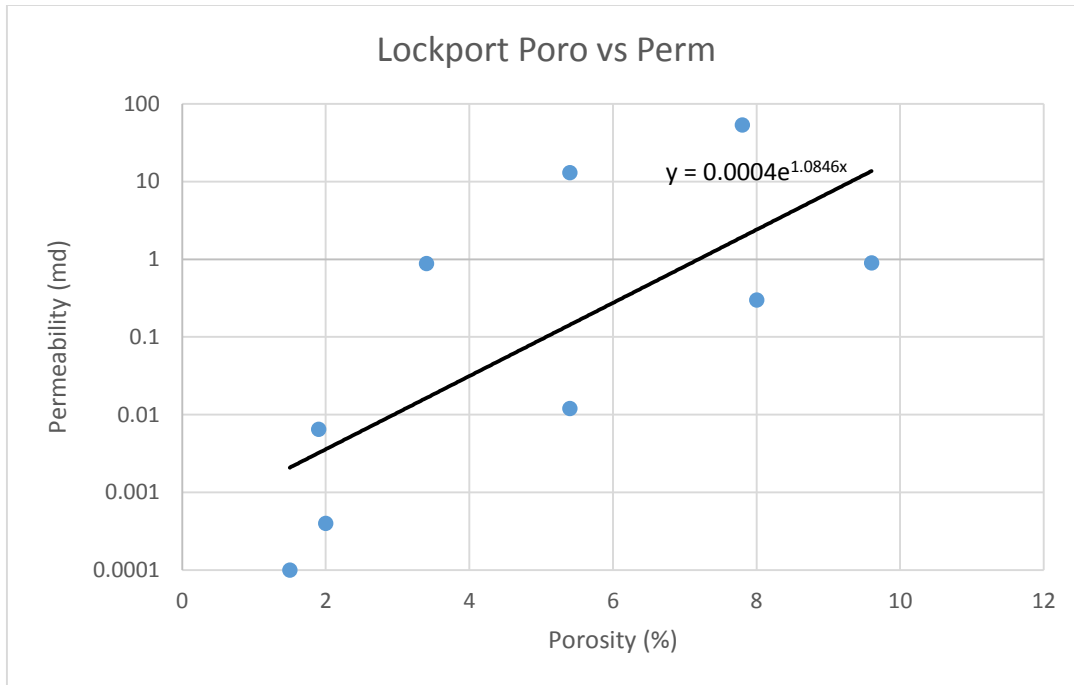


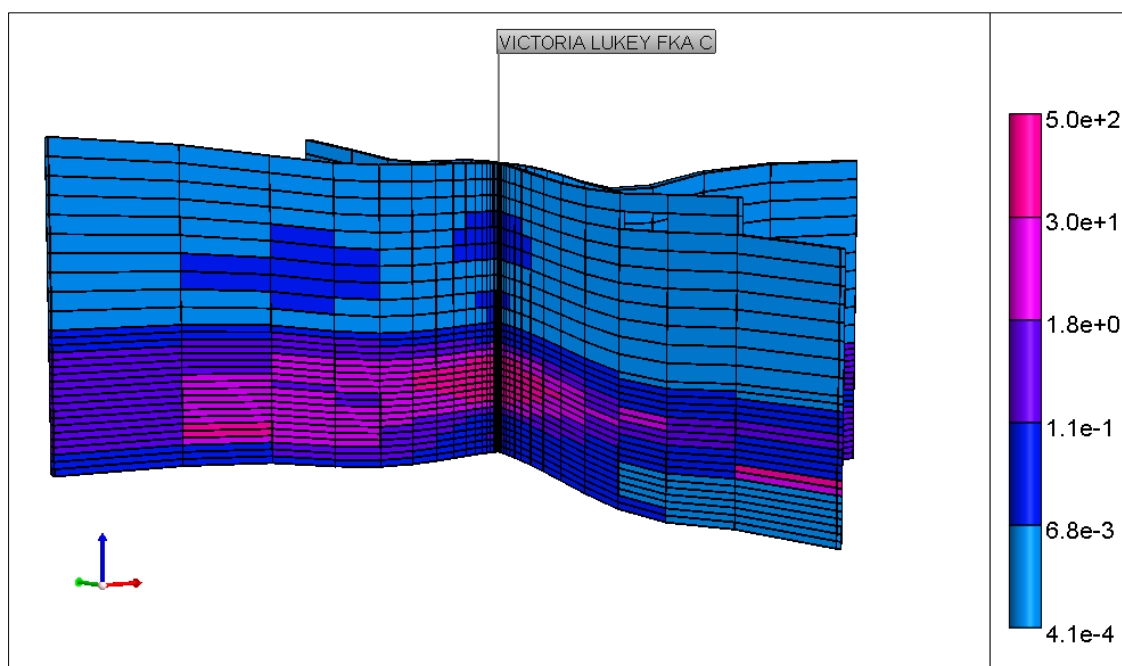
Figure 5-16. Porosity-to-permeability transform from Johnson #1 (Pennsylvania) and Ocel #1 (Ohio) Lockport core data.

5.2.2 Lockport-Newburg Simulation

5.2.2.1 Input Parameters

Brine injection into the Lockport-Newburg dolomite formation zones was modeled to analyze brine displacement dynamics in the subsurface. Porosity values were obtained from available well log data, and permeability values were obtained from available core data. The 3D static earth model grid with the porosity and permeability values was then imported into CMG-GEM® in a Rescue model format. Generalized Equation of state Model (GEM) by the Computer Modeling Group (CMG) is an industry-standard fully-compositional reservoir simulator that is widely used to model the flow of multi-phase, multi-component fluids in multi-dimensional systems. We utilized the Peng-Robinson equation of state for our model. Brine phase densities and viscosities were calculated as a function of pressure, temperature, and salinity; the Rowe and Chou correlation was used for densities and the Kestin correlation was used for viscosities.

The Lockport-Newburg injection model consisted of 36,750 grids that spanned about 4,500 feet in either direction from the injection well. The 344-foot-thick model was split into an upper zone and a lower zone; the 10-layer upper zone is less porous and more confining than the 20-layer lower zone. The upper zone has an average of 2% porosity and 0.009 mD permeability, while the lower zone has an average of 7% porosity and 43 mD permeability. Figure 5-17 shows the model permeability field along with the injection well location. Our model assumed an isometric permeability field for a conservative estimate of the brine displacement. A tartan grid, used for more resolution closer to the injection well, can also be seen in Figure 5-17.



Note: The color scale to the right gives the permeability values (mD) represented in the map.

Figure 5-17. Lockport-Newburg model permeability (cross section).

We initialized the model to be at hydrostatic pressure (assuming a pressure gradient of 0.45 psi/ft) and to be filled with native brine. The native brine salinity was assigned based on produced water data from Newburg wells in the area. Brine was injected into the Victoria Lukey Fka C well, which is perforated between 3,315 feet and 3,351 feet in the model (lower zone). In our case, the injected brine was of lower salinity than the native brine. Table 5-2 lists the parameter values considered in our dynamic model.

Table 5-2. Lockport zone brine injection simulation input parameters.

Parameter	Value	Comment
Model	CMG-GEM	Transient simulation
Domain	9,000 ft × 9,000 ft × 344 ft	Centered on Lukey well
Rows	35	Resolution increased near injection well
Columns	35	Resolution increased near injection well
Grid Spacing	Max = 200 x 200 m Min = 25 x 25 m	Variable grid spacing with grid increased grid resolution increased near injection wells (tartan grid)
Layers	30 -2,070 ft to -2,414 ft	Variable thickness based on structure maps: Upper zone (1) = 10 layers Lower zone (2) = 20 layers
Permeability	Heterogeneous $K_x:K_y = 1:1$	Upper zone (1) = 0.009 mD Lower zone (2) = 43 mD

Table 5-2. Lockport zone brine injection simulation input parameters. (Continued)

Parameter	Value	Comment
Porosity	6% average porosity in model	Upper zone (1) = 2% Lower zone (2) = 7%
Bulk Compressibility	Constant rock compressibility	5E-6 1/psi
Initial Reservoir Pressure, psia	(14.7 psi + 0.45 psi/ft × 2,070 ft)	Hydrostatic based on 0.45 psi/ft gradient
Injection Well	Perforations in layers 15-22	Victoria Lukey Fka C operated at a constant injection rate of 300 STB/day with minimum BHP constraint of 2,000 psi
Variable Density Model	CMG-GEM Compositional Simulator	Species = Salt (Na+)
Initial Salt Concentration	278,000 mg/L	Model filled with water initially (aquifer). Native brine salinity based produced water data for Newburg.
Source Term	Constant concentration source	Injected brine salinity = 250,000 mg/L

Two well schedules were investigated for the rate-constrained injection operations: a constant injection rate scenario and a more realistic variable injection rate scenario (Figures 5-18 and 5-19). The well schedule details were as follows:

1. A constant brine injection rate of 300 stock-tank barrels (STB) a day with a minimum BHP constraint of 2,000 psi.

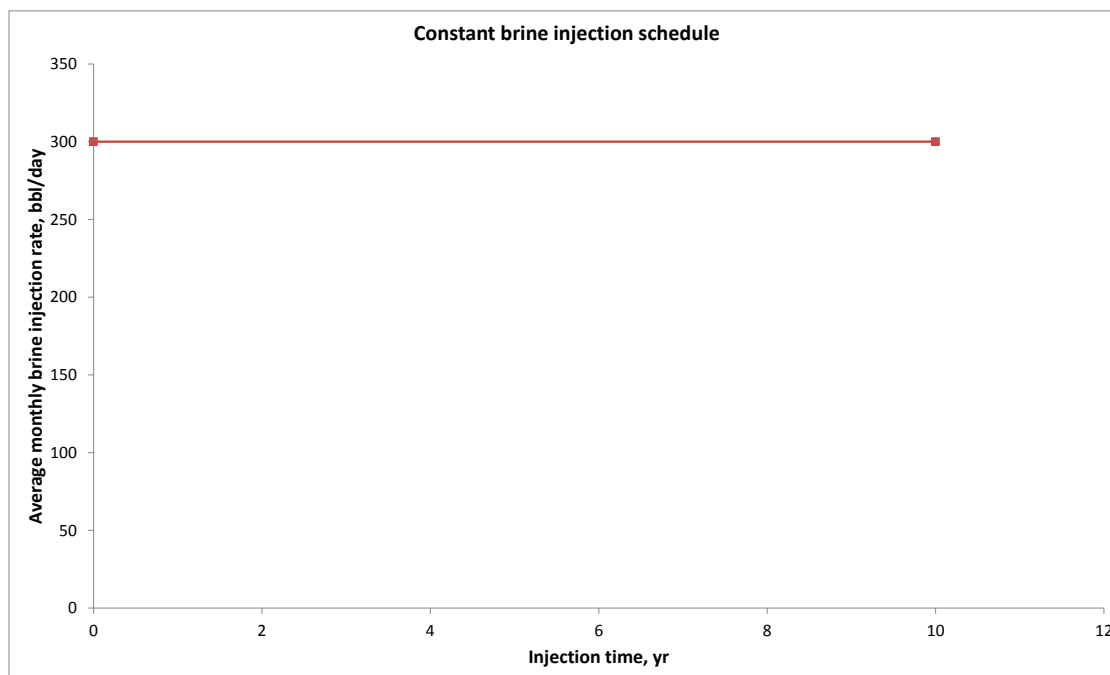


Figure 5-18. Constant brine injection schedule trial.

The constant rate injection simulation was run for a 10-year injection period followed by 40 years of post-injection monitoring.

1. A variable brine injection rate up to a maximum of 195 bbl/day.

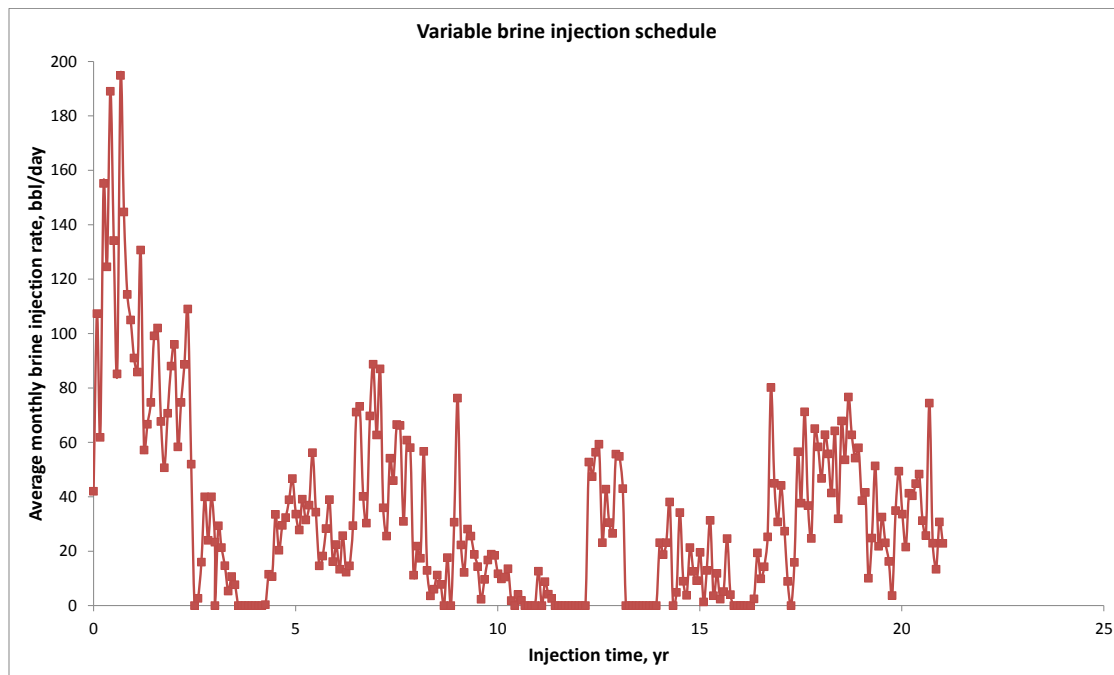


Figure 5-19. Variable brine injection schedule trial.

The variable-rate injection simulation was run for a 20-year injection period followed by 20 years of post-injection monitoring.

The initial pressure map is shown in Figure 5-20. Post-processing was conducted and the results were mapped to assess the injectivity of the Lockport-Newburg zone for the realistic injection volumes considered in both cases.

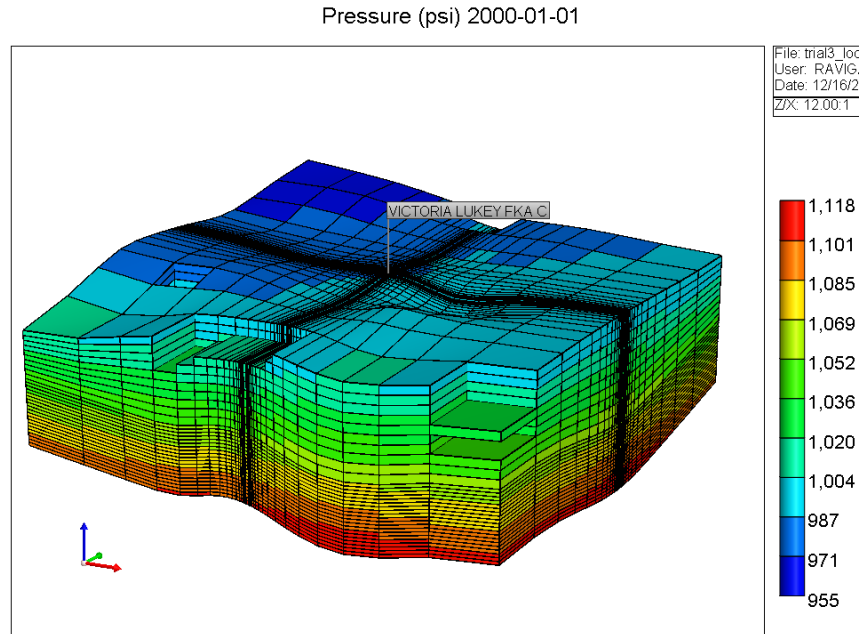
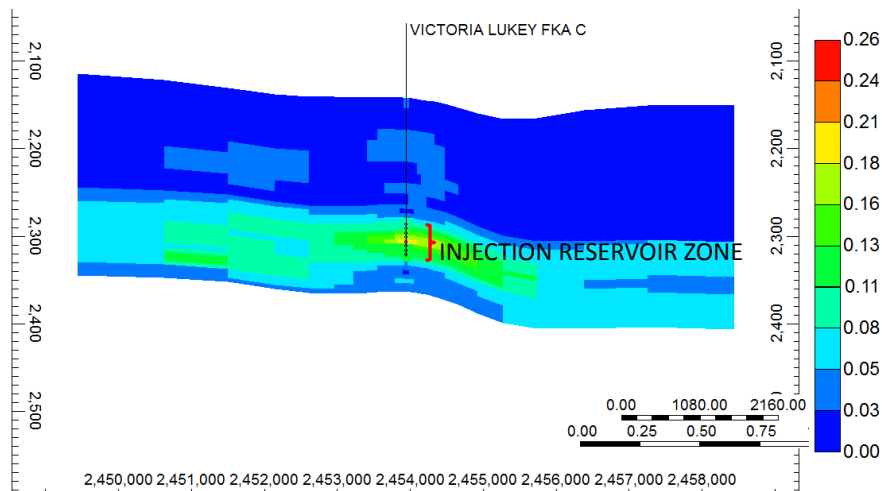


Figure 5-20. Lockport model initial pressure map.

5.2.2.2 Lockport-Newburg Simulation Output

The Lockport-Newburg model was initialized to be filled with brine (278,000 ppm salinity) based on produced water data from the Newburg formation. The model was at a corresponding initial hydrostatic pressure reflective of the denser formation brine. Injection water into this reservoir was considered to have lesser salinity (250,000 ppm) than the native brine. The injection reservoir was overlain by less porous and less permeable confining rock layers (upper model zone). Figure 5-21 shows the injection reservoir zone with respect to the model domain.



Note: Surrounding regions and overlying layers are less porous and less permeable compared to the injection reservoir zone.

Figure 5-21. Lockport porosity map indicating the injection zone (cross section).

We began with the simple constant injection rate scenario to analyze the injectivity and pressure-constrained capacity of the injection reservoir. For the constant injection schedule trial, brine was continuously injected into the reservoir at 200 bbl/day for 10 years, followed by a post-injection monitoring period of 40 years (Figure 5-22). The injection well also had a BHP monitoring constraint not to exceed 1,700 psi. Pressure and salinity were tracked through time in the model domain to examine the effects of subsurface injection.

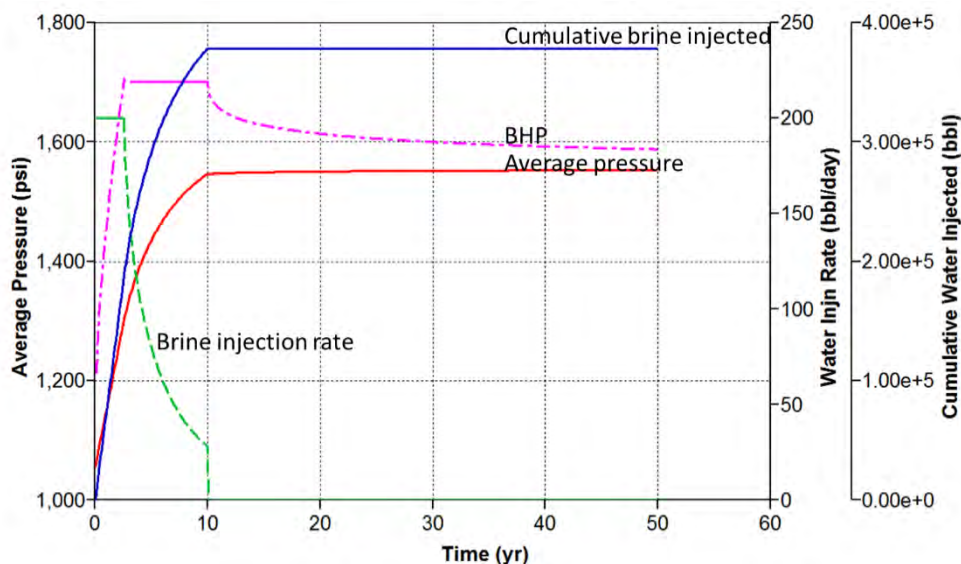


Figure 5-22. Lockport-Newburg brine injection simulation results at a constant injection rate over time.

Figure 5-23 shows the salinity profile for a chosen model slice. We observed that the injected brine filled the reservoir, with minimal brine migration after injection stopped. Figure 5-24 shows the salinity at the end of the 40-year post-injection monitoring period.

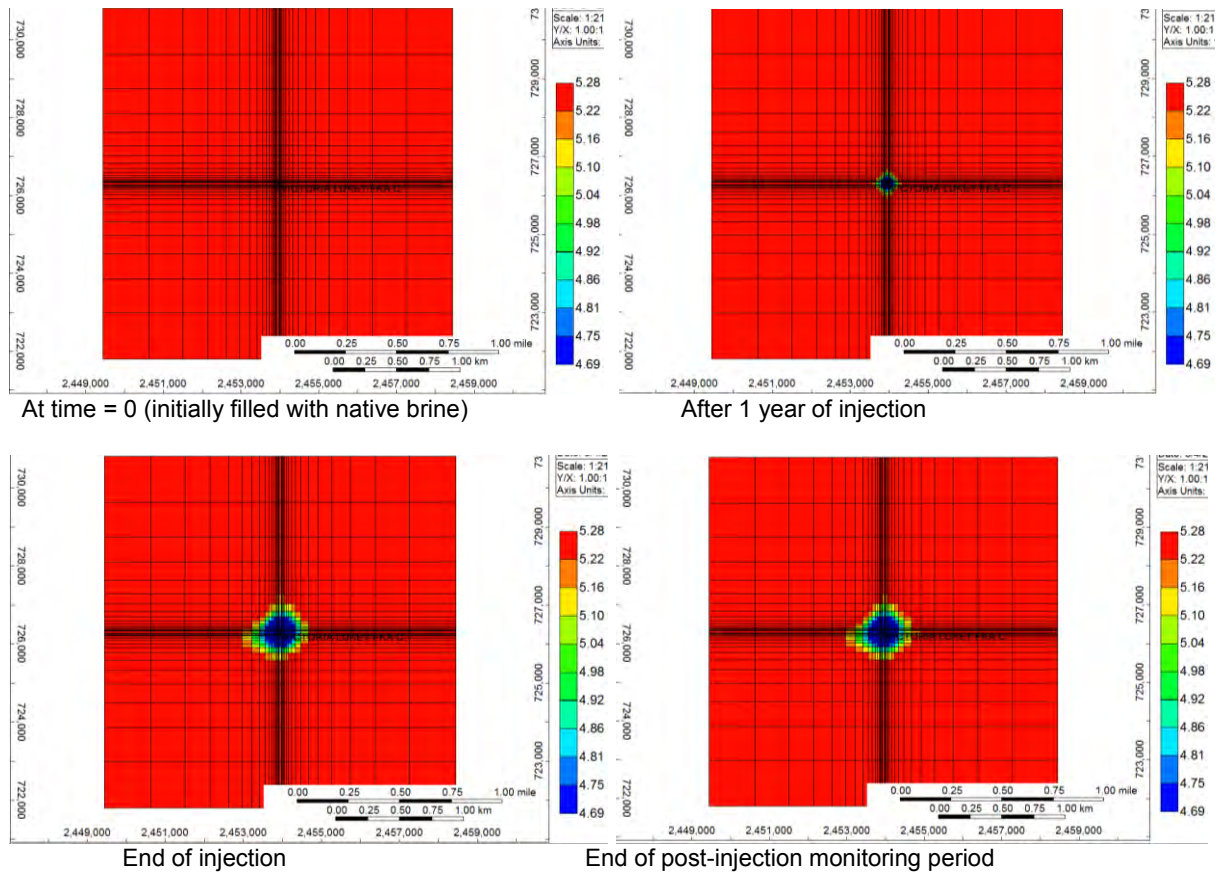


Figure 5-23. Salinity profile snapshots for the constant injection Lockport-Newburg GEM model (cross section).

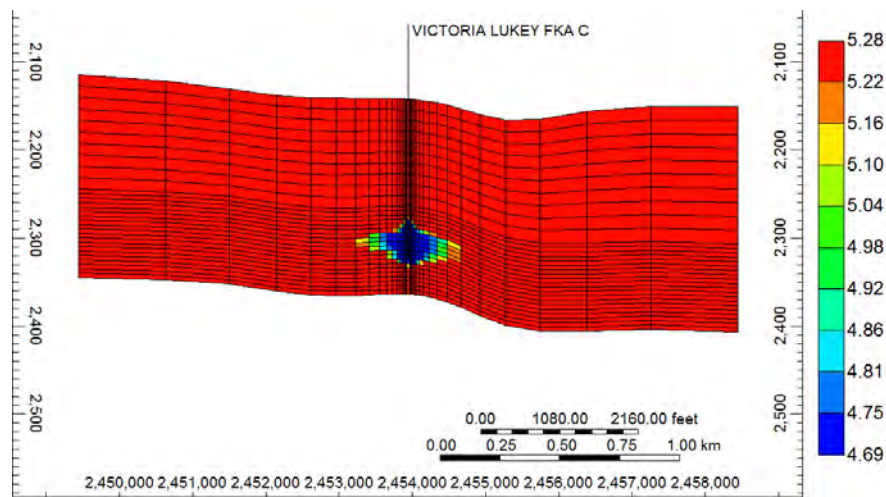


Figure 5-24. Aqueous salinity at the end of the 40-year post-injection monitoring period for the constant-injection Lockport-Newburg GEM model (cross section).

Since we observed extremely high BHP after a few years into our continuous injection schedule, we simulated a more realistic intermittent or variable brine injection schedule based on field data for the Victoria Lukey well to evaluate the pressure-constrained reservoir behavior (Figure 5-25). We simulated 20 years of brine injection followed by a 20-year post-injection monitoring period.

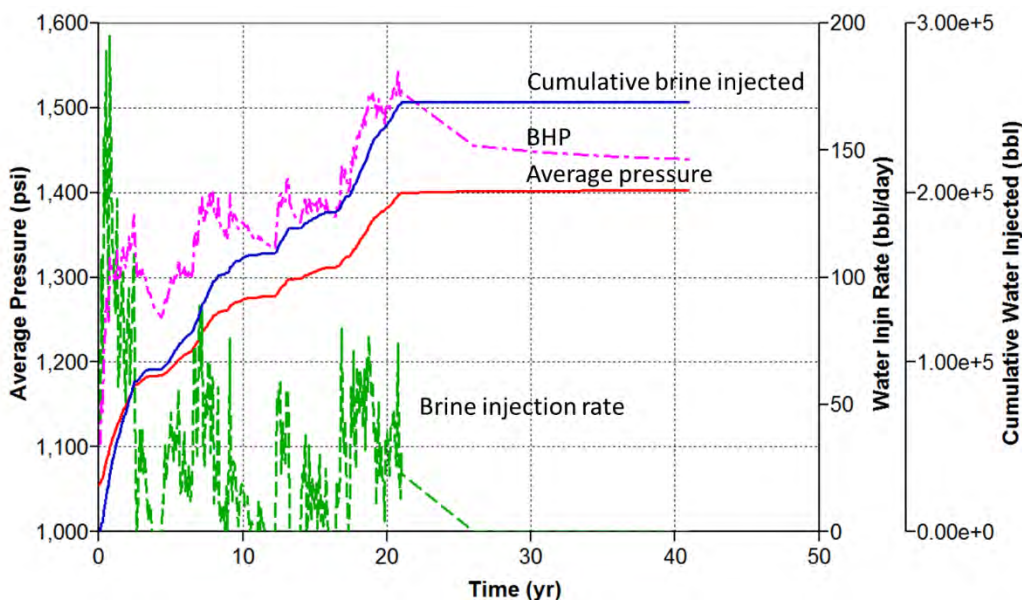


Figure 5-25. Lockport-Newburg brine injection simulation results at variable injection rates over time.

Figure 5-26, the salinity profile for a chosen model slice, shows that the injected brine filled the reservoir, with minimal brine migration after injection stopped. Figure 5-27 shows the salinity at the end of the 20-year post-injection monitoring period.

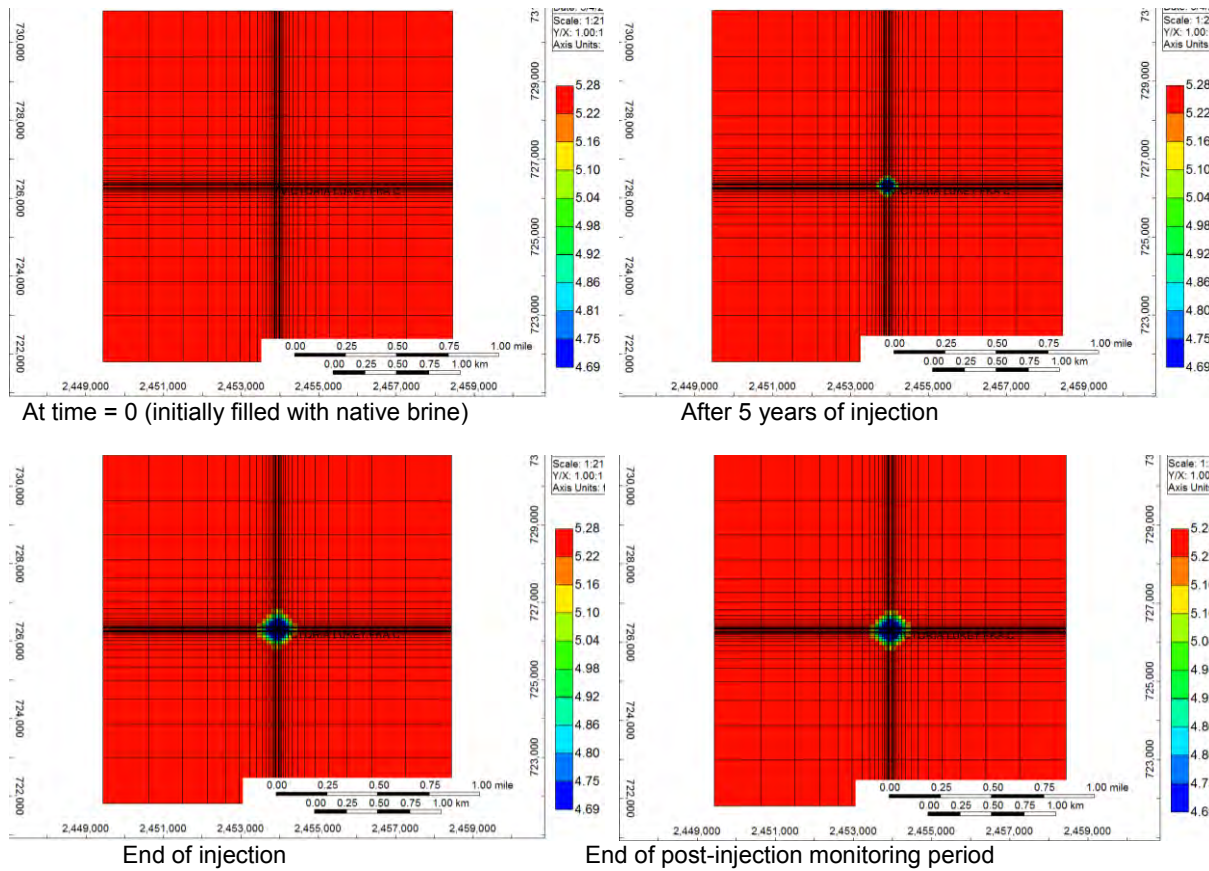


Figure 5-26. Salinity profile snapshots for the variable-injection Lockport-Newburg GEM model (cross section).

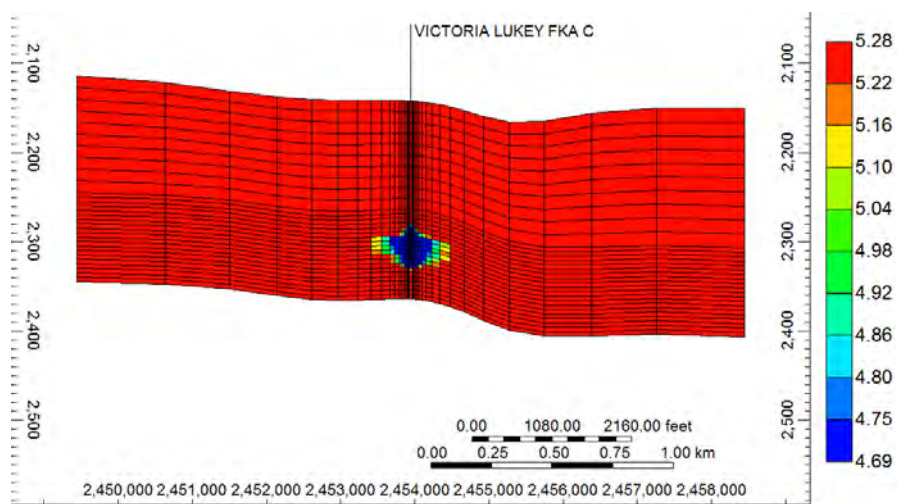
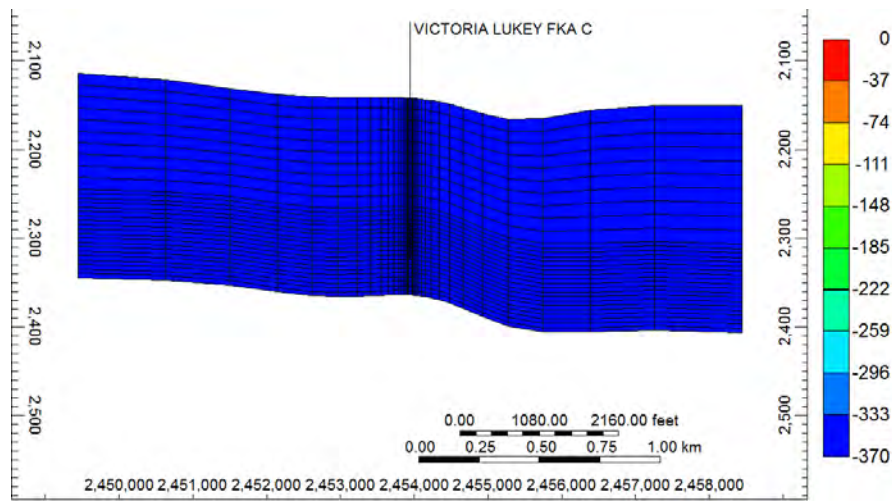


Figure 5-27. Salinity at the end of the 20-year post-injection monitoring period for the variable-injection Lockport-Newburg GEM model (cross section).

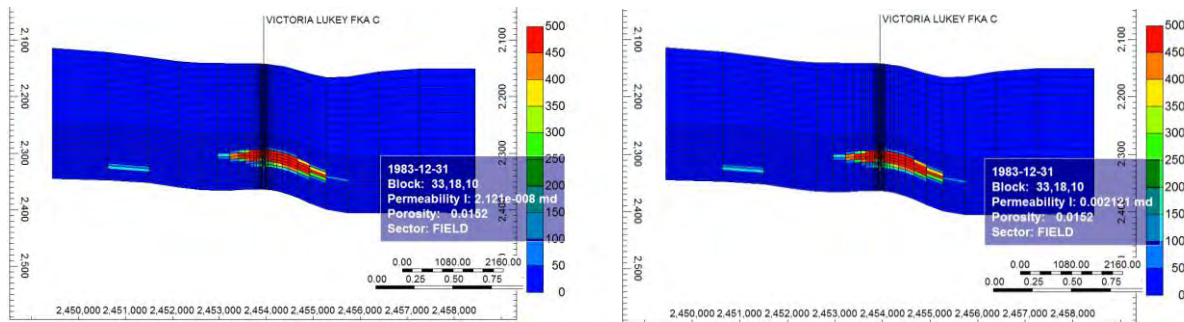
For 250,000 bbl of brine injected into the reservoir, Figure 5-28 shows the resulting pressure profile at the end of post-injection monitoring for same chosen model slice.



Note: Pressure buildup in psi, calculated as (initial pressure – final pressure).

Figure 5-28. Pressure buildup at the end of the post-injection monitoring period in the variable-injection Lockport-Newburg GEM model.

In this model, pressure migrated to the boundaries and overlying formations, leading to a higher average pressure compared to the initial conditions (i.e., residual pressure of 360 psi was present 20 years after injection was stopped for this model). In order to evaluate the sensitivity of pressure propagation to the overlying formation properties, we decreased the overlying confining zone permeability by 5 orders of magnitude; this adjustment allowed us to compare an average isotropic permeability on the order of $1\text{e-}8$ mD to the base-case average isotropic permeability on the order of $1\text{e-}3$ mD (Figure 5-29). We then compared the pressure propagation to confirm that a better confining formation (shale quality analog) would be more restrictive to brine injection.

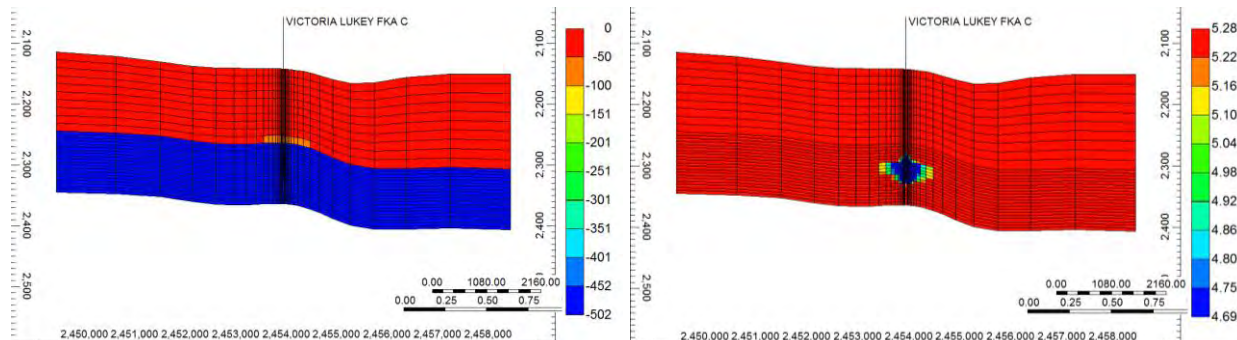


Note: Left panel is the lower-permeability case; right panel is the base case.

Lower zone permeabilities are the same between the two models. Color legends indicate permeability in millidarcy.

Figure 5-29. Results of the Lockport-Newburg model upper confining layer permeability sensitivity trial.

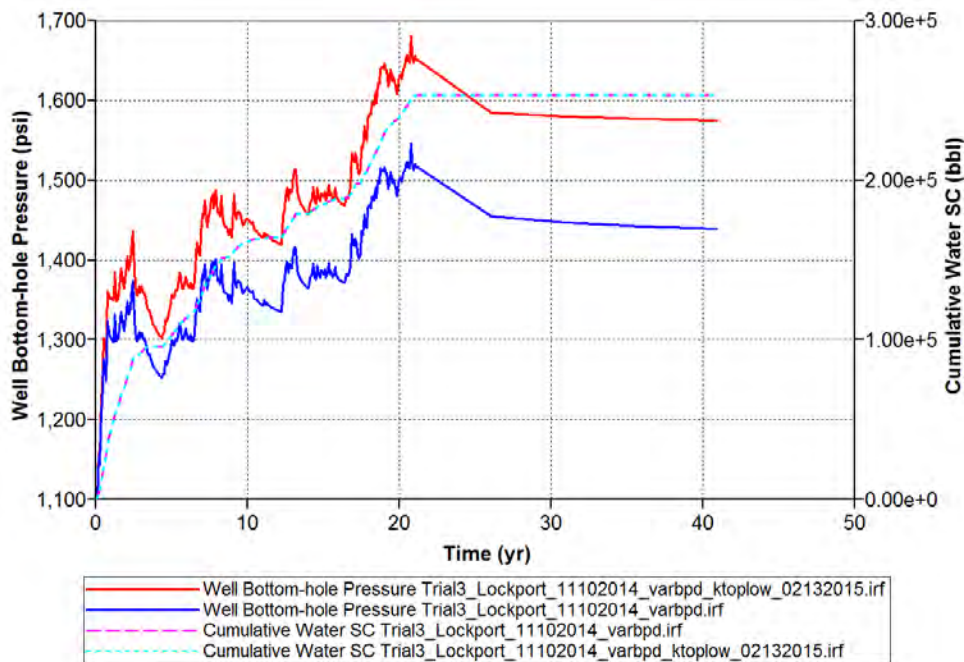
Figure 5-30 shows the resulting minimal pressure propagation through the less-permeable layers overlying the injection zone and the consequent increased injection reservoir and injector BHPs.



Note: Left panel = original pressure – final pressure (negative values indicate pressure buildup); right panel is salinity.

Figure 5-30. Pressure and salinity at end of 20-year post-injection monitoring period in the variable-injection Lockport-Newburg GEM model.

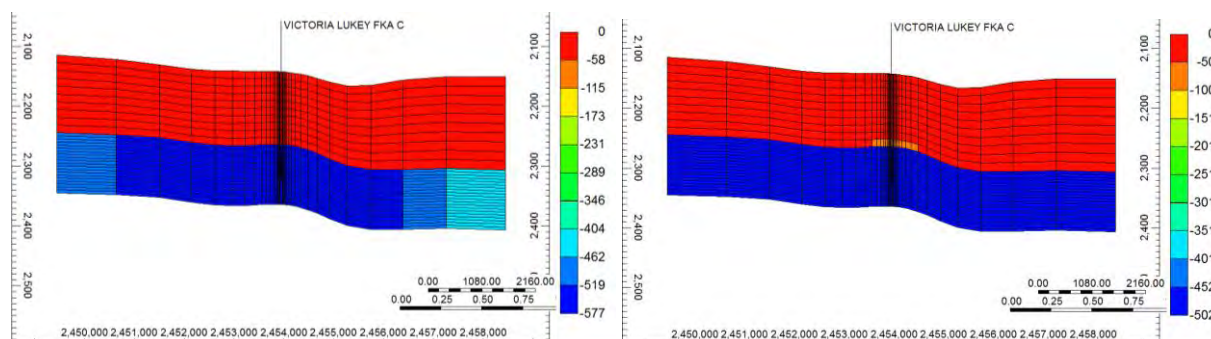
Figure 5-31 compares injector BHPs through time for the base case permeability and the low overlying zone permeability variable injection rate trials.



Note: The same amount of brine was injected in both models.

Figure 5-31. BHP through time for low and base-case variable-injection-rate trials.

For 250,000 bbl of brine injected into the reservoir, Figure 5-32 shows a cross section of the resulting pressures in this closed system at the end of injection and at the end of post-injection monitoring for the same chosen model slice.



Note: Left panel = original pressure – final pressure (negative values indicate pressure buildup); right panel is salinity.

Figure 5-32. Pressure and salinity at 10 years of post-injection monitoring in the variable-injection Lockport-Newburg GEM model.

The simulation indicated that, as expected, radial pressure buildup was greatest closer to the injection well. After injection was stopped, the simulation showed pressure gradually equilibrating over time and a residual pressure of 500 psi remaining 10 years after injection.

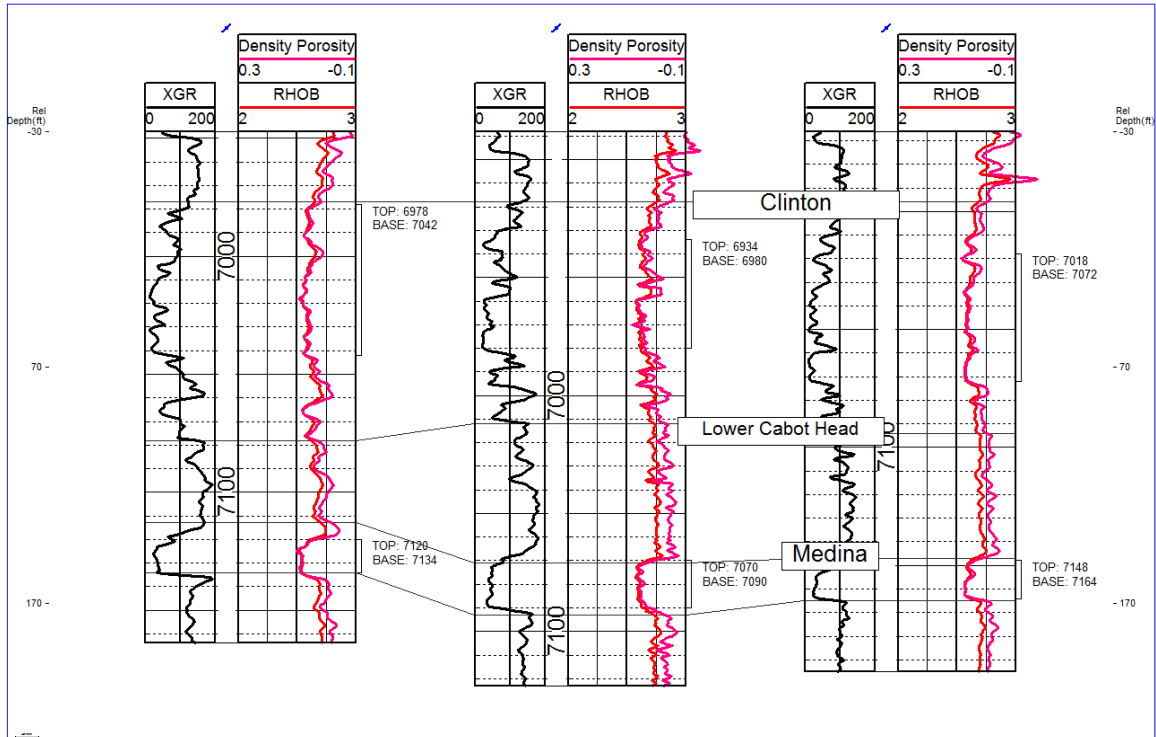
5.3 Clinton-Medina

The Clinton-Medina formation was heavily drilled in the 1980s, and many Class II brine injection wells were installed in association with the activities. Consequently, many of the Clinton-Medina injection wells are converted producers. However, the formation is also used for injection in other areas since it is fairly well defined in the region.

5.3.1 Clinton-Medina Geocellular Model

The Clinton-Medina Sandstone model was based on a general area in southeastern Ohio. This area was selected for injection modeling due to the relatively deep Clinton-Medina section, the potential as an analog for the Medina-Whirlpool section in northwestern Pennsylvania, and the availability of log and injection data.

The data set consisted of well logs and formation tops data for five wells. A density porosity curve was calculated from the bulk density log using a matrix density of 2.68 grams per cubic centimeter (g/cc). The Clinton Sandstone section is separated from the Medina Sandstone in this area by approximately 35 to 50 feet of Lower Cabot Head Shale (Figure 5-33). The basal Medina Sandstone is approximately 20 feet thick and has porosity values in the 6% to 12% range. The typical Clinton Sandstone porosity is in the 5% to 8% range based on the logs in the study. In the final model, an averaged section from the four wells was used due to the relative similarity of the Clinton-Medina section in the four wells.



Note: Depth track labeled in measured depth (MD) feet. Injection intervals noted on log with top and base.

Figure 5-33. Clinton-Medina section hung on top of the Clinton.

5.3.2 Clinton-Medina Simulation

5.3.2.1 Input Parameters

The Clinton-Medina simulation was based on the geocellular model described in the previous section. Table 5-3 summarizes the model setup parameters. The model domain was specified as 10 km by 10 km. A total of 20 model layers were defined across approximately 300 meters from the Rochester Shale to the Queenston Shale at a depth range of -1,800 to -2,100 meters msl. Layer thickness was based on data from five wells in the area that penetrate the Clinton-Medina zone (Figure 5-34). Overall, these layers follow the main zones defined in the geocellular model. Formation structure was determined by nearby wells. Based on these data, a constant dip to the east-southeast was prescribed, as shown in Figure 5-35. Since there were few other Clinton-Medina wells beyond the model area to define reservoir boundaries such as pinch-outs or lithology changes, layers were given constant thickness.

The model grid consisted of 117 rows and 117 columns centered on the injection well. Grid resolution was increased from 200 meters by 200 meters at the edges of the model domain to 25 meters by 25 meters near the injection well (Figure 5-36). Total grid cells in the model numbered 273,780.

Permeability was input as homogeneous by layer, as shown in Table 5-3. Permeability for the Clinton-Medina zones was specified as 5 mD, based on injection test data obtained from a Clinton well under this project and on model calibration. Other zones were assigned permeability based on log analysis. General model calibration was completed to observed wellhead pressures for brine disposal wells in the area, which had wellhead pressures in the range of 1,300 to 1,900 psi. Storage parameters in the injection interval included porosity of 10% and compressibility of 1E-5 1/m.

Table 5-3. Clinton Sandstone simulation input parameters.

Parameter	Value	Comment
Flow model	MODFLOW/SEAWAT	MODFLOW 2000, transient simulation, total simulation time = 7,300 days (20 years)
Domain	10 x 10 km x 300 m	Centered on injection well
Rows	117	Resolution increased near injection well
Columns	117	Resolution increased near injection well
Grid Spacing	Max = 200 x 200 m Min = 25 x 25 m	Variable grid spacing with grid increased grid resolution increased near injection wells
Layers	20	Variable thickness based on structure maps: Layer 1-3 = Rochester Shale Layer 4-5 = Dayton/Packer Shell Layer 6-12 = Clinton Sandstone Layer 13-14 = Cabot Head Shale Layer 15-17 = Medina Sandstone Layer 18-20 = Queenston Shale
Permeability (mD)	Homogeneous by layer $K_x:K_z = 1:1$	Layer 1-3 = 0.0005 Layer 4-5 = 0.1 Layer 6-12 = 5 Layer 13-14 = 0.1 Layer 15-17 = 5 Layer 18 = 0.01 Layer 19-20 = 0.0001
Bulk Compressibility	Constant value for layers 1-20	1E-5 1/m
Boundaries	Constant head, no flow	Constant head nodes specified at N,S,E,W model boundaries based on 0.433 psi/ft gradient
Injection Well	Row 58 Col 59	1,250 bbl/day for 3,650 days
Solution Parameters	WHS, head change criterion = 0.003	<0.05% cumulative volumetric budget error
Transport Model	SEAWAT2KT	Species = Salt
Initial Salt Concentration	150,000 mg/L	Based on regional salinity maps for Clinton Sandstone in southeast Ohio
Reservoir Temperature	Not applied	Not applied
Source Term	Constant Concentration Source	Low density salinity = 50,000 mg/L Baseline salinity = 125,000 mg/L High density salinity = 200,000 mg/L

Salt was input as the constituent species. Fluid density range was 1.00 to 1.25 with a density/concentration gradient of 0.7143. Initial salinity was set at 150,000 mg/L based on produced water for the Clinton sandstone in the general region. Initial pressure was set at hydrostatic conditions based on 0.433 psi/ft pressure gradient. Constant head boundary conditions were assigned at the model edges based on this pressure gradient.

The injection well was assigned to the middle of the model domain in row 58, column 59 with the well module in the SEAWAT program. The well was screened across the Clinton in layers 6-12 and the Medina in layer 15-17, which is similar to brine injection wells in the area. A pumping rate of 1,250 bbl/day was scheduled for 10 years followed by 10 years of post-injection. A point source was assigned at the well location with salt concentrations of 50,000 mg/L, 125,000 mg/L, and 200,000 mg/L to investigate low, medium, and high fluid density behavior.

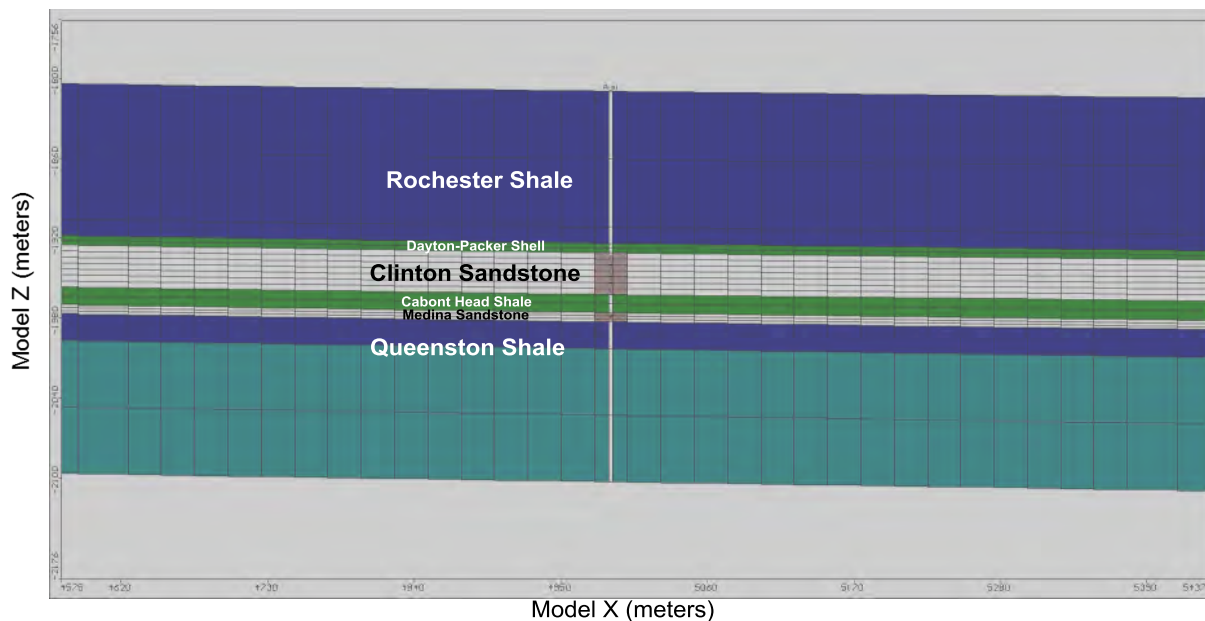


Figure 5-34. Model layers and thicknesses (cross section).

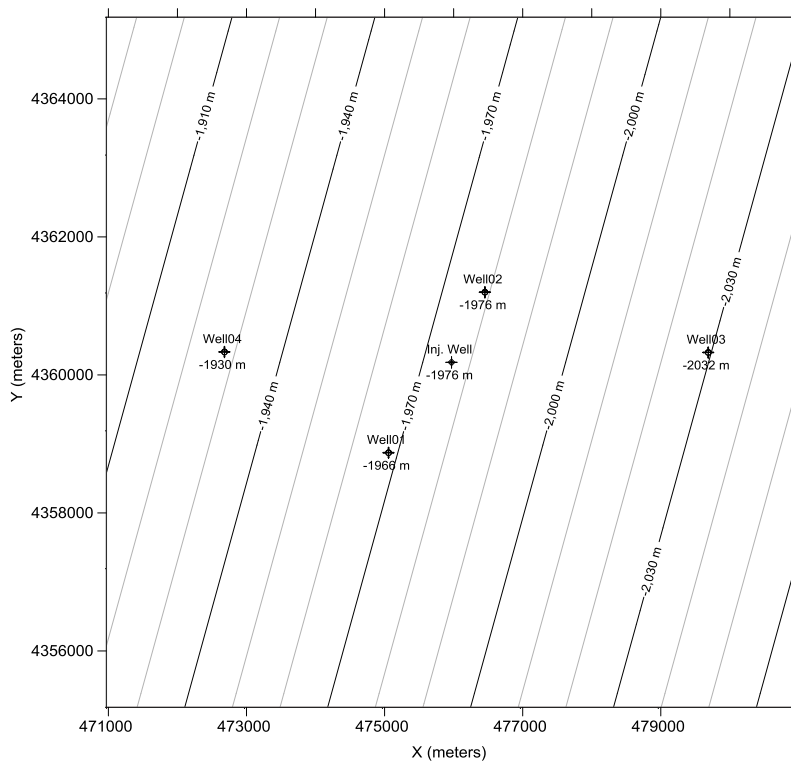


Figure 5-35. Model elevation of the Medina Sandstone surface.

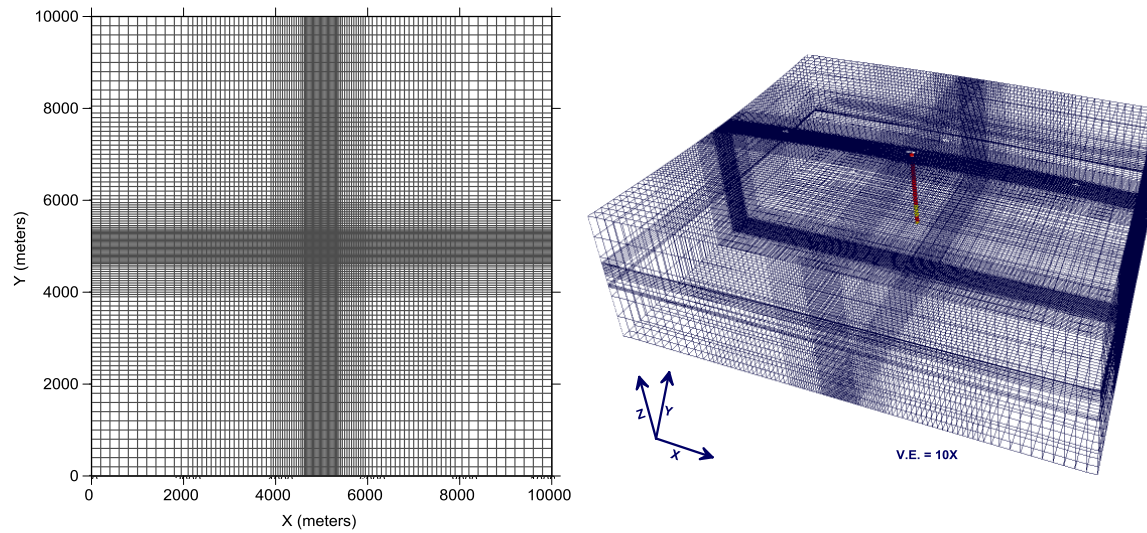


Figure 5-36. Clinton Sandstone simulation grid.

5.3.2.2 *Clinton-Medina Sandstone Simulation Output*

Clinton Sandstone simulation runs were set up to simulate commercial injection rates. There are no oil and gas fields in the general area where the model was based, so the simulation represents injection into a native deep saline formation. It should be noted that in other portions of the Appalachian Basin, Clinton-Medina fields are depressurized due to oil and gas production. Since there are few wells that penetrate the Clinton-Medina, the model was set up with homogeneous layers. No fractures or faults were included in the simulation. The model domain was large (10 km by 10 km) to ensure that model boundaries did not affect simulation results.

The SEAWAT model was run in transient solution mode for 10 years of injection at 1,250 bbl/day followed by a 10-year post-injection period. A central-in-space weighted algorithm solution scheme was used to calculate fluid density terms. Model mass balance showed an ‘in-out’ cumulative mass error of less than 0.05% for all simulation runs. Simulations were run for injection fluid with a salinity of 50,000 mg/L for a light injection fluid, 125,000 mg/L as a baseline, and 200,000 mg/L as a heavy injection fluid scenario. The model generally calibrated to nearby Clinton injection wells, which have historical wellhead pressures of 1,300 to 1,900 psi and brine injection rates ranging from 500 to 2,000 bbl/day.

Simulation pressure, salinity, and flow vectors were output at various time steps to examine the effects of subsurface injection. The maximum simulated pressure change at the injection well ranged from 1,523 psi for the 200,000-mg/L scenario, to 1,569 psi for the 125,000-mg/L scenario, to 1,582 psi for the 50,000-mg/L scenario. Overall, this calibrates to the historical wellhead pressures measured in Class II disposal wells in the area, which ranged from 1,300-1,900 psi. The model simulates pressure change in the reservoir, so there may be some additional pressure at the wellhead due to friction loss through the tubing.

Figure 5-37 shows the simulated pressure change over time in model layer 10 for the 125,000-mg/L injection scenario. As shown, the simulation indicates a fairly radial pressure buildup greatest near the injection well, extending approximately 600 meters from the injection well at greater than 200 psi after 10 years of injection. After injection was stopped, the simulation showed pressure decreasing to near initial conditions within approximately 5 years. Figure 5-38 shows the pressure profile at 3,650 days after 4,562,500 bbl total injection volume. As shown, the pressure front is contained within the reservoir zone, with the greatest pressure near the injection well.

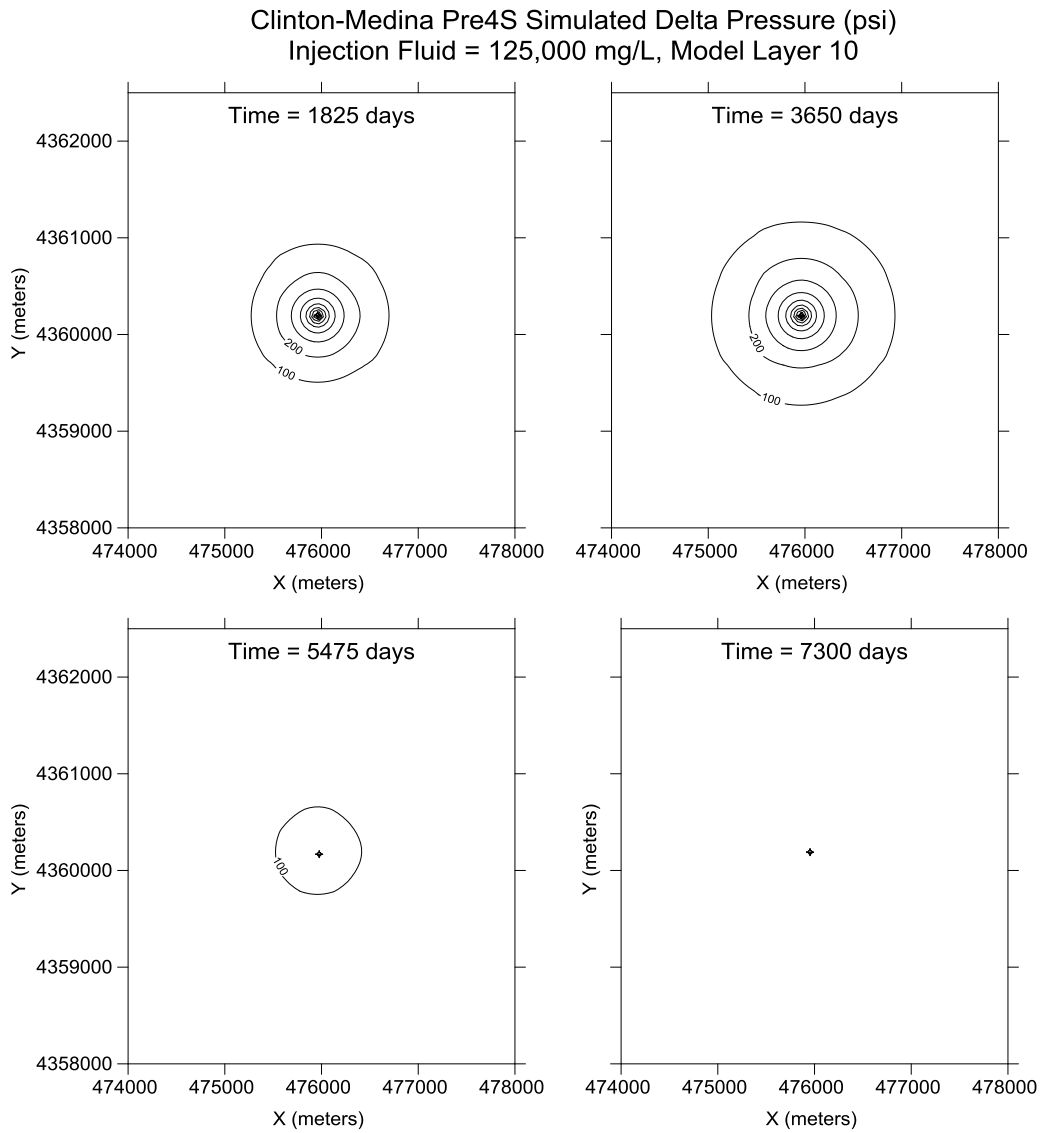


Figure 5-37. Clinton-Medina simulated delta pressure (psi) over time.

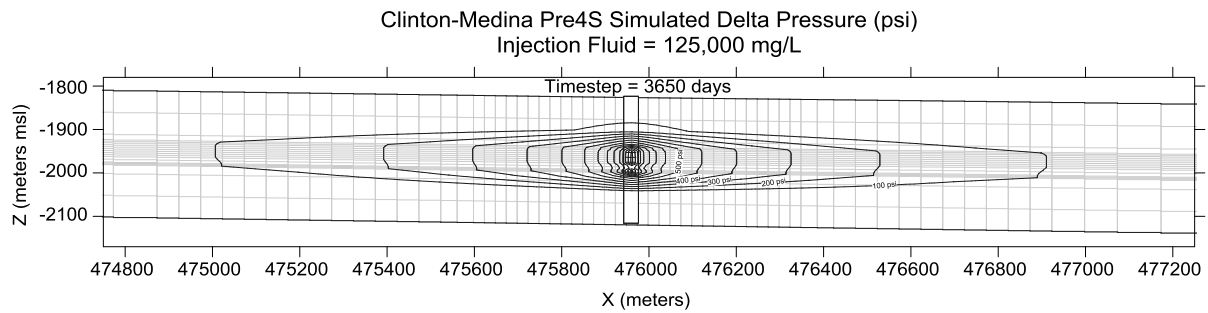


Figure 5-38. Clinton-Medina simulated delta pressure over time (cross section).

To illustrate the variable density effects of injection, simulated changes in salinity were analyzed for the 50,000-mg/L injection scenario. This scenario illustrates brine movement related to the injected fluid in the subsurface. Figure 5-39 shows simulated salinity over time. As shown, the salinity front appeared to extend only 350 meters from the injection well, and brine migration appeared to be minimal after injection stopped. Figure 5-40 shows the simulated salinity at time step 3,650 days. As shown, brine moved into the more permeable Clinton and Medina intervals. There also appeared to be potential for vertical brine displacement near the injection well due to the high pressure gradient in this area.

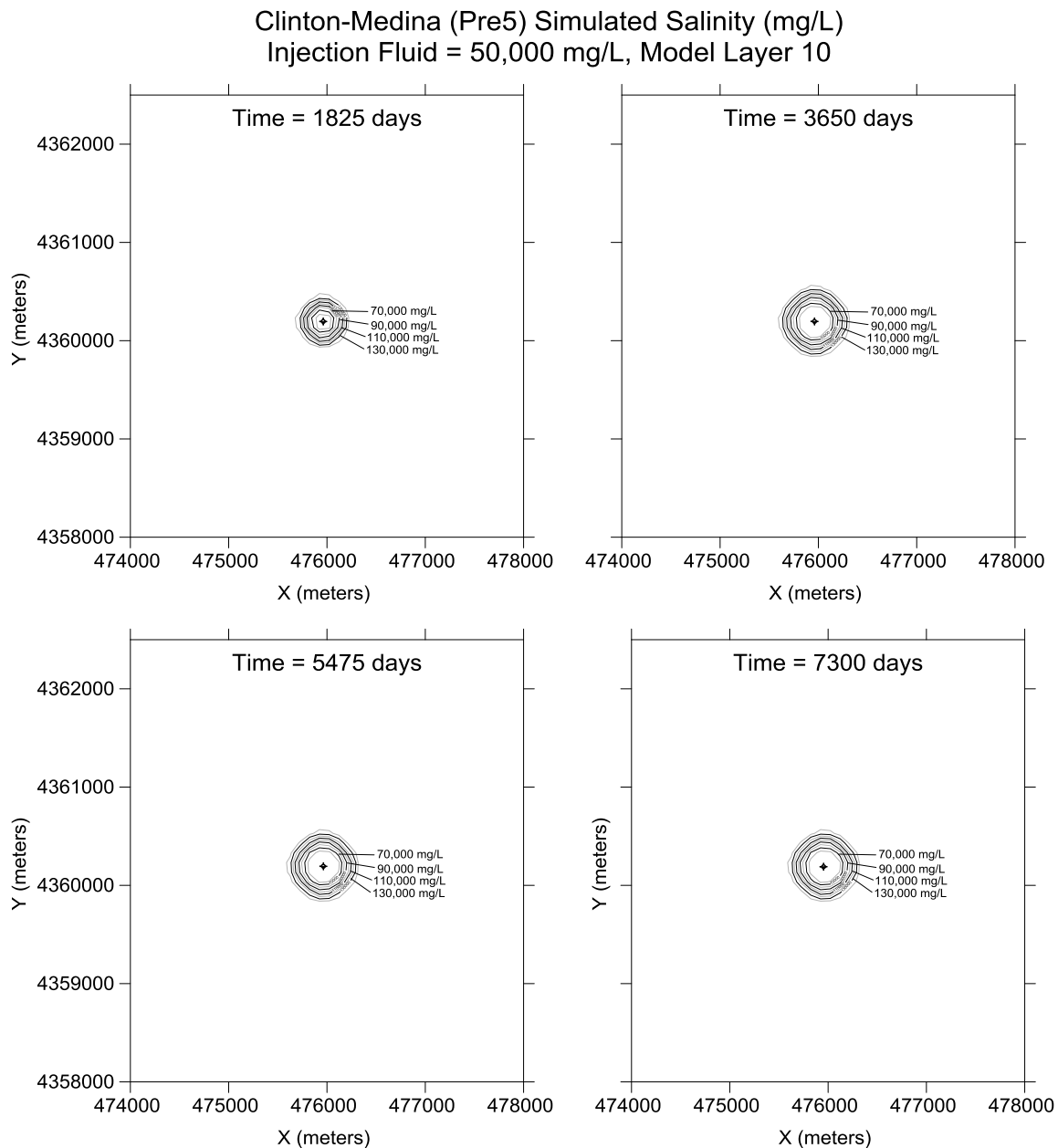


Figure 5-39. Clinton-Medina simulated salinity (mg/L) over time.

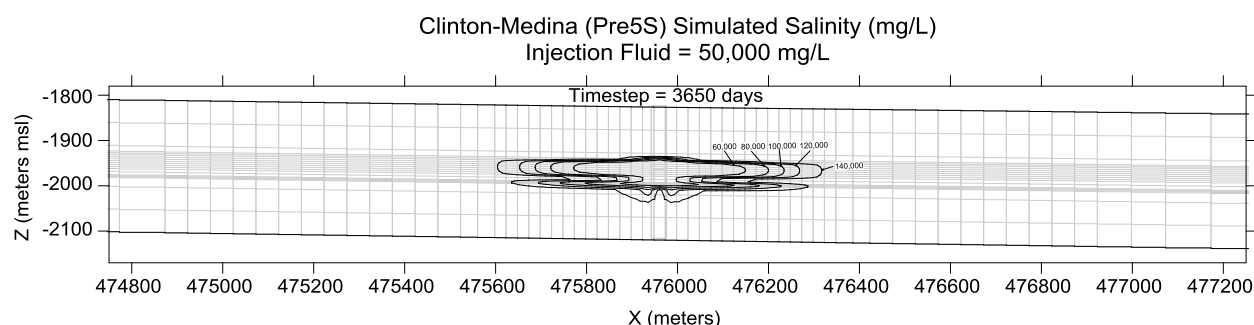


Figure 5-40. Clinton-Medina simulated salinity (cross section).

5.4 Knox-Basal Sandstone

The Knox-Basal Sandstone interval includes several formations utilized for brine disposal in the region. Many of these wells are completed as open-hole completions and inject large volumes as commercial operations.

5.4.1 Knox-Basal Sandstone Geocellular Model

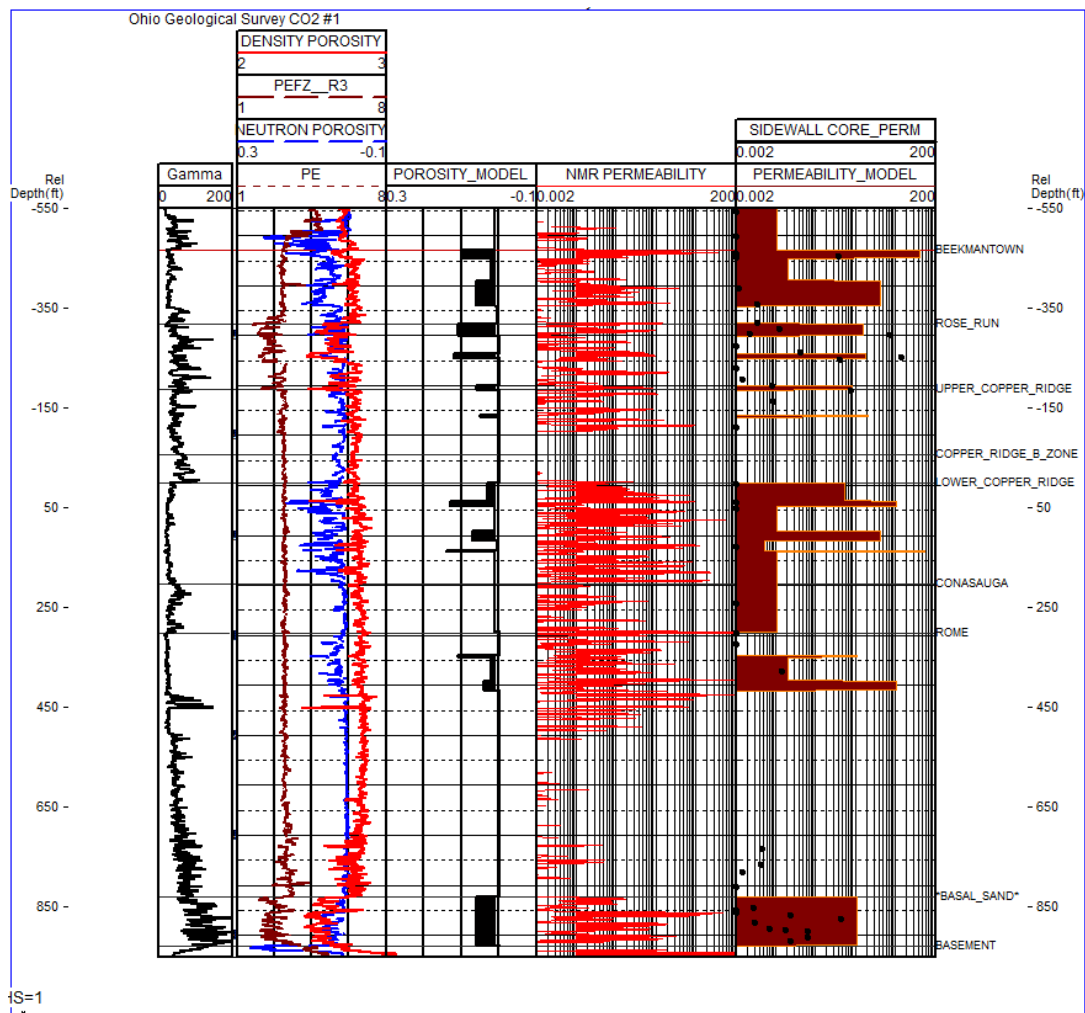
The Upper Copper Ridge Dolomite to Basal Cambrian Sandstone geocellular model was developed in an effort to evaluate the current brine injection practices being used in the industry. These wells include a variety of open-hole completion scenarios where injection occurs into the open hole below the casing point into the Ordovician and Cambrian section. In some wells, the Beekmantown and Rose Run Sandstones are cased off, and only the Upper Copper Ridge to top of the Basal Cambrian Sandstone is used for injection. Regional hydrocarbons are produced from the Beekmantown and Rose Run zones surrounding many of these injection wells, so these zones are cased off to protect offset production. The potential for induced seismicity from injection into the Precambrian has also made drilling into the Precambrian basement in the newer wells uncommon.

The Upper Copper Ridge to Basal Cambrian Sandstone model was built from log data collected in the Ohio Geologic Survey CO₂ #1 well API 3415725334 located in Tuscarawas County, Ohio. This well was drilled in 2007 as part of the regional characterization efforts for deep CO₂ injection. Extensive log sets were collected on this well, and it is in the same geologic setting where many of the new deep injection wells are located in eastern Ohio.

The main zones of interest for injection in the well occur in the Lower Copper Ridge dolomite, Rome Dolomite, and Basal Cambrian Sandstone (Figure 5-41). While the Rose Run and Basal Cambrian Sandstone units are regionally thick, stratigraphically continuous zones, the permeability in these units is lower than the thin, high-permeability reservoir zones in the carbonate units. This has a profound impact on reservoir analysis and on efforts to identify the most promising injection zones over several thousand feet of open-hole logs. Injection test flow or spinner logs and radioactive tracer tests performed prior to operation of the wells are critical in identifying high injection rate zones.

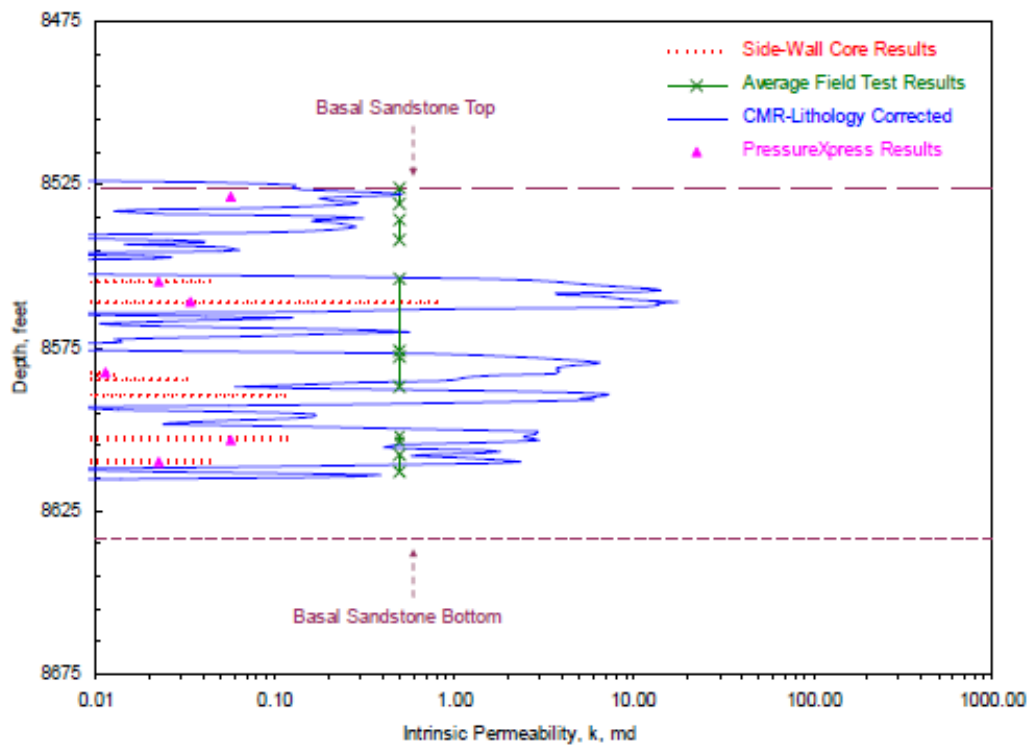
An open-hole single well model that included both clastic and carbonate lithologies was constructed to assess the overall performance and differences in brine invasion in the different units. A single-well layered model was built using the neutron and bulk density averaged

porosity and the nuclear magnetic resonance (NMR)-derived permeability (Figure 5-42). The NMR-derived permeability for the Rose Run and Basal Sandstone was compared to the sidewall core-derived and reservoir injection permeability values by Wickstrom et al. (2011) (Figure 5-42). While the permeability values have wide ranges between the methods, Wickstrom et al. concluded that the NMR values may be a viable tool for identifying permeability in sandstone reservoirs. The final coarsened layers exported to the model were created in an effort to include both thick moderate-permeability zones along with thin high-permeability zones (Figure 5-42).



Note: Plotted points on the permeability model curve are from sidewall core permeability measurements from previous study.

Figure 5-41. Log curves and final porosity and permeability values from Knox to Basal Sandstone injection model.



Source: Wickstrom et al., 2011.

Figure 5-42. Basal Sandstone permeability derived from sidewall core, injection reservoir testing, and NMR logs.

5.4.2 Knox-Basal Sandstone Simulation

5.4.2.1 Input Parameters

Input for the Knox-Basal Sandstone simulation was based on the geocellular model described in Section 5.4.1. The simulation was designed to account for open-hole injection across a thick interval with many different layers. Model setup parameters are listed in Table 5-4. The model domain was specified as 3 km by 3 km covering a depth range of approximately 600 meters from the Trenton-Black River to the Precambrian at a depth range of -1,800 to -2,400 meters msl. Layer thickness was based on the geocellular model data, which are mostly based on geophysical logs from a single well. Consequently, the simulation is more of a single-well model. Input model layers were approximated as flat lying, because there is low dip (approximately 15 meters per kilometer [m/km] to the east-southeast) across the model domain (Figure 5-43).

Table 5-4. Knox-Basal Sandstone simulation input parameters.

Parameter	Value	Comment
Flow Model	MODFLOW/SEAWAT	MODFLOW 2000, transient simulation, total simulation time = 7,300 days (20 years)
Domain	3 x 3 km x 600 m	Centered on injection well
Rows	50	None
Columns	50	None
Grid Spacing	50 x 50 m	Resolution increased near injection well
Layers	32	Variable thickness based on type log for Knox-Basal sandstone well: Layer 1-2 = Trenton Layer 3-7 = Beekmantown Layer 8-12 = Rose Run Layer 13-15 = Upper Copper Ridge Layer 16-22 = Lower Copper Ridge Layer 23-24 = Conasauga Layer 25-29 = Rome Layer 30-31 = Basal Sandstone Layer 32 = Precambrian
Permeability (mD)	Homogeneous by layer $K_x:K_z = 1:1$	Vary by layer: 0.001-75 Based on NMR geophysical log interpretation
Bulk Compressibility	Constant value for layers 1-21	1E-6 1/m
Boundaries	Constant head, no flow	Constant head nodes based on 0.433 psi/ft gradient
Injection Well	Row 25 Col 25	+480 bbl/day for 3,650 days Based on average rate for Basal Sandstone wells
Solution Parameters	WHS, head change criterion = 0.001	<0.05% cumulative volumetric budget error
Transport Model	SEAWAT2KT	Species = Salt
Initial Salt Concentration	200,000 mg/L	Based on regional salinity maps for Basal Sandstone
Source Term	Constant Concentration Source	Baseline salinity = 125,000 mg/L High-density salinity = 250,000 mg/L

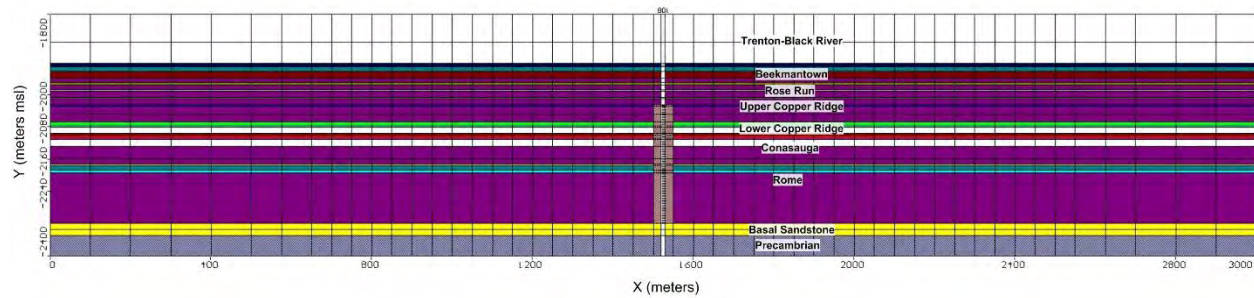


Figure 5-43. Knox-Basal Sandstone simulation model layers.

The model grid consisted of 50 rows, 50 columns, and 32 layers, for 80,000 grid cells. Figure 5-44 shows the grid layout with finer resolution near the injection well. Grid size ranged from 100 meters by 100 meters at the edges of the model domain to 50 meters by 50 meters near the injection well.

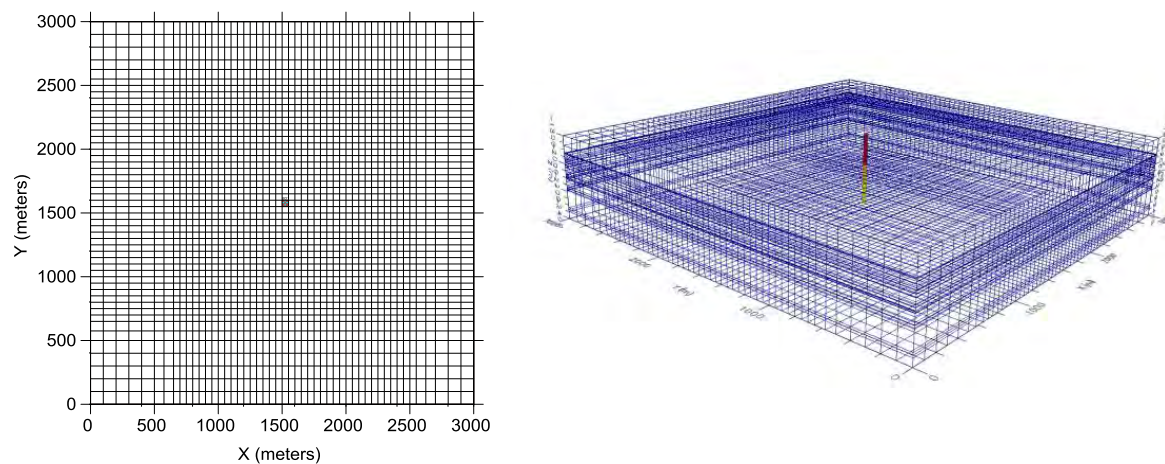


Figure 5-44. Knox-Basal Sandstone simulation grid.

Permeability was input as homogeneous by layer. The permeability was based on NMR geophysical log estimated permeability. In general, model layers were input to match the major NMR log data, but some layers were combined to decrease computational complexity in low-permeability zones. Conversely, some of the high-permeability zones were assigned multiple layers to capture variable density effects. Overall, the model layers follow the permeability zones delineated in the NMR estimate.

The constituent species was specified as salt. Fluid density range was 1.00 to 1.25 with a density/concentration slope of 0.7143. Initial salinity was set at 200,000 mg/L based on analytical data from produced water in the area. Initial pressure was set at hydrostatic conditions based on 0.433 psi/ft pressure gradient. Constant head boundary conditions were assigned at the model edges based on this pressure gradient.

The injection well was designated to row 25, column 25 with the well module in the SEAWAT program. The injection interval was specified across the Rose Run to Copper Ridge zone interval in layers 14-29. A pumping rate of 480 bbl/day was scheduled for 10 years followed by

10 years of post-injection. At the injection well, a point source was assigned with salt concentrations of 125,000 mg/L based on data on injection fluid for brine disposal wells in the area. A separate high-density fluid scenario was also studied with a point source assigned concentration of 250,000 mg/L.

5.4.2.2 Knox-Basal Sandstone Simulation Output

The Knox-Basal Sandstone simulation was set up to simulate moderate injection rates into a thick, Ordovician-Cambrian open-hole section, which reflects a well completion method used in many commercial brine disposal wells in the western Appalachian Basin. Model layers were specified as constant thickness and homogeneous based on permeability from a geophysical NMR log. No fractures or faults were included in the simulation. No formation dip was included in the model since layers are relatively flat-lying at the model location.

The SEAWAT model was run in transient mode for 10 years of injection at 480 bbl/day, followed by a 10-year post-injection period. The injection rate was the average from operational data for Basal Sandstone Class II wells in 2012. A central-in-space weighted algorithm solution scheme was used to calculate fluid density terms. Model mass balance showed an ‘in-out’ cumulative mass error of less than 0.05% for all simulation runs. Simulations were run for injection fluid with a salinity of 125,000 mg/L for a light injection fluid and 250,000 mg/L as a heavy injection fluid scenario. The model generally calibrated to average wellhead pressures for Knox-Basal Sandstone injection well operational data compiled under this project, which had average wellhead pressure in the range of 240 to 800 psi in 2012.

Simulation pressure, salinity, and flow vectors were output at various time steps to examine the effects of subsurface injection. The maximum simulated pressure change ranged from approximately 560 psi for the 125,000-mg/L scenario to 420 psi for the 200,000-mg/L scenario. Overall, this calibrates to the wellhead pressures operational data for Knox-Basal Sandstone wells, which ranged from 240 to 800 psi in 2012. The model simulated pressure change in the reservoir, so there may be some additional pressure at the wellhead due to friction loss through the tubing. Similar to other simulations, the results suggest that operations may be affected by the density of the injection fluid. Lighter fluid would require higher injection pressures.

Figure 5-45 shows simulated pressure change over time in model layer 22 for the 125,000-mg/L injection scenario. The simulation indicated that radial pressure buildup was greatest near the injection well. After injection was stopped, the simulation showed pressure gradually decreasing over time and a residual pressure of 100 to 200 psi remaining 10 years after injection. The sustained nature of the residual pressure was likely related to low-permeability layers which impede pressure dissipation. Figure 5-46 shows the pressure profile at 3,650 days. As shown, the pressure front extends in the higher-permeability layers, extending approximately 200 meters from the injection well at greater than 200 psi after 10 years of injection. However, the pressure front extends to a radius of over 1,000 meters at a 100 psi change. Again, the pressure front is greatest near the injection well.

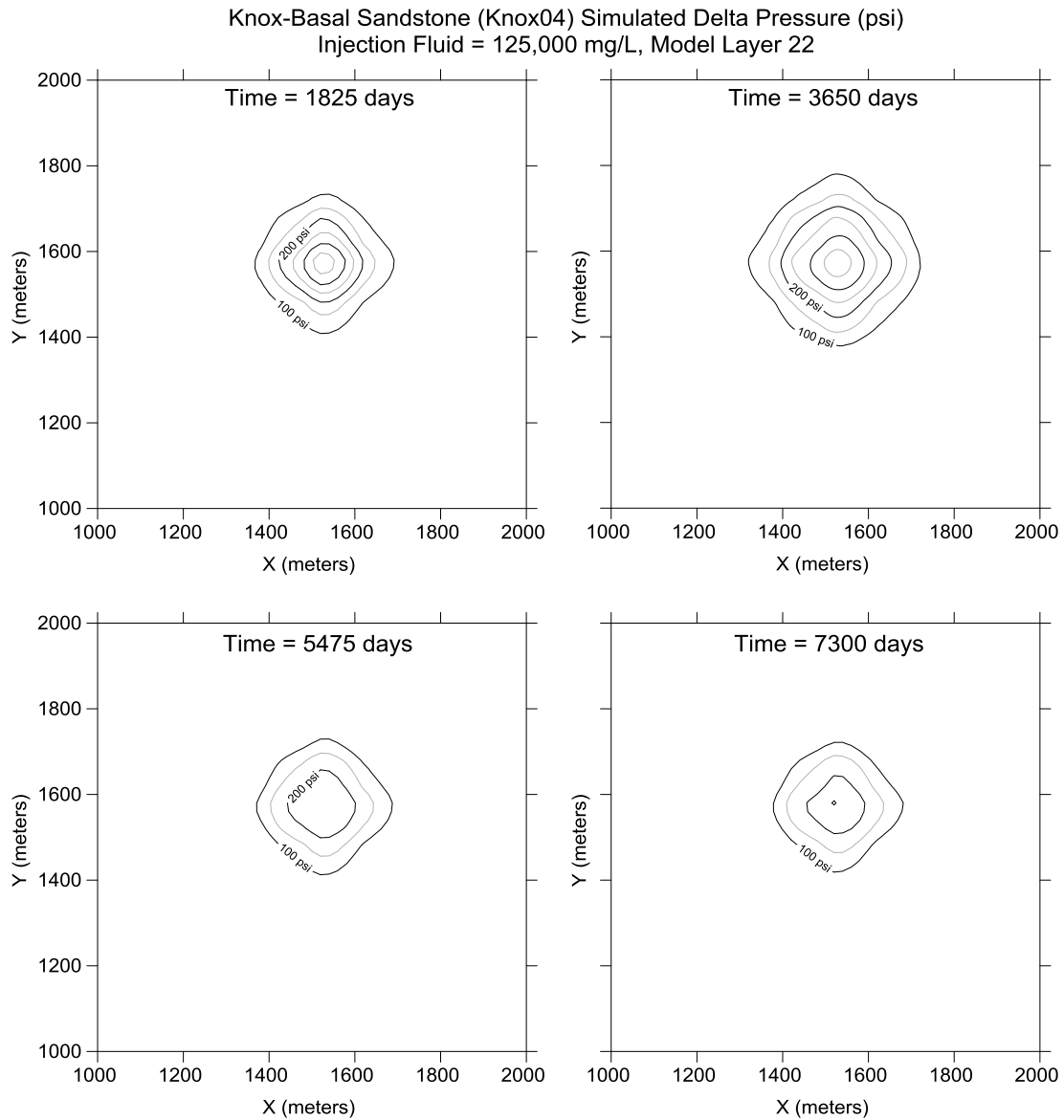


Figure 5-45. Knox-Basal Sandstone simulated delta pressure (psi) over time.

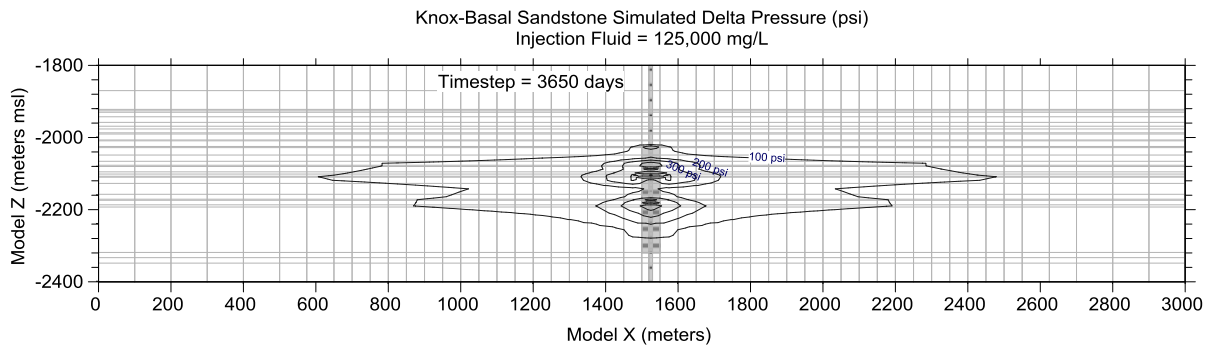


Figure 5-46. Clinton-Medina simulated delta pressure over time model cross section.

To illustrate the variable density effects of injection, simulated changes in salinity were analyzed for the injection scenarios. Figure 5-47 shows simulated salinity over time for the 125,000-mg/L injection scenario. The simulated results showed a mainly radial pattern with some evidence of grid effects imparting a slight diamond pattern. Again, there was minimal indication of brine migration after injection stopped. Figure 5-48 shows the simulated salinity at time step 3,650 days. As shown, the salinity front extended approximately 230 meters from the injection well, with preferential flow into the more-permeable intervals. There appeared to be less potential for vertical brine displacement near the injection well due to the presence of multiple confining layers above and below the injection interval.

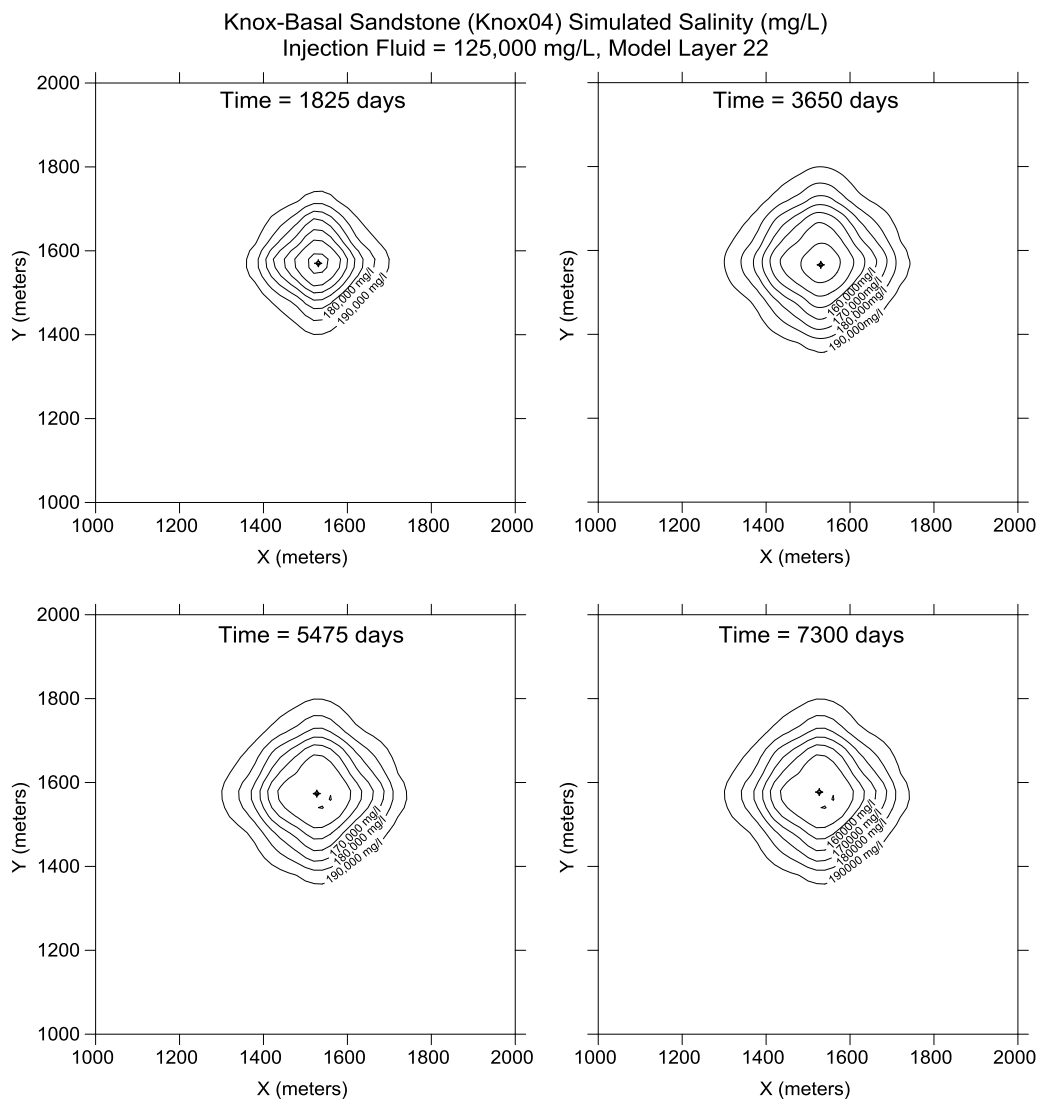


Figure 5-47. Knox-Basal Sandstone simulated salinity (mg/L) over time.

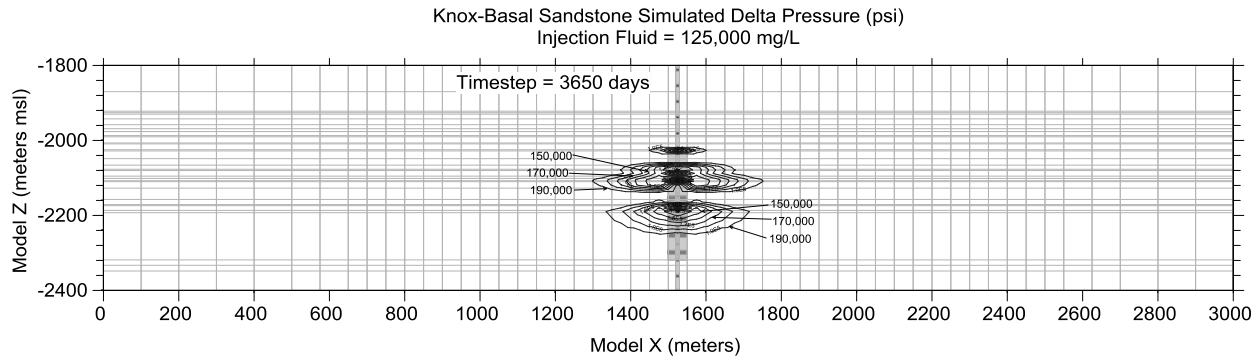


Figure 5-48. Knox-Basal Sandstone simulated salinity cross section.

5.5 Geomechanical Analysis of Brine Injection

The objective of the geomechanical analysis was to determine the potential for fracturing and stress changes in the subsurface related to brine injection. This section describes the methodology used in the analysis and presents analysis results for three representative injection zones of varying geologic complexity.

5.5.1.1 Methods

Pore pressure variation in response to brine injection into the geological formations induces effective stress perturbation in a target reservoir and surrounding formations. The effective stress field can be changed by pore pressure or temperature changes in the reservoir and surrounding rocks. The stress change produced as a function of brine injection could generate hydraulic fractures in the target reservoir or cap-rock and provide a leakage pathway. The stress changes determined by hydromechanical modeling can be combined with Mohr-Coulomb analysis to investigate failure potential (Fjar et al., 2008). The Mohr-Coulomb criterion describes separation between a safe region from a failure region in the shear-normal stress plane. The failure line is represented by the following equation (5.1) (Jaeger et al., 2009):

$$|\tau| = S_0 + \mu\sigma' \quad (5.1)$$

where S_0 = rock cohesion
 μ = coefficient of friction
 σ' = the effective normal stress, and
 τ = the shear stress.

The effective stress is calculated as follows:

$$\sigma' = \sigma - \alpha p \quad (5.2)$$

where α is Biot coefficient and p is pore pressure.

A Mohr circle (Figure 5-49) spans the difference between maximum and minimum effective normal stresses in the reservoir. All possible combinations of shear and normal stress lie within the area of the Mohr circle. When the circle is below the failure line for a cohesion less fracture (as in Figure 5-49), there is no potential for failure in the reservoir. As pore pressure increased, the effective stress was reduced (Figure 5-49a). The Mohr circles shifted to the left (represented

by the green circles in Figure 5-49) and approached both the shear and tensile failure envelope when total stress was kept constant.

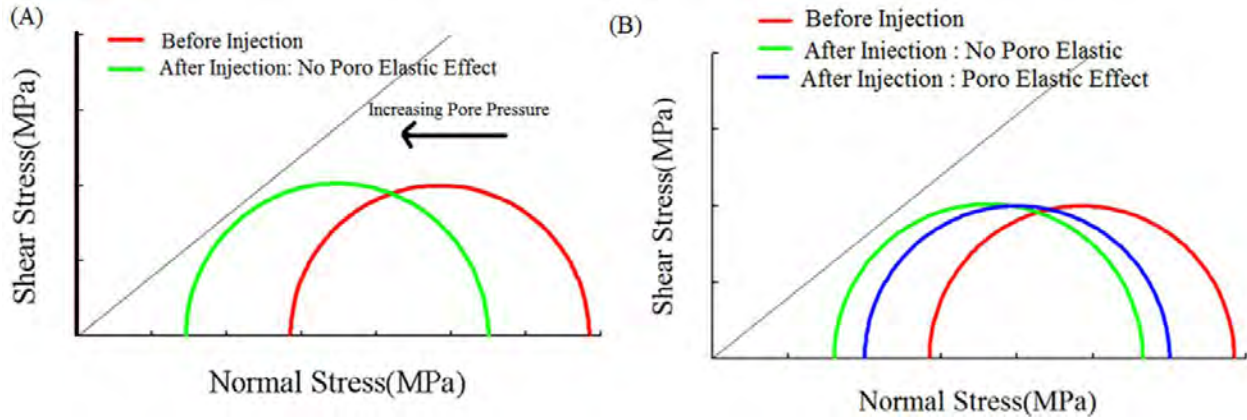


Figure 5-49. The effect of increasing pore pressure on rock failure (a), and the effect of poro-elasticity (b).

Poro- and thermo-elastic effects can also be evaluated when looking at failure criteria. By considering the poro-elastic effect of injection, the Mohr circle shifts to the right of the green circle (shown by the blue circle in Figure 5-49b), and the potential for hydraulic fracturing is reduced due to the counteraction on the pore pressure effect. On the other hand, the temperature difference between injection fluid and the formation could cause the Mohr circle to shift left and increase the potential of rock failure.

To avoid hydraulic fracturing (tensile fracturing) and shear failure of the target reservoir and cap-rock, it is necessary to estimate elastic parameters, minimum horizontal stress, and stress changes by fluid injection.

5.5.1.2 Estimating Elastic Parameters

Geomechanical properties of reservoirs and confining layers (i.e., elastic parameters) and initial stress magnitude (fracture gradient) play an important role in the evolution of stress fields in space and time. As a result, the maximum injection pressure to avoid hydraulic fracture initiation and propagation depends on rock mechanical properties. These properties include Young's modulus of elasticity, which is a measure of the stiffness of the rock, and Poisson's ratio, which is a measure of lateral expansion relative to longitudinal contraction of the rock under stress.

Rock static elastic parameters can be obtained from laboratory core tests of either uniaxial or triaxial compressive experiments by analyzing the strain-stress curve. Rock dynamic elastic parameters can be determined from knowing the rock elastic compressional and shear wave velocities obtained from a sonic well log. The dynamic elastic modulus can be converted into a static modulus by calibrating experimental data obtained from a triaxial test. Dynamic Poisson's ratio is calculated from the following relationship between P wave velocity and S wave velocity (Fjar et al., 2008):

$$\nu = \frac{V_p^2 - 2V_s^2}{2(V_p^2 - V_s^2)} \quad (5.3)$$

where V_p is compression and V_s is shear velocity.

Dynamic Young's modulus (E) is calculated from rock density, shear wave velocity, and Poisson's ratio as follows (Fjar et al., 2008):

$$E = 2\rho V_s^2(1 + \nu) \quad (5.4)$$

Rock dynamic elastic parameters should be calibrated by static elastic parameters provided by laboratory core tests (i.e., uniaxial or triaxial compressive experiment) for a more constrained analysis.

5.5.1.3 Estimating Overburden Stress

Overburden stress is required to calculate minimum horizontal stress. Overburden stress is induced by the weight of the overlying formations and can be calculated, with a high degree of certainty, by integrating rock density (from density logs) from the surface to the depth of interest (Zoback, 2010):

$$\sigma_v = \int_0^z \rho(z) dz \quad (5.5)$$

where $\rho(z)$ is the rock density and σ_v is vertical stress.

5.5.1.4 Estimating Minimum Horizontal Stress

The magnitude of minimum horizontal stress can be determined by the simplifying assumption that horizontal stress results from an inability of rock to deform laterally in response to vertical stress because of constraints imposed by the surrounding rock. That assumption is applied in relaxed basin settings (Fjar et al., 2008; Zoback, 2010):

$$\sigma_h = \frac{\nu}{1 - \nu} \sigma_v + \frac{1 - 2\nu}{1 - \nu} \alpha P_p \quad (5.6)$$

where ν = Poisson's ratio
 α = the Biot coefficient
 σ_h = minimum horizontal stress, and
 P_p = pore pressure.

5.5.2 Geomechanical Core Testing

As described in Section 3.5, rock core tests were performed to better define geomechanical properties of injection zones in the Northern Appalachian Basin. The tests provide static parameters (Poisson's ratio, Young's modulus, and compressibility) that reflect rock strength. Ten samples from state rock core libraries were selected and sent to a geotechnical laboratory for geomechanical testing. Table 5-5, 5-6, and 5-7 summarizes the geomechanical testing results. The test data were used to provide calibration for the geomechanical analysis in terms of derived static parameters.

Table 5-5. Geomechanical static properties of rock samples from key injection intervals.

Sample No.	Formation	Depth (ft)	Confining Pressure (psi)	Compressive Strength (psi)	Static Young's Modulus ($\times 10^6$ psi)	Static Poisson's Ratio
5-RMV	Big Injun	2186.87	730	30749	5.53	0.15
6-RMV	Clinton	2543.00	850	18882	3.65	0.23
7-RMV	Trempealeau	2950.50	1050	17473	5.43	0.16
1-RMV	Rose Run	3312.81	1350	24111	5.43	0.19
2-RMV	Copper Ridge	3790.30	1350	24544	8.33	0.19
3-RMV	Mount Simon	4686.35	1560	23254	4.56	0.30
8-RMV	Newburg	5155.76	1720	39265	6.63	0.16
9-RMV	Oriskany	5292.00	1760	50279	7.13	0.16
10-RMV	Rose Run	6926.70	2310	32949	5.78	0.16
11-RMV	Medina	8885.65	3160	43004	7.09	0.28

Table 5-6. Geomechanical dynamic properties of rock samples from key injection intervals

Sample No.	Depth (ft)	Formation	Confining Pressure (psi)	Bulk Density (g/cc)	Dynamic Elastic Parameter			
					Young's Modulus ($\times 10^6$ psi)	Poisson's Ratio	Bulk Modulus ($\times 10^6$ psi)	Shear Modulus ($\times 10^6$ psi)
5-RMV	2186.87	Big Injun	730	2.65	9.28	0.15	4.40	4.04
6-RMV	2543.00	Clinton	850	2.25	4.44	0.16	2.17	1.92
7-RMV	2950.50	Trempealeau	1050	2.65	7.04	0.32	6.49	2.67
1-RMV	3312.81	Rose Run	1100	2.41	5.89	0.32	5.41	2.23
2-RMV	3790.30	Copper Ridge	1350	2.71	11.74	0.33	11.38	4.42
3-RMV	4686.35	Mount Simon	1560	2.35	5.96	0.17	3.01	2.55
8-RMV	5155.76	Newburg	1720	2.56	6.39	0.18	3.29	2.71
9-RMV	5292.00	Oriskany	1760	2.55	6.59	0.09	2.65	3.03
10-RMV	6926.70	Rose Run	2310	2.58	8.78	0.25	5.86	3.51
11-RMV	8885.65	Medina	3160	2.59	8.48	0.23	5.21	3.45

Table 5-7. Tensile strength of rock samples from key injection intervals

Sample No.	Depth (ft)	Formation	Thickness (inch)	Diameter (inch)	Density (g/cc)	Max. Load (lb)	Brazilian Tensile Strength (psi)
5-BZ	2,186.87	Big Injun	0.599	0.996	2.64	1597	1704
6-BZ	2,543.17	Clinton	0.565	0.972	2.21	542	628
7-BZ	2,950.58	Trempealeau	0.552	0.973	2.62	913	1081
1-BZ	3,312.84	Rose Run	0.532	0.972	2.14	586	721
2-BZ	3,790.57	Copper Ridge	0.529	0.973	2.78	1064	1315
3-BZ	4,686.45	Mount Simon	0.567	0.972	2.26	362	419
8-BZ	5,155.81	Newburg	0.603	0.973	2.55	1416	1538
9-BZ	5,292.08	Oriskany	0.456	0.973	2.53	1233	1771
10-BZ	6,926.74	Rose Run	0.588	0.972	2.61	1012	1127
11-BZ	8,885.73	Medina	0.597	0.974	2.37	1233	1351

5.5.3 Modeling Potential of Fracture Propagation

Coupled fluid-flow, geomechanical, and fracture mechanics modeling can be used to predict and avoid the potential for fracturing in reservoirs and surrounding formations. Such numerical modeling can be carried forward to study stress changes during brine injection and determine whether the changes in stress compromise the capability of reservoirs to store brine. To study the potential for hydraulic fracturing by water injection, a finite element-based hydraulic fracture simulator (StimPlanTM) was used. StimPlanTM is equipped with the most rigorous fracture geometry modeling. A range of fracture geometry simulation options is available with StimPlanTM, from quick-look pseudo-3D methods to fully 3D-gridded methods for more complex problems.

Three models with increasing levels of geologic complexity were constructed using logs and operational data from injection wells. The Big Injun Sandstone model included a single, shallow injection zone; the Clinton-Newburg model included two injection zones; and the Knox Group model was an open-hole scenario with multiple stacked injection zones. Each mechanical earth model investigated the stress changes and potential of hydraulic fracturing by brine injection.

5.5.3.1 *Big Injun Sandstone*

The Big Injun Sandstone represents a shallow Pennsylvanian-Upper Devonian injection interval similar to the Weir Sandstone injection simulation.

5.5.3.2 *Geomechanical Model*

The Big Injun Sandstone is a thick, shallow-depth, moderate-porosity sandstone that is used extensively across the southern portion of the study region as a low-volume injection target, with some wells injecting at higher rates where the unit is deeper. The Raynor D #1 API 34053209890000 well was selected for geomechanical modeling due to its location relative to the current injectors and the availability of high-quality acoustic logs.

5.5.3.3 Geomechanical Analysis

Dynamic parameters were derived from sonic logs and density logs. A limited triaxial test was performed on the available cores from a reservoir section to calibrate the dynamic data and convert it to static data. The log-based minimum stress data for the reservoir and surrounding formations were also determined in order to build a simple mechanical model.

To model the poro-elastic effect, we input main fluid flow parameters such as porosity and permeability from log data and available core measurements. The fluid pressure gradient was equal to 0.433 psi/ft. The Biot coefficient was assumed to be 1.0. To model thermo-elasticity and investigate the effects of water injection, we applied a temperature gradient of 1 degree Fahrenheit ($^{\circ}$ F) per 100 feet and a thermal expansion coefficient of $3\text{E-}6$ $1/^{\circ}$ F.

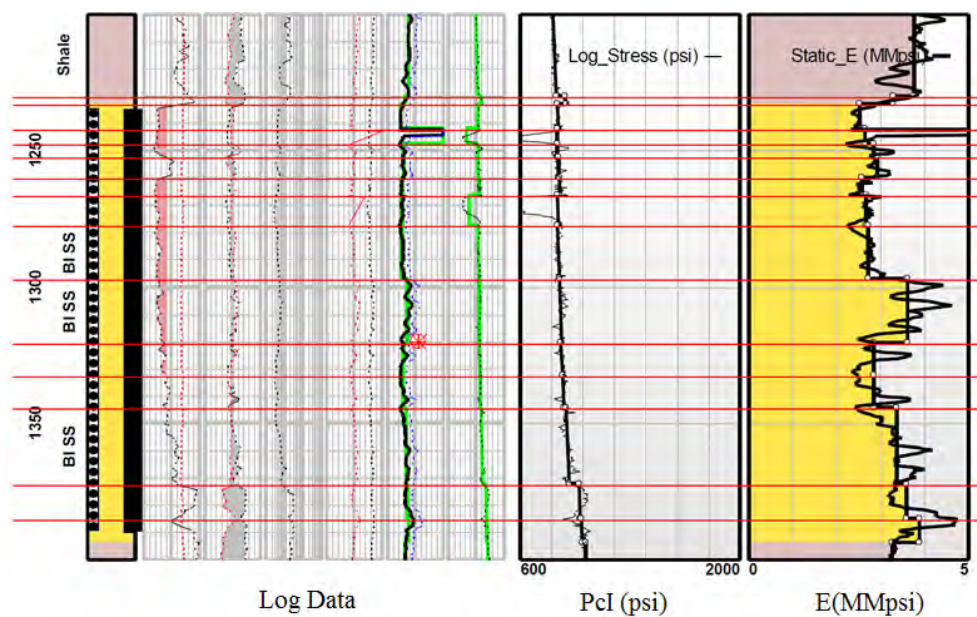
The main wellbore boundary condition was based on a constant injection rate and BHP. The available field data were used to input the injection rate and total injection volume. A long-term simulation was performed to represent typical brine injection operations for each scenario. Table 5-8 shows the input data used to build the Big Injun geomechanical model.

Table 5-8. Input data for the Big Injun geomechanical model.

Parameter	Value
Depth	1,233-1,394 feet
Porosity	15-20%
Permeability	10-20 mD
Fluid Pressure Gradient	Assumed freshwater 0.433 psi/ft
Reservoir Temperature	68 $^{\circ}$ F
Brine Viscosity	1.15 cp
Poro-elastic Constant	1.0
Thermal Expansion Coefficient	$3\text{E-}6$ $1/^{\circ}$ F
Median Injection Rate	682 bbl/month

Detailed layering was applied based on variations of the elastic modulus and the minimum horizontal stress. The advanced, fully 3D finite element simulation ensured that the fracture geometry was rigorously modeled, giving more accurate geometry estimates, particularly in complex multi-layered formations. Figure 5-50 shows the layering, elastic modulus, and calculated horizontal stress for the reservoir.

The results of the injection modeling are presented in Figures 5-51 and 5-52. Figure 5-51 shows the increasing of BHP, potential for geomechanical effects, and stress changes due to fluid injection at the rate of 0.2 barrels per minute (bpm). By increasing the stress around the wellbore due to fluid injection, the potential for fracturing decreases. Figure 5-52 shows that there is no fracture initiation since the BHP is much lower than the minimum horizontal stress by brine injection after 122 months.



Note: Red lines indicate layering.

Figure 5-50. Minimum horizontal stress (Pcl) and Young's modulus of reservoir and surrounding formations (Big Injun Sandstone).

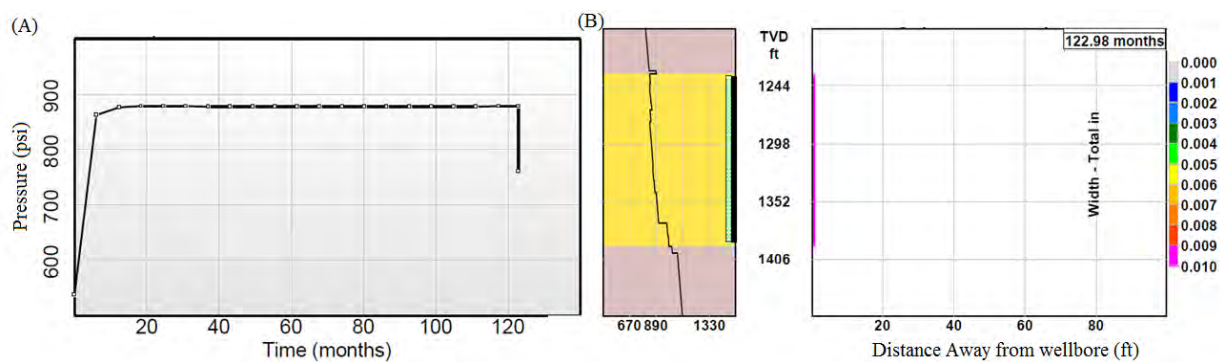
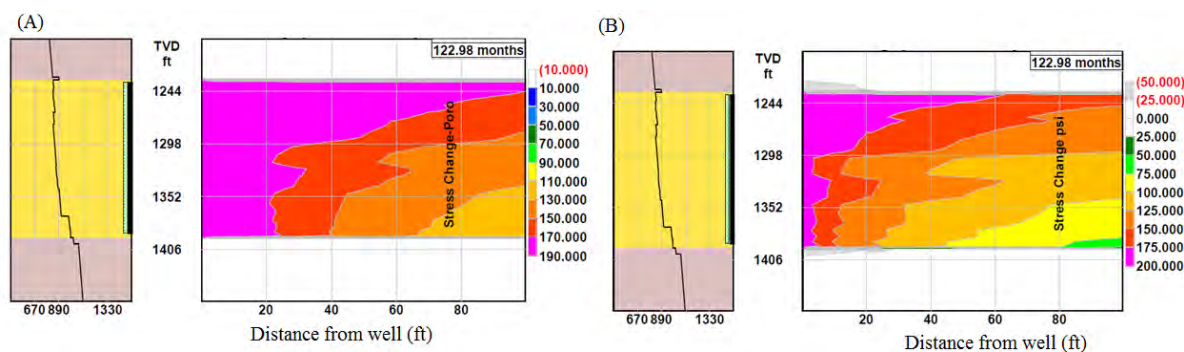


Figure 5-51. BHP increase by water injection (a) and width and length of near borehole effects (b).



Note: Black numbers show stress increase, red numbers show stress decrease.

Figure 5-52. Poro-stress changes away from wellbore (a) and total-stress changes away from wellbore (b).

5.5.3.4 Clinton-Newburg Zone

The Clinton-Newburg geomechanical model was set up to examine both the Clinton and Newburg zones. This allowed more flexibility in running injection scenarios.

5.5.3.5 Geomechanical Model

The Clinton Sandstone and Lockport Dolomite Newburg zone model well is located in Tuscarawas County, Ohio. The Tusc CO2 #1 well API 34157253340000 well was selected for geomechanical modeling because of its proximity to both Clinton and Lockport injection wells. It was also selected based on its potential to simulate injections both in the individual reservoirs and in the combined Clinton and Newburg injection zone. The combined injection zone is a common practice in wells in northern Ohio where the original Clinton producer was recompleted for injection into both zones.

5.5.3.6 Geomechanical Analysis

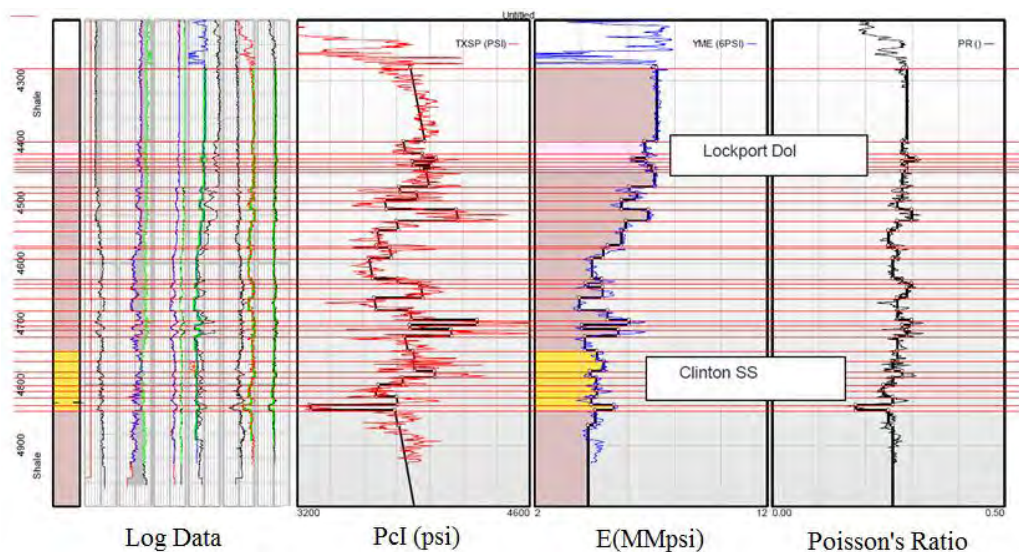
To model the poro-elastic effects, the main fluid flow parameters were porosity, permeability, fluid pressure, and poro- and thermo-elastic coefficients. The fluid pressure was equal to 0.4 psi/ft. The Biot coefficient was equal to 1.0. To model thermo-elasticity and investigate the effects of cold water injection, we applied a temperature gradient of 1° F per 100 feet and a thermal expansion coefficient of $3\text{E-}6$ 1/° F. The available field data were used to input the injection rate and total injection volume. Table 5-9 shows the input data used to build the Clinton-Newburg geomechanical model.

A triaxial test was performed on the available cores from a reservoir section to calibrate the dynamic data and convert it to static data. The log-based minimum stress data for the reservoir and surrounding formations were also determined in order to build a simple mechanical model. Detailed layering was applied based on variations of the elastic modulus and the minimum horizontal stress. Figure 5.53 shows the layering, elastic modulus, and calculated horizontal stress for the reservoir.

Table 5-9. Input data for the Clinton-Newburg geomechanical model.

Parameter	Value
Clinton Sandstone	
Depth	4,744-4,842 ft
Porosity	5-10%
Permeability	5-10 mD
Fluid Pressure Gradient	Assumed 0.40 psi/ft
Reservoir Temperature	103° F
Poro-elastic Constant	1.0
Thermal Expansion Coefficient	3E-6 1/° F
Newburg	
Depth	4,400-4,450 feet
Porosity	3-5% (vuggy carbonate)
Permeability	50-200 mD (vuggy carbonate)
Fluid Pressure Gradient	Assumed 0.40 psi/ft (may go on vacuum)
Reservoir Temperature	99° F
Poro-elastic Constant	1.0
Thermal Expansion Coefficient	3E-6 1/° F
Median Injection Rate	4,054 bbl/month
Injected Brine	
Fine Concentration	0.000190 (volume fraction)
Leak-off Coefficient	14.26 (ft/sqrt(min))

The results of the injection modeling are presented in Figures 5-54 through 5-56. Figure 5-54 and Figure 5-55 show the increasing of BHP, potential for fracturing, and stress changes due to fluid injection at the rate of 0.7 bpm. By increasing the stress around the wellbore due to fluid injection, the chance of fracturing decreases due to poroelastic effects. On the other hand, decreasing temperature could counteract the effect of the pressure increase. The effect of pressure and temperature changes on total stress is shown in Figure 5-55, which indicates that poro-elasticity is the dominant effect as compared to thermo-elasticity. Figure 5-54 shows simulated results for injection in the lower permeability Clinton Sandstone, which suggests some limited near borehole effects after 173 months of injection. Output suggests near wellbore sand fines prevent clear leak-off from the initial assumed fractured surface to the reservoir formation. The concentration of fines in the injected brine and leak-off coefficient is shown in Table 5-9. In the case where no fines are in the injected brine, there is no fracturing in either the Clinton or Newburg injection zones (Figure 5-56).



Note: Red lines indicate layering.

Figure 5-53. Minimum horizontal stress (Pcl) and Young's modulus of reservoir and surrounding formations (Clinton-Newburg zone).

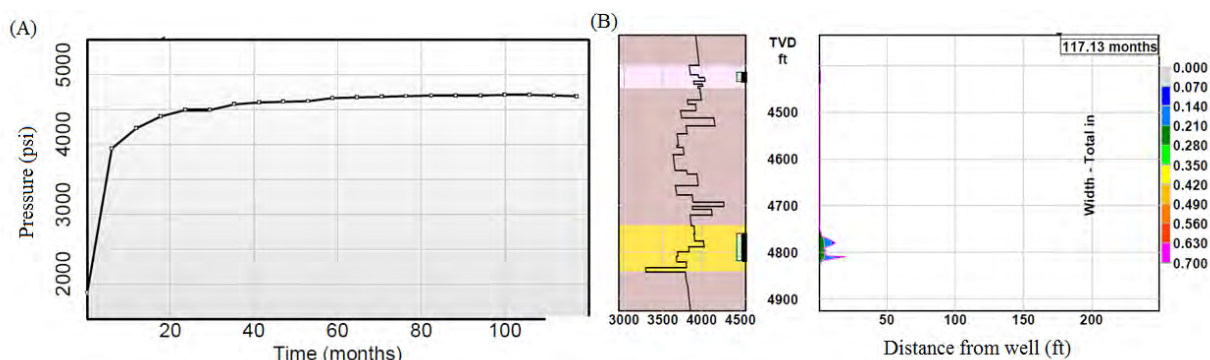
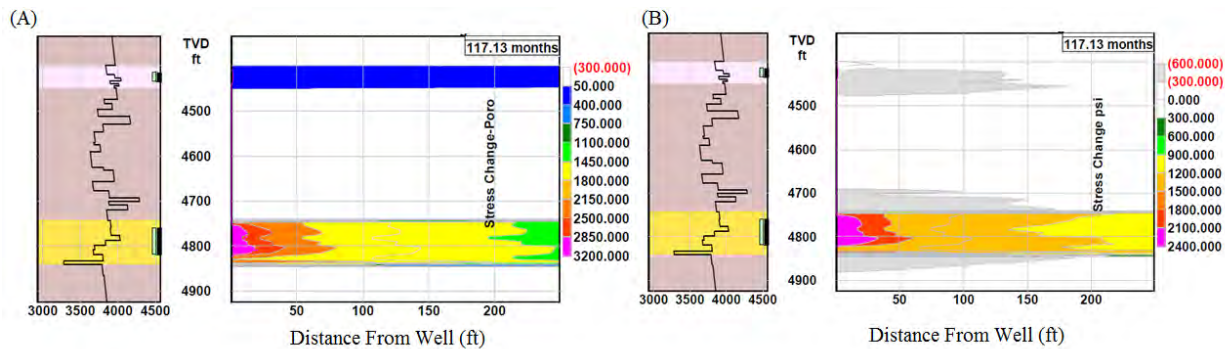
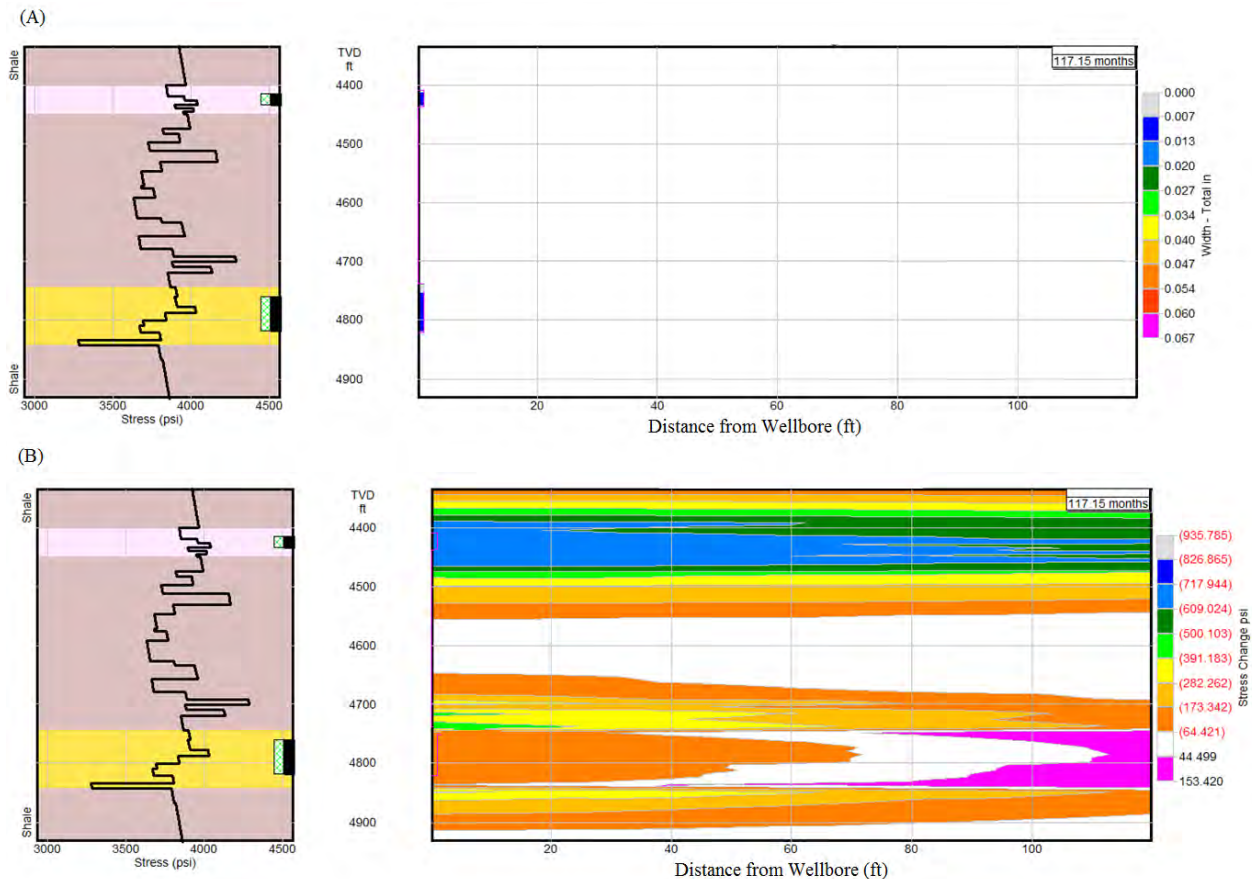


Figure 5-54. BHP increase by water injection (a) and width and length of near borehole effects (b).



Note: Black numbers show stress increase; red numbers show stress decrease.

Figure 5-55. Poro-stress changes away from wellbore (a) and total-stress changes away from wellbore (b).



Note: Black numbers show stress increase, red numbers show stress decrease.

Figure 5-56. Width and length of near borehole effects (a) and total-stress changes away from wellbore (b).

5.5.3.7 Knox Group Multiple Zone

The Knox Group multiple zone model reflects a well configuration being used in many recent, large-capacity Class II brine disposal wells in the Appalachian Basin. Many of these wells are completed as open-hole or long perforation intervals in the Cambrian Age rock layers.

5.5.3.8 Geomechanical Model

The Knox Unconformity to Copper Ridge Dolomite injection model is located in Kentucky. This location was selected to model injection into a moderate-depth (3,000 to 4,000-foot) open-hole section into the Beekmantown Dolomite, Rose Run Sandstone, and Copper Ridge Dolomite. Within the overall study area, many operators are currently disposing of large volumes of brine into the sub-Knox Unconformity formations at depths below 6,500 feet. This model was constructed to evaluate the geomechanical response during injection in the same formations at shallower depths where there is potential for injection on the western flank of the Appalachian Basin.

The Rose Run section in the modeled well generally consists of a single sandstone member, as opposed to the layered dolomite and sandstone units in the central portion of the study area. The Beekmantown Dolomite and Upper Copper Ridge Dolomite sections are similar to the same formations in deeper portions of the study area. They generally consist of low-porosity dolomites punctuated by thin, high-permeability injection zones. Porosity values were estimated for the model layers from the density and neutron porosity-derived logs, and permeability estimates were used for the layers based on injection tests performed on the well.

5.5.3.9 *Geomechanical Analysis*

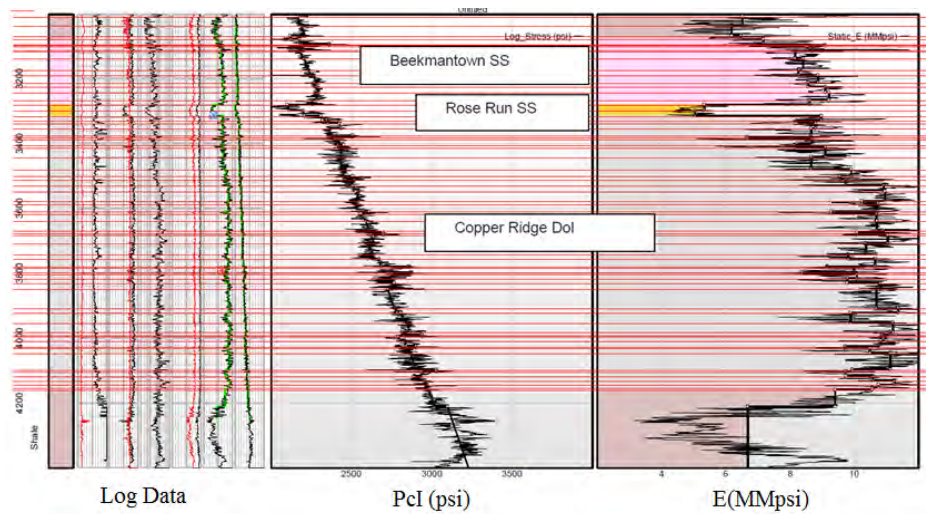
To model the poro-elastic effects of fluid injection into the Beekmantown Dolomite/Rose Run Sandstone/Copper Ridge Dolomite, the fluid pressure was assumed to be 0.48 psi/ft. The Biot coefficient was equal to 1.0. To model thermo-elasticity and investigate the effects of cold water injection, we applied a temperature gradient of 1° F per 100 feet and a thermal expansion coefficient of 3E-6 1/° F. The available field data were used to input the injection rate and total injection volume. Table 5-10 shows the input data used to build the Rose Run-Copper Ridge geomechanical model.

A limited triaxial test was performed on the available cores from a reservoir section (Rose Run Sandstone and Copper Ridge Formation) to calibrate the dynamic data and convert it to static data. The log-based minimum stress data for the reservoir and surrounding formations were also determined in order to build a simple mechanical model. Detailed layering was applied based on variations of the elastic modulus and the minimum horizontal stress. Figure 5-57 shows the layering, elastic modulus, and calculated horizontal stress for the reservoir.

The results of the injection modeling are presented in Figures 5-58 through 5-60. Figure 5-58 and Figure 5-59 show the increasing of BHP, potential for fracturing, and stress changes due to fluid injection at the rate of 2.8 bpm. By increasing the stress around the wellbore due to fluid injection, the chance of fracturing decreases (Figure 5-59a). On the other hand, the larger injection volumes, as compared to the previous models, decreases the reservoir temperature, which counteracts the effect of the pressure increase. The effect of pressure and temperature on total stress changes is shown in Figure 5-59b, which shows the effect of lower temperature on decreasing stress immediately adjacent to the wellbore, and the effect of increase of pressure on increasing stress away from the wellbore. Figure 5-58 shows that there is a small chance of near wellbore effects after 173 months of injection, assuming the brine includes some fine sand particles that prevent clear leak-off from fracture to formation. The concentration of fines in the brine and the leak-off coefficient are shown in Table 5-10. The analysis results show that if there are no fines in the brine, a fracture cannot propagate near the wellbore (Figure 5-60).

Table 5-10. Input data for the Rose Run-Copper Ridge geomechanical model.

Parameter	Value
Beekmantown	
Depth	3,077-3,280 feet
Porosity	Negligible as listed in the logs
Permeability	Assumed negligible
Poro-elastic Constant	1.0
Thermal Expansion Coefficient	3E-6 1/° F
Rose Run	
Depth	3,280-3,313 feet
Porosity	9.9±6.6% (n= 31)
Permeability	163 mD
Poro-elastic Constant	1.0
Thermal Expansion Coefficient	3E-6 1/° F
Fluid Pressure Gradient	0.48 psi/ft
Reservoir Temperature	87° F
Copper Ridge	
Depth	3,313-4,160 feet
Porosity	4.1±2.6% (n= 13)
Permeability	2.7±8.1 mD
Poro-elastic Constant	1.0
Thermal Expansion Coefficient	3E-6 1/° F
Median Injection Rate	15,073 bbl/month
Injected Brine	
Fine Concentration	0.000322 (Volume Fraction)
Leak off Coefficient	4.38 (ft/sqrt(min))



Note: Red lines indicate layering.

Figure 5-57. Minimum horizontal stress (Pcl) and Young's modulus of reservoir and surrounding formations (Knox-Basal Sandstone).

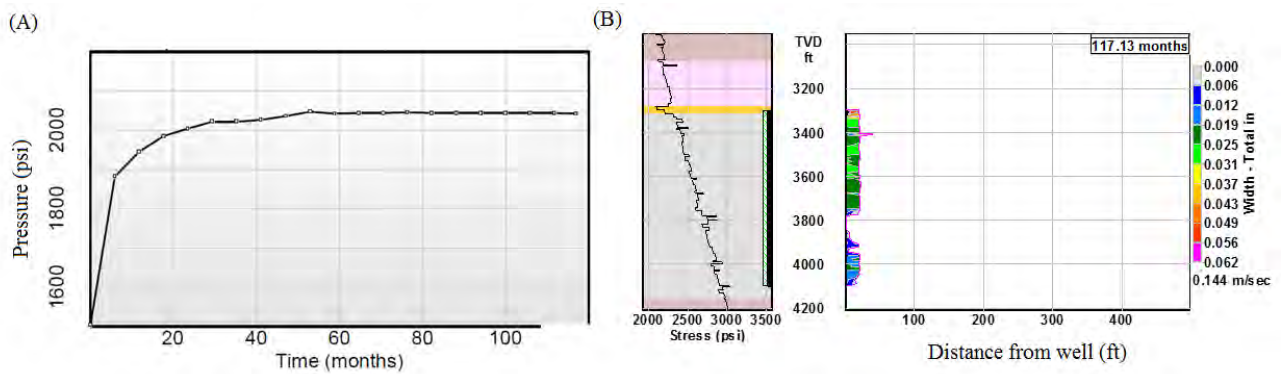
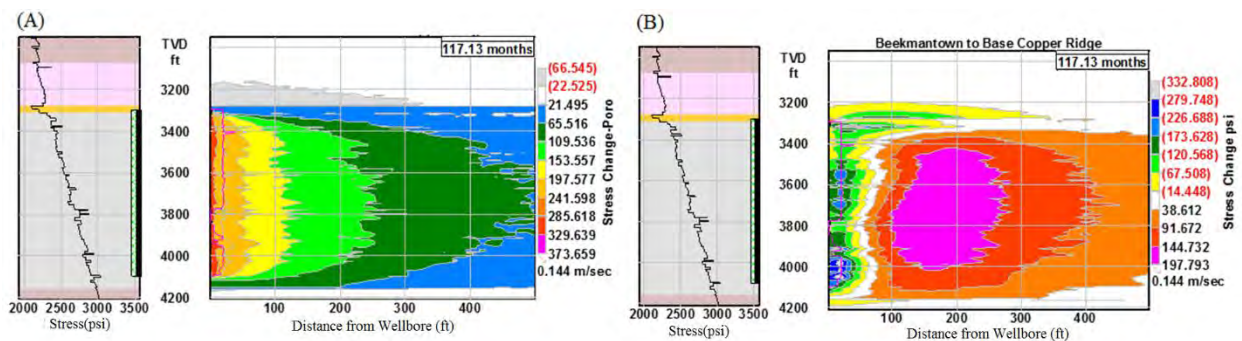
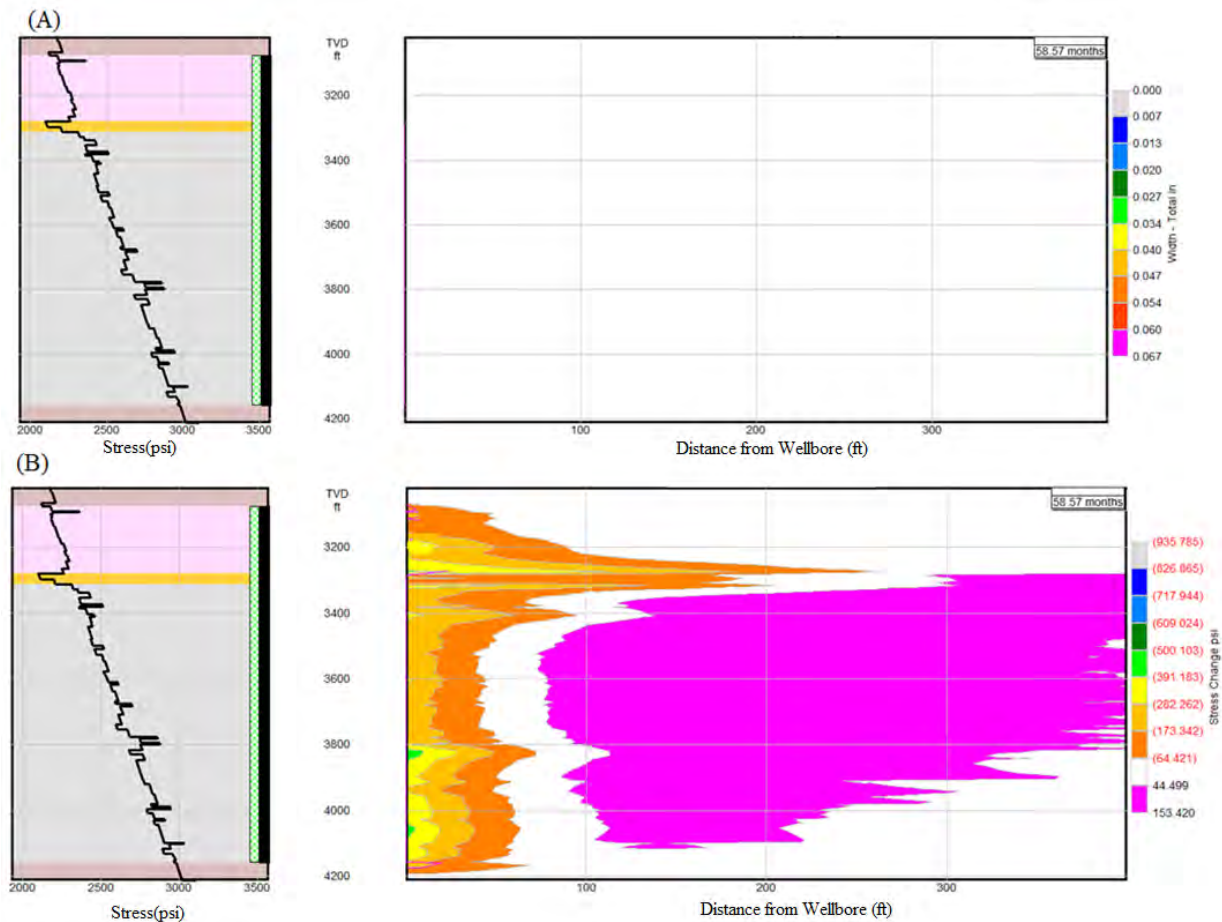


Figure 5-58. BHP increase by water injection (a) and width and length of near borehole effects (b).



Note: Black numbers show stress increase; red numbers show stress decrease.

Figure 5-59. Poro-stress changes away from wellbore (a) and total-stress changes away from wellbore (b).



Note: Black numbers show stress increase; red numbers show stress decrease.

Figure 5-60. Width and length of near borehole effects (a) and poro-stress changes away from wellbore (b).

5.5.4 Estimating Injectivity in Relation to Geomechanical Parameters in Western Flank of Appalachian Basin

To examine the effect of regionally variable geological and geomechanical parameters on brine injectivity, the region's geomechanics were characterized and analyzed. We selected eight wells in which the depth of the injection intervals in the Knox Group and the overlying cap-rock formations is progressively deeper to the east of Appalachian Basin to study petro-physical and rock mechanical behavior with increasing depth. Figure 5-61 shows the study area of interest with depth variation that was used to build the model.

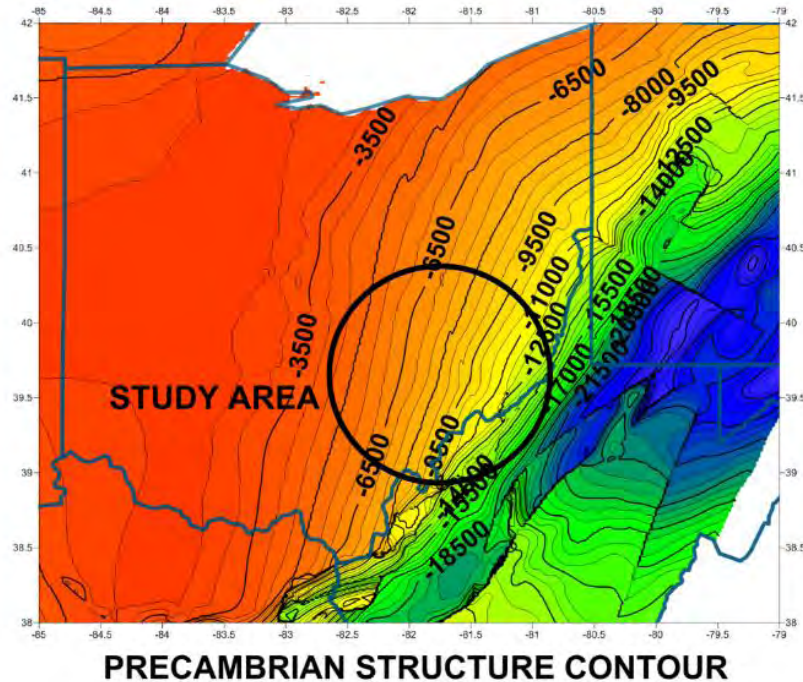


Figure 5-61. Study area of interest for investigation of Knox group reservoir injectivity.

5.5.4.1 Statistical Approach for Driving the Dynamic Rock Mechanical Parameters

While the dipole sonic log is needed to derive the dynamic elastic module of injection intervals and overburden, its availability was limited to selected wells. When the dipole sonic log was not available, a statistical approach was used to derive the dynamic elastic modulus. Eight wells were identified in which the depth of the injection intervals (Rose-Run Sandstone and Copper Ridge Dolomite) ranged from 6,000 to 14,000 feet (Figure 5-62). The first step was to build cross plots to understand how sonic wave velocity changes as a function of other available parameters such as density-neutron porosity and gamma logs. Figure 5-63 shows that the sonic wave velocity has the highest correlation to the density log. The shear wave velocity was also strongly related to the compression wave velocity (Figure 5-63).

The appropriate multivariate linear correlation was then built to determine compressional and shear wave velocity as a function of relevant parameters by evaluating the confidence level of prediction. The correlation between compression slowness and density log and shear – compression slowness is shown in Figure 5-64. The predicted-versus-correlated values are shown in Figure 5-65. Using the predicted model, the elastic modulus in the region could be derived with limited data with good accuracy.

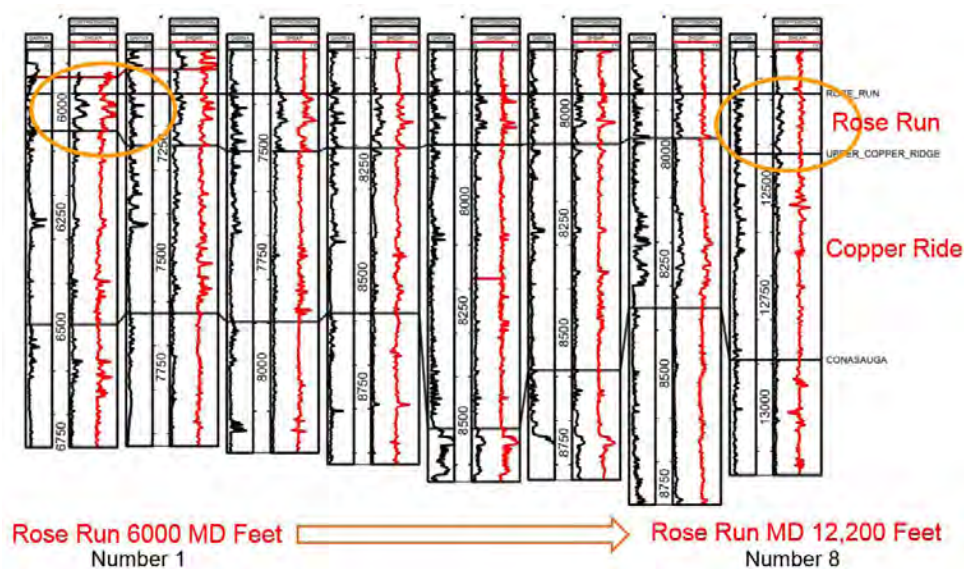
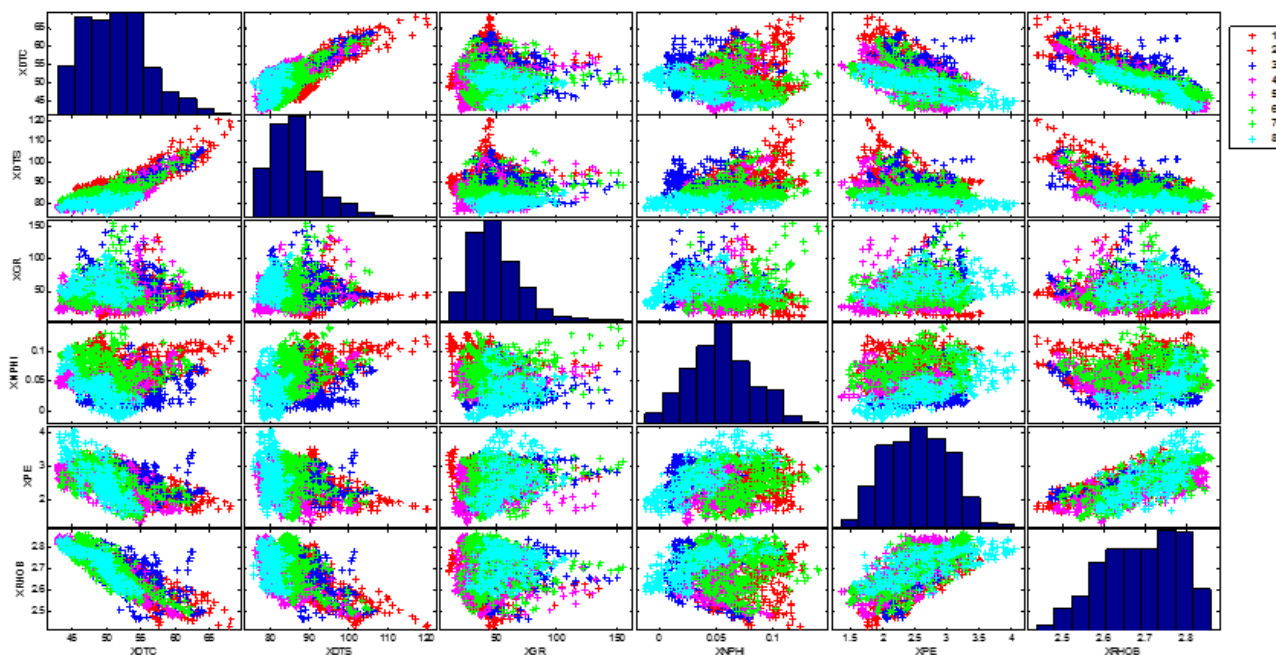


Figure 5-62. Depth variation of Rose Run and Copper Ridge across eight wells.



Note: XDTC = compression slowness, XDTS = shear slowness, XGR = gamma ray, XNPHI = neutron porosity, XPE = Photo electric log XRHO B = density.

Figure 5-63. Relationships among different petro-physical parameters.

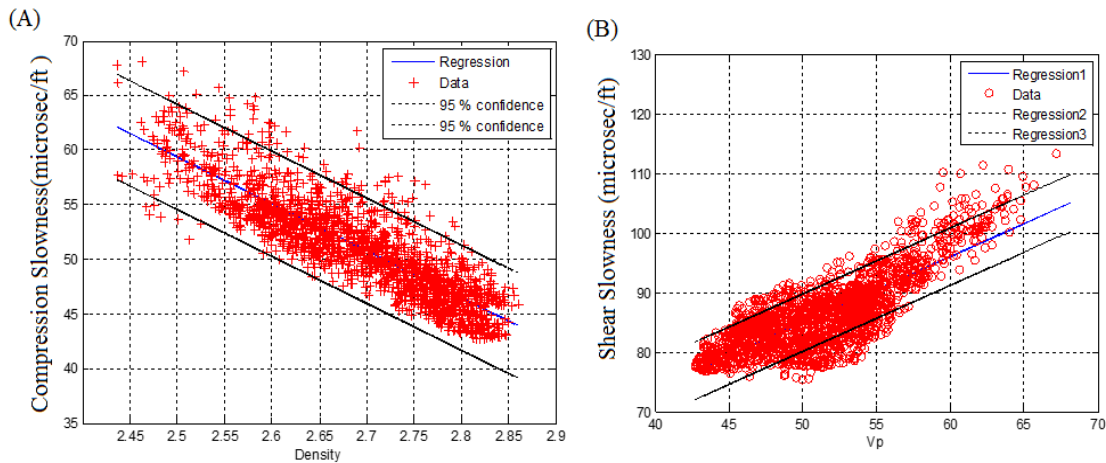


Figure 5-64. Relationship between compression – shear slowness and density.

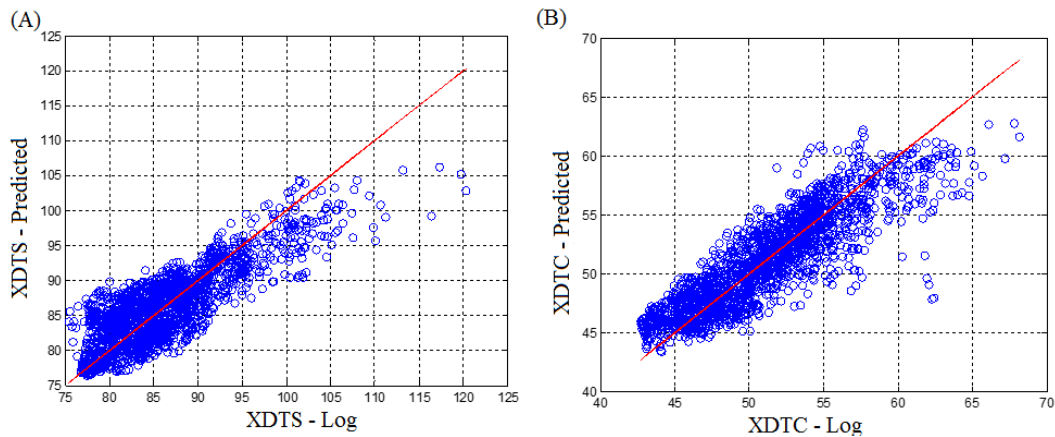


Figure 5-65. The predicted vs. measured compression and shear slowness.

We also analyzed the effect of depth on the relationship between petrophysical parameters and variations in trends that may be caused by geological events. The large variation of petrophysical parameters in the Rose Run Sandstone shows the important effect of formation cementation and consolidation with increasing depth. Figure 5-66 shows that shear and compressional slowness decrease with increasing depth in the Rose Run Sandstone. On the other hand, the limited variability of the bulk petrophysical parameters in the Copper Ridge Dolomite injection interval proves that its characteristics are not as dependent on depth. Within the Copper Ridge Dolomite there are thin, heterogeneous zones that show sharp changes in sonic wave velocity in all wells, which could signal the presence of vuggy zones and natural fractures.

The effect of petrophysical variations on the calculated dynamic rock mechanical properties is shown in Figure 5-67. The dynamic Young's modulus in the Rose Run Sandstone increases, indicating a more consolidated Rose Run in the deep portions of the basin (Figure 5-67a). On the other hand, the dynamic Young's modulus is more consistent with increasing depth in the Copper Ridge Dolomite (Figure 5-67b).

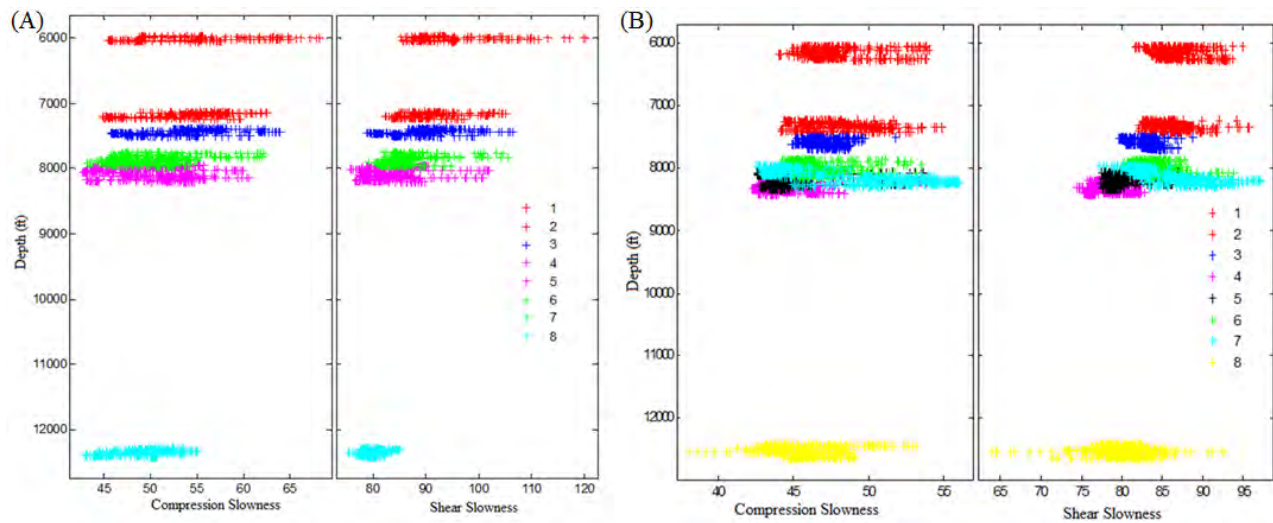


Figure 5-66. Compression and shear slowness at increasing depth in the Rose Run Sandstone (a) and Copper Ridge Dolomite (b).

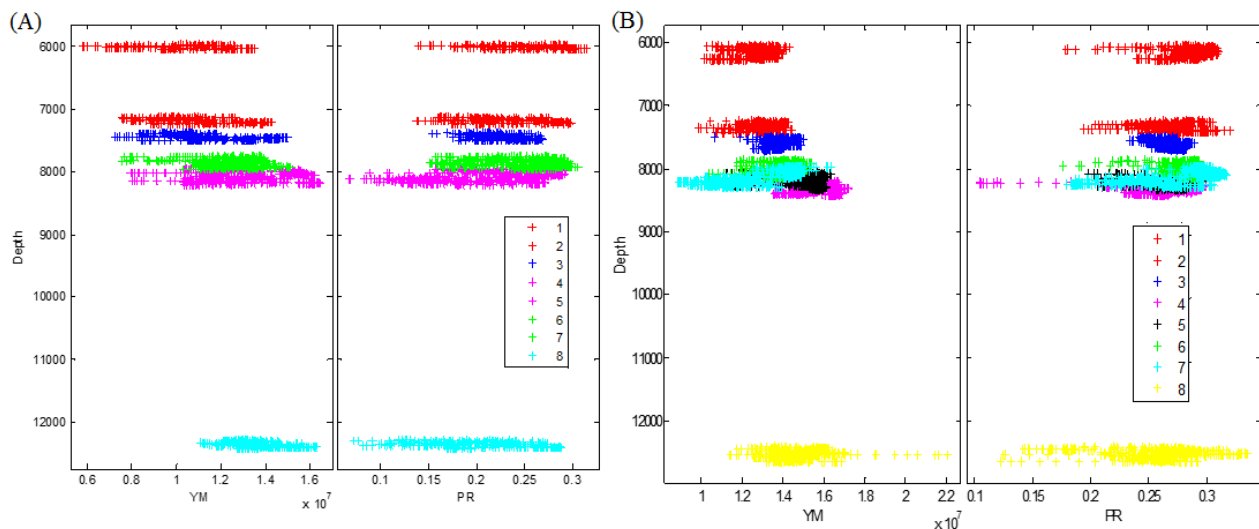


Figure 5-67. Dynamic Young's modulus and Poisson's ratio as a function of depth in the Rose Run Sandstone (a) and Copper Ridge Dolomite (b).

5.5.4.2 Injectivity Potential in Different Zones of Appalachian basin

When applying the coupled modeling, we also studied stress changes in specific reservoirs during fluid injection and predicted injection pressures that do not compromise the capability of reservoirs to store injected fluid by considering the poro-elastic effect of injection. We considered the effect of depth variation of two potential reservoir formations within the Cambrian-Ordovician Knox Group, the Rose Run Sandstone and Copper Ridge Dolomite, on stress response of fluid injection in the Northern Appalachian Basin and its injectivity. Geomechanical properties of reservoirs and confining layers play an important role in the evolution of stress field in space and time. In addition, changes with depth of the geological

parameters of formations, such as permeability, were reviewed in multiple numerical scenarios to evaluate poro-stress responses to fluid injection and determine the maximum injection rates that avoid unwanted hydraulic fracture initiation.

In general, deeper formations have a higher margin between pore pressure and minimum horizontal stress if there is not any change in pore pressure and fracture gradient by depth (Figure 5-68). Depth factors were addressed to see if the shallower injection intervals with higher permeability have the better injectivity, or whether the deeper interval with higher minimum effective horizontal stress could tolerate higher rates of brine injection before potential fracture initiation.

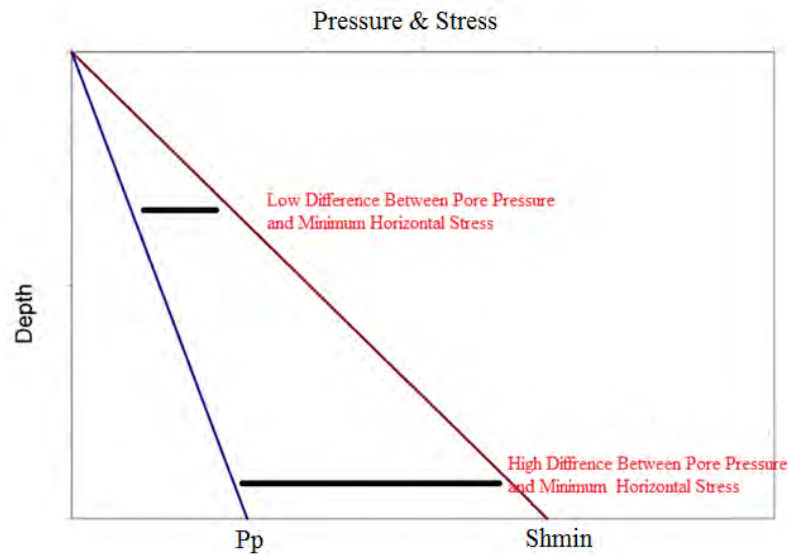


Figure 5-68. Higher depth and higher margin between pore pressure and minimum horizontal stress.

A 3D fluid flow simulator, CMG–GEM, was used to model the pressure rise following fluid injection. Next, the geomechanics module of CMG–GEM was used to simulate the poro-elastic response during injection periods. We assumed isothermal conditions during wastewater injection into the reservoir. We neglected hydrodynamic dispersion and chemical reactions between the components in the system. Based on the value of pressure at every time step, the geomechanics module computed stress and deformation in the storage formation and its surrounding formations to determine if and where rock failure might occur. An iterative coupling approach was used for coupling fluid flow and geomechanics. The pressure solution obtained in the reservoir simulator was passed on to the geomechanics module to compute deformation, strain, and stress. The solution from the geomechanical module was then passed on to the reservoir simulator via a coupling variable (such as porosity) to obtain new values of pressure. The process continued in a given time step until a convergence criterion was satisfied. The criterion of pressure, porosity, or total stress could be used for the loop of coupling iteration, which provides enough feedback to obtain a solution that is quite close to the solution obtained by the fully coupled method.

The mechanical parameters to build the coupled models for eight injection zones were derived from sonic and density logs of eight wells. The input included the Young's modulus and Poisson's ratio (Figure 5-69). The initial fracture gradient of reservoirs in all eight injection zones (from shallow to deep zone) was derived from a mini-frac test in one of the wells in the medium depth range. Table 5-11 shows model dimension, geomechanics, and fluid flow parameters to build models for all eight injection zones. Figure 5-70 shows the model schematic for one medium-depth well as well as two main parameters—permeability and effective minimum horizontal stress—that are variant. The constraint on the wells located in the middle of each simulation model was based on constant BHP determined by the minimum horizontal stress in the weakest formation, which is Rose Run. The eight models were run to evaluate the reservoir fluid flow and geomechanics response after one year of brine injection. The injection depth, initial pore pressure, and initial effective stress which limit the BHP of the injection well in each of the eight models are shown in Table 5-11.

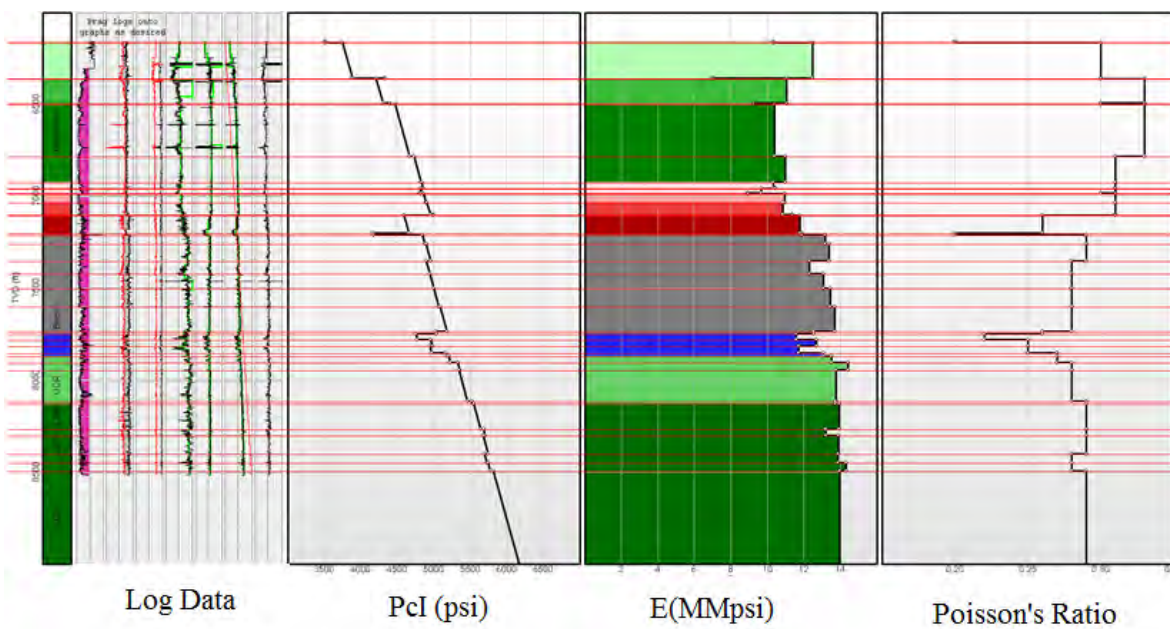


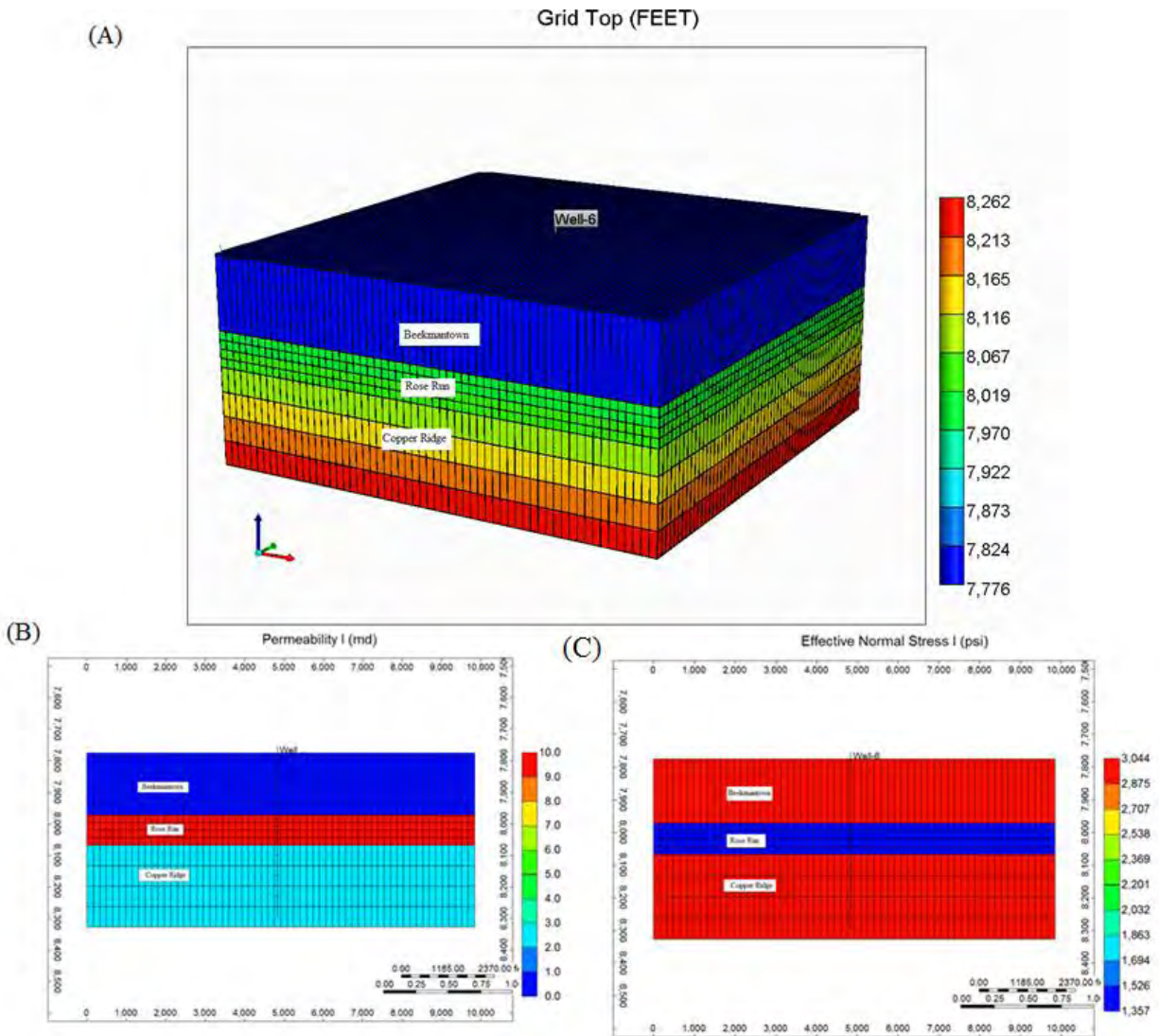
Figure 5-69. Construction of a model for geomechanics of one medium-depth-range well.

Table 5-11. Parameters for building eight models at different depths.

Geomechanical Parameters	
Young's Modulus	Derived by Log
Poisson's Ratio	Derived by Log
Poro-elastic Constant	1.0
Fluid Pressure Gradient	0.45 psi/ft
Minimum Horizontal Stress Gradient Rose Run Sandstone	0.65 psi/ft
Minimum Horizontal Stress Gradient Copper Ridge	0.8 psi/ft
Vertical Stress Gradient	1 psi/ft
Fluid Flow Model Parameters	
Number of Grids	60 * 60 * 9
Model Dimension	3 km * 3 km * 168 m
Permeability of Rose Run	10-30 mD
Permeability of Copper Ridge	2.5 mD
Permeability of Cap Rock	0.00001 mD
Porosity of Injection Zone	0.05
Injection Period	1 year

Table 5-12. Injection depth, initial pressure, and initial effective stress for building eight models at different depths.

Parameter	Well 1	Well 2	Well 3	Well 4	Well 5	Well 6	Well 7	Well 8
Model Top Depth (m)	1,808	2,150	2,248	2,370	2,382	2,424.7	2,450	3,744.5
Initial Pressure (kpa)	19,626	23,338	24,402	25,726	25,857	26,320	26,595	40,598
Effective Stress (kpa)	7,195	8,510	8,887	9,356	9,402	9,566	9,663	14,622
Permeability (mD) Same K model	10	10	10	10	10	10	10	10
Permeability (mD) Different K model	30	30	30	10	10	10	10	10



Note: 3D schematic of one of eight models (a); permeability variation from one formation to another formation in one injection case (b) and; effective minimum horizontal stress variation from one formation to another formation in one injection case (c).

Figure 5-70. Model schematic for one medium-depth-range well and variations in permeability and effective minimum horizontal stress between formations.

The pressure distribution and decreasing effective stress after one year of water injection in one of the simulation cases are shown in Figure 5-71. Figure 5-72 shows that the well with deeper reservoir formations has higher injectivity, assuming the same permeability of the Rose Run formation in the study area, due to a large margin between pore pressure and minimum horizontal stress. In fact, in the deepest well (well 8), the injectivity of brine could be as high as 4 bpm without any danger of hydraulic fracturing of the formation.

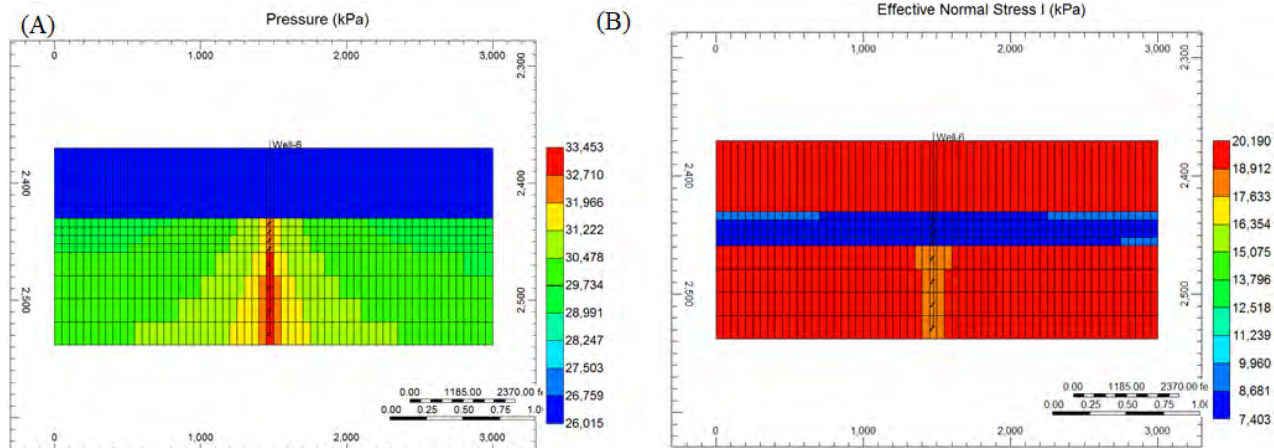


Figure 5-71. Pressure distribution after one year of injection (a) and effective stress reduction after one year of injection (b).

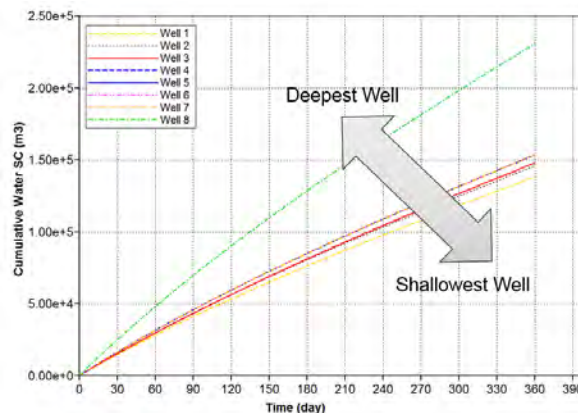


Figure 5-72. Injection capacity of different wells.

We considered higher permeability for a shallower well, as shown in the last row (different permeability model) of Table 5-12. Our simulations (Figure 5-73) show the important role of a higher-permeability formation in a shallower injection zone (well 2) on significantly higher injectivity of formations. Figure 5-73 shows that the shallower wells with higher permeability (well 1, well 2, well 3) could have higher injectivity (5 bpm) than the deepest well.

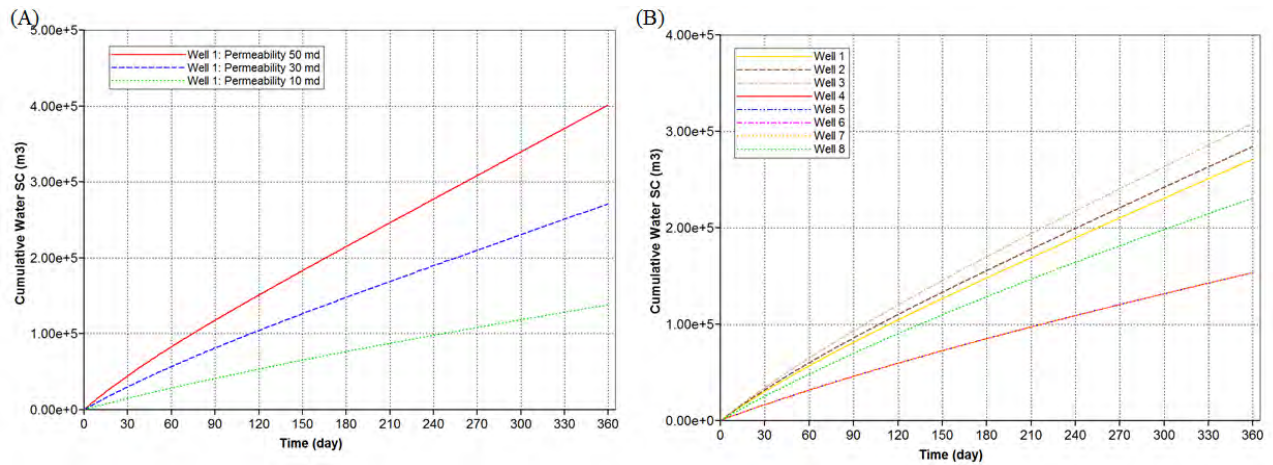


Figure 5-73. Effect of higher Rose Run permeability on increased injectivity (a) and comparison of injectivity of different wells (b).

Figure 5-74 shows the poro-elastic effect of injection in the Rose Run formation of wells 2, 4, and 8. The effective stress is higher than tensile fracturing pressure (0 psi) in all cases because of increasing total stress by fluid injection. In fact, the poro-elastic effect of injection prevents tensile fracturing of the reservoir.

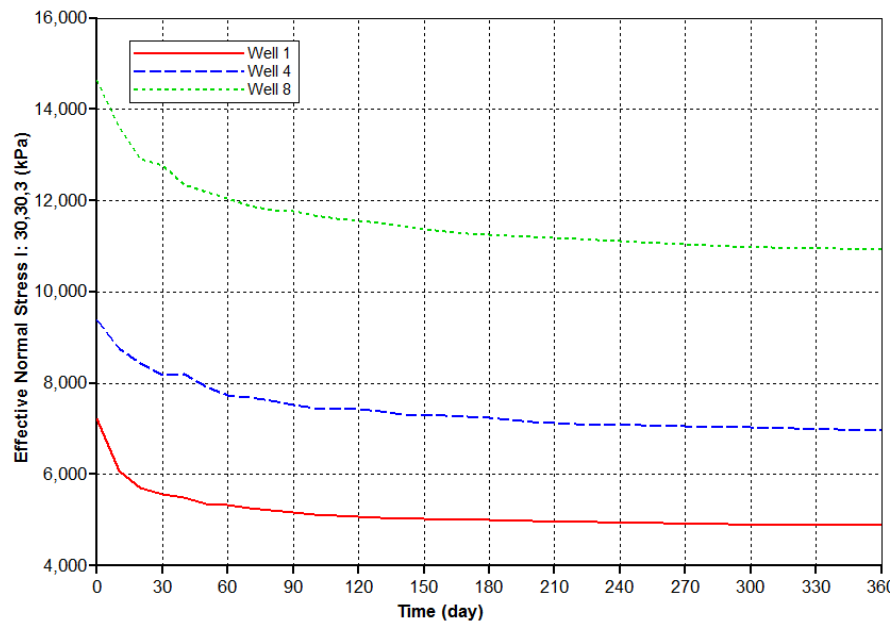


Figure 5-74. Effective stress in three wells after one year of brine injection.

6. Source-Sink Analysis

The overall objective of the source-sink analysis was to estimate the demand for brine disposal and capacity in injection zones in the Appalachian Basin. The sources of wastewater routed to Class II brine disposal wells were reviewed in relation to unconventional shale gas wells, hydrocarbon production, brine injection trends, and potential long-term demand for brine disposal. Sink capacity in depleted oil and gas fields and in deep saline formations is also described for the region.

6.1 Brine Disposal Source Analysis

The source analysis was focused on describing recent trends in the rates of hydrocarbon production and brine disposal. These rates may be used to estimate future demand for brine disposal when paired with resource estimates for unconventional plays. Sink capacity analysis was focused on looking at the physical dimensions and hydraulic properties of deep rock formations to calculate the volumetric storage capacity for brine. Based on the results of each research task, the source-sink volumes were compared for several scenarios.

Input data were compiled from a variety of sources that collect information from USEPA Class II UIC programs, oil and gas agencies, operators, drillers, and service companies. Efforts were made to review the quality of the data, but the accuracy of much of the information relies on external sources. Of note, Class II brine disposal operational data were not available for West Virginia for 2008-2011. Therefore, the brine disposal volume for West Virginia for 2008-2011 was estimated by the 2012 volume ratio of West Virginia to the combined volume for Eastern Kentucky, Ohio, and Pennsylvania, which was 28%. Other information on hydrocarbon production, unconventional wells, and oil and gas fields was obtained from state oil and gas agencies. Much of the geological information used to estimate capacity for brine disposal was based on research from other DOE projects (Wickstrom et al., 2005; Patchen et al., 2006; MRCSP, 2005) and USGS resource assessments for the Marcellus and Utica shale (USGS, 2011, 2012).

6.1.1 Assumptions and Limitations

The analysis described in this study was based on the physical properties of geologic layers and historical trends in brine injection, drilling activity, and hydrocarbon production. Estimates related to brine disposal demand and capacity in this study are general in nature. Site-specific projects would require field work such as seismic surveys, drilling, geophysical logging, reservoir tests, detailed reservoir modeling, and system design. The results of this study shall not be viewed or interpreted as a definitive assessment of the suitability of candidate geologic injection formations, the presence of suitable caprocks, or sufficient injectivity to allow brine disposal to be carried out cost effectively.

The status of Class II brine disposal wells is highly variable. This study focused on wells with operational data in the 2008-2012 time interval. When this study started, only operational data from 2012 and earlier were available. Many new Class II brine disposal wells have been permitted since this time, although they are not all actually drilled or operating. Therefore, the data from this study may be considered a ‘snapshot’ of Class II activity. Data should not be

considered a definitive list of Class II wells. This information is maintained by state or regional USEPA UIC programs and changes frequently.

Many factors may affect brine disposal in the Appalachian Basin, including technology, economics, politics, regulations, weather, climate, world conflicts, public perception, transportation corridors, surface developments, and other factors. This study was focused on the geology and operations information, since other factors are more difficult to predict.

Several major items affect analysis of brine disposal demand in the Appalachian Basin:

- **Brine disposal regulatory agencies** – Brine disposal is regulated by separate regulatory agencies for Pennsylvania (Region 3 USEPA UIC Program), Kentucky (Region 4 USEPA UIC Program), and West Virginia (West Virginia Department of Environmental Protection [WVDEP] UIC Program). There were some differences in the availability, attributes, and arrangement of injection records. Hydrocarbon production is regulated by state oil and gas agencies for Kentucky, Ohio, Pennsylvania, and West Virginia. Ohio is the only state where the Class II UIC program resides within the state Oil and Gas Division within the ODNR.
- **Interstate transport of wastewater** – Significant volumes of brine are transported across state lines for disposal in the Appalachian Basin. Ohio and Pennsylvania track out-of-state wastewater disposal volumes, while Kentucky and West Virginia do not distinguish between in-state and out-of-state wastewater volumes. Therefore, it was not possible to conclusively track the origin and destination of brine disposal volumes throughout the region.
- **Wastewater management** – Currently, only Pennsylvania requires detailed tracking of wastewater management in terms of flowback water, recycled water, produced water, and drilling fluids. These data are reported by various operators. Analysis of advances in recycle and reuse of drilling fluids was based solely on Pennsylvania.
- **Drilling operations** – Each operator has a different strategy for managing its drilling operations. Most operators have the goal of minimizing wastewater to reduce costs related to wastewater trucking and disposal. These operations may affect brine disposal trends, but they were not directly addressed in this research. The intent of this research was not to provide operators with wastewater management guidance at the wellpad.
- **Unconventional versus conventional wastewater production** – Prior to unconventional resource development in the Appalachian Basin, there was a baseline of brine disposal from traditional oil and gas production. Most of the increased demand for brine disposal may be attributed to unconventional production, but the source of brine is not explicitly tracked across the region. Therefore, brine disposal operations reflect combined conventional and unconventional operations across the region.

6.1.2 Unconventional Resource Development in Northern Appalachian Basin

Most of the increased demand for brine disposal in the Appalachian Basin has been related to unconventional shale gas development in the region. This activity has focused on the Marcellus and Utica-Point Pleasant shale, but unconventional completion methods have recently been

expanded to other organic shales. To identify source locations, unconventional shale wells were mapped. Data reflect state records as of approximately 2013. Figure 6-1 shows locations of unconventional wells in the study area. Overall, records indicate that 10,164 unconventional wells had been drilled in the Appalachian Basin as of fall 2013. Not all the wells drilled were completed for production, a process which would produce large volumes of wastewater. Also, some wells were temporarily shut-in. Once the wells are put online for hydrocarbon production, they may generate a portion of produced water that would require disposal.

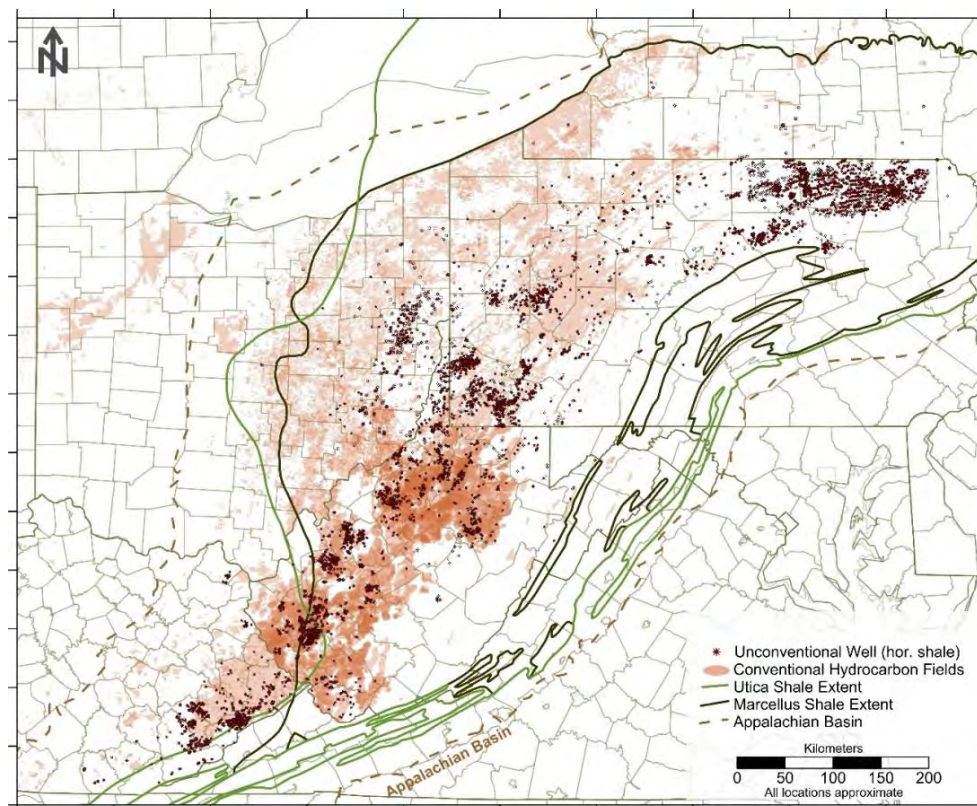


Figure 6-1. Locations of unconventional wells in the study area (circa fall 2013).

Data from eastern Kentucky were obtained from the Kentucky Geological Survey. Records indicated that there were 957 unconventional wells as of 2013. Most of the unconventional wells in the Appalachian Basin portion of Kentucky are drilled into Devonian-age shale formations in the far eastern portion of the state near the Kentucky-Tennessee state line. In general, the wells have horizontal completions into organic shales. Most of the wells were not completed with large, high-volume, multi-stage hydraulic fracturing. Therefore, there may be less wastewater produced and lower demand for brine disposal in the immediate area.

Data on unconventional wells in Ohio were obtained from the ODNR Division of Oil and Gas Resources. Records as of October 2013 listed 616 unconventional wells. Most of the unconventional activity in Ohio has been in the middle Ordovician Utica-Point Pleasant formation. Activity has been focused on a northeast-southwest trend along Columbiana, Carroll, Harrison, Guernsey, and Noble counties. Exploration in Ohio started later than other portions of the Appalachian Basin, and less production data were available for these wells.

Data on unconventional wells in Pennsylvania were obtained from the Pennsylvania Department of Environmental Protection (DEP) Office of Oil and Gas Management. Pennsylvania has the highest number of unconventional wells in the study area, with over 6,616 unconventional wells drilled in the state as of 2013. Many of these wells have been drilled but were not completed for production. Many more wells have been permitted in the state but not drilled. There are clusters of wells in Susquehanna, Bradford, Tioga, Lycoming, Armstrong, Westmoreland, Fayette, Greene, Washington, and several other counties. The Devonian-age Marcellus is the most common unconventional formation in Pennsylvania, but other organic shales were also targeted for production.

Data on unconventional wells in West Virginia were obtained from the West Virginia Geological and Economic Survey. As of 2013, West Virginia had 1,975 unconventional wells drilled. These wells are located throughout the northwestern half of the state. The wells are almost entirely completed in the Marcellus formation.

New York records indicated that about 24 wells were drilled into the Marcellus formation from 2004-2010. However, a moratorium on high-volume hydraulic fracturing was imposed in the state in 2008 and was recently extended into 2020.

To better depict the spatial distribution of unconventional wells, a well density map was prepared. Areas with higher well density are more likely to have a higher volume of wastewater. To prepare the density map, a density raster grid contour map was created using ESRI geographic information system (GIS) software. The data source for the density contour was the unconventional well locations from Ohio, West Virginia, Eastern Kentucky, Pennsylvania, and New York. The number of wells per 1-kilometer by 1-kilometer grid cell was gridded. The output units were number of completed unconventional wells per square kilometer. The well density map (Figure 6-2) shows that there are several areas with a high density of wells. Well fields in eastern Ohio and Central West Virginia are the only locations with many nearby brine disposal wells.

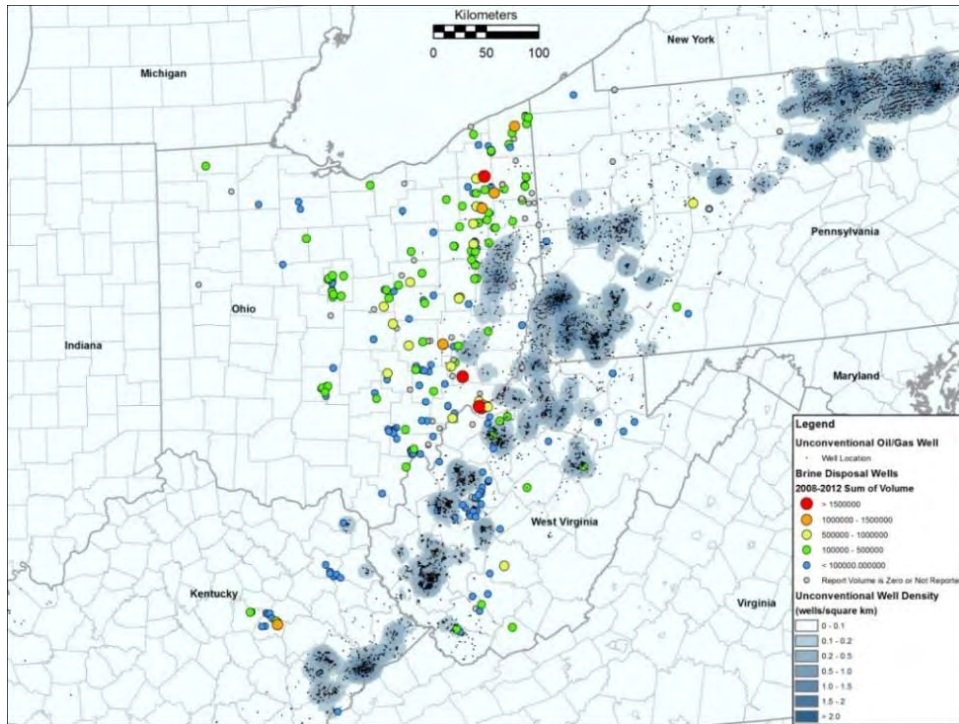


Figure 6-2. Density of unconventional wells in the study area.

To show the relationship between unconventional well locations and brine disposal well capacity, simple descriptive statistics were run on direct distances between the two items. Analysis indicated that there was a mean distance from the unconventional wells of 297 kilometers, a minimum distance of 2.87 kilometers, and a maximum distance of 922.5 kilometers to the disposal location (Figure 6-3). These statistics reflect direct distances; over-the-road distances are likely to be greater.

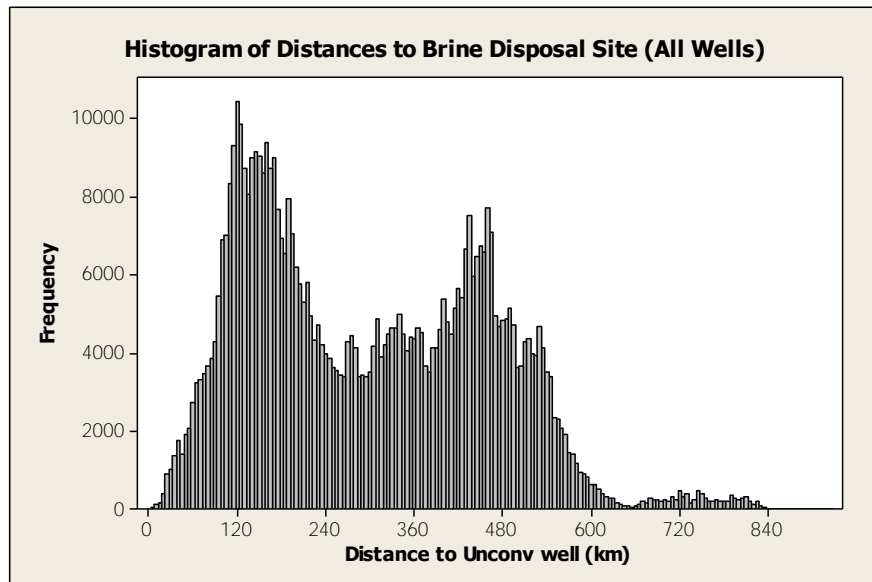


Figure 6-3. Direct distance between unconventional wells and Class II brine disposal wells in Appalachian Basin.

Figure 6-4 shows the broad spatial distribution of locations of unconventional and brine disposal wells across Ohio, Kentucky, West Virginia, and Pennsylvania. The larger dots represent brine injection wells with varying degrees of storage capacity, while the small black dots represent individual unconventional wells. The shaded regions are contours showing unconventional well densities per square kilometer. The pink lines generated from unconventional well locations to disposal wells represent the shortest path taken to the disposal site. These wells were selected from a table of wells closest to major injection sites. This map was generated using ESRI GIS software; all coordinate projections were in Universal Transverse Mercator (UTM) Zone 16 units in meters.

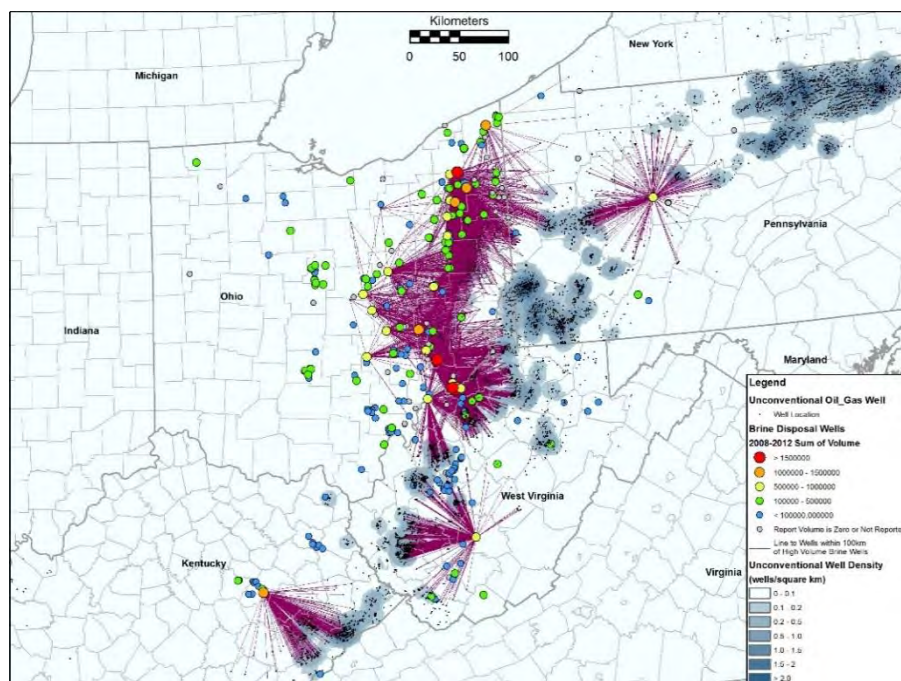


Figure 6-4. Distance between unconventional wells and Class II disposal wells.

6.1.3 Wastewater Production and Trends in Brine Disposal

Class II brine disposal wells inject fluids associated with oil and natural gas production. These fluids may include water mixed with hydrocarbon production, also referred to as ‘produced water.’ Produced water in the Appalachian Basin has high salinity (50,000 to 250,000 ppm) because there are salt layers present in the rocks, the rocks are very old (250 million to 540 million years ago), the formations are isolated from the surface, and diagenetic processes have occurred over time. Many Class II disposal wells simply inject produced water back into the same formations where it was produced. Class II brine disposal wells also inject drilling fluids used to control the well and circulate drilling cuttings, as well as fluids used to complete the well for production. Together, these wastewater streams contribute to the total volume routed to the Class II brine disposal wells. An increase in drilling activity, related hydrocarbon production, and adoption of high-volume hydraulic fracturing methods has increased wastewater volumes in the Appalachian Basin.

In the Appalachian Basin, studies suggest that a horizontal Marcellus well may use approximately 50,000 to 200,000 bbl of water (Arthur, Bohm, and Layne, 2009; Tiemann et al., 2012; Kakadjian et al., 2013; USGS, 2013). Conventional vertical wells typically use 5,000 to 20,000 bbl of water. Some water may be used to control the well and circulate drill cuttings to the surface. Hydraulic fracturing used for well completion requires large volumes of water delivered through high-pressure pump trucks. The water fractures the rock and carries proppant into the induced fractures. After the fracturing process, some of the fracture water and formation waters return as flowback fluid. A well may also generate produced water over a long period of time along with hydrocarbon production. The wastewater may be either disposed of in treatment plants or injection disposal wells or recycled/reused for additional hydraulic fracturing.

Tracking wastewater at drilling sites can be challenging. Many wells may be drilled from a single well pad and use the same water impoundment. Water may also be transferred from one well pad to another. Management of source water and wastewater may be affected by seasonal stream levels, economics, or other logistical considerations. It may be difficult to discern flowback water from formation water. In the project study area, only Pennsylvania requires unconventional operators to track their wastewater streams according to drilling fluids, flowback fluids, and produced water. Ohio requires injection wells to note if wastewater is from in-district or out-of-district. Other states do not track the source of water for Class II disposal wells.

This research focuses on wastewater volumes being routed to Class II disposal wells across the Appalachian Basin. On-site wastewater management methods, source water, wastewater treatment, and other solid waste associated with drilling were not addressed. Because not all states differentiate between the nature of the wastewater (flowback, drilling, or produced), total volumes injected into wells were used as the main measure of injection performance.

To assess brine injection trends in the Appalachian Basin, brine disposal rates were analyzed in relation to drilling activity and hydrocarbon production. Class II brine disposal operational data from 2008-2012 were collected from UIC agencies as described in a report titled *Development of Subsurface Brine Disposal Framework in the Northern Appalachian Basin Data Collection Topical Report (2013)*. Data included monthly injection volumes on a per-well basis. Table 6-1 summarizes annual brine disposal volumes for each state. Records indicate that the total volume of brine being routed to Class II injection wells increased from 9.2 million bbl in 2008 to 17.6 million bbl in 2012.

Table 6-1. Annual Class II brine disposal volumes (2008-2012).

Year	E. KY	OH	PA	WV ^a	Total Brine
	(bbl)				
2008	135,815	6,946,806	138,723	2,007,534	9,228,878
2009	545,014	7,587,157	215,608	2,320,683	10,668,462
2010	220,667	8,469,500	169,149	2,462,890	11,322,206
2011	621,723	12,419,849	190,934	3,678,637	16,911,143
2012	709,835	12,980,726	110,488	3,838,821	17,639,870

a. Data for West Virginia were unavailable for 2008-2011. West Virginia volumes for those years (shaded cells) were estimated to be 28% of Kentucky, Ohio, and Pennsylvania totals based on 2012 data.

The number of brine disposal wells in the Appalachian Basin has generally corresponded to historical production trends from key oil and gas fields. Figure 6-5 shows the number of brine disposal wells drilled by date in the study area. As shown, many of the wells were drilled in the 1980s, mostly related to ‘Clinton’-Medina production in Ohio. Thus, many of the existing wells were utilized for disposal in the early phases of unconventional production in the region. More wells have been installed recently to meet demand for brine disposal.

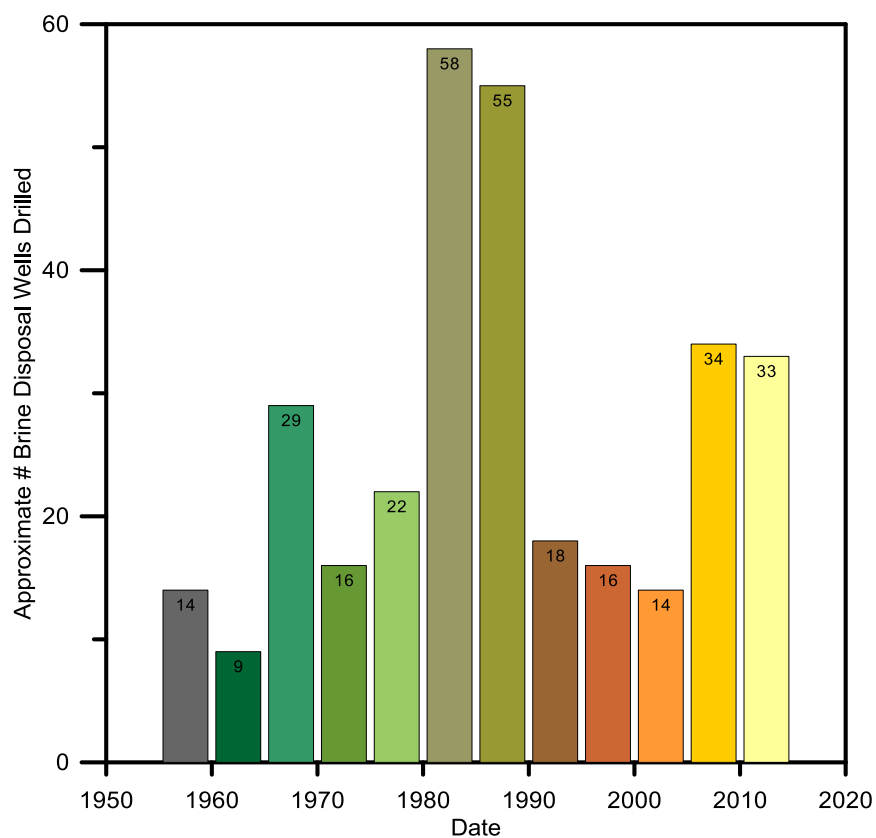


Figure 6-5. Approximate number of brine disposal wells drilled by date.

Recently, concerns over water resources have prompted an evaluation of basin wide/watershed impact of wastewater management on hydrologic systems (Ferguson, 2015; Lutz et al., 2013; Rahm et al., 2013; Tsang et al., 2013; Vidic et al., 2013). To depict the effect of brine disposal on overall hydrologic budgets, water use volumes were reviewed for the study area (Table 6-2). As shown, total water use for the study area was estimated at 221,000 million bbl in 2010 by the USGS (2014). Brine disposal in 2012 was approximately 0.008% of total water use in the region. The largest water use for the region was listed as thermoelectric power generation. Municipal wastewater treatment was estimated at roughly 14,000 million bbl per year, and many city wastewater treatment plants treat more wastewater on a weekly basis than is routed to all brine disposal wells in the Appalachian Basin over an entire year. Annual oil consumption for Kentucky, Ohio, Pennsylvania, and West Virginia exceeds 600 million bbl per year; most of this oil is imported from other regions. Natural gas consumption in the states is about 2.1 billion cubic feet per year.

Table 6-2. Summary of water use volumes for study area.

State	2010 Population (million) ^a	2010 Total Water Use (MMBBL/yr) ^b	2010 ThermoElectric Water Use (MMBBL/yr) ^b	2013 Wastewater Treatment (MMBBL/yr) ^c	2013 Natural Gas Production (MMBBL/yr) ^{d,e}	2012 Brine Disposal Volume (MMBBL/yr) ^f
KY	4.4	37,630	29,200	1,078	42	0.7
OH	11.5	82,038	62,745	6,518	83	13.0
PA	12.8	70,654	46,842	6,127	1,451	0.1
WV	1.9	30,677	21,465	404	320	3.8
Total	30.6	220,999	160,252	14,126	1,896	17.6

a. 2010 U.S. Census.

b. USGS, 2014.

c. Biogas Data, 2013.

d. EIA, 2015.

e. Dry gas to market converted to reservoir conditions based 0.0025 formation factor.

f. This study.

Following methods applied by Ferguson (2015), the total pore volume in the Appalachian Basin was compared to brine disposal volume over time. Based on brine disposal trends from 1978-2014, at total of about 308 million bbl of brine (or 0.05 cubic kilometers [km³]) have been injected into Class II brine disposal wells in the study area (before 1978 and the USEPA Clean Water Act, brine disposal was not tracked so it is difficult estimate volumes in the region). Using a simplified volumetric estimate based on area, thickness, and porosity of the major geologic layers in the Appalachian Basin, the total pore volume in the basin is on the order of 60,000 km³ (Table 6-3 and Table 6-4). As such, total brine disposal volume is 0.00005% of total pore volume based on USGS studies on groundwater recharge in the region.

Table 6-3. Total pore volume estimate for Appalachian Basin.

Layer	Porosity	Total Volume (km ³)					Net Pore Volume (km ³)				
		App. Basin	KY	OH	PA	WV	App. Basin	KY	OH	PA	WV
Surficial Deposits	10%	15,534	1,568	2,795	4,059	2,809	1,553	157	280	406	281
Post-Devonian	8%	171,588	15,995	12,587	37,070	38,711	13,727	1,280	1,007	2,966	3,097
Devonian Shale	3%	346,149	7,391	50,741	132,518	85,676	10,384	222	1,522	3,976	2,570
Silurian Carbonates	5%	63,775	507	1,754	12,049	11,080	3,189	25	88	602	554
Clinton-Medina	8%	118,292	1,346	3,565	81,805	7,101	9,463	108	285	6,544	568
Ordovician Shale	3%	807,543	74,698	67,411	227,234	234,434	24,226	2,241	2,022	6,817	7,033
Ordovician-Cambrian	5%	11,516	1,331	1,672	3,299	604	576	67	84	165	30
Total		1,534,397	102,836	140,526	498,034	380,415	63,119	4,099	5,288	21,476	14,133

Note: All values approximate estimates, including porosity. State data only include Appalachian Basin portion.

Table 6-4. Estimated total pore volume, brine disposal volume, and annual recharge to groundwater in Appalachian Basin study area.

Appalachian Basin Study Area	BBL	km ³
Total Sedimentary Volume	9.4E+15	1,500,000
Total Pore Volume	3.8E+14	60,000
Annual Recharge	4.5E+11	72
Historical Brine Disposal	3.0E+8	0.05

6.1.4 Ratio of Oil and Gas Production to Brine Disposal Volumes

Because brine disposal is a function of oil and gas activity, hydrocarbon production was also analyzed for the study area. There is a long history of oil and gas production in the Appalachian Basin, and over 1 million wells have been drilled in the region over time. While early production records are uncertain in many areas, state estimates suggest that over 43 trillion cubic feet (TCF) of natural gas and 3.8 billion bbl of oil have been produced in Kentucky, Ohio, Pennsylvania, and West Virginia (MRCSP, 2005). Production removed fluids in rock pore space, depressurizing the reservoirs and leaving a fraction of void space in the rocks. This void space volume is equivalent to approximately 47 billion bbl of brine. As such, there appears to be large capacity for brine disposal in depleted oil and gas reservoirs. Table 6-5 summarizes historical oil and gas production statistics for the study area.

Table 6-5. Historical oil and gas production in the study area.

State	Total Number of Wells	Total Historical Gas Production (MCF)	Total Historical Oil Production (bbl)	Approximate Brine Equivalent Volume ^a (bbl)
KY	250,000	5,388,675,103	772,532,160	6,161,207,263
OH	260,000	>8,009,749,438	1,105,000,000	9,114,749,438
PA	~350,000	>11,026,657,000	1,380,944,000	12,407,601,000
WV	~150,000	18,650,000,000	584,024,000	19,234,024,000
Total	>1,000,000	43,075,081,541	3,842,500,160	46,917,581,701

Source: MRCSP, 2005.

a. Assuming gas formation volume factor = 0.001 reservoir barrel/standard cubic foot gas.

To better define the relationship between hydrocarbon production and wastewater injection, more detailed oil and gas production data were tabulated from state oil and gas agencies for 2001-2012. Data for Kentucky were obtained from the Kentucky Geological Survey, which assesses data from the Kentucky Division of Oil and Gas. The Kentucky data include the Appalachian Basin portion of the state only. Data for Ohio were obtained from the ODNR Division of Oil and Gas Resources Management's *2012 Ohio Oil and Gas Summary* report. Ohio data include the entire state, but most production is from the Eastern Appalachian Basin portion of the state. Data from Pennsylvania were obtained from the Pennsylvania DEP Office of Oil and Gas Management's annual production reports, including both conventional and unconventional wells for the whole state. West Virginia data were obtained from the West Virginia Geological and Economic Survey summary data on oil and gas production for the whole state. Table 6-6 summarizes production data. As shown, gas production increased from 525 billion cubic feet in 2001 to 2,428 billion cubic feet in 2012. The total number of oil and gas wells peaked in 2007 at 9,313, then decreased to 3,517 in 2012.

Table 6-6. Hydrocarbon production and oil and gas wells drilled in the study area (2001-2012).

Year	E. Kentucky			Pennsylvania			Ohio			West Virginia			Total			
	Gas	Oil	Wells Drilled	Gas	Oil	Wells Drilled	Gas	Oil	Wells Drilled	Gas	Oil	Wells Drilled	Gas	Oil	Eq. Gas ^b	Total Wells
2001	80.9	1.02	633	148.9	1.49	2296	98.3	6.05	599	197.0	1.34	1226	524.9	9.9	582.5	4754
2002	87.1	1.06	633	151.7	1.65	2207	97.2	6.00	432	202.1	1.36	1126	538.1	10.1	596.6	4398
2003	86.3	0.96	657	162.0	1.95	2729	93.6	5.65	454	202.1	1.37	1251	544.0	9.9	601.7	5091
2004	92.4	1.04	718	159.3	1.88	3115	90.3	5.79	534	210.5	1.57	1528	552.5	10.3	612.3	5895
2005	91.0	1.06	902	182.5	1.95	3995	84.1	5.65	658	216.9	1.59	1676	574.6	10.2	634.2	7231
2006	93.3	0.83	1,104	198.0	2.08	4702	86.3	5.42	914	223.1	1.73	2176	600.8	10.1	659.2	8896
2007	93.9	1.18	953	170.0	1.41	4954	88.1	5.46	1022	234.0	1.97	2384	586.0	10.0	644.2	9313
2008	112.1	1.15	764	222.1	2.49	4990	84.9	5.55	1026	257.3	2.13	2210	676.3	11.3	742.1	8990
2009	298.4	1.26	397	288.0	2.39	2842	88.8	5.01	517	265.3	1.28	1109	940.6	9.9	998.3	4865
2010	288.3	1.27	260	493.7 ^a	2.68	3335	78.1	4.79	386	297.9	1.85	743	1158.0	10.6	1219.6	4724
2011	242.9	1.08	116	834.6	2.37	3234	73.3	4.85	423	407.5	2.20	514	1558.3	10.5	1619.4	4287
2012	277.0	1.67	14	1524.9	2.29	2370	86.8	4.97	641	538.9	2.57	492	2427.6	11.5	2494.5	3517

Note: Gas in billion cubic feet gas (BCFG), oil in million barrels oil (MMbbo).

a. Provisional based on partial data.

b. Assuming 5,814 SCFG per bbl oil.

Table 6-7 summarizes the total volume of wastewater routed to Class II brine disposal wells, the number of unconventional wells drilled per year, and hydrocarbon production. As shown, the total equivalent gas production has increased from 742 BCF in 2008 to 2,495 BCF in 2012 (Figure 6-6). The amount of brine injected for all oil and gas wells steadily increased from 1,026 bbl/well in 2008 to 5,016 bbl/well in 2012, which is likely the result of unconventional wells. Similarly, the annual volume of brine injected per unconventional well drilled shows a large degree of fluctuation. However, the amount of brine injected per year per BCF equivalent gas produced is more consistent, suggesting this may be a more suitable method for estimating the amount of brine produced.

Table 6-7. Class II brine injection volumes and hydrocarbon production (2008-2012).

Year	Total Class II Brine (BBL)	# Oil&Gas Wells Drilled	# Unconv. Wells Drilled	Total Eq. Gas ^a (BCF)	BBL Brine/#O&G Wells	BBL Brine/#Unc. Wells	BBL Brine/BCF
2008	9,228,877	8,990	1,031	742	1,026	8,951	12,436
2009	10,668,462	4,865	1,590	998	2,193	6,710	10,686
2010	11,322,206	4,724	2,268	1,220	2,397	4,992	9,284
2011	16,911,143	4,287	2,523	1,619	3,945	6,703	10,443
2012	17,639,870	3,517	2,193	2,495	5,016	8,044	7,071
Average	13,154,111	5,277	1,921	1,415	2,915	7,080	9,984

a. Assuming 5,814 SCFG per bbl oil.

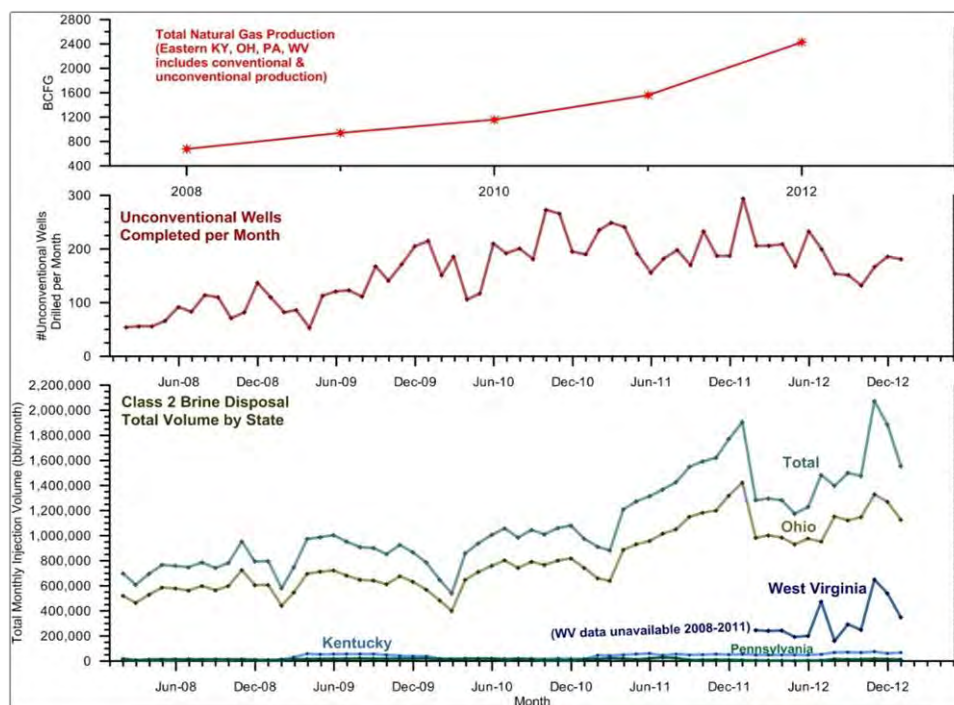


Figure 6-6. Class II brine disposal, natural gas production, and unconventional wells drilled (2008-2012).

Based on hydrocarbon production and brine disposal volumes from 2008-2012, an average of 9,984 barrels of brine were injected in Class II wells per billion cubic feet equivalent gas production (this figure includes all hydrocarbon production from both conventional and unconventional oil and gas wells). Continued demand for brine disposal is likely in the region, because there are thousands of unconventional wells in the basin that will have some produced water associated with hydrocarbon production. Economic issues complicate efforts to predict future trends in oil and gas production in the Appalachian Basin. However, resource estimates for unconventional shale gas plays provide a basis for estimating long-term brine disposal volumes.

6.2 Marcellus/Utica Resource Estimates and Long-Term Brine Disposal Demand

USGS resource estimates for the Marcellus and Utica-Point Pleasant shales indicate 70 to 229 TCF equivalent gas in the formations (USGS, 2011, 2012). Assuming 9,984 bbl brine per BCF gas, there may be ultimate demand for 706 million to 2,290 million bbl brine disposal related to production from these unconventional shale plays (Table 6-8). While many factors may affect development of these resources, these demand estimates provide a value to gauge against brine disposal sink capacity within the various injection intervals in the region.

Table 6-8. Brine disposal total demand estimates for Marcellus and Utica shale.

USGS Resource Estimates	Utica			Marcellus			Combined		
	Low (F95)	Mean	High (F5)	Low (F95)	Mean	High (F5)	Low (F95)	Mean	High (F5)
Gas (BCFG)	21,106	38,212	60,932	42,954	84,198	144,145	64,060	122,410	205,077
Natural Gas Liquid (MMBNGL)	590	940	1,386	1,554	3,379	6,162	2,144	4,319	7,548
Oil (MMbbo)	75	208	398	---	---	---	75	208	398
Total Equiv. Gas ^a (BCFG)	23,257	42,153	67,273	47,470	94,017	162,052	70,726	136,170	229,325
Brine Disposal Demand ^b (MMbbl brine)	232	421	672	474	939	1,618	706	1,360	2,290

Note: BCFG=billion cubic feet of gas; MMBNGL=million barrels natural gas liquid; MMbbo=million barrels of oil; MMbbl=million barrels.

- Assuming 5,814 CFG per bbl oil and 2,907 CFG per BNGL equivalent.
- Based on 9,984 bbl brine per 1 BCF total equiv. gas.

6.2.1 Brine Disposal Sink Capacity Analysis

The sink analysis task includes a description of Class II brine injection rock formations, sink capacity calculations for depleted oil and gas reservoirs, and sink capacity in deep saline formations. The objective of the analysis was to summarize volumetric capacity for brine disposal in the Appalachian Basin. Many different intervals are used for Class II brine disposal in the Appalachian Basin. Geologists have classified the injection zones into distinct formations based on rocks penetrated by oil and gas wells in the region. Overall, the injection zones fall within the Pennsylvanian-Cambrian interval, which consists of rock layers deposited 290 million to 540 million years ago.

A correlation chart (Figure 6-7) displays the nomenclature used in the project area of Ohio, eastern Kentucky, West Virginia, and Pennsylvania. Primary brine injection zones in the project area include the Cambrian basal sandstone, the Cambrian Copper Ridge Dolomite and Rose Run sandstone, the Silurian Medina Group/‘Clinton’ sandstone, the Silurian Lockport dolomite, the Devonian Oriskany sandstone, and Mississippian sandstone units. These reservoirs comprise a heterogeneous assemblage of carbonates and siliciclastics with complex porosity development and variable geographic distribution and thickness. Key factors that influence reservoir quality and injection potential are effective porosity and pore size distribution, permeability, reservoir heterogeneity, lithology, diagenesis, and presence and orientation of faults and fractures.

Class II brine disposal wells are distributed throughout the region (Figure 6-8). As shown, many of the wells were installed near hydrocarbon fields to accommodate produced water generated from oil and/or gas production. Therefore, many of the injection wells penetrate depleted oil and gas formations. Other injection wells penetrate deep saline formations that are mostly saturated with dense brine fluid.

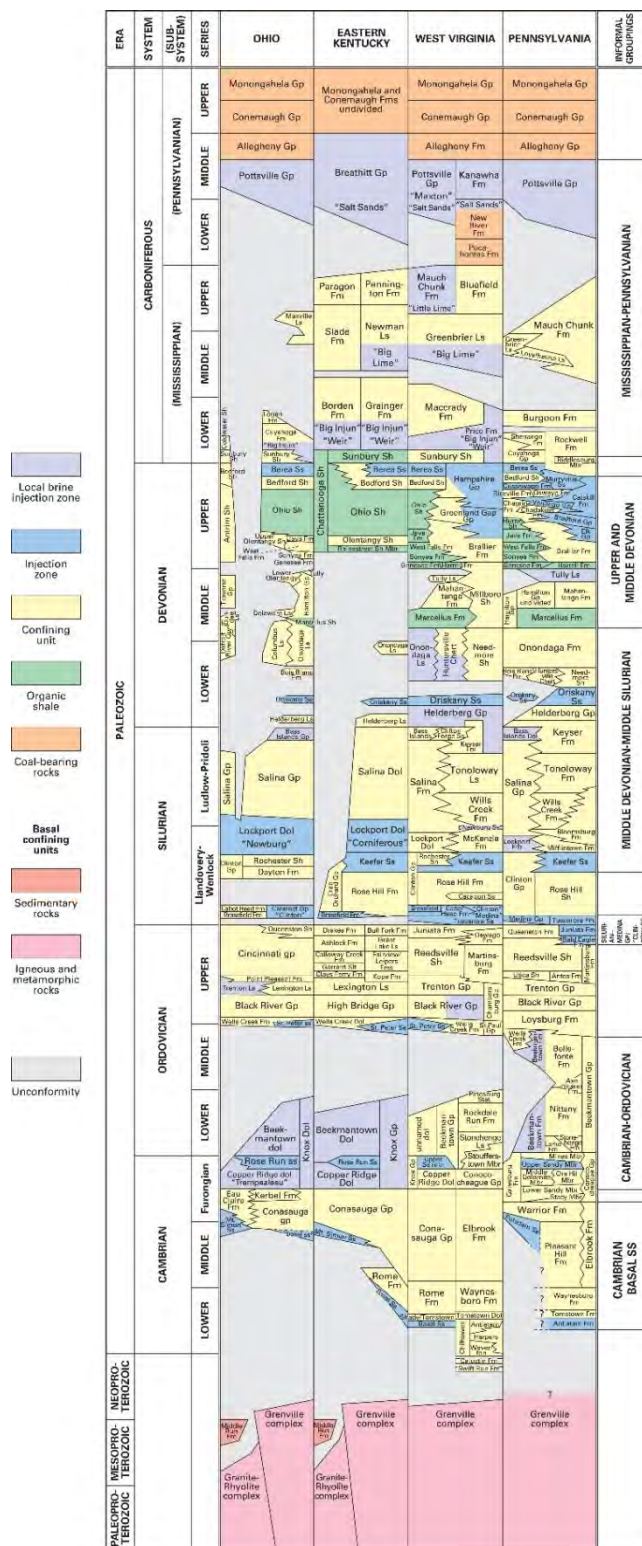


Figure 6-7. Stratigraphic correlation chart for the study area.

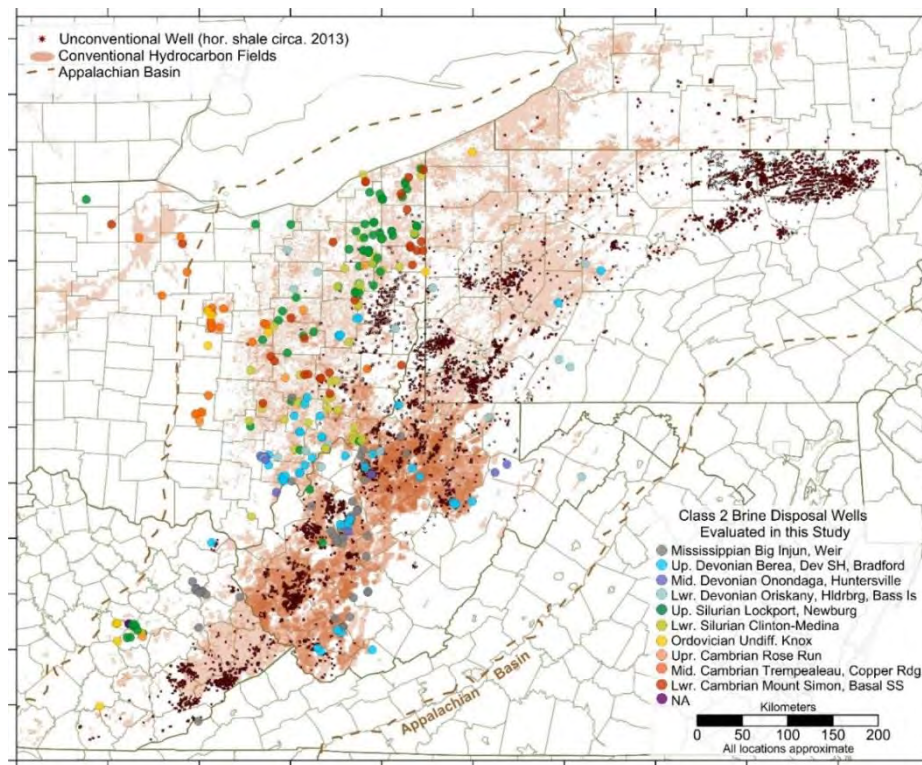


Figure 6-8. Distribution of Class II brine disposal wells, hydrocarbon fields, and unconventional wells.

6.2.2 Depleted Oil and Gas Formations

Sink capacity for brine disposal in depleted oil and gas reservoirs was estimated using the conventional methodology in the oil and gas industry to estimate the original oil in place STB, technically recoverable reserve, and volumetric capacity of reservoirs. Most of these reservoirs are depleted oil and gas reservoirs, while some are still in production through primary or secondary recovery means. The basis behind this effort is to systematically estimate the volume of brine that could be disposed of via Class II injection well into depleted oil and gas reservoirs, since brine disposal via Class II wells remains the preferred method for wastewater management. The data used to estimate the volumetric capacity of these reservoirs were primarily derived from the Petroleum Technology Transfer Council (PTTC) Tertiary Oil Recovery Information System (TORIS) database (PTTC, 2005). The data provided petrophysical parameters such as porosity, water saturation, area, thickness, and recovery factor (RF) required to make volumetric estimations.

The process of injection into depleted fields involves water being injected into the reservoir unit, where it is expected to occupy free portions of the pore space. In the case where other fluid types already occupy part of the pore space, the injected water is expected to displace residual fluid present within pores, since water is known to be denser than other fluids (such as gas or oil) that may be present. Furthermore, since the fields are no longer in production, the depleted

reservoirs are expected to be saturated with residual water, underpressurized due to hydrocarbon production, and the available pore space could be used for brine disposal.

Equation (6.1) (shown below) was used to calculate original oil in place (OOIP) for the different reservoirs; the result is estimated to be proportional to the wastewater storage capacity. The equation was modified only to exclude the shrinkage factor, since water volume is not expected to change significantly due to temperature or pressure changes both in reservoir or surface conditions.

$$OOIP = A * H * 7758 * \Phi * (1 - S_w) \quad (6.1)$$

where

OOIP	= $\sim Q_{\text{Brine}}$
OOIP	= original oil in place (STB)
Q_{Brine}	= volumetric capacity for brine disposal
A	= area (acre)
H	= thickness (ft.)
7758	= API bbl per acre-foot (used to convert acre-feet to STB)
Φ	= porosity, and
S_w	= water saturation.

Since it is not possible to access the entire reservoir column, a net-to-gross ratio could not be derived, so the entire reservoir thickness was used for the calculation. The various parameters used were sourced from data available for the Class II injection wells drilled in Kentucky, Ohio, Pennsylvania, and West Virginia fields. A total of approximately 324 Class II wells were used: 211 wells in Ohio, 30 in Kentucky, 7 in Pennsylvania, and 76 in West Virginia, drilled into various fields across the Appalachian Basin. Figure 6-9 shows all the oil and gas fields (including respective locations of the active Class II injection wells) in the Appalachian Basin. Figure 6-10 shows only the fields within the Appalachian Basin where active Class II injection wells have been drilled.

To complete the calculation for the volumetric capacity, it was important that we multiply the total capacity by an RF. The factor used was based upon the additional production and reserve estimates available in the TORIS database. The data were used to compute the RFs from various fields in the Appalachian Basin. We also calculated the 10th, 50th, and 90th population percentiles based on the series of data. A graph summarizing how p10, p50, and p90 were derived is shown in Figure 6-11. The derived values were then used to compute a recoverable reservoir volume with p10 (high), p50 (medium), and p90 (low) (Table 6-9).

Wells drilled within similar fields and into the same reservoir were accounted for, and the estimating process ensured that volumes were not double-counted by using the deepest formation penetrated, so the reservoirs could easily be sorted and summed up. Based on the available database, Table 6-9 shows the results of volumetric estimation in million barrels, for each formation in different states. Note that these estimates account only for oil and gas fields penetrated by Class II brine disposal wells. Additional capacity may be present in other depleted oil and gas fields in the region. Overall, results suggest that there may be brine disposal capacity for a median value estimate of 2,792 million bbl of brine in depleted oil and gas fields penetrated

by Class II brine disposal wells. Given the fact that total brine disposal volume in 2012 was 17.6 million bbl, the capacity may accommodate more than 150 years of injection.

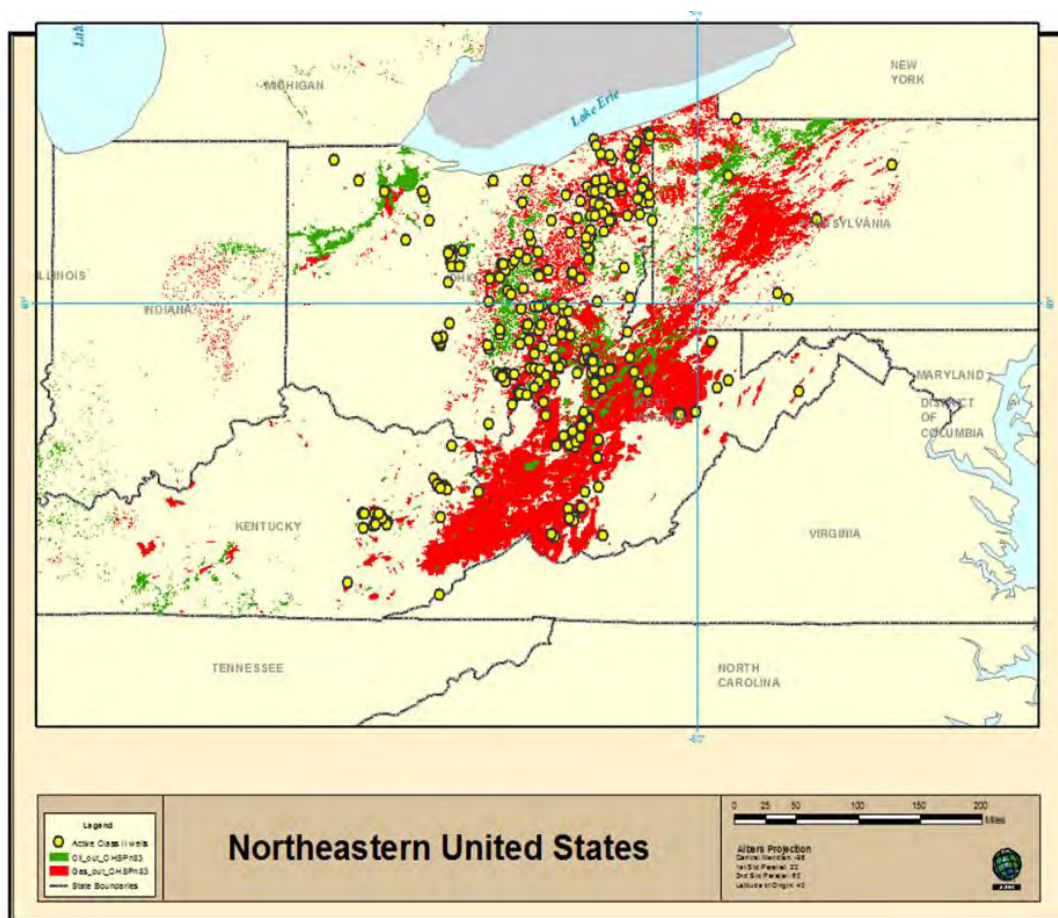


Figure 6-9. Oil and gas fields in the Appalachian Basin and locations of active Class II injection wells.

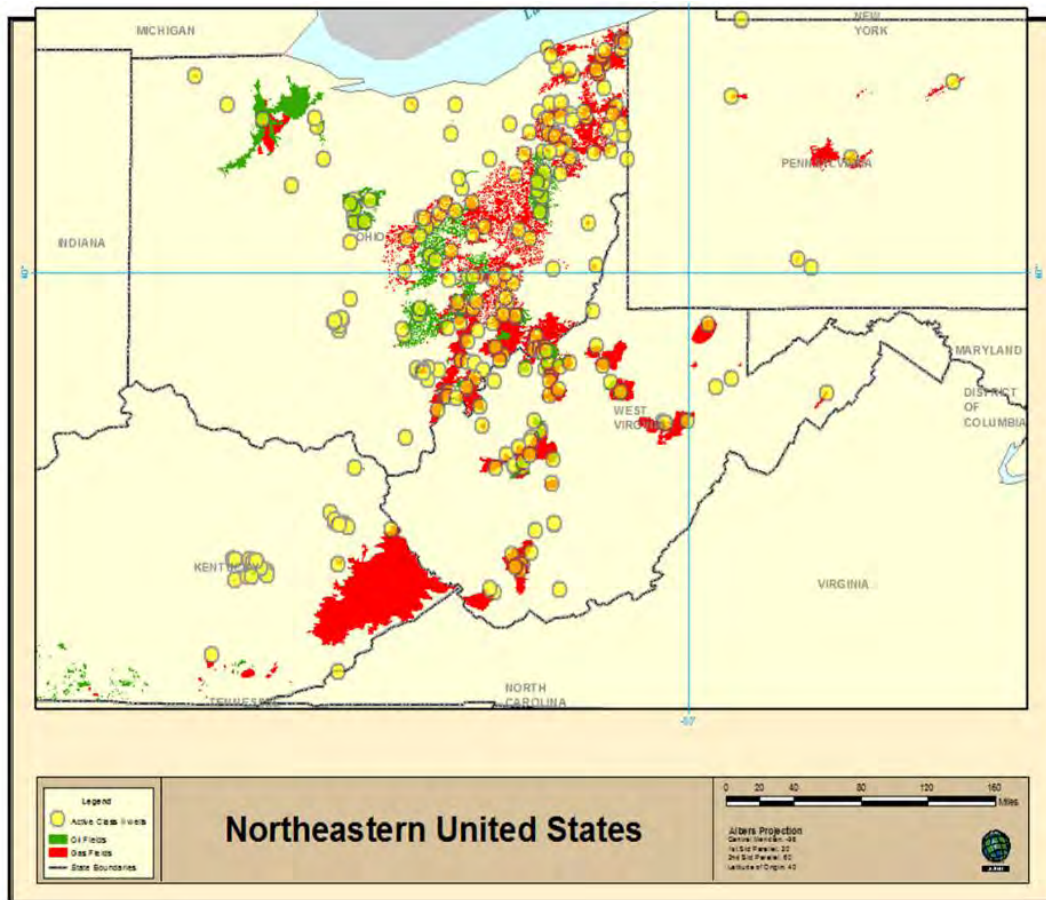


Figure 6-10. Locations of active Class II injection wells and related oil and gas fields in the Appalachian Basin.

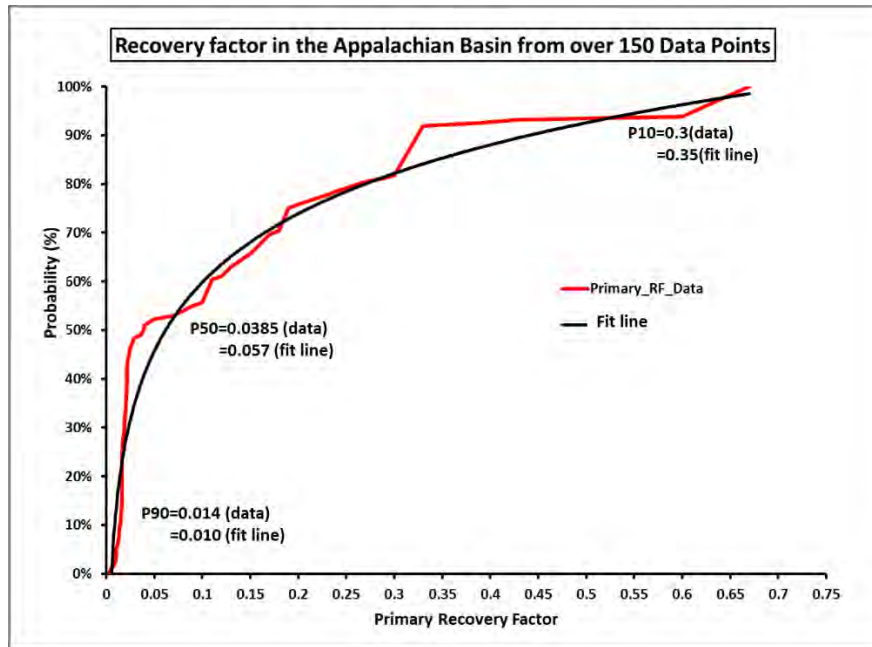


Figure 6-11. Recovery rate in the Appalachian Basin.

Table 6-9. Volumetric capacity in depleted oil and gas reservoirs penetrated by existing Class II brine disposal wells.

Well Injection Interval ^a	Total Pore Space	RF_High P10	RF_Med P50	RF_low P90
	(MMbbl)			
Pennsylvanian-Mississippian (Big Injun, Weir, Maxton, etc)	2,141	642.3	82.1	30.0
Upper Dev. (Berea, Dev SH, Bradford)	8,846	2653.9	340.0	123.7
Mid. Dev. Ondondaga, Huntersville	4,093	1228.2	157.7	57.5
Lwr Dev. Oriskany-Helderberg-Huntersville, Bass ls.)	4,215	1264.3	161.9	58.6
Upper Sil. Lockport, Newburg, Corniferous	16,944	5083.4	651.9	237.4
Lwr Silurian Clinton-Medina	18,585	5575.1	715.0	260.4
Undiff. Knox	2,639	791.9	101.7	36.8
Rose Run	2,145	644.1	82.9	29.7
Copper Ridge, Trempealeau	2,508	752.0	96	35.0
Mount Simon, Basal SS	10,444	3133.0	402	146.0
N/A-other	7.91	2.4	0.3	0.11
Total	72,567	21,770	2,792	1,015

Note: MMbbl = million barrels RF = recovery factor.

a. Based on deepest formation in the well's injection interval.

Other depleted oil and gas fields not currently used for brine disposal may offer additional capacity. Since the depleted oil and gas fields have demonstrated the ability to contain hydrocarbons and are depressurized, they may be appealing targets for brine injection. However, many of the fields are still targets for additional oil and gas production. The fields may also be penetrated by many oil and gas wells.

6.2.3 Deep Saline Formations

Many other deep saline rock formations in the region are suitable for brine disposal. These formations are typically saturated with saline formation fluids. The data used for deep saline formation volumetric capacity were collected from the report *Characterization of Geologic Sequestration Opportunities in the MRCSP Region* (Wickstrom et al., 2005). The report documented estimates of CO₂ storage capacities (in gigatonnes [GT]) for various deep saline formations. Capacity was estimated with a volumetric calculation based on formation areal coverage, thickness, and porosity. The total pore space was multiplied by a 1% low-end and 4% high-end efficiency factor (EF) to account for water saturation, gross-net reservoir thickness, and other factors (Goodman et al., 2011; DOE, 2012). A general conversion factor of 1 metric ton of CO₂ to 9 bbl water was used to convert the storage capacity into barrels of water; results were assumed to be proportional to wastewater storage capacity:

$$1 \text{ metric ton } CO_2 = \frac{1 \text{ m}^3 CO_2}{0.7 \text{ metric ton } CO_2} * \frac{6.3 \text{ bbl brine}}{1 \text{ m}^3 \text{ brine}} = 9 \text{ bbl brine} \quad (6.2)$$

(based on average CO₂ density of 0.7 metric ton/m³ at supercritical conditions)

The deep saline formation capacity estimates are based on formation coverage across broad areas throughout the region. Many of the formations are present throughout entire state areas. Thus, the capacities are more of a “resource” rather than proven “reserve.” As such, fairly conservative EFs were applied to the capacity estimates. The estimates were also limited to rocks over 2800 ft deep, so these estimates do not account for some of the shallow brine injection intervals in the Appalachian Basin.

The results of the conversion are presented in Tables 6-10 through 6-16. Overall, these calculations suggest there is capacity for 480 billion bbl of brine injection in the deep saline formations based on a 2.5% EF. The capacity is several thousand times greater than the 17.6 million bbl of brine injected in 2012 in the Appalachian Basin. The capacity is distributed across large areas. However, accessing the capacity may be limited by the injectivity of the formations.

Table 6-10. Volumetric capacity of Medina sandstone.

Medina sandstone estimated storage capacity (in billion barrels)						
State	Area (mi ²)	Total (GT)	Total (MMMbbl)	4% EF	2.5% EF	1% EF
				(MMMbbl)		
E. Kentucky	420	0.89	7.98	0.32	0.20	0.08
Ohio	15,647	55.79	502.15	20.09	12.56	5.02
Pennsylvania	31,333	360.24	3,242.15	129.69	81.06	32.42
West Virginia	23,642	254.59	2,291.34	91.65	57.28	22.91
Total	71,042	672	6,044	242	151	60

Note: GT= Gigatonnes, 1Gigatonnes= 10⁹Metric tonnes, 1Metric tonne= 9bbl, 1Gigatonnes=9MMMbbl.

Table 6-11. Volumetric capacity of Rose Run sandstone.

Rose Run sandstone estimated storage capacity (in billion barrels)						
State	Area (mi ²)	Total (GT)	Total (MMMbbl)	4% EF	2.5% EF	1% EF
				(MMMbbl)		
E. Kentucky	13,146	54.4	490	19.60	12.25	4.90
Ohio	16,353	81.0	729	29.16	18.22	7.29
Pennsylvania	22,222	297.5	2,677	107.09	66.93	26.77
West Virginia	5,438	52.2	469	18.77	11.73	4.69
Total	57,159	485	4,365	174.6	218.3	43.6

Note: GT= Gigatonnes, 1Gigatonnes= 10⁹Metric tonnes, 1Metric tonne= 9bbl, 1Gigatonnes=9MMMbbl.

Table 6-12. Volumetric capacity of Oriskany sandstone.

Oriskany sandstone estimated storage capacity (in billion barrels)						
State	Area (mi ²)	Total (GT)	Total (MMMbbl)	4% EF	2.5% EF	1% EF
				(MMMbbl)		
E. Kentucky	7	0.019	0.171	0.01	0.005	0.00
Ohio	1,123	9.81	88.29	3.53	2.20	0.88
Pennsylvania	29,002	76.69	690.21	27.61	17.26	6.90
West Virginia	22,265	100.49	904.41	36.18	22.61	9.04
Total	52,397	187	1683	67.3	42.1	16.8

Note: GT= Gigatonnes, 1Gigatonnes= 10⁹Metric tonnes, 1Metric tonne= 9bbl, 1Gigatonnes=9MMMbbl.

Table 6-13. Volumetric capacity of Potsdam sandstone.

Potsdam sandstone estimated storage capacity (in billion barrels)						
State	Area (mi ²)	Total (GT)	Total (MMMbbl)	4% EF	2.5% EF	1% EF
				(MMMbbl)		
Ohio	18	0.02	0.19	0.00	0.00	0.00
Pennsylvania	9,280	17.04	153.35	6.13	3.83	1.53
Total	9,298	17.0	153.5	6.1	3.8	1.5

Note: GT= Gigatonnes, 1Gigatonnes= 10⁹Metric tonnes, 1Metric tonne= 9bbl, 1Gigatonnes=9MMMbbl.

Table 6-14. Volumetric capacity of unnamed Conasauga sandstone.

Unnamed Conasauga sandstones estimated storage capacity (in billion barrels)						
State	Area (mi ²)	Total (GT)	Total (MMMbbl)	4% EF	2.5% EF	1% EF
				(MMMbbl)		
E. Kentucky	25	0.02	0.14	0.00	0.00	0.00
Ohio	21,185	34.69	312.17	12.49	7.80	3.12
Pennsylvania	2,410	4.59	41.35	1.65	1.03	0.41
West Virginia	943	1.61	14.52	0.58	0.36	0.15
Total	24,563	40.9	368.2	14.7	9.2	3.7

Note: GT= Gigatonnes, 1Gigatonnes= 10⁹Metric tonnes, 1Metric tonne= 9bbl, 1Gigatonnes=9MMMbbl.

Table 6-15. Volumetric capacity of unnamed Rome Trough sandstone.

Rome Trough sandstone estimated storage capacity (in billion barrels)						
State	Area (mi ²)	Total (GT)	Total (MMMbbl)	4% EF	2.5% EF	1% EF
				(MMMbbl)		
E. Kentucky	13,157	10.00	90.05	3.60	2.25	0.90
Ohio	201	0.06	0.53	0.02	0.01	0.01
West Virginia	5,094	2.21	19.92	0.80	0.50	0.20
Total	18,452	12.3	110.5	4.4	2.8	1.1

Note: GT= Gigatonnes, 1Gigatonnes= 10⁹Metric tonnes, 1Metric tonne= 9bbl, 1Gigatonnes=9MMMbbl.

Table 6-16. Volumetric capacity of Mount Simon sandstone formation.

Mount Simon sandstone estimated storage capacity (in billion barrels)						
State	Area (mi ²)	Total (GT)	Total (MMMbbl)	4% EF	2.5% EF	1% EF
				(MMMbbl)		
E. Kentucky	6,661.00	43.36	390.25	15.61	19.51	3.90
Ohio	19,768.00	193.90	1,745.11	69.80	43.62	17.45
Total	26,429	237.3	2,135	85.4	53.4	21.4

Note: GT= Gigatonnes, 1Gigatonnes= 10⁹Metric tonnes, 1Metric tonne= 9bbl, 1Gigatonnes=9MMMbbl.

6.3 PA Recycle Reuse Case Study

Large volumes of water are used in the hydraulic fracturing process for unconventional shale wells. After the fracturing process, some of the water returns to the surface with formation water. In the early stages of unconventional shale development, much of this flowback water was sent to wastewater treatment plants or Class II disposal wells, but operators have increased emphasis on reusing and recycling fluids. Pennsylvania DEP's Office of Oil and Gas Management tracks wastewater streams in Pennsylvania. Other states in the study area do not track the source of wastewater in as much detail as Pennsylvania. However, since reuse/recycle methods reduce costs associated with wastewater disposal, it is likely that operators use similar methods in other states. Wastewater recycle/reuse trends in Pennsylvania are analyzed in the following study.

Between 2004 and 2012, more than 3,000 shale gas wells were completed in the Commonwealth of Pennsylvania. The number of wells completed annually was relatively low in the first few years but then increased dramatically, peaking in 2010 (Figure 6-12). These statistics represent only those wells for which completion reports with open flow and/or completion (perforation and stimulation) data had been received and processed by the PaGS as of January 2014 (PA*IRIS/WIS, 2014).

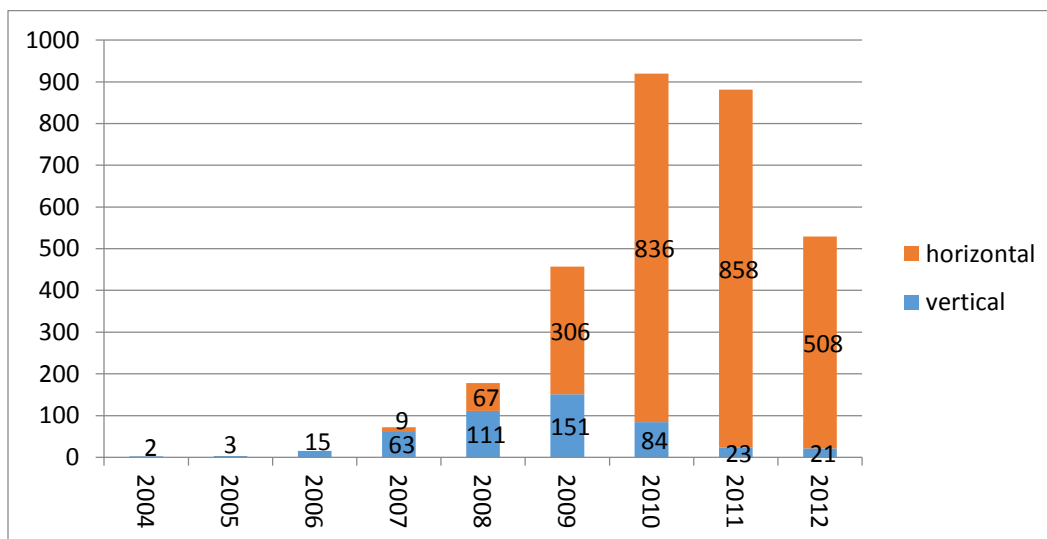


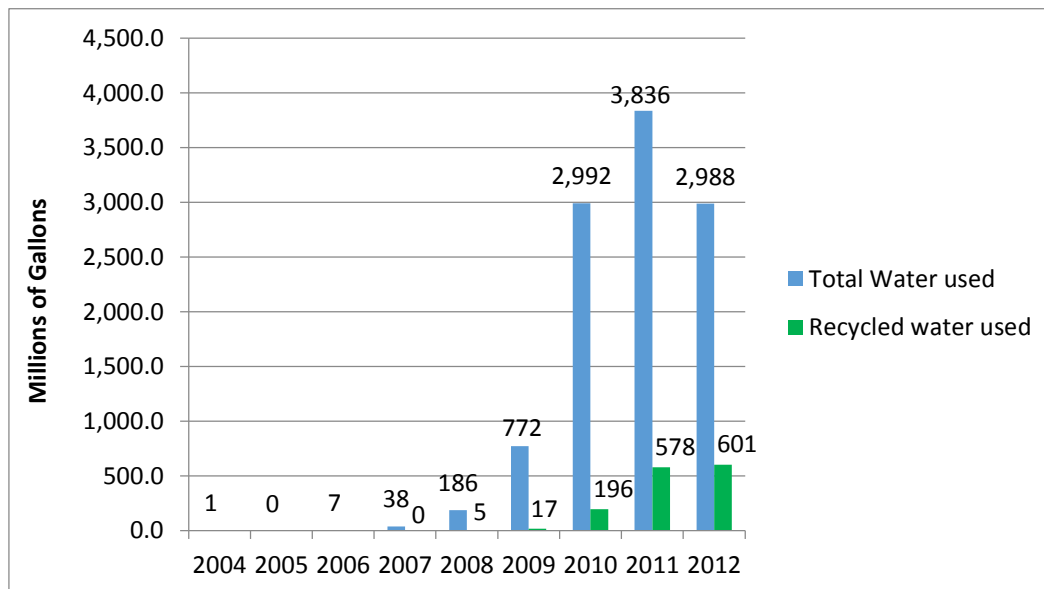
Figure 6-12. Annual horizontal and vertical shale well completion data for Pennsylvania.

Most, but not all, shale wells in the Appalachian Basin are stimulated by hydraulic fracturing to produce natural gas or oil. A limited number of wells produce gas naturally and do not need to be completed with hydraulic fracturing. The amount of water and other substances used to hydraulic fracture a well is reported on the completion report submitted to the Pennsylvania DEP. Figure 6-13 provides an example of fluid composition data included in such a report. Older reports are frequently not as detailed, as DEP did not require fracture fluid reporting for unconventional wells until 2012. In most cases, water is the main component used to treat a well, but other primary agents include nitrogen, foam, or carbon dioxide (CO₂). These would be reported under the 'Other Base Fluid(s) Used' section of the form.

STIMULATION BASE FLUID				
List Water Management Plan Source(s)		Water Management Plan ID	Volume (Gallons)	
1. Aqua		246326-4	3,228,456	
2. Parys Impoundment		246326-4		
3. Allen Impoundment		246326-4		
4. Neiley Impoundment		246326-4		
5. Cook N SUS 2H		246326-4		
6. Deer Park/MTN Energy		246326-4		
		DEP Biologist Review/Date	Total Gallons of Water Used 3,871,434	Water 3,228,456 Recycled 642,978
Other Base Fluid(s) Used			Quantity and /UOM	
1.			/	
2.			/	
			Total Quantity all Fluid(s)	/
STIMULATION/PRODUCTION INFORMATION (WELL)				

Figure 6-13. Example of hydraulic fracture water data included in a well completion report.

Annual water volumes used in the fracture treatment of shale gas wells from Pennsylvania from 2004-2012 are illustrated in Figure 6-14. As true vertical depths and lateral lengths increase for these unconventional shale wells, more water has been used to treat each well (Schmid, 2012), leading to a water use peak in 2011 due to increasing lateral lengths. Figure 6-14 also illustrates the increased use of water recycled from flowback or production water.



Note: The total volume will increase as more well completion reports are received and processed by PaGS.

Figure 6-14. Total volume and recycled volumes used to treat shale wells in Pennsylvania.

The amount of water used to complete a shale well depends on a variety of factors, including the orientation of the well (horizontal vs. vertical), the hydraulic fracture fluid composition, and the geologic unit targeted. For example, an average vertical Marcellus well in Pennsylvania uses 811,000 gallons of water, while a horizontal well averages 4.3 million gallons (PA*IRIS/WIS, 2014). In contrast, an average horizontal Marcellus well completed with foam uses 267,000 gallons of water. Horizontal Utica wells in Pennsylvania average 2.4 million gallons of fracture water per completion.

After a well has been hydraulically fractured, some of the treatment water returns to the surface with formation (brine) water. For the time period of July 2009 through December 2013, Pennsylvania's Marcellus wells averaged 724,000 gallons, and Utica wells averaged 656,000 gallons, of wastewater produced per well (PA DEP, 2014). A conversion factor of 42 was used to change units from barrels to gallons for easier comparison, as wastewater is reported to Pennsylvania's DEP in barrels and fracture water is usually reported in gallons.

Water returned to the surface after a fracture job needs to be handled in an environmentally responsible manner. The Pennsylvania DEP requires operators to measure and manage these fluids, as well as report the ultimate fate of these waters. As reported, 99% of the wastewater either is either disposed of in various treatment plants and injection disposal wells or recycled. The favored method for wastewater disposal has changed over time, as seen in Figure 6-15. Since 2009 (the year Pennsylvania DEP began tracking water management associated with shale gas well completions), the amount of wastewater disposed of at treatment plants has not changed appreciably. However, discharges to municipal waste treatment plants from shale wells have been eliminated altogether as a result of a voluntary ban that began in May 2011. This 'treatment plant' category includes centralized treatment plants for recycling or discharge, industrial waste treatment plants, municipal waste treatment plants, and residual waste processing facilities.

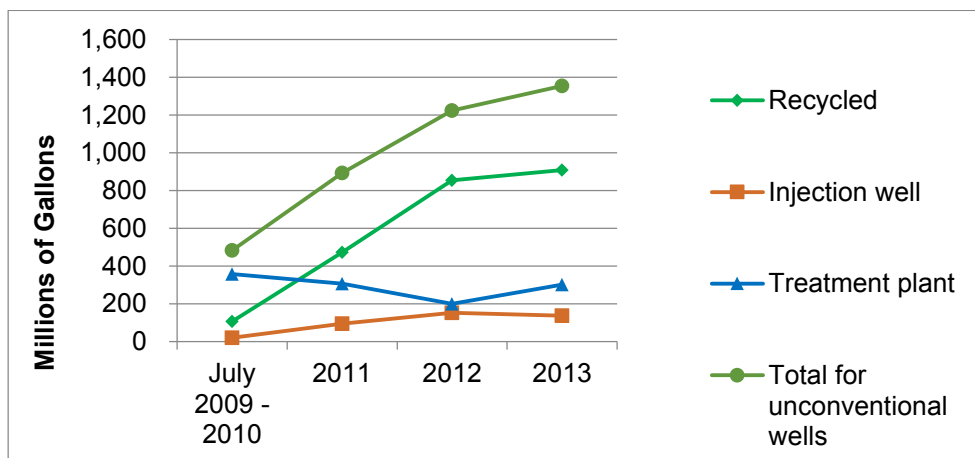
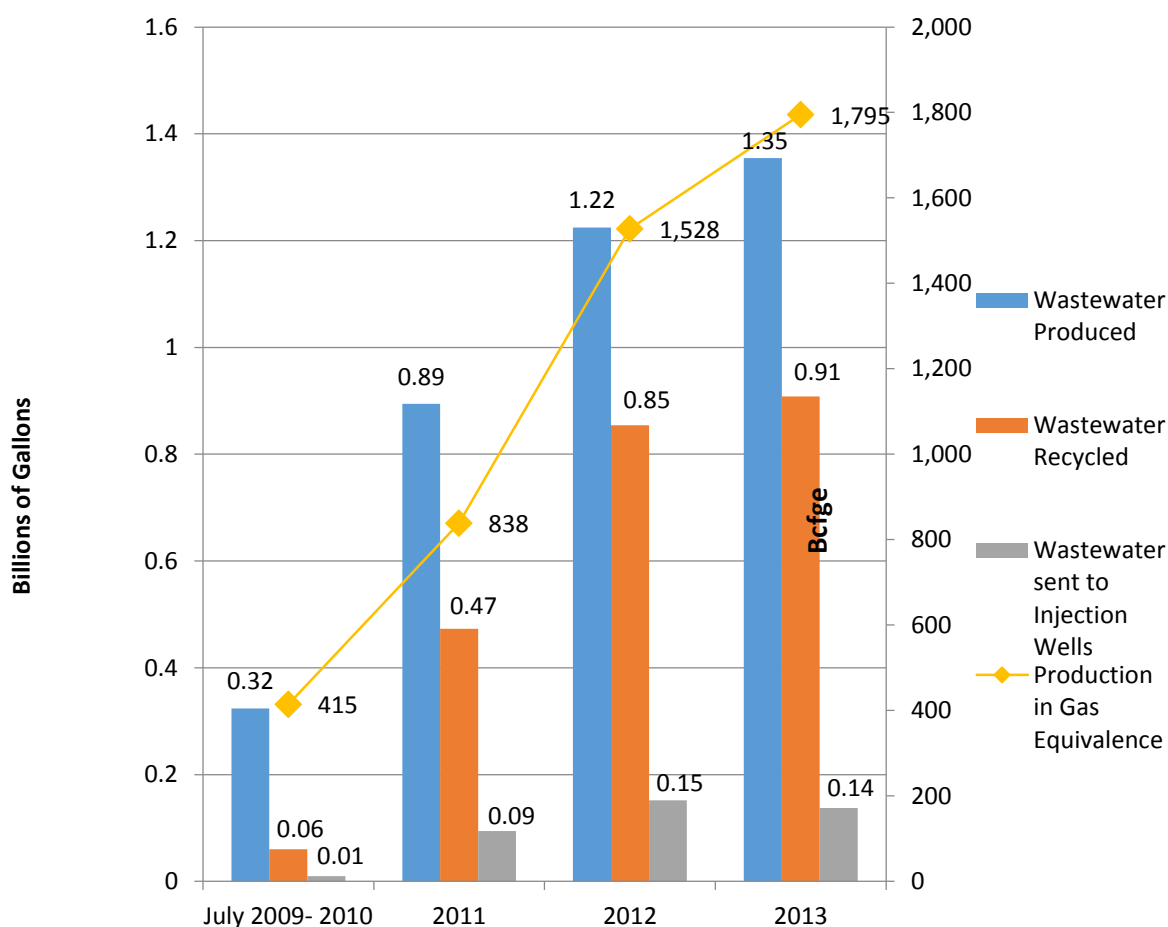


Figure 6-15. Disposal methods for wastewater from unconventional wells in Pennsylvania.

The practice of recycling and reusing water in drilling and completion operations has risen substantially in the last several years. Specifically, the amount of recycled water used to fracture shale gas wells has risen from 0% (0 gallons) in 2006 to about 20% (246 million gallons) in 2013 (PA*IRIS/WIS, 2014), and the amount of wastewater being recycled has risen from 22% (60 million gallons) in 2010 to 67% (908 million gallons) in 2013 (PA DEP, 2014). Disposal via injection wells has increased from 10 million gallons in 2010 to 138 million in 2013. As might be expected with the increase in the number of unconventional wells drilled during this time period, the volume of generated wastewater has nearly tripled over the past five years.

In summary, the volumes of both petroleum hydrocarbon products and associated wastewaters have increased substantially over the last five years in Pennsylvania (Figure 6-16). Much of this

water is being recycled to fracture new wells. The amount of wastewater from unconventional wells sent to injection wells in Pennsylvania has also increased appreciably, but appeared to stabilize in 2013.



Note: BCGE = billion cubic feet gas equivalent.

Figure 6-16. Annual natural gas equivalent production and wastewater production from Pennsylvania shale gas wells.

6.4 Update of Brine Disposal Activity: 2012-2014

As described in Section 2.0, operational data were compiled for the 2008-2012 time period, because at the time only 2012 and older data were available. To provide an update on the status of Class II brine disposal in the region, information was compiled to identify UIC Class II brine disposal wells permitted between 2012 and 2014 in Ohio, West Virginia, Kentucky, and Pennsylvania. This information was collected to update and supplement the 2008-2012 data for the 324 brine disposal wells previously incorporated in the RPSEA database.

Information for Class II brine disposal wells permitted post-August 2012 was compiled from files provided directly by Kentucky, Pennsylvania, and West Virginia state departments/geological surveys and from online database searches. Key information gathered for each well included location, total depth (TD), injection formation, operator, permit issue date, and surface elevation. An attempt was made to obtain well status information, but it should be

noted that discrepancies and frequent status changes were observed on status reports for wells in all four states.

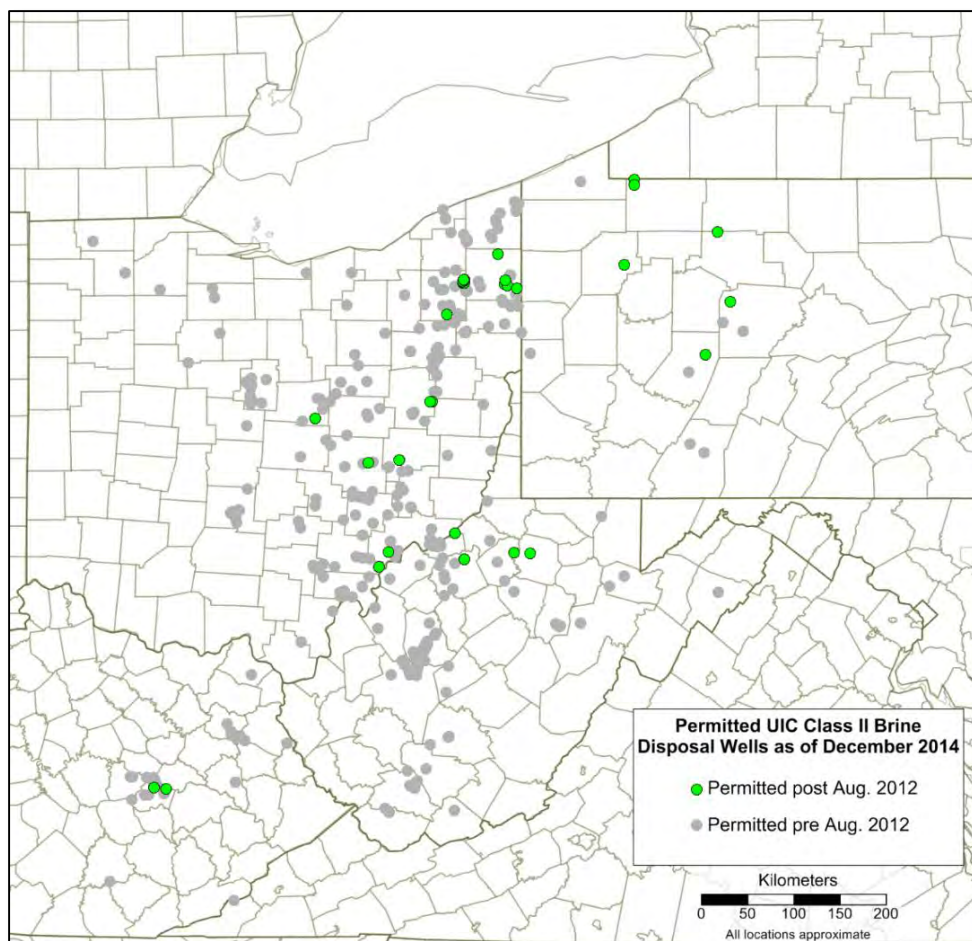
Since August 2012, approximately 34 new UIC Class II brine disposal wells have been issued in the Northern Appalachian Basin study area (Figure 6-17). Targeted injection zones for these wells include the Devonian System (sandstones and shales), the Onondaga Limestone, Huntersville Chert, Oriskany sandstone, Lockport dolomite, the Clinton-Medina group, the Knox group, the Rose Run sandstone, and basal Cambrian sandstones (Table 6-17). Silurian formations are reported as the targeted injection zones for a majority (56%) of these recently permitted wells, followed by Ordovician and deeper formations (29%), and Devonian sandstones and shales (15%).

The number of wells permitted in each state and the targeted injection zones are listed in Table 6-18. Twenty-two of the 34 wells permitted since August 2012 are in Ohio, and 6 of those 22 permitted wells were reported as actively injecting as of December 2014. The interval extending from the Silurian Lockport dolomite to the basal Cambrian sandstones is the injection target for 21 of the 22 Ohio wells. The well permitting timeframe is approximately 8 to 16 months in Pennsylvania and Kentucky, in contrast to 2 to 3 months in Ohio and West Virginia (McCurdy, 2011; Platt, 2009; Skoff and Billman, 2013; Yoxtheimer, 2015). Permitting is based on performance (initial test injection results, well operation), requiring wells to be emplaced in porous and permeable zones separated from underground sources of drinking water by a confining zone free of faults or fractures within a defined area near the injection well. Public notification and opportunity for a public hearing may also be required (USEPA, 2002).

The USEPA has issued six UIC permits for Class II brine disposal wells to be drilled and operated in Pennsylvania since August 2012, with two wells each targeting the Upper Devonian System, the Huntersville Chert, and Oriskany Sandstone, and the Clinton-Medina Group for storage. The Oriskany Sandstone is reported to have potential for becoming a major brine injection zone in Pennsylvania.

Four Class II brine injection wells permitted post-August 2012 were identified in West Virginia. Upper Devonian sandstones are reported as the target storage zone for two of the wells. One well each is emplaced in the Oriskany Sandstone and the Clinton-Medina Group for storage. Due to limitations imposed by greater basin depths in West Virginia relative to Ohio, Kentucky, and Pennsylvania, it is unlikely that zones deeper than the Silurian will be targeted for brine injection in the future. Three of the four wells in West Virginia are reported as actively injecting.

Two UIC Class II brine disposal wells have been permitted in Kentucky since August 2012, targeting dolomite units within the Knox Group for storage. As of December 2014, neither of these newly permitted Kentucky wells was reported to be actively injecting.



Note: Well locations shown in green. Gray dots represent wells with operational data previously incorporated in the RPSEA database.

Figure 6-17. Locations of UIC Class II brine injection wells permitted since August 2012 in the Northern Appalachian Basin.

Table 6-17. Number of UIC Class II brine injection wells permitted post-August 2012 and the targeted injection zones reported in the study area.

Age (period)	Injection Zone	Wells Permitted 2012-2014		
		#	%	
Devonian	Venango Sandstone	3	15%	
	Elk Sandstone	1		
	Undiff. shales	1		
Silurian	Onondaga / Huntersville / Oriskany	3	56%	
	Lockport Formation	12		
	Clinton-Medina Group	4		
Ordovician	Knox Group	8	29%	
Cambrian		Rose Run Sandstone		1
		Basal Sandstone.		1
TOTAL		34		

Table 6-18. Number of UIC Class II brine injection wells permitted post-August 2012 and the targeted injection zones reported in each state.

Age (period)	Injection Zone	No. of Permitted Wells				
		PA	WV	OH	KY	
Devonian	Venango Sandstone	1	2			
	Elk Sandstone	1				
	Undiff. shales			1		
Silurian	Onondaga / Huntersville / Oriskany	2	1			
	Lockport Formation			12		
	Clinton-Medina Group	2	1	1		
Ordovician	Knox Group			6	2	
Cambrian		Rose Run Sandstone			1	
		basal sandstones			1	
Subtotal		6	4	22	2	
TOTAL		34				

7. Tools/Products for Industry/Operators

The objective of the tool and product development effort was to translate the RPSEA project results into practical products and tools for industry application. The audience for these tools may include operators, regulators, and the research community. Products generated under the task included an informational pamphlet on injection zones, a wellhead pressure estimator, a summary of well logging options for Class II brine disposal wells, and a review of monitoring methods for injection operations.

7.1 Injection Zone Summary

To summarize injection zones in the Appalachian Basin, a series of maps, cross sections, and tables were prepared and integrated into an informational pamphlet. As described in Section 3.0, regional stratigraphic correlations were compiled across Eastern Kentucky, Ohio, Pennsylvania, and West Virginia. The correlations were depicted in a stratigraphic chart that identifies injection intervals, confining units, and organic shales. The chart illustrates terminology across state borders and the informal ‘drillers’ names’ for injection zones. Based on the chart, key formations were identified for mapping. Structure and isopach maps were developed for these formations (see Section 3.0). The maps were based on other mapping efforts for projects on CO₂ storage and oil and gas research, but the maps were updated to honor formation data for brine disposal wells. Maps included structure maps, isopach maps, and more detailed local analysis of facies and other geological features. Geologic cross sections were also prepared in association with the geocellular model discussed in Section 5.0. Overall, it was determined that local cross sections were more useful for evaluating injection zones.

The informational pamphlet provides end users with an easy-to-use product summarizing the distribution, operational data, and geologic properties of the injection zones in the Appalachian Basin. The pamphlet includes an injection zone geologic description, an example of a geophysical log, a graph illustrating monthly injection rates, and a map of the well locations (Figure 7-1). A full version of the pamphlet is provided in Appendix. The pamphlet was provided to industry and operators.

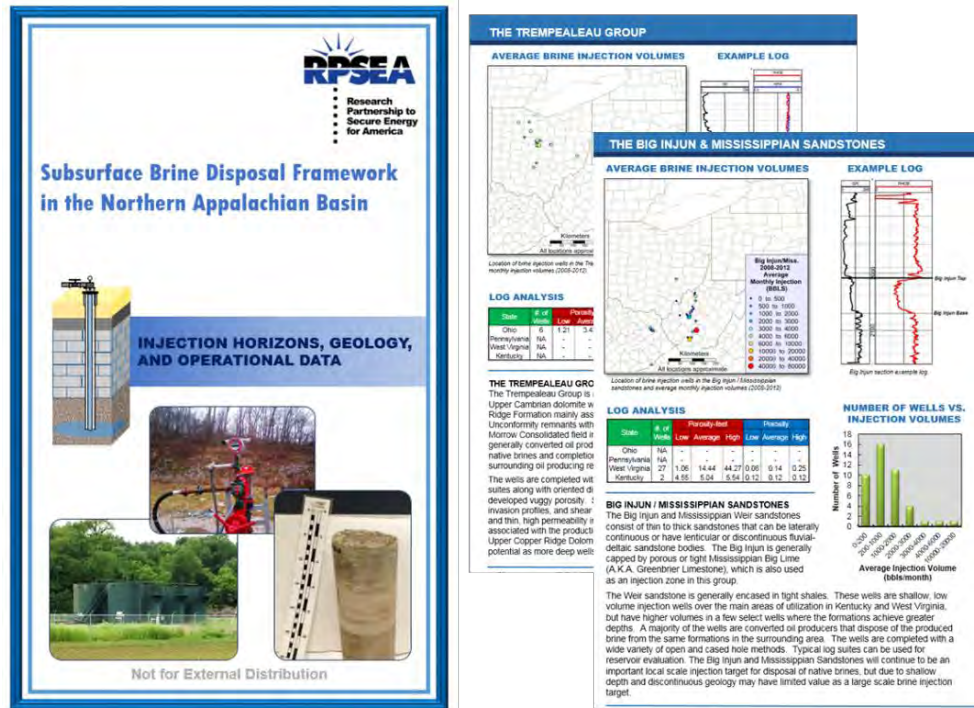


Figure 7-1. Informational pamphlet for Class II brine disposal wells in the Appalachian Basin.

7.2 Wellhead Pressure Regression Estimator

One objective of the tool and product development effort was to develop calculation tools for operating parameters related to brine disposal in key injection horizons using spreadsheet formats. The calculation tools incorporated items such as flow rates, wellhead pressure, BHP, temperature, and reservoir parameters. Typical data made available for brine injection operations include the injection zone depth, injection volumes per month, and the corresponding wellhead pressures. Several options are available to analyze injection flow rates and pressures, ranging from simple analytical equations (Horner, 1951; Matthews and Russell, 1967; Earlougher, 1977; Lee, 1982) to complex numerical models (Saripalli et al., 2000; Nicot and Chowdhury, 2005). However, many of the key parameters necessary for these methods were based on assumptions (permeability, porosity, reservoir boundaries), because these properties are not always well-defined for the injection zones in the region or are only available after a well has been drilled and tested for these properties. To provide general guidance on expected injection rates or operating pressures for Class II brine disposal wells in our study area, a basic regression analysis was completed to correlate the average tubing pressures as a function of the typically available monthly injection rates and injection depths. This empirical analysis was utilized to provide some basic guidance on injection rates that may be expected in the region.

The estimator was based on a simple linear regression using average injection rate, average wellhead pressure, and maximum depth of the injection interval from monthly operational data compiled from 324 wells for 2008-2012 under this project. Figure 7-2 shows wellhead pressure

versus maximum injection depth interval for wells analyzed. There is a large amount of variability in the data. The wells show a general trend of increasing pressure with depth. This trend is likely related to the pressure necessary to overcome hydrostatic pressure with depth, which may be higher in formations with dense brines. Figure 7-3 shows a graph of average wellhead pressure versus average injection rate for operational data from 2008-2010. While the data show a general trend of higher injection rate with higher wellhead pressures, there is much variability. Many wells operate at low pressure and rates, likely on an intermittent basis, which may bias data to the lower-end injection rates. Additional efforts to investigate the relationship between reservoir thickness, porosity, and permeability to injection performance are limited by sparse data availability for any formation-specific analysis discussed in Chapter 2.0.

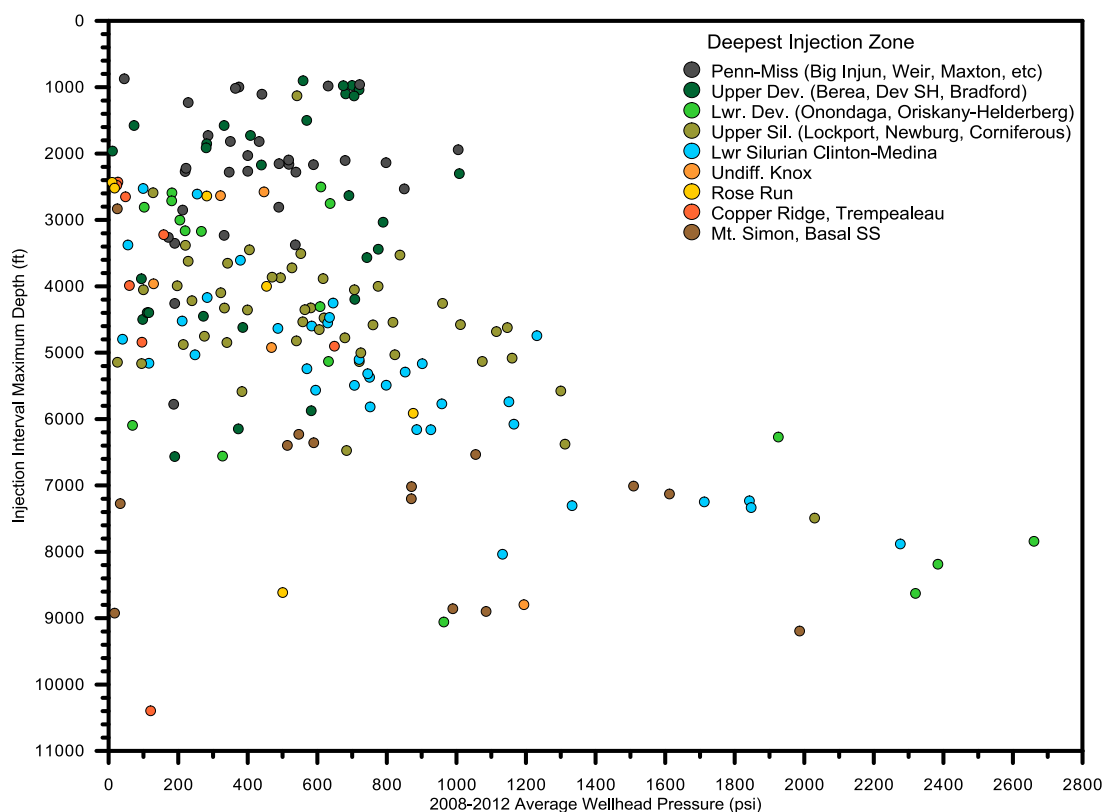


Figure 7-2. 2008-2012 average wellhead pressure versus depth.

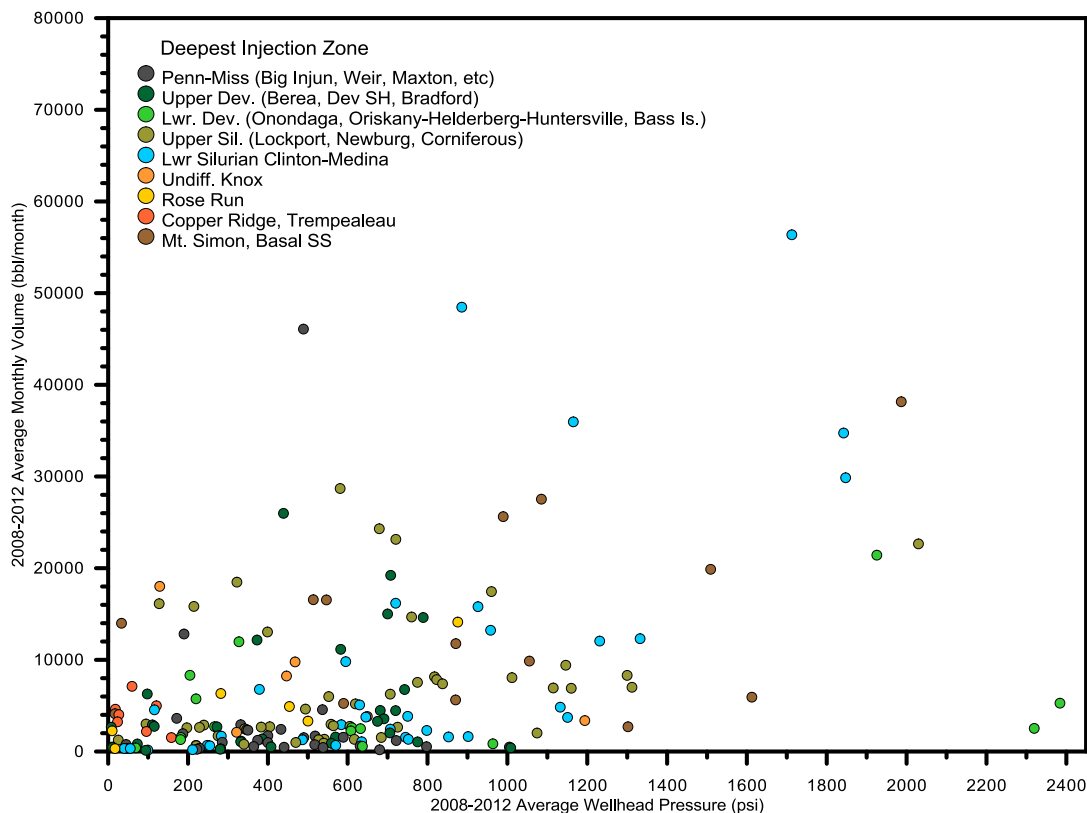


Figure 7-3. 2008-2012 average wellhead pressure versus average monthly injection rate.

To provide general guidance on expected wellhead pressures for injection intervals in the Appalachian Basin, a basic regression model was developed. This analysis was strictly based on operational data from 2008-2012. It assumes injection into one of the typical injection zones in the region. Overall, the analysis provides some general guidance that may be used to predict pressures for injection rates at depth based on generally available historical operational data. More site-specific characterization, analysis, drilling, and testing would be necessary to support the planning and completion of a Class II brine disposal well.

Average wellhead tubing pressure (P) was determined as a function of the depth of formation (D) and injection rate (Q) from the injection data. Lower value responses were excluded from the analysis based on injection rate of 100 bbl per month and wellhead tubing pressure of 100 psi cutoffs, because these wells did not significantly pressure the reservoir. After applying cutoffs, there were 135 responses to perform the analysis. The cutoffs were applied to screen out wells that inject at lower rates, which do not have enough injection to generate significant reservoir response.

Table 7-1 shows the resulting correlation matrix for all three parameters. The value of a matrix is its ability to show how each parameter correlates with other two. The matrix is the measure of linear relationship between two parameters. It shows a stronger relationship between pressure

vs. depth (0.58) and pressure vs. injection rate (0.49). Physically, formation depth is not responsive to higher or lower injection rate. Formation depth is an independent parameter; nevertheless, we see the linear relationship with correlation coefficient of 0.40 for injection rate vs. depth.

Table 7-1. Correlation coefficients for regression analysis.

	Total Depth (ft)	2008-2012 Avg. Monthly Volume (bbl/mo)	2008-2012 Avg. Monthly Tubing Pressure (psi)
Total Depth (ft)	1	---	---
2008-2012 Avg. Monthly Volume (bbl/mo)	0.402	1	---
2008-2012 Avg. Monthly Tubing Pressure (psi)	0.584	0.491	1

The regression fit for estimating wellhead tubing pressure (P) as function of formation depth (D) and injection rate (Q) was developed as follows:

$$P(\text{Avg Tubing Pressure, psi}) = c_1 \times D(\text{Depth, ft}) + c_2 \times Q \left(\text{Avg Inj. Rate, } \frac{\text{BBL}}{\text{Month}} \right) + c_0 \quad (7.1)$$

Table 7-2 summarizes descriptive statistics for the regression analysis performed for the selected data, including lower and upper confidence intervals for reference.

Table 7-2. Summary of regression fit coefficients.

	Coefficients	Standard Error	t Stat	P-value	Lower 95%	Upper 95%
Intercept	162.3	71.1	2.28	0.0240	21.7	302.9
Depth (ft)	0.103	0.0162	6.36	2.97E-09	0.0709	0.135
Avg Inj (bbl/mo)	0.0102	0.00242	4.21	4.6E-05	0.00541	0.0150

The resulting regression (equation 7.2) is summarized as follows:

$$P = 0.103 \times D + 0.0102 \times Q + 162.3 \quad (7.2)$$

The analysis includes data from different formations in the region. The resulting equation (7.2) attempts to quantify the general trend of operational pressures in the study area. This regression equation has the coefficient of regression (i.e., R-squared value [R^2]) of 0.42 (Figure 7-4).

Considering the physical complexity of the problem, the R^2 value shows decent agreement. Overall, the regression equation may be useful for site screening and general planning for Class II brine disposal wells in the Appalachian Basin. Because lower injection rates and wellhead pressures were screened out in the regression, the model would not be appropriate for scenarios with injection rates less than 100 bbl per month or those that result in 100 psi wellhead pressure.



Figure 7-4. Observed average wellhead pressure versus regression model prediction.

Geologic properties of the injection zone may have a significant effect on injection performance. We expect that the predictability of wellhead pressures would improve if a formation-specific analysis were attempted. To investigate these effects, a regression analysis was performed on the Lower Silurian Clinton-Medina injection interval wells. Using the previous methodology, the wellhead pressures for Lower Silurian Clinton-Medina were evaluated resulting in the following regression model (equation 7.3):

$$P = 0.234 \times D + .00877 \times Q - 547 \quad (7.3)$$

As shown in Figure 7-5, the formation-specific regression model fit had a better coefficient of regression (R^2 value) of 0.77 compared to equation (7.1). This model suggests that some operational similarities could be tied to the formations and hence improve predictability. Unfortunately, there were not enough observations for other injection intervals to perform meaningful regression analysis.

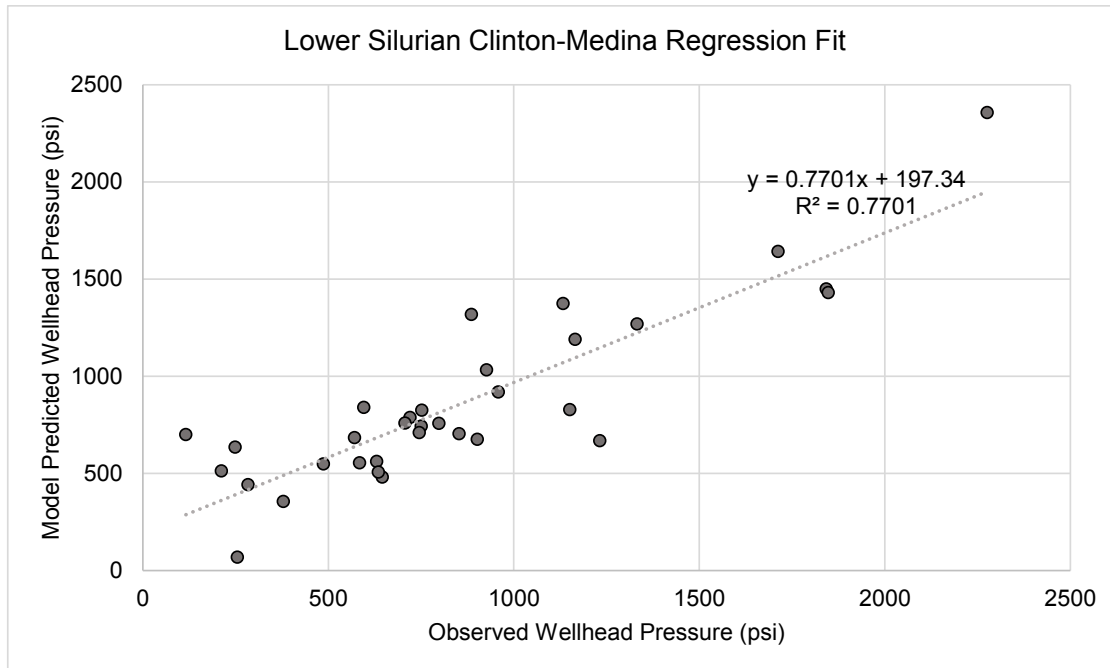


Figure 7-5. Observed average wellhead pressure versus regression model prediction for Clinton Sandstone Wells.

7.3 Well Logging Options

7.3.1 Well Log Data Analysis

Advanced open-hole well log data collection and analysis are critical for understanding the nature and extent of injection zones in cased and open-hole completions. Non-isolation of injection zones in the open-hole completions makes exploration for injection wells difficult if individual injection zones cannot be characterized with log analysis. Of interest in open-hole wells is the analysis of sandstone and carbonate injection zones with different petrophysical characteristics. A variety of common and advanced logging tools can be run in injection wells that provide a higher level of detail for injection zone analysis (Table 7-3). Porosity and permeability determination in the different lithologies requires different approaches to adequately characterize the reservoirs and seals. This section generally reviews some of the standard and advanced logging data that can be used for injection reservoir analysis.

Table 7-3. Logging tools and analysis results.

Logging Tool	Units	Analysis Results
Caliper	Inches	Borehole Dimensions
Compensated Neutron Porosity	PU	Porosity, Hydrocarbon Detection
Acoustic Bond Log	Various	Cement Bond, Completion Design
Monopole Acoustic	μS/ft	Compressional Wave Slowness, Porosity
Dipole Acoustic	μS/ft	Compressional and Shear Wave Slowness, Slow and Fast Shear Wave Slowness and Azimuth, Geomechanical Formation Stress

Table 7-3. Logging tools and analysis results. (Continued)

Logging Tool	Units	Analysis Results
Shallow Resistivity	Ohmm	Water Saturation, Permeability (est.), Fluid Conductivity
Medium Resistivity	Ohmm	Water Saturation, Permeability (est.)
Deep Resistivity	Ohmm	Formation Water Saturation, Permeability (est)
Photo Electric Cross Section	B/E	Formation Mineralogy
Bulk Density	g/cc	Formation Porosity and Mineralogy (grain density)
Gamma	API Units	Correlation and Mineralogy (radioactivity)
Nuclear Magnetic Resonance	Various	Porosity, Permeability, Fluid Composition, Bound vs Moveable Formation Water
Acoustic And Resistivity Image	Image	Stratigraphic Features and Fracture Identification
Production Logging	Various	Temperature and Fluid Flow for Injection Zone Identification
Elemental Spectroscopy	Various	Mineralogy (est.), Elemental Composition

Density and Neutron Logs

Bulk density and neutron tools are used mainly to derive porosity values and are the most common methods used to estimate porosity in the Appalachian Basin region. Typically, in clastic sandstones and siltstones the bulk density-derived porosity using equation (7.4) is used as the main porosity estimate, and changes in neutron porosity are used to identify fluid composition (in particular, gas effect where the neutron porosity is below the density porosity). Typical matrix density used for sandstones and siltstones in the Appalachian Basin ranged from 2.65 to 2.71 g/cc (Table 7-4). The deeper sandstones such as the Rose Run have high proportions of dolomitic cement so using a 2.71 instead of a 2.65 matrix density may be more appropriate.

$$\phi_D = (\rho_{ma} - \rho_b) / (\rho_{ma} - \rho_{fl}) \quad (7.4)$$

where ϕ_D = density porosity
 ρ_{ma} = matrix density
 ρ_b = bulk density from wireline log density
 ρ_{fl} = fluid density in borehole.

Fresh water mud=1.0 g/cc, brine mud=1.1 g/cc for ρ_{fl}

Table 7-4. Standard matrix density values for porosity calculations.

Lithology	ρ_{ma} g/cc	Commonly Used ρ_{ma} g/cc
Sandstone	2.65-2.71	2.68
Limestone	2.71	2.71
Dolomite	2.83-2.88	2.83

The neutron tool-derived porosity is critical in understanding carbonate reservoirs and injection zones. The complex network of porosity and permeability in carbonates, along with the thin zones present in these reservoirs, require that multiple tools be used to estimate and constrain porosity values within a reservoir. The neutron-derived porosity from modern neutron logs can be used directly in limestones if run on a limestone matrix. If dolomites are the actual formations of interest, a correction needs to be made using charts or calculations for sidewall neutron porosity (SNP) and compensated neutron porosity (CNP) in order to determine absolute values (Asquith and Gibson, 1982).

Average porosity using both density and neutron values can be used to estimate final reservoir porosity. Average porosity is calculated using standard oil and gas quick-look procedures, as follows:

$$\phi_A = (\phi_D + \phi_N)/2 \quad (7.5)$$

where ϕ_A = average porosity
 ϕ_D = density porosity
 ϕ_N = neutron porosity.

The average porosity is appropriate when trying to identify zones where matrix and fluid changes have effects on the final porosity. Along with these two porosity estimates, acoustic and NMR log porosity can also be derived.

Nuclear Magnetic Resonance Log

The NMR log, combined with other logs such as image logs, is widely used to evaluate reservoirs. NMR tools utilize pulsed radio frequency in polarizing and spinning hydrogen protons of formation fluids occupying pore space. The spin echo generated from tipping the nuclei and the decay rate (known as relaxation time) of the echo are measured by an antenna located on the tool. The measured relaxation time is auto-processed and transformed into fractions of fluid types that can be used to compute permeability values by applying Timur Coates or the Schlumberger Doll Research (SDR) model. The fractional fluid types provided in NMR processing include clay-bound water (CBW), bulk volume irreducible (BVI) fluid (also known as capillary bound fluid), and bulk volume movable (BVM) fluid (Figure 7-6). The measured amplitude from the generated echoes contributes to evaluation of pore sizes within the formation matrix. Generally, the higher the amplitude, the larger the pore size.

The primary purpose of running the NMR tool is to acquire data on porosity, pore size distribution, fluid type, transition zones (such as oil-water contact) and permeability. The major benefit of an NMR measurement over other conventional porosity logs is its ability to separate effective and total porosity using relaxation time cutoffs.

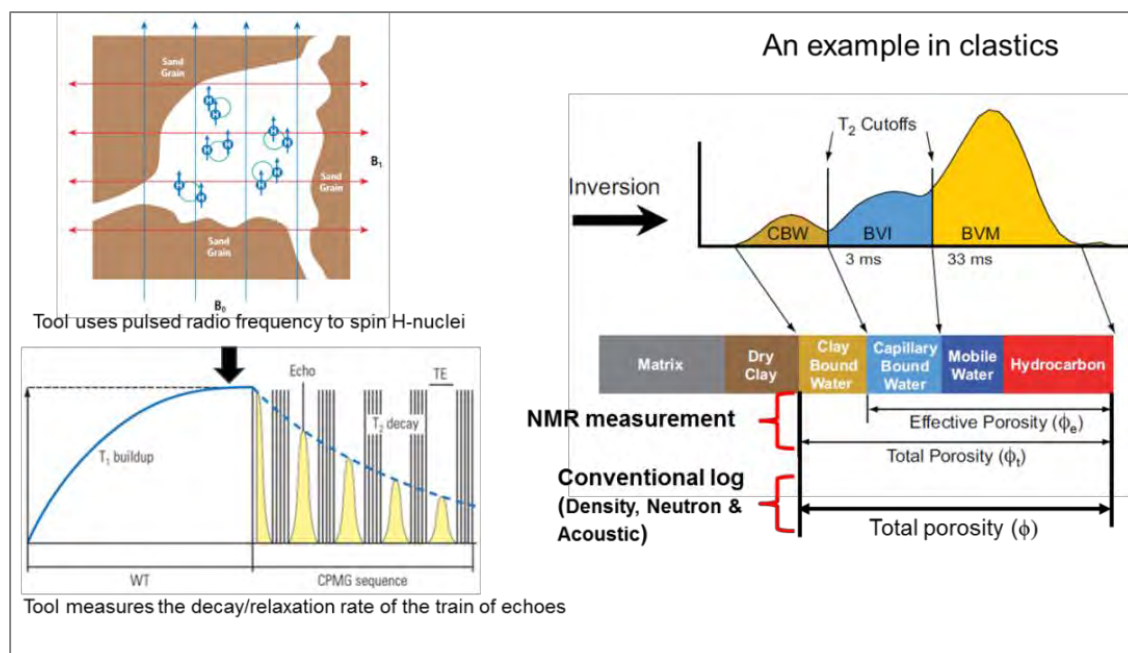


Figure 7-6. NMR water molecule response and processed log products.

The NMR tool can be used to identify zones of porosity and permeability and estimate their ultimate values in the absence of coring. In the Rose Run Sandstone, the total effective porosity and computed permeability from the NMR log was plotted against sidewall core-derived values for porosity and permeability (Figure 7-7). The NMR values closely approximate the core values and could be used to model or evaluate zones of injection with confidence.

In the Lower Copper Ridge Dolomite, the sidewall core porosity and permeability values are all extremely low, but the NMR log porosity and permeability values show thin zones of high porosity and permeability (Figure 7-8). The complex nature of thin vuggy or fractured zones within the carbonate unit makes collecting accurate values for these parameters from core difficult. While the ultimate magnitude derived from the NMR log may be difficult to quantify, the NMR log is valuable in identifying thin injection zones and placing a range of potential values on the porosity and permeability within these zones.

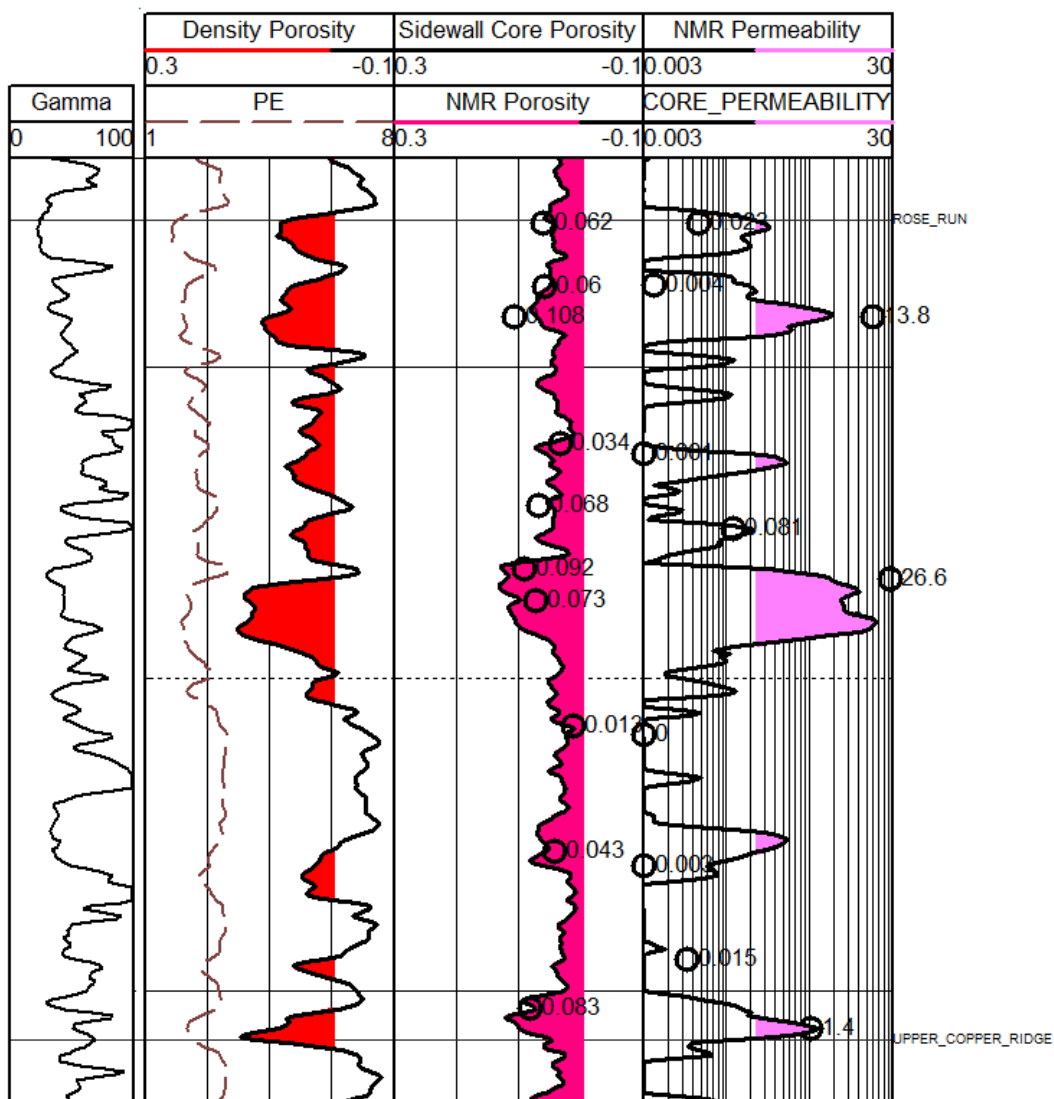


Figure 7-7. NMR-derived porosity and permeability with plotted sidewall core-derived porosity in Rose Run Sandstone.

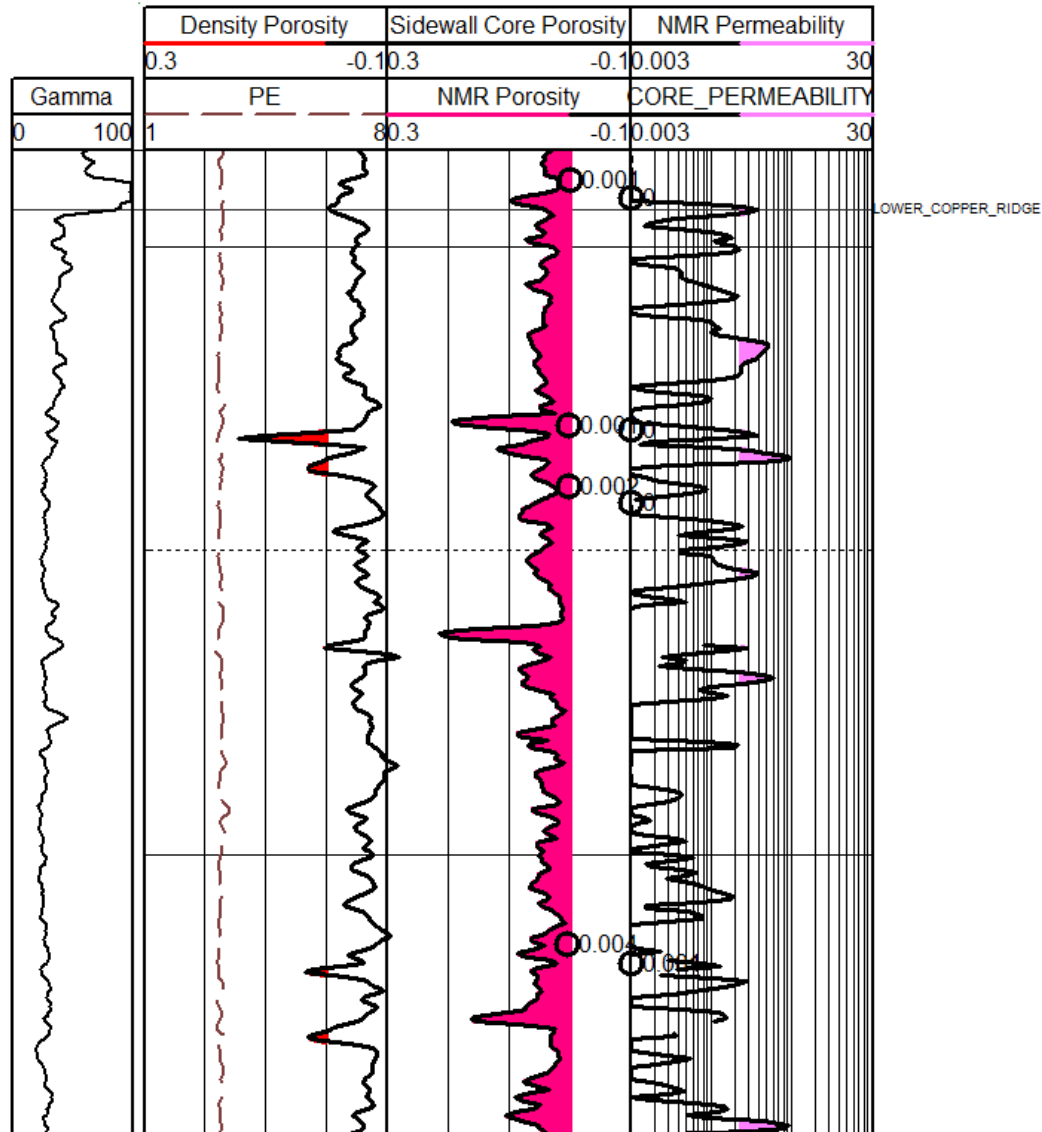


Figure 7-8. NMR-derived porosity and permeability with plotted sidewall core-derived porosity in Lower Copper Ridge Dolomite.

Image

Typical image logs are run with multiple-arm resistivity tools or with acoustic imaging tools. The image logs can provide information on structural and sedimentary structures such as bed forms, primary and secondary porosity networks, fracture orientation and type, and potential pore sizes in vugular carbonates. The ability to distinguish these features in the image logs and correlate them to other log signatures provides the opportunity to explore for potential new wells in areas with limited log data. The image logs in carbonates in particular show vug zones and instances where vugs are further connected by fracture networks (Figure 7-9 and 7-10). Orientations of drilling-induced fractures and borehole breakouts, along with natural fractures, can also be interpreted and used to identify zones of open fractures and their orientation in relation to regional stress fields (Figure 7-11). In central Ohio, the Maximum Horizontal Stress

(Shmax) direction interpreted from drilling-induced fractures is N59E (Figure 7-12). The identification of natural fractures within injection zones is potentially important in understanding how the existing natural fractures and drilling-induced or stimulation fractures react geomechanically to large-volume injections of water.

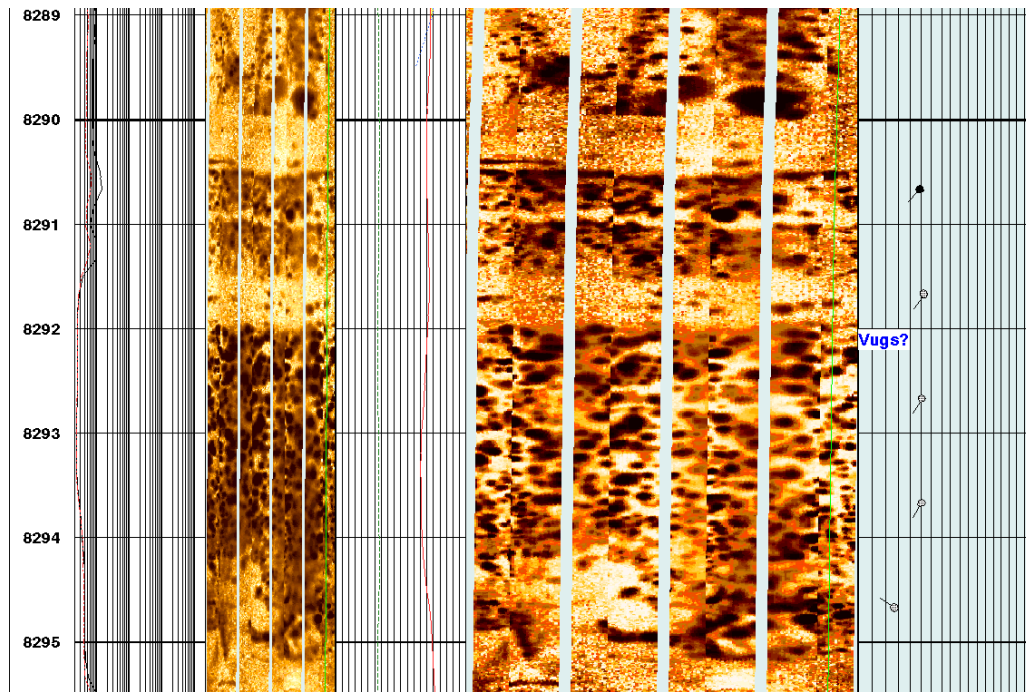


Figure 7-9. Vugular carbonate zone in Lower Copper Ridge Knox Group dolomite.

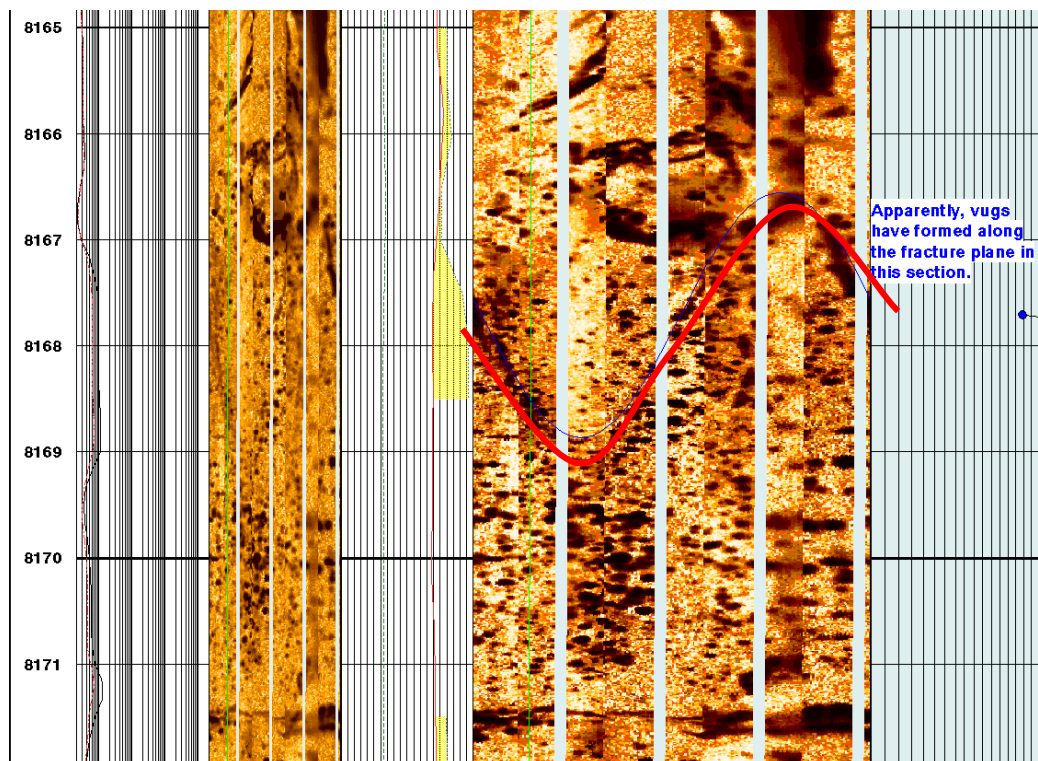


Figure 7-10. Natural fracture within vugular zone in Lower Copper Ridge Knox Group dolomite.

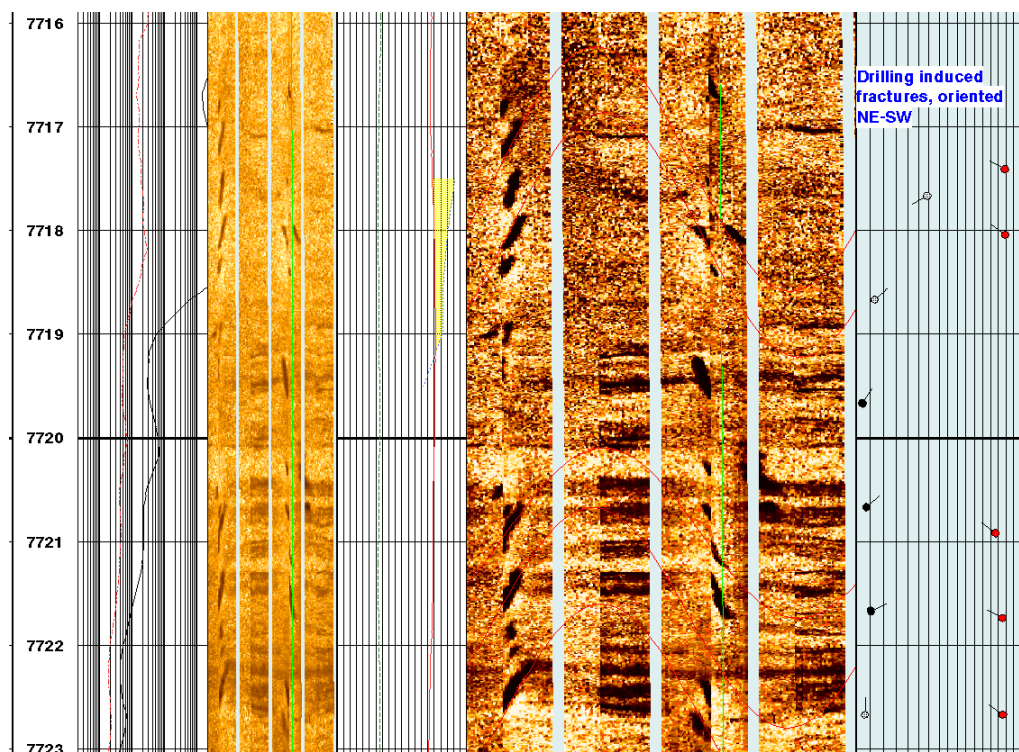


Figure 7-11. Drilling-induced fractures.

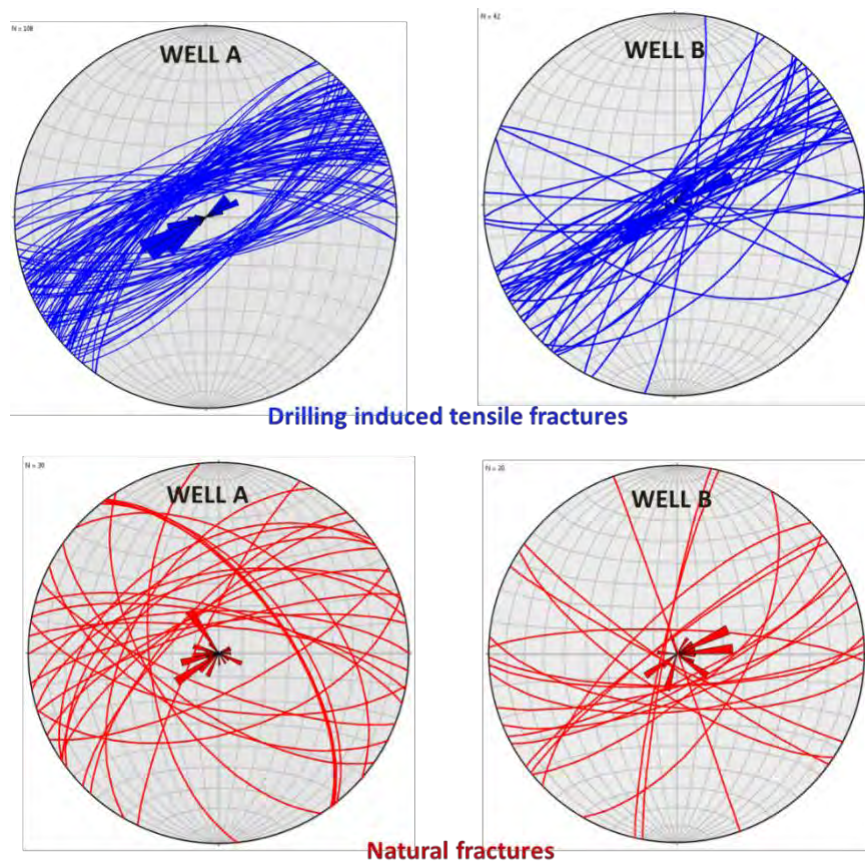


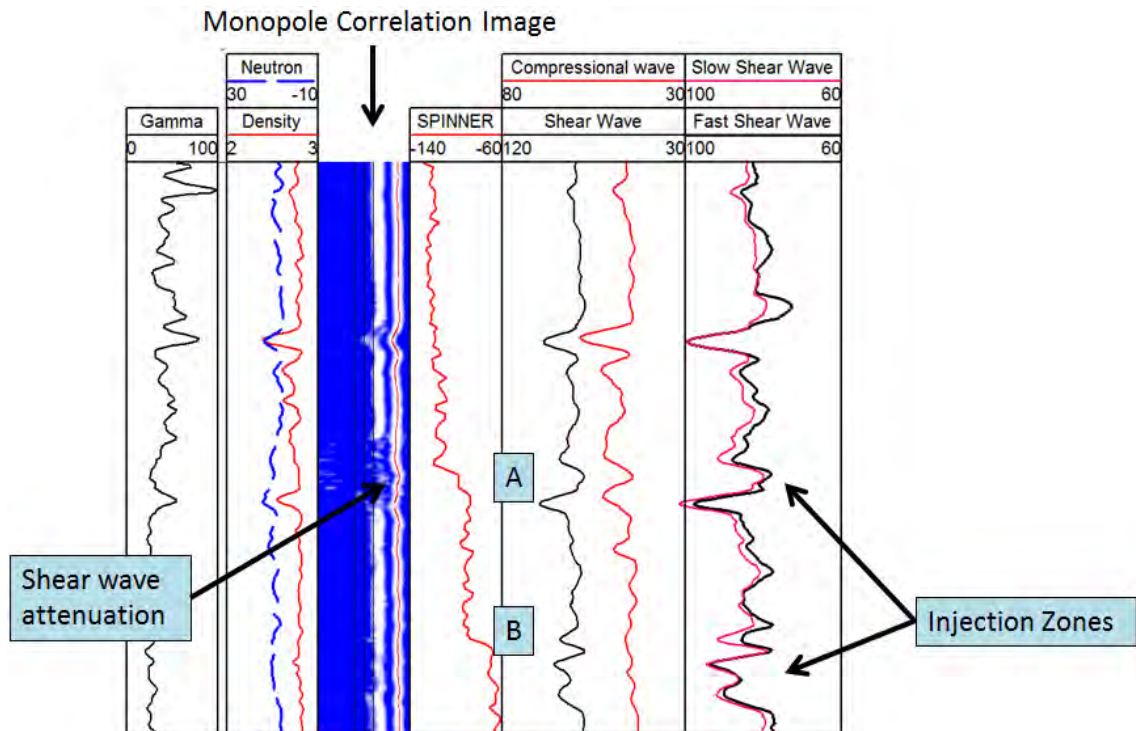
Figure 7-12. Drilling-induced and natural fractures identified on image logs from central Ohio wells.

Acoustic Logging

Typical acoustic logging suites include oriented dipole and monopole sonic tools to evaluate the acoustic response of the formations and to further characterize the nature of the porosity and the overall physical properties of the reservoirs and seals. The processed acoustic logs provide the compressional wave slowness (V_p), shear wave slowness (V_s), the fast (V_{fs}) and slow (V_{ss}) shear wave slowness, the azimuthal direction of fast shear wave, the 24-inch depth of investigation formation slowness, Stoneley waveforms, and the correlation coherence and variable density image logs. The correlation coherence images provide a confidence image of not only the changes in slowness of the reservoir, but also the presence of complete attenuation of the shear or compressional waves in the reservoir. The acoustic logs and images, in combination with the other log suites, can be used to interpret the orientation of high-permeability fractures or facies changes, discern matrix porosity from vuggy or fracture porosity, and discriminate between potential gas-charged and fluid-charged zones in the well. The acoustic logs are also used to calculate the dynamic stresses of formations to evaluate the rock mechanical properties of the reservoirs and seals as discussed in Section 5.5.

The acoustic responses of two carbonate injection zones, A and B, in the same formation are different (Figure 7-13). Where the spinner log shows injection, zone A shows minimal or no

compressional and shear slowness changes, but zone B shows a slowing of the fast and slow shear wave. While these two zones are in close proximity, the differences in acoustic response indicate that they are not identical in nature. Integration of image and other logs can be used to evaluate whether zones are fractured and/or vuggy to target injection zones.



Note: Notice differences in compressional and shear wave responses in injection zone A and B.

Figure 7-13. Acoustic log responses in injection zones identified from spinner log.

Acoustic porosity can be derived from the interval transit time of the formation by equation (7.6). This formula can be used in consolidated sandstones and carbonates with intergranular porosity, but it may underpredict porosity in carbonate formations with fractures or irregular vugs (Asquith and Gibson, 1982).

$$\phi_{\text{Sonic}} = (\Delta t_{\text{log}} - \Delta t_{\text{ma}}) / (\Delta t_{\text{fl}} - \Delta t_{\text{ma}}) \quad (7.6)$$

where ϕ_{Sonic} = sonic porosity
 Δt_{ma} = interval transit time of matrix
 Δt_{log} = interval transit time of formation
 Δt_{fl} = interval transit time of fluid in wellbore
 Fresh water mud = 189; salt water mud = 185

Table 7-5. Standard matrix travel time values for sonic porosity calculation.

Lithology	Δt_{ma} μsec/ft	Commonly Used Δt_{ma} μsec/ft
Sandstone	55.5-51.0	55.5-51.0
Limestone	47.6-43.5	47.6
Dolomite	43.5-38.5	43.5

Figures 7-14 and 7-15 show the sidewall core analysis porosity compared to that derived from the density, NMR, sonic, and neutron porosity in the Rose Run Sandstone and the Lower Copper Ridge Dolomite. As can be seen in the Rose Run, the density, NMR, and sonic porosity values correlate relatively well with the sidewall core porosity. In the lower Copper Ridge, the porosity zones observed in the density, NMR, and neutron logs do not readily correlate to the sonic or sidewall core porosity. The complex nature of porosity in fractured or vuggy carbonates makes porosity determination from core samples or logs difficult, but the log-derived porosity zones are valuable for identifying zones of injection and the potential ranges of porosity.



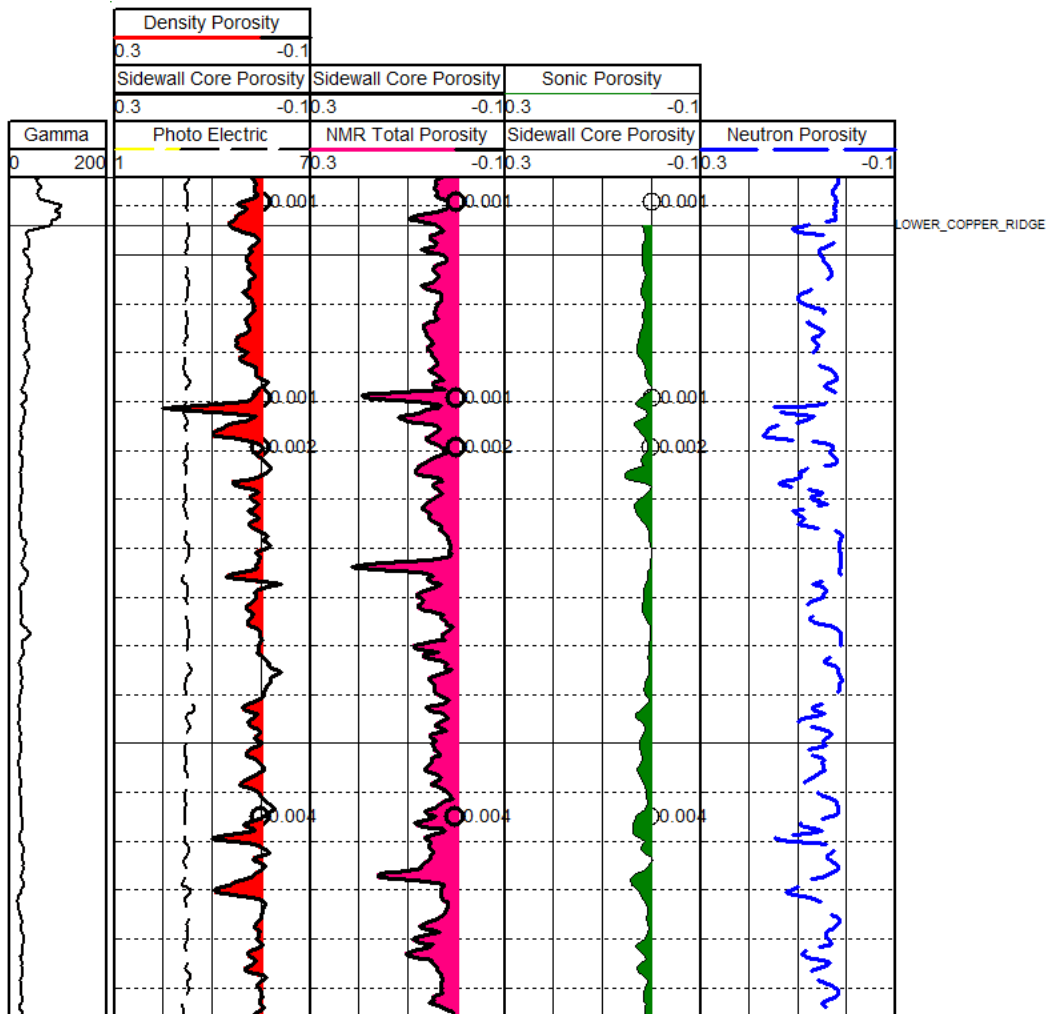


Figure 7-15. Comparison of porosity derived from density, NMR, acoustic, and neutron to sidewall core porosity in the Lower Copper Ridge Dolomite.

Elemental Spectroscopy

Elemental spectroscopy is used to determine mineralogy within formations in order to better estimate petrophysical properties in heterogeneous clastic and carbonate formations. Natural gamma rays emitted from radioactive decay of thorium, potassium, and uranium are measured. Gamma rays can also be sourced from the tool, and the returning gamma ray spectra can be processed to obtain elemental yields from the formations. The lithology and mineralogy determinations can then be used to better define bulk matrix density for porosity calculations, determine total organic carbon, define clay mineral compositions, and better define mineralogy for geomechanical analysis.

The mineralogy percentages calculated from the logs can be used to discern changes in lithology within the formations that effect porosity and permeability. Figure 7-16 shows the mineralogy changes within the Rose Run Sandstone. Relative changes in dolomite and other mineralogy percentages within the individual sandstone members can impact porosity calculations if an

assumed matrix density is used. Figure 7-17 shows the differences in porosity estimates calculated using equation (7.5) with an assumed and mineralogic matrix density; to perform the calculation, the mineral weight percentages from the elemental spectroscopy log were used to generate the mineralogic matrix density. While both values are similar, the variable matrix density calculated porosity matches the core-derived porosity values better than the single matrix density. The mineralogy data become increasingly important when evaluating formations with variable clay mineralogy. The elemental spectroscopy data can also be used to evaluate completion procedures or fluid interaction with different mineral types.

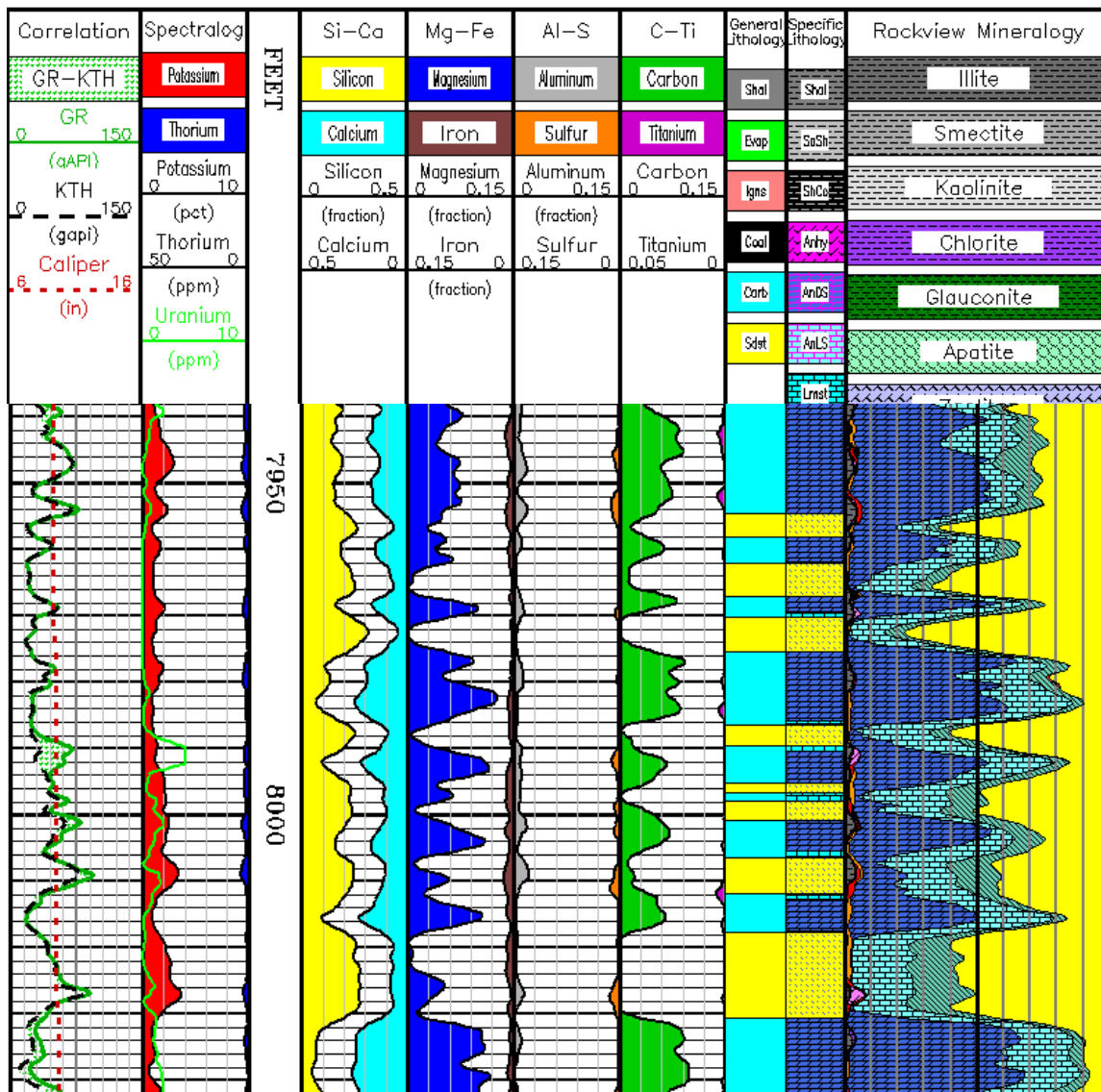


Figure 7-16. Baker Hughes elemental spectroscopy RockView™ mineralogy log.

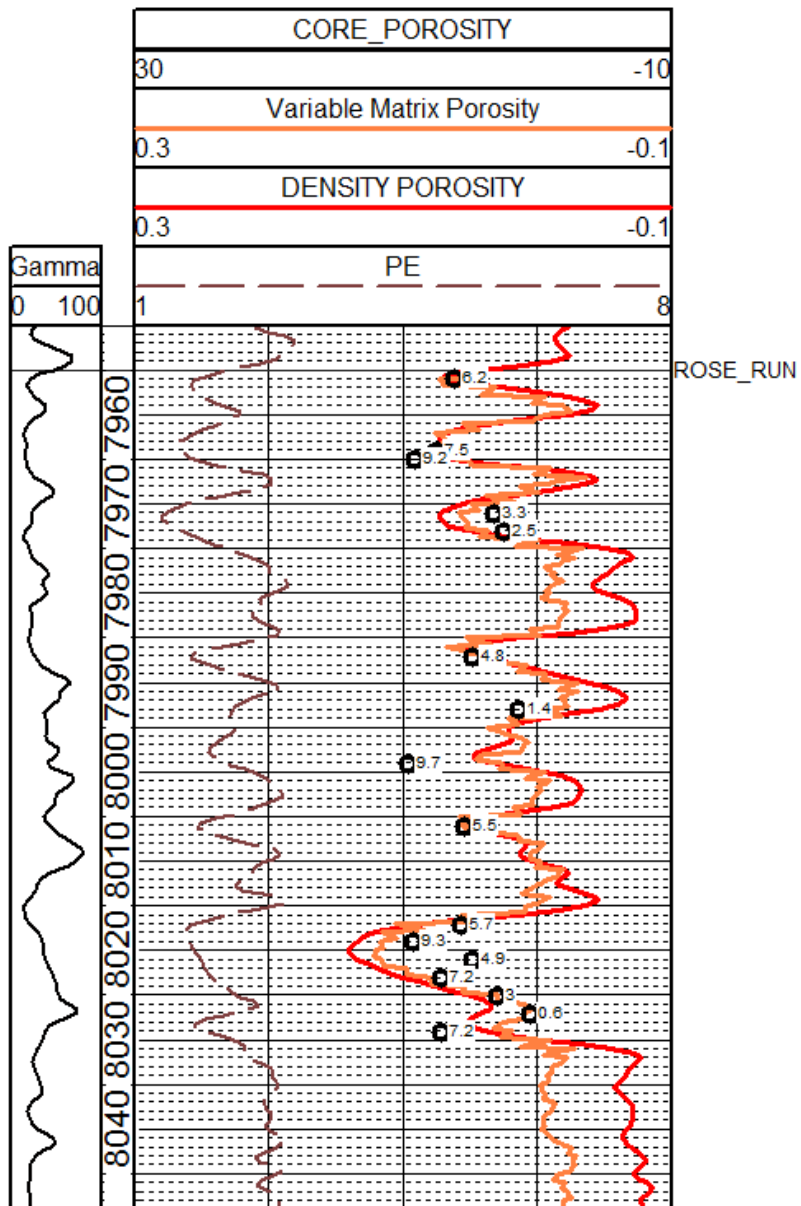


Figure 7-17. Porosity logs calculated from a matrix density porosity of 2.68 and a mineralogic matrix (variable matrix porosity) with core-derived porosity values plotted.

7.4 Well Testing Options (Pre-Injection)

Pre-injection testing can be performed in the drilling/development phase of a well, before a well is completed, to identify geologic intervals with injection potential and to assess the approximate injectivity of the candidate injection intervals. If the well is going to be completed with casing, the operator can use this information to decide where to perforate the casing. Alternatively, an operator may decide to plug and abandon the well if pre-injection testing shows the well has insufficient injectivity to support the intended operation. An open-borehole flow-meter test is a type of pre-injection test that can be used for this purpose.

A flow-meter test involves logging a section of open borehole (i.e., below casing) using a wireline-deployed mechanical flow-meter (spinner logging-tool) while injecting water into the well. Flow-meter tests conducted inside perforated casing while pumping from the well is a common technique used by the oil industry to identify productive intervals; the industry refers to this practice as production logging. The type of flow-meter testing discussed here refers to testing conducted in an open-borehole before the well is completed for the purpose of identifying potential injection intervals. While this discussion focuses on mechanical-type flow-meter logging, other types of flow-logging tests are possible, including: tracer logging (e.g., using a short-lived radioactive tracer), thermal logging (i.e., heat-pulse sensing), and electromagnetic logging.

The mechanical flow-meter logging tool (spinner) uses an impeller that revolves in response to fluid flow. As fluid moves through and rotates the impeller blades, the number of impeller revolutions per second (RPS) is automatically recorded and used to calculate the velocity of the fluid. Most impeller flowmeters incorporate a lightweight three- or four-bladed impeller that rotates a magnet mounted on the same shaft. The magnet actuates a sealed microswitch, so that one or more pulses are impressed on low-voltage direct current that is connected across the switch. The impeller is protected from damage by a basket or housing, and the probe is centralized with bow springs (arms), or similar devices. For this reason, this type of spinner-logging tool is referred to as a caged full-bore spinner. Caged full-bore spinners fold down to pass restrictions (e.g., tubing or casing) and open when in the open borehole. Figure 7-18 shows a typical four-arm spinner-logging tool.

Spinner measurements can be made while trolling at a constant logging speed in order to generate a continuous flow profile over a certain depth, or while stationary in order to measure flow at a specific location in the borehole. Spinners can make measurements over a wide range of flow rates, although the tool often has poorer resolution at very low flow rates. Baskets and impellers of different diameters are available and are easily changed, so the maximum size for a well can be used to increase sensitivity. The most commonly used impeller flowmeters usually stall at vertical velocities of 1.2 to 1.5 meters per minute, although it is possible to measure velocities as low as one-half those velocities under some conditions. The addition of a packer or other flange-like device to divert most of the flow through the basket will improve sensitivity to low velocity, particularly in large-diameter wells. An advantage of spinner logging is that most major logging companies (e.g., Baker Hughes) and some small independent logging companies provide this service. Some companies will also interpret the logging data.



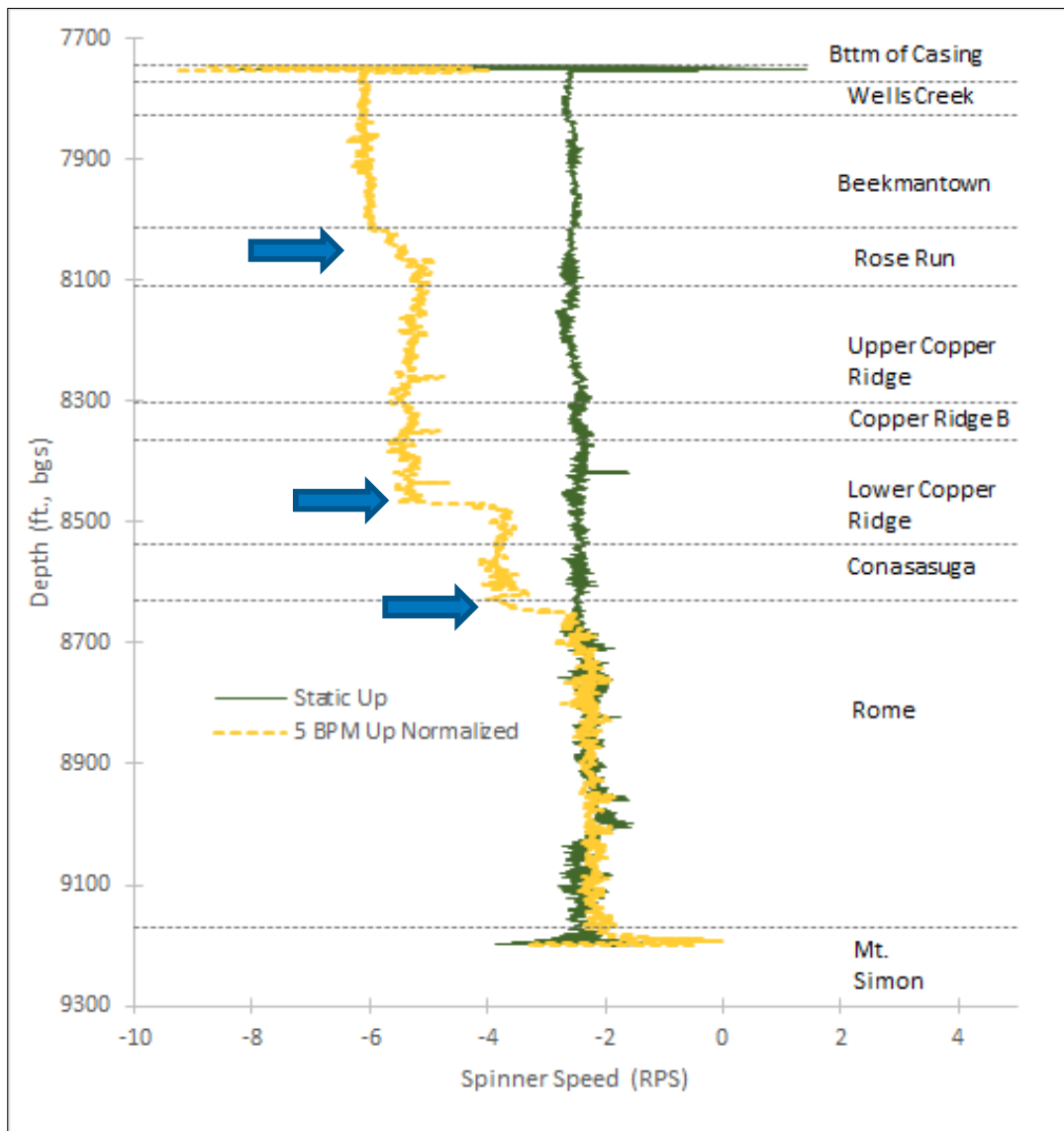
Figure 7-18. Four-arm caged full-bore spinner-logging tool.

Figure 7-19 shows an example flow profile for a 1,455-foot-long open-borehole section in a well in eastern Ohio. This figure shows the spinner-logging data for a log obtained while injecting water into the well at a rate of 5 barrels per minute (BPM) (yellow curve) compared to a log obtained under static (no injection) conditions (green curve). Both logging runs were made in the upward direction, starting at the bottom of the open borehole, to increase the flow-measuring sensitivity of the tool. Results, in RPS, are plotted as a function of depth to identify injection zones.

A positive RPS reading indicates an upward flow direction, while a negative RPS indicates a downward flow direction. Under static (no flow) conditions, a downward logging run will create an apparent upward flow direction as the tool moves downward through a stagnant water column and thus produce a positive RPS reading. Conversely, an upward logging run will produce a negative RPS reading due to an apparent downward flow direction as the tool moves upward through a stagnant water column (e.g., the green curve in Figure 7-19). The RPS curves for upward and downward passes, made at the same logging speed, should be similar except the downward curve will be shifted in the positive direction relative to the upward curve. For spinner-logs obtained in the upward direction while injecting water into the well, such as the example in Figure 7-19, the entire RPS curve will be negative because the combined effects of the downward direction of flow and the upward direction of the tool will produce an apparent downward flow direction everywhere along the open borehole. When reading the RPS curves from the top down, inflow zones in the open borehole are indicated by a shift to the right (in the positive direction), which indicates a decrease in the amount of water moving past the tool.

In Figure 7-19, three injection zones are indicated by the blue arrows: one in the Rose Run Formation; a second in the Lower Copper Ridge Formation, and a third in the uppermost Rome Formation. The lower two injection zones are very thin, as indicated by the abrupt decrease in the RPS curve at these depths, while the gradual decrease in the RPS curve across the Rose Run Formation indicates that this injection zone is thicker. Also, based on a comparison of the amount of decrease in the RPS curve associated with each of the three injection zones, it can be concluded that the Lower Copper Ridge zone was responsible for taking the greatest amount of injection.

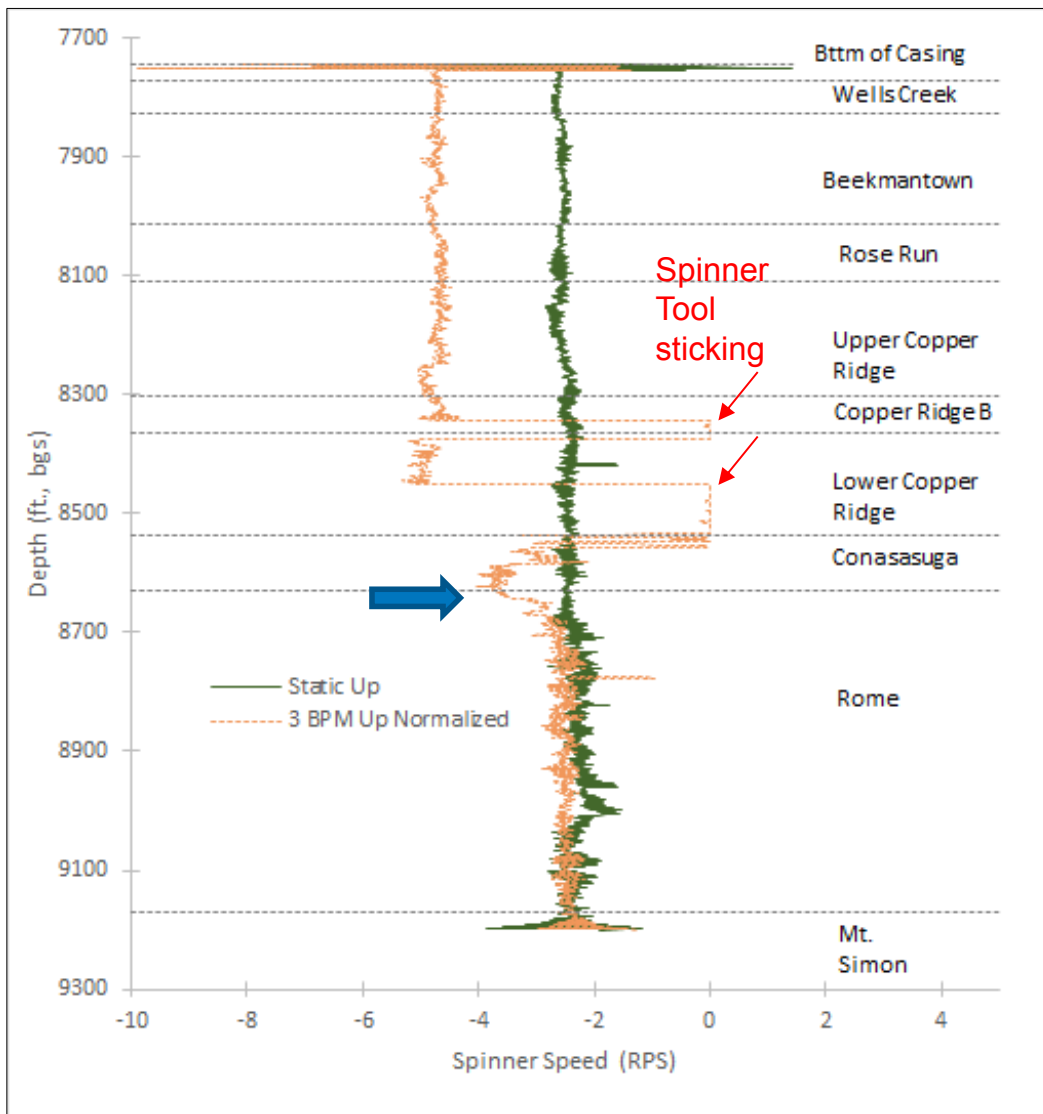
Several factors can affect the RPS readings, including borehole diameter (enlargement in the diameter of the borehole will result in a decrease in the RPS reading, giving the impression that water was lost to the formation), logging speed, and flow rate. Raw RPS data can be corrected for variations in borehole diameter by normalizing the results to a common diameter. The results can be further processed by smoothing the data using moving average or other similar techniques.



Note: Interval from 7,745 feet to 9,200 feet.

Figure 7-19. Example spinner-log flow profile for a 1,455-foot-long open-borehole interval, acquired at a 5-BPM injection rate.

When doing a flow-meter test, spinner logs should be acquired at multiple injection rates because an injection zone with low transmissivity may not be detected at a low injection rate due to the resolution characteristics of the spinner tool. To illustrate this point, Figure 7-20 is a spinner log for the same borehole shown in Figure 7-19; however, it was acquired for an injection rate of 3 BPM instead of 5 BPM. Only one injection zone, the Rome Formation, is evident in Figure 7-20. The Lower Copper Ridge injection zone is likely masked by the spinner-tool malfunction at this depth, so it is not possible to say whether this zone was an active injection zone at the 3 BPM injection rate. However, it is clear that the Rose Formation was not acting as an injection zone at 3 BPM.



Note: Interval from 7,745 feet to 9,200 feet.

Figure 7-20. Example spinner-log flow profile for a 1,455-foot-long open-borehole interval, acquired at a 3-BPM injection rate.

In addition to the spinner-logging tool, other companion logging tools should be included in the tool string to provide supporting information for processing or confirming the results of the spinner-logging. A collar locator tool and a gamma-ray tool should be included for depth correlation with other logs. A caliper tool (preferably a six-arm caliper) should be included if a recent high-quality caliper log is not available because these data are needed to correct the RPS results for borehole-size variations. A temperature sensor should be included because temperature data can help identify injection zones. Specifically, a post-injection fluid temperature log obtained after the dynamic flow-meter logging test can be compared to a baseline fluid temperature log obtained before the flow-meter logging test to help identify injection zones where cooling in the wellbore persists.

Figure 7-21 shows a baseline and repeat temperature log obtained before and after the flow-meter logging tests shown in Figures 7-19 and 7-20. As can be seen in Figure 7-21, the temperature log run after injection shows that the borehole above a depth of approximately 8,725 feet underwent cooling, indicating that there are no injection zones below this depth. The repeat temperature log (green) shows several temperature anomalies that may coincide with inflow zones, including the three zones identified from the spinner-logging data. The others that are not corroborated by the spinner logs may be minor inflow zones that could not be detected with the spinner-logging tool. The uppermost anomaly that occurs within the Wells Creek Formation may be associated with thermal cooling/heating of the casing which terminates just above this point. This application of fluid temperature log surveys assumes that the temperature of the injected fluid is significantly different than the ambient formation fluid temperature.

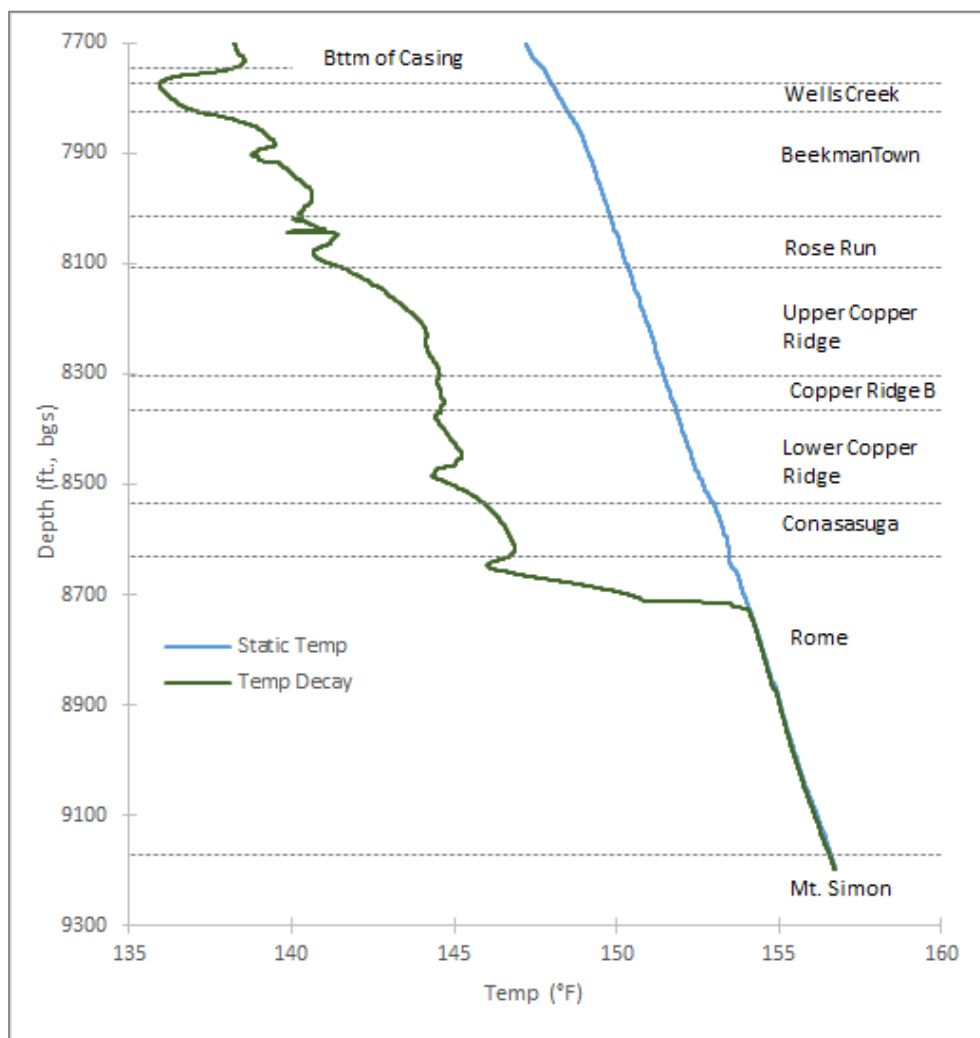


Figure 7-21. Example temperature logs collected before and after flow-meter logging.

If possible, a pressure probe should also be included in the tool string with the spinner tool. Pressure data obtained after the injection can be analyzed to estimate the total transmissivity of the injection zones identified within the open-borehole. Prior to starting the flow-meter test, the

logging tool with the attached pressure sensor should be lowered into the open borehole interval to obtain a measurement of baseline (pre-injection) pressure. Then, following the final flow-meter logging run, with the tool string positioned at the same depth where the baseline pressure data was obtained, injection is terminated and the tool string is left in place at this depth to record post-injection pressure recovery (i.e., fall-off). The pressure fall-off data can be analyzed using established PTA techniques. In order to analyze the BHP data, a time-history record of the injection rate and surface injection pressure during the flow-meter test should also be collected. Figure 7-22 is an example illustrating injection rate and injection pressure data recorded during a flow-meter logging test along with BHP fall-off data collected following the end of injection. Surface injection pressure recorded during the flow-meter test (blue curve) was converted to estimated BHP (green curve) and combined with the measured fall-off data (yellow curve) to create an injection/fall-off data set for analysis. A PTA of the injection/ fall-off pressure data, shown in Figure 7-23, determined that the injection zones within the tested borehole have a transmissivity (permeability-thickness product) of 185,000 mD-ft.

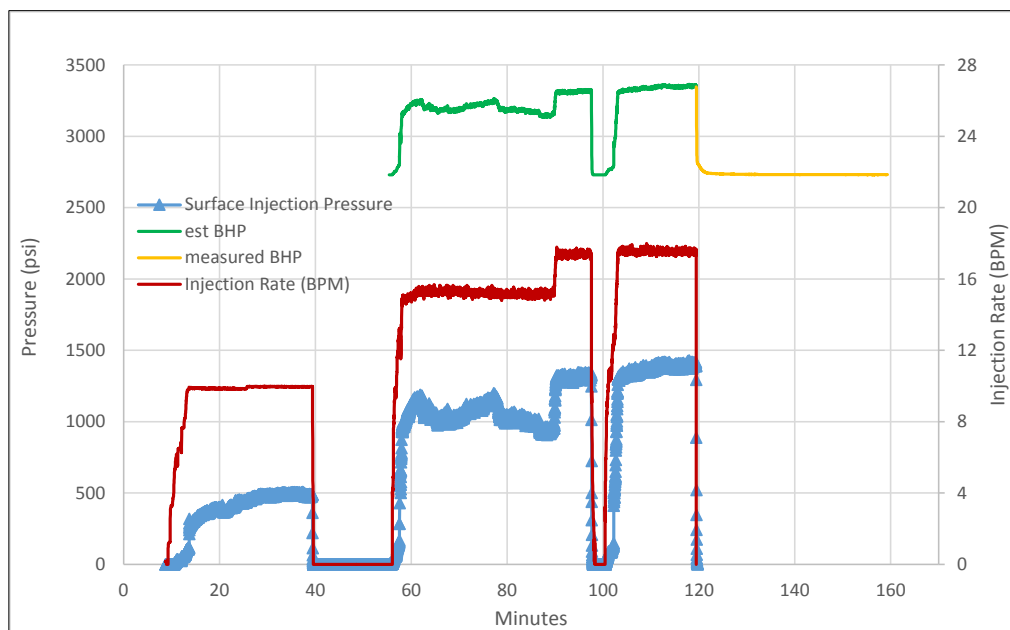


Figure 7-22. Injection rate and pressure history for a flow-meter logging test along with BHP fall-off data.

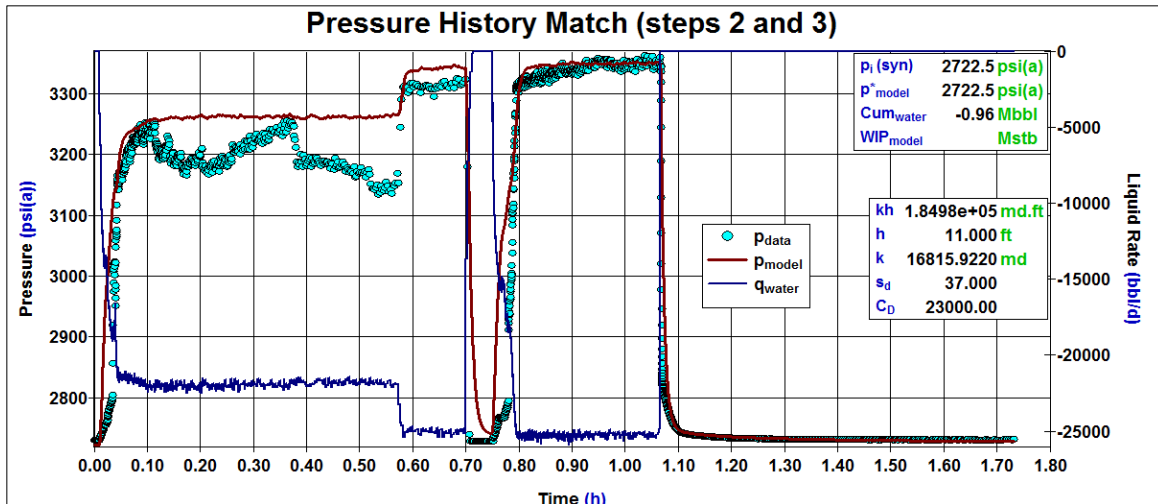


Figure 7-23. Time-history match analysis of injection/fall-off test to determine transmissivity of injection intervals.

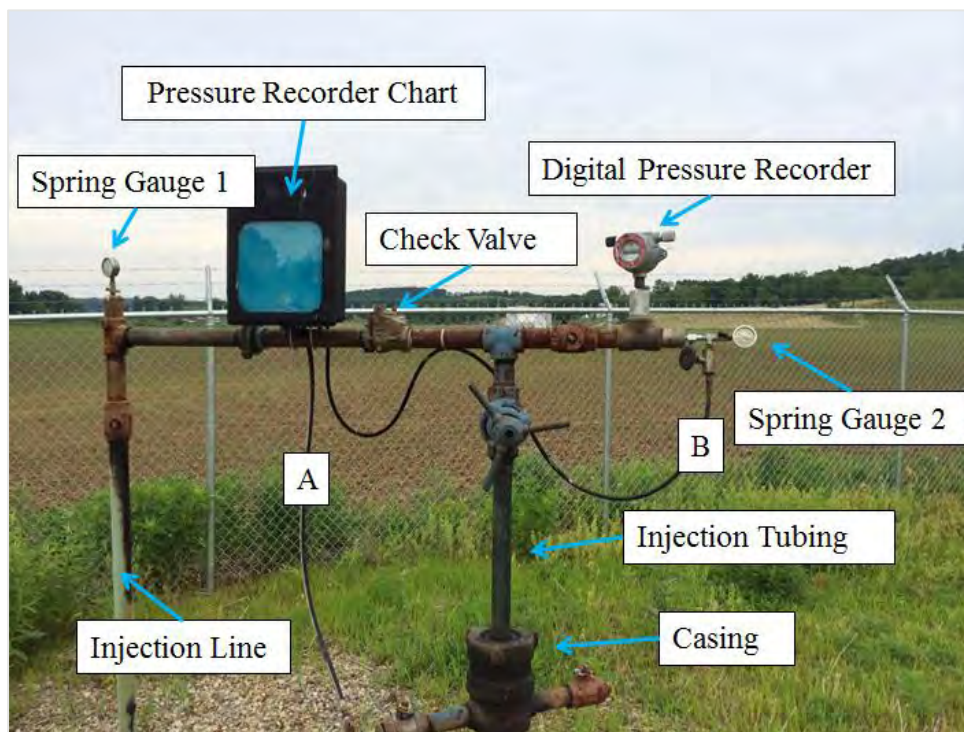
7.5 Injection Monitoring Options

Monitoring the surface injection pressure and the injection tubing/casing annulus pressure are both requirements of the Class II UIC permit. In order to avoid hydraulically fracturing the injection zone, a maximum allowable wellhead injection pressure is assigned to the well at the time the permit is issued. The maximum allowable surface pressure can be calculated by using the regulatory agency's formula, or it can be determined by performing injection/pressure fall-off tests as approved by the regulatory agency. Injection pressure is not allowed to exceed the maximum allowable surface injection pressure at any time during injection operations. (The operator of a Class II Injection well is allowed to exceed the maximum allowable injection pressure during stimulation treatments and work-over operations.)

7.5.1 Injection Tubing Monitoring

The operator is required to monitor the injection volume and the surface injection pressure on a daily operational basis. The pressure can be monitored several ways. One common monitoring tool is the spring gauge. The spring gauge can be installed on the injection tubing and will give a constant readout of the current pressure. The date and time of the pressure reading can be logged by the operator to meet record-keeping requirements. Another option for injection tubing monitoring is the pressure recorder chart. This chart draws a continuous record of the tubing injection pressure on paper, which can then be stored in the well file. The pressure recorder chart makes it easy for the operator to see trends and anomalies in the injection pressure. A third option for monitoring the injection tubing pressure is the digital pressure recorder, which stores pressure and time data electronically and can be downloaded to a computer by the operator. The digital pressure recorder can be programmed to take time and pressure readings at many different frequencies, from several times per second to once an hour or even one or two times a day. Figure 7-24 shows an injection well where all three types of pressure monitoring devices are installed to monitor tubing and annulus data.

In addition to monitoring the injection tubing pressure, it is recommended that a pressure switch be installed near the injection pump. The pressure switch will automatically turn the injection pump off if the pressure exceeds the high pressure setting or if the pressure drops below the low pressure setting. Shutting the pump down on the high pressure setting will avoid injecting at a pressure above the maximum allowable surface injection pressure. Shutting the pump down for a sudden loss of pressure can save the operator the cost of cleaning up a spill in the event of a catastrophic mechanical failure at the injection pump, in the injection line, or at the well head.



Note: Spring gauge 1 monitors pressure on the injection line side of the check valve; spring gauge 2 monitors pressure on injection tubing side of check valve. The digital pressure recorder monitors pressure on the tubing. The pressure recorder chart monitors pressure on the tubing and annulus between the tubing and casing. Pressure hose "A" is connected to the annulus, and hose "B" is connected to tubing. The check valve prevents backflow to the pump.

Figure 7-24. Injection well head configured with pressure monitoring equipment.

7.5.2 Injection Tubing/Casing Annulus Monitoring

The operator is also required to monitor the annular space between the injection tubing and the casing during injection operations. The type and frequency of monitoring required may vary depending on the regulatory agency and the date the well was permitted. Some regulatory agencies will assign a positive pressure to be maintained on the annulus. If positive pressure is not maintained and monitored on the injection tubing/casing annulus, the regulatory agency might request the operator to perform periodic pressure tests, or some other kind of test to confirm the mechanical integrity of the system.

The pressure can be monitored in a number of ways. One common monitoring tool is the spring gauge. The spring gauge can be installed on the casing head outlet and will give a constant readout of the current pressure. The date and time of the pressure reading can be logged by the operator to meet record-keeping requirements. Another option for injection tubing/casing annulus monitoring is the pressure recorder chart. This chart draws a continuous record of the tubing/casing annulus pressure on paper, which can then be stored in the well file. The pressure recorder chart makes it easy for the operator to see trends and anomalies in the injection tubing/casing annulus pressure. It is not uncommon for the injection tubing/casing annulus pressure to vary as a result of ambient temperature or the temperature of the injection fluid. A third option for monitoring the injection tubing/casing annulus pressure is the digital pressure recorder, which stores pressure and time data electronically and can be downloaded to a computer by the operator. The digital pressure recorder can be programmed to take time and pressure readings at many different frequencies, from several times per second to once an hour or even one or two times a day.

If the injection tubing/casing annulus will not hold positive pressure, or if the pressure increases unexpectedly, it is assumed that there is a lack of mechanical integrity in the injection tubing, the injection packer, or the casing. In that case, the operator should terminate injection operations until the failure has been corrected and mechanical integrity has been restored.

8. Survey of Information Sources for Produced Water Disposal

This task was focused on evaluating existing information sources on produced water disposal activities in the continental United States. Currently, no centralized source of information on produced water/brine injection is being generated by the regulatory, industry, and academic programs involved in oil and gas production. The task included a survey of Class II well regulations, research, and practices. Based on this review, data distribution methods were summarized for organizing and distributing information on Class II brine disposal wells for operators and other stakeholders.

8.1 Class II Well Survey

Since Edwin Drake drilled the first commercial oil well near Titusville, Pennsylvania, in 1859 (Harper, 1998), the disposal of produced water has posed an economic and site management problem for the oil and gas industry. Produced water is the largest source of waste, by volume, generated by oil and gas drilling (Veil et al., 2004; Veil and Clark, 2010). Producing formations can yield as much as 10 times more saltwater than oil and/or gas (Mace et al., 2005). During the oil and/or gas extraction process, additional fluids are injected into an active well to enhance production. Some of this injectate comes back up during production. These fluids are referred to as flowback and are also considered produced water. Returning produced water back into the subsurface has become a common industry practice to dispose of the water, maintain reservoir pressure, or increase the amount of oil and gas produced. The Government Accountability Office (GAO) (2012) estimates that 56 million barrels of produced water are generated per day from onshore oil and gas production; approximately 90% of the water is injected underground for disposal or EOR. Underground disposal of produced water is regulated by the USEPA through the Safe Drinking Water Act (SDWA) UIC program established in 1980. Under this program, when fluids associated with oil and gas production are to be injected into wells for the purpose of disposal or EOR, those wells are classified as Class II injection wells (USEPA, 2002).

Management of produced water is the subject of many records documenting regulations, legal decisions, research and development, and other activities and information related to the oil and gas industry. The current status of drill records, well data, injection records, and construction information across the United States is contained in disparate state, federal, and industry databases. Finding information and data pertaining to Class II injection wells can be challenging, because there is neither a consistent method for organizing nor a consistent procedure for disseminating the information, and the entity responsible for compiling and maintaining the records is not always identified.

Development of a subsurface brine disposal framework is necessary to support the development of safe and reliable locations to dispose of wastes associated with energy resources. In the Northern Appalachian Basin, for example, the discovery of economically feasible drilling techniques to access the natural gas stored in Marcellus and Utica formations has resulted in a large increase in drilling-related fluids. It is important that the drilling and injection records be meticulously tracked, updated, and disseminated.

This section reviews and summarizes existing information sources on produced water disposal activities in the continental United States (Figure 8-1). Available records from regional and state regulatory agencies and significant published papers and reports were reviewed. Options for distributing the dispersed information were studied to develop a conceptual framework to make data readily available to end users.

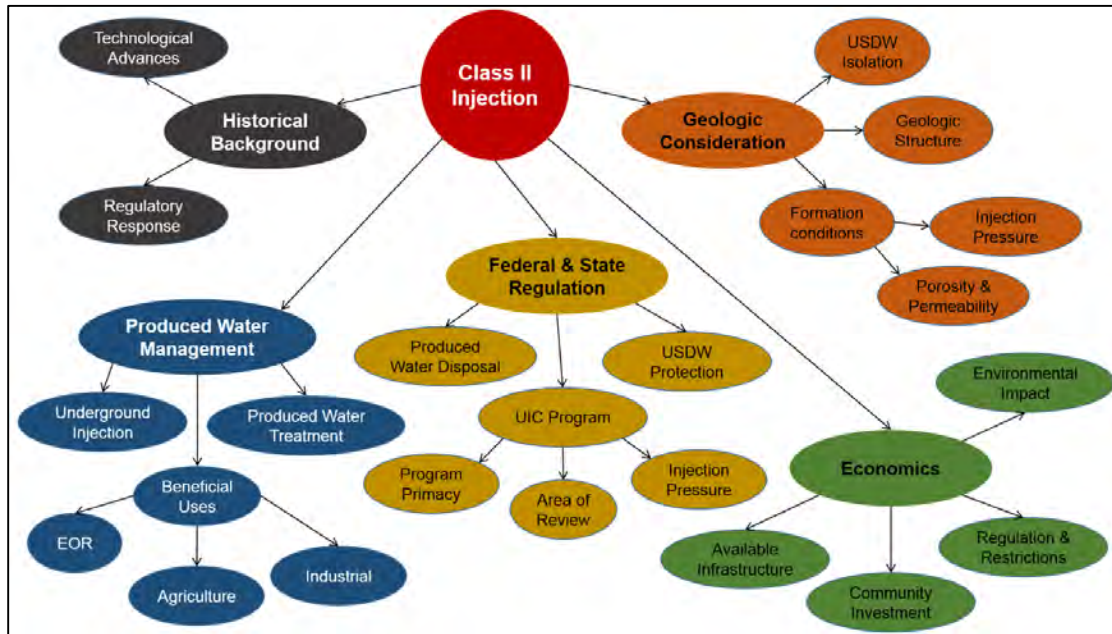
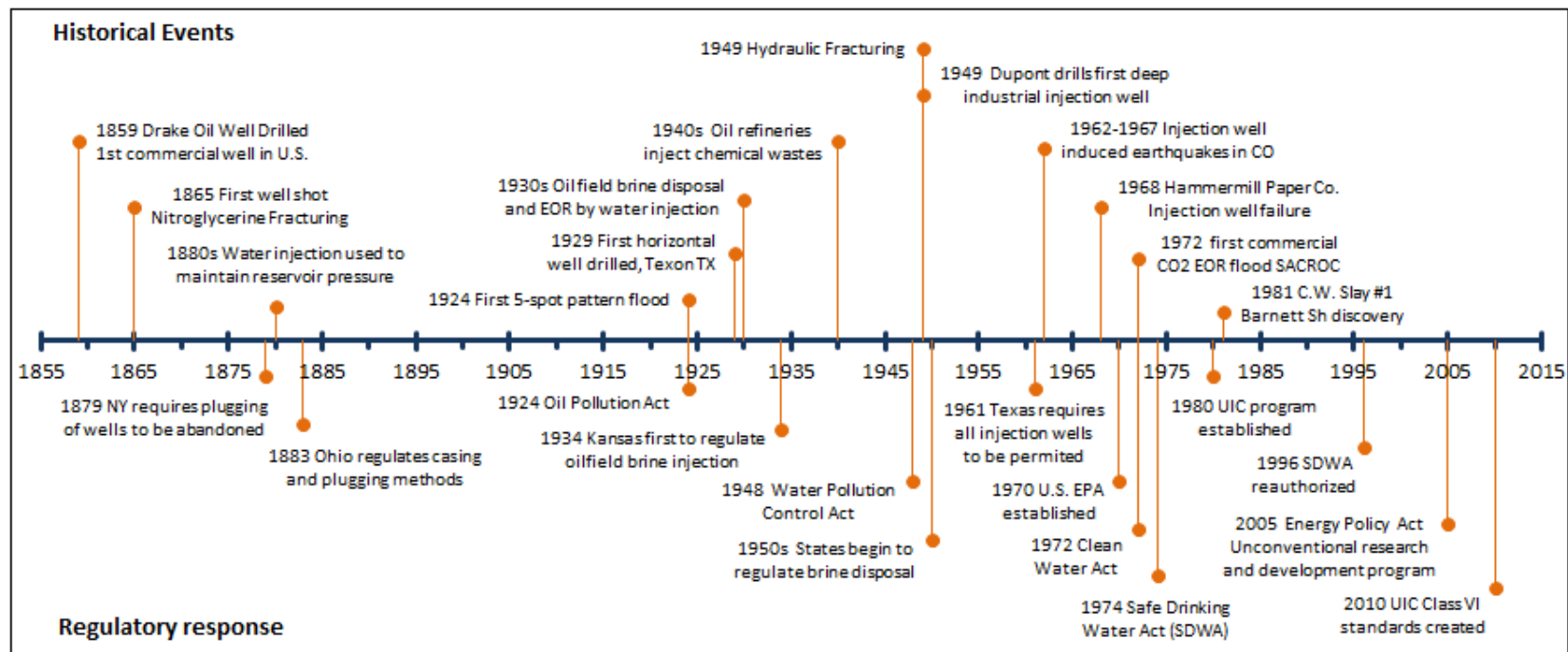


Figure 8-1. Topics related to Class II injection summarized in this literature review

8.1.1 Historical Background

Since 1859, the oil and gas industry has experienced numerous advances in drilling technologies and in methods of produced water management. Along with the technological and management advances, federal and state governments have, over time, developed regulations to enforce environmental stewardship associated with oil and production and waste management. Figure 8-2 shows major oil- and gas-related events and discoveries and regulatory responses by governmental agencies.



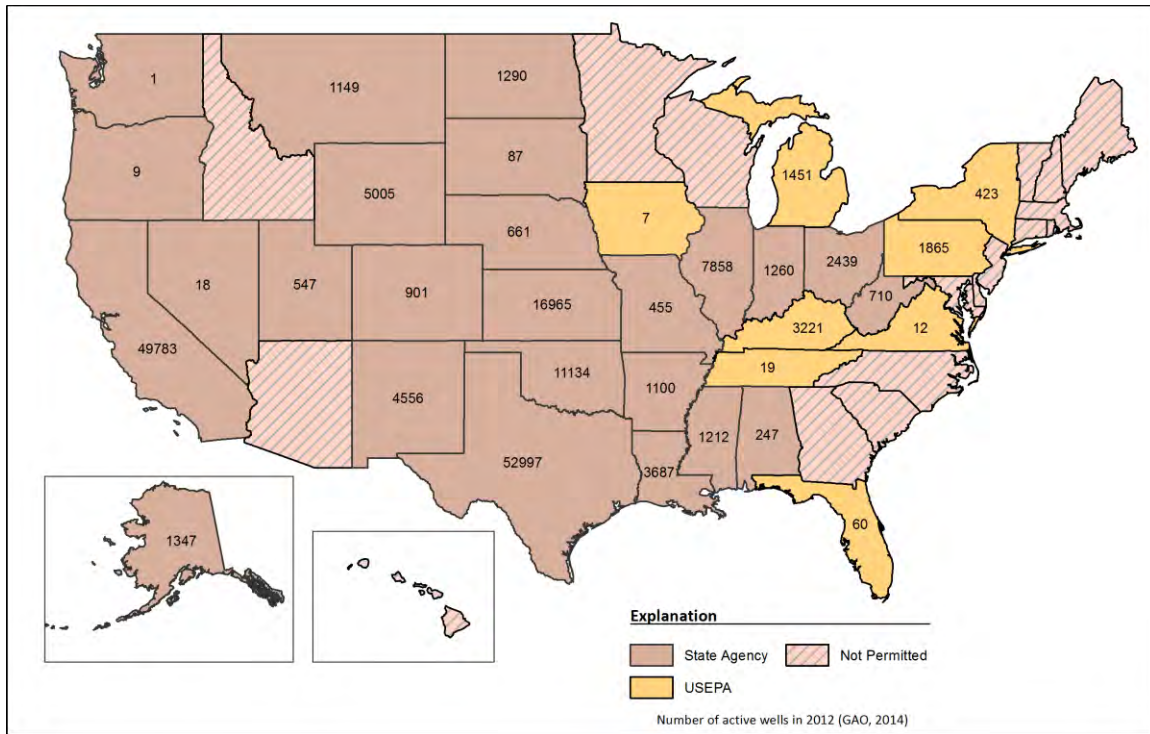
Note: The time markers above the line are major oil field events and discoveries; the markers below the line show how regulation has developed.

Figure 8-2. Generalized timeline showing major oil- and gas-related events and regulatory response by government agencies.

Prior to the 1930s, the oil and gas industry generally operated without much oversight from state or federal government agencies, and produced water was discharged into surface waters. As early as 1879, states began regulating how wells should be cased, plugged, and abandoned (GWPC, 2009). During the 1880s, water injection was first used to maintain reservoir pressure and to extend oil production (Satter et al., 2007). Disposal of oilfield brine by underground injection to enhance oil recovery, maintain reservoir pressure, and avoid contamination of surface waters began in the 1930s (Clark et al., 2005; GWPC, 2009). Kansas was the first state to regulate brine disposal through its State Corporation Commission in 1934 (Wilson et al., 2003). During the 1940s, oil refineries began to inject their liquid waste underground. In 1948, Congress enacted the Federal Water Pollution Control Act, the first comprehensive legislation addressing the issue of surface water pollution. In 1949, Stanolind Oil introduced hydraulic fracturing to the oil and gas industry; this technology replaced fracturing by explosives, which was first introduced by Colonel E.A.L. Roberts in 1862 (Bowman, 1911; Montgomery and Smith, 2010).

During the 1950s, many oil-producing states started to regulate brine disposal. In 1950, there were 4 operating industrial waste injection wells; by 1963, 30 wells were operating (Donaldson, 1964; Tsang et al., 2007). The 1960s marks the first time induced earthquakes and contamination of sources of drinking water were documented, and state agencies became actively involved with ground water pollution issues (Evans, 1966; Wesson and Nicholson, 1987). The earliest documented case of induced seismic activity related to fluid injection occurred at the Rocky Mountain Arsenal disposal well near Denver, Colorado, over a five-year period from 1962 to 1967 (Evans, 1966; Nicholson and Wesson, 1990; Veil, 2013). In 1968, casing failed in Hammermill Paper Company's well No. 1 near Erie, Pennsylvania, contaminating the ground water (USEPA, 2001).

Federal authority for ground water and injection wells began in 1972 with the Clean Water Act (CWA) of 1972. In 1974, with the enactment of the SDWA, the federal government took an active role in UIC. In response to the SDWA, the USEPA established the UIC regulations in 1980. The UIC program classifies wells used to inject fluids associated with oil and gas production, for the purpose of disposal or EOR, as Class II injection wells (USEPA, 2002). According to the GAO (2014), in 2012 there were 172,476 active Class II disposal wells in the continental United States (excluding tribal lands and territories). Figure 8-3 shows the number of active wells for each state. A total of 33 states have operating Class II injection wells; the remaining 17 states do not permit Class II injection due to unsuitable geology. Figure 8-3 also shows that of the 33 states with active wells, 25 have been given primary UIC enforcement authority (primacy) by the USEPA and 8 are under USEPA authority.



Source: GAO (2014)

Figure 8-3. Number of active Class II wells and regulatory enforcement authority, by state, as of 2012.

8.1.2 Organizational Challenges and Current Data Availability

State and federal agencies collect large amounts of data concerning oil and gas operations; these data are contained in a variety of different databases. Table 8-1 illustrates the multiplicity of regulatory agencies across states; Table 8-2 illustrates the types of data available.

Table 8-1. Primary regulatory agencies and active Class II well inventories.

State	Class II Primary Regulatory Enforcement Agency	Effective Date	Well Inventory		
			2010	2011	2012
States with UIC primacy					
Alabama	State Oil and Gas Board	1982	240	247	247
Alaska	Oil and Gas Conservation Commission	1986	1,347	1,347	1,347
Arkansas	Oil and Gas Commission	1982	1,093	1,085	1,100
California	Department of Conservation, Division of Oil, Gas, and Geothermal	1984	29,505	47,624	49,783
Colorado	Oil and Gas Conservation Commission	1984	874	901	901
Illinois	Illinois Environmental Protection Agency	1984	7,843	7,858	7,858
Indiana	Department of Natural Resources	1991	2,091	1,260	1,260
Kansas	Department of Health and Environment	1984	16,658	15,919	16,965
Louisiana	Department of Natural Resources	1982	3,731	3,676	3,687
Mississippi	State Oil and Gas Board	1989	1,110	1,180	1,212
Missouri	Department Natural Resources	1983	282	282	455
Montana	Board of Oil and Gas Conservation	1996	1,062	1,062	1,149
Nebraska	Oil and Gas Conservation Commission	1984	661	661	661
Nevada	Division of Environmental Protection	1988	18	18	18
New Mexico	Energy and Minerals Department, Oil Conservation Division	1982	4,585	4,616	4,556
North Dakota	Industrial Commission-Oil and Gas Division	1983	1,023	1,171	1,290
Ohio	Department of Natural Resources, Division of Oil and Gas Resources	1983	2,455	2,459	2,439
Oklahoma	Corporation Commission	1981	10,629	10,854	11,134
Oregon	Department of Environmental Quality	1984	9	8	9
South Dakota	Department of Environment and Natural Resources	1984	87	87	87
Texas	Railroad Commission	1982	52,016	52,501	52,997
Utah	Department of Natural Resources, Division of Oil, Gas, and Mining	1982	428	462	547
Washington	Department of Ecology	1984	1	1	1
West Virginia	Division of Environmental Protection	1983	779	779	710
Wyoming	Oil and Gas Conservation Commission	1982	4,978	5,005	5,005
States where USEPA Regions have primacy					
Florida	USEPA Region 4	1984	58	56	60
Iowa	USEPA Region 7	1984	3	7	7
Kentucky	USEPA Region 4	1984	3,403	3,165	3,221
Michigan	USEPA Region 5	1984	1,460	1,432	1,451
New York	USEPA Region 2	1984	532	481	423
Pennsylvania	USEPA Region 3	1984	1,861	1,857	1,865
Tennessee	USEPA Region 4	1988	18	16	19
Virginia	USEPA Region 3	1984	11	12	12

Sources: 40 CFR Part 147 (2011); USEPA (2002, 2011); GAO (2014).

Table 8-2. Primary regulatory agencies and data availability.

State	Regulatory Agency	Website	GIS	RBDMS	Forms on-line	
					Permits	Inventory
States with UIC primacy						
Alabama	Geological Survey, State and Oil Gas Board	✓			✓	✓
Alaska	Oil and Gas Conservation Commission					
Arkansas	Oil and Gas Commission	✓	✓	✓	✓	✓
California	Department of Conservation, Division Oil, Gas, and Geothermal Resources	✓	✓		✓	✓
Colorado	Oil and Gas Conservation Commission	✓	✓	✓	✓	✓
Illinois	Department of Natural Resources, Oil and Gas Resource Management	✓		✓	✓	✓
Indiana	Department of Natural Resources, Division of Oil and Gas	✓	✓	✓	✓	✓
Kansas	Corporation Commission	✓	✓	✓	✓	✓
Louisiana	Department of Natural Resources, Office of Conservation	✓			✓	✓
Mississippi	State Oil and Gas Board	✓	✓	✓		
Missouri	Oil and Gas Council	✓		✓	✓	✓
Montana	Board of Oil & Gas Conservation	✓	✓	✓	✓	✓
Nebraska	Nebraska Oil and Gas Conservation Commission	✓	✓	✓	✓	✓
Nevada	Division of Environmental Protection, Bureau of Water Pollution Control		✓	✓	✓	✓
New Mexico	Oil Conservation Division	✓	✓	✓	✓	✓
North Dakota	Industrial Commission-Oil and Gas Division			✓	✓	✓
Ohio	Department of Natural Resources, Division of Oil and Gas Resources	✓	✓	✓	✓	✓
Oklahoma	Corporation Commission	✓		✓	✓	✓
Oregon	Department of Environmental Quality	✓	✓		✓	✓
South Dakota	Department of Environment and Natural Resources	✓	✓		✓	✓
Texas	Railroad Commission	✓	✓			
Utah	Department of Natural Resources, Division of Oil, Gas, and Mining	✓	✓	✓	✓	✓
Washington	Department of Ecology	✓				
West Virginia	Department of Environmental Protection	✓			✓	✓
Wyoming	Oil & Gas Conservation Commission	✓	✓	✓	✓	✓
States where USEPA Regions have primacy						
Florida	USEPA Region 4					
Iowa	USEPA Region 7					
Kentucky	USEPA Region 4					
Michigan	USEPA Region 5					
New York	USEPA Region 2	✓				
Pennsylvania	USEPA Region 3					
Tennessee	USEPA Region 4					
Virginia	USEPA Region 3					

Finding information and data pertaining to Class II injection wells can be challenging. Agencies are responsible for administering injection permits, inspections, and well closures and for compiling monitoring data on injection operations (volumes and pressures). Determining which agency is responsible for data access is not always straightforward. For example, according to Code of Federal Regulations (CFR) (2011) Title 40, Volume 23, Part 147, the ODNR was given primacy over the state's Class II wells in 1983. The agency given regulatory authority by the state of Ohio was the Division of Oil and Gas. Since 1983, this division has undergone name changes through departmental reorganization. Over a period of time, the Division of Oil and Gas was part of the Division of Reclamation, which later became the Division of Mineral Resources Management, and has now come full circle to be called the Division of Oil and Gas again. This creates confusion in identifying the proper regulatory agency. Even if the proper state agency can be identified, not all agencies provide data access via the internet. Furthermore, while many agencies do provide internet access to their data, some of the information (primarily confidential and pre-digital legacy data) is inaccessible.

Another problem encountered during this review was finding up-to-date statistics. For example, the USEPA posts well inventories from 2010 and 2011 on its website. These inventories do not differentiate between the numbers of brine disposal, EOR, or hydrocarbon storage wells. The most current and comprehensive national summary on produced water volumes and management was compiled by Clark and Veil (2009) using 2007 data.

8.1.3 Geologic Considerations

One of the principal considerations in siting a Class II injection well is the local geology (Arthur et al., 2009b). Geologic formations used for produced water disposal vary by state, but in general they are required to meet similar criteria. Injection wells operators target permeable strata below the USDW that can reasonably accept injected fluids at pressures less than the formation fracture pressure of the confining strata. Traditionally, existing hydrocarbon wells with a successful history of production and a depleted reservoir have been transformed into produced water disposal wells, but a well integrity factor is crucial when such wells are considered for such operations (discussed in more detail in Section 8.1.12). The rationale behind the transformation is that a depleted reservoir that has formerly produced hydrocarbon would have the capability and storage potential of accepting injected fluid at a suitable rate that satisfies disposal objectives. This practice is most common in Texas and Alaska, which have a large number of licensed Class II injection wells.

The presence of numerous licensed Class II wells in specific states is largely due to political factors, geological constraints, and a history of exploration activities (Zoback et al., 2010). Geologic constraints related to porosity, permeability, geological structures, and other factors play a significant role in the current shortage of Class II wells in the Marcellus Shale regions.

Another important factor in siting and permitting Class II injection wells is the target interval, which must be adequately isolated from the USDW. A sufficient interval of impermeable strata (approximately 250 feet of clay or shale) capable of containing the injected fluids must be present above and below the injection zone in order to successfully permit injection wells (Arthur et al., 2009b). Criteria used in choosing a geologic formation for injection of produced water include, but are not limited to, permeability, porosity, thickness, and reservoir state (i.e.,

whether the formation is hydrocarbon-bearing or a depleted reservoir). A detailed requirement is provided in application packs for injection wells provided by state agencies. An example of suitable geologic formations with properties adequate for injection purposes is provided in Table 8-3. The information and parameters provided in the table were obtained from the Alaska Oil and Gas Conservation Commission website.

Table 8-3. Geologic properties of injection zones in Alaska formations.

Formation	Estimated porosity range (%)	Estimated permeability (mD)	Estimated injection pressure (psig)
Beluga (fluvial/lacustrine/alluvial sandstone)	1.9-29.7	0.001-128	1,200-3,000
Kingak (Barrow Sandstone)	—	0.01-3295	400-800
Sterling	28	1,000	1,600-2,800
Torok	21	—	1,800-2,300
McArthur River unit	—	—	3,000-3,300
North Trading Bay unit	—	—	3,000

Source: Alaska Oil and Gas Conservation Commission (2013)

8.1.4 Economics

Across the United States, several large shale developments that are comparable in resource quantity or size have impacted the surrounding economies. Among them are the Bakken Shale in North Dakota and Montana, the Eagleford Shale in Texas, the Barnett Shale in Texas, and now the Marcellus Shale in Ohio, West Virginia, Pennsylvania, and New York. The location of shale development plays a key role in the economic success of the well. In areas where geological exploration and production are already significant, there is an existing infrastructure and community familiarity with drilling. In new locations or less-developed locations, there is a larger initial investment into the community to develop the infrastructure to support drilling and production activities. Furthermore, in areas that are not rich in resource extraction, there can be economic restrictions and regulations due to the community. For example, the Marcellus Shale is spread through several states with different regulatory bodies and regulations (Table 8-4). West Virginia has implemented minor new regulations related to shale gas, while New York has implemented a moratorium on hydraulic fracturing shale formations while the environmental impact of the technology is considered.

Table 8-4 State distribution of the Marcellus Shale play.

State	Area % of Marcellus
Maryland	1.09
New York	20.06
Ohio	18.19
Pennsylvania	35.35
Virginia	3.85
West Virginia	21.33

Source: USEIA (2011)

Ohio is experiencing an increase in drilling, production, and waste disposal. This has resulted in several new bills. Senate Bill 315, signed into law in 2012, imposed new restrictions and controls on oil and natural gas drilling in Ohio. As of March 2014, a House Bill was proposed for a 2.75% severance tax, and House Bill 375, passed in May, seeks a 2.25% tax revenue which will go to local governments impacted by drilling in the shale (Benham, 2014). The oilfield business in Ohio is not as developed as it is in Texas, and the costs associated with drilling and waste disposal are higher in Ohio than in Texas. These legislative developments and the cost of drilling may impact Marcellus and Utica shale development in Ohio. To understand all the economic factors, it is important to compare similarities and differences in different shale plays and analyze the economic opportunities and challenges of northeastern shale development.

As the Marcellus Shale is developed, there are numerous economic impacts to consider. As of 2011, almost 7 million acres of land over the Marcellus Shale play has been leased to 19 companies. Overall, the general location of the shale influences economic expenditures and the success of exploration. In addition, the Marcellus and Utica shale creates more hydraulic fracturing waste than any other U.S. shale play (USEIA, 2011). This increases waste disposal costs, which are already higher in this part of the country due to pre-existing regulation, community opposition, and the lack of existing salt water disposal wells.

Approximately 98% of oilfield fluids in Ohio are disposed of through injection in disposal wells. The remaining 2% is spread legally for dust and ice control. In 2011, more than half of the liquids disposed of in Ohio's disposal wells came from out of state (Fort, 2013).

The cost of disposal is adjusted by the distance the flowback is transported. According to Chesapeake Energy's 2011 economics report, commercial produced water disposal is typically \$0.50 to \$2.50 per barrel, determined by supply and demand. Trucking costs across the country average \$1 per barrel per hour. In areas with a large number of salt water disposal wells, such as Texas, the trucking costs are \$0.50 to \$1. In areas where produced water disposal is less common (for example, Pennsylvania), these costs range from \$4 to \$8 per barrel (McCurdy, 2013).

8.1.5 Environmental Regulations (Policy Issues)

Across the United States, the impact of produced water from oil and gas operations on the environment has been a concern for federal and state regulatory agencies. Unconventional extraction of oil and gas resources, such as hydraulic fracturing of tight shale formations for natural gas, could produce water that may contain organic chemicals, inorganic chemicals, naturally occurring radioactive materials (NORM), and toxic metals (Abdalla et al., 2011; Tiemann et al., 2012). These chemicals and materials can be potentially harmful to the public if they are disposed of improperly at the surface. For example, recent studies by Thamke et al. (1996) and Thamke and Smith (2014) investigated the contamination of USDW in and near the East Poplar field in northeastern Montana. The studies concluded that the likely source of contamination was from brine produced with crude oil. These studies illustrate the contamination risks to the USDW from produced water that is not managed responsibly (Thamke et al., 1996; Thamke and Smith, 2014). This particular incidence (and other examples discussed later) suggests that the handling and disposal of produced water are of paramount importance in the oil and gas industry. The production of 1 gallon of oil may result in the production of up to

10 gallons of water (Mace et al., 2005; USEPA, 2005). By injecting the produced water deep underground, via Class II wells, into their source formation or into similar formations at significant depths below the USDW, the contamination of surface soil and of shallow ground water can be prevented (Tiemann et al., 2012).

To contain and minimize the effect of produced water on the environment, stringent regulations have been put in place and newer ones are emerging. In the United States, the CWA is the primary federal law enacted to protect surface water quality. It establishes pollutant limits on the discharge of oil- and gas-related produced water (GWPC, 2009).

In 1974, Congress passed the SDWA with the goal of protecting public health (GWPC, 2009; Arthur et al., 2009b). One of the Act's primary goals is to ensure that current (and possibly future) water sources that could serve as public drinking water supplies are not polluted. To that end, the SDWA establishes a framework for the UIC program to prevent contamination of USDW from injection of liquid wastes such as the produced water from oil and gas operations (GWPC, 2009). For almost 40 years, the SDWA has promoted the preservation of USDW and the regulation of injected wastes at federal and state levels through the USEPA UIC program. The USEPA works closely with states and other key holders to help ensure that oil and natural gas extraction does not come at the expense of public health and the environment.

8.1.6 Unconventional Resources

Recent advances in technology have introduced techniques such as horizontal drilling and reservoir stimulation (also referred to as “hydraulic fracturing”). These techniques have made the exploitation of unconventional shale resources in over half of the lower 48 states (Figure 8-4) economically viable (Arthur et al., 2009b; Tiemann et al., 2012; Vengosh et al., 2013). One of the potentially largest unconventional natural gas resources in the United States is the Marcellus shale of the Appalachian region. Significant interest in the Marcellus shale as a major gas play is reflected in the increased drilling activity in Pennsylvania and West Virginia, combined with increased industry presence in New York and Maryland (Tiemann et al., 2012). The growth in development of natural gas from the unconventional shale play comes with challenges related to environmental considerations and water management issues. Hydraulic fracturing in conventional vertical wells may use as little as 50,000 gallons of water, while multi-stage fracturing in horizontal wells may require 3 million to 8 million gallons per well within the Marcellus shale play (Arthur et al., 2009a; Tiemann et al., 2012; Kakadjian et al., 2013; USGS, 2013).



Source: Vengosh et al. (2013)

Figure 8-4. Shale gas basins in the United States.

Generally, most of the water used to fracture a well will remain deep underground; approximately 9% to 35% will return to the surface within a few weeks to 30 days (Abdalla et al., 2011; Tiemann et al., 2012). This amounts to about 300,000 to 800,000 gallons of wastewater per well drilled in the Marcellus or Barnett shale play, assuming that 10% of the fluid returns to the surface. Because of the increase in drilling activities and in produced water from shale gas in the United States, managing produced water could pose a significant challenge to operators and lawmakers in years to come. For instance, managing the wastewater produced from the hydraulic fracturing process has become a major water resource issue for the Marcellus shale play (Tiemann et al., 2012; USGS, 2013).

Environmental considerations associated with the development of these unconventional plays are gradually receiving nationwide attention from lawmakers. Some of this attention is focused on the management of the brine produced following hydraulic fracturing. Flowback fluid emerges at the surface within 30 days after a hydraulic fracturing procedure (Abdalla et al., 2011). Flowback fluid is a mixture of the naturally occurring saline formation fluid and the hydraulic fracturing fluid, which may contain concentrations of sand, heavy metals, oils, grease, and naturally occurring compounds from within the fractured formation (Abdalla et al., 2011; Tiemann et al., 2012). Carter et al. (2013) studied the different organic compounds contained in fracturing fluids

that are injected into formation, their possible life cycle after the process, and difficulties encountered when analyzing these compounds. Continued analyses of both the hydraulic fracturing fluid and the produced water have shown that not all organic compounds that were injected into the well return to the surface (Carter et al., 2013). According to Tiemann et al. (2012), the additives in 3 million gallons of water used for a fracturing process (and 300,000 gallons of produced waste) could yield about 15,000 gallons of chemicals in the produced waste, accounting for 0.5% of water used and 5% of fluid that resurfaces.

Produced water from hydraulic fracturing is managed differently from state to state (Veil, 2011), depending on the economics, local geology, existing regulations, and availability of disposal facilities

8.1.7 Produced Water Management Practices

Produced water can be described as waste fluids produced during drilling, reservoir stimulation, and production associated with oil and gas operations. It could be produced from conventional oil and gas wells, unconventional reservoir stimulation operations (hydraulic fracturing), and other processes such as EOR and oil and gas processing. Improper surface disposal of produced water from such activities could result in the contamination of shallow ground water aquifers. Traditionally, these produced fluids have been either injected into deep wells or treated before disposal into surface water (GWPC, 2009; Tiemann et al., 2012).

Underground Injection of Produced Water

Underground injection of produced water via Class II wells still remains the preferred disposal practice (Tiemann et al., 2012). In some states (for example, Texas), there are tens of thousands of licensed Class II injection wells (Zoback et al., 2010) (see Figure 8-3), making underground injection a common practice in this state; however, underground injection is not possible in every shale play due to the unavailability of suitable injection zones (GWPC, 2009). On the other hand, in states such as Pennsylvania, there are limited numbers of Class II injection wells and there are regulations limiting these wells to accepting a particular type of wastewater in some areas (Abdalla et al., 2011). Hence, produced water is disposed of at municipal waste water treatment facilities where the water is treated, then either discharged into surface water bodies such as rivers and streams or exported to Class II wells (Zoback et al., 2010).

Handling and Treatment of Produced Water

Innovative technologies for handling produced water have been tested in the past. Examples of such technologies include the AltelaRain technology, which was applied in the Marcellus Basin for treatment of produced water. Details and benefits of the technology are discussed more extensively by Bruff and Jikich (2011). Another method that has been applied to encourage water reuse could preclude the need to use fresh water in the fracturing fluid system. This potentially revolutionary method would reuse 100% produced water for the hydraulic fracturing process by introducing a stable fracturing fluid (Kakadjian et al., 2013). In other documented cases, produced water has been reused to recover chemicals (Grimaldi et al., 2010).

These recent innovations have not been used on a broad scale; however, they could hold the solution to mitigate the challenges of managing produced water from hydraulic fracturing by

reducing waste volumes, reducing the need for more Class II injection wells, and reducing operational costs for oil and gas operators.

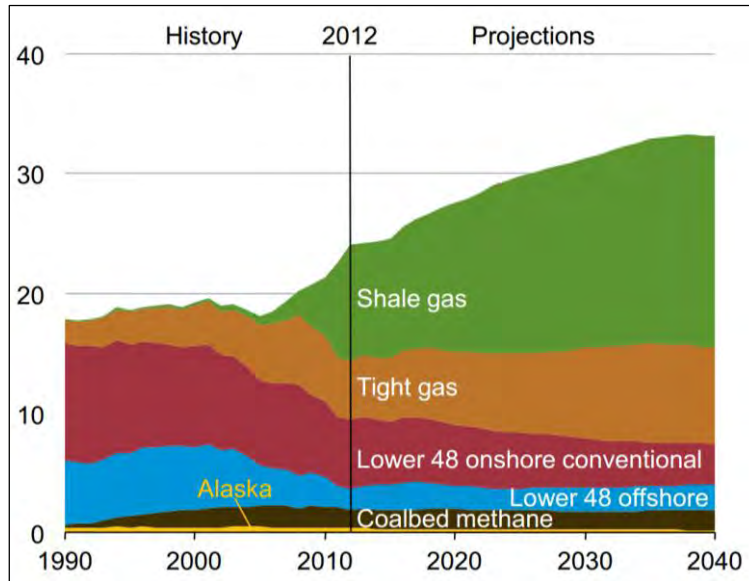
Beneficial Use

Some information sources have discussed the potential for beneficial use of the produced water from oil and gas operations in the western United States, but such use would depend on factors such as water quality criteria, water quantity, ownership of produced water, and acquisition of permits (Guerra et al., 2011). The produced water may contain salt, organic constituents, inorganic constituents, chemical additives, or NORM that can contaminate soil, ground water, and surface water (Abdalla et al., 2011; Tiemann et al., 2012; Guerra et al., 2011). Depending on the need and potential use, and given the quality of produced water, treatment would be required to meet most beneficial use scenarios. Examples of beneficial uses include livestock watering, irrigation, stream flow augmentation, rangeland restoration, industrial uses (such as reuse in oil and gas operations: EOR, fracturing water, dust suppression, fire protection, cooling towers), and, in some cases, domestic purposes (Guerra et al., 2011).

8.1.8 Underground Injection Program (Class II injection)

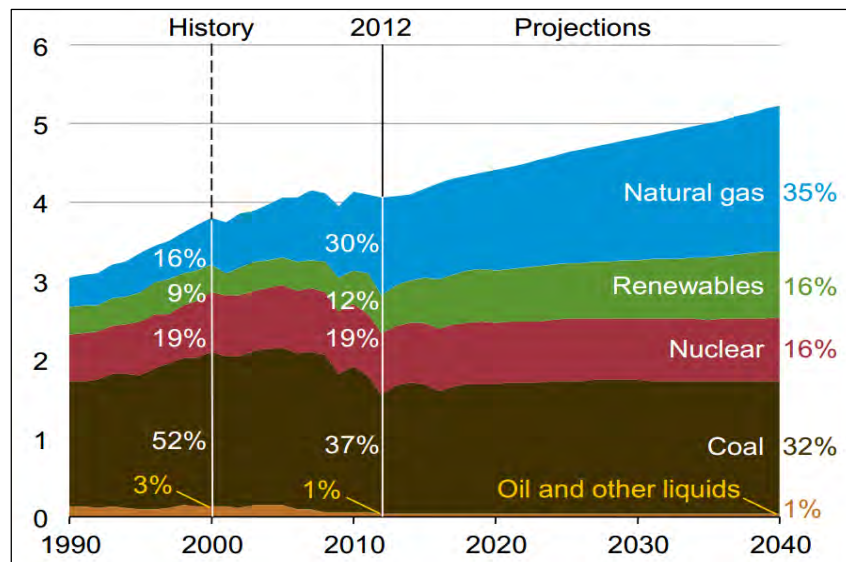
The SDWA authorizes the UIC program to protect existing USDW, as well as aquifers having the potential for future use as USDW, from unsafe injection practices (Arthur et al., 2009b; USEPA, 2002). In recent years, all aspects of hydrocarbon exploration and production activities have drawn closer scrutiny in terms of existing and potential impairment of the environment (Moody, 1994). A substantial volume of liquid and solid waste generated from oilfield operations is salt water (brine), and most of the liquid waste is reinjected into the underground via a Class II injection well. Because of the enormous volume of produced water injected into the ground, specifically in hydrocarbon-producing states, the USEPA continues to reassess the UIC program, reviewing the existing regulations and updating them.

Factors limiting this particular method of disposal are the availability of adequate numbers of disposal wells, maximum injection pressures (MIP), and limitations on the allowable daily volume of water that can be injected per well. Emerging shale development plays such as the Marcellus shale may require additional capacity of Class II wells in the Appalachian region if underground injection is to be used for disposal of flowback and produced water (Gaudlip et al., 2008). There are currently only about 7 to 10 Class II injection wells in Pennsylvania (Abdalla et al., 2011; Zoback et al., 2010), and only one is commercial. Compounding the issue of disposal in Pennsylvania is the fact that the single commercial well has limited or no available capacity and is not permitted for Marcellus wastewater disposal (Abdalla et al., 2011). The situation could potentially get worse because projections (Figure 8-5) show shale gas production increasing over the coming years. In addition, the reliance on natural gas for electricity generation (Figure 8-6) is expected to increase over the coming years, with natural gas generating nearly 35% of the electricity used in the United States by 2040. Such an increase in the production of shale gas will require more Class II wells in the shale play regions, particularly in the Marcellus area and in areas close to the state of Pennsylvania (such as northeastern Pennsylvania) where geologic constraints have limited the underground injection of produced water (Tiemann et al., 2012; Zoback et al., 2010).



Source: USEIA, 2014.

Figure 8-5. Past and projected (1990-2040) U.S natural gas production (TCF).



Source: USEIA, 2014.

Figure 8-6. Past and projected (1990-2040) electricity generation by fuel (trillion kilowatt-hours).

In Arkansas, there are approximately 528 Class II injection wells; 28 of these wells are operated as commercial wells and approximately 500 operate as non-commercial (producer-owned) disposal wells (STRONGER, 2012). The Fayetteville Shale play has an estimated technically recoverable resource of 32 TCF of gas (USEIA, 2011). Within the Fayetteville shale

development area, there are approximately six commercial and nine non-commercial wells. Despite the presence of 28 licensed commercial Class II injection wells and over 500 non-commercial in the Arkansas region, exploration and production waste still needs to be trucked to disposal wells in nearby Oklahoma City. On the other hand, the Marcellus region has an estimated technically recoverable resource of 84 to 144 TCF (USEIA, 2011; USGS, 2011) and 324 licensed Class II injection wells (August 2012 data), some of which are commercial and non-commercial, serving the region. Recognizing the relatively low number of Class II wells serving the Marcellus region, which has approximately three times more estimated resource than Fayetteville, it is clear that there is still a huge gap to fill in the near term if operators plan to use underground injection only for disposal in the Marcellus.

8.1.9 Issues Related to Underground Injection

Ground Water Quality

No systematic survey has documented the extent of shallow ground water contamination from disposal by underground injection; however this practice is recognized as a major potential pollution source in leading hydrocarbon-producing states (McLin, 1986). In the past, citizens have alleged that underground fluid injection related to hydraulic fracturing of coal bed methane reservoirs is affecting the quality of ground water (USEPA, 2004). Many believe that this contamination is occurring through leakages. However, underground injection is one of the most promising and applied methods for disposal of produced brine in the oil and gas industry (Tiemann et al., 2012), and the challenge to contain the disposed fluid in the target injection zone is regulated by the UIC program. The UIC program prevents contamination that could occur via the following pathways (USEPA, 2012):

- Faulty well construction: Leaks in well casing or fluid escaping from space between well's outer casing and wellbore.
- Nearby wells: Fluids from pressurized area in injection zone escaping through wells in injection area.
- Faults or fractures in confining strata: Fluids leaking out of pressurized area through faults/fractures in confining beds.
- Direct injection: Fluids injected into or above USDW.
- Displacement: Fluid displaced from injection zone into hydraulically connected USDW.

Seismic Events

Another issue related to underground injection is the potential for seismic events. This issue has been receiving wider attention in regions of underground injection. With regard to cases such as those in the Fayetteville shale region, investigators identified a possible correlation of seismic events occurring within the shale development area to underground injection at a disposal well located near a previously unknown deep fault system (STRONGER, 2012). Other seismic events related to underground injection have also been studied by different information sources, and such events are becoming a major concern. Some sources have linked seismic events to fault

systems located near an injection area, while others have linked them to some other subsurface mechanism (see Section 8.1.14).

8.1.10 Other Associated Environmental Issues

Other environmental issues associated with Class II brine disposal include wastewater treatment, storage, and transportation; well siting; the use of chemicals; and the preservation of rare species and natural communities.

Wastewater Treatment, Storage, and Transportation

Wastewater from gas well drilling is known to be treated in sewage treatment plants in some places (for example, the state of Pennsylvania) prior to disposal into surface water (Tiemann et al., 2012; Zoback et al., 2010). The wastewater is noted to contain high concentrations of total dissolved solids (TDS), which are not considered a major human health risk if present in allowable amounts (PA DEP, 2008; WSC, 2007). However, high TDS concentrations may indicate elevated levels of ions (aluminum, arsenic, copper, lead, nitrate, etc.) that pose a health concern. In the past, elevated TDS concentrations have been recorded in Pennsylvania's Monongahela River, which supplies drinking water to the city of Pittsburgh (PA DEP, 2008; Zoback et al., 2010; Tiemann et al., 2012). The TDS increases were traced to a treatment facility; as a result, the Pennsylvania Department of Environmental Protection (PA DEP) ordered the facility to temporarily restrict its intake of drilling wastewater. PA DEP reported other possible influences on the TDS levels (e.g., mine drainage, stormwater runoff, and discharges from industrial or sewage treatment plants), and similar occurrences were reported again twice in 2009 (Zoback et al., 2010).

Managing produced brine (flowback fluid) sometimes requires temporary storage and transport of such fluids prior to treatment or disposal. A review of the literature shows that operators have used a variety of storage options for flowback fluid and produced water. Some service companies that perform hydraulic fracturing stimulation work for operators are working to design systems that allow fluids to be contained within closed fluid-capture systems to mitigate the risk of spills and subsequent exposure to the environment (Arthur et al., 2008). Other operators store flowback fluid and produced water in open evaporation pits. Produced fluids that are stored in pits could leak and penetrate into the surface, presenting a risk of contaminating shallow ground water or even a poorly constructed drinking water well within the locality (Tiemann et al., 2012). In Pennsylvania, impoundment incidents have been reported in Dimock Township in Susquehanna County and Hopewell Township in Washington County. Steps have been taken and precautions applied to prevent or mitigate such incidents (for example, impoundments used only for a limited duration to reduce risk).

There is also an associated risk that a pit could overflow during a period of rainfall, resulting in contaminated runoff. Storing produced flowback water in enclosed tanks could significantly lessen the risk of such contamination. Unsecure hoses on equipment could also lead to fluid spilling onto bare soil; therefore, onsite equipment requires frequent monitoring and testing before it is used. Adequate measures must also be taken while transporting produced water via pipelines and trucks. To reduce the risk of leaks and spills due to human error, equipment malfunction, and other operational issues, the industry has established many inspection and management practices for day-to-day operations.

Given the shortage of injection facilities in the Marcellus region, where shale development is booming, there is a growing need to transport produced flowback water by truck to nearby states, such as Ohio, that have a greater number of licensed Class II injection wells. However, trucks pose threats to the environment from two major, quantifiable sources: air pollution and noise (OECD, 1997; THE Impact Project, 2012). Heavy-duty trucks that transport produced water use diesel fuel, and emissions from these trucks contain diesel particulate matter (DPM). Some places, such as the state of California, regulate DPM as a toxic air contaminant (THE Impact Project, 2012). In addition, the gases emitted increase air pollution and degrade the atmosphere, thereby directly (and adversely) affecting human health and the environment (Corbett and Winebrake, 2007; Zoback et al., 2010). Other concerns related to trucking include the environmental impacts of accidents and road damage (OECD, 1997, THE Impact Project, 2012).

Well Siting

The siting of Class II injection wells primarily considers proximity to current and future drilling and production facilities (Arthur et al., 2009b). In cases where shale development wells are constructed in remote locations, roads must be constructed to accommodate truck transport and provide access to other facilities. Construction-related activities and oil and gas operations increase the likelihood that sediments will become polluted; therefore, some states (e.g. Pennsylvania and New York) require well operators to develop an erosion and sedimentation plan for any construction activities (Arthur et al., 2009b; Tiemann et al., 2012).

Use of Chemicals

The public has expressed concerns regarding the chemicals used for natural gas production ever since a report analyzing such chemicals showed possible health effects, especially when encountered in high concentrations (Arthur et al., 2009a). The fluid used for hydraulic fracturing varies state by state and company by company. In addition, because the composition of each fracturing fluid varies to meet needs specific to a well, it is not possible to provide a single amount or volume present in each additive (Arthur et al., 2008). Some information sources (such as the website of the Arkansas Oil and Gas Commission) provide examples of chemical lists used by service companies for operators. The mixture of fracturing fluid used for hydrofracturing is also governed by the geologic characteristics of the affected formation and the chemical characteristics of the water used. In most cases, the fluids consist of water mixed with proppants and chemicals. Depending on the state, companies may be required to submit a detailed composition of fluids used for their hydraulic fracturing jobs. An example of fracturing fluid additives, main compounds, and common uses is provided in Table 8-5.

Table 8-5. Fracturing fluid additives, main compounds, and common uses.

Additive Type	Main Compound	Common Use of Main Compound
Acid	Hydrochloric acid or muriatic acid	Swimming pool chemical and cleaner
Biocide	Glutaraldehyde	Cold sterilant in health care industry
Breaker	Sodium chloride	Food preservative
Corrosion inhibitor	N, n-dimethyl formamide	Used as a crystallization medium in pharmaceutical industry
Friction reducer	Petroleum distillate	Used in cosmetics, including hair, make-up, and nail and skin products
Gel	Guar gum or hydroxyethyl cellulose	Thickener used in cosmetics, sauces, and salad dressings
Iron control	2-hydroxy-1,2,3-propanetricarboxylic acid	Citric acid used to remove lime deposits Lemon juice ~7% citric acid
Oxygen scavenger	Ammonium bisulfite	Used in cosmetics
Proppant	Silica, quartz sand	Play sand
Scale inhibitor	Ethylene glycol	Automotive antifreeze and deicing agent

Source: Arthur et al. (2008)

Preservation of Species and Natural Communities

Other environmental concerns relate to the preservation of rare species and peculiar natural communities. Some states take these concerns into consideration before a Class II injection well is permitted. For example, the state of New York requires that a proposed disposal well location be characterized by the New York Natural Heritage Program before a disposal facility is constructed (Arthur et al., 2009b).

8.1.11 State and Federal Regulations

Prior to the 1930s, the oil and gas industry generally operated without much regulation from the state or federal government. Most early regulations were not designed to protect ground and surface water from the impacts of oil and natural gas production. In the 1970s, the U.S. Congress passed two federal laws governing the disposal of drilling waste: the CWA (1972) and the SDWA (1974). The CWA prohibits the discharge of oil and gas field produced water, including flowback, into navigable waters; the SDWA governs underground disposal and injection of fluids to ensure the protection of USDWs. In 1980, the USEPA, under authority of the SDWA, established the UIC program to protect current and future USDW through proper site location, construction, and operation of injection wells (GAO, 2012). The federal requirements and standards for the UIC program are found in 40 CFR Parts 145-147.

The UIC program is designed to ensure that:

- injection activities are performed safely,
- the current USDWs that supply 90% of all public water systems are protected, and
- future sources of underground water are preserved.

The USEPA may grant a state agency primary enforcement authority for the UIC program if the agency meets or exceeds the federal requirements established by the program. If approved, the

state is responsible for executing the program, permitting and monitoring wells, and enforcing underground injection operations (GAO, 2012). This responsibility is referred to as primacy. For Class II wells, only states with existing oil and gas programs can be granted primacy by the USEPA. If a state does not have primacy, the state's USEPA region will directly implement the program and retain primary enforcement authority (USEPA, 2002; Arthur et al., 2009b). Currently, Class II wells are operating in 33 states; of these, 24 states have been granted primacy, while primacy for 9 states resides with USEPA regional offices. Table 8-1 lists the states and the state agencies granted primacy over Class II wells by the USEPA and the states where USEPA regions have enforcement primacy.

States may have different requirements than the federal program regarding different sizes of areas of review (AORs) and different MIPs. The AOR is the region surrounding an injection well that is reviewed during the permitting process to determine if there is a potential for USDW contamination from injection activities. Under federal regulations, AORs are delineated by determining the zone of endangering influence either by a circle with a minimum fixed radius of ¼ mile from the well or an area determined by calculating the pressure change (Thornhill et al., 1982). Table 8-6 shows the different AORs and MIP gradients required by the states. These requirements may be key considerations for operators in well permitting, installation, and operations.

Table 8-6. Class II well permitting requirements by state.

State	AOR (Mile)	MIP Gradient
Alabama	0.25	—
Alaska	0.25	0.8 psi/ft
Arkansas	0.50	Calculated by agency
California	0.25	By formation, SRT
Colorado	0.25	0.6 psi/ft
Florida	0.25	0.8 psi/ft
Illinois	0.25	<10% BP
Indiana	0.25	0.8 psi/ft
Iowa	0.25	0.8 psi/ft
Kansas	0.25	—
Kentucky	0.25	0.8 psi/ft
Louisiana	0.25	90% CFP
Michigan	0.25	0.8 psi/ft
Mississippi	0.25	75% CFP
Missouri	0.50	—
Montana	0.25	—
Nebraska	0.50	—
Nevada	1.00	—
New Mexico	0.50	0.2 psi/ft
New York	0.25	0.8 psi/ft
North Dakota	0.25 < 200 bbl/day > 0.5	—
Ohio	0.25 < 200 bbl/day > 0.5	0.75 psi/ft

Table 8-6. Class II well permitting requirements by state. (Continued)

State	AOR (Mile)	MIP Gradient
Oklahoma	0.25 (non-com) 0.5 (com)	0.5 psi/ft
Oregon	—	—
Pennsylvania	0.25	0.8 psi/ft
South Dakota	0.50	—
Tennessee	0.25	0.8 psi/ft
Texas	0.25	0.5 psi/ft
Utah	0.50	—
Virginia	0.25	0.8 psi/ft
Washington	—	—
West Virginia	0.25	0.8 psi/ft
Wyoming	0.25	—

Note: BP = breakdown pressure
 CFP = calculated formation fracture pressure
 SRT = step rate test

Under the UIC program, operators are required to apply for a permit to drill an injection well from the primary regulatory agency. After the UIC permit is issued, the operator must observe and record the injection pressure, flow rate, and cumulative volume each month and report this information to the permitting agency annually. The injection well permit also requires producers to conduct mechanical integrity tests on the wells at least once every five years (GAO, 2012).

8.1.12 Wellbore Integrity

Recently, wellbore integrity has been subject of research as a risk factor for carbon capture, utilization, and storage (CCUS) applications. Poor wellbore construction could result in the development of a migration pathway for fluid in any injection operation (underground brine injection, for example). Hundreds of thousands of oil and gas wells have been drilled in the Midwest United States because it has some of the oldest oil and gas fields in the world.

However, the risk in relation to the zones being targeted for CCUS is not well defined. Shallow, old wells may not present actual risk to CCUS projects in deeper formations. In addition, the technical and economic feasibility of mitigating old wellbores has not been well studied. Many areas may have few wellbores and may be more suitable for CO₂ storage fields. Processes related to the age of wells, materials, and construction procedures may also help define risk related to well integrity in old boreholes. For example, analysis of annulus/casing pressure data from gas storage and/or injection wells can help determine issues related to borehole integrity such as microannulus, cement degradation, channeling, casing leaks, and other factors.

Wellbore integrity focuses on defining upper and lower wellbore pressure limits and identifying the optimum mud weight window. Monitoring the integrity of the wellbore is extremely important in protecting ground water throughout the life cycle of a well. Both state and federal regulatory agencies have testing standards to ensure the safety of our wells and aquifers (USEPA, 2013b). The Ground Water Protection Council (GWPC), a national association of state agencies, has recommended a full suite of life cycle analysis procedures aimed at protecting the

environment from hydraulic fracturing materials. This recommendation would result in three acceptable parameters: the existing parameters, those which can be established at installation, and those which can be controlled during execution.

8.1.13 Risk Based Data Management Solutions

Many states catalogue oil and gas data using the GWPC's Risk Based Data Management Solutions (RBDMS) database. The RBDMS is an online data management system designed for regulatory agencies to access and manage all their oil- and gas-well information databases in order to track and map oil, gas, injection well, and ground water protection activities. The GWPC began developing the RBDMS in 1992, under grant funding administered by the U.S. Department of Energy (DOE). Initially, the system was created to meet the USEPA's tracking requirements for UIC class to programs.

The RBDMS is designed to help state regulatory agencies:

- track well locations and construction details,
- track production and injection activities,
- track inspection, compliance, enforcement programs,
- track complaints and spill investigations,
- assess AOR impacts to protect USDW,
- manage operator and bonding information,
- manage permitting,
- schedule hearings, and
- generate reports on demand.

Currently, 21 member regulatory state agencies are using the RBDMS system (Table 8-7). Many of these state agencies provide operator and public internet access to the RBDMS data (Table 8-2). RBDMS web applications allow the public to access, and facilitate the ability to mine, data such as well locations; permits; completion, production, and injection reports; field inspections; and geophysical logs (Belieu et al., 2003; GWPC, 2005; McDonald et al., 2005; Jehn and Grunewald, 2007; National Petroleum Council, 2011; RBDMS.Net, 2014).

Table 8-7. States and regulatory agencies using the RBDMS.

State	Agency
Alabama	Geological Survey of Alabama , State Oil and Gas Board
Alaska	Oil and Gas Conservation Commission
Arkansas	Oil and Gas Commission
Colorado	Oil and Gas Conservation Commission
Illinois	Department of Natural Resources
Indiana	DNR Division of Oil and Gas
Idaho	Department of Lands
Kansas	Corporation Commission
Kentucky	Department of Natural Resources, Division of Oil and Gas
Mississippi	State Oil and Gas Board
Missouri	Department Natural Resources
Montana	Department of Natural Resources and Conservation, Board of Oil and Gas Conservation
Nebraska	Department of Environmental Quality
	Oil and Gas Conservation Commission
New York	Department of Environmental Conservation, Division of Mineral Resources
New Mexico	Oil Conservation Division
Nevada	Division of Environmental Protection
North Dakota	Department of Mineral Resources, Oil and Gas Division
Ohio	Department of Natural Resources, Division of Oil and Gas Resources
Oklahoma	Corporation Commission
Pennsylvania	Department of Conservation and Natural Resources
	Department of Environmental Protection
Utah	Department of Natural Resources, Division of Oil, Gas, and Mining

Source: RBDMS.Net (2014)

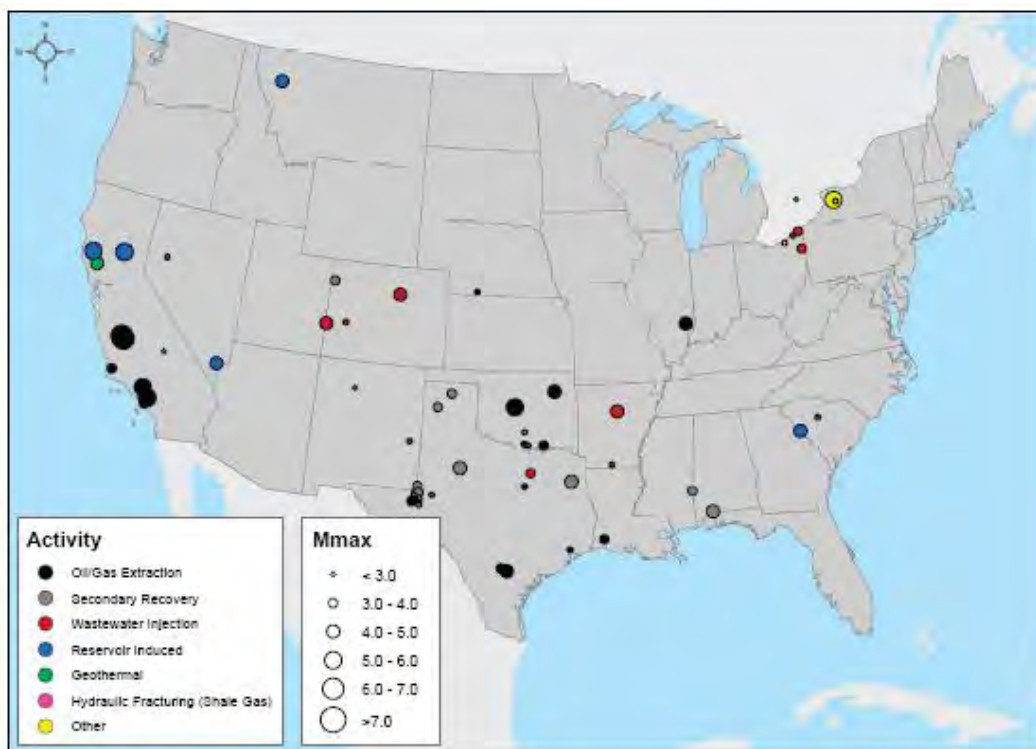
8.1.14 Induced Seismicity

Since the 1960s, induced seismic events related to energy development projects have drawn increasing public and regulatory attention. Seismic events related to energy development have been observed across the United States in Alabama, Arkansas, California, Colorado, Illinois, Louisiana, Mississippi, Nebraska, Nevada, New Mexico, Ohio, Oklahoma, Texas, and West Virginia (National Research Council, 2012; Ellsworth, 2013). Deep well injection has a history of triggering small-scale seismic activity and, in some cases, moderate earthquakes. The earliest documented case of induced seismic activity related to fluid injection occurred at the Rocky Mountain Arsenal disposal well near Denver, Colorado. Induced seismic events occurred over a five-year period from 1962 to 1967 (Evans, 1966; Nicholson and Wesson, 1990; Veil, 2013). A deep disposal well pressure-injected wastewater into impermeable fractured Precambrian gneiss. The volume and pressure of the fluid injection opened existing fractures, causing rock movement. Table 8-8 shows the number of probable induced seismic events in the United States as of 2012; Figure 8-7 shows the locations of these events (National Research Council, 2012).

Table 8-8. Number of induced seismic events in the United States by technology

Technology	No. of Events
Wastewater injection	9
Oil and gas extraction	20
Secondary recovery (water flooding)	18
Geothermal energy	4
Hydraulic fracturing (shale gas)	1
Surface water reservoirs	6
Other (e.g., coal mining, solution mining)	3
Total	61

Source: National Research Council (2012)



Source: National Research Council (2012)

Figure 8-7. Locations of induced seismic events in the United States.

Studies by Wesson and Nicholson (1987), the National Research Council (2012), and Sminchak and Gupta (2003) examined the scale, scope, and consequences of induced seismicity from fluid injection and extraction. In most cases, the risk for induced seismic events occurs in seismically unstable areas with a history of faulting and earthquakes and where the pore fluid pressure and/or stress are high. The factor that seems to have a direct effect is total balance of fluid injected or removed from the subsurface. Most oil- and gas-related projects that maintain a balance between fluid injected and extracted produce fewer seismic events than those that do not maintain a

balance. Wastewater disposal wells that inject into porous aquifers at relatively low pressures generally do not appear to pose a hazard for induced seismicity. Current regulations for Class II disposal were designed to protect ground water reservoirs from contamination and do not address seismic safety (Ellsworth, 2013). As the number of wastewater disposal wells increases in the future, the long-term effects for induced seismicity will be uncertain and will require further study.

8.1.15 Current Research on Oil and Gas Wastewater Management

Sustainable Management of Flowback Water during Hydraulic Fracturing of Marcellus Shale for Natural Gas Production

DOE is currently funding a project aimed at developing a sustainable system for water management in the production of the Marcellus shale. Under this project, flowback water would be treated onsite and reused in adjacent wells for hydraulic fracturing. The project will also investigate the effects of precipitated barium sulfate (BaSO_4) on fractures and well surfaces. The lead performers on this project are the University of Pittsburgh and Carnegie Mellon University. DOE's contribution to the project, from October 1, 2009, to September 30, 2014, is \$794,226; the performers are to contribute an additional \$284,010. Dr. Radisav Vidic (University of Pittsburgh) is the principal investigator (PI) for this project.

NORM Mitigation and Clean Water Recovery from Marcellus Frac Water

RPSEA, along with GE Water & Process Technologies and Endicott Interconnect Technologies Inc., is funding a project to develop a process to recover distilled water and a salable salt product from water produced from the hydraulic fracturing process of the Marcellus shale. The first stage is to develop a process that removes NORM through pretreatment and enables NORM concentrate to be disposed of in an environmentally friendly manner. The second stage is to use membrane distillation to develop a cost-effective brine concentrator suitable for desalinating hydraulic fracturing flowback water. The total project cost is \$1,884,591, with \$1,488,827 being RPSEA's share and the remaining \$376,918 being cost-shared. The project started January 27, 2012, and will continue through April 30, 2014. Dr. James Silva (GE Global Research) is the PI for this project.

Novel Engineered Osmosis Technology: A Comprehensive Approach to the Treatment and Reuse of Produced Water and Drilling Wastewater

This RPSEA funded project was completed by the Colorado School of Mines to investigate osmotically driven membrane processes that utilize osmosis as a mechanism to extract water from highly impaired solutions. The research focused on the development and implementation of this novel engineered osmosis technology in treating wastewater associated with well drilling and stimulation.

Treatment and Beneficial Reuse of Produced Waters Using a Novel Pervaporation-Based Irrigation Technology

RPSEA funded a recent project with WyoTex Ventures LLC, DTI Group, and Imperial College London that explored a novel pervaporation-based irrigation technology and its potential for

treating and reusing water associated with oil and gas production. The research showed potential for the hydrophilic pervaporation membranes to be used to treat produced water as an irrigation system and identified necessary improvements to be made before it could be a viable method for treating wastewater from well production. The project started March 16, 2011, and ended March 15, 2014. Dr. Jonathan Brant (University of Wyoming) was the PI for this project.

Evaluation of Fracture Systems and Stress Fields within the Marcellus Shale and Utica Shale and Characterization of Associated Water Disposal Reservoirs: Appalachian Basin

RPSEA recently funded a project with the University of Pittsburgh, Chesapeake Energy Corporation, Jeter Field Service, RARE Technology, AscendGeo, AOA Geophysics Inc., Austin Powder Company, and Seismic Source Company (subcontractors: The University of Texas at Austin, Bureau of Economic Geology). The project goal was to evaluate fracture systems and stress fields in the Marcellus and Utica shales. The study emphasized the importance of multicomponent seismic data acquisition based on the higher resolution it provides (compared to conventional, single-component data). It explored the orthorhombic nature of the Marcellus shale, characterizing its orthogonal joint sets and other fracture properties to advance current knowledge of how the formation can act as a deep-water disposal reservoir. This study showed that the presence of orthogonal joint systems (in which the Marcellus shale has two sets) may be overlooked in seismic data due to orthogonal joint sets causing azimuth variations in P and S reflection amplitudes to be small compared to a medium where a single set of fractures occurs. These findings suggest that an alternative approach is necessary to accurately estimate fracture densities of orthogonal joints in the Marcellus by using converted S-seismic data. The implementation of this work could allow operators to optimize production of fractured shale-gas reservoirs and more accurately screen potential reservoirs for disposal of flowback water. The project started on September 29, 2009, and ended on January 31, 2013. Dr. Bob Hardage (University of Texas at Austin) was the PI for this project.

Pilot Testing: Pretreatment Options to Allow Reuse of Frac Flowback and Produced Brine for Gas Shale Resource Development

DOE, along with Norse Energy, Range Resources, BG Exco Partnership, and Escondido Resources, funded a project aimed at identifying cost-effective pretreatment methods to treat and reuse oilfield brines and fracture flowback waters (performers: Texas A&M University, Argonne National Laboratory, Los Alamos National Laboratory, Houston Advances Research Center, Sam Houston State University, and Rensselaer Polytechnic Institute) in collaboration with New York State Research Development Authority and M-I SWACO. The project developed a “chemicals-free” method for removing contaminants from saline brines. The study developed a methodology for removing contaminants from oil field brines without the use of chemicals. Spiral-wrapped polymeric membranes were tested in the field and were able to remove tall suspended solids, hydrocarbons, and bacteria from brine (of greater than 140,000 TDS), producing a stable water suitable for reuse in well operations. This methodology promises a more environmentally responsible way to manage flowback water from the Marcellus. The project started on October 1, 2009, and ended December 31, 2012. David Burnett (Texas A&M University) was the PI for this project.

GIS and Web-Based Water Resource Geospatial Infrastructure for Oil Shale Development

DOE, in collaboration with the USGS Energy Resources Program, Los Alamos National Laboratory, and USGS Colorado Water Science Center, recently funded a project aimed at developing a GIS and web-based geospatial infrastructure for water resources (performers: Colorado School of Mines, the University of Oklahoma, and Idaho National Laboratory). A water resource geospatial infrastructure was developed, creating a repository for water resource, geological, topological, and other data types to allow for collaborative regional assessments for future energy development that can be based on the same “baseline.” The project started on October 1, 2008, and ended September 30, 2012. Dr. Wei (Wendy) Zhou (Colorado School of Mines) was the PI for this project.

8.2 Class II Well Data Distribution Methodology

Annual brine injection in the Appalachian Basin has more than tripled from about 5 million to 6 million barrels in the early 2000s to over 17 million barrels in 2012, due to the shale gas activity in the region. The challenge of handling a growing volume of brine for disposal has to be handled responsibly and safely by the industry. The consequently rising number and density of saltwater disposal wells in the region now start to face interference and capacity restrictions as operators confront this challenge.

An associated aspect of this challenge to the brine disposal industry is record-keeping and timely analysis of the operational data in a convenient setting. The quality and frequency of operational data that is reported is, however, found to be highly variable and heavily dependent on the regulatory agency and the injection well operators. To enable well-characterized, reliable, and environmentally responsible brine disposal operations in the region, a convenient platform for data assimilation and analysis of the publicly available data is sorely needed. This system would enable better outreach in the wake of widespread public concern in the study region and encourage responsible brine disposal operations.

As more factors and data are collected on each well, a system that can be expanded is critical. After a review of different methods to distribute brine disposal information, three conceptual models are presented:

- Model 1: Use an existing, off-the-shelf document management software
- Model 2: Use an existing database structure
- Model 3: Develop a web-based evaluation tool

All these models will require a high level of upfront labor to find, document, and organize the existing data, with a more minimal level of maintenance to continue to log and enter new data received from lease holders, drilling companies, and permit files. The current status of geological information varies widely by state; therefore, the amount of funding necessary to help bring each state/region up to par with their existing data will vary greatly.

Each of these models would offer a system where access to data can be expanded (to allow for direct upload of information by users) or restricted (to install a process by which information is submitted to, and then uploaded by, a database manager). If new, off-the-shelf document management software were to be used, some degree of user training would be necessary to consolidate all data into one large-scale database. Alternatively, using a system that is already in

place would help reduce upfront costs because one state or regional office would already be actively storing and dispersing information this way. A system of checks and balances would also need to be implemented to ensure that all necessary data has been collected; the current record system has missing data, either from lack of collection or lack of proper storage (lost information). This system could trigger an automatic check based on the date of a permit, to provide a reminder to the permit holder and to the state agency that follow-up must be completed on the work. Creating and automating this process would help to lower long-term costs of a data manager and decrease the time-intensive work that searching the database would create.

The web-based system would provide easier access to forms, regulations, and geological data to both agencies and data users, decreasing the level of request and the quantity of lost data. This system would be able to grow with the end user's needs to provide controllable access to research institutions, drillers, and the general public based on the needs of the community and the agency.

Sections 8.2.1 through 8.2.3 analyze the models in detail, including a breakdown of effective tools to implement the changes under each model.

8.2.1 Model 1: Off-the-Shelf Document Management Software

Health care, legal, accounting, and other professions use document management software to organize and secure large amounts of sensitive data. Those software programs have been developed with an internal structure to support the routine documents associated with each of those professions. The structure includes search functions, headings, predefined tags, indexing, accessibility, user control, and remote access.

Numerous document management software programs have been developed for the oil and gas industry, leading to competition and lower prices. The large number of options has also led to a standard structure and usability. In general, the Model 1 option would provide readily available, inexpensive software, with a reliable format. However, under this option, the predefined tagging and indexing functions would not accommodate the storage of geological information that is fundamental to the oil and gas industry. Creating a custom group of indexes and tags within these software programs is possible, but the effort would take time. In addition, each office that chose to use this software program may need to buy its own copy; at the lower price point, this would not be a significant monetary burden, but a coordinating effort to match tags and indexing would be required.

Analysis of Document Management Software

Table 8-9 lists nine off-the-shelf document management software programs that contain the appropriate tools to customize and adjust the storage options to fit geological information. To limit our analysis to these nine options, we reviewed numerous document management software programs and several websites that evaluated these software programs for their functions and capabilities. This process involved reviewing capabilities, determining which software programs would be usable for our data, and eliminating those programs that were incompatible with our data needs. Because some software was designed to meet the specific needs of other professions (for example, health care information and regulations), several features were not useful to our proposed design.

Analysis of Functions/Features

In the past, a significant amount of well data was handwritten in the field or was manually typed; therefore, much historical data is not available in digital form. Optical character recognition (OCR) allows typewritten/printed text to be converted from images into encoded, computer-readable text. The OCR function allows users to search data that were manually handled.

Version control is the efficient management and recording of changes to documents, programs, files, etc., over time as different state offices continually update their records. The version control function records changes, backs up multiple versions, and handles several changes occurring at the same time. The most commonly used office computer programs are Microsoft (MS) products; therefore, using a document management software program that is compatible with the Microsoft suite and operating system would facilitate the transfer of computer files to a document management system. Although all 50 states use English, compatibility with other languages can help us extend our data to other local territories and allow us to share data across borders. Geology transcends state and country borders; therefore, being able to share data with, and receive data from, Canada or Mexico may extend knowledge north and south of the United States.

Because the software used would not be limited to a single office or small group of users, an enterprise database would provide cloud software/services and continued management of the quality and performance of continuous and growing data volumes. At any given time, several users may need to enter/edit data, and other users may need to access data. Multiple-author software allows records to be added, amended, and/or accessed by several contributors. User access controls provide security and administrative features to prevent data users from altering documents and software settings without the proper permissions.

In addition to natural resource and oil and gas offices, a significant amount of physical geological data is stored at alternative locations. A remote document access interface allows users to access, search, and retrieve documents from any location via an internet connection for easy upload from any storage site. Once manually handled text has been OCR'ed, full-text searches allow users to search for and retrieve text from all of the words in every stored document. Multi-condition search queries allow users to search for and retrieve information based on multiple, specified conditions/search criteria. Some forms of data incorporate metadata (map layers, MS Excel sheets, etc.). These internal data can be searched through a metadata search. This capability allows users to find data/information about data content/structures.

Each of the programs in Table 8-9 contains a predefined indexing/profiling structure. A customizable structure would allow data and metadata to be grouped and stored by category in order to optimize document accessibility, search speed, and performance. This tool allows users to drill down into data based on type, location, or source, instead of using a search field. Finally, a tagging tool allows an index parameter to be assigned to a specific piece of information.

Table 8-9. Existing Document Management Software Options

Feature/Function	Software								
	Document Locator	Tallega	Alfresco One	Worldox	FileHold	GoFileRoom	Conterra	FileCabinet CS	SAFE
OCR	✓	✓	•	•	✓	✓	✓	✓	✓
Version Control	✓	✓	✓	✓	✓	✓	✓	✓	✓
MS Compatible	✓	✓	✓	✓	✓	✓	✓	✓	✓
Multi-Language	•	✓	✓	•	✓	✓	•	✓	•
Enterprise Database	✓	✓	✓	✓	✓	•	•	✓	✓
Multiple Author	✓	✓	✓	✓	✓	✓	•	✓	✓
User Access Control	✓	✓	✓	✓	✓	✓	✓	✓	✓
Custom User Views	✓	•	•	•	✓	✓	•	•	•
Remote Document Access	✓	✓	✓	✓	✓	✓	✓	✓	✓
Full Text Search	✓	✓	✓	✓	✓	✓	✓	✓	✓
Multi-Condition Search Queries	✓	✓	✓	✓	✓	✓	✓	•	✓
Metadata Search	✓	✓	✓	✓	✓	✓	✓	✓	✓
Indexing/Profiling	✓	✓	✓	✓	✓	✓	✓	✓	✓
Tagging	✓	✓	✓	✓	✓	✓	✓	✓	✓
Annual Pricing (per 5 users)	Contact for quote	\$3,000	Contact for quote	Contact for quote	\$750	\$750	Contact for quote	\$750	\$1,395
Manufacturer	ColumbiaSoft	Tallega	Alfresco Software, Inc	World Software, Inc	FileHold Systems, Inc	Thomson Reuters	Orienge	Thomson Reuters	Cabinet

8.2.2 Model 2: Existing Database Structure

Oil and gas data have become highly sought after, not only by oil and gas associations and government offices, but also by drillers, environmental organizations, and lawmakers. Furthermore, the amount and types of data have increased dramatically. In addition to permits and basic logs, technology has allowed for more in-depth data collection, including numerous drilling logs, core samples, and fluid samples.

The growth in data and in the need to access those data has resulted in the development of several website-based oil and gas databases. These existing databases generally contain only specific types of data that are in a specific geological area. The following databases have developed user-friendly search capabilities and organizational structures for complex geological information.

FracFocus.org

Overview

FracFocus.org (Figure 8-8) is a chemical disclosure registry for hydraulic fracturing fluids managed by the Ground Water Protection Council and Interstate Oil and Gas Compact Commission. The website provides public access to information and data related to hydraulic fracturing in the United States (including ground water protection), chemical use, regulations by state, and a “Find a Well” feature.

The chemical registry for fracturing fluids is distributed on FracFocus.org via two main tables. One table explains why chemicals are used, with three headings that describe an additive, its purpose, and the downhole result. The second table lists the chemicals used and is organized by chemical name, Chemical Abstracts Service (CAS) number, chemical purpose, and product function.

The database of regulation information by state is accessed via an interactive map of the United States that links users to the contact information for their state and to each state’s regulations.

The site’s “Find a Well” feature includes a database of wells organized by state. Wells can be searched by state and county or API number. The search can be further narrowed by operator, well name, or build date. Well data and the associated hydraulic fracturing fluid composition can be viewed in a PDF table.

Pros

FracFocus.org includes headings along the top of the page that are easy to find and read, with links that direct users to resources/databases. The chemical registry tables, including headings and subheadings, are well organized. The site’s maps display well and regulation data by state, helping to eliminate pages with overcrowded text. Its map information is tied to Google, providing regularly updated maps to display information. Regulation information is tied directly to the regulator website. Once a search has been performed, the column headings can be clicked to reorganize the results by the original criteria. PDF downloads are available for certain information/resources and are organized in the same format to allow easy comparison.



Figure 8-8. FracFocus.org home page.

Cons

The display table of wells in each state shows only 20 results at a time, and with no export function the user must flip between pages to review all of the well search results. There is no function to search for wells by depth, water volume used, or number of hydraulic fracturing events. The database on FracFocus.org does not include information for all existing wells in every state; rather, it is limited to the states and organizations that have voluntarily supplied

information to the website. There are 231 organizations that share hydraulic fracturing information with FracFocus, but the site does not list companies that have not supplied information to the site. This skews the available data because users are only looking at a certain percentage of the data.

Texas-drilling.com

Overview

Texas-drilling.com (Figure 8-9) is a comprehensive oil and gas online database that allows the public to access well, lease, operator, permit, and production data for the state of Texas. The home page displays the 100 highest-producing counties, along with a summary table for the state that includes the number of producing leases, producing operators, drilled wells, barrels of oil produced in the most recent timeframe for which data are available, and cubic feet (in millions) of gas produced in the most recent timeframe for which data are available. Links are available for each county, directing the user to a page that contains more links to various production information for the county, along with a Google map showing well locations.

Pros

Texas-drilling.com provides a wealth of information to users via links to graphs and large data tables. The design of graphs and tables is consistent throughout the website. Along the top of the site's web pages are links that offer easy access to permit, operator, and lease information. For every county, a summary table (similar to the state-wide summary table on the home page) is displayed. Overall, the website's display of production data and delivery of information are consistent, making site navigation and data comparison relatively straightforward and easy.

Cons

The production information is largely presented in the form of text links formatted as lists throughout the website. Although the links are well organized under headings, the numerous lists of links can be overwhelming to the user. The map of wells displayed for each county requires a user subscription to obtain more well information and "advanced mapping." A subscription is also often required to view all of the data presented in the tables. For example, the operator range and hydrocarbon production data are blurred in the tables for each lease and operator.

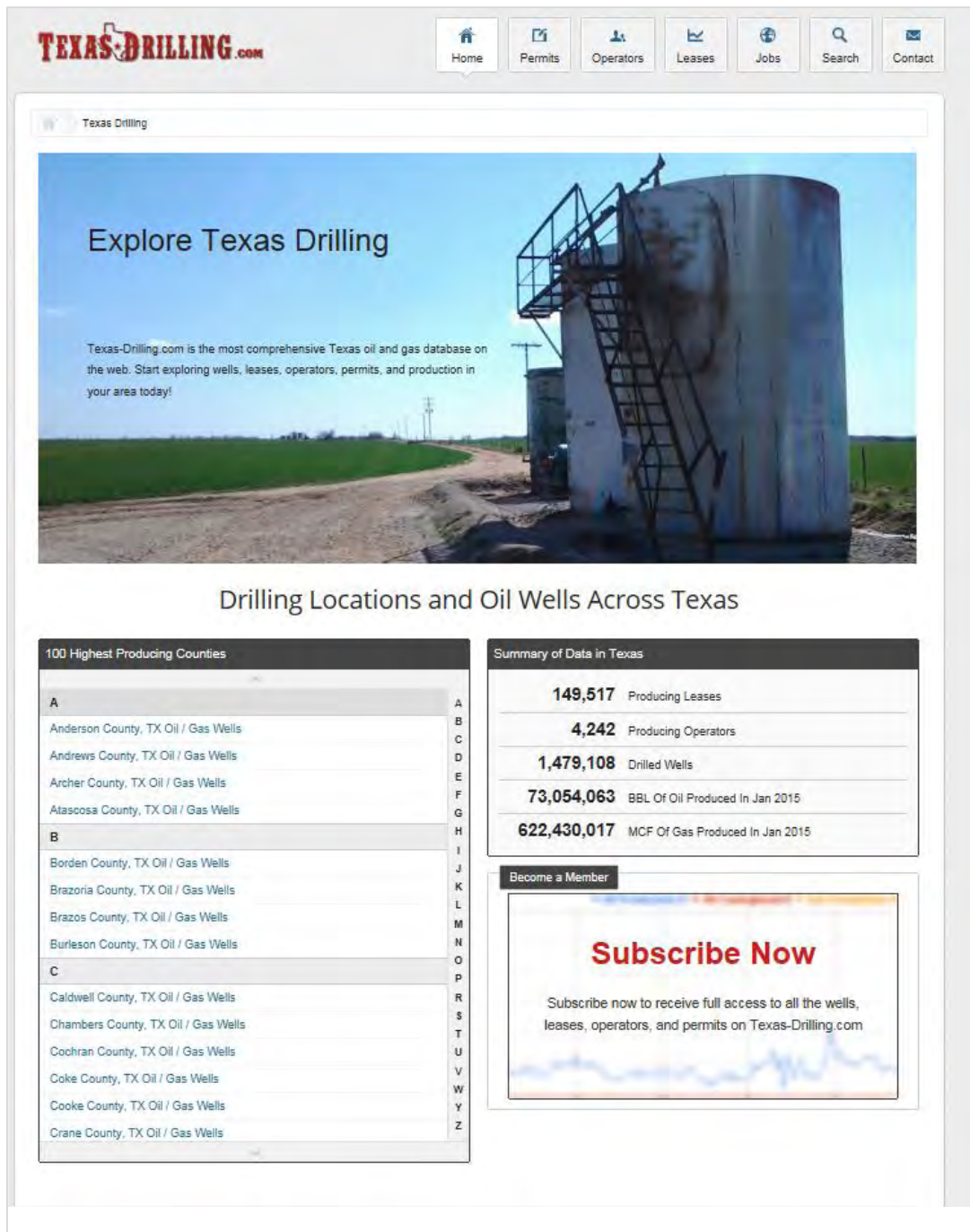


Figure 8-9. Texas-drilling.com home page.

rbdmsonline.org

Overview

The rbdmsonline.org site (Figure 8-10), developed by the GWPC, provides tools for regulatory agencies to analyze and manage oil, gas, and water resource data. The site also provides non-

proprietary software that can be used by regulatory agencies, industry, and the public to assess risks to USDWs and to access data related to oil and gas well locations, permits, and production. Site information is categorized into 10 main subject areas: RBDMS Classic, Electronic Permitting, Field Inspection, RBDMS.net, RBDMS Environmental, Electronic Reporting, Wellbore Schematic, Data Mining, Well Finder, and the Oil & Gas Gateway.

Electronic Reporting (“EReport”) is a web application used by industry operators to report production and UIC data directly to agency databases using an XML format. Well path information can be displayed on diagrams in Adobe Flash Player via the Wellbore Schematic application provided by site. The Data Mining web application provides a three-pane interactive display for accessing and searching RBDMS, GIS, and full-text data, with files that can be downloaded in csv or MS Excel formats. Well Finder is a mobile application that displays identification information, status, operator information, current and historical production data, and regulatory agency contact information for nearby wells. Data sets in the Oil and Gas Gateway are normalized and indexed in a query-able format for storage on the gateway’s central repository server.

Pros

The applications and data file formats provided by rbdmsonline.org are compatible with MS Office. Older versions of RBDMS continue to be supported during migration to the newer platform: RBDMS Classic is the original client server implementation of RBDMS, while RBDMS.net is the new data structure accommodating larger data sets with a customized.net front end for better speed, performance, and capabilities. The Wellbore Schematic utility is a free, open-access application. The Well Finder application (under development) will allow users to access maps and well data for nearby oil, gas, and UIC wells on smart phones and tablets using the internal GPS locations recorded on their mobile devices. The Oil and Gas Data Gateway provides continuous nation-wide regulatory and environmental sampling data feeds from participating RBDMS agencies. Data sets can be displayed in map and tabular formats.

Cons

A significant impediment to the utility of the site/database is that it is not immediately obvious to the user how to access the software, applications, and downloads. In most instances the technical director for the GWPC must be contacted in order to obtain more information regarding access to the RBDMS tools and applications.



Figure 8-10. rbdmsonline.org home page.

usgs.gov/water/

Overview

The *usgs.gov/water* site (Figure 8-11) maintained by the USGS is dedicated to providing data on water resources for the United States. The database consists of real-time, current, and past surface water and ground water data. Form-based and map-based access is available for water resource data from 1.5 million sites through the National Water Information Systems web interface. Links to information regarding streams, lakes reservoirs, ground water aquifers and wells, water quality, and water use are provided on the site, with data displayed in both maps and tables. Water resource data tables are available by county, state, and country in the form of MS Excel and tab-delimited ASCII files.

Pros

The *usgs.gov/water* site provides a large amount of water resource information and data that is well-organized into four main subject areas: Surface Water (Streams, Lakes, and Reservoirs), Groundwater Aquifers and Wells, Quality of Water Resources, and Water Use. All maps, data tables, and supporting documents/information are available for free download to the public. Notifications of newly available, real-time water resource data can be sent to users via email and/or phone through a free subscription. Users can customize data tables to display specific

parameters of interest, such as depth to water level, stream velocity, temperature, salinity, pH, nitrite concentration, etc.

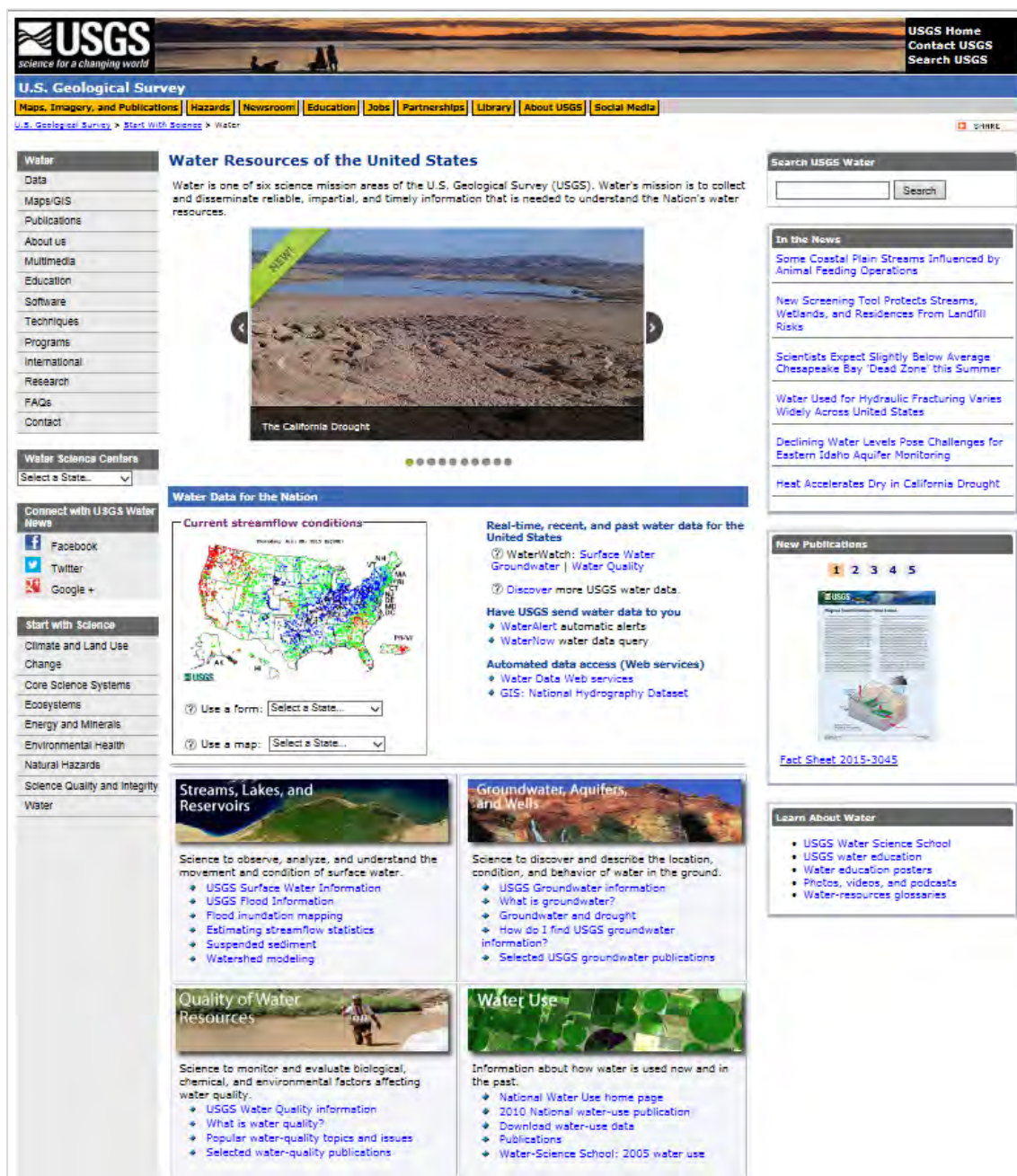


Figure 8-11. usgs.gov/water/ home page.

Cons

The large amount of data and various options for data display and user customization make it difficult to focus search efforts and results. Although water resource data are logically organized into four main subjects, the subheadings and links are different for each subject area, and page

format, data display, and data parameters between links lack consistency. Numerous links bound the main content of every page, changing from page to page and making navigation difficult. A user who is unfamiliar with the site and does not have specific direction may find it difficult to access the available data and resources.

8.2.3 Model 3: Web-Based Evaluation Tool

A web-based evaluation tool is an easy-to-use, interactive mobile computing tool to track operational data for outreach to the public and to industry. The tool would offer visualization and basic analytical capabilities to help evaluate where the best wells in the state operate and to evaluate the typical capacity and injectivity of wells in a given area. It could also be extended to evaluate, using simple flow calculations, the best sites to safely put new wells based on injectivity considerations.

The tool would have two basic modes of operation: a ‘resource’ mode for data assimilation and visualization and an ‘analysis’ mode for dynamic data analysis. The primary step—to compile and organize publicly available operational data—would offer the advantage of a comprehensive, standardized application programming interface that would provide easy data access. Visualization capabilities embedded in the tool would enhance interactive display of various parameters, such as injection volumes and injection pressures, which can be easily tracked to study time-varying trends in the data. Figure 8-12 shows the overall interface with operational information for a sample well selection. Figure 8-13 depicts typical well data available for active brine injection wells in the study region. Toggle would be enabled to switch between the operational history plots and general well information.

Parameter-based filtering capabilities would also be enabled for more meaningful analyses. A sample filter application would be to analyze brine injection volumes across the study region in specific formations of interest with a summary compilation of the analysis. Figure 8-13 shows a filter-enabled view displaying only the wells injecting into the Newburg dolomite formation in the study region.

A web-based evaluation tool can be useful as a screening tool for preliminary analyses and as a central resource for brine disposal operations in a region of interest. Table 8-10 summarizes features of the system. The tool would leverage and combine the fundamental knowledge of the regional geology and operational history in the Appalachian Basin gained through the current project. Overall, the web-based evaluation tool would have potential to support safe, reliable, and environmentally responsible brine disposal in the region.

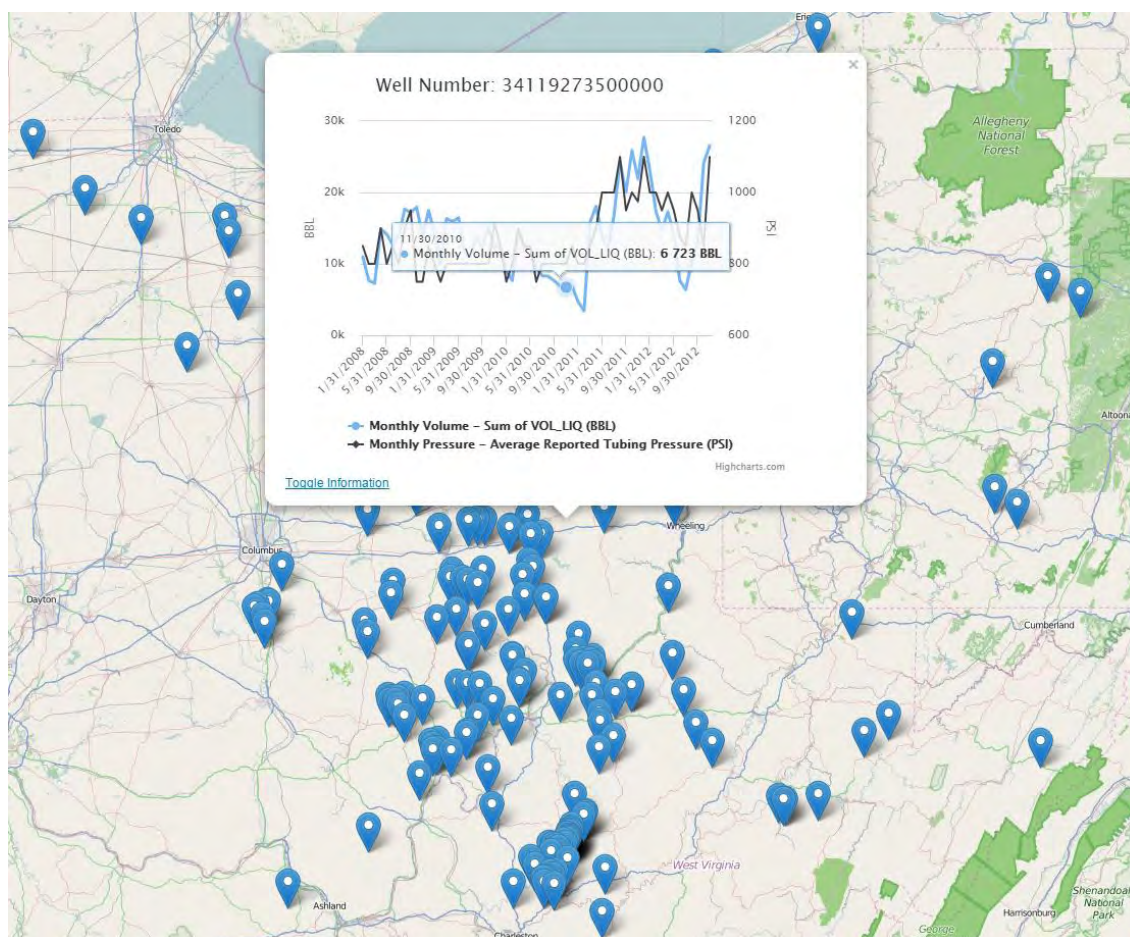
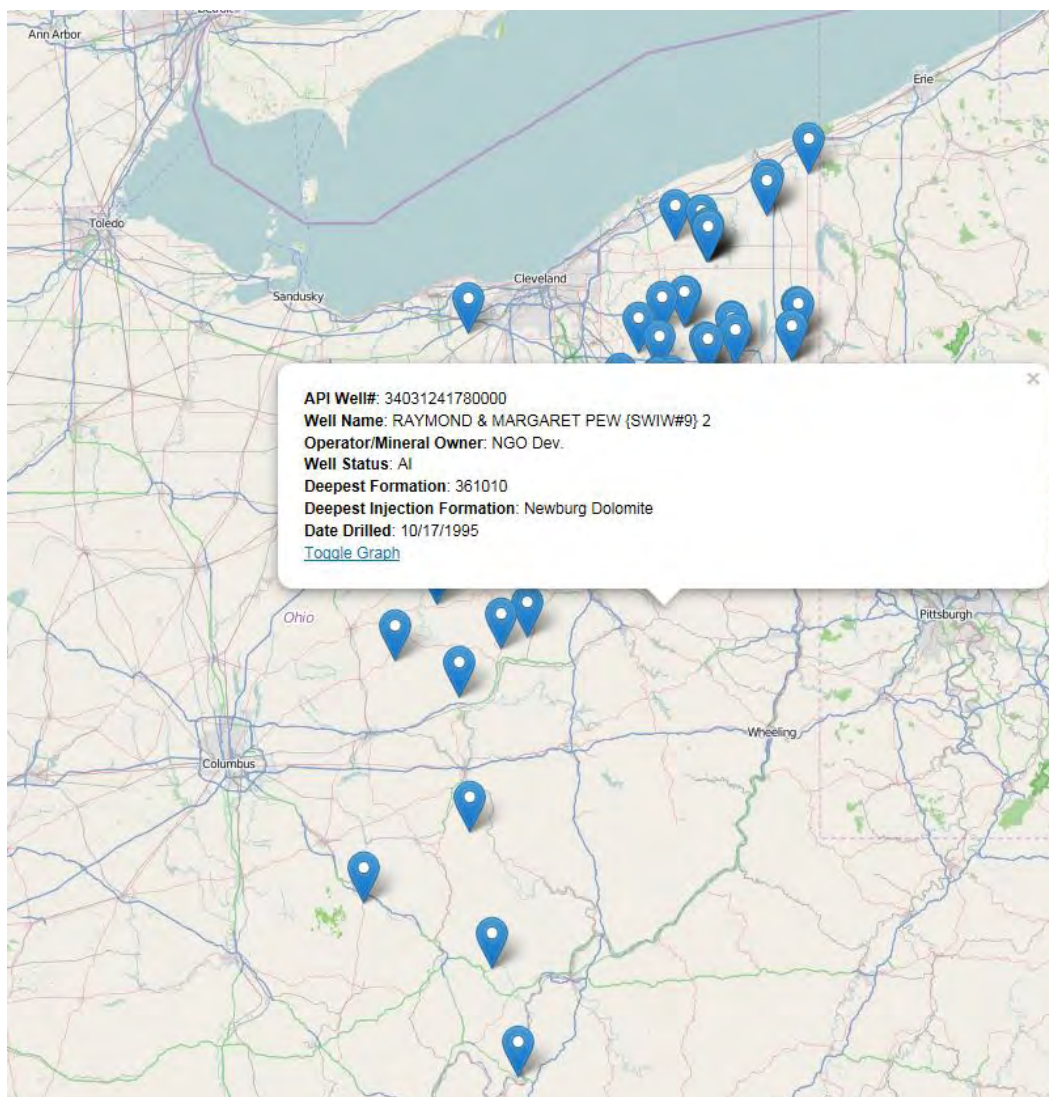


Figure 8-12. Example snapshot of the interface with operational data for a selected well



Note: View filtered to display only wells injecting brine into the Lockport-Newburg.

Figure 8-13. Example of pop-up for well details in a sample zoomed-in AOR.

Table 8-10. Web-based evaluation tool features.

Central resource for brine disposal operational data in Appalachian basin
<ul style="list-style-type: none">• Provides potentially standardized data access• Regulate operational data quality• Comprehensive database for operators and public
Statistical analysis of time-sensitive operational parameters
<ul style="list-style-type: none">• Primary resource mode feature• Interactive visualization and trend analyses of operational parameters such as injection volumes and pressures• Parameter-based filtering capabilities such as formation and county-specific statistical analysis
Simplistic injection analysis capability
<ul style="list-style-type: none">• Extension mode to proposed outreach tool for basic injectivity analysis during project planning• Simplified site-specific injectivity analysis to estimate pressure buildup due to injection
Ease of use
<ul style="list-style-type: none">• Simple, interactive platform with flexible visualization modes• Mobile computing interface for versatile data access

9. Results and Discussion

Overall, the project results describe operational ranges and geological properties for the Class II brine injection zones in the Northern Appalachian Basin. Data were collected on the status of brine disposal wells, geological conditions of injection zones, subsurface hydrologic conditions, geotechnical rock core test data, and operational data from injection wells. The information gathered was used to analyze injection performance, complete reservoir simulations of the injection process, and assess source-sink capacities.

9.1 Operational Data

Monthly operational data on injection volumes, wellhead pressure, and injection uptime were analyzed with statistics, graphs, and maps. The data were compiled from the 2008-2012 time period. The operating data were categorized by injection formation and depth. These products provide useful guidance for operators in relation to general operating conditions to be expected for different injection rock formations. However, some operational data merely reflect facility activity rather than reservoir performance.

The Appalachian Basin is a regional sedimentary basin that covers approximately 500,000 km² from Tennessee to Ontario, Canada. For the purposes of the research, the study area was defined as eastern Kentucky, Ohio, Pennsylvania, and West Virginia. There is a long history of oil and gas production in the Basin, and there are over 900,000 oil and gas wells in the region. Since 2003, approximately 9,375 unconventional horizontal shale gas wells have been drilled in the study area.

Much of the information available on Class II UIC brine disposal wells is shaped by the USEPA UIC program. The regulatory agencies are the USEPA Region 4 UIC Program for Kentucky, the ODNr Division of Oil & Gas for Ohio, the USEPA Region 3 UIC Program for Pennsylvania, and the West Virginia Department of Environmental Protection Office of Oil and Gas. Most of the information on wells relies on the quality of data reported to state agencies when the wells were drilled.

A survey of Class II UIC brine disposal wells in eastern Kentucky, Ohio, Pennsylvania, and West Virginia indicated that there are 324 wells with active permits as of August 2013. The majority of the wells are in Ohio (211) and West Virginia (76); Kentucky has 30 and Pennsylvania has 7. The status of injection wells is fairly variable, with many wells being permitted or taken off-line due to demand or maintenance. There are several thousand Class II UIC EOR wells and several hundred abandoned or inactive wells. The wells are completed in a variety of different rock formations related to the subsurface distribution of rock formations. Well construction records suggest that approximately 18% of the wells are open-hole completions and that most wells are fractured and acidized before injection.

Geological data on the injection zones showed that rock formations used for injection can be correlated across the Appalachian Basin. Maps of these formations were compiled to depict the distribution of injection intervals. A total of 690 well logs were collected from the injection wells to better define the geologic layers and parameters. Hydrologic data were collected on reservoir conditions, but these data suggest that subsurface conditions must be evaluated on a

site-specific basis. Data on injection fluids suggest that these fluids vary based on geographic location.

Geotechnical data were available from many wells in the study area, but it is difficult to generalize formation properties since they cover such a large area. Each state in the project team reviewed its rock core repositories and identified core that may be suitable for geomechanical tests (Poisson's ratio, Young's modulus, and compressibility). A total of 10 samples were selected for laboratory testing.

Finally, operational data from the active Class II brine disposal wells in the Northern Appalachian Basin were collected to help gauge injection performance. Data were collected for wells with active Class II UIC brine disposal permits for the study area from regulatory agencies. Data were generally available in terms of monthly injection volume, pressure, and rates.

Injectivity analysis was performed for 24 Class II brine disposal wells in the study area. Injectivity index calculations were helpful in evaluating the injection performance of these wells. Trends in injectivity index observed with time were analyzed to explain monitored well behavior. Efforts to study the correlation of well injectivities with specific formations had mixed results. Review of injectivity over time for individual wells provided some indication of trends in reservoir performance. However, data often reflected items like well conditions, scale buildup, well workovers, injection activity, and other factors.

9.2 Geologic Properties of Injection Zones

Data on the geologic setting and injection operations were analyzed for Class II UIC brine disposal wells in the Northern Appalachian Basin. Analysis involved compiling geologic cross sections and maps, analyzing geophysical well logs, integrating seismic survey data, reviewing geomechanical data, and analyzing regional operational injection data and individual well performance. Results from the data integration and analysis task were used to develop site-specific geocellular models, complete reservoir simulations of the injection process, and assess source-sink capacities.

Injection zones were analyzed in a systematic manner to provide indicators of injection performance and better outline the most suitable injection zones to meet demand for brine disposal in the region. Geophysical well logs were reviewed using a similar method so the injection zones could be compared. Operational injection data were evaluated for indicators of injection performance in individual wells. Together, these two classes of data were analyzed to determine injection performance in the various injection intervals/formations in the study area.

The regional framework depicts the general depth and distribution of formations, reservoir parameters, and injected fluid volumes for Class II brine disposal wells in the region. Wells generally penetrate older Silurian-Cambrian age formations on the northwestern flank of the Appalachian Basin where injection intervals above the Precambrian basement are above 9,000 feet. Wells in the eastern portion of the Appalachian Basin are generally restricted to younger Mississippian-Devonian age formations because of depth, structural complexity, and the lack of deep formational analysis in the central portion of the Basin. The Upper Silurian Lockport Dolomite, Lower Silurian Clinton-Medina Sandstone, and Cambrian Basal Sandstone injection formations have the highest total injection volumes.

A systematic analysis of 732 geophysical logs was completed for Class II brine disposal wells in the study area. Gross and net thickness, average porosity, and porosity-feet estimates for each injection zone were calculated with the injection data for analysis. The bulk-density-derived porosity was used to evaluate general reservoir parameters for most formations within the study area. Some of the carbonate units are difficult to detect in typical log suites run in the Appalachian Basin (i.e. ‘triple-combo’) for reservoir evaluation, because thin zones of irregular porosity constitute the majority of the injection intervals. The porosity and net thickness data was used as an indicator of reservoir general performance for the individual injection zones. The carbonate units with thin net thicknesses and low porosity-feet values can have larger cumulative fluid injection numbers than sandstone units at similar depths with larger net thicknesses and porosity-feet values.

The regional seismic lines in eastern Ohio can be correlated with changes in porosity and thickness in Cambrian Basal Sandstone. There are also regions in southeast Ohio that have sections faulted from the Precambrian Basement through the Devonian Onondaga.

A wide variety of injection zones are used for Class II brine disposal in the Northern Appalachian Basin. Consequently, it is challenging to group information on the geological properties and injection performance, because many formations change in character with location. Further well and site-specific analysis is required to understand the quality of various injection formations.

9.3 Source-Sink Analysis

The source analysis task included review of unconventional shale wells, Class II wastewater production, trends in recycle/reuse of drilling fluids, and brine injection. The objective of the analysis was to summarize trends in wastewater being delivered to Class II brine disposal wells in the Appalachian Basin. Major conclusions of the source analysis are summarized as follows:

- Drilling records indicated that 10,164 unconventional horizontal shale wells have been drilled in the study area as of 2013.
- Unconventional wells are clustered in several areas that are located large distances from existing Class II brine disposal wells. A well density map illustrates areas of higher well activity that could benefit from closer injection wells.
- Review of wastewater production practices indicates that Class II disposal wells may inject a mixture of drilling fluids used to control the well and circulate drilling cuttings, as well as fluids used to complete the well for production.
- Trends in wastewater management in Pennsylvania indicate that more than 90% of unconventional operators were recycling/reusing fluids in their operations. Research on wastewater disposal methods in Pennsylvania unconventional wells suggests that the amount of wastewater recycled from 2010 to 2013 increased from 22% to 67%. Pennsylvania data indicated that operators used about 20% recycled wastewater for hydraulic fracturing treatment in 2013, versus 0% in 2006.

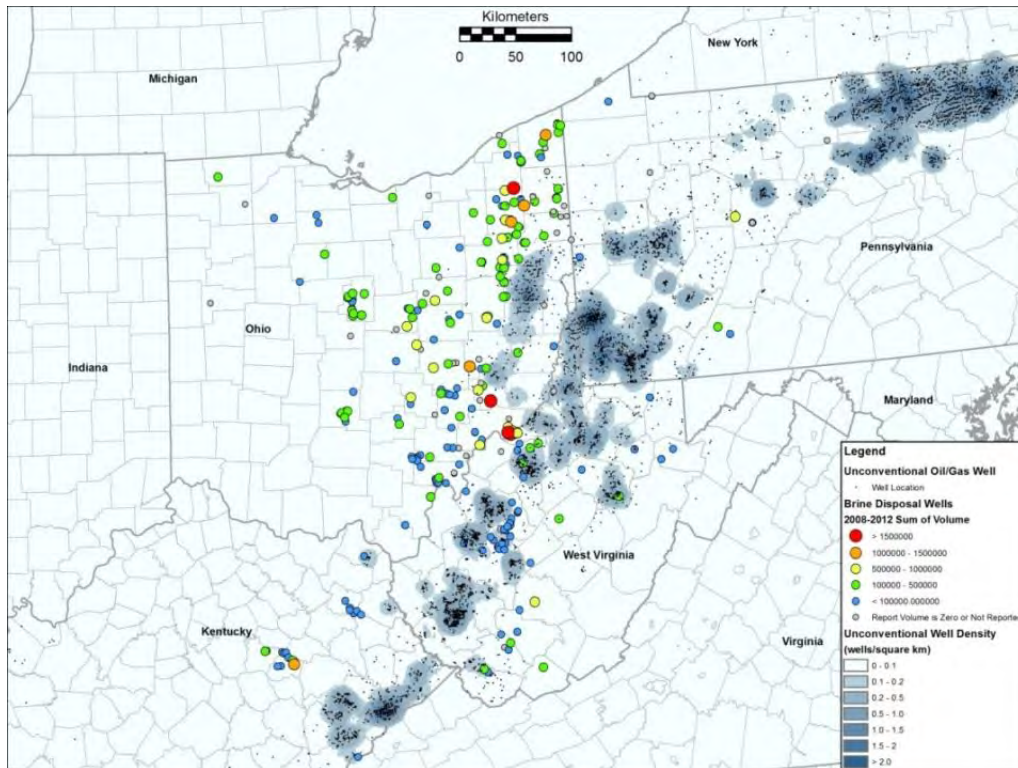


Figure 9-1. Map Showing Class II Brine Disposal Wells and Unconventional Well Density.

- Operational records compiled under this study indicate that the total volume of brine being routed to Class II injection wells increased from 9.2 million barrels in 2008 to 17.6 million barrels in 2012. Provisional data from 2013 suggest that disposal volumes continued to increase to over 20 million barrels in 2013.
- Brine injection trends appear to correlate best to total hydrocarbon production in the region. Data from 2008-2012 suggest that, on average, 9,984 bbl of brine were injected per BCF of equivalent gas produced.
- Based on USGS resource estimates for the Marcellus and Utica shales, ultimate brine disposal demand for these unconventional plays may range from 706 million bbl to 2,290 million bbl. Many factors (such as drilling technology, economy, etc.) may affect the actual development of these resources.

The sink analysis task described Class II brine injection rock formations, calculated sink capacity for depleted oil and gas reservoirs, and estimated sink capacity in deep saline formations. The objective of the analysis was to summarize volumetric capacity for brine disposal in the Appalachian Basin:

- Many different intervals are used for brine disposal in the region, including the Cambrian basal sandstone, the Cambrian Copper Ridge Dolomite and Rose Run Sandstone, the Silurian Medina Group/'Clinton' sandstone, the Silurian Lockport Dolomite, the Devonian Oriskany Sandstone, and Mississippian sandstone units.
- Injection volumes and rates vary with location, geologic formation, and well location.

- Class II brine disposal wells are distributed throughout the region. Many of the wells were installed near hydrocarbon fields to accommodate produced water generated from oil and/or gas production. Other wells are completed within deep saline formations that are mostly saturated with dense brine fluid.
- Historical oil and gas production in Kentucky, Ohio, Pennsylvania, and West Virginia has totaled approximately 43 TCF of gas and 3.8 billion bbl of oil, which is equivalent to approximately 47 billion bbl of brine void pore space in the depleted oil and gas reservoirs.
- Estimates for sink capacity based on areal coverage, thickness, porosity, and typical recovery factors suggest that there may be brine disposal capacity for a median value estimate of 2.8 billion bbl in depleted oil and gas fields penetrated by Class II brine disposal wells (*this does not include other oil and gas fields that are not penetrated by existing Class II disposal wells*). Given the fact that total brine disposal volume in 2012 was 17.6 million bbl, the capacity may accommodate more than 150 years of injection. Additional capacity may be present in other depleted oil and gas fields not currently penetrated by brine disposal wells.
- The capacity for brine disposal in deep saline formations was estimated at 480 billion bbl based on a 2.5% EF, areal coverage of the formation, porosity, and thickness. The capacity is several thousand times greater than the 17.6 million bbl of brine injected in 2012 in the Appalachian Basin.
- Based on the ratio of brine volume versus hydrocarbon production from 2008-2012, approximately 10 bbl brine were disposed of in Class II wells per million cubic feet equivalent gas produced.
- Based on this ratio and USGS combined resource estimates for the Marcellus and Utica-Point Pleasant shales (70 to 229 TCF), total brine disposal demand may be 0.7 billion to 2.3 billion bbl. Since resource estimates are greater than technically recoverable reserves, it is likely that only a fraction of the resource will be developed with a corresponding fraction of brine disposal demand.

Table 9-1 summarizes source-sink estimates. As shown, the capacity for brine disposal in the region appears to be very large. A comparison of sink capacity to recent brine injection volumes and estimates for ultimate demand for brine disposal related to Marcellus/Utica plays suggests that there is adequate capacity to meet demands related to unconventional production in the Northern Appalachian Basin. The capacity is distributed across large areas in both depleted oil and gas fields and deep saline formations. However, accessing the capacity may be limited by the injectivity of the formations, which is ultimately related to geological properties and features of the rock layers.

- Oil and gas production in the region has increased substantially to nearly ~8 TCF of gas and ~22 million bbl of oil in 2014, which represents a ~10-fold increase since 2008. However, brine disposal has not seen quite the same rate of increase, such that the more recent ratio of brine disposal volume to hydrocarbon production appears to have declined to more like 5 to 6 bbl brine per million cubic feet of gas, possibly because fewer wells are being drilled and more are coming online for production.

- From 2013-2014, over 30 new Class II disposal wells were permitted in the study area, including five new permits in Pennsylvania. Four commercial wells in Ohio had reported injection volumes over 1 million bbl per year each in 2014. Combined, these four wells provided a 33% increase in capacity over 2012.
- In general, it appears that brine disposal capacity is not a major limiting factor on unconventional hydrocarbon resource development in the Appalachian Basin. Depleted oil and gas reservoirs and deep saline formations offer very large capacity for brine disposal in the region. Increased demand has been met with installation of 10 to 20 new Class II wells per year.

Table 9-1. Summary of source-sink estimates for brine disposal.

Description	Low (MMbbl)	Medium (MMbbl)	High (MMbbl)	Comment
Brine disposal volumes in 2008-2012	9.2 (2008)	13.1 (average)	17.6 (2012)	Based on UIC Class II brine disposal operational data
Resource-based ultimate demand from Marcellus & Utica Shale	706 (F95)	1,360 (mean)	2,290 (F5)	Based on 9,984 bbl brine/BCF gas equivalent
Historical oil & gas production in study area	3,842 (oil only)	43,075 (gas only)	46,918 (combined)	Based on conversion to brine volumes
Capacity in depleted oil & gas fields	1,015 (P90 RF)	2,792 (P50 RF)	21,770 (P10 RF)	Based on fields penetrated by Class II brine disposal wells
Capacity in deep saline formations	148,000 (1% EF)	480,000 (2.5% EF)	594,000 (4% EF)	Volumetric estimate for all deep saline formations

- There are still some limiting factors related to transportation and costs of Class II wastewater disposal. The model of commercial disposal wells requires costly transport from well pads to distant injection wells. Trucking wastewater also creates a perception issue for the oil and gas industry because the trucks are visible to the general public along major interstates and especially to local residents near injection wells.
- Overall, the volumes of fluid routed to Class II disposal wells in the Appalachian Basin are much lower than other oil and gas regions in North America (Table 9-2). The total volume of hazardous wastewater injected into the Mount Simon Sandstone in Class I disposal wells in the Midwest has been over 500 million bbl of wastewater over the last 40 years (Sminchak, 2012).

Table 9-2. Class II Brine Disposal Volumes for North American oil and gas regions.

Oil and Gas Region	Volume of Fluid per Year (MMbbl)
Anadarko Basin	~2,000 ^a
Appalachian Basin	~9.2-17.6
Texas	~7,000 ^b
California	~2,500 ^b
Western Canadian Basin	~200 ^c

a. Murray, 2014.

b. Clark and Veil, 2009.

c. Ferguson, 2015.

10. Impact to Producers

Results of this project were aimed at helping ensure safe, reliable, and environmentally responsible oil and gas production in the Appalachian Basin. In general, brine disposal is a byproduct of oil and gas development in this area. Since 2005, hydrocarbon production in the region has seen about a 10-fold increase, mostly due to unconventional shale play development in the Marcellus and Utica-Point Pleasant plays. During this period, demand for brine disposal has also increased about 3 to 4 times the rates in effect before 2005. As such, there was increased demand for disposal, and many of the injection zones were not well characterized. The new demand for brine disposal created stress on the system, especially with much of the brine being trucked to distant injection wells. This project's impact to producers is summarized in the following products:

- Review of operational parameters for various injection zones in the region, helping operators select the most appropriate injection zone based location, geologic setting, and required injection rates for siting and operating brine disposal wells.
- Production of geologic maps, cross sections, and geophysical log analysis that help operators understand the thickness, porosity, permeability, subsurface distribution, and features in the various injection zones in the region.
- Collection and analysis of field operational data from six Class II brine disposal wells in the study area. Pressure transient analysis was completed on three of the wells, providing valuable hydraulic parameters for these zones which are not often tested.
- Systematic analysis of brine disposal volumes versus production to help estimate future demand related to unconventional resource estimates. Results indicated approximately 10 bbl brine were disposed of in Class II wells per million cubic feet equivalence natural gas produced.
- Based on this ratio and USGS combined resource estimates for the Marcellus and Utica-Point Pleasant shales (70-229 TCF), total brine disposal demand may be in the range of 0.7-2.3 billion barrels. Since resource estimates are greater than technically recoverable reserves, it is likely that only a fraction of the resource will be developed with a corresponding fraction of brine disposal demand.
- Given prices for brine disposal in the region, this market will be at minimum several billion dollars over the long term.
- Source-sink analysis for depleted oil & gas reservoirs and deep saline formations, demonstrating capacity for nearly 500 billion barrels brine disposal.
- A study was accomplished on brine reuse/recycle trends in Pennsylvania, documenting how 90% of operators reuse/recycle flowback water, and 67% of wastewater is recycled for use in operations.
- Injection simulations for typical operations in the Appalachian Basin. These simulations show the pressure increase and fluid migration effects of brine injection in the subsurface. The simulations also show the effect of geologic features and hydraulic parameters on injection performance over time.

- National survey of Class II brine disposal information sources, regulatory items, and technical research to aid operators and stakeholders on aspects of injection well. Also, an example data distribution system to estimate hydraulic parameters by location and geologic unit.
- The products and tools for operators included an informational pamphlet summarizing geologic and operational data for injection zones, wellhead pressure estimator, and guidance on logging, testing, and monitoring Class II wells. The field monitoring of Class II injection wells has provided new and valuable information on the nature of injection zones in the Appalachian Basin.
- Utilizing a wide variety of injection intervals in both depleted oil and gas reservoirs and deep saline formations may reduce potential for issues such as high costs for wastewater disposal, long trucking distances, induced seismicity, and improper injection well operations.

11. Technology Transfer Efforts

Technology transfer efforts included technical presentations, development of informational products, and project team meetings. Since the state geological surveys of Kentucky, Ohio, Pennsylvania, and West Virginia were part of the project team, the output of the work will be embedded in these agencies for future support on Class II brine disposal in the region.

Technology transfer activities are summarized as follows:

- Dr. Neeraj Gupta presented a project overview titled *Development of a Brine Disposal Framework for the Northern Appalachian Basin* at the SPE Workshop on Reducing Impact of Unconventional Resource Development, Denver, Colorado, April 24, 2013.
- A project team meeting was held on June 26, 2013, at Battelle in Columbus, Ohio. The meeting was attended by the Kentucky Geological Survey (Marty Parris and Tom Sparks), the Ohio Geological Survey (Mike Angle and Ron Riley), the Pennsylvania Bureau of Topographic & Geologic Survey (Kris Carter and Katie Schmid), the West Virginia Geological and Economic Survey (Phil Dinterman), and Battelle technical staff (Joel Sminchak and John Miller).
- Battelle responded to an inquiry from the Columbus Dispatch on September 11, 2013, regarding brine disposal activity in Ohio. On September 23, 2013, an article titled *Sites sought for region's fracking residue* was published in the Columbus Dispatch. The article subsequently led to interviews with the National Public Radio (NPR) radio station in Cleveland, The Allegheny Front (an environment-focused radio program for Pittsburgh-area NPR stations), and the Shale Daily.
- A project review was presented by Joel Sminchak at the Groundwater Protection Council Annual UIC Meeting (January 21-23, 2014, New Orleans, Louisiana). The review was titled *Development of a Framework for Brine Disposal Wells in the Northern Appalachian Basin Based on Operational and Geologic Information*.
- A project review was presented to Exxon/XTO water management personnel on March 3, 2014, at Battelle, Columbus, Ohio.
- Dr. Gupta gave a technical presentation at the SPE Unconventional Resources Technology Conference (August 25-27, 2014, Denver, Colorado): *Geologic and Reservoir Assessment for Brine Disposal in the Northern Appalachian Basin*. Joel Sminchak, Mark Moody, and John Miller provided technical support.
- A technical paper was prepared and submitted for the SPE Unconventional Resources Technology Conference: *Geologic and Reservoir Assessment for Brine Disposal in the Northern Appalachian Basin*, Neeraj Gupta, Joel Sminchak, Mark Moody, and John Miller.
- A presentation was made by K.W. Schmid on *Production and Water Use in Pennsylvania's Organic Shales*, on March 25, 2014, at The Geological Society of America Northeastern Section Meeting, Lancaster Pennsylvania.

- A project team meeting was held on October 14, 2014, at Salt Fork State Park, Cambridge, Ohio. The team meeting was focused on local-scale analysis of key injection zones, geocellular modeling, injection simulations, and geomechanical analysis:
 - The Kentucky Geological Survey presented a review on the status of brine disposal wells and the Weir Sandstone injection zone in Elliot and Lawrence counties.
 - The Ohio Geological Survey presented an analysis of the Lockport-Newburg injection zone in northeastern Ohio based on horizon mapping and injection data.
 - The Pennsylvania Geological Survey presented a review of brine injection wells, Upper Devonian Sand injection interval, Oriskany injection interval, Medina injection zone, and risk factors related to brine disposal wells in Pennsylvania.
 - The West Virginia Geologic and Economic Survey presented an analysis of the Big Injun injection zone for Roane and Kanawha counties, West Virginia.
 - Battelle project team members presented a review of the source-sink estimates, geocellular models, and injection simulation progress.
 - NSI presented a summary of the StimPlan geomechanical analysis work.
- A project review meeting was held on January 27, 2015, at the offices of the U.S. Department of Energy National Environmental Technology Laboratory (DOE-NETL) in Pittsburgh, Pennsylvania. At the meeting, Battelle presented an update on project activities to DOE-NETL and RPSEA.
- A presentation was given by Joel Sminchak at the Ground Water Protection Council Annual UIC meeting in Austin, Texas, on February 10, 2015. The presentation was titled *Brine Disposal Reservoirs in the Appalachian Basin: Injection Performance and Geological Properties*.
- An abstract was submitted to the SPE Eastern Section Meeting on *Petrophysical and geomechanical analysis of Knox Group Reservoirs and Caprocks across the western flank of the Northern Appalachian Basin as a Function of Depth*, Samin Raziperchikolaee (scheduled for October 2015).
- A presentation was given by Samin Raziperchikolaee at the 14th Annual Carbon Capture Utilization and Storage conference in Pittsburgh, Pennsylvania, on May 30, 2015, *Constraining Injectivity of Knox Group Formations with Varying Depth across the Northern Appalachian Basin Using Coupled Fluid Flow-Geomechanics Modeling*, Samin Raziperchikolaee, John Miller, and Joel Sminchak.
- A project overview presentation was given by Neeraj Gupta at the Pennsylvania Independent Oil & Gas Association Technical Seminar on *Analysis of Brine Disposal in the Appalachian Basin - Linking Injection Operations and Geologic Reservoirs*, July 29, 2015, Seven Springs, Pennsylvania.

In addition to these items, an informational pamphlet was developed summarizing geological and operational data for brine disposal zones in the region. These pamphlets were distributed to various end users. Overall, the technology transfer task was able to highlight the actual operational data and geological factors for Class II brine disposal in the Appalachian Basin.

12. Recommendations

Based on the analyses completed for this project, this section provides recommendations for Class II brine disposal wells in the Northern Appalachian Basin. It should be noted that the project team is not responsible for overseeing brine injection, and these recommendations are general in nature. They are mostly intended to help operators and stakeholders understand the relationship between injection operations and the geologic setting for injection zones in the region. State and regional UIC programs regulate Class II wells on a continuous basis and are better equipped to manage these operations. Many of these recommendations have already been implemented by operators of newer injection wells.

- There are many different injection zones in the Appalachian Basin, so review of the operational data compiled in this project may help operators understand the typical injection rates, pressures, and volumes that have been achieved for the different injection intervals.
- It is valuable to review local geologic features and parameters of the injection intervals. For example, the Lockport-‘Newburg’ zone may have reservoir boundaries and may be limited in size, so detailed geologic characterization of the formation’s local features may aid in understanding operational limitations.
- If possible, injection wells should be located near areas with a high density of oil and gas wells. This approach may be challenging for unconventional wells, because they are spread out over large areas as opposed to conventional production fields. In addition, permitting a brine disposal well in an area with pre-existing opposition to shale development may be difficult because there is a more substantial permitting process for Class II wells. This permitting process is open to 30-day public comment period.
- Occasional pressure transient analysis of operational data may be useful to understand reservoir permeability, transmissivity, skin-effects, and geologic features. Other injection performance indicators may be tracked based on operational parameters (injection rate, pressure, volumes). This analysis may be especially useful on a periodic basis to see decrease in injection performance. These methods generally require more continuous monitoring of injection pressures and rates (every 10 minutes to every 60 minutes), but otherwise would not interrupt normal operations.
- A study on recycle/reuse of produced/flowback water in Pennsylvania Marcellus formation illustrates the benefit of recycle/reuse in well completion operations. These methods should be considered by operators, since they may provide additional cost benefit by reducing amount of wastewater sent to disposal wells. Operators in Pennsylvania have increased reuse/recycle of wastewater to reduce need for subsurface brine disposal such that 90% of unconventional operators report reuse/recycle. In Pennsylvania, the amount of recycled water used to fracture shale gas wells has risen from 0% (0 gallons) in 2006 to about 20% (246 million gallons) in 2013, and the amount of wastewater being recycled has risen from 22% (60 million gallons) in 2010 to 67% (908 million gallons) in 2013.

- Basin-wide review of hydrocarbon production and wastewater injection is useful to better understand hydrologic budgets across the geologic province. This approach may also consider other hydrologic water inputs/outputs (thermoelectric, municipal water, municipal wastewater treatment, agriculture, industrial water use, groundwater recharge).

13. REFERENCES

- Abdalla, C.W, Drohan, J.R., Blunk, K.S, and Edson, J., 2011. Marcellus Shale wastewater issues in Pennsylvania- Current and emerging treatment and disposal technologies: Pennsylvania State University, College of Agricultural Sciences, 9 p.
- AEP Mountaineer CCS II Project. 2011. Mountaineer CCS II Project: BA-02 Summary Characterization Report, prepared for AEP by Battelle, September 2011.
- Alaska Oil and Gas Conservation Commission, 2013. Disposal Injection Orders: <http://doa.alaska.gov/ogc/orders/dio/dioindex.html> (accessed August 2014).
- AMTV, LLC. 2012. Marcellus Shale Water Management Study. Catalyst Connection, M-RIC, Pittsburgh Gateways Corporation.
- Ammerman, M.L., and Keller, G.R. 1979. Delineation of Rome Trough in eastern Kentucky by gravity and deep drilling data: American Association of Petroleum Geologists Bulletin, v. 63, no. 3, p. 341–353.
- Anderson, W. H., 1991, Mineralization and hydrocarbon emplacement in the Cambrian–Ordovician Mascot Dolomite of the Knox Group in south-central Kentucky: Kentucky Geological Survey Report of Investigations 4, 31 p.
- Arthur, D.J, Bohm, B., Coughlin, B.J., and Layne, M., 2008. Hydraulic fracturing considerations for natural gas wells of the Marcellus Shale: Groundwater Protection Council, 2008 Annual Forum, Cincinnati, Ohio, September 21-24, 2008, 21 p.
- Arthur, D.J., Dutnell, P.E., and Cornue, P.G., 2009b. Siting and permitting of class II brine disposal wells associated with development of the Marcellus Shale: Society of Petroleum Engineers Paper 125286, presented at the Eastern Regional Meeting, Charleston, WV, 23-25 September, 2009, 10 p.
- Arthur, D.J, Bohm, B., and Layne, M. 2009. Considerations for development of Marcellus Shale gas, completion and stimulation technology, World Oil, p. 65-68.
- Asquith G., and Gibson, C. 1982. Basic well logging analysis for geologists, American Association of Petroleum Geologists, Methods in Exploration Series, p. 1-216.
- Baranoski, M.T., Riley, R.A., and Wolfe, M.E. 1996. Play COK: Cambrian-Ordovician Knox Group unconformity play, in Roen, J.B., and Walker, B.J., eds., The atlas of major Appalachian Basin gas plays: West Virginia Geological and Economic Survey Publication V25, p. 181–188.
- Baranoski, M.T. 2002. Structure contour map on the Precambrian unconformity surface in Ohio and related basement features: Ohio Division of Geological Survey Map PG-23, scale 1:500,000, (18 p. text).

- Baranoski, M.T. 2013. Structure contour map on the Precambrian unconformity surface in Ohio and related basement features: Ohio Department of Natural Resources, Division of Geological Survey Digital Map Series PG-23, Version 2.0, scale 1:500,000, and 17 p.
- Barlow, C.A. 1996. Play Mmc: Upper Mississippian Mauch Chunk Group and equivalent strata, in Roen, J.B., and Walker, B.J., eds., *The atlas of major Appalachian Basin gas plays*: West Virginia Geological and Economic Survey Publication V25, p. 31–36.
- Bartholomew, M.J., Hatcher, R.D., Jr., 2010, The Grenville orogenic cycle of southern Laurentia: Unraveling sutures, rifts, and shear zones as potential piercing points for Amazonia (invited paper), p.4-20 in Casquet, C., Cordani, U., Pankhurst, R.J., eds., *The Grenville Orogen of Central and South America: Special Issue 1*, *Journal of South American Earth Sciences*, 159p.
- Basan, P.B., Kissling, D.L., Hemsley, K.D., Kersey, D.G., Dow, W.G., and Chaiffetz, M.S. 1980. Geological study and reservoir evaluation of Early Devonian formations of the Appalachians: Houston, Texas, Robertson Research, Inc. (U.S.A.), v. 1., pt. 1, 262 p.
- Battelle. 2013. Conducting Research to Better Define the Sequestration Options in Eastern Ohio and the Appalachian Basin. Final Report: Ohio Developmental Services Agency Agreement CDO-D-10-7a.
- Beardsley, R.W., and Cable, M.S. 1983. Overview of the evolution of the Appalachian basin. *Northeastern Geology*, Vol. 5, No. 3/4, p. 137–145.
- Beardsley, R.W., Campbell, R.C., and Shaw, M.A. 1999. Appalachian plateaus, in Shultz, C.H., ed., *The geology of Pennsylvania*: Pennsylvania Geological Survey, 4th ser., Special Publication 1, p. 287-289.
- Belieu, S., Jehn, P., Kerr, T., and Gillespie, D., 2003. Electronic Applications of EIMS Available to the Oil and Gas Industry: Society of Petroleum Engineers, SPE/EPA/DOE Exploration and Production Environmental Conference, San Antonio, Texas
- Benham, S., 2014. Ohio Legislative Service Commission: Bill Analysis, H.B 375. Downloaded from, <http://www.lsc.state.oh.us/analyses130/h0375-i-130.pdf>
- Bickford, M.E., Van Schmus, W.R., and Zietz, I. 1986. Proterozoic history of the mid continent region of North America: *Geology*, v. 14, p. 492-496.
- Biogas Data, 2013. <http://www.resourcerecoverydata.org/biogasdata.php>
- Black, D.F.B. 1986. Basement faulting in Kentucky, in Aldrich, M.J., and Laughlin, A.W., eds., *Proceedings of the 6th International Conference on Basement Tectonics*, Salt Lake City, Utah: International Basement Tectonics Association, p. 125–139.
- Black, D.F.B., and Haney, D.C. 1975. Selected structural features and associated dolostone occurrences in the vicinity of the Kentucky River Fault System (roadlog for Geological Society of Kentucky 1975 field conference): Kentucky Geological Survey, ser. 10, 27 p.

- Boswell, R. 1996. Play UDs: Upper Devonian black shales, in Roen, J.B., and Walker, B.J., eds., The atlas of major Appalachian gas plays: West Virginia Geological and Economic Survey Publication V-25, p. 93–99.
- Boswell, R., Heim, R.L., Wrightstone, G.R., and Donaldson, A. 1996a. Play Dvs: Upper Devonian Venango sandstones and siltstones, in Roen, J.B., and Walker, B.J., eds., The atlas of major Appalachian Basin gas plays: West Virginia Geological and Economic Survey Publication V25, p.63–69.
- Boswell, R., Thomas, B.W., Hussing, R.B., Murin, T.M., and Donaldson, A. 1996b. Play Dbs: Upper Devonian sandstones and siltstones, in Roen, J.B., and Walker, B.J., eds., The atlas of major Appalachian Basin gas plays: West Virginia Geological and Economic Survey Publication V25, p. 70–76.
- Bowman, I., 1911. Well-drilling methods: U.S. Geological Survey, Water-supply Paper 257, 139 p.
- Brett, C.E., Tepper, D.H., Goodman, W.M., LoDuca, S.T., and Eckert, B. 1995. Revised stratigraphy and correlations of the Niagaran Provincial Series (Medina, Clinton, and Lockport Groups) in the type area of western New York: U.S. Geological Survey Bulletin 2086, 66 p.
- Bruff, M.J., and Jikich, S.A., 2011. Field demonstration of an integrated water treatment technology solution in Marcellus Shale: Society of Petroleum Engineers paper 149466, SPE Eastern Regional Meeting, 1 October, Columbus, Ohio, 9 p.
- Butts, C. 1918. Geologic section of Blair and Huntington Counties central Pennsylvania; American Journal of Science, v. 46, p. 523–537.
- Butts, C. 1940. Geology of the Appalachian Valley in Virginia; Part 1: Virginia Geological Survey Bulletin, no. 52, 568 p.
- Campbell, M.R. 1893. Geology of the Big Stone Gap coal field of Virginia and Kentucky: U.S. Geological Survey Bulletin 111, 106 p.
- Cardwell, D.H., and Avary, K.L. 1982. Oil and gas fields of West Virginia: West Virginia Geological & Economic Survey Mineral Resources Series 7B, 119 p.
- Carman, J.E. 1927. The Monroe division of rocks in Ohio: Journal of Geology, v. 35, no. 6, p. 481–506.
- Carpenter, T.W. 1976. Stratigraphy and sedimentation of middle Mississippian rocks of Gilmer and Braxton counties, West Virginia: Morgantown West Virginia University, M.S. Thesis, 205 p.
- Carter, K.E., Hammack, R.W., and Hakala, J.A., 2013. Hydraulic fracturing and organic compounds- Uses, disposal and challenges: Society of Petroleum Engineers paper 165692, SPE Eastern Regional Meeting, 20-22 August, Pittsburgh, Pennsylvania, 11 p.

- Carter, K.M. 2007. Subsurface rock correlation diagram, oil and gas producing regions of Pennsylvania: Pennsylvania Geological Survey, 4th ser., Open-File Report OFOG 07-01.1, Available online.
- Carter, K.M., Kostelnik, J., Laughrey, C.D., and 14 others. 2010. Characterization of geologic sequestration opportunities in the MRCSP region: Middle Devonian-Middle Silurian formations: MRCSP Phase II Topical Report under DOE cooperative agreement no. DE-FC26-05NT42580, 150 p., 4 appendices.
- Carter, K.M., Schmid, K.W., Harbert, W., and Parrish, J.B. 2014. Using geophysical and remote sensing techniques to evaluate deep geologic formations in Indiana County, Pennsylvania—Geologic structure from 2D seismic data: Pennsylvania Geological Survey, 4th ser., Open-File Report OFOG 14–01.0, 8 p.
- Castle, J.W. 1998. Regional sedimentology and stratal surfaces of a Lower Silurian clastic wedge in the Appalachian foreland basin: *Journal of Sedimentary Research*, V. 68, No. 6, p. 1201-1211.
- Castle, J.W. 2001a. Foreland-basin sequence response to collisional tectonism: *GSA Bulletin*, Vol. 113, No. 7, p. 801-812.
- Castle, J.W. 2001b. Appalachian basin stratigraphic response to convergent-margin structural evolution. *Basin Research*, Vol. 13, No. 4, p. 1365–2117.
- Castle, J.W., and Byrnes, A.P. 1998. Petrophysics of low-permeability Medina sandstone, northwestern Pennsylvania, Appalachian basin: *The Log Analyst*, V. 39, No. 4, 1998, p. 36-46.
- Castle, J.W., and Byrnes, A.P. 2005. Petrophysics of Lower Silurian sandstones and integration with the tectonic-stratigraphic framework, Appalachian basin, United States: *The American Association of Petroleum Geologists Bulletin*, V. 89, No. 1, p. 41-60.
- Chaplin, J.R. 1980. Stratigraphy, trace fossil associations and depositional environments in the Borden Formation (Mississippian), northeastern Kentucky: Guidebook and roadlog for Geological Society of Kentucky 1980 field conference, Kentucky Geological Survey, 114 p.
- Clark, W.B. 1897. Untitled [Preliminary account of physiography, geology, and mineral resources]: Maryland Geological Survey, v. 1, p. 172–188.
- Clark, C.E., and Veil, J.A. 2009. Produced Water Volumes and Management Practices in the United States. Report ANL/EVS/R-09/1. Prepared under U.S. Department of Energy (DOE) Contract DE-AC02-06CH11357.
- Clark, J.E., Donura, D.K., and Voorhees, R.F., 2005. An overview of injection well history in the United States of America: In, C.F. Tsang and J.A. Apps (eds.) *Underground Injection Science and Technology: Developments in water science*, v. 52, pp. 3-12.

- Clifford, M.J. 1973. Hydrodynamics of Mount Simon Sandstone, Ohio and Adjoining Areas. *Underground Waste Management and Artificial Recharge*, Vol 1, p 349-356.
- Clifford, M.J. 1975. Subsurface liquid-waste injection in Ohio: Ohio Department of Natural Resources, Division of Geological Survey Information Circular 43, 27 p.
- Computer Modeling Group (CMG). 2012. GEM Technical Manual: General Adaptive Implicit Equation of State Compositional Model. Computer Modeling Group, Ltd., Alberta, Canada.
- Corbett, J. and Winebrake, J., 2007. Environmental implications of trucks, trains, ships, and planes: Air and Waste Management Association, p 8-12, downloaded from <https://ritdml.rit.edu/bitstream/handle/1850/7582/JWinebrakeArticle11-2007%20final.pdf?sequence=1>
- Cramer, J.W. 2011. Post-frac Flowback Analysis and Reuse Implications. Ohio Oil and Gas Association, Fall Technical Meeting, December 7, 2011.
- Dever, G.R., Jr. 1999. Tectonic implications of erosional and depositional features in upper Meramecian and lower Chesterian (Mississippian) rocks of south-central and east-central Kentucky: Kentucky Geological Survey, ser. 11, Bulletin 5, 67 p.
- Dickas, A.B. 1986. Comparative Precambrian stratigraphy and structure along the Midcontinent Rift. *AAPG Bulletin* 70, 225-238.
- Diecchio, R.J. 1985. Regional controls of gas accumulation in Oriskany Sandstone, central Appalachian basin: *American Association of Petroleum Geologist Bulletin*, v. 69, p. 722–732.
- Dietz, R.S. 1972. Geosynclines, mountains, and continent-building. *Continents Adrift*, Scientific American, p. 124-132.
- DOE (U.S. Department of Energy). 2012. Carbon Utilization and Storage Atlas, fourth edition (Atlas IV). U.S. Department of Energy, Office of Fossil Energy, National Energy Technology Laboratory (NETL).
- Donaldson, A., Boswell, R., Xiangdong Z., Cavallo, L., Heim, R.L., and Canich, M. 1996. Play Des: Upper Devonian Elk sandstones and siltstones, in Roen, J.B., and Walker, B.J., eds., *The atlas of major Appalachian Basin gas plays*: West Virginia Geological and Economic Survey Publication V25, p. 77–85.
- Donaldson, E.C, 1964. Surface disposal of industrial wastes in the United States: U.S. Bureau of Mines, Information Circular 8212, 32 p.
- DOGRM (Division of Oil and Gas Resources Management). 2014. Risk-Based Data Management System (RBDMS) [Access Database]: Ohio Department of Natural Resources, Division of Oil and Gas Resources. Available at <http://oilandgas.ohiodnr.gov/well-information/oil-gas-well-database>.

- Drahovzal, J.A., Harris, D.C., Wickstrom, L.H., Walker, D., Baranoski, M.T., Keith, B.D., and Furer, L.C., 1992, The East Continent Rift Basin: A new discovery: Kentucky Geological Survey, ser. 11, Special Publication 18, 25 p.
- Drahovzal, J.A., and Noger, M.C. 1995. Preliminary map of the structure of the Precambrian surface in eastern Kentucky: Kentucky Geological Survey, ser. 11, Map and Chart 8, scale 1:500,000.
- Drahovzal, J.A., 1997, Proterozoic sequences and their implications for Precambrian and Cambrian geologic evolution of western Kentucky: evidence from seismic-reflection data: Seismological Research Letters, v. 68, p. 553-566.
- Drahovzal, J.A. and Harris, D.C., 2004, Potential Reservoirs for Geologic Sequestration in the East Continent Rift Basin: Kentucky Geological Survey Website, 6 p.
- Dresel, P.E., and Rose, A.W. 2010. Chemistry and Origin of Oil and Gas Well Brines in Western Pennsylvania. Pennsylvania Department of Conservation and Natural Resources, Open File Report OFOG 10-01.0.
- Driese, S.G., Byers, C.W., and Dott, R.H., Jr., 1981, Tidal deposition of the basal Upper Cambrian Mt. Simon Formation in Wisconsin: Journal of Sedimentary Petrology, v. 51, p. 367-381.
- Earlougher R. 1977. Advanced Well Test Analysis: Monograph Series, Vol 5. Society of Petroleum Engineers.
- EIA (U.S. Energy Information Administration). 2010. 2010 State Energy Profiles. www.eia.gov/state/.
- EIA (U.S. Energy Information Administration). 2011. 2011 State Energy Profiles. www.eia.gov/state/.
- EIA (U.S. Energy Information Administration). 2012. 2012 State Energy Profiles. www.eia.gov/state/.
- EIA (U.S. Energy Information Administration). 2015. U.S. State Profiles and Energy Estimates. <http://www.eia.gov/state/>
- Ellsworth, W.I., 2013. Injection-induced earthquakes: Science, v. 341, pp. 142-149.
- Emmons, E. 1838. Report of the second geological district of the State of New York: New York Geological Survey Annual Report, no. 2, p. 185–252.
- Ettensohn, F.R. 2008. Chapter 4: The Appalachian Foreland Basin in the Eastern United States, in: Miall, A., ed., in The Sedimentary Basins of the United States and Canada: Sedimentary Basins of the World, p. 105–179. Elsevier, Amsterdam, Netherlands.

- Evans, D.M., 1966. Denver area earthquakes and the Rocky Mountain Arsenal disposal well: *Mountain Geologist*, v. 3 no. 1, pp. 23-36.
- Fekete Associates, Inc., 2013. F.A.S.T. WellTest™, Pressure Transient Analysis software.
- Ferguson, G. 2015. Deep Injection of Waste Water in the Western Canada Sedimentary Basin. *Groundwater*, vol. 53, no. 2, p. 187-194.
- Fjar, E., Holt, R.M., Raaen, A.M., Risnes, R., and Horsrud, P. (2008). *Petroleum related rock mechanics* (Vol. 53). Elsevier.
- Flaherty, K.J. 1996. Play Dho: Fractured Middle Devonian Huntersville Chert and Lower Devonian Oriskany Sandstone, in Roen, J.B., and Walker, B.J., eds., *The atlas of major Appalachian Basin gas plays: West Virginia Geological and Economic Survey Publication V25*, p. 103–109.
- Floto, B.A. 1954. The possible presence of buried Niagaran reefs in Ohio and their relationship to the Newburg oil and gas zone, in *Oil and gas developments in Ohio: Ohio Department of Natural Resources, Division of Geological Survey Report of Investigations no. 24*, p. 41–53.
- Fort, J., 2013. Exploring the Disposal of Fracking Waste Water – UIC Class II Wells in Ohio, prepared by porter wright for the Oil & Gas Law Report
<http://www.oilandgaslawreport.com/2013/04/13/exploring-the-disposal-of-fracking-waste-water-uic-class-ii-wells-in-ohio/>
- Freeman, L.B. 1949. Regional aspects of Cambrian and Ordovician subsurface stratigraphy in Kentucky: *American Association of Petroleum Geologists Bulletin*, v. 22, p. 1655–1681.
- GAO (U.S. Government Accountability Office), 2012. *Energy-Water Nexus: Information on the quantity, quality, and management of water produced during oil and gas production*: U.S. Government Accountability Office, GAO-12-156, 56 p.
- GAO (U.S. Government Accountability Office), 2014. *Drinking Water, EPA program to protect underground sources from injection of fluids associated with oil and gas production needs improvement*: U.S. Government Accountability Office, GAO-14-555, 103 p.
- Gaudlip, A.W., Paugh, L.O., and Haynes, T.D., 2008. Marcellus Shale water management challenges in Pennsylvania: Society of petroleum Engineers paper 119898, presented at the 2008 SPE Shale Gas Production Conference held in Fort Worth Texas, 16-18 November 2008, 12 p.
- Glohi, B.V. 1984. Petrography of Upper Devonian gas bearing sandstones in the Indiana 71/2-minute quadrangle, well #1 1237 Ind25084, Indiana County, Pennsylvania: University of Pittsburgh, unpublished Master's thesis, 143 p.
- Goodman, A., Hakala, A., Bromhal, G., Deel, D., Rodosta, T., Fraily, S., Small, M., Romanov, V., Fazio, J., Huerta, N., McIntyre, D., Kutcho, B., and Guthrie, G. 2011. U.S.

- Department of Energy (DOE) methodology for the development of geologic storage potential for carbon dioxide at the national and regional scale. *Int. Jour. of Greenhouse Gas Control* 5, p. 952-965.
- Greb, S., Harris, D.C., Solis, M.P., Anderson, W.H., Drahovzal, J.A., Nuttall, B.C., Riley, R.A., Solano-Acosta, W., Rupp, J.A., and Gupta, N. 2009. Cambrian-Ordovician Knox carbonate section as integrated reservoirs and seals for carbon sequestration in the eastern mid-continent United States, in Grobe, M., Pashin, J., and Dodge, R.L., eds., *Carbon dioxide sequestration in geologic media - state of the science*: Tulsa, Okla., American Association of Petroleum Geologists, p. 241-259.
- Greb, S.F., Riley, R. A., Bowersox, J.R., Solis, M.P., Rupp, J.A., Kelley, M., Harris, D.C., and Gupta, N., 2012, Ordovician Knox carbonates and sandstones of the eastern midcontinent: Potential geologic carbon storage reservoirs and seals, in Derby, J.R., Fritz, R.D., Longacre, S.A., Morgan, W.A., and Sternbach, C.A., eds., *The Great American Carbonate Bank: The Geology and Economic Resources of the Cambrian-Ordovician Sauk Megasequence of Laurentia*: AAPG Memoir 98, no. 45, p. 1077-1101.
- Greb, S.F., and Solis, M.P. 2010. Chapter 4: Geologic carbon storage (sequestration) potential in Kentucky, in Parris, T.M., Greb, S.F., Nuttall, B.C., eds., *Evaluation of geologic CO₂ sequestration potential and CO₂ enhanced oil recovery in Kentucky*: Kentucky Geological Survey, ser. 12, Report of Investigation 21, p. 55–212.
- Green, J.C. 1982. Geology of Keweenaw extrusive rocks. In Wold, R.J, and Hinz, W.J. eds. *Geology and tectonics of the Lake Superior Basin*: Geological Society of America Memoir 156, p. 47-55.
- Grider, J., and Parris, T.M. 2014. Updating the fresh-saline water interface map in eastern Kentucky: Kentucky Academy of Sciences 100th annual meeting, Lexington, Kentucky, November 14, 2014.
- Gupta, N. 2013. Conducting Research to Better Define the Sequestration Options in Eastern Ohio and the Appalachian Basin: Final Report prepared under OCDO Grant Agreement No. CDO/D-10-7a.
- GWPC (Ground Water Protection Council), 2005. The effects of the RBDMS/e-commerce initiative on domestic oil and gas production and water resource protection: Groundwater Protection Council Annual Report to U.S. DOE and Congress, 37 p.
- GWPC (Ground Water Protection Council), 2009. State oil and natural gas regulations designed to protect water resources: Ground Water Protection Council Report to U.S. DOE, National Energy Technology Laboratory, 63 p.
- Haddox, C.A., and Dott, R.H. 1990. Cambrian shoreline deposits in northern Michigan. *Journal of Sedimentary Petrology*, 60 (5), p. 697-716.
- Hall, J.A. 1839/ Third annual report of the Fourth Geological District of New York: New York State Geological Survey Annual Report 3: p. 287–347.

- Harbaugh, A.W., Banta, E.R., Hill, M.C., and McDonald, M.G. 2000. *MODular three-dimensional finite-difference ground-water FLOW model* (MODFLOW-2000). U.S. Geological Survey modular ground-water model.
- Harper, J.A. 1989. Effects of recurrent tectonic patterns on the occurrence and development of oil and gas resources in western Pennsylvania: *Northeastern Geology*, V. 11, p. 225-245.
- Harper, J.A. 1991. Preliminary assessment of the stratigraphy and structure of the Cambro-Ordovician carbonate sequence in western Pennsylvania, in *Exploration strategies in the Appalachian basin: 22nd Annual Appalachian Petroleum Geology Symposium*, Morgantown, WV, I.C. White Memorial Fund Publication 3, p. 30–32.
- Harper, J.A., 1998. Why the Drake Well: Bureau of Topographic and Geological Survey, *Pennsylvania Geology*, V. 29, no.1, p. 2-4.
- Harper, J.A., and Laughrey, C.D. 1987. Geology of the oil and gas fields of southwestern Pennsylvania: Pennsylvania Bureau of Topographic and Geologic Survey, Mineral Resources Report M 87, 166 p.
- Harper, J.A., and Patchen, D.G. 1996. Play Dos—Lower Devonian Oriskany Sandstone structural play, in Roen, J.B., and Walker, B.J., eds., *The atlas of major Appalachian gas plays: West Virginia Geological and Economic Survey*, Publication V-25, p. 109–117.
- Harper, J.A. 1999. Devonian, in Shultz, C.H., ed., *The Geology of Pennsylvania: Pennsylvania Geologic Survey*, p. 109-127.
- Harris, D.C., and Baranoski, M.T. 1996. Play Cpk: Cambrian pre-Knox Group play, in Roen, J.B., and Walker, B.J., eds., *The atlas of major Appalachian gas plays: West Virginia Geological and Economic Survey Publication V-25*, p. 188–192.
- Harris, D.C., and Drahovzal, J.A. 1996. Cambrian hydrocarbon potential indicated in Kentucky's Rome Trough: Kentucky Geological Survey, Ser. 11, Information Circular 54, 11 p.
- Harris, D.C., Hickman, J.B., Baranoski, M.T., Drahovzal, J.A., Avery, K.L., and Nuttall, B.C., 2004, Rome Trough Consortium final report and data distribution: Kentucky Geological Survey, ser. 12, Open File Report 04-06.
- Hatcher, R.D., Jr., Thomas, W.A., Geiser, P.A., Snoke, A.W., Mosher, S., and Wiltschko, D.V. 1989. Alleghanian Orogen, in Hatcher, R.D., Jr., Thomas, W.A., and Viele, G.W., eds., *The Appalachian-Ouachita Orogen in the United States: Geological Society of America, The Geology of North America*, v. F-2, p. 233–318.
- Hayes, T. 2011. Characterization of Marcellus and Barnett Shale Flowback Waters and Technology for Water Reuse. Hydraulic Fracturing Technical Workshop #4. Arlington, Virginia: Gas Technology Institute, 30 March 2011.

- Heyman, L. 1977. Tully (Middle Devonian) to Queenston (Upper Ordovician) correlations in the subsurface of western Pennsylvania: Pennsylvania Geological Survey, 4th ser., Mineral Resource Report 73, 16 p.
- Hohn, M.E. 1996. Play Paf: Middle Pennsylvanian Allegheny Formation/Group sandstone play, in Roen, J.B., and Walker, B.J., eds., The atlas of major Appalachian Basin gas plays: West Virginia Geological and Economic Survey Publication V25, p. 23–25.
- Hohn, M.E., Matchen, D.L., Vargo, A.G., McDowell, R.R. 1993. Petroleum geology and reservoir characterization of the Big Injun sandstone (Price Formation) in the Rock Creek (Walton) field, Roane County, West Virginia: West Virginia Geological & Economic Survey Bulletin 43, 76 p.
- Hopkins, H.T. 1966. Fresh-saline water interface map of Kentucky: U.S. Geological Survey–Kentucky Geological Survey, ser. 10, Hydrogeologic Map 21, 19 p. plus 1 sheet, scale 1:500,000.
- Hoppe, W.J., Montgomery, E.W., and Van Schmus, W.R., 1983, Age and significance of Precambrian basement samples from northern Illinois and adjacent states: Journal of Geophysical Research, v. 88, p. 7270-7286.
- Hoskins, H.A. 1947. Analysis of West Virginia Brines: West Virginia Geologic and Economic Survey Publication, Reports of Investigation RI-1, p. 22.
- Horner, D.R. 1951. Pressure build-up in wells, Proceedings of the Third World Petroleum Congress, The Hague, Session II:503-523.
- Horvath, A.L. 1970. The Silurian of southern Ohio, in Silurian stratigraphy, central Appalachian basin: Roanoke, VA, Appalachian Geological Society Field Conference, 17–18 April 1970, p. 34–41.
- Hussing, R.B. 1994. Structure and sedimentation of Upper Devonian Bradford Group “Kane” sandstone of the Cush Cushion Field, west-central Pennsylvania: West Virginia University, unpublished Master’s thesis, 84 p.
- Jaeger, J.C., Cook, N.G., and Zimmerman, R. 2009. Fundamentals of rock mechanics. John Wiley & Sons.
- Janssens, A. 1973. Stratigraphy of Cambrian and Lower Ordovician rocks in Ohio: Ohio Department of Natural Resources, Division of Geological Survey, Bulletin 64, 197 p.
- Jehn, P, and Grunewald, B., 2007. Facilitating oil industry access to federal lands through interagency data sharing: Ground Water Protection Research Foundation, Final Report, DOE No. DE-FC26-06NT15542, 25 p.
- Jillson, W.R. 1937. Natural gas in eastern Kentucky: A summary account of the occurrence of natural gas in the eastern part of this commonwealth coupled with brief statements as to the production and geology of each separate field: The Standard Printing Co., Inc., 237 p.

- Johnson, K. 2015. Underground Injection Control Program, Penn State Webinar, January 2015. Available at <http://extension.psu.edu/natural-resources/natural-gas/webinars>.
- Kakadjian, S., Thompson J., Torres R., Trabelsi, S., and Zamora, F. 2013, Stable fracturing fluids from waste water: Society of Petroleum Engineers (SPE) paper 167175, presented at the SPE Unconventional Resources Conference – Canada in Calgary, Alberta, Canada, 5-7 November 2013, 17 p.
- Kauffman, M.E. 1999. Eocambrian, Cambrian, and transition to Ordovician, in Shultz, C.H., ed., *Geology of Pennsylvania: Pennsylvania Geological Survey and Pittsburgh Geological Society, Special Publication 1*, p. 59–73.
- Kahle, C.F., and Floyd, J.C. 1972. *Geology of Silurian rocks northwestern Ohio: Ohio Geological Society Fieldtrip Guidebook*, 91 p.
- Kelley, D.R., and McGlade, W.G. 1968. Medina and Oriskany production along the shore Lake Erie, Pierce Field, Erie County, Pennsylvania. In *Ontario Petroleum Inst. Conf.*, Windsor.
- Kelley, D.R., and McGlade, W.G. 1982. Medina and Oriskany production along the shore of Lake Erie, Pierce Field, Erie County, Pennsylvania: *Pennsylvania Geological Survey, 4th ser., Mineral Resource Report 60*, 38 p.
- KGS (Kentucky Geological Survey). 2015. Tertiary Oil Recovery Information System (TORIS) Database Enhancement in Kentucky: Kentucky Geological Survey, accessed January 21, 2015. Available at www.uky.edu/KGS/emsweb/toris/toris.html.
- Kestin, J., Khalifa, E.H., and Correia, R.J. 1981. Tables of the Dynamic and Kinematic Viscosity of Aqueous NaCl Solutions in the Temperature Range 20-150 C and the Pressure Range 0.1-35 MPa. *Journal of Physical Chemistry Reference Data*, 71-87.
- Kim, W.Y. 2013. Induced seismicity associated with fluid injection into a deep well in Youngstown, Ohio. *Journal of Geophysical Research: Solid Earth*, 118, no 7, 3506-3518.
- Kostelnik, J., and Carter, K.M. 2009a. The Oriskany Sandstone Updip Permeability Pinchout: A Recipe for Gas Production in Northwestern Pennsylvania: *Pennsylvania Geology*, v.39, no.4, p. 19-24.
- Kostelnik, J., and Carter, K.M. 2009b. Unraveling the stratigraphy of the Oriskany Sandstone: A necessity in assessing its site-specific carbon sequestration potential: *Environmental Geosciences*, v. 16, no.4, p. 187-200.
- Krebs, C.E., and Teets, D.D.S., Jr. 1914. Kanawha County: West Virginia Geological and Economic Survey, *County Geologic Report CGR-11a*, 679 p.
- Lane, A.C., Prosser, C.S., Sherzer, W.H., and Grabau, A.W. 1909. Nomenclature and Subdivision of the Upper Silurian strata of Michigan, Ohio, and Western New York: *Geological Society of American Bulletin*, v. 19, p. 553–556.

- Langevin, C.D., Thorne, D.T., Dausman, A.M., Sukop, M.C., and Guo, W. 2008. SEAWAT Version 4: A Computer Program for Simulation of Multi-Species Solute and Heat Transport. U.S. Geological Survey Techniques and Methods Book 6, Chapter A22.
- Larese, R.E. 1974. Petrology and stratigraphy of the Berea Sandstone in the Cabin Creek and Gay-Fink trends, West Virginia: Unpublished Ph.D. dissertation, West Virginia University, 246 p.
- Laughrey, C.D. 1984. Petrology and reservoir characteristics of the Lower Silurian Medina Group sandstones, Athens and Geneva fields, Crawford County, Pennsylvania: Pennsylvania Geological Survey, 4th ser., Mineral Resource Report 85, 126 p.
- Laughrey, C.D., and Harper, J.A. 1986. Comparisons of Upper Devonian and Lower Silurian tight formations in Pennsylvania - geological and engineering characteristics, in Spencer, C.W., and Mast, R.F., eds., *Geology of tight gas reservoirs: American Association of Petroleum Geologists Studies in Geology* 24, p. 9–43.
- Laughrey, C.D., Kostelnik, J., Carter, K.A., and Harper, J.A. 2007. Petrologic and petrophysical evaluation of the Lockport Dolomite (Middle Silurian) for geological sequestration of CO₂ in the central Appalachian basin (abs.): American Association of Petroleum Geologists - Eastern Section, 36th Annual Meeting, Program with Abstracts, 16-18 September 2007, Lexington, Kentucky, p. 42.
- Lee, W.J. 1982. Well Testing. Society of Petroleum Engineers: Textbook Series No. 1.
- Lewis, J.E. 2013. Evaluation of the Newburg Sandstone of the Appalachian Basin as a CO₂ Geologic Storage Resource; *Environmental Geosciences*, v. 20, p. 137-150.
- Lidiak, R.G., and Zietz, I. 1976. Interpretation of aeromagnetic anomalies between latitude 37 N and 38 N in Eastern and Central U.S. Geological Society of America Special Paper 167, 37p.
- Lundegard, P.D., Samuels, N.D. and Pryor, W.A. 1985. Paleogeography, paleoclimate, and sedimentary processes of the Late Catskill Delta in Woodrow, D.L. and Sevon, W.D., eds., *The Catskill Delta: The Geological Society of America*, p. 107-121.
- Lutz, B.D., Lewis, A.N., and Doyle, M.W. 2013. Generation, transport, and disposal of wastewater associated with Marcellus Shale gas development. *Water Resources Research* 49, 647-656.
- Lytle, W.S., Heyman, L., Kelley, D.R., and Wagberm W.R. 1971. Future petroleum potential of western and central Pennsylvania, in Cram, I.H., ed., *Future petroleum provinces of the United States – their geology and potential: American Association of Petroleum Geologists Memoir* 15, V. 2, p. 1232-1242.
- Mace, R.E., Nicot, J.P., Chowdhury, A.H., Dutton, A.R., Kalaswad, S., 2005. Please pass the salt: using oil fields for the disposal of concentrate from desalination plants: *Texas Water*

- Development Board, Bureau of Economic Geology, Desalination and Water Purification Research and Development Program, Report 112, 229 p.
- McCormac, R., Mychkovsky, G.O., Opritza, S.T., Riley, R.A., Wolfe, M.E., Larsen, G.E., and Baranoski, M.T. 1996. Lower Silurian Cataract/Medina Group ('Clinton') sandstone play in The atlas of major Appalachian gas plays: West Virginia Geological and Economic Survey Publication V-25, p. 156-163.
- McCurdy, R. 2011. Underground Injection Wells for Produced Water Disposal. United States Environmental Protection Agency Technical Workshop Proceedings: Hydraulic Fracturing Technical Workshop 4.
- McCurdy, R., 2013. Underground Injection Wells for Produced Water Disposal – presentation to the U.S. Environmental Protection Agency, downloaded from http://www2.epa.gov/sites/production/files/documents/21_McCurdy_-_UIC_Disposal_508.pdf
- McDonald, J., Wickstrom, L.H., Steck, C.D., and Wells, J.G., 2005. Conversion of the Ohio oil- and gas-well township-location maps to a geographical information system: history and methodology: Ohio Department of Natural Resources, Division of Geological Survey, Information Circular 61, 34 p.
- McGuire, W.H., and Howell, P. 1963. Oil and gas possibilities of the Cambrian and Lower Ordovician in Kentucky: Lexington, Kentucky., Spindletop Research Center for the Kentucky Department of Commerce, 216 p.
- McFarlan, A.C. 1943. Geology of Kentucky: The University of Kentucky, 531 p.
- McLelland, J., Selleck, B., Bickford, M. 2010. Review of Proterozoic evolution of the Grenville Province, its Adirondack outlier, and the Mesoproterozoic inliers of the Appalachians. Geological Society of America Memoir 206, p. 21-49.
- McLin, S.G, 1986. Evaluation of aquifer contamination from salt water disposal wells: Proceedings Oklahoma Academy of Science, V. 66 pp. 53-61.
- Matchen, D.L., and Vargo, A.G. 1996. Play Mws: Lower Mississippian Weir sandstones, in Roen, J.B., and Walker, B.J. eds., The atlas of major Appalachian gas plays: West Virginia Geological and Economic Survey, Publication V-25, p. 46–50.
- Martens, J.H.C. 1939. Petrography and correlation of deep-well sections in West Virginia and adjacent states: West Virginia Geological Survey, v. XI, 255 p.
- Matthews, C.S., and Russell, D.G. 1967. Pressure Buildup and Flow Tests in Wells. Henry L Doherty Series Vol 1. New York: Society of Petroleum Engineers.
- Meglan, J.F., and Noger, M.C. 1996. Play Dsu: Lower Devonian—Upper Silurian unconformity, in Roen, J.B., and Walker, B.J., eds., The atlas of major Appalachian gas plays: West Virginia Geological and Economic Survey, Publication V. 25, p. 133–138.

- Milici, R. C. 1980. Relationship of regional structure to oil and gas producing areas in the Appalachian basin. U.S. Geological Survey Miscellaneous Investigations Series Map I-917-F, 5 sheets, scale 1:2,500,000.
- Milici, R.C., and de Witt, W., Jr., 1988, The Appalachian basin, in Sloss, L.L., ed., *Sedimentary Cover- North American Craton*: Geological Society of America, Boulder, Colorado, p. 506.
- Montanez, I.P., 1994, Late diagenetic dolomitization of Lower Ordovician, Upper Knox carbonates: a record of the hydrodynamic evolution of the southern Appalachian Basin: *American Association of Petroleum Geologists Bulletin* 78, p. 1210-1239.
- Montgomery, C.T., and Smith, M.B., 2010. Hydraulic fracturing history of an enduring technology: Society of Petroleum Engineers, JPT Online, <http://www.spe.org/jpt/print/archives/2010/12/10Hydraulic.pdf> (accessed January 2014).
- Moody, T., 1994. Current and Proposed Regulations for Salt-Water Disposal Wells: Gulf Coast Association of Geological Societies, Vol. 44, p. 515-520.
- MRCSP (Midwest Regional Carbon Sequestration Partnership). 2005. Characterization of Geologic Sequestration Opportunities in the MRCSP Region: Phase I Task Report Period of Performance: October 2003–September 2005, Open File Report 2005-1. Prepared under DOE Cooperative Agreement No. DE-PS26-05NT42255, 152 p.
- MRCSP (Midwest Regional Carbon Sequestration Partnership). 2008. Characterization of Geologic Sequestration Opportunities in the MRCSP Region: Middle Devonian-Middle Silurian Formations. MRCSP Phase II Topical Report prepared under DOE Cooperative Agreement No. DE-FC26-05NT42589 and OCDO Grant Agreement No. DC-05-13.
- Muffler, L.P.J. 1979. Assessment of geothermal resources of the United States–1978, U.S. Geological Survey Circular 790, 163 p.
- Murin, T.M. 1988. Sedimentology and structure of the First Bradford Sandstone in the Pennsylvania Plateau Province: University of Pittsburgh, unpublished Master's thesis, 95 p.
- Murray, K.E. 2014. Fluid Injection Inventory for Class II UIC Wells of Oklahoma. Ground Water Protection Council Annual UIC Meeting, 23 January 2014, New Orleans, Louisiana.
- Mussman, W.J., and Read, J.F., 1986, Sedimentology and development of a passive- to convergent-margin unconformity: Middle Ordovician Knox unconformity, Virginia, Appalachians: *Geological Society of America Bulletin*, v. 97, p. 282-295.
- Mussman, W.J., Montanez, I.P., and Read, J.F. 1988. Ordovician Knox paleokarst unconformity, Appalachians, in James, N.P., and Choquette, P.W., eds., *Paleokarst*: Springer-Verlag, New York, p. 211–229.

- National Petroleum Council, 2011. Regulatory data management: National Petroleum Council, North American Resource Development Study, Paper 2-20, 13 p.
- National Research Council, 2012. Induced seismicity potential in energy technologies: National Academies Press, Washington, DC, 300 p.
- Nicholson, C., and Wesson, R.L., 1990. Earthquake hazard associated with deep well injection-A report to the U.S. Environmental Protection Agency: U.S. Geological Survey Bulletin 1951, 74 p.
- Nicot, J.P., and Chowdhury, A.H. 2005. Disposal of brackish water concentrate into depleted oil and gas fields: a Texas study. *Desalination*, Vol. 181, No. 1–3, 5 September 2005, p. 61-74.
- Noger, M.C., Meglen, J.F., Humfreys, M., Baranoski, M.T. 1996. Upper Silurian Lockport Dolomite-Keefer (Big Six) Sandstone, in Roen, J.B., and Walker, B.J., eds., *The atlas of major Appalachian basin gas plays: West Virginia Geological and Economic Survey Publication v. 25*, p. 145-150.
- NREL (National Renewable Energy Laboratory). 2013. Geothermal Dynamic Maps, GIS Data, & Analysis Tools. Available at <http://www.nrel.gov/gis/geothermal.html>.
- NYSM (New York State Museum). 2013. Empire State Oil and Gas Information System. Available at <http://esogis.nysm.nysed.gov/esogis/index.cfm>.
- OECD (Organisation for Economic Co-operation and Development), 1997. *The Environmental Effects of Freight: Organization for Economic Co-operation and Development*, 35 p., <http://www.oecd.org/trade/envtrade/2386636.pdf>
- Oliver, W.A. 1967. Stratigraphy of the Bois Blanc Formation in New York: U.S. Geological Survey Professional Paper 584–A, 8 p.
- General Land Office Rept., p. 170.
- ODNR (Ohio Department of Natural Resources). 2012. Preliminary report on the Northstar 1 Class II injection well and the seismic events in the Youngstown, Ohio, area: Ohio Department of Natural Resources preliminary report, March 2012, 23 p.
- ODNR (Ohio Department of Natural Resources). 2013. Shale Well Drilling and Permitting, ODNR Oil and Gas Division. Available at <http://oilandgas.ohiodnr.gov/shale>.
- Opritz, S.T. 1996. Play Dop: Lower Devonian Oriskany Sandstone updip permeability pinchout, in Roen, J.B., and Walker, B.J., eds., *The atlas of major Appalachian gas plays: West Virginia Geological and Economic Survey, Publication V-25*, p. 126–129.
- Owen, D.D. 1847. Preliminary report of the geological survey of Wisconsin and Iowa: U.S.

- PA DEP (Pennsylvania Department of Environmental Protection), 2008. DEP investigates source of elevated total dissolved solids in Monongahela River: Pennsylvania Department of Environmental Protection, News Release, Harrisburg, PA, 22 October, 2008, <http://s3.amazonaws.com/propublica/assets/monongahela/10.22.08PADEPPressReleaseonTDSInvestigation.pdf> .
- PA DEP (Department of Environmental Protection). 2014. Pennsylvania Department of Environmental Protection Oil and Gas Reporting Website: <https://www.paoilandgasreporting.state.pa.us/publicreports/Modules/Welcome/Welcome.aspx>, accessed February 2015.
- PA*IRIS/WIS (Pennsylvania Internet Record Imaging System/Wells Information System). 2014. Well completion data and location data, Pennsylvania Geological Survey database. Available at <http://www.pairis.state.pa.us>, accessed February 2015.
- Parrish, J.B., and Lavin, P.M. 1982. Tectonic model for kimberlite emplacement in the Appalachian Plateau of Pennsylvania. *Geology*, v. 10, p. 377-347.
- Patchen, D.G., Avary, K.L., and Erwin, R.B., coords. 1985. Correlation of stratigraphic units in North America, northern Appalachian region correlation chart. Tulsa, Okla., American Association of Petroleum Geologists, 1 sheet.
- Patchen, D.G., and Harper, J.A. 1996. Play Doc: The Lower Devonian Oriskany sandstone combination traps play, in Roen, J.B., and Walker, B.J., eds., *The atlas of major Appalachian gas plays: West Virginia Geological and Economic Survey, Publication V-25*, p. 118–125.
- Patchen, D., Hickman, J., Harris, D., et al. 2006. A Geologic Play Book for Trenton-Black River Appalachian Basin Exploration. Final Report prepared under U.S. Department of Energy (DOE) Award Number: DE-FC26-03NT41856.
- PA*IRIS/WIS (Pennsylvania Internet Record Imaging System/Wells Information System). 2015. Well completion data and petroleum production data, Pennsylvania Geological Survey database. Available at <http://www.pairis.state.pa.us>, accessed January 22, 2015,
- Pepper, J.F., deWitt, W., Jr., and Demarest, D.F. 1954. Geology of the Bedford Shale and Berea Sandstone in the Appalachian basin: U.S. Geological Survey Professional Paper 259, 111 p.
- Perry, C., Erenpretss, M., Leftwich, T., Riley, R., Schumacher, G., Solis, M., and Wolfe, M. 2013. Conducting Research to Better Define the Sequestration Options in Eastern Ohio and the Appalachian Basin: Final Report prepared under OCDO Grant Agreement No. CDO/D-10-7b and the Ohio Department of Natural Resources State of Ohio.
- Piotrowski, R.G., and Harper, J.A. 1979. Black shale and sandstone facies of the Devonian “Catskill” clastic wedge in the subsurface of western Pennsylvania: US Department of Energy, Eastern Gas Shales Project, Series 13, Morgantown Energy Technology Center, 40 p.

- Piotrowski, R.G. 1981. Geology and natural gas production of the Lower Silurian Medina Group and equivalent rock units in Pennsylvania: Pennsylvania Geological Survey, 4th ser., Mineral Resource Report 82, 21 p.
- Platt, S. 2009. EPA's Underground Injection Control Program Brine Disposal Well Regulation in Pennsylvania. Pennsylvania Department of Education UIC Advisory Council.
- Pratt, T., Culotta, R., Hauser, E., Nelson, D., Brow, L., Kaufman, S., Oliver, J., and Hinze, W. 1989. Major Proterozoic basement features of the eastern Midcontinent of North America revealed by recent COCORP profiling: *Geology*, v. 17, p 505-509.
- Price, P.H. 1929. Pocahontas County: West Virginia Geological Survey, 531 p.
- ProChemTech International. 2013. Marcellus Gas Well Hydrofracture Wastewater Disposal by Recycle Treatment Process. Available at http://www.prochemtech.com/Literature/TAB/PDF_TAB_Marcellus_Hydrofracture_Disposal_by_Recycle_1009.pdf, accessed August 22, 2013.
- PTTC (Petroleum Technology Transfer Council). 2005. TORIS Database for the Appalachian Region: <http://karl.nrcce.wvu.edu/TORIS.html>, accessed February 2015.
- Quinlan, G.M., and Beaumont, C. 1984. Appalachian thrusting, lithospheric flexure, and the Paleozoic stratigraphy of the eastern interior of North America. *Canadian Journal of Earth Sciences*, Vol. 21, No. 9, p. 973–996.
- RBDMS.Net, 2014. About RBDMS.Net: Ground Water Protection Council, <http://rbdmsonline.org/GWPC/About.aspx> (accessed 1/27/2014).
- Read, 1989a, Controls on evolution of Cambrian-Ordovician passive margins, U.S. Appalachians, in Crevello, P.S., ed., Controls on carbonate platform and basin development: Society of Economic Mineralogists and Paleontologists Special Publication 44, p. 147-162.
- Rennick, G., and Whieldon, C. 1970. Bottom-hole Pressure Testing in the East Canton Oilfield of Ohio. Presented at the Winter Meeting of the Ohio Oil and Gas Association, 6 March 1970, Columbus, Ohio.
- Rahm, B.G., Bates, J., Bertoia, L., Galford, A., Yoxtheimer, D., and Riha, S. 2013. Wastewater management and Marcellus Shale gas development: Trends, drivers, and planning implications. *J. of Environmental Management* Vol. 120, p. 105-113.
- Rhinehart, J.C. 1979. Lithofacies and paleoenvironmental study of the Lockport-Guelph Group in the subsurface of western Pennsylvania: Master's thesis, SUNY Fredonia, New York, 109 p.
- Riley, R.A., Harper, J.A., Baranoski, M.T., Laughrey, C.D., and Carlton, R.W. 1993. Measuring and predicting reservoir heterogeneity in complex deposystems: The Late Cambrian Rose Run sandstone of eastern Ohio and western Pennsylvania. *Appalachian Oil and Natural*

- Gas Research Consortium, West Virginia University, Morgantown, West Virginia, U.S. Department of Energy, Contract No. DE-AC22-90BC14657, 257 p.
- Roen, J.B., and Walker, B.J. (eds). 1996. The Atlas of Major Appalachian Gas Plays. U.S. Department of Energy, Gas Research Institute, and West Virginia Geological and Economic Survey.
- Rogers, W.B. 1879. Virginia and West Virginia, in Macfarlane, J., An American geological railway guide: New York, D. Appleton and Company, 219 p.
- Rogers, P., and Pitzer, K.S. 1982. Volumetric properties of aqueous sodium chloride solutions. *Journal of Physical Chemical Reference Data*, 15-81.
- Ryder, R.T. 1991. Stratigraphic framework of Cambrian and Ordovician rocks in the Central Appalachian basin from Richland County, Ohio, to Rockingham County, Virginia: U.S. Geological Survey, Miscellaneous Investigations Series, Map I-2264.
- Ryder, R.T. 1992. Stratigraphic framework of Cambrian and Ordovician rocks in the Central Appalachian basin from Morrow County, Ohio, to Pendleton County, West Virginia: U.S. Geological Survey Bulletin 1839-G, 25 p., 1 pl.
- Ryder, R.T. 1994. The Knox unconformity and adjoining strata, western Morrow County, Ohio: in Shafer, W.E., ed., *Ohio Geological Society Anthology, The Morrow County, Ohio "Oil Boom" 1961–1967 and the Cambro-Ordovician reservoir of central Ohio*: Ohio Geological Society, p. 249–271.
- Ryder, R.T., Repetski, J.E., and Harris, A.G. 1996. Stratigraphic framework of Cambrian and Ordovician rocks in the central Appalachian basin from Fayette County, Ohio, to Botetourt County, Virginia: U.S. Geological Survey Miscellaneous Investigations Series Map I-2495.
- Ryder, R.T., Repetski, J.E., and Harris, A.G. 1997. Stratigraphic framework of Cambrian and Ordovician rocks in the Central Appalachian basin from Campbell County, Kentucky, to Tazewell County, Virginia: U.S. Geological Survey, Miscellaneous Investigations Series, Map I-2350.
- Sanders, L.L. 1991. Geochemistry of formation waters from the Lower Silurian Clinton Formation (Albion Sandstone), eastern Ohio: *American Association of Petroleum Geologists Bulletin*, v. 75, no. 10, p. 1593-1608.
- Santos, J.O., Potter, P.E., Easton, R.M., Hartmann, L.A., McNaughton, N.J., and Rea, R., -Joao-Orestes, 2001, Proterozoic Middle Run Formation of eastern Midwest, USA; a Torridonian equivalent? (abs): *Geological Society of America*, v. 33, p. 93.
- Saripalli, K.P., Sharma, M.M., and Bryant, S.L. 2000. Modeling injection well performance during deep-well injection of liquid wastes. *Journal of Hydrology*, Vol. 227, No. 1–4, p. 41-55.

- The Salt Institute. 2013. Physical Properties of Salt. Available at <http://www.saltinstitute.org/salt-101/chemical-physical-properties/>, accessed June 13, 2015.
- Satter, A., Iqbal, G.M., and Buchwalter, J.L., 2007. Practical enhanced reservoir engineering: assisted with simulation software: PennWell Corp., Tulsa, OK, 688 p.
- Schmid, K.W. 2012. The Marcellus Shale gas play – Geology and production and water management, Oh my! Pennsylvania Geology, Vol. 42, No. 2. p. 3-12.
- Seeber, L., Armbruster J.G., and Kim, W. 2004. A Fluid-Injection-Triggered Earthquake Sequence in Ashtabula, Ohio: Implications for Seismogenesis in Stable Continental Regions: Bulletin of the Seismological Society of America, Vol. 94, No. 1, p. 76-87.
- Sevon, W. D. 1968. Lateral continuity of the Ridgeley, Schoharie-Esopus and Palmerton Formations in Carbon and Schuylkill counties, Pennsylvania: Pennsylvania Academy of Science Proceedings, Vol. 42, p. 190–192.
- Shearrow, G.C. 1987. Maps and cross sections of the Cambrian and Lower Ordovician in Ohio. Columbus Ohio Geological Society, 31 p.
- Shrake, D.L., Wolfe, P.J., Richard, B.H., Swinford, E.M., Wickstrom, L.H., Potter, P.E., and Sitler, G.W. 1990. Lithologic and geophysical description of a continuously cored hole in Warren County, Ohio, including description of the Middle Run Formation (Precambrian?) and a seismic profile across the core site: Ohio Department of Natural Resources, Division of Geological Survey Information Circular 56.
- Silin, D.B., Holtzman, R., Patzek, T.W., and Brink, J.L. 2005. Monitoring Waterflood Operations: Hall's Method Revisited (SPE 93879). Society of Petroleum Engineers (SPE) Western Regional Meeting Irvine, California. 30 March – 1 April, 2005.
- Skoff, D., and Billman, D. 2013. Facilitating Shale Play Development in Pennsylvania - Meeting the Need for Nearby Brine Disposal Wells. American Association of Petroleum Geologists 2013 Annual Convention and Exhibition, Search and Discovery Article #80304.
- Shumaker, R.C. 1996. Structural history of the Appalachian basin, in Roen, J.B., and Walker, B.J., eds., The atlas of major Appalachian gas plays: West Virginia Geological and Economic Survey Publication V25, p. 8–22.
- Sminchak, J.R. 2012. Simulation Framework for Regional Geologic CO₂ Storage Along Arches Province of Midwestern United States. Final Report prepared under DOE/NETL Cooperative Agreement No. DE-FC0001034 and OCDO Grant Agreement No. CDO/D-10-03.
- Sminchak, J. and Gupta, N., 2003. Aspects of induced seismic activity and deep-well sequestration of carbon dioxide: Environmental Geosciences, v. 10, no. 2, pp. 81-89.

- Sminchak, J.R., Jagucki, P., and Meggyesy, D. 2006. Rock Core Testing Results in the Mountaineer CO₂ Storage Test Well. Proceedings of the Geological Society of America North-Central Section Annual Meeting, Akron, Ohio, 20-21 April 2006.
- Smosna, R.A. 1983. Diagenetic history of the Silurian Keefer Sandstone in West Virginia and Kentucky: *Journal of Sedimentary Petrology*, Vol. 53, No. 4, p. 1319–1329.
- Smosna, R.A. 1996. Play Mgn: Upper Mississippian Greenbrier/Newman limestones, in Roen, J.B., and Walker, B.J., eds., *The atlas of major Appalachian Basin gas plays: West Virginia Geological and Economic Survey Publication V25*, p. 37–40.
- Smosna, R.A., Conrad, M.J., and Maxwell, T. 1989. Stratigraphic traps in Silurian Lockport Dolomite of Kentucky: *American Association of Petroleum Geologists Bulletin*, Vol. 73, No. 7, p. 876–886.
- Smosna, Richard, Bruner, K.R., and Riley, R.A. 2005. Paleokarst and reservoir porosity in the Ordovician Beekmantown dolomite of the central Appalachian Basin: in *Carbonates and Evaporites*, Vol. 20, No. 1, p. 50–63.
- Sparks, T.N., Harris, D.C., and Bowersox, J.R. 2013. Class I waste-disposal wells and Class II brine-injection wells in Kentucky: Kentucky Geological Survey, ser. 12, Map and Chart 204, scale 1:1,000,000.
- Stose, G.W. 1908. The Cambro-Ordovician limestones of the Appalachian Valley in southern PA: *Journal of Geology*, Vol. 16, p. 698–714.
- STRONGER, 2012. Arkansas Hydraulic Fracturing State Review, report by State Review of Oil and Natural Gas Environmental Regulations. 30 p., downloaded from http://www.aogc.state.ar.us/notices/AR_HFR_FINAL.pdf
- Thamke, J.N., Craigg, S.D., and Mendes, T.M., 1996. Hydrologic data for the East Poplar oil field, Fort Peck Indian Reservation, northeastern Montana: U.S. Geological Survey Open-File Report 95–749, 92 p., downloaded from <http://pubs.er.usgs.gov/publication/ofr95749> .
- Thamke, J.N., and Smith, B.D., 2014. Delineation of brine contamination in and near the East Poplar oil field, Fort Peck Indian Reservation, northeastern Montana, 2004–09: U.S. Geological Survey Scientific Investigations Report 2014–5024, 40 p., downloaded from <http://pubs.usgs.gov/sir/2014/5024/pdf/sir2014-5024.pdf>
- Thomas, W.A. 2006. Tectonic inheritance at a continental margin: *GSA Today*, v. 16, no. 2, p 4-11.
- Thomas, W.A., and Astini, R. 199 Simple-shear confugate rift margins of the Argentine Precordillera and Ouachita embayment of Laurentia: *Geological Society of America Bulletin*, v. 111, p 1069-1079.

- THE Impact Project, 2012. Driving harm: Health and community impacts of living near truck corridors: Trade, Health and Environment Impact project, 11 p., downloaded from <http://hydra.usc.edu/scehsc/pdfs/Trucks%20issue%20brief.%20January%202012.pdf>
- Thornhill, J.T., Short, T.E., and Silka, L. 1982. Application of the area of review concept: Ground Water, v. 20, no. 1, pp. 32-38.
- Tiemann, M., Andrews, A., Copeland C., Folger, P., Brougher, C., and Meltz, R. 2012. Marcellus Shale Gas: Development potential and water management issues and laws: Congressional Research Service Report R42333, 44 p.
- Tomastik, T.E. 1996. Play MDe: Lower Mississippian-Upper Devonian Berea and equivalent sandstones, in Roen, J.B., and Walker, B.J., eds., The atlas of major Appalachian Basin gas plays: West Virginia Geological and Economic Survey Publication V25, p. 56–62.
- Tomastik, T.E. 2013. Ohio Dept. of Natural Resources UIC Program, personal communication, April 20-25, 2013.
- Tsang, C-F., Birkholzer, J., Rutqvist, J., 2007. A comparative review of hydrologic issues involved in geologic storage of CO₂ and injection disposal of liquid waste: Environmental Geology, v. 54, no. 8, pp. 1723-1737.
- Tsang, C-F., and Neimi, A. 2013/ Deep hydrogeology: A discussion of issues and research needs. Hydrogeology Journal, Vol. 21, No. 8, p. 1687-1690.
- Ulrich, E.O. 1911. Revision of the Paleozoic systems: Geological Society of America Bulletin, Vol. 22, p. 281–680.
- URS Corporation. 2011. Water-Related Issues Associated with Gas Production in the Marcellus Shale. Fort Washington, Pennsylvania: NYSERDA.
- U.S. Census, 2010. United States Census Bureau State Population. <http://www.census.gov/topics/population.html>
- USEIA (U.S. Energy Information Administration), 2011. Review of Emerging Resources: U.S. Shale Gas and Shale Oil Plays: U.S. Energy Information Administration, U.S. Department of Energy, 105 p., downloaded from <http://www.eia.gov/analysis/studies/usshalegas/pdf/usshaleplays.pdf>.
- USEIA (U.S. Energy Information Administration), 2014. Annual Energy Outlook 2014 with projections to 2040: U.S. Energy Information Administration, U.S. Department of Energy, DOE/EIA-0383 (2014), 269 p.
- USEPA (U.S. Environmental Protection Agency), 2001. Class I underground injection control program: study of the risks associated with class I underground injection wells: Environmental Protection Agency, Washington DC, Office of Ground Water and Drinking Water, Report No. EPA 816-R-01-007, 113 p

- USEPA (U.S. Environmental Protection Agency), 2004. Evaluation of impacts to underground sources of drinking water by hydraulic fracturing of coalbed methane reservoirs, final report: Environmental Protection Agency, Washington DC, Office of Ground Water and Drinking Water, Report No. EPA 816-R-04-003, 424 p.
- USEPA (U.S. Environmental Protection Agency), 2005. Underground injection control program: 30 years protecting ground water through the Safe Drinking Water Act: U. S. Environmental Protection Agency, Washington DC, Office of Ground Water and Drinking Water, Poster No. 816-H-05-001A.
- USEPA (U.S. Environmental Protection Agency). 2011. UIC Inventory by State – 2011. <http://water.epa.gov/type/groundwater/uic/upload/uicinventrybystate2011.pdf>.
- USEPA (U.S. Environmental Protection Agency), 2012. Protecting drinking water through underground injection control: U. S. Environmental Protection Agency, Washington DC, Office of Ground Water and Drinking Water, Pocket guide EPA 816-K-10-004, 36 p.
- USEPA (U.S. Environmental Protection Agency), 2013b. Draft UIC program guidance on transitioning Class II wells to Class VI wells: U.S. Environmental Protection Agency, Washington D.C, Office of Water, EPA 816-P-13-004, 57 p.
- USEPA (U.S. Environmental Protection Agency). 2013. Water: Underground Injection Control Classes of Wells. Available at <http://water.epa.gov/type/groundwater/uic/wells.cfm>.
- USEPA (U.S. Environmental Protection Agency). 2015a. Water: Underground Injection Control, classes of wells. Available at www.water.epa.gov/type/groundwater/uic/wells.cfm, accessed January 30, 2015.
- USEPA (U.S. Environmental Protection Agency). 2015b. Water: Class II wells–Oil and gas related injection wells. Available at www.water.epa.gov/type/groundwater/uic/class2/index.cfm, accessed January 30, 2015.
- USGS (U.S. Geological Survey). 2002. Produced Waters Database. Available at <http://energy.cr.usgs.gov/prov/prodwat/>, accessed August 22, 2013.
- USEPA (U.S. Environmental Protection Agency). 2002. Technical Program Overview: Underground Injection Control Regulations. U.S. Environmental Protection Agency. Office of Water 4606 EPA 816-R-02-025 Technical Reference.
- USGS (U.S. Geological Survey). 2011. Assessment of Undiscovered Oil and Gas Resources of the Devonian Marcellus Shale of the Appalachian Basin Province, 2011. Fact Sheet 2011-3092.
- USGS (U.S. Geological Survey). 2012. Assessment of Undiscovered Oil and Gas Resources of the Ordovician Utica Shale of the Appalachian Basin Province, 2011. Fact Sheet 2012-3116.

- USGS (U.S. Geological Survey). 2013. Water resources and shale gas/oil production in the Appalachian Basin—Critical issues and evolving developments: U.S. Geological Survey, Open-File Report 2013-1137, 11 p.
- USGS (U.S. Geological Survey). 2014. Estimated Use of Water in the United States in 2010. U.S. Geological Survey Circular 1405, 56 p.
- Van Schmus, W.R., and Hinze, W.J., 1985, The Midcontinent Rift System: Annual Reviews of Earth and Planetary Sciences, v. 13, p. 345-383.
- Vanuxem. 1842. Oriskany Sandstone in Oneida County. Geol. N.Y. pt3. 1842.
- Vanuxem. 1840. Medina Sandstone in Orleans County. Geol. N.Y. pt3. 1840.
- Vargo, A.G., and Matchen, D.L. 1996. Play Mws: Lower Mississippian Weir sandstones, in Roen, J.B., and Walker, B.J., eds., The atlas of major Appalachian Basin gas plays: West Virginia Geological and Economic Survey Publication V25, p. 51–55.
- Veil, J.A., 2011. Water management practices used by Fayetteville shale gas producers: ANL/EVS/R-11/5, prepared by the Environmental Science Division, Argonne National Laboratory, for the U.S. Department of Energy, 26 p., downloaded from http://www.veilenvironmental.com/publications/pw/Water_Mgmt_in_Fayetteville_Shale.pdf
- Veil, J.A., 2013. White paper II summarizing a special session on induced seismicity: Ground Water Protection Council, White Paper II on Induced Seismicity, 33 p.
- Veil, J.A., and Clark, C.E., 2010. Produced water volume estimates and management practices: Society of Petroleum Engineers 125999, presented at International Conference on Health, Safety and Environment in Oil and Gas Exploration and Production, Rio de Janeiro, Brazil, 12-14 April, 2010, 8 p.
- Veil, J.A., Puder, M.G., Elcock, D., and Redweik, R.J., Jr., 2004. A white paper describing produced water from production of crude oil, natural gas, and coal bed methane: ALL Consulting, LLC, US DOE Repot W-31-109-Eng-38, 79 p.
- Vengosh, A., Warner, N., Jackson, R., and Darrah, T., 2013. The effects of shale gas exploration and hydraulic fracturing on the quality of water resources in the United States: Procedia Earth and Planetary Science, V. 7, p. 863-866.
- Venteris, E.R., and Carter, K.M. 2009. Assessing spatial uncertainty in reservoir characterization for carbon sequestration planning using public well-log data: A case study: Environmental Geosciences, Vol. 16, No. 4, p. 211-234.
- Vidic, R., Brantley, S., Vandenbossche, J., and Yoxtheimer, D. 2013. Impact of shale gas development on regional water quality. Science, vol. 340, p 6134.

- Vogel, P.N., King, S.M., and Seaton, W.J. 2010. Seismic survey report, carbon sequestration storage investigatory activity: Project No. DGS A 171-4 Indiana County, Pennsylvania: ARM Geophysics, 25 p. (unpublished report on file at BTGS).
- Wagner, W.R. 1976. Growth faults in Cambrian and Lower Ordovician rocks of western Pennsylvania: American Association of Petroleum Geologists, Vol. 60, No. 3, p. 414-427.
- Walcott, C.D. 1914. Cambrian geology and paleontology: Smithsonian Misc. Coll., v. 57, p. 345–412.
- Warner, D. L. 1988. Hydrogeologic and Hydrochemical Assessment of the Basal Sandstone and Overlying Paleozoic Age Units for Wastewater Injection and Confinement in the North Central Region. Underground Injection Practices Council, Oklahoma City, Oklahoma.
- Wesson, R.L., and Nicholson, C., 1987. Earthquake hazard associated with deep-well injection: U.S. Geological Survey Open-file Report no. 87-331, 112 p.
- Whieldon, C.E., and Eckard, W. 1963. West Virginia oil fields discovered before 1940: U.S. Bureau of Mines Bulletin 607, 187 p.
- White, I.C. 1904. Petroleum and natural gas—Precise levels: West Virginia Geological and Economic Survey, Volume V-1A, 625 p.
- White, T.M., and Drahovzal, J.A. 2002. Fault kinematics of the Rome Trough [abs.]: Geological Society of America Abstracts with Programs, Vol. 33, No. 4, p. A-42.
- Whitmeier, S.J. and Karlstrom, K.E. 2007. Tectonic model for the Proterozoic growth of North America. *Geosphere*, v. 3, p 220-259.
- Wickstrom, L.H., Drahovzal, J.A., Keith, B.D. [coordinators], 1992, The geology and geophysics of the east Continent Rift Basin: Indiana Geological Survey Open-File Study 92-04, 103 p., 32 fig., 23 pl.
- Wickstrom, L.H., Riley, R.A., Spane, F.A., McDonald, J., Slucher, E.R., Zody, S.P., Wells, J.G., and Howat, E. 2011. Geologic assessment of the Ohio Geological Survey CO₂ No.1 well in Tuscarawas County and surrounding vicinity. Ohio Department of Natural Resources, Division of Geological Survey, Open-File Report 2011-3, 81 p.
- Wilson, E.J., Johnson T.L., and Keith, D.W., 2003. Regulating the ultimate sink: managing the risks of geologic CO₂ storage: *Environmental Science and Technology*, v. 37, no. 16, pp. 3476-3483.
- Woodrow, D.L. 1985. Paleogeography, paleoclimate, and sedimentary processes of the Late Catskill Delta, in Woodrow, D.L. and Sevon, W.D., eds., *The Catskill Delta: The Geological Society of America*, p. 51-63.
- Woodward, H.P. 1961. Preliminary subsurface study of southeastern Appalachian Interior Plateau: American Association of Petroleum Geologists Bulletin, v. 45, p. 1634-1655.

- WSC, 2007. Wellcare information for you about Total Dissolved Solids: Water Systems Council Factsheet, 4 p., downloaded from http://www.watersystemscouncil.org/VAiWebDocs/WSCDocs/2010920TDS_FINAL.pdf
- WVGES (West Virginia Geologic and Economic Survey). 2013. Selected References about Devonian Shales. Available at <http://www.wvgs.wvnet.edu/www/datastat/devshales.htm>.
- WVGES (West Virginia Geologic and Economic Survey). 2013. Selected References about Devonian Shales. Available at <http://www.wvgs.wvnet.edu/www/datastat/devshales.html>.
- Yoxtheimer, D. 2015. Shale Energy Produced Fluids Management and UIC Well Disposal Trends. Ground Water Protection Council Annual UIC Conference, Austin, Texas.
- Zagorski, W.A. 1991. Model of local and regional traps in the Lower Silurian Medina Sandstone Group Cooperstown gas field, Crawford and Venango counties, Pennsylvania: M.S. thesis, University of Pittsburgh, 131 p.
- Zenger, D.H. 1965. Stratigraphy of the Lockport Formation (Middle Silurian) in New York State: New York State Museum and Science Service Bulletin 404, 210 p.
- Zheng, C., and Wang, P.P. 1999. MT3DMS - A modular three-dimensional multispecies transport model for simulation of advection, dispersion and chemical reactions of contaminants in ground-water systems: Documentation and user's guide: U.S. Army Corps of Engineers Contract Report SERDP-99-1.
- Zoback, M. D. 2010. Reservoir Geomechanics. Cambridge University Press.
- Zoback, M., Kitasei, S., and Copithorne, B., 2010. Addressing the environmental risks from shale gas development: World Watch Institute, Washington, DC 18 p., downloaded from <http://blogs.worldwatch.org/revolt/wp-content/uploads/2010/07/Environmental-Risks-Paper-July-2010-FOR-PRINT.pdf>